The Role of Phosphate Acquisition in Promoting Stress Resistance and Virulence in a Major Human Fungal Pathogen

Yasmin Ahmed

Thesis submitted in accordance with the regulations of Newcastle University for the degree of Doctor of Philosophy

Faculty of Medical Sciences
Newcastle University Institute for Biosciences
Newcastle University

January 2021

Declaration

I certify that this thesis contains my own work, except where acknowledged, and that no part of this material has been previously submitted for a degree or any other qualification at this or any other university.

Some of this work has also been presented in the following publication:

Ikeh, M[+]., Ahmed, Y[+]. and Quinn, J. (2017) 'Phosphate Acquisition and Virulence in Human Fungal Pathogens', *Microorganisms*, 5(3).

Acknowledgments

Firstly, I would like to thank my supervisor Professor Jan Quinn for her constant support, encouragement, and guidance. I ended up doing my PhD in the JQ lab by chance following a project withdrawal and I think it was the luckiest turn of events. I cannot emphasise enough how thankful I am for all the opportunities you have given me, and I hope you do not regret too much giving me a mug in my first year which said, “shy bairns get nowt”.

Secondly, I would like to thank my progress panel, Dr David Bolam and Dr Julian Rutherford for their expertise and guidance throughout my annual reviews. I would also like to thank the other supervisors in the yeast lab, Dr Elizabeth Veal, Dr Simon Whitehall, and Professor Brian Morgan, for all their help and suggestions throughout my PhD. Thank you also to Dr Peter Banks from the High Throughput Screening Facility at Newcastle University for all his help with the drug screen.

It goes without saying that I have been incredibly lucky to have worked with some of the best and funniest people during my PhD, I feel very fortunate to call them friends. Thank you, Faye, Clement, Callum, Grace, Martin, Katie, Ashleigh, Min, Zoe and Elise! I would also like to thank other JQ lab members past and present including, Dr Alison Day for all her help and a special thank you to Dr Katharina Trunk for all her help, constructive criticism, and support. A big thank you also to Dr Alessandra da Silva Dantas for patiently teaching me how to do the *Galleria* virulence assays.

Also, I would like to thank my friends outside of the lab, for being so supportive even though at times I have spent far too much time in the lab at the detriment of spending time with them.

I would like to say thank you to my parents and sisters for all their love and encouragement over the years to get me here. A special thankyou to my Grandad Stan for all his support and belief in me. Also, all of my animals for (mostly) always making me laugh and de-stress after a long day in the lab.

Finally, I would like to thank Michael, for making me take breaks and for always helping me keep things in perspective. Thank you for all your love and support, I could not have done it without you.

Abstract

The ability of pathogenic fungi to obtain essential nutrients from the host is vital for virulence. In *Candida albicans*, acquisition of the macronutrient phosphate (Pi) is regulated by the Pho4 transcription factor, which is important for both virulence and resistance to diverse and physiologically important stresses. A key aim of this work was to investigate the regulation of Pho4, and the roles of Pho80-Pho85 cyclin dependent kinase (CDK) signalling and inositol polyphosphates were explored. As reported in the model yeast *Saccharomyces cerevisiae,* the Pho80 cyclin functions as a negative regulator of Pho4 in *C. albicans*. However, in contrast to *S. cerevisiae*, the CDK inhibitor Pho81 also negatively regulates *C. albicans* Pho4; Pho4 accumulates in the nucleus in *pho81Δ* cells and Pi acquisition strategies are activated under Pi replete conditions. With regard to inositol polyphosphates, in contrast to that reported in *S. cerevisiae,* IP_7 synthesis by the Kcs1 inositol pyrophosphate synthase was found to be largely dispensable for Pi homeostasis with Vip1-derived IP_7 synthesis playing a more prominent role in *C. albicans*.

The synthesis of the Pi storage molecule polyphosphate (polyP) is also regulated by Pho4. Previous work found that mobilization of Pi from polyP is one of the first responses evoked in response to Pi starvation and precedes activation of the Pho4 transcription factor. A further aim of this thesis was to investigate the importance of polyP mobilisation in the pathobiology of *C. albicans*. It was found that two polyphosphatases, Ppn1 and Ppx1, function redundantly in *C. albicans* to release Pi from polyP. Strikingly, it was shown that polyP mobilisation plays a role in Pho4 activation and stress resistance in *C. albicans*. Blocking polyP mobilisation also resulted in significant morphological defects. Consistent with these findings, data is also presented illustrating that polyP mobilisation is important for the virulence of *C. albicans*.

Given the links between Pi acquisition and virulence, a further aim was to explore whether Pi acquisition could be exploited as a novel antifungal strategy. High-throughput screening of compound libraries revealed potential candidates directly targeting the PHO pathway, which present an exciting avenue for future work.

Taken together, the findings presented in this thesis reveal novel insight into Pi homeostasis mechanisms in *C. albicans* and the potential of targeting this important virulence trait in the development of future therapeutic strategies.

Abbreviations

ABC	ATP-binding cassette
Als	Agglutinin-like sequence
ARG	Arginine
ATP	Adenine Triphosphate
B cell	B lymphocytes
bHLH	Basic helix-loop-helix
C. albicans	*Candida albicans*
C. galbrata	*Candida galbrata*
CDK	Cyclin dependent kinase
C. elegans	*Caenorhabditis elegans*
C. neoformans	*Cryptococcus neformans*
Cu	Copper
DNA	Deoxyribonucleic acid
dNTP	Deoxyribonucleotide triphosphate
E. coli	*Escherichia coli*
EGRF	Epidermal growth factor receptors
Fe	Iron
g	Gram
GFP	Green fluorescent protein
GroPCho	Glycerophosphocholine
G. mellonella	*Galleria mellonella*
Glr1	Gluthathione reductase
GPI	Glycosylphosphatidylinositol
GSNO	S-nitrosoglutathione
GSSG	Gluthathione, producing glutathione disulphide
Gxp	Glutathione peroxidases
H^+	Hydrogen
HIS	Histidine
Hu	Hydroxyurea

Hwp	Hyphal wall protein
H_2O	Water
H_2O_2	Hydrogen peroxide
IP	Inositol pyrophosphate
K^+	Potassium
Kb	Kilobase
KCl	Potassium chloride
KDa	kilodalton
K_m	Michaelis constant
L	Litre
LiAC	Lithium acetate
LOH	loss of heterozygosity
M	Molar
MAPK	Mitogen activated protein kinase
Mg	Magnesium
Min	Minuet
mM	Millimolar
Mn	Manganese
MF	Major Facilitator
MTL	Mating type locus
MLST	Multilocus strain typing
OD	Optical density
ORF	Open reading frame
Na^+	Sodium
NaCl	Sodium chloride
NADPH	Nicotinamide adenine dinucleotide
PCR	Polymerase chain reaction
PEG	Polyethylene glycerol
PHO	Phosphate
Pi	Phosphate

Plb	Phospholipase family
PNMC	Peptone NaCl Magnesium Chloride
PolyP	Polyphosphate
Ppn1	Endopolyphosphatase
Ppx1	Exopolyphosphatase
PTM	Post translational modification
RNS	Reactive nitrogen species
ROS	Reactive oxygen species
RPM	Revolutions per minuet
SDS	Sodium dodecyl sulphate
SDS-Page	Sodium polyacrylamide gel electrophoresis
Saps	Secreted aspartyl proteases
S. cerevisiae	*Saccharomyces cerevisiae*
SP	Serine-Proline residues
SPX	Syg1, Pho81, XPR1 domain
SODs	Superoxide dismutase enzymes
T cell	T lymphocytes
Trr1	Thioredoxin reductase
T. cruzi	*Trypanosoma cruzi*
Trx1	Reductant thioredoxin
URA	Uridine
UV	Ultraviolet
VTC	Vacuolar chaperone complex
YPD	Yeast Peptone Dextrose
YRE	Yap-1 response element
Zn^{2+}	Zinc
µ	Micro

Table of Contents

List of Figures

Chapter 1

Chapter 2

Chapter 3

Chapter 4

Chapter 5

Chapter 6

List of Tables

Chapter 1: Introduction

1.1 Human fungal pathogens

Fungal pathogens are often overlooked despite the major health threat they pose (Brown *et al*., 2012). Severity of disease ranges from superficial to invasive infections (Köhler *et al*., 2017). Alarmingly, incidence of invasive fungal infections is rising. This is due to increases in immunocompromised individuals as medical advancements increase survival of previously fatal conditions/diseases (Köhler *et al*., 2017). There are three main pathogenic fungal species which cause most invasive infections; *Aspergillus fumigatus*, *Cryptococcus neoformans* and *Candida albicans* (Pfaller and Diekema, 2007). *A. fumigatus* is a filamentous, environmental fungi (Brown, et al. 2012). It produces asexual spores called conidiosphores. In immunosuppressed individuals, inhaled conidia can become trapped in the lungs, leading to germination and invasive infection (van de Veerdonk *et al*., 2017). Similarly, *C. neoformans* is also an environmental fungus causing infection by inhalation (Köhler *et al*., 2017). It can cause pulmonary disease or following dissemination from the lung, cross the blood-brain barrier, infecting the central nervous system leading to meningitis (Brown *et al*., 2012). The third fungal pathogen, *C. albicans* is the focus of this work and thus is discussed in greater detail below.

1.1.1 Candida albicans an opportunistic pathogen

In most healthy individuals the fungus *C. albicans* resides as a benign commensal in the oral cavity, skin microflora and gastrointestinal and urogenital tracts (Caldrone and Clancy, 2012). Unlike other members of the digestive tract microbiome, *C. albicans* can colonise any segment of the digestive tract. Transmission of *C. albicans* occurs from mother to baby during birth, thus, playing a role in the early education of the immune system (Willnger *et al*., 1994). However, the benefit of *C. albicans* as a commensal organism remains ambiguous (Poulain, 2013).

The inherent plasticity of *C. albicans* to adapt to a broad range of microenvironments within the host leaves it poised to rapidly proliferate and become pathogenic in the immunocompromised (Scaduto and Bennett 2015). The numbers of immunocompromised individuals are rising because of the AIDs epidemic, chemotherapy, increases in transplantation and antibiotic usage, resulting in an increasing global burden of *Candida* infections (Sellam and Whiteway, 2016). Disease severity ranges from superficial to life

threatening sepsis. Superficial infections including vaginal candidiasis are estimated to affect 75 % of women at some point during their lifetime, 10% of which will experience persistent recurrent infections (Sobel, 2007). Recurrent superficial infections are also typical in AIDS patients with approximately 90% suffering from oropharyngeal candidiasis at least once (de Repentigny *et al*., 2004). Dissemination to the internal organs has a disturbing mortality rate of >40% (Morgan, 2005). Globally, invasive candidiasis has been estimated to be more than 250,000 cases and lead to an excess of 50,000 deaths per year (Zeng *et al*., 2019). Furthermore, *C. albicans* has been recorded as the main infection acquired in a hospital setting and accounts for approximately 15% of all sepsis cases (Nobile and Johnson, 2015). This is despite availability of antifungal drugs such as the azoles, echinocandins and polyenes (Odds *et al*., 2003; Brown *et al*., 2012). The situation is set to be exacerbated by the spread of antifungal resistance (Sharpio *et al*., 2011). Thus, a greater understanding of the pathobiology of *C. albicans* promoting survival within different host niches is warranted to direct new antifungal strategies.

The genome of *C. albicans* is composed of 8 chromosomes with 6,200 genes (Poulain, 2013). Multilocus strain typing (MLST) has discovered 18 clades (Poulain, 2013). *C. albicans* was historically referred to as an obligate diploid, until recently when a complex parasexual cycle was uncovered (Hickman *et al*., 2013). The cycle involves homozygosis at the mating type locus (*MTL*) and epigenetic switching of *C. albicans* to an 'opaque' state (Forche *et al*., 2008). This allows mating and the formation of tetraploids (Hickman *et al*., 2013). Subsequent chromosome reductions result in diploid progeny (Forche *et al*., 2008). This genetic plasticity allows *C. albicans* to adapt to changes within host microenvironments facilitating its pathogenicity.

C. albicans belongs to the ascomycete phylum alongside the model yeast *Saccharomyces cerevisiae* (Berman and Sudbery, 2002). The model yeast paradigm has contributed to the rapid advancement in knowledge of some aspects of *C. albicans* biology including, cell wall biosynthesis, cell cycle regulation and signal transduction (Asleson *et al*., 2001; Berman and Sudbery, 2002). However, the divergence of *C. albicans and S. cerevisiae* 140-841 million years ago (Heckman *et al*., 2001) has led to a myriad of differences. For example, *C. albicans* has developed greater phenotypic plasticity enabling it to overcome challenges encountered within different regions within the host, facilitating survival and proliferation (Mallick *et al*., 2016).

The overall aim of this thesis is to investigate the mechanisms underlying phosphate (Pi) homeostasis in *C. albicans*, to understand the importance of this process in mediating stress resistance and virulence and to explore whether our knowledge of Pi homeostasis can be exploited to identify novel lead compounds for antifungal development. Therefore, in this introduction, an overview of current antifungal strategies is presented, followed by a summary of *C. albicans* virulence traits with specific focus on stress sensing and signalling mechanisms. Finally, an overview of current knowledge pertaining to Pi homeostasis in fungi and links to stress resistance and virulence is presented.

1.2 Antifungal detection and treatment

One of the greatest challenges posed by pathogenic fungi is detection and treatment. The most common methods of detection include blood culturing methods and microscopy. These conventional methods give a 40 % success rate of diagnosing an infection caused by *Candida* species (Pfaller and Diekema, 2007). Furthermore, diagnosing infection using a blood culture approach is less successful at earlier stages of infection. This is a major issue given that the earlier the diagnosis and treatment, the better the prognosis. Increased diagnostic sensitivity is provided by newer methods including PCR and β-glucan detection (Pfaller and Diekema, 2007; Pappas *et al*., 2016). However, these approaches are more costly and are not universally available.

Currently, there are three main classes of antifungals available, azoles, echinocandins and polyenes to treat invasive *Candida* infections. Despite the threat posed by *Candida* species, there have been no new approved antifungal drugs since anidulafungin in 2006 which can also be used against to treat *Aspergillus* infections (Kofla and Ruhnke, 2011). The main issue with developing drugs against fungal pathogens is that there is an evolutionary relationship between them and their hosts thus, limiting the number of druggable targets (Fuentefria *et al*., 2017). Current antifungal targets for *C. albicans* are either its cell wall, which host cells do not possess, or the cell membrane which is ergosterol rich in fungi but cholesterol rich in animal cells (Fisher *et al*., 2020). However, both the fungal cell wall and membrane pose permeability challenges for compounds (Lee *et al*., 2020). Moreover, the development of novel antifungals attracts limited attention from the pharmaceutical industry (Lee *et al*., 2020). Furthermore, some of the most effective antifungals have poor oral bioavailability and therefore need to be administered intravenously. This is both a logistical and financial issue, particularly in low-income countries (Loyse *et al*., 2019).

An additional challenge for antifungals is biofilms. A biofilm is defined as a microbial community enclosed by a secreted polymer matrix (Sardi *et al*., 2014). Most biofilms are mixed species, presenting a more complex problem requiring either broad spectrum antimicrobials or a combination of drugs (Funetefria *et al*., 2007). Biofilms including *Candida* species often colonise voice prosthesis devices (Pentland *et al*., 2020), pacemakers (Sardi *et al*., 2014) and catheters (Funetefria *et al*., 2027), but can form biofilms on any artificial device located within the host (Fuentefria *et al*., 2017). Compared to planktonic cells, those found in a biofilm can be 1000 x more resistant to antimicrobials (Chandra *et al*., 2001). Thus, the development of novel antimicrobial compounds is warranted.

The oldest group of antifungals is the polyenes, many of which were originally isolated from *Streptococcus* species (Chandrasekar, 2010). Most polyenes are no longer used to treat systemic infections other than amphotericin B and its derivatives (Mathew and Nath, 2009). One of the advantages of amphotericin B is its broad-spectrum activity against several species of *Aspergillus*, *Candida,* and *Cryptococcus* (Lee *et al*., 2020). Originally, amphotericin B was thought to directly target the fungal membrane via binding of ergosterol, increasing membrane permeability (Chandrasekar, 2010). However, recent biophysical studies have proposed that amphotericin B causes the extraction of ergosterol from the cell membrane via the formation of extramembranous aggregates (Anderson *et al*., 2014). Thus, it has been dubbed a “sterol sponge” (Anderson *et al*., 2020). Drawbacks of amphotericin B occur due to its ability to interact with the lipid component of human membranes (Van Daele *et al*., 2019). There is also an issue of toxic side effects with amphotericin B treatment (Grela *et al*., 2018). Resistance against azoles is becoming an increasing clinical issue (Verweij *et al*., 2007). Resistance mechanisms include the expansion of target enzyme genes, alterations in ergosterol synthesising enzymes and development of pathways which bypass drug targets (Pemàn *et al*., 2009).

The azoles were first used clinically in the 1980s (Lee *et al*., 2020). Currently there are three generations of azole available. However, most of the first generation have been phased out due to their lack of specificity (Girmenia, 2009). The second and third generation of azoles, including, fluconazole have increased target specificity and are less toxic because they are based on a triazole ring instead of an imidazole structure (Mast et al., 2013). A major advantage of azoles is that most can be effectively administered orally as well as intravenously (Lee *et al*., 2020). Azoles prevent ergosterol biosynthesis via inhibition of the

fungal cytochrome P450 Erg11, thus altering the integrity of the fungal membrane (Mast *et al*., 2013). Furthermore, azoles also trigger the accumulation of sterol intermediates such as, 14-α-methy-3,6-diol which is toxic (Lee *et al*., 2020). However, due to their widespread frequent usage, as well as their fungistatic mode of action, they are susceptible to resistance being generated against them (Revie *et al*., 2020).

The echinocandins are the newest class of antifungals, being licenced for medical use in the early 2000s (Glökner *et al*., 2009). They are currently recommended as the treatment of choice against *Candida* species due to their safety and low drug-drug interaction profile (Lee *et al*., 2020). However, they have a very limited affect against *Cryptococcus* (Lee *et al*., 2020). Echinocandins are derivatives of natural products. Structurally, they are made up of an N-linked fatty-acyl side-chain joined onto a cyclin hexapeptide core (Lee *et al*., 2020). Echinocandins target the synthase of (1,3)-β-D-glucan, a major carbohydrate component of the fungal cell wall encoded by *FSK1* in *C. albicans* (Wagener and Loiko, 2017). Whilst relatively low concentrations of echinocandins are fungicidal, there have been paradoxical reports of strains able to grow at high concentrations but unable to grow at lower doses (Wagener and Loiko, 2017). Whether this phenomenon is only found *in vitro* remains unclear. Inevitably, due to the frequency of their use, resistance against echinocandins is rising (Lee *et al*., 2020). A further drawback of treating invasive Candidiasis with echinocandins is that they are solely delivered intravenously (Van Danele *et al*., 2019).

1.2.1 Antifungal resistance

Antifungal drug resistance in *C. albicans* can occur via various mechanisms including, alteration in drug targets, overexpression of efflux pumps, and genomic modifications. An extensive review of these mechanisms is beyond the scope of this work; thus, a brief summary will be presented for each. A comprehensive review is provided by Lee and colleagues (Lee *et al*., 2020).

One of the most common mechanisms underpinning azole resistance in *C. albicans* is the overexpression of *ERG11*, encoding lanosterol 14-α-demethylase which functions in ergosterol biosynthesis (Revie *et al*., 2018). Thus, there is an increase in target abundance causing a decrease in drug susceptibility. Commonly, resistance against echinocandins in *C. albicans* is conferred by mutations in the glucan synthase gene, *FSK1* (Pfaller *et al*., 2011). Mutations in *FSK1* can decrease drug susceptibility. Antifungal resistance generated against

polyenes via an alteration in the drug target is considerably rarer. However, when it does occur, it is due to either depletion of ergosterol in the membrane or via reduction in enzyme binding affinity. For example, susceptibility of *C. albicans* to amphotericin B occurs when there are mutations in enzymes involved in ergosterol biosynthesis such as, *ERG2, ERG3, ERG5* and *ERG11* (Sanglard *et al*., 2003).

The overexpression of efflux pumps is a further mechanism for antifungal resistance against azoles. However, based on their mode of action, efflux pump overexpression is less of an issue for echinocandins and polyenes (Lee *et al*., 2020). There are two major families of plasma membrane efflux pumps which are implicated in azole resistance. Both deliver substrates across the fungal cell membrane; the ATP-binding cassette (ABC) family and the major facilitator (MF) family (Revie *et al*., 2018). Overexpression of these efflux pumps is underpinned by gain of function mutations in the transcription factors which regulate them, Tac1 and Mrr1 (Lohberger *et al*., 2014). In patients receiving long-term azole treatment, the up-regulation of *CRD1* and *CRD2* in *C. albicans* encoding ABC transporters has been frequently reported in resistant isolates (Revie *et al*., 2018).

One of the key traits of *C. albicans* is its genomic plasticity. It can undergo large scale genomic alterations including aneuploidies, chromosomal rearrangements, and loss of heterozygosity (LOH) (Lee *et al*., 2020). All of which can have an impact on the resistance mechanisms described above. For example, fungistatic azoles can select for aneuploidy by causing atypical cell cycle rounds, altering the DNA content of the fungal cell (Coste *et al*., 2007). In *C. albicans*, it has been found that there is close correlation between azole resistance and gaining an aneuploidy to the left arm of chromosome 5 (Selmecki *et al*., 2006). Karyotype analysis revealed that this specific aneuploidy is an isochromosome comprised of a single centromere flanked by two left arms of chromosome 5 (Selmecki *et al*. 2006). The resistance associated with this includes, LOH, gain of function mutations and an increased copy frequency of *TAC1* and *ERG11* (Coste *et al*., 2007). The occurrence of antifungal resistance to echinocandins and polyenes generated via genomic abnormalities is less frequent. However, it has been reported that chromosome 5 monosomy in *C. albicans* confers a decrease in susceptibility to echinocandins (Yang *et al*., 2013). This is underpinned by changes in the cell wall; the amount of the echinocandin target, β-1,3-glucan diminishes but chitin levels are elevated (Yang *et al*., 2013). Furthermore, resistance to caspofungin is linked to chromosome 2 trisomy (Niimi *et al*., 2010).

1.2.2 Novel strategies to combat antifungal resistance

Given the rise in the number of immunocompromised individuals, the social and economic impact of fungal diseases alongside current antifungal limitations and rising resistance, developing new strategies is paramount. Novel strategies for treating fungal infections include combinational therapy, drug repurposing, targeting virulence determinants and targeting the host immune system.

Combinational therapy, the use of more than one drug at a time, provides an attractive strategy for expanding the fungal armamentarium. It is already employed as a strategy in combating other infectious diseases such as tuberculosis, HIV and malaria (Lee *et al*., 2020). Benefits include a reduction in the likelihood of the fungi acquiring resistance due to more efficiently reducing the pathogen population size (Spitzer *et al*., 2017). Additionally, by combining drugs with distinct modes of actions there is an increase in intracellular targets and thus, a reduction in the probability of resistance emerging (Robbins *et al*., 2017). For example, several mutations are generally needed to accumulate for resistance against two different drugs to occur (Spitzer *et al*., 2017). Furthermore, some drug combinations can be synergistic. For example, when an indole derivative was used with fluconazole the resistance of fluconazole resistant *C. albicans* isolates was overcome (Youngsaye *et al*., 2012).

High-throughput screening of compound collections provide an efficient opportunity to identify synergistic, fungistatic and fungicidal compounds which can be used in combination with existing antifungals (Spitzer *et al*., 2017). Furthermore, high throughput screening of non-antifungal licenced drug libraries can lead to the re-purposing of drugs to combat fungal infections (Stylianou *et al*., 2014). Although a fairly new concept, it has the potential to negate some of the time-consuming processes in the development of antifungals. For example, licenced drugs already have identified and characterised cell targets, mechanisms of action and safety profiles (Kim *et al*., 2019).

A relatively unexploited area is targeting known fungal virulence determinants as an antifungal strategy thus, preventing the pathogen from harming the host. An advantage of this strategy is it expands the number of intracellular targets and provides a weaker selection pressure for developing resistance (Pierce and Lopes-Ribot, 2013). Furthermore, targeting fungal virulence determinants provides good candidates for combinational therapy with traditional antifungals and also may improve their efficiency (Lee *et al*., 2020).

However, the specificity of this strategy means that compounds targeting these virulence determinants may not depending on target have broad spectrum activity against different fungal species. This may prove problematic given the current limitations in diagnosing early invasive *Candida* infections (Pierce and Lopes-Ribot, 2013).

Strategies of targeting the host immune system to treat Candidiasis have had limited success (Lee *et al*., 2020). Studies have investigated the fungal cell wall component, β-glucan, as a vaccine candidate. This is an attractive candidate as this would immunise against a broad spectrum of fungal pathogens, but a caveat is that it has poor immunogenic properties (Armstrong-James *et al*., 2017). However, its immunogenic potential can be increased by conjugating β-glucan to diphtheria toxoids (Torosantucci *et al*., 2005). Initial reports have shown in murine models that vaccines based on β-glucan conjugates can prolong survival (Torosantucci *et al*., 2005). Another vaccine candidate with potential includes the hyphal specific glycophosphatidylinositol cell wall protein agglutinin-like sequence (ALS) protein Als3 (Ibrahim *et al*., 2013). Studies using murine models have found that the immune system mounts robust B and T cell responses to Als3 based vaccines (Ibrahim *et al*., 2013). However, despite initial promising lab results, the pipeline to develop a licenced vaccine is a time-consuming process requiring rigorous testing (Ibrahim *et al*., 2013). Furthermore, the reality of a vaccine against candidiasis relies on interest and prioritisation from pharmaceutical companies.

1.3 Virulence determinants of *C. albicans*

The pathogenic success of *C. albicans* depends on its ability to adhere to and penetrate host tissues and to rapidly respond to changing environments encountered during the infection process within the host. This ability is conferred by a battery of virulence factors. Notably, the expression of virulence factors is not constitutive, rather they are tissue specific and dependent upon infection stage (Brown *et al*., 2007). This section provides a brief overview of the main arsenal of virulence factors expressed by *C. albicans* during different stages of infection.

1.3.1 Adhesins

Central to the colonisation of host tissue are adhesins, biomolecules which facilitate the adherence of *C. albicans* to host cell ligands (Calderone and Fonzi, 2001). The significance of adhesins to the virulence of *C. albicans* is highlighted by the fact that *C. albicans* has greater

adhesive qualities than other members of *Candida* species (Calderone and Braun, 1991). One of the best studied families of adhesins is the agglutinin-like sequence family (Als) which is composed of 8 glycosylphosphatidylinositol (GPI) anchored proteins on the cell surface (Hoyer *et al*., 2008). Structurally, the Als are composed of a single peptide with an N-terminal domain, a 103 amino acid non-repeat Thr-rich region, with a variable central region of 36 amino acid repeats and a C-terminal domain which is Ser/Thr/Asn rich but varying in length (Salgado *et al*., 2011). The C-terminal domain is responsible for attachment of the Als protein to the cell wall. Both the central and C-terminal region are highly glycosylated (Salgado *et al*., 2011). The N-terminus has been shown to be associated with ligand binding (Salgado *et al*., 2011).

The expression of Als is differential depending upon host tissue and conditions (Brown *et al*., 2007). For adherence to epithelial cells the genes encoding Als4 and Als9 have been reported to be preferentially expressed (Hoyer *et al*., 2008). Whereas Als1, Als2, Als3 and Als5 expression appears to be induced by other cell types (Hoyer *et al*., 2008). It has been reported that Als6 binds to gelatine, whereas the ligand that Als7 adheres to remains ambiguous (Hoyer *et al*., 2008). Research has shown that one of the most crucial family members is Als3 which alongside its adhesive role for cell invasion, also functions in biofilm promotion (Nobbs *et al*., 2010), and assimilation of iron (Almedia *et al*., 2009).

Another family of adhesins are the hyphal wall protein family (Hwp) which includes Hwp1, Hwp2 and Rbt1 (Calderone and Fonzi, 2001). The most extensively studied family member is Hwp1, a mannoprotein located on the cell surface (Brown *et al*., 2007). The N-terminal domain of Hwp1 function as a substrate for mammalian transglutaminase (Naglik *et al*., 2006). Expression of *HWP1* occurs in hyphal cells with next to none detected in yeast cells (Naglik *et al*., 2006). Other families of adhesion proteins in *C. albicans* include the Iff/Hyr family. An extensive review of adhesion proteins is beyond the scope of the work but can be found in (Zhu and Filler, 2010).

1.3.2 Secreted proteins and peptides

1.3.2.1 Candidalysin

The intestinal epithelial cells are the first contact point between *C. albicans* and the host immune defence (Naglik *et al*., 2017). They play a crucial role against invading microbes by providing a physical and biochemical barrier distinguishing between pathogen and

commensal (Allert *et al*., 2018). Indeed, the ability of *C. albicans* to adhere and penetrate the epithelial cell barrier is key to establishing blood stream infection (Allert *et al*., 2018).

Peptide toxins and cytolytic enzymes have been extensively characterised in bacterial pathogens such as *Bacillus anthracis* (Fribere *et al*., 2016), *Escherichia coli* (Wang and kim, 2013), *Shigella* (Gray *et al*., 2015) and *Vibrio cholerae* (Queen and Satchell, 2013). However, until recently none were documented in *C. albicans*. An exciting recent discovery by Moyes and colleagues revealed the presence of a novel lytic factor, found to be a 31 amino acid peptide derivative of the *ECE1* gene, named Candidalysin (Moyes *et al*., 2016). *ECE1* is a gene associated with hyphae expressed under most conditions associated with hyphal induction (Naglik *et al*., 2019). The peptide was found to be amphipathic, with an α-helical structure and two amyloidogenic regions, that has pore-forming properties (Moyes *et al*., 2016).

Candidalysin causes damage to epithelial cells by disrupting the integrity of the plasma membrane and induces the immune response by the activation of protein 1 (AP1) transcription factor c-FOS mitogen activated protein kinase (MAPK) signalling pathway (Richardson *et al*., 2018). Induction of this pathway occurs via activation of epidermal growth factor receptors (EGFR) on epithelial cells indirectly by Candidalysin. Indirect mechanism of this activation was found to be by the induction of epiregulin and epigen which are both EFRG ligands, calcium fluxes and induction of matrix metalloproteins (Ho *et al*., 2019). Strains with mutations in the *ECE1* gene can still form hyphae; however, their pathogenicity is impaired as they are unable to stimulate an epithelial cell immune response (Moyes *et al*., 2016).

1.3.2.2 Secreted hydrolytic enzymes

Another important virulence determinant of *C. albicans* is the secretion of hydrolytic enzymes. Such enzymes are secreted to breakdown complex macromolecules to readily make available nutrients for the cell. However, they have been adapted in *C. albicans* to aid pathogenicity by carrying out specific functions during infection (Naglik *et al*., 2003). The key secreted hydrolytic enzymes in *C. albicans* are the secreted aspartyl proteases (Saps), phospholipases and lipases (Abegg *et al*., 2010). Such enzymes are responsible for the digestion and distortion of host cell membranes, enhancing tissue invasion and the assimilation of nutrients (Biswas *et al*., 2007). They further contribute to virulence by

degrading complement proteins, cytokines and immunoglobulins all of which are important to the host immune defence (Kantarcioglu and Yucel, 2002).

There are 10 proteins in the Sap family which are encoded by *SAP*1-*10* and range in molecular weight form 35-50 KDa (Naglik *et al*., 2003). The Sap proteins have been reported as being associated with adhesion, hyphal formation, and phenotypic switching (Monod and Zepelin, 2002; Naglik *et al*., 2003; Naglik *et al*., 2004). Expression of Saps is dependent upon environmental cues such as pH (Sorgo *et al*., 2012). For example, the optimum pH for Sap1-3 is 3-4, whereas, Saps 4-6 which are vital for systemic infection have an optimal pH of 5-7, correlating with their function (Naglik *et al*., 2003). Research by Sorgo and colleagues showed by analysing the secretome of *C. albicans,* that Saps4-6 were only present in filamentous cultures with a pH of 7.4 in the presence of N-acetylglucosamine (Sorgo *et al*., 2012). The fact that a large number of Saps are present in *C. albicans*, with different pH optima, is a good example of how *C. albicans* can adapt to numerous anatomical niches within the host.

Another family of hydrolytic enzymes is the phospholipase family which has four members. However, to date only Plb1 has been shown to be required for virulence in *C. albicans* (Ghannoum, 1998). Plb1 penetrates the host cell membrane by hydrolysis of glycophospholipid ester linkages (Mukherjee *et al*., 2003). Expression of *PLB1* is dependent upon environmental conditions (Naglik *et al*., 2003). Interestingly, albeit at low levels, the phospholipase B, Plb3 was reported to be secreted in cultures stressed with fluconazole (Sorgo *et al*., 2011). However, this requires further investigation.

Although substantially less characterised, a further family of secreted enzymes implicated in tissue penetration is the extracellular lipases. There are 10 members of the lipase family with 80% amino acid conservation between them. Functionally, they promote the hydrolysis of the ester bonds of glycerols and phospholipids (Schaller *et al*., 2005). All 10 lipase genes have been shown to be expressed dependent upon environmental cues (Hube *et al*., 2000). Results from transcript profiling studies suggest that lipase genes play roles in morphogenesis and pathogenesis (Hube *et al*., 2000).

1.3.3 Morphological switching

C. albicans can reversibly switch morphogenetic growth forms between yeast, pseudohyphae, and hyphae, dependent upon environmental conditions (Saville *et al*., 2003).

Each form has specific roles to play at different stages of infection. Genetically manipulating cells so that they can only adopt a single morphology either attenuates or renders the cell avirulent in the murine systemic infection model (Lo *et al*., 1997; Murad *et al*., 2001; Saville *et al*., 2003; Lu *et al*., 2013). Yeast cells have been shown to facilitate dissemination (Saville *et al*., 2003) and function in biofilm development (Finkel and Mitchell, 2011). A study by Grubb and colleagues demonstrated that yeast cells have superior ability to adhere to epithelial cells under flow conditions compared to hyphal cells (Grubb *et al*., 2009). Filamentous *C. albicans* cells contribute to the penetration of tissues which has been suggested to be a thigmotropic response (Brand, 2012). The transition from yeast to filamentous form has been extensively investigated because of its intimate link with pathogenicity (Zheng *et al*., 2004; Saville *et al*., 2006; Carlisle *et al*., 2009; Witchley *et al*., 2019).

The induction of hyphal growth in *C. albicans* is elicited by various environmental cues such as ambient temperature, neutral pH, nutrient starvation, presence of N-acetylglucosamine and serum (Biswas *et al*., 2007). These stimuli trigger signal transduction pathways such as the cyclic AMP/protein kinase A and mitogen activating protein kinase (MAPK) pathways (Sudbery, 2011). These pathways regulate transcription factors required for hyphal growth including, *CPH1, CZF1, CPH1* and *EFG1* (Cleary *et al*., 2012). An additional layer of regulation is provided by the transcriptional repressors *NRG1, RFG1* and *TUP1* which repress inappropriate hyphal growth (Cleary *et al*., 2012). The DNA binding protein, *NRG1* is vital for the suppression of filamentation, working in concert with *TUP1* a global transcription repressor (Lu *et al*., 2011). Studies investigating the overexpression of *NRG1* have demonstrated that it suppresses all hyphal growth (Saville *et al*., 2003). In contrast *NRG1* and *TUP1* deficient cells display constitutive hyphal growth (Murad *et al*., 2001).

1.4 Adaptations of *C. albicans* to the host environment

The dynamic interplay between host and pathogen has not only shaped the host immune response but also the molecular strategies of the pathogen to overcome immune defences (Naglik *et al*., 2004). Success of *C. albicans* infection is determined by the effectiveness of the host immune response and in immunocompetent individuals is routinely cleared (Richardson *et al*., 2019).

This section provides an overview of the stresses encountered by *C. albicans* within host environments, and the mechanisms evoked to sense, respond, and survive such stresses. Comprehensive reviews on the innate and adaptive response are beyond the scope of this work and can be found in the work by Neeta and colleagues (Neeta *et al*., 2015).

1.4.1 The host environment

Conditions within the host differ depending upon the precise microenvironment colonised, providing changing challenges which *C. albicans* must negate to survive and proliferate. For example, in the mouth and kidneys there are fluctuations in osmolarity (Barelle *et al*., 2006) and the pH and availability of nutrients is highly niche-dependent (Du and Huang, 2016; Hood and Skarr, 2012). Additional stresses are elicited by the immune system, including increases in host temperature caused by the inflammatory response (Basso *et al*., 2019) and the hostile antimicrobial environment of the phagosome (Brown *et al*., 2012).

Within the host, *C. albicans* must adapt to survive pH fluctuations. Dependent upon the niche, pH can range from pH 2 to pH 10 (Davis, 2003). The gut, oral cavity and within the phagosome are acidic, whereas, the blood stream is weakly alkaline/neutral (Du and Huang, 2016). Fluctuations in pH are not solely niche dependent. For example, pH in the vagina is acidic but can become alkaline during menstruation (Davis, 2003). *C. albicans* also encounters pH fluctuations within the phagosome (Brown *et al*., 2009). When encountering pH stress, *C. albicans* induces pH responsive genes which has been shown during liver invasion (Thewes *et al*., 2007).

Another challenge encountered by *C. albicans* within the host is nutrient limitation. Access of essential nutrients can be restricted in certain niches. Furthermore, *C. albicans* must also compete with members of the microbiota for nutrient availability (Fourie *et al*., 2018). Levels of glucose, the preferred carbon source of *C. albicans,* have been shown to differ between niches within the host (Barelle *et al*., 2006). Moreover, transcriptome profiling studies identified that iron and phosphate (Pi) were both limited in the liver as iron and Pi transporters were up-regulated following invasion (Thewes *et al*., 2007). Nutritional challenges are also faced by *C. albicans* within the phagosome. The up-regulation of ammonium permeases (Fradin *et al*., 2005), glyoxylate cycle genes (Lorenz *et al*., 2004) and genes involved in amino acid synthesis and transport (Rubin-Bejerano *et al*., 2003) indicates a glucose and nitrogen poor environment within the phagosome.

Within the phagosome one of the major fungicidal mechanisms is the generation of toxic reactive oxygen species (ROS), via the NADPH oxidase complex (da Silva Dantas *et al*., 2015). In phagocytosed *C. albicans* cells there is rapid up-regulation of genes involved in detoxifying and repairing oxidative stress including *CAP1*, *CTA1*, *GPX1*, *GPX3*, *TRX1, TRR1* and *TSA1* (Enjalbert *et al*., 2007; Fadin *et al*., 2005; Lorenz *et al*., 2004; Rubin-Bejerano *et al*., 2003). Within the phagosome, *C. albicans* also encounters nitrosative stress from reactive nitrogen species (RNS). A hallmark of this response is the up-regulation of the nitric oxide dioxygenase, Yhb1 which is involved in detoxifying and scavenging nitric oxide (Lorenz *et al*., 2004). *C. albicans* also encounters nitrosative stress during epithelial cell infection indicated by the induction of RNS detoxifying genes (Hromatka *et al*., 2005).

Phagocytes do not just pose an oxidative and nitrosative stress threat; they also inflict cationic stress on *C. albicans* (Brown *et al*., 2014). This is accounted for by the generation of superoxide anions leading to an accumulation of anionic charge which is balanced by an increased influx of K^+ cations into the phagosome (Fang *et al*., 2004). As with osmotic stress, cationic stress leads to the rapid loss of H_20, turgor pressure and reduction of cell size (Brown *et al*., 2014). Many studies have dissected the stress resistance mechanisms of *C. albicans* to individual stresses (Enjalbert *et al*., 2007; da Silva Dantas *et al*., 2010; Komalapyria *et al*., 2015). However, a better representation of the problems *C. albicans* encounters within host niches has been shown in studies investigating the effects of combinations of stresses (Kaloriti *et al*., 2014; Kos *et al*., 2016). Phagocytic potency has been shown to be attributed in part by the synergistic combination of oxidative and cationic stress (Kaloriti *et al*., 2014). A summary of stress encountered by *C. albicans* within the phagosome is shown in Figure 1.1.

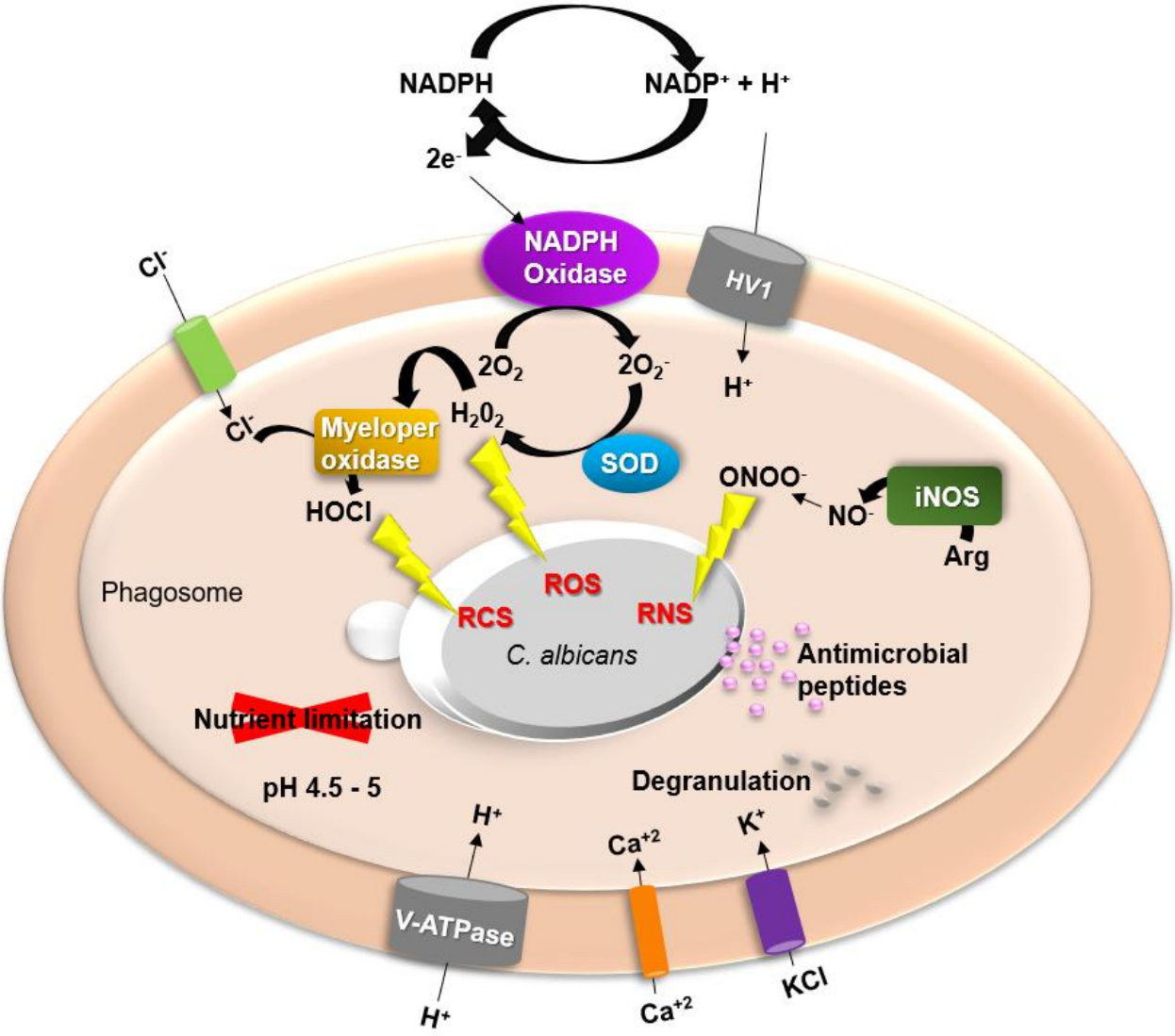

Figure 1.1. *C. albicans* encounters a hostile environment within the phagosome.
C. albicans encounters stress within the phagosome including acidification, antimicrobial peptides, cationic fluxes, reactive oxygen, nitrogen and chloride species, and nutrient limitation. Adapted from (Brown *et al*., 2009; Brown *et al*., 2012).

1.4.2 C. albicans response to oxidative stress

1.4.2.1 ROS as mediators of oxidative stress

At high levels the effects of ROS are cytotoxic (Lushchak *et al.,* 2010). Above threshold levels ROS such as hydrogen peroxide (H_2O_2) and superoxide trigger an imbalance in redox homeostasis causing DNA damage, lipid peroxidation and protein oxidation (Lushchak *et al*., 2010). This damage can cause changes to cell function and lead to apoptosis. DNA damage by ROS causes nucleotide changes or single and double strand breaks and cross linkages resulting in mutations, errors in replicating, genome instability and ultimately cell death (da Silva Dantas *et al*., 2015). In *C. albicans,* exposure to H_2O_2 activates the DNA damage Rad53 checkpoint kinase resulting in cell cycle arrest and the formation of hyperpolarised buds (da Silva Dantas *et al*., 2010). Lipid peroxidation occurs when electrons are removed from lipids by free radical species resulting in a chain reaction and ROS (Lushchak *et al*., 2010). Particularly, this is an issue for cell membranes which are rich in polyunsaturated fatty acids resulting in significant damage, loss of integrity and ultimately cell death (Lushchak *et al*., 2010). The interaction of ROS with proteins can cause oxidation of the peptide backbone, protein to protein cross-links and oxidation of amino side chains which can be reversible or irreversible. Oxidation of regulatory proteins occurs to activate oxidative stress responses, although high levels of ROS can impact on protein stability which can decrease or alter protein function (da Silva Dantas *et al*., 2015). Thus, to attempt to overcome the effects of oxidative stress, *C. albicans* has developed resistance mechanisms and an elaborate antioxidant system.

1.4.2.2 Sources of ROS encountered by C. albicans

There are several different sources of ROS encountered by *C. albicans*. Endogenously, *C. albicans* produces ROS during aerobic respiration. One of the main exogenous sources of ROS encountered by *C. albicans* is from the oxidative burst generated by the host immune system (Komalapriya *et al*., 2015). This occurs following the recognition and engulfment of *C. albicans* by phagocytes which activates the Nicotinamide Adenine Phosphate (NADPH) phagocyte oxidase (Warris and Ballou, 2019). The NADPH phagocyte oxidase releases superoxide into the phagosome (Warris and Ballou, 2019). The toxic environment of the phagosome is exacerbated further as ROS reacts spontaneously with other molecules generating reactive chlorine species (RCS) and reactive nitrogen species (RNS) (Frohner *et al*., 2009). Additionally, phagocytes have also been shown to secrete ROS into the

surrounding external environment (Frohner *et al*., 2009). A further source of ROS encountered by *C. albicans* is from commensal organisms such as *Enterococcus faecalis* and *Lactobacillus acidophilus* which secrete ROS into the external milieu for interspecies competition (Huycke *et al*., 2008; Hertzberger *et al*., 2014).

Furthermore, some antifungal drugs have also been suggested to induce ROS. For example, miconazole has been reported to induce an accumulation of ROS in targeted fungal cells (Delattin *et al*., 2014). Moreover, a correlation has been found between fungicidal activity of miconazole and induced ROS in *C. albicans* and *Candida glabrata* (François *et al*., 2006). Furthermore, treatment with amphotericin B has also been shown to produce ROS against fungal pathogens including *C. albicans* (Mesa-Arango *et al*., 2014).

1.4.2.3 C. albicans antioxidant defence system

Depending on environment, such as in the presence of glucose, *C. albicans* can withstand over 20 mmol 1^{-1} H_2O_2 (Rodaki *et al*., 2009; Nikolaou *et al*., 2009). This is a lot higher than other eukaryotic microbes such as *S. cerevisiae* (Nikolaou *et al*., 2009). Transcript profiling studies have shown that following exposure to H_2O_2 a significant number of antioxidant and detoxifying enzymes are rapidly up-regulated (Enjalbert *et al*., 2003; Enjalbert *et al*., 2006). However, it is noteworthy that exposure to H_2O_2 induces a similar set of genes involved in antioxidant defence in *C. albicans*, *S. cerevisiae* and *Schizosaccharomyces pombe* (Enjalbert *et al*., 2003; Enjalbert *et al*., 2006). Thus, transcriptional responses to H_2O_2 are not underpinning the increased resistance to oxidative stress in *C. albicans*. Whilst these antioxidant defence genes are up-regulated following phagocytosis they are not induced during infection within other host niches (Thewes *et al*., 2007; Enjalbert *et al*., 2007; Walker *et al*., 2009). Thus, induction of oxidative stress response genes is important for survival against assault by phagocytes but are less vital once systemic infection is established (Enjalbert *et al*., 2007).

The response to oxidative stress includes those non-enzymatic ROS scavenging molecules and antioxidant enzymes. Non-enzymatic ROS scavenging molecules include trehalose, glutathione, ascorbic acid, and tocopherols. These function by directly binding ROS detoxifying the harmful free radicals. Enzyme antioxidant defences include catalases, peroxidases, and superoxide dismutases (SODs) (da Silva Dantas *et al*., 2015).

Trehalose is a non-reducing disaccharide which accumulates in response to oxidative stress preventing apoptosis. The accumulation is via the activation of trehalose-6-phospahte synthase (Alvarez-Peral *et al*., 2002). In cells with impaired trehalose production there is increased sensitivity to killing my neutrophils (Mayer *et al*., 2012) and macrophages (Martinez-Esparza *et al*., 2007; Matrinez-Esparza *et al*., 2009) and attenuated virulence in murine models (Zaragoza *et al*., 1998).

Glutathione breaks down H_2O_2 in a reaction catalysed by glutathione peroxidises (Gpx1, Gpx2, Gpx3) (Komalapriya *et al*., 2015). ROS and RNS produced by the host immune response react with glutathione, producing glutathione disulphide (GSSG) and S-nitrosoglutathione (GSNO) respectively (Tillman *et al*., 2015). Consequently, the glutathione reductase (Glr1) then reduces GSSG using NADPH (Komalapriya *et al*., 2015). The glutaredoxins (Grx1, Grx3, Ttr1 and Orf19.4150) present in the glutathione system also function to repair protein thiols that have been damaged by oxidation (Komalapriya *et al*., 2015). The reducing activity of glutathione reductase appears to be specifically induced by being phagocytosed by neutrophils (Enjalbert *et al*., 2007). In murine models, cells defective in glutathione reductase have attenuated virulence (Chaves *et al*., 2007).

One of the most important set of enzymes involved in detoxifying ROS are the SODs which are metalloproteins that convert superoxide into molecular oxygen and H_2O_2. Thus, negating the toxicity of superoxide as H_2O_2 is less harmful (Frohner *et al*., 2009). In *C. albicans* Pi acquisition has been shown to play an important role in superoxide resistance (Ikeh *et al*., 2016). Interestingly, there is an expansion in the genes encoding for SODs in *C. albicans* compared to the model yeast *S. cerevisiae* (Broxton and Cullotta, 2016). This is probably a reflection of *C. albicans* pathogenicity and diversity of environments it can exploit. Sod1 and Sod3 are both cytoplasmic whereas Sod2 is in the mitochondrial matrix. Sod4, Sod5 and Sod6 are extracellular and are exclusively copper (Cu) dependent (Frohner *et al*., 2009). Sod1 is a Cu/zinc (Zn) dependent SOD whereas Sod2 and Sod3 are dependent on manganese (Mn) (Broxton and Cullotta, 2016). The transition to stationary phase from exponential phase represses *SOD1* and induces *SOD3* (Lamarre *et al*., 2001). This is a mechanism for ensuring continuous oxidative stress protection in the face of diminishing Cu levels as the cells approach stationary phase (Lamarre *et al*., 2001). Such effects of Cu fluctuation is mitigated by the switching between Cu dependent and independent SODs and is mediated by the Cu sensing regulator Mac1 (Li *et al*., 2015). At low copper concentrations *C. albicans* switches

from Cu dependent Sod1 to Mn dependent Sod3 (Li *et al*., 2015). With regard to the extracellular Sods, *SOD4* has been shown to be up-regulated in yeast cells and in response to iron (Fe) starvation (Schatzman *et al*., 2020). Whereas induction of *SOD5* is seen during osmotic stress, high pH, and hyphal growth (Martchenko *et al*., 2004; Schatzman *et al*., 2020). Furthermore, Sod5 has been shown to play an important role in detoxifying ROS secreted from phagocytes into the external milieu (Frohner *et al*., 2009). Cells lacking *SOD1* are sensitive to menadione, killing by macrophages and have attenuated virulence in mice (Hwang *et al*., 2002). Similarly, Sod5 has been shown to be required for virulence in mice (Martchenko *et al*., 2004) and for survival in neutrophils (Fradin *et al*., 2005).

In addition to the SODs, catalase, glutathione peroxidases and thioredoxin peroxidases all detoxify H_2O_2. Activation of the *CAT1* gene induces catalase which catalyses the dismutation of H_2O_2 (Znaidi *et al*., 2009). There is an increase in the up-regulation of *CAT1* during phagocytosis (Fradin *et al.*, 2005; Enjalbert *et al*., 2007). Detoxification of H_2O_2 occurs by glutathione peroxidases when the thiol groups of glutathione are oxidised (Miramón *et al*., 2014). The thioredoxin detoxification system is composed of redox regulated thioredoxin peroxidase enzymes, thioredoxin and thioredoxin reductase (da Silva Dantas *et al*., 2010). Induction of the oxidoreductase enzymes, glutaredoxins has been shown to occur following exposure to oxidative, osmotic and heat stress. They also play an important role in the repair protein thiols that have been damaged by oxidation (Komalapriya *et al*., 2015).

1.4.2.4 Signalling pathways activated by ROS

1.4.2.4.1 Cap1

Resistance to H_2O_2 is provided by Cap1 which is an Ap-1-like transcription factor (Alarco and Raymond, 1999), working in concert with Skn7 a response regulator transcription factor (Singh *et al*., 2004). For Cap1 to accumulate in the nucleus, redox-sensitive cysteine residues present near the carboxy terminus must be oxidised (Patterson *et al*., 2013). Nuclear accumulation of Cap1 leads to activation of key oxidative stress response genes. Cap1 activates these genes by binding to the Yap-1 response element (YRE) present within their promoters (Znadidi *et al*., 2009). Genes targeted by Cap1 include *SOD1*, *CAT1*, *GCS1*, *GLR1* and *TRX1* which function together to facilitate *C. albicans* adaptation to oxidative stress and detoxification (Brown *et al*., 2014). Confirmation of the importance of Cap1 is shown by inactivation leading to reduction in oxidative stress response gene induction, increased

sensitivity to oxidative stress, and sensitivity to macrophage killing (Alarco and Raymond, 1999; Enjalbert *et al*., 2006; Patterson *et al*., 2013).

In the presence of combinations of cationic stress and H_2O_2, Cap1 is hyperoxidized and is unable to accumulate in the nucleus and mount an oxidative stress response (Kaloriti *et al*., 2014; Kos *et al*., 2016). This perhaps explains the antimicrobial potency of combinatorial osmotic and oxidative stresses elicited by the host innate immune cells against *C. albicans* (Kos *et al*., 2016). Whilst Cap1 has been shown to be important for survival in neutrophils and macrophages it is, however, dispensable for virulence in systemic murine infection models (Patterson *et al*., 2013; Jain *et al*., 2013).

1.4.2.4.2 Hog1

The stress activated protein kinase (SAPK) Hog1 plays a role in mediating the response to a variety of stresses in *C. albicans*. Whilst beyond the scope of this thesis, a comprehensive review of Hog1 is provided in a recent review (Day and Quinn, 2019). In response to oxidative stress Hog1 is phosphorylated and translocates to the nucleus (Smith *et al*., 2004). However, Hog1 does not play a significant role in oxidative stress induced gene expression (Enjalbert *et al*., 2006). Cells lacking Hog1 are sensitive to ROS (Alonso-Monge *et al*., 2003; Smith *et al*., 2004), so Hog1 function is essential for *C. albicans* to survive this stress. However, the precise role of Hog1 in mediating oxidative stress protection remains unclear (Day and Quinn, 2019). Regarding the relay of oxidative stress signals to the Hog1 module a number of regulators have been identified and include the thioredoxin peroxidase Tsa1, the thioredoxin Trx1 (da Silva Dantas *et al*., 2010) and the response regulator Ssk1 (Chauhan *et al*., 2003). The involvement of the thioredoxin pathway is similar to that reported for activation of the analogous Sty1 MAPK pathway in the model yeast *Schizosaccharomyces pombe* (Veal *et al*., 2004). Although Hog1 activation in response to oxidative stress in impaired in cells lacking the response regulator Ssk1, and *ssk1Δ* cells are sensitive to H_2O_2 and have impaired virulence (Chauhan *et al*., 2003), it is yet to be established whether two component signalling is important for the Ssk1 mediated regulation of Hog1 (Day and Quinn, 2019).

1.4.2.4.3 Rad53

As described above ROS can induce DNA damage. This leads to the activation of the Rad53 DNA checkpoint pathway resulting in cell cycle arrest and the formation of hyperpolarised

buds (da Silva Dantas *et al*., 2010). A range of genotoxic stresses in addition to ROS, including UV, hydroxyurea (HU, an inhibitor of ribonucleotide reductase) and methyl methanesulfonate (MMS) also lead to the activation of Rad53 kinase in *C. albicans* (Shi *et al*., 2007). The hyperpolarised bud is morphologically distinct from pseudohyphae and hyphae cells and is formed independently of Cph1 and Efg1 which are key regulators of hyphae (Shi *et al*., 2007; da Silva Dantas *et al*., 2010). Instead, hyperpolarised bud formation is dependent on the DNA damage checkpoint kinase Rad53 kinase and its upstream regulators (Shi *et al*., 2007). Moreover, cells lacking Rad53 kinase are acutely sensitive to H_2O_2 (da Silva Dantas *et al*., 2010). An important protein in regulating activation of Rad53 and hyperpolarised bud formation, in response to H_2O_2, is the thioredoxin Trx1. Trx1 is a negative regulator of Rad53 in *C. albicans,* which has led to a model whereby exposure to H_2O_2 induces the oxidation and inactivation of Trx1 necessary to allow Rad53 activation and hyperpolarised bud formation (da Silva Dantas *et al*., 2010).

1.4.3 C. albicans response to cationic stress

1.4.3.1 Sources of cationic stress

Within the host there are significant fluctuations in osmolarity particularly within the oral cavity, kidney, and gastrointestinal tract. For example, in the kidney the concentration of NaCl can be up to 600 mmol L^{-1} and the osmolarity can reach 1200 mOsm/kg (Ohno *et al*., 1997). Whereas osmolarity in serum is significantly less ranging from 285 to 295 mOsm/kg (Verbalis, 2003). Thus, the kidney is a highly hypertonic niche within the host. *C. albicans* will also encounter cationic stress following phagocytosis. Within the phagosome the concentration of potassium ions (K^+) can reach up to 200-300 mM (Reeves *et al*., 2002). This is because there is an influx of K^+ into the phagosome to neutralise the anionic charge generated by high levels of superoxide radicals following phagocytosis (Reeves *et al*., 2002).

1.4.3.2 Response to cationic stress

Following exposure to high osmolarity cells experience ion gradient disruption, dehydration, and loss of viability (Brown *et al*., 2017). Transcript profiling studies exposing cells to high concentrations of NaCl resulting in hyperosmotic stress have shown that *C. albicans* responds by inducing osmo-protective genes (Enjalbert *et al*., 2003; Enjalbert *et al*., 2006; Marotta *et al*., 2013). These genes include cation transporters *ENA21* and *ENA22*, genes involved in glycerol synthesis *GDP1* and *RHR2* and genes encoding sugar transporters such as

STL1 (Enjalbert *et al*., 2003; Enjalbert *et al*., 2006). Activating the synthesis of intracellular osmolytes such as glycerol is one of the mechanisms by which *C. albicans* counteracts hyperosmotic stress and restores turgor pressure (Day and Quinn, 2019). Glycerol synthesis occurs when Gpd1 mediates the reduction of the glycolytic intermediate dihydroxyacetone phosphate to glycerol-3-phosphate which is the dephosphorylated by Rhr2 releasing glycerol (Fan *et al*., 2005). Whilst the main osmolyte produced is glycerol there is also accumulation of D-arabitol (Kayingo *et al*., 2005). However, its role in the osmotic stress response remains ambiguous.

Central to the regulation of the response to cationic/osmotic stress in yeast is the Hog1 (High Osmolarity Glycerol) MAPK originally described in *S. cerevisiae* (Brown *et al*., 2017). As in *S. cerevisiae*, in *C. albicans* in response to osmotic stress Hog1 is activated via dual phosphorylation of conserved Thr and Tyr residues by the MAP kinase kinase Pbs2 which, in turn, is activated by the upstream MAP kinase kinase kinase Ssk2 (Day and Quinn, 2019). Phosphorylation of Hog1 leads to Hog1 nuclear accumulation and the up-regulation of genes involved in the osmotic stress response (Smith *et al*., 2004). This includes genes involved in glycerol accumulation *GDP1* and *RHR2* (Enjalbert *et al*., 2006). However, it has been shown that Hog1 nuclear accumulation is dispensable for osmotic stress resistance and Hog1 dependent stress induced gene expression (Day *et al*., 2017). Deletion of *HOG1* leads sensitivity to osmotic stress and impaired virulence (Alonso-Monge *et al*., 1999; Cheetham *et al*., 2011).

Cells grown *in vitro* in the presence of lactate have increased resistance to osmotic stress (Ene *et al*., 2012). However, this increased resistance is attributed to the effects of utilizing an alternative source of carbon and the impact it has upon cell wall architecture and the proteome rather than being Hog1 dependent (Ene *et al*., 2012).

Although Hog1 mediated expression of osmotic stress protective genes is essential for *C. albicans* to respond to fluctuations in osmolarity, the transcription factors involved remain elusive (Day and Quinn, 2019). Screening of a transcription factor deletion collection for mutants which were sensitive to cationic stress identified Pho4 as the transcription factor most sensitive to cationic stress (Ikeh *et al*., 2016). However, transcript profiling revealed that Pho4 does not regulate genes involved in the response to cationic stress (Ikeh *et al*., 2016). As Pho4 regulates Pi homeostasis this suggests instead that Pi acquisition may be an important determinant in mediating resistance to cationic stress.

1.4.4 C. albicans response to pH induced stress

A further stress that *C. albicans* faces within niches in the host is variations in pH. High extracellular pH poses challenges relating to ATP synthesis and nutrient acquisition both needed for growth and survival. This is because proton gradients essential for transport of nutrients across the plasma membrane are harder to establish in alkaline conditions (Brown *et al*., 2017). Furthermore, at an alkaline pH there is a reduction in the bioavailability and solubility of essential nutrients such as Pi (Lev and Djordjecvic, 2018). In *S. cerevisiae*, alkaline pH has been found to trigger a Pi starvation response (Serrano *et al*., 2002; Sambade *et al*., 2005). Moreover, the Pi acquisition factor Pho4 has been shown to accumulate in the nucleus in response to alkaline pH in *S. cerevisiae* (Serra-Cardona *et al*., 2015) and *C. albicans* (Ikeh *et al*., 2016). Furthermore, in *C. neoformans* and *C. albicans* cells unable to acquire Pi via deletion of *PHO4* are acutely sensitive to alkaline conditions (Lev *et al*., 2017; Ikeh *et al*., 2016).

Genes under pH regulation include the putative glycosidases *PHR1* and *PHR2* which are expressed differentially at pH >5.5 and <5 respectively (Berandis *et al*., 1998). Therefore, they are expressed during different infection types; *PHR1* is induced during systemic infection (pH 7.4) and *PHR2* during vaginal infection (pH4) (Hube, 2004). Mutations in *PHR2* lead to strains which can cause systemic infection but are impaired in their ability to establish vaginal candidiasis (Hube, 2004). The pH-dependent expression of *PHR1* and *PHR2* is under the control of Rim10, a zinc finger transcription factor which is activated by upstream signalling from Rim2 and Rim8 (Bensen *et al*., 2004).

Microarray experiments focusing on liver invasion revealed that *DFG16* is vital for pH sensing and pH-dependent hyphal formation (Thewes *et al*., 2007). Whilst mutants lacking *DFG16* grow similar to wild type in an acidic pH environment when the pH is alkaline they exhibit reductions in osmotic tolerance (Wilson *et al*., 2009) and hyphal growth (at pH8>) (Wilson *et al*., 2009) as well as attenuated virulence (Thewes *et al*., 2007). Furthermore, in an alkaline pH environment where Pi or iron is scarce there is growth impairment (Wilson *et al*., 2009).

1.4.5 C. albicans response to nutritional stress

For *C. albicans* to establish a successful infection it must be physiologically robust enough to rapidly adapt to different metabolic niches within the host (Ene *et al*., 2014). Whilst there is

some conservation between regulatory networks there is evolutionary rewiring of metabolic pathways in *C. albicans* compared to *S. cerevisiae* (Lavoie *et al*., 2009). Thus, facilitating plasticity to allow *C. albicans* to colonise and proliferate in almost any niche within the host (Childers *et al*., 2016). Within many niches that *C. albicans* encounters during infection there are low levels of glucose. For example, there is 0.5% glucose in vaginal secretion (Owen and Katz, 1999) and 0.06-0.1% present in the blood stream (Barelle *et al*., 2006). Survival in these environments relies on the ability of *C. albicans* to assimilate complex carbohydrate alternatives such as amino acids, fatty acids, and carboxyl acids (Brown *et al*., 2014 b). Pathways in *C. albicans* to utilise these alternative sources include the glyoxylate cycle and gluconeogenesis (Barelle *et al*., 2006; Brown *et al*., 2014). These pathways have been shown to be intimately linked to the ability of *C. albicans* to be fully virulent (Brown *et al*., 2007). Studies investigating metabolic flexibility have shown that unlike *S. cerevisiae*, *C. albicans* can exploit alternative carbon sources at the same time as assimilating sugars (Childers *et al*., 2016). This is underpinned by a lack of ubiquitin sites in key enzymes of the gluconeogenic and glyoxylate cycle preventing their degradation in the presence of glucose (Childers *et al*., 2016).

Following phagocytosis, alternative carbon assimilation pathways are induced in *C. albicans* (Lornez *et al*., 2004; Barelle *et al*., 2006). Similar pathways are activated in *C. albicans* cells infecting the kidneys (Barelle *et al*., 2006). Post phagocytosis there is up-regulation in genes associated with gluconeogenesis, the glyoxylate cycle, carbon starvation and enzymes functioning in β-oxidation of fatty acids (Rodaki *et al*., 2009). Intriguingly, stimulation of glucose-sensing pathways by transient glucose exposure elicits transcription of oxidative stress response genes (Rodaki *et al*., 2009). This is proposed to be an adaptive prediction of *C. albicans* to account for the likelihood of phagocytic assault on *C. albicans* when it disseminates into the blood stream (Brown *et al*., 2014).

1.4.6 C. albicans response to nutritional immunity

Another facet of the host immune response repertoire is the manipulation of micronutrients. This can be through either attempting to withhold essential micronutrients or through increasing potentially toxic elements (Hood and Skarr, 2012). Copper is crucial for life and plays a role in *C. albicans* oxidative stress resistance and virulence. However, when copper levels are too high it can be cytotoxic, this is because it leads to the accumulation of protein and lipid peroxidation via the generation of free radicals via the Fenton reaction

(Ehrensberger and Bird, 2011). A prime example is the influx of copper into the phagosome as an antimicrobial mechanism (Douglas and Konopka, 2019). To maintain copper homeostasis *C. albicans* cells sense shifts in copper levels. For example, during kidney infection by differentially regulating the copper transporter Ctr1 and copper efflux pump Crp1 (Mackie *et al*., 2016). During early renal infection there is up-regulation of Crp1 to counteract the increasing levels of copper triggered by the host (Mackie *et al*., 2016). Expression of Crp1 is low during early infection (Mackie *et al*., 2016). However, during later infection stages Ctr1 is up-regulated and Crp1 down regulated to account for the decreased copper levels present in the host renal environment (Mackie *et al*., 2016). *C. albicans* also mitigates the effects of copper fluctuations by switching between copper dependent and independent SODs as discussed in section 1.4.2.3.

In cells the assimilation and intracellular mobility of iron is dependent on the bioavailability of copper, which is an evolutionary conserved dependency (Collins *et al*., 2010). *C. albicans* activates transcription of the copper ferroxidase Fet3 to sequester iron (Eck *et al*., 1999). Nutritional immunity is the restriction of essential metals by the host (Hood and Skarr, 2012). An example of this is during disseminated *Candida* infection in the liver, the host has been shown to respond by synthesising more hepcidin in the liver to inhibit tissue stores releasing iron (Portykus *et al*., 2013). Furthermore, haem oxygenases infiltrate the liver to prevent the iron released during erythrocyte recycling from reaching *C. albicans* leading to iron starvation zones (Portykus *et al*., 2013). To negate this *C. albicans* adopts an iron oxygen mechanism dependent upon the haem oxygenase, Hmx1 rather than an iron acquisition mechanism dependent on the high affinity iron permease Ftr1 (Portykus *et al*., 2013). A homozygous deletion of either *FTR1* (Ramanan and Wang, 2000) or *HMX1* (Navarathna and Roberts, 2010) results in attenuated virulence. Thus, highlighting the mechanisms *C. albicans* has to facilitate iron acquisition and circumvent the nutritional immunity strategies of the host.

Access to zinc (Zn) is also restricted within certain niches in the host. However, access to zinc is important for *C. albicans* as it plays a role as the co-factor for certain metalloproteins and Zn dependent transcription factors (Hood and Skaar, 2012). *C. albicans* scavenges Zn from the extracellular environment via the secretion of the zincophore, Pra1 (pH Regulated Antigen) (Citiulo *et al*., 2012). Uptake of Zn into the cells is then mediated by the membrane transporter Zrt1 (Citiulo *et al*., 2012). Infection of the kidney leads to the up-regulation of

PRA1 and *ZRT1* suggesting that *C. albicans* experiences Zn limitation during kidney invasion (Nobile *et al*., 2009; Xu *et al*., 2001).

1.5 Phosphate homeostasis

The high affinity Pi symporter, Pho84 has been found to be up-regulated in several transcript profiling studies examining how *C. albicans* responds to different host niches (Fradin *et al*., 2005; Enjalbert *et al*., 2006; Thewes *et al*., 2007; Zakikhany *et al*., 2007; Walker *et al*., 2009; Hebecker *et al*., 2016; Muñoz *et al*., 2019). Furthermore, previous work has shown that Pi acquisition in *C. albicans* is essential for virulence (Ikeh *et al*., 2016; Liu *et al*., 2018). Moreover, Pi acquisition plays an important role in stress resistance (Ikeh *et al*., 2016; Liu *et al*., 2018). In all organisms Pi is a vital nutrient requirement for nucleic acids, membrane phospholipids, energy storage and transfer (ATP) and signal transduction via protein phosphorylation (Jimenez *et al*., 2016). Therefore, there is tight regulation of its acquisition, storage, and release, to maintain homeostasis. In ascomycetes this is governed by the PHO pathway (Tomah and Sinah, 2014). Whilst knowledge of the PHO pathway in *S. cerevisiae* is well established, in *C. albicans* it remains to be fully elucidated.

In the following sections the well characterised PHO pathway in *S. cerevisiae* will be described first of all. This will be followed by a summary of what is known regarding PHO pathway regulation in several fungal pathogens and the evidence that supports a role of Pi homeostasis in stress resistance and virulence. Finally, two further aspects of Pi homeostasis will be discussed; the role and regulation of the Pi storage molecule polyphosphate (polyP), and the emerging role of inositol polyphosphates in regulating Pi homeostasis.

1.5.1 The PHO pathway in S. cerevisiae

In the model yeast, *S. cerevisiae,* the PHO pathway regulates a number of Pi homeostasis mechanisms including scavenging extracellular Pi and transporting Pi into the cell, as well as regulating Pi storage. The membrane transportation system promotes survival in differing Pi concentrations due to the presence of both high and low affinity transporters (Tomah and Sinah, 2014). Pi is stored in the cell as polyP; a linear polymer composed of inorganic phosphate molecules linked together with high energy phosphoanhydride bonds (Moreno and Docampo, 2013). Initial Pi demands are met by the mobilization of polyP stores (Ogawa *et al*., 2000). The PHO regulatory system monitors cytoplasmic Pi and controls the expression

of genes involved in sensing, uptake, and mobilisation (Tomah and Sinah, 2014). Known proteins involved in the PHO pathway are shown in table 1.

The PHO pathway includes two transcription factors, Pho2 and Pho4, the Pho80-Pho85 cyclin dependent kinase (CDK) complex, and the CDK complex inhibitor Pho81 (Ogawa *et al*., 2000). A member of the myc-family, Pho4 has a basic helix-loop-helix (bHLH) structural motif (Yoshida *et al*., 1989). Pho2 is a homeodomain transcription factor which co-operatively interacts exclusively with unphosphorylated Pho4 during Pi starvation (Yoshida *et al*., 1989). A major aspect of PHO pathway regulation is the cellular location of the Pho4 transcription factor. Following Pi starvation, Pho4 accumulates in the nucleus where it up regulates genes involved in Pi acquisition (Kaffman *et al*., 1994).

When Pi levels are replete (~10 mM) the Pho80-Pho85 CDK complex phosphorylates specific serine residues on Pho4 preventing its nuclear accumulation (Kaffman *et al*., 1994). In *S. cerevisiae*, it has been shown that there are five specific Serine-Proline residues on Pho4 which are targeted by the CDK complex. These include SP1, SP2, SP3, SP4 and SP6; all of which have a distinctive role in Pi regulation (Komeili and O'Shea, 1999). For example, nuclear import of Pho4 is promoted via phosphorylation at SP4, whereas nuclear export is promoted by phosphorylation at SP2 and SP3. Under Pi replete conditions, the interaction of Pho4 with Pho2 is prevented by phosphorylation at SP6 (Komeili and O'Shea, 1999). In *S. cerevisiae*, under Pi limiting conditions, the inositol pyrophosphate IP_7 produced by the enzyme Vip1, binds to the **S**yg1, **P**ho81, **X**PR1 (SPX) domain on Pho81 (Lee *et al*., 2007). Subsequently, Pho81 inhibits the Pho80-Pho85 CDK complex resulting in an accumulation of unphosphorylated Pho4 which can accumulate in the nucleus (Figure 1.2) (Schneider *et al*., 1994). Consequently, Pho4 targets genes involved in Pi homeostasis that are characterised by conserved motifs within their promoter region (CACGTT and/or CACGTG) (Komeili and O'Shea, 1999). These genes encode proteins involved in Pi acquisition and polyP synthesis (Ogawa *et al*., 2000).In *S. cerevisiae*, there are 22 genes which have been identified as being regulated by the PHO pathway (Ogawa *et al*., 2000).

The activation of the PHO pathway is hallmarked by the up-regulation of extracellular Pi acquisition and transport systems which work concurrently. This includes the induction of *PHO5*, *PHO11* and *PHO12* which are secreted acid phosphatases that scavenge Pi from the extracellular milieu (Kennedy *et al*., 2005) (Figure 1.2). In *S. cerevisiae* it has been shown that Pho5 is accountable for almost 90% of acid phosphatase activity (Svaren and Hörz, 1997).

Localisation of the secreted acid phosphatases has been shown to be either at the cell wall or periplasmic space (Kennedy *et al*., 2005). Under Pi replete conditions, low affinity transporters maintain Pi homeostasis. However, during Pi starvation, their activity is down-regulated in favour of increased expression of the high affinity Pi transporters, Pho84 and Pho89 (Kennedy *et al*., 2005) (Figure 1.2). In *S. cerevisiae*, Pho84 is thought to contribute the most significantly to Pi import (Perrson *et al*., 2003). Pho84, has a K_m for external Pi of 1-15 µM, coupling the import of Pi with H^+ (Martinez *et al*., 1998). The stoichiometry of this symporter is 3 H^+ for each Pi anion (Petersson *et al*., 1999). The other high affinity Pi transporter Pho89, couples Pi import with Na^+, with a K_m for external Pi of 0.5 µM and a stoichiometry of 2 Na^+ for every monovalent Pi anion (Petersson *et al*., 1999). Pho84 and Pho89 operate in alternative pH conditions, thus, facilitating the up-take of scavenged external Pi across a broad range of environments. Optimal pH for Pho84 activity is pH 5 whereas, Pho89 activity is optimal under alkaline conditions (Perrson *et al*., 2003).

Feedback loops provide an additional layer of complexity to PHO pathway regulation which is underpinned by Pi availability. Following Pho4 activation, both a positive and negative feedback loop are triggered. A positive feedback loop which elicits Pho4 activation occurs due to the reduction in Pi uptake by the low affinity Pi transporters (Wykoff *et al*., 2007). This follows the Pho4 dependent induction of *SPL2*, encoding a negative regulator of Pho87 and Pho90 (Wykoff *et al*., 2007). Whereas a negative feedback loop inactivating Pho4 occurs by the up-regulation of high affinity Pi transporters, importing Pi into the cell (Wykoff *et al*., 2007).

In addition to Pi acquisition through the dual action of secreted acid phosphatases and phosphate transporters, Pi is also scavenged from phospholipids. This is coordinated by the activation of the Git1 permease (Almaguer *et al*., 2003) and the Gde1 phosphodiesterase (Fisher *et al*., 2005). Phospholipases catalyse the deacylation of phosphatidylcholine generating glycerophosphocholine (GroPCho) which is subsequently imported by Git1 into the cell (Almaguer *et al*., 2003). Gde1 hydrolyses GroPCho to glycerolphosphate which can be utilised as a Pi source and choline (Fisher *et al*., 2005) (Figure 1.2). Other genes up-regulated in response to PHO pathway activation include those involved in polyP synthesis and hydrolysis, discussed in further detail in the section 1.8. Furthermore, many components of the PHO pathway have SPX domains which can bind IP_7 molecules which are suggested to

be play a role in regulating Pi homeostasis. IP signalling molecules are discussed in further detail in section 1.9.

Gene	*S. cerevisiae* function	*C. albicans* homologue/orthologue	Ref.
PHO2	Homeodomain transcription factor. Targets genes which are involved in Pi metabolism.	*GRF10* (C5_05080W_A)	Komeili and O'Shea, 1999
PHO4	Member of the myc-family with a bHLH structure. In response to Pi limiting conditions, it accumulates in the nucleus to up-regulate genes involved in	*PHO4* (C4_05680W_A)	Ogawa *et al*., 2000
PHO5, PHO10, PHO11	Secreted acid phosphatases. Regulated by Pho2 and Pho4 in phosphate limited conditions.	*PHO100* (C1_07430W_A) *PHO112* (CR_02400W_A) *PHO113* (CR_02400W_A)	Ogawa *et al*., 2000
PHO80	Cyclin which interacts with Pho85 to form the Pho80-Pho85 CDK complex. In Pi rich conditions the Pho80-Pho85 CDK complex phosphorylates Pho4 to prevent it from accumulating in the nucleus.	*PHO80* (C6_03810W_A)	Ogawa *et al*., 2000
PHO84	High affinity Pi transporter which has been shown to be localised to the outer membrane.	*PHO84* (C1_11480W_A)	Wykoff *et al*., 2007
PHO85	Forms complex with Pho80. See Pho80 function description.	*PHO85* (C1_04520C_A)	Ogawa *et al*., 2000
PHO87	Low affinity Pi transporter.	*PHO98* (C1_05940W_A)	Ogawa *et al*., 2000
PHO90	Low affinity Pi transporter.	*PHO91* (C1_02050C_A)	Ogawa *et al*., 2000
GIT1	Plasma membrane permease. Facilitates the uptake of GroPCho and glycerophosphinositol as a source of Pi and inositol. Regulated by Pi and inositol levels.	*GIT1* (C2_06590C_A)	Almaguer *et al*., 2003
GDE1	Phosphodiesterase, hydrolyses GroPCho to choline and glycerolphosphate.	*GDE1* (C5_04510W_A)	
MSN5	Involved in nuclear export and import.	*MSN5* (C4_3280W_A)	Ogawa *et al*., 2000
PPX1	Functions as both an endopolyphosphatase and an exopolyphosphatase splitting orthophosphate from the ends of polyP.	*PPX1* (C2_06110W_A)	Ogawa *et al*., 2000
PPN1	Endopolyphosphatase which cleaves long polyP chains.	*PHM5* (C7_00980W_A)	Ogawa *et al*., 2000
VTC1	VTC complex subunit.	*VTC1* (C3_00170C_A)	Ogawa *et al*., 2000

VTC2/3	VTC complex subunit.	*VTC3* (CR_03610C_A)	Ogawa *et al*., 2000
VTC4	VTC complex subunit. Vacuole membrane polyphosphate polymerase. Functions in the synthesis and transfer of polyP to the vacuole.	*VTC4* (C4_03360C_A)	Ogawa *et al*., 2000

Table 1.1. PHO pathway genes.

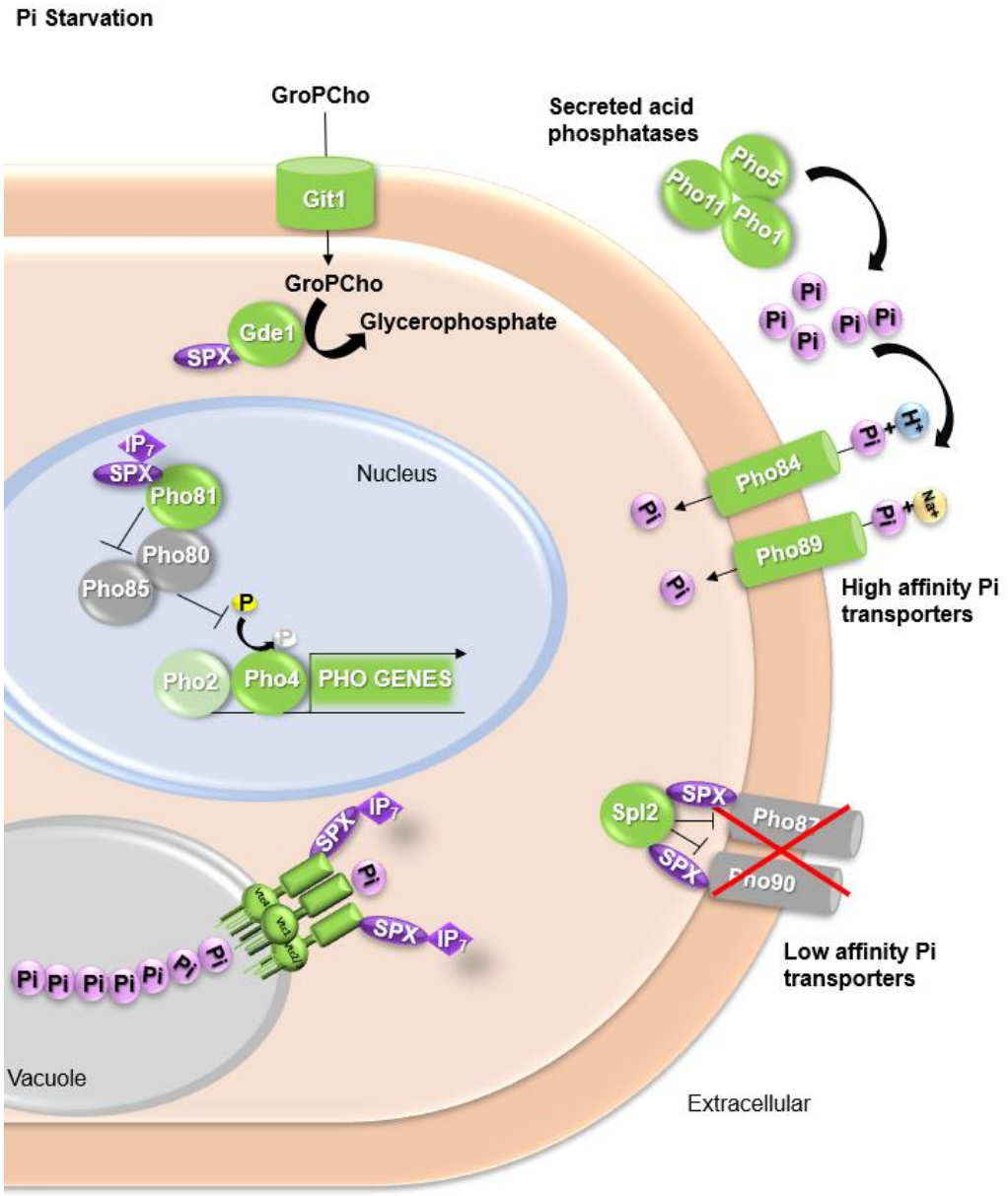

Figure 1.2. The Pi starvation response in *Saccharomyces cerevisiae*.
Under Pi starvation conditions, the CDK inhibitor Pho81 inhibits the Pho80-Pho85 CDK complex allowing the transcription factor Pho4 to become de-phosphorylated and accumulate in the nucleus to up-regulate genes involved in Pi acquisition (shown in green). Pi acquisition genes include; secreted acid phosphatases, high affinity Pi transporters and genes which mobilise Pi from phospholipids. Further induced genes include those involved in polyphosphate synthesis. The activity of the low affinity Pi transporters is inhibited by Spl2. In *S. cerevisiae*, the transcription factor Pho2 works co-operatively with Pho4, however Pho2 has been shown to be largely dispensable for PHO pathway activation in pathogenic fungi. Several PHO pathway targets have SPX domains (shown in purple) which can bind IP_7 molecules which have been reported to play a role in regulating Pi homeostasis. Adapted from (Ikeh *et al*., 2017).

1.5.2 The role of Pho85-Pho80 in yeast

Crucial to regulation of the cell cycle is the activity of cyclin dependent kinases (CDKs) and cyclins which are regulatory subunits that provide domains for enzymatic activity (Lim and Kaldis, 2013). CDks are serine/threonine kinases which were discovered through studies in yeast which using genetic and biochemical approaches (Nurse *et al*., 1976; Reed *et al*., 1982; Beach *et al*., 1982). Pioneering work investigating the role of Cdc28 in *S. cerevisiae* and Cdc2 in *Schizosaccharomyces pombe* found that they promoted the transition between the different phases of the cell cycle via interactions with specific cyclins (Beach *et al*., 1982; Reed *et al*., 1982). The role of CDKs and cyclins is not exclusive to cell cycle control. Moreover, they play a role in regulating a diverse array of cellular processes including DNA damage repair, metabolism, morphogenesis, and epigenetic regulation (Lim and Kaldis, 2013).

Fundamentally, there is similarity in the activity and substrates of CDKs in *C. albicans* and *S. cerevisiae*. However, the cell cycle transcription programme significantly differs between the two organisms (Ihmels *et al*., 2005). Furthermore, cell cycle differs dependent on morphology. Although in terms of size, shape, and order of cell cycle events *C. albicans* yeast and pseudohyphae are similar to those in *S. cerevisiae* (Ihmels *et al*., 2005). There are lots of similarities between the G1 cyclins of *S. cerevisiae* and *C. albicans*. However, there are differences in distribution of roles between them (Berman, 2006). For example, *S. cerevisiae* cells lacking G1 cyclins can be rescued by the sole introduction of Cln3 from *C. albicans* (Sherlock *et al*., 1994). Furthermore, in *C. albicans* the cyclin Hgc1 is most similar to the G1 cyclins Cln1 and Cln2 in *S. cerevisiae*. Expressing *C. albicans* Hgc1 in a S*. cerevisiae* G1 cyclin mutant stain only partially rescued growth (Zheng *et al*., 2004). However, in *S. cerevisiae*, only re-introduction of one of the three G1 cyclin (Cln1, Cln2 or Cln3) is needed for growth be to restored to wild type levels (Zheng *et al*., 2004).

There are several features of the Pho85-Pho80 complex which distinguish it from canonical cell cyclin CDK-cyclin complexes. For example, for the activation of cell cycle CDK-cyclin complexes a conserved serine/threonine residue on the kinase activation loop is phosphorylated however, this is not essential for Pho85-Pho80 kinase activity (Nishizawa *et al*., 1999). Furthermore, there is a significant degree of difference in the +3 position of the consensus sequence of the phosphorylation sites of the Pho85-Pho80 substrate Pho4 compared to many cell cycle CDK-cyclin complex substrates (O'Neill *et al*., 1996). Moreover,

a distal site from the phosphorylation sites on Pho4 is important for the interaction with Pho80 enhancing catalytic efficiency (Byrne *et al*., 2004). CDK inhibitors of cell cycle CDK-cyclin complexes typically interact with the kinase or both kinase and cyclin. However, Pho81 the CDK inhibitor or Pho85-Pho80 has been found to mainly interact via association with Pho80 (Schneider *et al*., 1994). Interestingly, although inactive during Pi replete conditions, Pho81 has been found to be associated with Pho85-Pho80 irrespective of Pi condition (Schneider *et al*., 1994).

One of the most notable and studied roles of Pho85 in *S. cerevisiae* is its role in regulating the PHO pathway (Schneider *et al*., 1994). However, it has a range of targets other than Pho4 which play roles outside of mediating Pi homeostasis (Toh-e and Nishizawa, 2001). For example, it has been linked to playing a role in cell cycle progression, cell polarity, glycogen metabolism and the response to environmental changes (Huang *et al*., 2007). Thus, Pho85 has been dubbed as a 'multifunctional' kinase. Furthermore, as well as Pho80, there are 9 other cyclins have also been shown to form complexes with Pho85 (Toh-e and Nishizawa, 2001). However, despite the range of multiple roles Pho85 has been shown to function in, it is non-essential in *S. cerevisiae*.

In *S. cerevisiae*, Pho85 has been shown to target substrates involved in the cell cycle. For example, Pho85 has been reported *in vitro* to target Swi5 and Ace2 which are transcription factors involved in late M and early G1 phase (Measday *et al*., 2000). Moreover, *S. cerevisiae* cells lacking Pho85 display hyperactivated Swi5 suggesting that Pho85 negatively regulates Swi5 (Measday *et al*., 2000). Consistent with this, *S. cerevisiae* cells lacking *PHO85* have also been shown to display a range of defects linked to cell cycle impairment (Carroll and O'Shea, 2002). It is noteworthy however, that whilst the CDK, Cdc28 plays an essential role in the cell cycle, Pho85 has been found to only been required to maintain viability when the activity of Cdc28 is compromised (Huang *et al*., 2007).

In *S. cerevisiae*, the transcription factor, Gcn4 which is responsible for the activation of genes involved in the biosynthesis of amino acids in response to amino acid starvation is regulated by Pho85 in complex with the cyclin Pcl5 (Shemer *et al*., 2002). When amino acids are abundant the Pho85-Pcl5 complex phosphorylates Gcn4 thus, targeting it for degradation (Shemer *et al*., 2002).

In *C. albicans* significantly less is known about the roles of Pho85 and Pho80. There is currently no published work directly investigating the role of Pho80 in *C. albicans*. Pho85 in *C. albicans* has been shown to be a functional homologue of Pho85 in *S. cerevisiae* (Miyakawa *et al*., 2000). Indeed, deletion of Pho85 in *S. cerevisiae* has been shown to be rescued by the introduction of Pho85 from *C. albicans* (Miyakawa *et al*., 2000). Furthermore, unlike *S. cerevisiae* in *C. albicans* Pho85 is essential. Work in *C. albicans* has shown that Pho85-Pcl1-Hms1 plays an important role in the filamentation response to inhibition of Hsp90 and temperature increase (Shapiro *et al*., 2012). However, the precise role of Pho85 in mediating Pi homeostasis in *C. albicans* remains to be elucidated.

1.5.3 The PHO pathway in pathogenic yeast

The transcription factor Pho4 has recently been implicated in stress resistance and virulence in two prominent fungal pathogens, *C. albicans* and *C. neoformans* (Ikeh *et al*., 2016; Lev *et al*., 2017), and has also been partially characterised in *Candida glabrata*. However, knowledge of PHO pathway regulation in pathogenic yeast is limited compared to *S. cerevisiae*.

1.5.3.1 C. glabrata

C. glabrata is a commensal organism which has the potential to become pathogenic in immunocompromised individuals (Kerwin and Wykoff, 2009). There is a high degree of conservation of the PHO pathway between *S. cerevisiae* and *C. glabrata*, this is perhaps underpinned by the fact that *C. glabrata* is more closely related to *S. cerevisiae* than *C. albicans* (Kerwin and Wykoff, 2009). However, in *C. glabrata*, Pho2 has been shown to be dispensable for Pho4 activation of genes involved in Pi acquisition (He *et al*., 2017). This study, which ectopically expressed *C. glabrata PHO4* in *S. cerevisiae,* showed that this negated the need for Pho2 in the activation of the *S. cerevisiae* PHO pathway (He *et al*., 2017). It has also been suggested that the gene expansion of Pho4 regulated genes seen in *C. glabrata* is underpinned by the lack of dependence on Pho2 to co-activate genes (He *et al*., 2017). In *C. glabrata,* of the genes directly activated by Pho4, only 16 are involved in Pi acquisition (He *et al*., 2017). The other 63 genes have been linked to adhesion, cell wall synthesis and stress resistance (He *et al*., 2017). Thus, it is an attractive hypothesis that removal of the requirement of the co-activator Pho2 has led to the expansion of genes regulated by Pho4 in *C. glabrata*.

1.5.3.2 C. neoformans

In *C. neoformans*, Pho4 has been found to accumulate in the nucleus in response to Pi starvation and to up-regulate genes involved in Pi acquisition including those encoding high affinity Pi transporters and secreted acid phosphatases similar to *S. cerevisiae* (Lev *et al*., 2017). However, the sequence of Pho4 in *C. neoformans* has greater homology to *C. albicans* Pho4 than *S. cerevisiae* (Lev *et al*., 2017). Furthermore, compared to *S. cerevisiae* there is an expansion in Pho4 target genes, with *C. neoformans* Pho4 being shown to bind to more than 110 genes some of which are not directly linked to Pi acquisition (Toh-e *et al*., 2015). However, the physiological relevance of this gene expansion in *C. neoformans* requires further investigation. Akin to Pho4 in *S. cerevisiae*, Pho4 in *C. neoformans* plays a vital role in the response to alkaline pH stress leading to the induction of Pi acquisition genes (Lev *et al*., 2017).

C. neoformans has homologues of the key Pho4 regulators including components of the CDK complex, Pho80 and Pho85, and the CDK inhibitor Pho81. Indeed, deletion of *PHO80* results in the PHO pathway being constitutively active (Toh-e *et al*., 2015). This suggests that the role of Pho80 in Pho4 regulation in *C. neoformans* is the same as in *S. cerevisiae*. Furthermore, similar to Pho81 in *S. cerevisiae*, Pho81 in *C. neoformans* positively regulates Pho4, as its deletion prevented key Pi acquisition mechanisms such as the production of secreted acid phosphatases (Toh-e *et al*., 2015). However, it is noteworthy that in *C. neoformans*, Pi starvation also led to the up-regulation of additional regulatory proteins as well as those found in *S. cerevisiae* (Toh-e *et al*., 2015). Chromatin immunoprecipitation studies in *C. neoformans* revealed that under Pi starvation, Pho4 binds to its own promoter, thus self-regulating expression, which has not been reported for Pho4 in *S. cerevisiae* (Toh-e *et al*., 2015). In *C. neoformans*, there is evidence of functional redundancy in the high affinity Pi transporters, Pho84, Pho840 and Pho89 as all three had to be deleted before growth was impaired under Pi starvation conditions (Kretschmer *et al*., 2014). This has not been reported in other yeast. Moreover, cells lacking *PHO4* in *C. neoformans* have also been shown to have wild type levels of polyP unlike that in *S. cerevisiae* and *C. albicans* (Lev *et al*., 2017). Thus, although there is a high degree of conservation in how Pho4 is regulated in *C. neoformans* compared to *S. cerevisiae* there are also key differences regarding Pi homeostasis.

1.5.3.3 C. albicans

The sequence homology between Pho4 in *S. cerevisiae* and *C. albicans* is almost exclusively restricted to the C-terminal DNA binding domain (Urrialde *et al*., 2016). Moreover, the specific Serine-Proline residues on *S. cerevisiae* Pho4 targeted by the CDK complex are largely non-conserved in *C. albicans* (Ikeh *et al*., 2016). Furthermore, Pho2 has been shown to be non-essential for Pho4 activation of genes involved in Pi acquisition in *C. albicans* (Homann *et al*., 2009). It has been shown in *C. albicans* that, similar to that seen in *C. glabrata* and *C. neoformans*, that loss of *PHO4* impacts on the transcription of an additional set of genes outside of the PHO pathway (Ikeh *et al*., 2016). In total, 150 genes were reported as being dependent upon Pho4 for induction (Ikeh *et al*., 2016) (Figure 1.3). Alongside genes which were involved in Pi accumulation, additional biological process categories included response to stress, response to chemical, response to drug, DNA metabolic process, and filamentous growth (Figure 1.3). Thus, it is an attractive hypothesis that removal of dependence on Pho2 to co-activate has also led to the expansion of genes regulated by Pho4 in *C. albicans* (Ikeh *et al*., 2017). Furthermore, as Pho4 has been found to play a role in the response to a pleiotropy of stresses, it may be that gene expansion has facilitated the adaptation of *C. albicans* to survive within different niches in the host. Analysis using GO Slim terms of biological processes using DNA microarray data of Pho4 dependent genes in *S. cerevisiae* (Ogawa *et al*., 2000) revealed that some genes alongside playing a role in Pi accumulation were involved in other processes. Similar to *C. albicans*, genes were found to function in the cell cycle, lipid metabolic process, signal transduction, carbohydrate metabolic process, transport, and cellular homeostasis (Figure 1.3). However, it is notable that unlike Pho4 target genes in *C. albicans* none in *S. cerevisiae* were found to have GO Slim terms relating to stress response/resistance (Figure 1.3).

Similar to *S. cerevisiae*, cells lacking Pho4 in *C. albicans* have no polyP present (Ikeh *et al*., 2016). However, whether Pho4 in *C. albicans* is regulated by the Pho80-Pho85 CDK complex and the CDK inhibitor Pho81, like in *S. cerevisiae,* remains to be investigated.

Recent work in *C. albicans* discovered an additional role for Pi homeostasis in the regulation of the Target of Rapamycin (TOR) pathway which was also shown to be conserved in *S. cerevisiae* (Liu *et al*., 2017). The TOR pathway is key for controlling cell growth and metabolism (Liu *et al*., 2017). The high affinity Pi transporter, Pho84 was shown to be

required for the activity of The Target of Rapamycin Complex 1 (TORC1) (Liu *et al*., 2017). Thus, as well as monitoring carbon and nitrogen availability, TORC1 also monitors Pi.

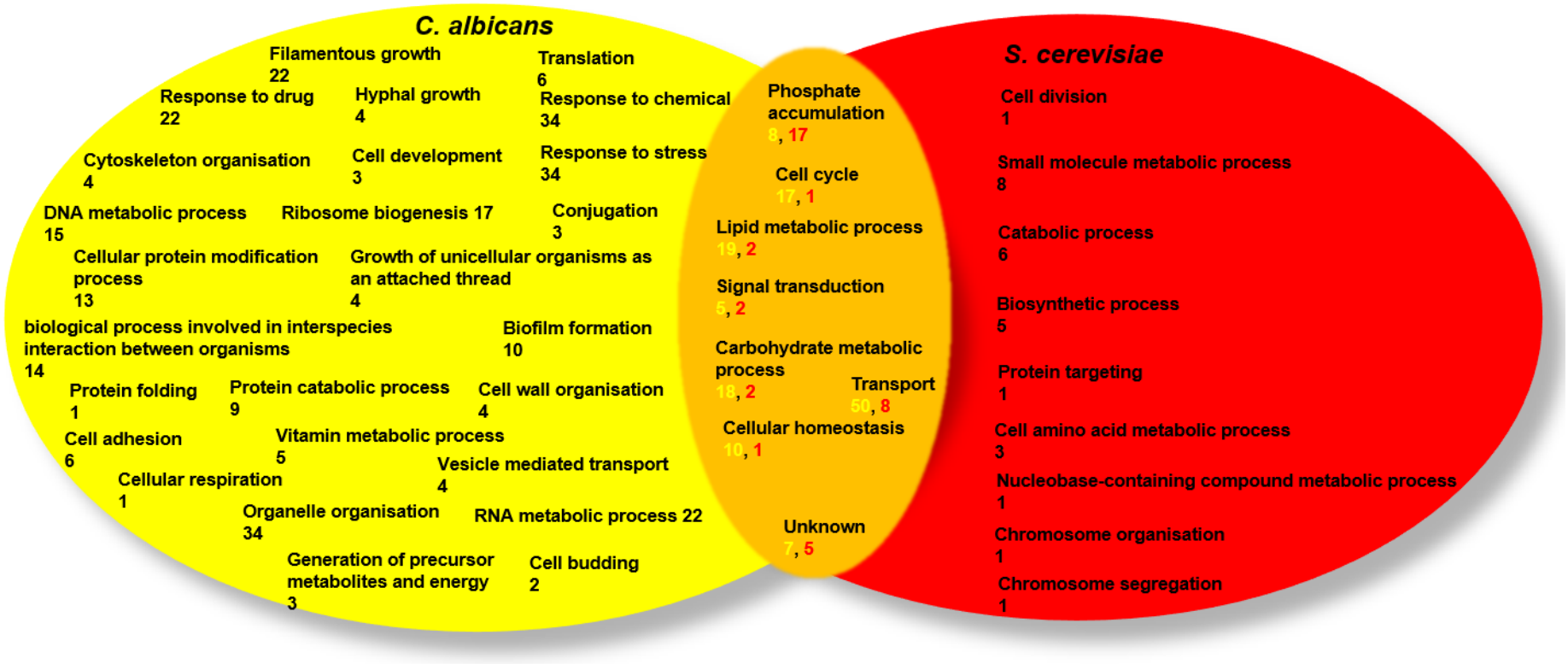

Figure 1.3. The Pho4 Regulon is Expanded in *C. albicans* compared to *S. cerevisiae*.
GO Slim terms of biological processes that are regulated by Pho4 in *C. albicans* (shown in yellow) and *S. cerevisiae* (shown in red). RNA-sequencing data was used for *C. albicans* (Ikeh *et al.*, 2016) and DNA microarray data for *S. cerevisiae* (Ogawa *et al.*, 2000). For both organisms, several genes map to more than one GO Slim term.

1.6 Phosphate homeostasis and fungal virulence

The intimate link between Pi acquisition and virulence has been well established in a wide array of bacterial pathogens (Chakraborty *et al*., 2011; Chekabab *et al*., 2014; Lamarche *et al*., 2008). However, less is known about its contribution in eukaryotic pathogens, in particular fungi.

In the pathogenic fungus, *C. neoformans* transcript profiling studies revealed that upon co-culture with macrophages, genes involved in activating the high affinity Pi transporters were up-regulated (Fan *et al*., 2005; Griffiths *et al*., 2012). Furthermore, in mutants lacking all three high affinity Pi transporter genes (*PHO840*, *PHO84* and *PHO89*) there is a reduction in the production of the virulence factors melanin and capsule and impaired virulence (Kretschmer *et al*., 2014). To complement this, Lev and colleagues showed that cells lacking the transcription factor Pho4 had attenuated virulence in a murine inhalation model (Lev *et al*., 2017). Cells lacking Pho4 displayed a reduced ability to disseminate to the brain compared to wild type cells (Lev *et al*., 2017), and to have impaired proliferation in the presence of monocytes (Lev *et al*., 2017). The gene, *APH1* which encodes the secreted acid phosphatase Aph1 is regulated by Pho4 and has also been shown to be key contributor to *C. neoformans* virulence (Lev *et al*., 2014).

C. albicans cells lacking Pho4 also display a reduction in virulence leading to increased survival times of *Caenorhabditis elegans* infected with cells lacking Pho4 compared to wild type (Ikeh *et al*., 2016). Furthermore, cells lacking Pho4 were found to have impaired virulence in mice using the 3-day intravenous challenge model (Ikeh *et al*., 2016). It was also shown that *C. albicans* cells lacking Pho4 were extremely sensitive to killing by macrophages (Ikeh *et al*., 2016). Complementary to this, *GIT3*, *PHO100* and *PHO84* which are target genes of Pho4 have been demonstrated to contribute to the virulence of *C. albicans* cells (Bishop *et al*., 2013; MacCallum *et al*., 2009; Liu *et al*., 2018). Moreover, it is noteworthy that in multiple infection models *PHO84* has been shown to be induced (Fradin *et al*., 2005; Enjalbert *et al*., 2006; Thewes *et al*., 2007; Zakikhany *et al.*, 2007; Walker *et al*., 2009; Hebecker *et al*., 2016; Muñoz *et al*., 2019). Furthermore, it has been reported in *C. albicans* that Pi limitation leads to increased filamentation in a *C. elegans* infection model, which was interpreted as lack of Pi acting as a virulence cue (Romanowski *et al*., 2012). In concert, these studies indicate one of the key facets affecting the pathogenic potential of *C. albicans* and *C. neoformans* at multiple infection sites is their ability to sense and regulate Pi homoeostasis.

1.7 Phosphate homeostasis and stress resistance

In *C. albicans*, Pho4 has been shown to be vital for resistance to alkaline, cationic and superoxide stresses (Ikeh *et al*., 2016). This section will give an overview of current knowledge regarding how Pi acquisition promotes resistance to cationic, superoxide and alkaline pH stress.

1.7.1 Phosphate homeostasis and resistance to cations

Intracellular Pi levels impact upon the metal cations (Rosenfled *et al*., 2010; Pontes and Groisman, 2018). Many of these metal cations are important for a variety of cellular processes (Hood and Skarr,2012) . In *S. cerevisiae*, cytosolic Pi has been shown to play a critical role in mediating metal homeostasis (Rosenfled *et al*., 2010). Indeed, Pi has been suggested as playing an important role in maintaining an intracellular charge balance (Rosenfled *et al*., 2010). In support of this, cells deficient in Pho80, the negative regulator of Pho4 have increased cytosolic Pi levels which correlates with significantly increased intracellular levels of sodium and calcium (Rosenfled *et al*., 2010). The dramatic increase in the influx of calcium and sodium in these cells has been suggested as a counter mechanism to negate the negative charge of increased Pi levels (Rosenfled *et al*., 2010). Moreover, *S. cerevisiae* cells lacking Pho80 displayed increased toxicity to copper, cobalt, manganese, and zinc (Rosenfled *et al*., 2010). In *S. cerevisiae*, high Pi levels have also been shown to induce an iron starvation response, this is underpinned by the binding of Pi to iron, decreasing its bioavailability (Rosenfled *et al*., 2010).

Whilst there has been some investigatory work done on metal-Pi interactions in *S. cerevisiae*, few have been carried out on pathogenic fungi. However, a study in *C. neoformans* where mutations were made in all three high affinity Pi uptake transporter genes (*PHO840*, *PHO84* and *PHO89*) led to low intracellular Pi levels yet high iron, sodium, and zinc levels (Kretchemer *et al*., 2014). In *C. neoformans*, the triple high affinity Pi transporter mutant was sensitive to manganese, sodium, and calcium cations (Kretchemer *et al*., 2014). *C. albicans* cells lacking Pho4 have significantly lower levels of Pi, magnesium, manganese (Ikeh *et al*., 2016). Furthermore, *C. albicans* cells deficient in Pho4 have sensitivity to non-metal cations such as spermidine in addition to a vast range of metal cations (Ikeh *et al*., 2016). PolyP has also been shown to play a role in the resistance to cations which will be discussed below in section 1.8.3.

1.7.2 Phosphate homeostasis and superoxide resistance

Screening a *C. albicans* transcription factor library revealed *pho4*Δ cells to be acutely sensitive to the superoxide generator menadione (Ikeh *et al*., 2016). This is likely attributed to the observation that cells deficient in Pho4 have impaired Sod1 activity (Ikeh *et al*., 2016). This phenotype is suggested to be attributed to copper bioavailability defects in *pho4Δ* cells, as the addition of excess copper to growth media leads to the restoration of wild type Sod1 activity levels and resistance to superoxide stress (Ikeh *et al*., 2016). Further evidence in support of this is the observation that *C. albicans* cells lacking *PHO4* are resistant to copper (Homann 2009; Ikeh *et al*., 2016). In *C. albicans* cells lacking Pho84 are superoxide sensitive which is partially due to low levels of Sod3 due to disruption in TORC1 signalling (Liu *et al*., 2018).

1.7.3 Phosphate homeostasis and the response to alkaline pH

The blood stream and various organs within the body have an alkaline pH. The cellular responses to alkaline pH have been best studied in *S. cerevisiae,* and exposure to alkaline pH triggers a Pi starvation response including the rapid utilisation of intracellular polyP stores (Serrano *et al*., 2002). Interestingly, the Pi starvation response to alkaline stress is significantly quicker than when cells are switched to Pi limiting media (Serrano *et al*., 2002). This is attributed to the fact that the uptake of Pi by symporters such as Pho84 rely on a proton gradient which is disrupted under alkaline conditions triggering a Pi starvation response (Lev and Djordjevic, 2018). Work by Serra-Cardona and colleagues suggests that following alkaline pH exposure the Pi/H+ symporters in *S. cerevisiae* are less effective (Serra-Cardona *et al*., 2014; Serra-Cardona *et al*., 2015). For example, the activity of the high affinity transporter Pho84 is rapidly decreased once pH reaches 7.5 or above (Lagerstedt *et al*., 2002). Work in the model yeast, *S. cerevisiae*, has also shown that alkaline pH conditions elicit induction of the VTC complex and Pho12, both of which are Pho4 effector genes (Serrano *et al*., 2002; Serra-Cardona *et al*., 2014). Moreover, the synthesis of polyP by the VTC complex is dependent on the proton gradient by the V-ATPase (Tomashevski and Petrov, 2015).

Alkaline conditions have also been shown to trigger rapid mobilisation of intracellular polyP stores in *C. albicans* (Ikeh *et al*., 2016). In *C. neoformans*, as in *C. albicans,* cells deficient in Pho4 were acutely sensitive to alkaline conditions (Lev *et al*., 2017). In *C. albicans*, Pho4 has

also been shown to rapidly accumulate in the nucleus in response to alkaline stress (Ikeh *et al*., 2016). In *C. neoformans*, the potency of this alkaline pH tolerance defect in Pho4 lacking cells is thought to underpin the reduced ability of the mutant to disseminate in a murine infection model when compared to wild type cells (Lev *et al*., 2017). Similarly, in *C. albicans* it has been shown that the defect in alkaline pH tolerance in Pho4 lacking cells results in growth impairment and delayed filamentation in response to serum (Ikeh *et al*., 2016). This indicates that Pi acquisition is key for the ability of *C. albicans* to grow in alkaline conditions and thus colonise various niches within the host.

1.8 Phosphate storage as polyP

1.8.1 PolyP introduction

There needs to be tight control of cytosolic Pi levels within the cell so that biosynthetic and signalling requirements are met but balanced against rising elevated Pi levels in the cytosol. This is essential as metabolism can be stalled when Pi levels are too high (Austin and Mayer, 2020). Within cells Pi is stored as polyP, a linear polymer composed of inorganic Pi molecules together with high-energy phosphoanhydride bonds (Moreno and Docampo, 2013). In yeast there is significantly more polyP than in mammalian cells, with approximately up to 10% of dry weight attributed to polyP molecules in *S. cerevisiae* (Lonetti *et al*., 2011). The vast majority of polyP in fungal cells is stored in the vacuole to prevent cytotoxicity (Lonetti *et al*., 2011). However, the presence of low levels of polyP has also been reported in the cytoplasm, mitochondria, and nucleus (Moreno and Docampo, 2013). It remains to be elucidated how optimal Pi levels are maintained within cells by co-ordinating the balance of polyP synthesis and mobilisation.

1.8.2 PolyP synthesis and mobilisation

Within the model yeast *S. cerevisiae*, the synthesis of polyP is mediated by the vacuolar membrane protein assembly known as the vacuolar transporter chaperone (VTC) complex (Figure 1.4). Regulation of the VTC complex is under control of the PHO pathway. The VTC complex is composed of the synthetase Vtc4 along with the subunit Vtc1 and either Vtc2 or Vtc3 (Desfougères *et al*., 2016). The subunits are all composed of three transmembrane helices (Hothorn *et al*., 2009). The smallest subunit, Vtc1 does not contain hydrophilic domains whereas, Vtc2, Vtc3 and Vtc4 have two hydrophilic domains facing the cytosol (Hothorn *et al*., 2009). Furthermore, Vtc2, Vtc3 and Vtc4 also have a central domain and an

SPX domain which will be discussed further in section 1.9 (Figure 1.4). The central domain of Vtc4 contains the active site and synthesises polyP from ATP (Hothorn *et al*., 2009). Metal ions are required for the synthesis of polyP from ATP, with Mn^{2+} being the most preferential (Hothorn *et al*., 2009). Alongside its role in polyP synthesis, the VTC complex has also been shown to play a role in vacuole fusion (Muller *et al*., 2002), microautophagy (Uttenweiler *et al*., 2007) and V-ATPase trafficking and stability (Cohen *et al*., 1999). However, it remains ambiguous whether these are mechanistically distinct roles or involve polyP.

Following Pi starvation, initial Pi demands are met by the mobilisation of polyP stores by polyphosphatases including Ppn1 and Ppx1 (Figure 1.4). Ppn1 is a vacuolar endopolyphosphatase which cleaves long chains of polyP. Ppx1 functions dually as an endo- and exo-polyphosphatase that splits the orthophosphate from the ends of polyP (Tammenkoski *et al*., 2007). Ppx1 activity has been detected in the cytosol, nucleus, and mitochondrial matrix (Gerasimaite *et al*., 2014). Pi starvation induces the expression of *PPN1* whereas *PPX1* is constitutively expressed (Ogawa *et al*., 2000). Ppn1 requires activation by vacuolar proteases as it is initially expressed as a 78 KDa precursor peptide (Shi and Kornberg, 2005). Structurally, following activation Ppn1 is a 35 KDa homotetramer (Shi and Kornberg, 2005). The activity of Ppn1 is metal dependent, requiring either Mg^{2+} or Mn^{2+} (Shi and Kornberg, 2005). Ppx1 is a soluble 40 kDa member of the DHH phosphoesterase superfamily, which has been shown to be responsible for a significant amount of polyphosphatase activity in *S. cerevisiae* (Wurst and Kornberg, 1994). It releases Pi from polyP but discriminates against hydrolysing ATP (Wurst and Kornberg, 1994). Metal ions are a requirement of the polyphosphatase activity of Ppx1, of which Mg^{2+} is the preferred ion (Tammenkoski *et al*., 2007). Furthermore, the activity of Ppx1 spans a broad pH range from 5.5 – 9 (Tammenkoski *et al*., 2007). Structurally, between the interface of the N and C terminal domains there is a channel containing the active site of the enzyme (Ugochukwu *et al.*, 2007). The channel is lined with numerous charged amino acids (Ugochukwu *et al*., 2007). Interestingly, this is a conserved feature between different organisms with Ppx1 enzymes, including mammals (Ugochukwu *et al*., 2007; Gerasimaitė and Mayer, 2016). Although yet to be directly proven, the charged residues of the channel have been proposed to act as funnel, navigating polyP towards the active site (Ugochukwu *et al*., 2007). Following hydrolysation of vacuolar polyP, Pi molecules are thought to leave the vacuole via the intracellular low affinity Na/Pi symporter, Pho91 which is localised to the vacuolar

membrane and has an SPX domain dependent on IP_6/IP_7 regulation (Potapenko *et al*., 2018) (Figure 1.4).

Polyphosphatases in addition to Ppx1 and Ppn1 have been reported in *S. cerevisiae*. There is further enzyme, Ddp1 localised to the cytosol has been shown to mobilise polyP (Lonetti *et al*., 2011). There are also suggestions Ddp1 could mobilise polyP from the nucleus (Azevedo *et al.*, 2015). Ddp1 has endopolyphosphatase activity was found following reports that cells lacking Ppn1 and Ppx1 still had low levels of polyP mobilisation (Lichko *et al*., 2008; Lichko *et al*., 2010). Additionally, this 20 KDa enzyme also hydrolyses inositol pyrophosphate molecules discussed in section 1.9 which neither Ppn1 nor Ppx1 can do (Lonetti *et al*., 2011). It is noteworthy however, that the endopolyphosphatase activity of Ddp1 in hydrolysing polyP remains to be shown *in vivo*. Recently, another enzyme with endopolyphosphatase activity , Ppn2, was found in the vacuole of *S. cerevisiae* (Gerasimaitė and Mayer, 2017). The endopolyphosphatase activity of this enzyme, Ppn2 was found to be dependent on Zn^{2+} (Gerasimaitė and Mayer, 2017). However, in a strain lacking both Ppn1 and Ppn2 no accumulation of polyP was observed, suggesting mobilisation was not significantly impacted (Gerasimaitė and Mayer, 2017). Furthermore, results of the study suggest that whilst Ppn1 plays a role in polyP mobilisation to meet Pi demands during Pi starvation, Ppn2 functions to control the chain length of polyP (Gerasimaitė and Mayer, 2017). Indeed, polyP chain length has been shown to play various roles within the cells, for example metal ion chelation is more effective when polyP chains are longer (Lee and Whitesides, 2010; Gerasimaitė and Mayer, 2017). The lack of short chains and accumulation of long polyP chains has been suggested to be toxic to yeast (Sethuraman *et al*., 2001).

1.8.3 PolyP - not just a Pi storage molecule

Previously deemed a molecular relic, there has been a recent surge in studies investigating the roles of polyP outside its role as a Pi storage molecule. PolyP has been extensively studied in bacteria. The pioneering work of Arthur Kornberg and colleagues provided evidence for the role polyP plays in bacterial biofilm development, growth, stress responses, virulence, metal chelation and quorum sensing (Rao *et al*., 2009). Recently, polyP has been implicated in an array of processes including; antioxidant protection (Gray and Jakob, 2015), protein chaperoning (Gray *et al*., 2014), signalling (Azevedo *et al*., 2015), post-translational modification (PTM) as the novel PTM polyphosphorylation (Azevedo *et al*., 2015) and poly3-hydroxybutyrate production (Tumlirsch *et al*., 2015).

Although extensive work has been carried out investigating the role of polyP in prokaryotic cells, comparatively less is known for eukaryotes. In *S. cerevisiae*, polyP has been shown to play a role in cell cycle progression and the response to genotoxic stress (Bru *et al*., 2016). Intriguingly, in *Trypanosoma cruzi* in response to hyperosmotic stress polyP levels dramatically increase, whereas hyposmotic stress triggers rapid mobilization of polyP stores (Ruiz *et al*., 2001). Interestingly, in *C. neoformans*, cells which either have no polyP or an impairment in polyP mobilisation are sensitive to excess zinc (Kretschmer *et al*., 2014). In higher eukaryotic cells, polyP is a potent modulator of inflammation (Muller *et al*., 2009) and blood coagulation in mammalian cells (Smith *et al*., 2006). PolyP present on the surface of *S. cerevisiae* has also been suggested to be playing a role in chelating metal cations present on cellular surfaces (Keasling *et al*., 1997). Supportive evidence comes from a study which reported that uranium complexes found on the *S. cerevisiae* cell wall could be attributed to polyP (Rothstein *et al*., 1951). Phosphorus-31nuclear magnetic resonance revealed a signal which corresponded to *S. cerevisiae* cell surface polyP, which decreased in signal intensity when non-penetrative metal cations were added (Keyhani *et al*., 1996). The presence of polyP on the cell surface has also be reported in *C. neoformans* (Ramos *et al*., 2017).

PolyP synthesis and catabolism in *C. albicans* remains poorly defined. However, unlike reports from bacterial cells, polyP appears to be dispensable for resistance to host imposed stresses in *C. albicans* (Ikeh *et al*., 2016). To date the only phenotype associated with loss of polyP in *C. albicans* is sensitivity to manganese, suggesting it plays a role as a manganese storage reservoir (Ikeh *et al*., 2016). This is in keeping with the defined role of polyP in metal homeostasis in bacterial cells (Albi and Serrano, 2016). Intriguingly though, in *C. albicans* polyP as well as being mobilised in response to Pi starvation, is also hydrolysed in response to alkaline pH, hypo-osmotic and hyper-osmotic stress (Ikeh *et al*., 2016). The significance of the role of polyP mobilisation in *C. albicans* is addressed in this thesis.

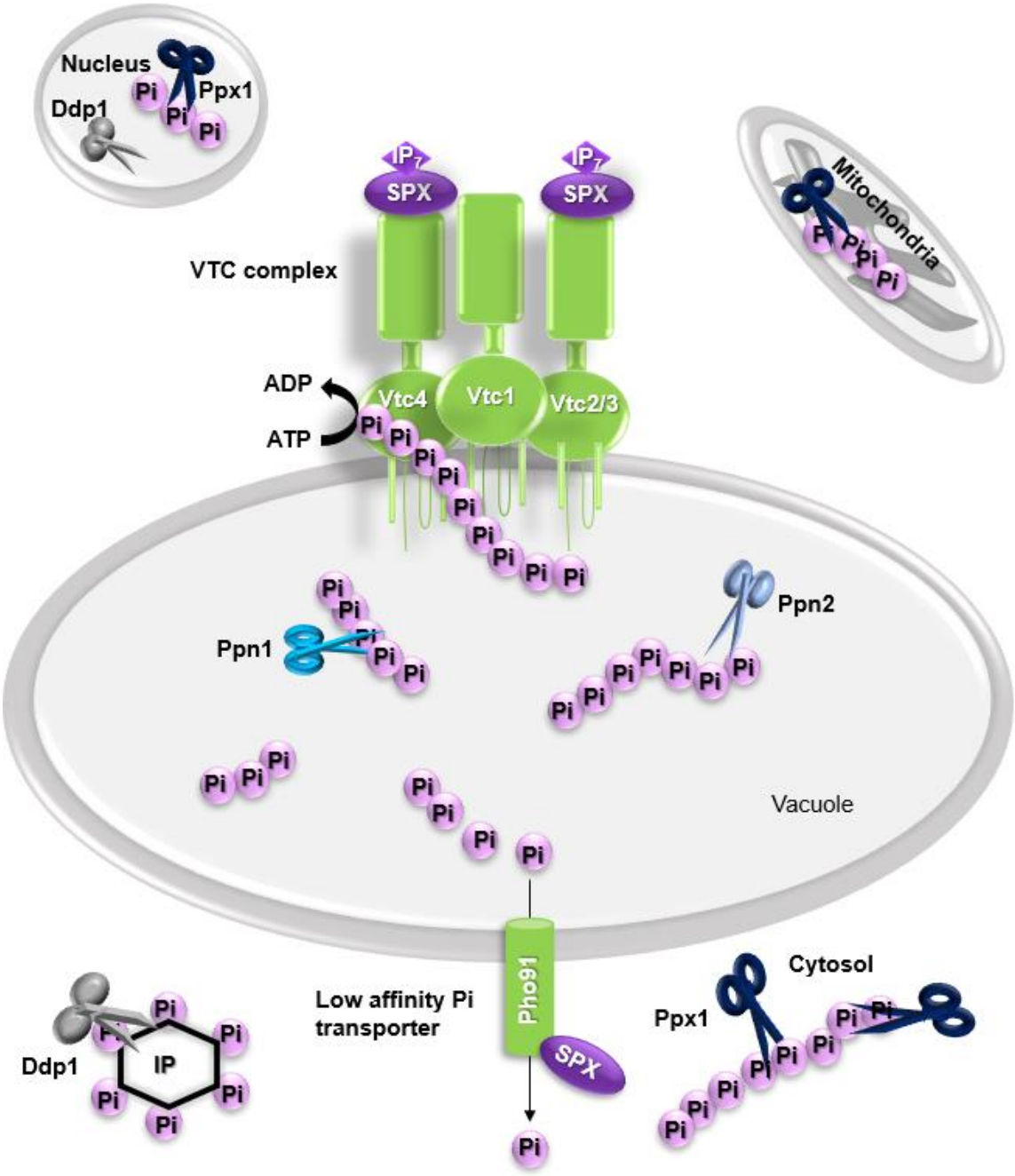

Figure 1.4. PolyP synthesis and mobilisation in *S. cerevisiae*.
The vacuole is the main reservoir of polyP in fungal cells; however, it is also found in the cytosol, nucleus, and mitochondria. The vacuolar chaperone complex (VTC) mediates polyP synthesis from free Pi within the cell which requires ATP. PolyP is mobilised by polyphosphatases, including Ppn1, Ppn2, Ppx1 and Ddp1. The low affinity Pi transporter Pho91 transports Pi from the vacuolar lumen into the cytosol. The VTC complex and Pho91 have been shown to have SPX domains (shown in purple) which have been reported to play a role in mediating Pi homeostasis.

1.9 Control of phosphate homeostasis by inositol polyphosphates (IPs)

One of the most poorly characterised aspects of cellular Pi homeostasis is how cells sense low Pi levels. However, recent studies have revealed new insight into the mechanism by which cells sense and respond to low Pi level. It has been appreciated for some time that the levels of IP_7 molecules fluctuate dependent on Pi conditions (Lee *et al*., 2007). New research suggests that such IPs function as intracellular Pi sensors by directly bind to SPX domains, which are found on many proteins involved in Pi homeostasis (Wild *et al*., 2016). SPX domains were originally characterised in yeast, and are named after **S**uppressor of yeast gpa1, **P**ho81 and human **X**enotropic and polytropic Retrovirus receptor 1 (Secco *et al*., 2012). As show in Figure 1.2, several PHO pathway components and targets in fungi have SPX domains. These include the CDK inhibitor Pho81, the low affinity Pi transporters Pho87 and Pho90, the GroPCho phosphodiesterase Gde1, and proteins involved in polyP synthesis, Vtc2, Vtc3 and Vtc4, as well as the low affinity vacuolar Pi transporter Pho91 (Ikeh *et al*., 2017). Structurally, SPX domains have a bundle of 3 helices and an interaction site, which has a high affinity for both IP_6 and IP_7 ligands, at the N-terminus (Wild *et al*., 2016).

Inositol polyphosphates (IP) are small, water soluble signalling molecules with multifaceted roles governing cellular processes. Significantly, they contain high energy Pi moieties participating in phosphotransfer reactions (Saiardi *et al*., 2004). Structurally, they are based on a six-carbon inositol ring, providing stability (Figure 1.5) (Shears, 2018). Added to the inositol ring are monophosphate and pyrophosphates which dictate their nomenclature. Briefly, IPs originate from inositol 1,4,5-tiphosphate (IP_3) generated through hydrolysis of the phosphoinositide, PtdIns(4,5)P_2 (PIP_2) (Figure 1.5). This hydrolysis is mediated via phospholipase C and releases IP_3 into the cytoplasm (Lev *et al*., 2015). In *S. cerevisiae*, the dual specificity enzyme, Arg82, phosphorylates IP_3 to IP_4 and then subsequently generates IP_5 (Shears, 2018). The generation of IP_6 from IP_5 is catalysed by Ipk1 (Shears, 2018). The generation of IP_7 from IP_6 can be catalysed by either Vip1 or Kcs1 resulting in 1-IP_7 or 5-IP_7 respectively (Lonetti *et al*., 2011). Depending upon the IP_7 isoform, IP_8 can be generated from IP_7 by either Vip1 or Kcs1 (Lonetti *et al*., 2011). In the reverse reaction, diphosphoinositol polyphosphate phosphohydrolases (DIPPs) hydrolyse IPs (Lonetti *et al*., 2011).

IP signalling molecules are ubiquitous throughout nature and have been shown to play roles in a myriad of processes including, apoptosis, cell wall integrity, DNA hyper-recombination,

transcription of ribosomal RNA, telomere length and vacuolar biogenesis (Bennett *et al*., 2006; Luo *et al*., 2002; Saiardi *et al*., 2000; Saiardi *et al*., 2002; Saiardi *et al*., 2004). Moreover, they have been implicated in numerous human diseases including, cancer, diabetes, and obesity (Charkaborty, 2018). The most extensively studied IPs in fungi are IP_6, IP_7 and IP_8, as they have been implicated as playing a role in either fungal stress responses, antifungal resistance in *C. neoformans* (Lev *et al*., 2015) or Pi homeostasis thus, the rest of this chapter and will focus on them. However, there are several excellent extensive reviews on the entire pathway and further signalling roles which can available (Bennett *et al*., 2006; Charkaborty, 2018; Shears, 2018).

A number of studies have indicated the importance of IP_7 molecules or SPX domains in Pi homeostasis. For example, in *S. cerevisiae*, the interaction of Vip1-derived IP_7 with Pho81 was shown to trigger the inhibition of the Pho80-Pho85 CDK complex (Lee *et al*., 2007). This facilitates the accumulation of dephosphorylated Pho4, which localises to the nucleus and up-regulates Pi acquisition genes. With regard to SPX domains, the negative regulation of the low affinity transporters, Pho87 and Pho90 by Spl2 in response to Pi starvation was shown to be SPX-domain dependent (Hürlimann *et al*., 2009). When mutant Pho87 and Pho90 proteins were generated lacking the SPX domain, there was an increase in their catalytic activity and thus in Pi accumulation which culminated in cell growth being prevented (Hürlimann *et al*., 2009). However, it was only recently discovered that SPX domains provide a basic binding surface for IP_7 signalling molecules, the concentrations of which change in response to cellular levels (Wild *et al*., 2016). So essentially SPX domains are eukaryotic sensors of Pi via the binding of IP_7 molecules. With regard to yeast, it was shown that IP_7 molecules bind with high affinity to SPX domains located on VTC components of the polyP synthetase and stimulate VTC-catalysed polyP synthesis (Wild *et al*., 2016). When conserved residues in the SPX domains within VTC components were mutated, the binding of IP_7 was prevented *in vitro* and the synthesis of polyP abolished *in vivo* (Wild *et al*., 2016). Such findings explain previous observations that cells lacking the IP_7 synthase, Kcs1, contain no polyP (Lonetti *et al*., 2011).

Interestingly, there are some conflicts in the literature. For example, in work from the O'Shea group it was shown that IP_7 levels increase following Pi starvation (Lee *et al*., 2007) whereas in other studies it has been shown that IP_7 levels decrease following Pi starvation (Lonetti *et al*., 2011; Wild *et al*., 2016). Moreover, in the original study which linked IP_7 to

Pho81 inhibition, it was the Vip1 generated IP_7 isoform, 1-IP_7 that was important (Lee *et al*., 2007). However, challenging this, other studies indicate a more prominent role for Kcs1 derived 5-IP_7 in PHO pathway regulation in *S. cerevisiae* (Lonetti *et al*., 2011; Desmarini *et al*., 2020). Furthermore, recent work in *C. neoformans* has shown that it is 5-IP_7, generated by Kcs1, which is responsible for binding to the SPX domain of Pho81 (Desmarini *et al*., 2020). Clearly, this is an emerging area of biology and much is left to learn about how IP interaction with different SPX domains influences protein function.

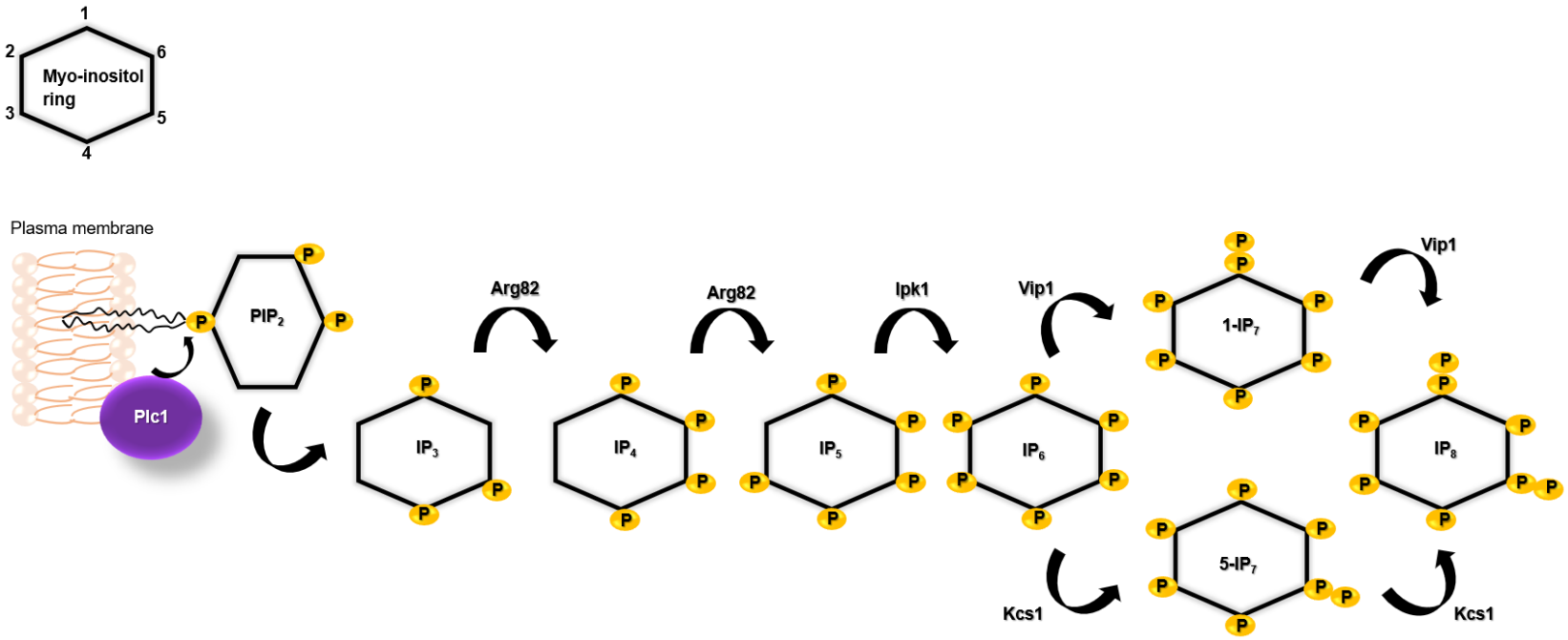

Figure 1.5. Diagrammatic representation of the inositol polyphosphate biosynthesis pathway in *S. cerevisiae*. The hydrolysis of PIP_2 by phospholipase C1 generates IP_3 which is converted to IP_4 by the enzyme Arg82. The kinase Arg82 is sometimes referred to as Ipk2 in some literature, it has dual specificity and can convert IP_4 to IP_5. The enzyme Ipk1 generated IP_6 from IP_5. IP_6 can be converted to IP_7 by either Vip1 or Kcs1 generating 1-IP_7 or 5-IP_7, respectively distinguished by which site is phosphorylated. IP_8 can be generated from Ip_7 by either Vip1 or Kcs1 depending upon IP_7 isoform. Adapted from (Lev *et al.*, 2015; Gu *et al.*, 2016).

1.10 Summary and aims

This chapter has introduced the major human fungal pathogen *C. albicans,* including an overview of current antifungal therapies, and key virulence determinants with a focus on stress response mechanisms to enable this pathogen to colonise multiple, often hostile, host environments. One of the most significant challenges faced by *C. albicans* is an ability to acquire essential nutrients, such as the essential macronutrient Pi, upon colonising different host niches.

Previous work in *C. albicans* has revealed that Pi acquisition by the transcription factor Pho4 plays a role in mediating a variety of stress responses, including those encountered within the phagosome (Ikeh *et al*., 2016). Consequently, *pho4Δ* cells are very sensitive to macrophage-mediated killing. Furthermore, virulence is reduced in systemic infection models in *C. albicans* cells lacking Pho4 (Ikeh *et al*., 2016), and many other proteins implicated in Pi homeostasis such as Pho84, Pho100, Gde1 and Git3 (Liu *et al*., 2017; MacCallum *et al*., 2009; Bishop *et al*., 2013). Similarly, in *C. neoformans* defects in Pi acquisition also have a negative impact on the ability to establish infection (Lev *et al*., 2017). Collectively, these studies show that investigations into Pi homeostasis in pathogenic fungi are warranted.

Most of the current knowledge on the control of Pi homeostasis in yeast comes from work in *S. cerevisiae* in which the PHO pathway has been extensively characterised (Komeili and O'Shea, 1999; Ogawa *et al*., 2000; Tomah and Sinah, 2014). Whilst, homologues of the PHO pathway are found in *C. albicans*, how Pho4 is regulated is unknown. Indeed, based on the limited studies investigating Pi acquisition in *C. albicans* diverges from the PHO pathway paradigm have been found. In addition, whilst IP signalling molecules have been shown to play a role in Pi homeostasis in both *S. cerevisiae* and *C. neoformans* (Lee *et al*., 2007; Wild *et al*., 2016; Desmarini *et al*., 2020), this remains to be studied in *C. albicans*. Investigating the regulation of the PHO pathway in *C. albicans* is one of the main aims of this thesis.

In various organisms, polyP has been shown to play a multitude of roles including stress resistance (Rao *et al*., 2009; Moreno and Docampo, 2013; Gray and Jakob, 2015). However, in *C. albicans*, the only role prescribed to the presence of polyP thus far is a manganese storage reservoir (Ikeh *et al*., 2016). However, Pho4 activation occurs only following polyP mobilisation (Ikeh *et al*., 2016). Furthermore, polyP stores have been shown to be mobilised

in *C. albicans* in response to Pi starvation, alkaline and cationic stresses (Ikeh *et al*., 2016). Thus, an additional aim of this thesis is to determine the physiological relevance of polyP mobilisation in *C. albicans*.

Finally, as discussed in this introduction, there is an urgent need for the development of novel antifungal strategies. One promising avenue is targeting fungal virulence determinants (Lee *et al*., 2020). Given that preventing Pi acquisition attenuates virulence, a further aim of this thesis is to attempt to identify small molecules that block Pi acquisition in *C. albicans*.

Thus, to summarise the three aims of this thesis:

1. To investigate mechanisms underlying PHO pathway activation in *C. albicans.*
2. To explore the role of polyP mobilisation in the pathobiology of *C. albicans*.
3. To investigate whether our knowledge of the PHO pathway can be exploited to identify compounds that prevent Pi acquisition.

Chapter 2: Materials and Methods

2.1 Yeast techniques

2.1.1 C. albicans growth conditions and strains

All *C. albicans* strains used in this study are shown in table 2.1 and were routinely grown at 30^0C in Yeast Peptone Dextrose (YPD) media containing 2% bacto-peptone, 1% bacto-yeast extract and 2% glucose (Sherman, 2002) in either liquid medium or on solid plates with the additions of 2% agar unless otherwise stated. Additionally, SD media was used, comprised of 0.67% bacto-yeast nitrogen base without amino acids, 2% glucose and supplemented with the appropriate amino acids respective of growth selection. When plating out *C. albicans* transformations, when an autotrophic marker was used for selection, SD was used as above with 2% agar.

For experiments requiring phosphate limitation, strains were grown in either YPD-Pi medium which contained yeast extract lacking phosphate supplemented with KCL (ForMedium) or PNMC medium (Peptone 2.5 g/L, NaCl 3 g/L, $MgSO_4$ 1 mM, $CaCl_2$ 1 mM and 2% glucose). For enriched phosphate conditions, both medium were supplemented with 10 mM KH_2PO_4 (pH 6), generating YPD+ Pi or PNMC+ Pi.

Strain		**Genotype**	**Source**
SN148	*wt*	*arg4Δ/arg4Δ leu2Δ/leu2Δ his1Δ/his1Δ ura3Δ::imm434/ura3Δ::imm434 iro1Δ::imm434/iro1Δ::imm434*	Noble *et al*., 2005
JC747	*wt SN148 + CIp30*	*arg4, leu2/leu2, his1/his1, ura3 ::λimm434/ura3::λimm434, iro1 ::λimm434/iro1::λimm434, CIp10*	da Silva Dantas *et al*., 2010
JC1936	*wt*	*his1Δ/ his1Δ, leu2Δ::C.dubliniensis HIS1/leu2Δ::C. maltose LEU2, arg4Δ/arg4, ura3/ura3Δ, IRO1 /iro1Δ, CIp10*	Ikeh *et al*., 2016
JC1991	*ppx1Δ + CIp10*	*SN148 ppx1::loxP-ARG4-ura3-loxP/ppx1::loxP-HIS1-loxP, CIp10*	Ikeh, 2015
JC1985	*ppn1Δ + CIp10*	*SN148 ppn1::loxP-ARG4-ura3-loxP/ppn1::loxP-HIS1-loxP, CIp10*	Ikeh, 2015
JC2016	*ppn1Δ + CIp10-PPN1*	*SN148 ppn1::loxP-ARG4-ura3-loxP/ppn1::loxP-HIS1-loxP, CIp10-PPN1*	Ikeh, 2015
JC2283	*ppx1Δ + CIp10-PPX1*	*SN148 ppx1::loxP-ARG4-ura3-loxP/ppx1::loxP-HIS1-loxP, CIp10-PPX1*	This work

JC2210	*ppn1Δ/ppx1Δ + CIp10*	*SN148 ppn1::loxP-ARG4-ura3-loxP/ppn1::loxP-HIS1-loxP, ppx1Δ::loxP/ppx1Δ::loxP, CIp10*	This work
JC2257	*ppn1Δ/ppx1Δ + CIp10-PPN1*	*SN148 ppn1::loxP-ARG4-ura3-loxP/ppn1::loxP-HIS1-loxP, ppx1Δ::loxP/ppx1Δ::loxP, CIp10-PPN1*	This work
JC2267	*ppn1Δ/ppx1Δ + CIp10-PPX1*	*SN148 ppn1::loxP-ARG4-ura3-loxP/ppn1::loxP-HIS1-loxP, ppx1Δ::loxP/ppx1Δ::loxP, CIp10-PPX1*	This work
JC2303	*ppn1Δ/ppx1Δ + PHO4-GFP*	*SN148 ppn1::loxP-ARG4-ura3-loxP/ppn1::loxP-HIS1-loxP, ppx1Δ::loxP/ppx1Δ::loxP/ pACT-PHO4-GFP:URA3*	This work
JC1928	*pho4Δ + CIp10*	*SN250 his1Δ/ his1Δ, leu2Δ ::C. dubliniensis HIS1/leu2Δ::C. maltose LEU2, arg4Δ/arg4, ura3/ura3Δ, IRO1/iro1Δ pho4Δ:: C. dubliniensis HIS1/pho4Δ:: C. maltose LEU2* CIp10	Ikeh *et al*., 2016
JC1917	*pho4Δ + CIp10-PHO4*	*SN250 pho4::loxP-ARG4-ura3-loxP/pho4 ::loxP-HIS1-loxP,* CIp10-*PHO*4	Ikeh *et al*., 2016
JC1977	*PHO4-GFP*	*SN148 pACT-PHO4-GFP:URA3*	Ikeh *et al*., 2016
JC1883	*PHO4-MH*	*SN148 PHO4/PHO4-MH:URA3*	Ikeh *et al*., 2016
JC1984	*vtc4Δ + CIp10*	*SN148 vtc4::loxP-ARG4-ura3-loxP/vtc4::loxP-HIS1-loxP,CIp10*	Ikeh *et al*., 2016
JC2014	*vtc4Δ + CIp10-VTC4*	*SN148 vtc4::loxP-ARG4-ura3-loxP/vtc4::loxP-HIS1-loxP,CIp10-VTC4*	Ikeh *et al*., 2016
JC2150	*pho81Δ + CIp10*	*SN250 pho81::loxP-HIS1-ura3-loxP/pho81::loxP-leu2-loxP,CIp10*	This work
JC2153	*pho80Δ + CIp10*	*SN148 pho80::loxP-ARG4-ura3-loxP/pho80::loxP-HIS1-loxP,CIp10*	This work
JC2374	*pho80Δ + CIp10-PHO80*	*SN148 pho80::loxP-ARG4-ura3-loxP/pho80::loxP-HIS1-loxP,CIp10-PHO80*	This work
JC2380	*pho81Δ + CIp10-PHO81*	*SN250 pho81::loxP-HIS1-ura3-loxP/pho81::loxP-leu2-loxP,CIp10-PHO81*	This work
JC2276	*pho80Δ + PHO4-MH*	*SN148 pho80::loxP-ARG4-ura3-loxP/pho80::loxP-HIS1-loxP/ PHO4-MH-URA3*	This work
JC2335	*pho81Δ + PHO4-MH*	*SN250 pho81::loxP-HIS1-ura3-loxP/pho81::loxP-leu2-loxP/ PHO4-MH-URA3*	This work
JC3350	*pho80Δ + PHO4-GFP*	*SN148 pho80::loxP-ARG4-ura3-loxP/pho80::loxP-HIS1-loxP/ pACT-PHO4-GFP:URA3*	This work

JC2154	*pho81Δ + PHO4-GFP*	*SN250 pho81::loxP-HIS1-ura3-loxP/pho81::loxP-leu2-loxP/ pACT-PHO4-GFP:URA3*	This work
JC2324	*ubp3Δ + Clp10*	*SN148 ubp3::loxP-ARG4-ura3-loxP/ubp3::loxP-HIS1-loxP,Clp10*	This work
JC2333	*ubp3Δ + PHO4-MH*	*SN148 ubp3::loxP-ARG4-ura3-loxP/ubp3::loxP-HIS1-loxP/ PHO4-MH-URA3*	This work
JC2539	*vip1Δ + Clp10*	*SN148 vip1::loxP-ARG4-ura3-loxP/vip1::loxP-HIS1-loxP,Clp10*	This work
JC2353	*kcs1Δ + Clp10*	*SN148 kcs1::loxP-ARG4-ura3-loxP/kcs1::loxP-HIS1-loxP,Clp10*	This work
JC2377	*kcs1Δ + Clp10-KCS1*	*SN148 kcs1::loxP-ARG4-ura3-loxP/kcs1::loxP-HIS1-loxP,Clp10-KCS1*	This work
JC2549	*vip1Δ + Clp10-VIP1*	*SN148 vip1::loxP-ARG4-ura3-loxP/vip1::loxP-HIS1-loxP,Clp10-VIP1*	This work

Table 2.1. *C. albicans* strains used in this study.

2.1.2 C. albicans transformations

To transform *C. albicans* cells with exogenous DNA the lithium acetate (LiAc) protocol was used, as described by Burk Braun (http://www.sacs.ucsf.edu/home/johnsonLab/burk/transformation.html). Strains were grown overnight to an OD_{660} between 1.0 and 4.0. Subsequently, 50 mL of cells were harvested by centrifugation for 2 minutes at 2500 rpm and re-suspended in 20 mL of Lithium acetate/ TE solution (LiAc/TE) (100 mM lithium acetate (pH 7), 1 mM EDTA (pH 8), 10 mM Tris (pH 7.5)). The re-suspended cells were pelleted again by centrifugation at 2500 rpm for 2 minutes following re-suspension in 1 mL of LiAc/TE solution. Per tube, 100 µL of cells, 10 µL of boiled carrier DNA salmon sperm (50 µg) and exogenous DNA were added and mixed well. To each transformation, 750 µL of LiAc/TE/PEG solution (LiAc/TE, 50% PEG 3350) and mixed well. The transformation mix was then incubated for 3 hours for disruption cassettes utilising autotrophic marker selection, or overnight for nourseothricin antibiotic selection, on a shaking platform at 30^0C. Following this, cells were heat shocked at 42^0C for 45 minutes. Cells were subsequently subjected to centrifugation at 8000 rpm for 1 minute and re-suspended in 100 µL of YPD. To select for transformants cells were either plated on SD agar containing the appropriate amino acids for selection or onto YPD plates containing 150 µg/mL nourseothricin, dependent on selective marker. Plates were incubated for 2-5 days at 30^0C. Successful transformation was confirmed via polymerase chain reaction (PCR) using extracted genomic DNA as template with appropriate check oligonucleotides. Positive

colonies were then re-streaked for single colonies on the appropriate selective plate and re-checked. Correctly transformed strains were maintained at 80^0C in YPD stocks containing 15% glycerol.

2.1.3 C. albicans genomic DNA extraction

Cells were taken directly from a plate by a sterile loop, washed in 1 mL of sterile nH_2O and centrifuged at 13,000 rpm for 1 minute. Pellets were re-suspended in 200 µL of chromosomal breakage buffer (10 mM Tris-HCL [pH 8], 1 mM EDTA [pH 8], 100 mM NaCl, 1% SDS (w/v), 2 % Triton X100 (v/v)) and transferred to Ribolyser tubes containing 200 µL of sterile glass beads. To each tube 200 µL of ice-cold phenol-chloroform was added. Subsequently, cells were disrupted by vortexing in a mini-bead beater (Biospec Products) for 30 seconds. Lysate was clarified by centrifugation at 13,000 rpm for 15 minutes. Following this, clarified lysate was removed into a fresh Eppendorf tube. To precipitate the DNA, 1 tenth volume of 3 M Sodium acetate (pH 7) and 2 volumes of ethanol was added to the clarified lysate and incubated for 30 minutes at -20^0C. Subsequently, lysates were centrifuged at 13,000 rpm for 15 minutes and washed in 400 µL of 70% ethanol before undergoing centrifugation at 13,000 rpm for 5 minutes. Pellets were re-suspended in 50 µL of nuclease-free H_2O.

2.1.4 C. albicans strain construction

The *C. albicans* strains used in this study are listed in table 2.1, at least two replicates were made for each strain but only one representative strain is listed. Oligonucleotide primers used in this study are listed in table 2.2.

Oligonucleotide	**Sequence 5'-3'**	**Restriction site**
PPX1 del F	CGTCATACGTGAAGAGGAAGCACGTTCTATTTAAAGATATC TTCTCTTTTCATAAAAAATAAAAATCATCTCCAGTAGGGTTG TTCTTAATACTACAGTCACGGCCAGTGAATTGTAATA	
PPX1 del R	TATATTTCTGGTATTTGTCAAATTACGGCCAAAGATACTCTTC ACATAGTTAACCATGACTATTAATAAATTAATCAATAGATTC GATGTGGATTCCAATTCGGAATTAACCCTCACTAA	
UBP3 del F	CACAGAACCAACAACACCCACCCTCTTTTTATAACGCCTGAA AAAAAAAGACCTTTTCCAACTGTTGAGCTTATCATTCCATGT TCTAATCCTGCCAGGGTTTTCCCAGTCACGACGTTG	
UBP3 del R	CCTCAAATGTCACAGTCATAGAGTCTAATGGTGCCAGCAAA TTAAACCTAAGGAGTTTAGCCGGTGCTGGCCTTGTCGCTGCT	

	ATCTTTATTGCTTTTATCCCTCACTAAAGGGAACAAAAGCTGGG	
VIP1 del F	CACTATCTTCACCAGCCATGACAAATAACTCAAAGTCTTTGCCTATTCCTGTCCCCAAGAAGGAAGATGCTAAACTGAACTCATTGAATATCCCCAAATCACGGCCAGTGAATTGTAATA	
VIP1 del R	TTTTAGATAACTGGGAACAATACGAATAAACTTAGAATGTATAGATAATAAATAAATGTATAAAATTTCTATTTACTTGCTATTTAAAGGACCTGTTATGTCGGAATTAACCCTCACTAA	
KCS1 del F	TTTGGGAAAACTTGTGGGAGATATTTCCATCTATTTTTTTTTAGTCACATTTGCACGATTTCTTACGATGGTGTTAATTGTAGTTGATGTACTTAGGAAAACGGCCAGTGAATTGTAATA	
KCS1 del R	ATTTCTCTGACTCGTTTATTTACTTCTCTCACTCACTCACTAATAATTAAAACTTGTAGAACCTTGTTACTCTGAAAGTCCTTCGTCTTCTTCTGGGGTATCGGAATTAACCCTCACTAA	
PPX1 Ch F	TTGTGGATATTTGTACCACGG	
PPX1 Ch R	TTGGATGTTGTTGTGATCAAC	
PPN1 Ch F	GCTTTACAACAATTTTATACTGG	
PPN1 Ch R	GGATTCCAAATCGGCATAGTAT	
UBP3 Ch F	ACCAACACCAAGAACGGATACG	
UBP3 Ch R	ACATCTGATTCATCATCATGGG	
VIP1 Ch F	CCTTTGATAAGTCCGTCTGTCTCC	
VIP1 Ch R	GACCACGCAAGATTGATGCACAGG	
KCS1 Ch F	TTCCTACCATCCCTTTATCATCCC	
KCS1 Ch R	GGATCCATTACTACCTTTATACC	
ARG R2	CCCATCTAATAGGTTGAGC	
HIS R2	AATGGTTGCGTAATAAA	
LOXP R	TTCGTATAATGTATGCTATACG	
CycTerm R	CGACAGCCATGTTGTAC	
PPX1 CI F	GCGCGGATCCGCACCGATCCAAGAAACCAGTATG	*BamH1*
PPX1 CI R	GCGCGGATCCGGCTTAAATGTGGTGATTGATGGG	*BamH1*
VIP1 CI F	GCGCGGATCCGACTATGATTCCGATTCCATGACC	*BamH1*
VIP1 CI R	GCGCGGATCCCCATTCTTCGTACTTGATGTCTGG	*BamH1*
KCS1 CI F	GCGCAAGCTTGCAAGGATTCCAAAAGGGAATGTG	*Hind III*
KCS1 CI R	GCGCAAGCTTGGGAGAGAAAAATAACGTCAATCC	*Hind III*
PHO80 CI F	GCGCGGATCCCAATCTACAACCACCAAAGAAGGC	*BamH1*
PHO80 CI R	GCGCGGATCCCTGGTGAAACTCAATTAGCACCAT	*BamH1*
PHO81 CI F	GCGCGGATCCCCAATGAAGAAGATGAGGAAGTCT	*BamH1*
PHO81 CI R	GCGCGGATCCCCATTACCAAAATTACCTATCCCT	*BamH1*

Table 2.2. Oligonucleotide primers used in this study.

2.1.4.1 Creation of a double ppn1Δ/ppx1Δ deletion strain

To create a double *ppn1Δ/ppx1Δ C. albicans* strain, *PPX1* was deleted in the previously generated *ppn1Δ* strain background (Ikeh, 2015) using the Clox deletion system utilising nourseothricin (NAT1) as a selective marker (Shahana *et al*., 2014). The NAT1-cassette and

100 base pairs 5’ and 3’ of the *PPX1* open reading frame (ORF) were PCR amplified using the oligonucleotides Ppx1delF and Ppx1delR. This was sequentially transformed into JC1975 (*ppn1Δ)* cells to disrupt both alleles of *PPX1*, generating JC2201 (*ppn1Δ/ppx1Δ*). Successful loss of each *PPX1* allele was confirmed via diagnostic PCR of genomic DNA with oligonucleotide primers Ppx1ChF and either LoxP-R or Ppx1ChR for the first and second *PPX1* allele, respectively. CIp10 was integrated at the *RSP10* locus generating JC2210. The strategy used to create the *ppn1Δ/ppx1Δ* double deletion strain is shown in Figure 2.1.

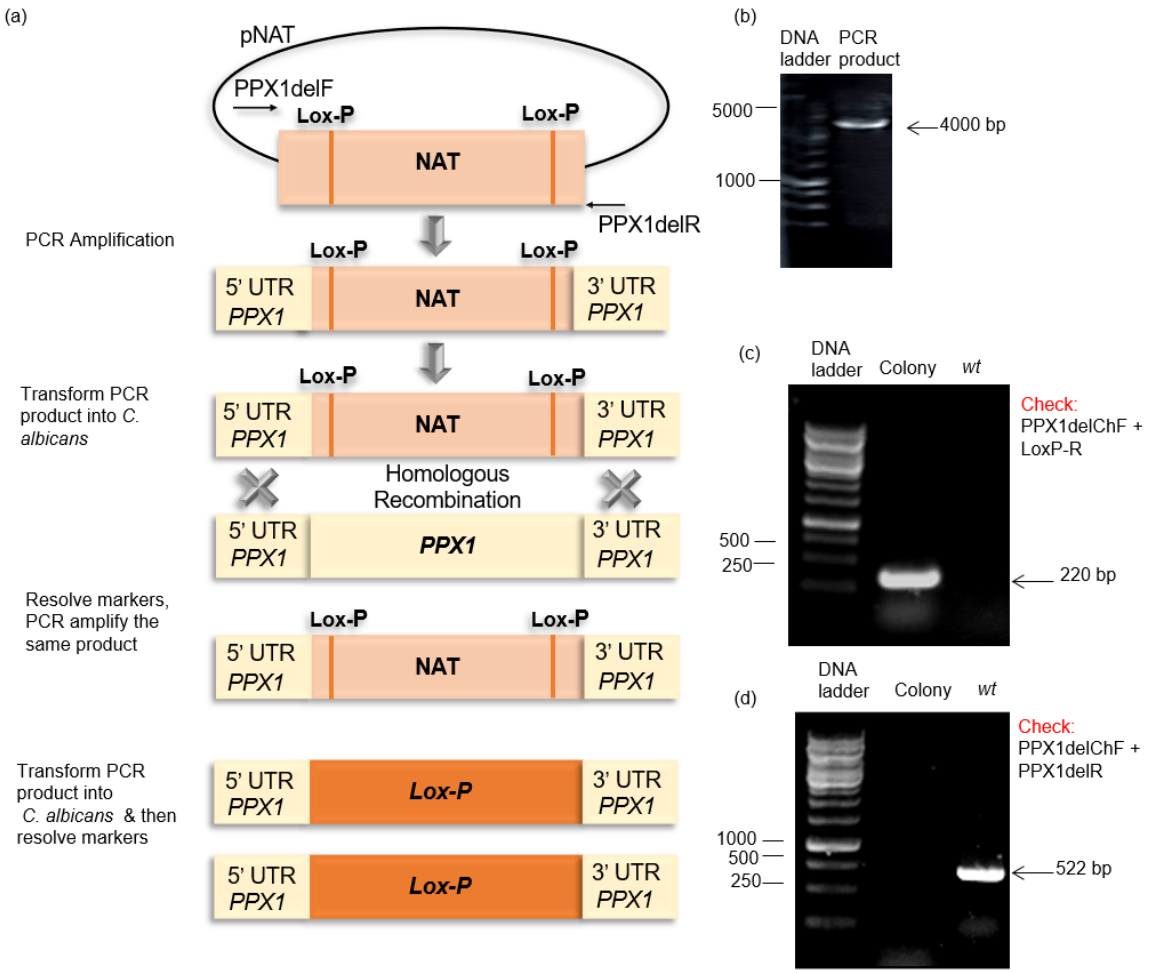

Figure 2.1. Creation of a double *ppn1Δ/ppx1Δ* deletion strain. (a) A diagrammatic illustration of the strategy used starting with the *ppn1Δ (*JC1975) strain background. **(b)** PCR check for correct deletion cassette integration following the first transformation using genomic DNA extracts and the oligonucleotides PPX1delChF and LoxP-R. **(c)** PCR check for correct deletion cassette integration following the second transformation using genomic DNA extracts and the oligonucleotides genomic DNA PPX1delChF and PPX1delChR. Both PCR products **(b)** and **(c)** were ran out onto a 1% agarose gel with a genomic extract from wild type cells (JC465) used as a control.

2.1.4.2 Deletion of UBP3, VIP1, KCS1

To delete *UBP3* in *C. albicans*, a disruption cassette was PCR amplified containing either the *ARG4* or *HIS1* gene flanked by *LoxP* sites and 100 base pairs 5' and 3' of the *UBP3* ORF using the plasmid templates pLAL or pLHL (Dennison *et al*., 2005) and the oligonucleotide primers Ubp3delF and Ubp3delR. Following PCR amplification, disruption cassettes were transformed sequentially into SN148 *C. albicans* cells yielding JC2323 (*ubp3Δ*). Successful disruption of either allele was confirmed using the oligonucleotide primers Ubp3ChF and either ARG-R2 or HIS-R2 dependent on the disruption cassette. Loss of both alleles was

confirmed using genomic DNA and oligonucleotide primers Ubp3ChF and Ubp3ChR. CIp10 was integrated at the *RSP10* locus generating JC2324. The disruption strategy used is shown in Figure 2.2. For disruption of *VIP1* and *KCS1* the same strategy was utilised. To delete *VIP1*, the oligonucleotide primers Vip1delF and Vip1delR were used. Loss of either *VIP1* allele was confirmed with the oligonucleotide primer Vip1ChF with either ARG-R2 or HIS-R2. Successful creation of a *vip1Δ* strain was confirmed with the oligonucleotide primers Vip1ChF and Vip1ChR. CIp10 was integrated at the *RSP10* locus generating JC2539. To delete *KCS1*, the oligonucleotide primers Kcs1delF and Kcs1delR were used. The disruption of either *KCS1* allele was confirmed with the oligonucleotide primers Kcs1ChF with either ARG-R2 or HIS-R2. Loss of both copies of *KCS1* was confirmed using the oligonucleotide primers Kcs1ChF and Kcs1ChR. CIp10 was integrated at the *RSP10* locus generating JC2353.

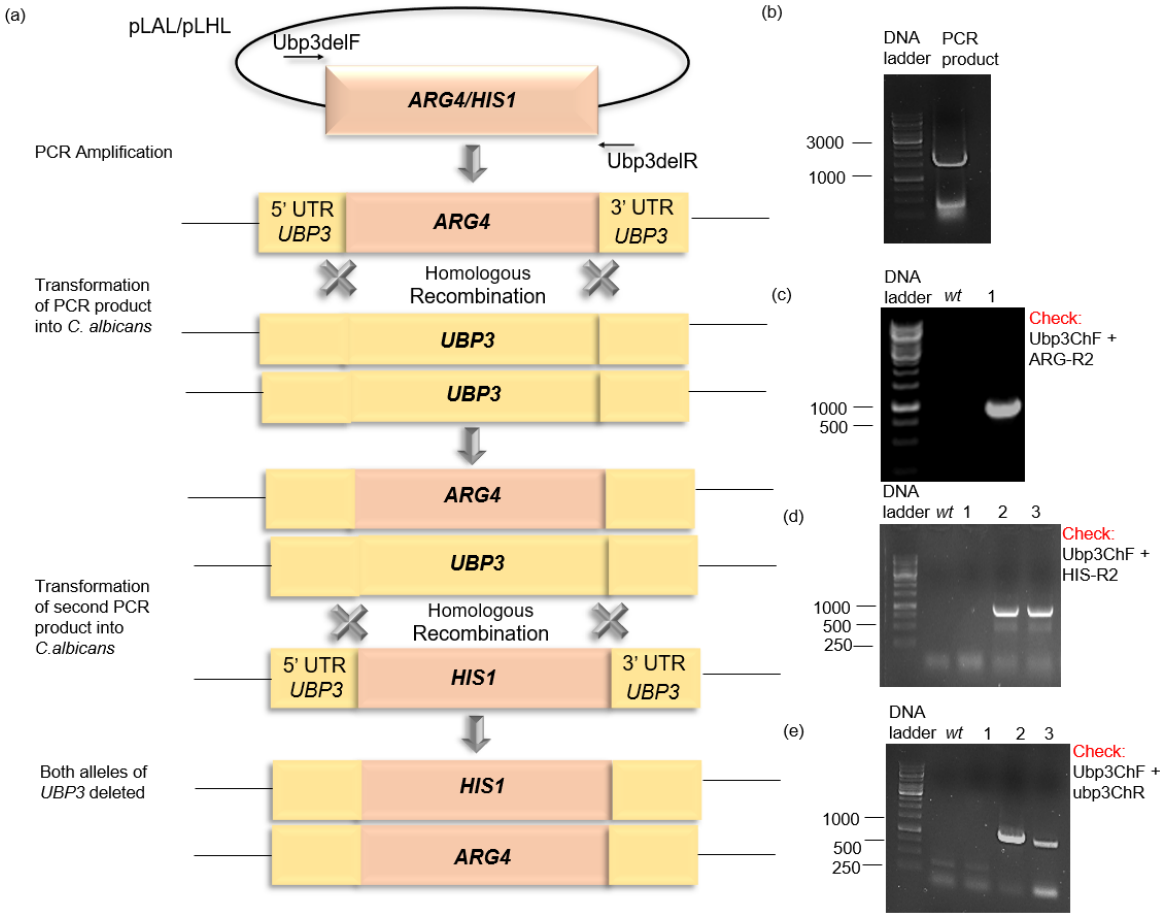

Figure 2.2. Creation of a strain lacking *UPB3*. (a) Diagrammatic representation of the strategy used. **(b)** Ubp3::ARG deletion cassette amplified by PCR using oligonucleotide primers Ubp3DelF and Ubp3DelR. **(c)** PCR check for correct deletion cassette integration following the first transformation using genomic DNA extracts and the oligonucleotides Ubp3ChF and ARG-R2. **(d)** PCR check for correct deletion cassette integration following the second transformation using genomic DNA extracts and the oligonucleotides genomic DNA Ubp3ChF and HIS-R2. **(e)** PCR check for correct deletion cassette integration following the second transformation using genomic DNA extracts and the oligonucleotides genomic DNA Ubp3ChF and Ubp3ChR. All PCR products were ran out onto a 1% agarose gel, for checks a genomic extract from wild type cells (JC465) used as a control.

2.1.4.3 Reintegration of PHO80, PHO81, PPN1, PPX1, VIP1, KCS1

To reintegrate *PHO80* into JC2138 (*pho80Δ*), the *PHO80* ORF plus promoter and terminator sequences were PCR amplified using the oligonucleotide primers PHO80CIBAMHIF and PHO80CIBAMHIR and the resulting fragment ligated into the *BamHI* site of CIp10 generating CIp10-*PHO80*. Subsequently, CIp10-*PHO80* was linearized by *Stu1* and integrated at the *RSP10* locus generating JC2374. Successful integration was confirmed by PCR using the oligonucleotide primers PHO80ChF and PHO80ChR. The same strategy was used to reintegrate *PHO81* into JC2131 (*pho81Δ*), *PPN1* into JC1975 (*ppn1Δ*), *PPX1* into JC1964

(*ppx1Δ*), *VIP1* into JC2538 (*vip1Δ*) using the oligonucleotide primer pairs, Pho81CIBAMHIF and PHO81CIBAMHIR, PPN1CIBAMHIF and PPN1CIBAMHIR, PPX1CIBAMHIF and PPX1CIBAMHIR and primer pair VIP1BAMHIF and VIP1BAMHIR, respectively. The only exception was that to reintegrate *KCS1* into JC2352 (*kcs1Δ*), the *KCS1* ORF plus promoter and terminator sequences were amplified by PCR using the oligonucleotide primers KCS1CIHINDIIIF and KCS1CIHINDIIIR and the subsequent product ligated into the *Hind III* site of CIp10, resulting in CIp10-*KCS1*. The successful integration of CIp10-*Pho81* into JC2131 generating JC2380, CIp10-*PPN1* into JC1975 generating JC2016, CIp10-*PPX1* into JC1964 generating JC2283, CIp10-*VIP1* into JC2538 generating JC2549 and CIp10-*KCS1* into JC2352 generating JC2379 was confirmed via PCR using the oligonucleotide primer pairs PHO81ChF and PHO81ChR, PPN1ChF and PPN1ChR, PPX1ChF and PPX1ChR, VIP1ChF and VIP1ChR and KCS1ChF with KCS1ChR, respectively. All reintegration plasmids generated were sequenced prior to transformation.

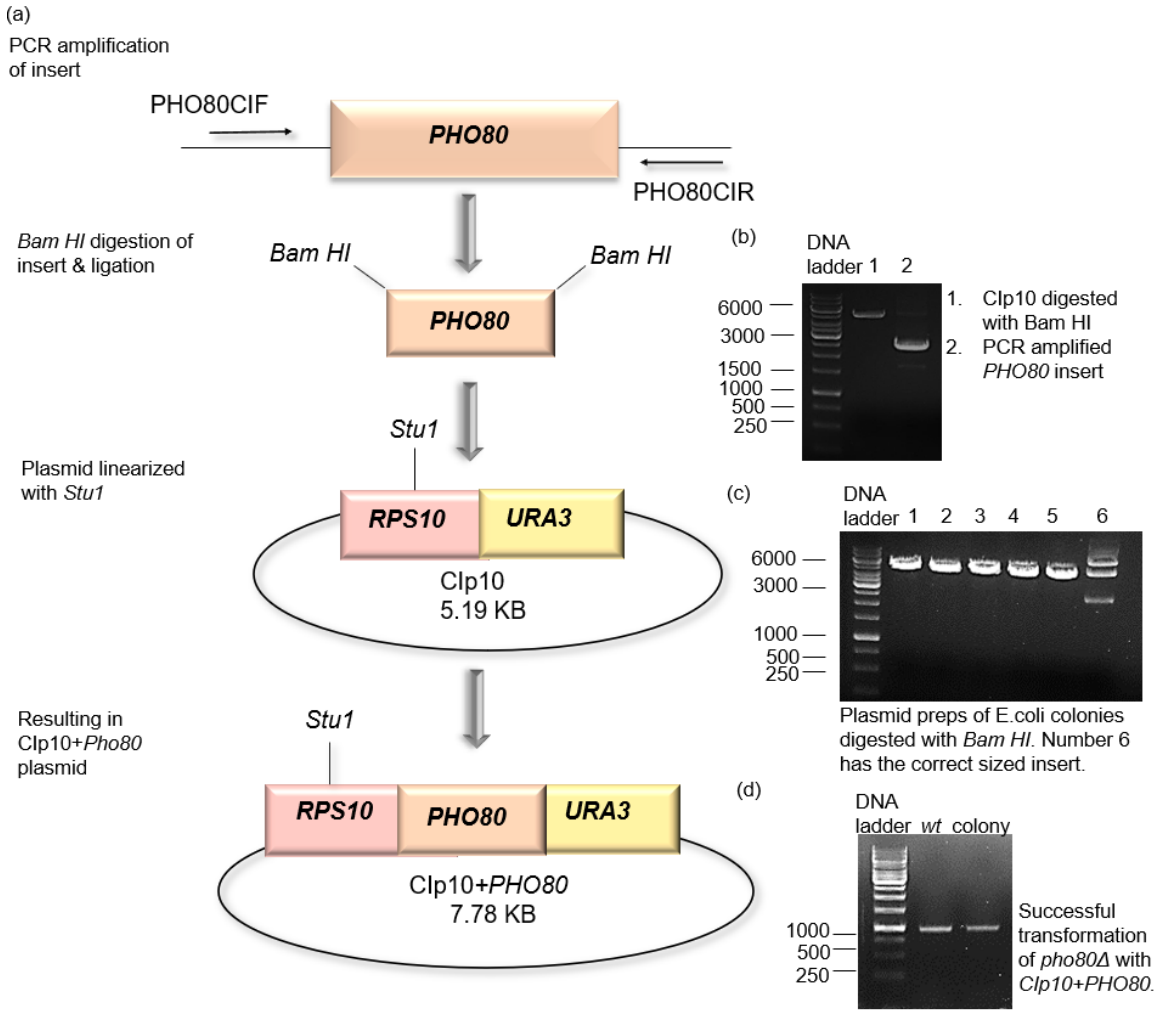

Figure 2.3. Diagram of strategy to create Clp10+*PHO80* plasmid. (a) Diagrammatic representation of the strategy used. *PHO80* ORF plus promoter and terminator sequences were PCR amplified from genomic DNA using the oligonucleotides Pho80CIF and Pho80CIR. The resulting fragment was cloned into the *BamHI* site of the integrating plasmid Clp10 to create Clp10-PHO80. This was then linearized with *Stu1* and integrated at the *RSP10* locus in *pho80Δ*. **(b)** 1 % agarose gel showing vector and insert prior to ligating. Vector was digested with *BamHI* and insert was generated by PCR using the oligonucleotide primers Pho80CIF and Pho80CIR and genomic DNA template. **(c)** 1 % agarose gel showing plasmids digested with *BamHI* to check whether transformed *E. coli* cells have the correct sized insert. **(d)** PCR check for successful transformation of *pho80Δ* using genomic DNA extracts and the oligonucleotides genomic DNA Pho80ChF and Pho80ChR. Genomic extract from wt cells (JC465) was used as a control.

2.1.4.4 Generating strains expressing tagged Pho4

To generate strains expressing Pho4 tagged with the myc-epitope, p-PHO4-MH (Ikeh *et al*., 2016) was linearized with *Age1* to integrate at the *PHO4* locus and transformed into JC2138 (*pho80Δ*), JC2131 (*pho81Δ*) and JC2201 (*ppn1Δ/ppx1Δ*), generating JC2276, JC2335 and

JC2451 respectively. PCR using the oligonucleotide primers Pho4TagChF and CycTermR was employed to confirm successful integration.

For the creation of strains expressing Pho4 tagged with GFP, pACT-PHO4GFP (Ikeh *et al*., 2016) was linearized with Stu1 and integrated at the *RSP10* locus in JC2201 (*ppn1Δ/ppx1Δ*), JC2138 (*pho80Δ*) and JC2131 (*pho81Δ*) cells, generating JC2303, JC2350 and JC2154 respectively. Successful integration was confirmed by PCR.

2.2 Yeast Phenotypic Analysis

2.2.1 Spot tests

Overnight *C. albicans* cultures grown in YPD were diluted back to OD_{660}=0.2 and then grown to mid-exponential phase (OD_{660}≈ 0.7) before being diluted back to OD_{660}=0.2 in fresh YPD or YPD-Pi and serial 10-fold dilutions were spotted onto YPD or YPD-Pi agar plates, containing the specified stress inducing compounds, using a 48-well replica plater (Sigma) . Plates were incubated for 24-48 hours at 30^0C. Oxidative stress was induced using stocks of 30% H_2O_2 (v/v) or 100 mM menadione. Cationic stress was stimulated using stocks of 5 M NaCl and 1 M KCl. For alkaline stress, YPD broth was adjusted to pH 8 using a 1 M stock of Tris (pH 8.25). Defects in the cell wall were examined using 30 mg/ml Calcoflour white, 30 mg/ml Congo red or 10% SDS. Genotoxic stress resistance was examined using stocks of 1 M HU, 99% MMS and 100 mg/ml Bleocin. To assess sensitivity to UV, cells were treated with the appropriate UV dose by Stratalinker. To investigate sensitivity to serum, 20% fetal calf serum (v/v) was used. All chemical agents were either obtained from Sigma or BDH unless otherwise stated.

2.2.2 Yeast-hyphae switch

Germ tube and hyphae formation was induced by diluting stationary phase cells grown overnight 1:10 in fresh YPD liquid media containing 10% fetal calf serum (v/v) (Invitrogen) and incubated at 37^0C for 6 hours at 180 rpm. Cells were fixed as described under microscopy analysis and captured on a Zeiss Axioscope with a 63X oil immersion objective using Axiovision software.

2.2.3 Hyperpolarised bud stimulation

Hyperpolarised bud formation was induced by diluting stationary phase cells grown overnight 1:10 in fresh YPD liquid media containing 40 mM HU and incubated at 30^0C for 6

hours at 180 rpm. Cells were fixed as described under microscopy analysis and captured on a Zeiss Axioscope with a 63X oil immersion objective using Axiosvision software.

2.2.4 Cell Volume Analysis

Overnight cultures were diluted back to OD_{660}=0.2 and then grown to mid-exponential phase (OD_{660}≈ 0.7). To avoid cell clumps, samples were sonicated at 35 kHz for 15 seconds. Cell volume was assayed using a Beckman Coulter counter using manufacturer's instructions.

2.3 Molecular Biology Techniques

2.3.1 Polymerase chain reaction

For synthesis of deletion cassettes using pLAL or pLHL (Dennison *et al*., 2005) PCR reactions were carried out using Dream Taq (Thermo Scientific). Reaction mixes were made to a final volume of 50 µL containing 0.5 µL of template DNA 100 ng/µL, 100 pmol of each oligonucleotide primer, 10 mM of each dNTP, 5 µL of 10X buffer (supplied by manufacturer) and 1 µL of Dream Taq polymerase (5 units/µl). Thermal cycling conditions were carried out under the following conditions: (1) initial denaturation: 94^0C for 5 minutes, (2) denaturation: 94^0C for 1 minute, (3) annealing: 52^0C for 2 minutes, (4) extension: 72^0C for 1 minute/kilobase, steps (2)-(4) were repeated 30 cycles (5) final extension: 72^0C for 8 minutes.

Synthesis of the Clox disruption cassette was carried out using the Extensor Master Mix (Thermo Scientific). Reaction mixes were made to a final volume of 50 µL containing 0.5 µL of template DNA of pNAT 20 ng/µL, 100 pmol of each oligonucleotide primer and 25 µL of extensor Master Mix containing the polymerase enzyme (supplied by manufacturer). Thermal cycling conditions were carried out under the following conditions: (1) initial denaturation: 94^0C for 5 minutes, (2) denaturation: 94^0C for 1 minute, (3) annealing: 54^0C for 1 minute, (4) extension: 68^0C for 1 minute/kilo base, steps (2)-(4) were repeated 35 cycles (5) final extension: 68^0C for 10 minutes.

Diagnostic PCR of genomic DNA extracts to check for successful integration following transformation was carried out using Dream Taq polymerase (Thermo Scientific). Reaction mixes were made to a final volume of 50 µL containing 0.5 µL of template DNA, 100 pmol of each oligonucleotide primer, 10 mM of each dNTP, 5 µL of 10X buffer (supplied by manufacturer) and 1 µL of Dream Taq polymerase. Thermal cycling conditions were carried

out under the following conditions: (1) initial denaturation: 95^{0}C for 2 minutes, (2) denaturation: 95^{0}C for 20 seconds, (3) annealing: 50^{0}C for 30 seconds, (4) extension: 72^{0}C for 1 minute/kilo base, steps (2)-(4) were repeated 35 cycles (5) final extension: 72^{0}C for 10 minutes.

DNA fragments for cloning were amplified using Phusion (New England Biolabs). Reaction mixes were made to a final volume of 50 µL containing 0.5 µL of template DNA, 100 pmol of each oligonucleotide primer, 10 mM of each dNTP, 5 µL of 10X HF buffer (supplied by manufacturer) and 0.5 µL of Phusion DNA polymerase (2 units/µl). Thermal cycling conditions were carried out under the following conditions: (1) initial denaturation: 98^{0}C for 30 seconds, (2) denaturation: 98^{0}C for 10 seconds, (3) annealing: 53^{0}C for 30 seconds, (4) extension: 72^{0}C for 0.5 minute/kilo base, steps (2)-(4) were repeated 35 cycles (5) final extension: 72^{0}C for 10 minutes.

2.3.2 Restriction endonuclease digestion, phosphatase treatment and DNA ligation reactions

All restriction enzymes used were purchased from either Promega (Southampton, UK) or New England Biolabs (Herts, UK) and reactions were carried out according to manufacturer's instructions.

To prevent self-ligation, plasmid vectors were treated with calf intestinal alkaline phosphatase, New England Biolabs (Herts, UK). Reaction mixes were set up according to manufacturer's instructions. Reactions were incubated at 37^{0}C for 30 minutes following 20 minutes at 65^{0}C to heat-deactivate the phosphatase.

DNA ligation reactions were set up in accordance with manufacturer's instructions using T4 ligase Promega (Southampton, UK). Each reaction contained approximately a molar ratio of 1 vector (20 ng): 3 or 5 insert and incubated at 4^{0}C overnight, before being transformed into competent *Escherichia coli* cells.

2.3.3 Analysis of DNA by agarose gel electrophoresis

DNA was analysed by electrophoresis on 1 % agarose (w/v)/TAE (40 mM Tris-acetate, 1 mM EDTA [pH 8.4]) gels containing 0.02% ethidium bromide in 1 X TAE buffer. Gels were visualised on a Gel Doc 1000 transilluminator system (Bio-Rad Laboratories, California) using

Quantity One software. To extract DNA fragments for cloning, a GeneJet gel extraction kit (Thermo Scientific, UK) was used in accordance with manufacturer's instructions.

2.3.4 Bacterial growth conditions, preparation of competent cells and transformations

E. coli (DH5α) cells were used to transform all of the plasmids created in this thesis. To prepare competent cells, cells were grown overnight in 5 mL Luria Broth (LB) (1% Bacto yeast extract (w/v), 2% Bacto tryptone (w/v) and 1% NaCl (w/v) pH 7.2) at 37^0C, 180 rpm. 125 µL of overnight cultures were inoculated into 25 mL of fresh LB and grown for 3 hours at 37^0C, 180 rpm. Cells were harvested by centrifugation at 2500 rpm for 3 minutes. Cell pellets were washed in ice-cold 100 mM $CaCl_2$ and incubated on ice for 15 minutes. Subsequently, cells were harvested at 8000 rpm for 2 minutes at 4^0C, then re-suspended in ice-cold 100 mM $CaCl_2$ and incubated on ice for 30 minutes prior to transformation.

To transform competent *E. coli*, 100 µL of cells were incubated with 10 µL of plasmid (~100 ng of plasmid DNA) on ice for 30 minutes before undergoing a heat shock treatment at 42^0C for 90 seconds. Subsequently, 1 mL of LB was added to the cell suspension and incubated at 37^0C, 180 rpm for 1 hour. Following this, cells were harvested at 8000 rpm for 1 minute, re-suspended in 100 µL of fresh LB and plated onto LB agar plates (LB media plus 2% Bacto agar (w/v)) containing 0.1 mg/mL ampicillin for plasmid selection. Plates were then incubated overnight at 37^0C.

2.3.5 Extraction of plasmid DNA

Plasmid extraction from *E. coli* cells was carried out using the standard alkaline lysis method (Birnboim and Doly, 1979). Briefly, 5 mL of *E. coli* was grown overnight in LB at 37^0C, 180 rpm. Cells were harvested at 3000 rpm for 5 minutes and re-suspended in 200 µL of solution 1 (50 mM glucose, 25 mM Tris-HCl [pH 8.0], 10 mM EDTA [pH8.0]) and 200 µL of solution 2 (0.2 M NaOH, 1% SDS (w/v)) and inverted 3-6 times to mix followed by an incubation at room temperature for 3 minutes or until the solution cleared. Following this, 350 µL of solution 3 (3 M KAC, 8% glacial acetic acid (w/v)) was added and inverted 3-6 times to mix before the addition of 400 µL of phenol: chloroform. The suspension was then centrifuged at 13,000 rpm for 5 minutes to separate the aqueous layer. Precipitation of plasmid DNA from the aqueous layer by adding 2 volumes 100% ethanol and $1/10^{th}$ volume 3 M NaAC [pH 7] and incubating for 30 minutes at -20^0C. Following incubation, samples were pelleted at

13,000 rpm for 15 minutes. Pellets were washed in 400 µL of 70% ethanol and centrifuged at 13,000 rpm for 5 minutes. Pellets were re-suspended in 50 µL of sterile nano H_2O.

Plasmids for sequencing were extracted using GeneElute™ MiniPrep Kit (Sigma, UK) in accordance to manufacturer's instructions.

2.3.6 DNA sequencing

DNA sequencing was performed by Eurofins (UK).

2.4 RNA techniques

2.4.1 RNA extraction

To collect samples for RNA extraction, cells were grown to mid-exponential phase and 25 mL were collected either treated or with the appropriate treatment for the designated amount of time and collected by centrifugation at 3000 rpm for 1 minute. To collect samples for qRT-PCR, cells were grown for 16 hours at 30˚C in YPD-Pi prior to being harvested and washed twice in ice-cold H_2O then snap frozen in liquid nitrogen. 10 mM KH_2PO_4 was added to Pi starved cultures and grown for a further 2 hours at 30°C before being harvested. Following this, harvested cells were washed in 1 mL of sterile nano H_20, pelleted by centrifugation at 13,000 rpm for 1 minute and then snap-frozen in liquid nitrogen. Samples were kept at -80^{0}C prior to processing.

For extraction, pellets were thawed on ice before being re-suspended in 750 µL TES (10 mM Tris-HCL [pH 7.5], 5 mM EDTA [pH 7.5], 1% SDS (w/v)) and 750 µL of acidic phenol: chloroform. Following this, samples were incubated at 65^{0}C for 1 hour with vortexing every 10 minutes. Subsequently, samples were in incubated on ice for 1 minute and centrifuged at 6000 rpm for 15 minutes 4^{0}C to separate the aqueous layer. To the aqueous layer, 700 µL of acidic phenol: chloroform was added and mixed by inversion before undergoing centrifugation at 13,000 rpm for 5 minutes 4^{0}C to separate the aqueous layer. Following this, 700 µL of phenol: chloroform was added to the aqueous layer, mixed by inversion and centrifuged at 13, 000 rpm for 5 minutes 4^{0}C. To the aqueous layer, 2 volumes of 100% ethanol and 1/10th volume 3 M NaAC [pH 7] was added and samples were incubated overnight at -80^{0}C to precipitate the RNA. Following incubation, samples were pelleted at 13,000 rpm for 15 minutes at 4^{0}C. Pellets were washed in 400 µL 70% ethanol, centrifuged at

13,000 rpm for 5 minutes at 4^0C and then re-suspended in 50 µL of sterile nano H_2O. Samples were stored at -80^0C until use.

2.4.2 DNAse treatment

RNA extracts for RT-qPCR were treated with Turbo DNA-free kit (Fisher Scientific, UK) according to manufacturer's instructions. Briefly, 0.1 volume of 10X TURBO DNAse buffer and 1 µL of TURBO DNAse (2 units/µL) was added to RNA extracts and mixed by inversion before being incubated at 37^0C for 30 minutes. Following this, 0.1 volume of DNAse inactivation reagent was added to the samples and vortexed. This was followed by incubation at room temperature for 5 minutes with frequent vortexing. Samples were the centrifuged at 13,000 rpm for 2 minutes. The aqueous layer containing the RNA was then transferred to a fresh tube.

2.4.3 Quantification of RNA

RNA was quantified at an absorbance of 260 nm using a nano drop spectrophotometer in accordance with manufacturer's instructions.

2.4.4 Primer design for real-time quantitative PCR

Targets selected were Pho4 dependent genes up-regulated following Pi starvation (Ikeh *et al*., 2016). Primers were designed using Primer3 websoftware (version 4.0.0) and synthesised by Eurogentec. *ACT1* was used as housekeeping gene.

Gene	Forward primer	Reverse primer
ACT1	ACCACCGGTATTGTTTTGGA	AGCGTAAATTGGAACAACGTG
PHO84	TTTGTTGGGTTTGTTCGTCA	GCAATAATGGCACCGACTTT
PHO100	GCTGGCCACAATBTTTTCTT	ACAGCAGATGAGGCTGGAGT

Table 2.3. Primer sequences for qPCR.

2.4.5 Real-time quantitative PCR

For each primer pair, melt curve analysis was performed to check for the presence of a single amplicon. Primer efficiency was validated by creating a standard curve using serial dilutions of wild type RNA extracted as described above (2.4.1).

For real-time qPCR, samples extracted as above (2.4.1) were diluted according to their concentration to be used as a template for one-step reactions using the SuperScript® III

Platinum® One-Step qRT-PCR Kit (Thermo-Fisher) in 96 well plates ran on a ABI machine. Reaction mixes were made to a final volume of 10 µl containing, 5 µl of 2X SYBR Green reaction mix, 0.5 µl of 10 µM forward and reverse primer, 0.2 µl ROX reference dye, 0.2 µl of SuperScript® III Platinum® Taq and 200 ng of RNA. Reactions were carried out with one cycle at 50^0C for 3 minutes to synthesise cDNA followed by one cycle at 95^0C for 5 minutes then 40 cycles of 95^0C for 15 seconds and 60^0C for 30 seconds then one cycle at 40^0C for 1 minute, followed by melt curve analysis. Threshold cycle (C_T) values were determined using ABI software. For the tested targets, the single enrichment for each target was calculated using the comparative C_T method. *ACT1* was used for normalisation. qRT-PCR was performed in 3 biological replicates in technical duplicate. Statistical significance was determined using Welch's two sample t-test.

2.5 Protein Analysis

2.5.1 C. albicans protein extraction

C. albicans cultures were grown to mid-exponential phase and either left untreated or treated with the appropriate stress treatment unless the stress was Pi starvation. When looking at Pi starvation, cultures were grown for 16 hours in YPD-Pi and incubated for a further 2 hours in the presence of 10mM KH_2PO_4 (pH 6) for YPD+Pi conditions. 25 mL of cells were harvested by centrifugation at 3000 rpm for 1 minute before being snap-frozen in liquid nitrogen. When investigating Pi starvation as a stress, 5 mL of cells were harvested to account for the high OD_{660} after 16 hours of growth. Pellets were stored at -80^0C until processing.

Pellets were thawed rapidly at room temperature prior to being washed in 1 mL of ice-cold lysis buffer (150 mM NaCl, 50 mM Tris-HCL [pH 7.5], 0.5% NP_4O (v/v), 10 mM Imidiazole) containing protease inhibitors (0.7 units/mL aprotinin, 10 µg/mL leupeptin, 10 µg/mL pepstatin A , 1mM phenylmethanesulfonyl fluoride (PMSF)) and phosphatase inhibitors (50 mM NaF, 2 mM Na_3VO_4). Washed cells were collected by centrifugation at 13,000 rpm for 1 minute and re-suspended in 200 µL of ice-cold lysis buffer and 1.5 mL of ice-cold glass beads on ice. Cells were disrupted by vortexing in a mini-bead beater (Biospec Products) for 2 X 15 seconds with a 1 minute incubation on ice in between. Following this, extracts were collected and the lysate clarified by centrifugation at 13,000 rpm for 10 minutes at 4^0C. Protein concentration was determined using the Bradford method (Bradford, 1976).

Samples were adjusted to the desired concentration and 4 X loading buffer (50 mM Tris-HCL [pH 6.8], 2% SDS (w/v), 10% glycerol (v/v), 12.5 mM EDTA, 1% β-mercaptoethanol) was added. Samples were either loaded onto an 8% SDS-PAGE gel or were stored at -20^{0}C. Prior to loading onto an SDS-PAGE gel, samples were incubated at 100^{0}C for 5 minutes to ensure protein denaturation. All chemicals were purchased from Sigma unless otherwise stated.

2.5.2 SDS-PAGE and Western blotting

Protein samples were subjected to electrophoresis on 8% SDS polyacrylamide gels (Laemmli, 1970) in TAE running buffer (2.5 mM Tris-HCL, 19.2 mM glycine, 0.01% SDS pH 8.3) for approximately 1 to 1.5 hours dependent on protein size. In order to assess correct running of the gel and protein size, 5 µL of pre-stained molecular weight marker (Page Rule, Thermo-Scientific) was loaded per gel. Proteins were transferred to a nitrocellulose membrane (Protan® Schleicher & Schuell Bioscience, DE) for 1 hour at 100 V in transfer buffer (2.5 mM Tris-HCL, 19.2 mM glycine, 0.01% SDS pH 8.3, 20% methanol (v/v)). Membranes were blocked in 10 % bovine albumin serum (BSA) in TBST (1 mM Tris-HCL [pH 8], 15 mM NaCl, 0.1% Tween 20 (v/v)) at room temperature for 30 minutes with gentle agitation. Following blocking, membranes were incubated with the appropriate primary antibody overnight at 4^{0}C with gentle agitation. Membranes were subsequently washed 3 times in TBST before being incubated with the appropriate secondary antibody for 1 hour at room temperature with gentle agitation. Following this, membranes were washed a further 3 times in TBST. Development of membranes was carried out manually using ECL™ Western Blot detection system (Amersham Pharma Biotech) and Fuji Medical X-ray film. Pho4 expressing 2myc 6His tag was detected by probing with an anti-myc mouse monoclonal primary antibody (Sigma, Dorset, UK) and an HRP-conjugated anti-mouse secondary antibody (Sigma, Dorset, UK). Tubulin was used as a loading control which was detected by probing with an ant-tubulin monoclonal primary antibody (DSHB, University of Iowa) and the same secondary antibody described above.

2.5.3 Stripping of membranes for re-probing

Membranes were incubated in stripping buffer (62.5 mM Tris-HCL [pH 6.7], 2% SDS (w/v), 100 mM β-mercaptoethanol) for 30 minutes at 50^{0}C with gentle agitation. Followed by washing 2X in TBST for 10 minutes each time at room temperature with gentle agitation.

Membranes were then blocked and probed with a primary antibody as described above (2.5.2).

2.6 Phosphate analysis

2.6.1 Polyphosphate

2.6.1.1 Growth conditions for PolyP extraction

C. albicans cultures were grown in YPD to mid-exponential phase OD_{660} = 0.8 and either left untreated or treated with the appropriate stress treatment. 25 mL of cells were harvested by centrifugation at 3000 rpm for 1 minute, washed 1 mL ice-cold sterile nano H_2O transferred to an Eppendorf and pelleted at 13,000 rpm for 1 minute before being snap-frozen in liquid nitrogen. Samples were stored at -80^{0}C until processing.

For detecting polyP levels following Pi starvation, cultures were grown for 16 hours in YPD-Pi. For detecting polyP levels following adding Pi back, cultures were incubated with 10mM KH_2PO_4 (pH 6) for 2 hours following 16 hours Pi starvation. For both conditions samples were then collected as described above.

2.6.1.2 PolyP extraction

Pellets were thawed on ice and re-suspended in 200 µL ice-cold RNA lysis buffer (50 mM Tris-HCL [pH 8], 100 mM EDTA [pH 8], 100 mM NaCl, 5 µL 20 % SDS (w/v)). To this suspension, 200 µL pf phenol: chloroform and 1 mL of ice-cold glass beads were added. Cells were disrupted by vortexing in a mini-bead beater (Biospec Products) for 30 seconds. Lysate was clarified by centrifugation at 13,000 rpm for 15 minutes at 4^{0}C. To the aqueous layer, 2 volumes of 100% ethanol and 1/10th volume 3 M NaAC [pH 7] was added and samples were incubated overnight at -80^{0}C to precipitate the RNA. Following incubation, samples were pelleted at 13,000 rpm for 15 minutes at 4^{0}C. Pellets were washed in 400 µL 70% ethanol, centrifuged at 13,000 rpm for 5 minutes at 4^{0}C and then re-suspended in 30 µL of sterile nano H_2O. Samples were stored at -80^{0}C until use.

2.6.1.3 PolyP analysis by UREA-PAGE

RNA was quantified for each sample as previously described (2.4.3). Each sample contained 20 µg RNA, to which 6 X loading dye was added (6X TBE, 15% Ficoll, 0.025% xylene cyanol FF). Samples were loaded onto pre-cast 12% polyacrylamide TBE-UREA (7M) gels (Bio-Rad,

Hercules, CA, USA). Samples were ran for 200 minutes at 100 V in TBE running buffer (89 mM borate, 2 mM EDTA, 89 mM Tris, pH 8). Samples were fixed for 15 minutes at room temperature in fixing buffer (5% glycerol, 25% methanol) with gentle agitation. Gels were then stained in staining buffer (5 % glycerol, 25% methanol, 0.05% toluidine blue) for 15 minutes at room temperature with gentle agitation. Following this, gels were washed 3 X in fixing buffer (Smith and Morrissey, 2007). Images of gels were obtained on a HP Scanjet flatbed scanner.

2.6.1.4 PolyP analysis by Neisser staining

Cells were grown to mid-exponential phase OD_{660}= 0.7-0.8 in YPD and either left untreated or treated with the appropriate stress before being fixed with paraformaldehyde as described (2.9.1). The only exception was for Pi starvation where instead cells were grown for 16 hours in YPD-Pi and a further 2 hours following the addition of 10mM KH_2PO_4 (pH 6).

Cells were fixed as described in 2.9.1. To fixed cells mounted onto slides, freshly prepared solution A (0.1% methylene blue, 5% Glacial acetic acid) and solution B (10% Crystal violet in 96% ethanol) were added to the slide for 15 seconds before being washed with H_2O. Solution C (1% Chrysoidin Y) was added to the slide for 45 seconds before being washed with H_2O (Gurr, 1965). Staining was visualised by light microscopy on Zeiss Axioscope with a 63X oil immersion objective analysed with Axiovision Imaging Software.

2.6.2 Secreted acid phosphatase assay agar overlay

Overnight *C. albicans* cultures in YPD were diluted back to OD_{660}=0.2 in PNMC+ Pi (2 mM KH_2PO_4 [pH 6]) then grown to mid-exponential phase O_{D660}=0.7. Cells were harvested at 2,500 rpm for 2 minutes before being washed 3X in PNMC. Cells were diluted back to OD_{660}=0.5 in fresh PNMC and 10 µL spotted onto either PNMC or PNMC+ 10 mM Pi agar plates. Plates were incubated overnight (16 hours) at 30^0C. Following incubation, 1% melted agar (~50^0C) plus staining solution (50 mM NaAc [pH 4], 18.65 µM I-napthyl phosphate, 105.2 µM Fast-blue salt dye) was laid over colonies on the PNMC and PNMC+ 10 mM Pi agar plates and incubated at 30^0C for 30 minutes (Toh-E *et al*., 1973). The presence of secreted acid phosphatase activity was visualised if the colony turned a reddish/brown colour. Images were taken on a HP Scanjet flatbed scanner.

2.6.3 Secreted acid phosphatase plate based assay

Overnight cultures were grown in YPD and diluted back to OD_{660}=0.2 in PNMC+ Pi (2 mM KH_2PO_4 [pH 6]) then grown to mid-exponential phase O_{D660}=0.7. Cells were harvested at 2,500 rpm for 2 minutes before being washed 3X in PNMC. Cells were diluted back to OD_{660}=0.05 in fresh PNMC or PNMC+ 10 mM Pi and 25 µL cells were seeded into 96 well plates and incubated overnight (16 hours) at 30^0C. Following incubation, to each seeded well, 1.5 µL of 1 M NaAc [pH 5.2] and 1.5 µL of 100 mM p-Nitrophenol phosphate was added. Plates were incubated at 37^0C for 20 minutes before reactions were stopped by the addition of 25 µL of 0.2 M NaOH. Cells were considered positive for presence of secreted acid phosphatase activity if a yellow colour was formed (via the release of the chromogenic compound p-nitrophenol from p-nitrophenol phosphate).

2.7 Inductively coupled mass spectrometry (ICP-MS)

Cells were grown in YPD to mid-exponential phase O_{D660}=0.7 and 25mL were harvested in triplicate by centrifugation at 2500 rpm for 2 minutes. Pellets were washed 2X in 25 mL wash buffer (50 mM Tris pH 7.5) then incubated in surface metal dissociation buffer (50 mM Tris [pH 7.5], 10 mM EDTA [pH 7.5]) at room temperature for 5 minutes. Pellets were then washed a further 2X in 25 mL wash buffer. Pellets were digested in triplicate in 1 mL 65% HNO_3 (w/v) (Merck) at room temperature for >48 hours. Following this, samples were centrifuged at 13,000 rpm for 20 minutes and diluted 1:10 with fresh 2% HNO_3 containing the internal standards Ag and Pt. ICP-MS analysis was then performed by Dr Kevin Waldron, Newcastle University as described in Tottey *et al*., 2008. Briefly, each sample was analysed for manganese (^{55}Mn), magnesium (^{24}Mg) and phosphorus (^{31}P) and the internal standards, silver (^{107}Ag) and platinum (^{195}Pt). Analysis was performed on a Thermo X-series ICP-MS operating system in collision cell mode (3 mL min^{-1} of 8% H_2 in He as collision gas). For each isotope, analysis was performed in peak-jump mode 100X with 25 ms dwell time on 3 channels with 0.02 atomic mass units separation, in triplicate. The concentration of each metal per sample was calculated by comparison to matrix-matched element standards (containing 0-100 µg/L of each element) which was analysed in the same analytical run. This was normalised to the OD_{660} recorded for each culture.

2.8 Drug Screening

2.8.1 Screen of secreted acid phosphatase assay

Samples were grown and prepared as described under secreted acid phosphatase plate based assay (2.6.3). The screen was carried out by Dr Peter Banks (High Throughout Screening Facility in the Faculty of Medical Sciences at Newcastle University) following the assay preparation described in (2.6.3), cells were seeded into 348 well plate containing 100 µM compounds from LifeArc Index Collection and Kinase Collection (Birchall *et al*., 2018). Plates were incubated overnight (16 hours) at 30^0C. Following incubation, to each seeded well, 1.5 µL of 1 M NaAc [pH 5.2] and 1.5 µL of 100 mM p-Nitrophenol phosphate was added. Plates were incubated at 37^0C for 20 minutes before reactions were stopped by the addition of 25 µL of 0.2 M NaOH. Growth was read at 600 nm and secreted acid phosphatase activity at 405 nm. Screening was repeated 4 times. Screening was repeated with compounds at the following concentrations 25 µM, 6.25 µM and 1.5625 µM.

2.8.2 pH 8 growth screening

Samples were grown to logarithmic phase in YPD before being washed 3 times in pH 8 media and diluted and seeded into a 384 well plate containing either 100 µM, 25 µM, 6.25 µM of each compound. Plates were incubated for 16 hours then growth was recorded at OD_{600}. The screen was carried out by Dr Peter Banks (High Throughout Screening Facility in the Faculty of Medical Sciences at Newcastle University).

2.9 Microscopy Analysis

2.9.1 Fixing cells with paraformaldehyde

Cells were fixed with paraformaldehyde as previously described (Enjalbert *et al*., 2006). Briefly, to 10 mL of cells, $1/10^{th}$ volume of 3.7% paraformaldehyde made in PEM (1 mM EGTA [pH 8], 100 mM piperazine- 1, 4-bis (2-ethanesulfonic acid) (PIPES) [pH 6.8], 1 mM $MgSO_4$) was added and mixed at room temperature for 30 minutes. Following this, samples were pelleted at 2500 rpm for 2 minutes and washed 3X in PEM. Samples were re-suspended in 100 µl of fresh PEM and stored at 4^0C.

2.9.2 Differential interphase contrast (DIC) microscopy

To fix cells to slides for microscopy, 10µL cells were spread onto slides coated with Poly-L-lysine and left for 20 minutes at room temperature. Following this, 5 µL of Vectashield® mounting medium (vector laboratories) was added prior to mounting the cover slip. Nail varnish was used to seal the coverslip to slide. Slides were imaged on a Zeiss Axioimager with a 63X oil immersion objective and analysed using Axiovision software.

2.9.3 Nuclear staining

For nuclear staining, cells and slides were prepared as described above (2.9.1 and 2.9.2) with the addition that Vectashield® mounting medium containing 1.5 mg/mL DAPI (4'-6-diamidino-2-phenylindole) (Vector laboratories) was used. DAPI fluorescence images were captured by excitation at a wavelength of 450-490 nm.

2.9.4 Cell wall straining

For cell wall staining, cells and slides were prepared as described above (2.9.1 and 2.9.2) but prior to the addition of mounting medium and cover slip, slides were incubated with 10 µg/mL Calcofluor white (CW) for 3 minutes at room temperature. Following this, slides were gently washed with H_2O. Samples were then prepared as described above. CW stained images were captures by excitation at a wavelength of 450-490 nm.

2.9.5 Vacuolar staining

For vacuolar staining, prior to fixing, cells were washed 3 X in phosphate buffered saline (PBS) to remove traces of YPD as this can interfere with the dye. Cultures were incubated with 100 mM 7-amino-4-chloromethylcoumarin (CMAC) for 30 minutes in the dark. Cells were subsequently fixed with paraformaldehyde as previously described (2.9.1). CAMC stained images were captured by excitation at a wavelength ~ 460 nm.

2.9.6 Pho4 localisation

Cells expressing Pho4-GFP were grown in YPD-Pi for 16 hours and incubated for a further 2 hours in the presence of 10mM KH_2PO_4 (pH 6) for YPD+ Pi conditions. 9 mL of cells were collected for each sample and fixed as described above (2.9.1). In order to determine whether Pho4-GFP located to the nucleus, Vectashield® mounting medium containing 1.5 mg/mL DAPI was used to locate the nucleus. GFP fluorescence was captured by excitation at

a wavelength of 356 nm and DAPI 450-490 nm. Images were captured at Newcastle University Bioimaging unit on a Zeiss Axioimager with a 63X oil immersion objective and analysed using Axiovision software.

2.10 Virulence assays

2.10.1.1 C. elegans strains

The *C. elegans* strain used in *C. albicans* virulence assays was wild type (N2) supplied by Dr Elizabeth Veal, Newcastle University.

2.10.1.2 Preparation of Nematode growth media lite (NGML)

C. elegans were maintained on Nematode growth media lite (NGML) (1 mM $CaCl_2$, 25 mM KH_2PO_4 (Biochemika), 1 mM $MgSO_4$, 50 mM NaCl, 0.25% peptone (w/v) (BD), 1.7% agar (w/v)) supplemented with 1 mL/L cholesterol (5 mg/mL stock in 95% ethanol) and streptomycin (300 ng/mL). Small petri dishes contained 7 mL of NGML and were seeded with 300 µL of overnight cultured *E. coli* OP50 (Brenner, 1974). *E. coli* was inoculated into 25 mL of LB supplemented with streptomycin (300 ng/mL) and grown overnight at 37^0C 180 rpm. NGML plates seeded with *E. coli* were allowed to grow for 48 hours prior to the seeding of *C. elegans*.

2.10.1.3 Maintenance of C. elegans stocks

C. elegans were maintained on NGML plates with *E. coli* OP50 as a food source. 20 worms at L4 life stage were moved weekly onto fresh NGML plates with a worm pick using a Binocular Stereo zoom Microscope (Nikon SMZ1000, Japan). Stocks were maintained at 15^0C.

2.10.1.4 C. elegans synchronisation & infection assay

To synchronise worms for virulence assays, 25 L4 stage worms were moved onto fresh NGML plates seeded with *E. coli* OP50 and incubated for 3 hours at 25^0C. Worms were then removed and plates incubated at 25^0C for 48 hours. The following day, small petri dishes containing Brain heart infusion (BHI) (Brain heart infusion (BD), 1.7% agar (w/v)) were seeded with 300 µL overnight cultured *C. albicans* strains and incubated overnight at 25^0C. Following overnight incubation, 150 µM 5-fluoro-2'-deoxyuridine (FUdR) (Sigma) was added to each *C. albicans* seeded BHI plate and incubated for 1 hour at room temperature to

prevent *C. elegans* reproduction during infection assay (He, 2011). From the NGML plates seeded with *E. coli* OP50 which had been incubated for 48 hours, 3 X 25 worms for each *C. albicans* strain assayed were moved to fresh unseeded NGML plates and incubated for 1 hour at room temperature to prevent contamination of *C. albicans* seeded BHI plates with *E. coli* OP50. Worms were then moved from the unseeded NGML plates to *C. albicans* seeded BHI plates. 3 X 25 worms were moved onto 3 *C. albicans* seeded BHI plates for each *C. albicans* strain being assayed. Plates were incubated at 25^0C. Daily checks were performed to monitor worm viability, worms were considered deceased if there was no pharynx contraction or response to touch with a worm pick and removed from the plate. Viability was monitored using a Binocular Stereo zoom Microscope (Nikon SMZ1000, Japan). Differences in *C. elegans* survival were determined by log-rank test with a P value of <0.05 considered as significant.

2.10.2 Galleria mellonella infection assay

Galleria mellonella was performed as described (Patterson *et al*., 2013). *Galleria mellonella* were maintained at 15^0C in the dark for no longer than 5 days. Only larvae which were approximately the same weight, height and had no signs of melanisation were used for inoculation. *C. albicans* strains for inoculation were grown overnight in YPD before being diluted back to OD_{660}=0.2 and grown to mid-exponential phase OD_{660}=0.7 and number of cells per mL determined using haemocytometer. 5 X 10^5 *C. albicans* cells in a final volume of 30 µL in PBS was used to inoculate *G. mellonella* by injecting into the left hind leg using a BD-microfine insulin syringe (Scientific Laboratories Supplies). 15 larvae were used per *C. albicans* strain. 30 µL PBS was used to inoculate the control group of 15 larvae. *G. mellonella* were maintained in 9 cm petri dishes without food at 37^0C for 5 days. Daily checks were performed to assess viability, larvae were considered deceased if no movement was observed following touch, or if there was complete melanisation, and removed from the plate. Differences in *G. mellonella* survival was represented by Kaplan-Meier curves and analysed by a Log-rank test. A P value <0.05 was considered significant.

Chapter 3: Regulation of the PHO Pathway in *C. albicans*

3.1 Introduction

Then PHO pathway in yeast is essential for maintaining Pi homeostasis, orchestrating Pi acquisition, polyP synthesis, storage, and mobilisation. To date, studies investigating the PHO pathway have largely focussed on *S. cerevisiae* (Komeili and O'Shea, 1999; Ogawa *et al*., 2000; Tomah and Sinah, 2014). However, in *C. albicans* it has been shown that loss of the PHO pathway transcription factor, Pho4, similarly impairs growth in Pi limiting conditions (Homann *et al*., 2009; Romanowski *et al*., 2012). Moreover, loss of Pho4 (Ikeh *et al*., 2016), the high affinity Pi transporter Pho84 (Liu *et al*., 2017) or the secreted acid phosphatase Pho100 (MacCallum *et al*., 2009) attenuates virulence. Furthermore, induction of *PHO84* has been shown to occur following phagocytosis (Fradin *et al*., 2005) and during infection of the kidney (Walker *et al*., 2009) and liver (Thewes *et al*., 2007). Collectively, these studies support a link between Pi acquisition and *C. albicans* pathogenicity.

In *S. cerevisiae*, Pho4 is regulated by the core signalling cascade composed of the CDK, Pho85, the cyclin Pho80, and the CDK inhibitor Pho81 (Tomah and Sinah, 2014). As described in Chapter 1, section 1.5.1, under Pi replete conditions the Pho85-Pho80 CDK complex phosphorylates Pho4 which triggers the nuclear export of this transcription factor (Kaffman *et al*., 1994) . However, in response to Pi starvation, Pho81 inhibits the CDK complex (Schneider *et al*., 1994), subsequently Pho4 becomes dephosphorylated, facilitating its nuclear accumulation and the Pho-dependent induction of genes involved in Pi acquisition (Kaffman *et al*., 1994). In *S. cerevisiae*, up-regulation of Pi acquisition genes occurs codependently with Pho2 (Komeili and O'Shea, 1999). However, in *C. albicans*, induction of Pi acquisition genes by Pho4 is Pho2 independent (He *et al*., 2017).

In *S. cerevisiae*, the CDK complex prevents Pho4 nuclear accumulation by phosphorylation of 5 specific Serine-Proline residues (SP1, SP2, SP3, SP4 and SP6) (Komeili and O'Shea, 1999). However, such phosphorylation sites do not appear to be conserved in *C. albicans* Pho4 (Ikeh *et al*., 2016). Indeed, conservation between *S. cerevisiae* and *C. albicans* Pho4 is mostly exclusive to the C-terminal DNA binding domain (Ikeh *et al*., 2016). Previous unpublished work from the Quinn lab revealed that Pho4 carries an unidentified, phosphorylation independent, post translational modification (PTM) present during Pi replete conditions (Ikeh, 2015). However, this PTM of Pho4 was no longer observed following Pi starvation. This is suggestive that such a PTM may also be involved in the regulation of Pho4. There is

growing appreciation that ubiquitination is a PTM that has vital signalling roles in addition to functioning in targeting proteins for degradation (Bhat and Greer, 2011). Ubiquitin-dependent signalling is modulated by deubiquitylating enzymes (DUBs), of which there are 20 in *S. cerevisiae* (Finley *et al*., 2012). Proteomic analysis of 9 DUB deletion strains revealed that deletion of the DUBs, Ubp3, Ubp10 and Otu2 all resulted in lower protein levels of the Pho4 regulated targets, Pho5, Pho84 and Vtc2-4 (Isasa *et al*., 2015). In addition, over-expression of Ubp3 resulted in the nuclear retention of Pho4 under Pi replete conditions (Isasa *et al*., 2015). Collectively, these data indicate that ubiquitination of Pho4 in *S. cerevisiae* negatively regulates this transcription factor. Therefore, a plausible candidate for the unidentified PTM of *C. albicans* Pho4 observed during Pi replete conditions could be ubiquitination.

A key question regarding PHO pathway regulation is how the CDK complex is differentially regulated depending on intracellular Pi levels. As discussed in Chapter 1, section 1.9, the sensing and signalling of Pi levels is thought to be via the interaction of IP_7 signalling molecules with SPX domains found in many proteins involved in Pi homeostasis (Wild *et al*., 2016; Lee *et al*., 2007). IP_7 is converted from IP_6 by either Vip1 or Kcs1, generating 1-IP_7 or 5-IP_7, respectively (Lonetti *et al*., 2011). Of particular relevance here is the CDK inhibitor Pho81, which has an SPX domain. A previous study in *S. cerevisiae* reported that, following Pi starvation, IP_7 produced by Vip1 binds to Pho81, leading to inhibition of Pho80-Pho85 complex kinase activity (Lee *et al*., 2007). However, other studies indicate that 5-IP_7, generated by Kcs1, is the key signalling molecule and that levels decrease rather than increase following Pi Starvation (Wild *et al*., 2016). Moreover, it has been shown in *S. cerevisiae* that loss of Kcs1 (and thus presumably 5-IP_7) results in constitutive activation of the PHO pathway. This is demonstrated by constitutive expression of secreted acid phosphatases and polyP mobilisation (Auesukaree *et al*., 2005). However, in *C. neoformans* cells lacking Kcs1, the opposite situation is observed as activation of Pho4 dependent genes is abolished and therefore *kcs1Δ* cells phenocopy cells lacking Pho4. This is because the binding of Kcs1 derived IP_7 molecules to the SPX domain of Pho81 promotes the interaction of this inhibitor with the Pho80-Pho85 CDK complex (Desmarini *et al*., 2020). However, neither Vip1 or Kcs1 enzymes have been investigated in *C. albicans* with regard to potential roles in Pi sensing and homeostasis regulation .

The main aim of this chapter is to characterise putative regulators of the PHO pathway in *C. albicans* and to determine their contribution to Pi homeostasis, Pho4 regulation and stress resistance.

3.2 Results

3.2.1 Pho80 and Pho81 in C. albicans

3.2.1.1 Cells lacking PHO80 have a growth defect

The PHO pathway has been extensively studied in *S. cerevisiae*; therefore, this knowledge was used to begin addressing how Pho4 is regulated in *C. albicans*. In *S. cerevisiae* Pho81 is the inhibitor of the CDK complex which phosphorylates Pho4, preventing its nuclear accumulation. Analysis of the Candida Genome Database revealed the presence of a gene CR_00590W_A, which shares 32% homology to the protein in *S. cerevisiae* and has a conserved SPX domain as well as an Ankyrin rich repeat domain and GP-PDE domain (Figure 3.1). A *C. albicans* strain lacking Pho81 was obtained from the Noble deletion library (Noble *et al*., 2010). In *S. cerevisiae* the CDK complex is composed of the cyclin Pho80 and the kinase Pho85, of which there are putative homologues in *C. albicans* (C6_03810W_A, C1_04520C_A) which share 49.4% and 68% homology respectively with those in *S. cerevisiae* (Figure 3.2 & 3.3). A *pho80Δ* strain was previously generated in the lab (M. Ikeh and J. Quinn, unpublished). Reconstituted *pho80Δ+PHO80* and *pho81Δ+PHO81* strains were generated in this study by the integration of the respective ORF plus promoter and terminator sequences at the *RSP10* locus of the deletion strain. With regard to the Pho85 cyclin dependent kinase, deletion of *PHO85* in *S. cerevisiae* has been shown to be rescued by the introduction of *C. albicans PHO85* (Miyakawa *et al*., 2000). However, unlike in *S. cerevisiae*, Pho85 is essential in *C. albicans* (Segal *et al*., 2018).

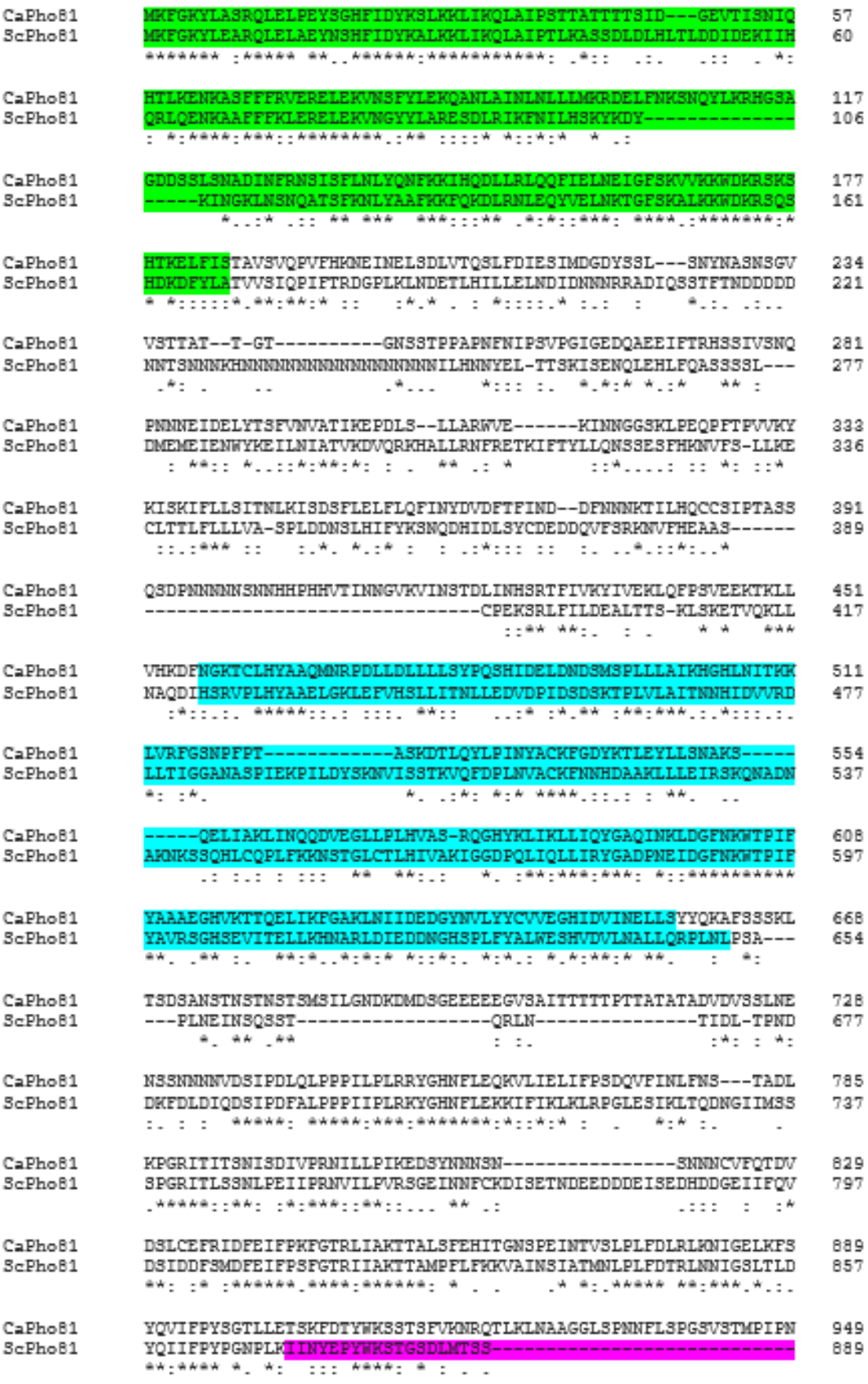
CaPho81 MKFGKYLASRQLELPEYSGHFIDYKSLKKLIKQLAIPSTTATTTTSID---GEVTISNIQ 57
ScPho81 MKFGKYLEARQLELAEYNSHFIDYKALKKLIKQLAIPTLKASSDLDLHLTLDDIDEKIIH 60
CaPho81 HTLKENKASFFFRVERELEKVNSFYLEKQANLAINLNLLLMKRDELFNKSNQYLKRHGSA 117
ScPho81 QRLQENKAAFFFKLERELEKVNGYYLARESDLRIKFNILHSKYKDY-------------- 106
CaPho81 GDDSSLSNADINFRNSISFLNLYQNFKKIHQDLLRLQQFIELNEIGFSKVVKKWDKRSKS 177
ScPho81 -----KINGKLNSNQATSFKNLYAAFKKFQKDLRNLEQYVELNKTGFSKALKKWDKRSQS 161
CaPho81 HTKELFISTAVSVQPVFHKNEINELSDLVTQSLFDIESIMDGDYSSL---SNYNASNSGV 234
ScPho81 HDKDFYLATVVSIQPIFTRDGPLKLNDETLHILLELNDIDNNNRRADIQSSTFTNDDDDD 221
CaPho81 VSTTAT--T-GT----------GNSSTPPAPNFNIPSVPGIGEDQAEEIFTRHSSIVSNQ 281
ScPho81 NNTSNNNKHNNNNNNNNNNNNNNNNNNNILHNNYEL-TTSKISENQLEHLFQASSSSL--- 277
CaPho81 PNNNEIDELYTSFVNVATIKEPDLS--LLARWVE------KINNGGSKLPEQPFTPVVKY 333
ScPho81 DMEMEIENWYKEILNIATVKDVQRKHALLRNFRETKIFTYLLQNSSESFHKNVFS-LLKE 336
CaPho81 KISKIFLLSITNLKISDSFLELFLQFINYDVDFTFIND--DFNNNKTILHQCCSIPTASS 391
ScPho81 CLTTLFLLLVA-SPLDDNSLHIFYKSNQDHIDLSYCDEDDQVFSRKNVFHEAAS------ 389
CaPho81 QSDPNNNNNSNNHHPHHVTINNGVKVINSTDLINHSRTFIVKYIVEKLQFPSVEEKTKLL 451
ScPho81 --------------------------------CPEKSRLFILDEALTTS-KLSKETVQKLL 417
CaPho81 VHKDFNGKTCLHYAAQMNRPDLLDLLLLSYPQSHIDELDNDSMSPLLLAIKHGHLNITKK 511
ScPho81 NAQDIHSRVPLHYAAELGKLEFVHSLLITNLLEDVDPIDSDSKTPLVLAITNNHIDVVRD 477
CaPho81 LVRFGSNPFPT------------ASKDTLQYLPINYACKFGDYKTLEYLLSNAKS----- 554
ScPho81 LLTIGGANASPIEKPILDYSKNVISSTKVQFDPLNVACKFNNHDAAKLLLEIRSKQNADN 537
CaPho81 -----QELIAKLINQQDVEGLLPLHVAS-RQGHYKLIKLLIQYGAQINKLDGFNKWTPIF 608
ScPho81 AKNKSSQHLCQPLFKKNSTGLCTLHIVAKIGGDPQLIQLLIRYGADPNEIDGFNKWTPIF 597
CaPho81 YAAAEGHVKTTQELIKPGAKLNIIDEDGYNVLYYCVVEGHIDVINELLSYYQKAFSSSKL 668
ScPho81 YAVRSGHSEVITELLKHNARLDIEDDNGHSPLFYALWESHVDVLNALLQRPLNLPSA--- 654
CaPho81 TSDSANSTNSTNSTSMSILGNDKDMDSGEEEEEGVSAITTTTTPTTATATADVDVSSLNE 728
ScPho81 ---PLNEINSQSST------------------QRLN---------------TIDL-TPND 677
CaPho81 NSSNNNNVDSIPDLQLPPPILPLRRYGHNFLEQKVLIELIFPSDQVFINLFNS---TADL 785
ScPho81 DKFDLDIQDSIPDFALPPPIIPLRKYGHNFLEKKIFIKLKLRPGLESIKLTQDNGIIMSS 737
CaPho81 KPGRITITSNISDIVPRNILLPIKEDSYNNNSN----------------SNNNCVFQTDV 829
ScPho81 SPGRITLSSNLPEIIPRNVILPVRSGEINNFCKDISETNDEEDDDEISEDHDDGEIIFQV 797
CaPho81 DSLCEFRIDFEIFPKFGTRLIAKTTALSFEHITGNSPEINTVSLPLFDLRLKNIGELKFS 889
ScPho81 DSIDDFSMDFEIFPSFGTRIIAKTTAMPFLFKKVAINSIATMNLPLFDTRLNNIGSLTLD 857
CaPho81 YQVIFPYSGTLLETSKFDTYWKSSTSFVKNRQTLKLNAAGGLSPNNFLSPGSVSTMPIPN 949
ScPho81 YQIIFPYPGNPLKIINYEPYWKSTGSDLMTSS---------------------------- 889

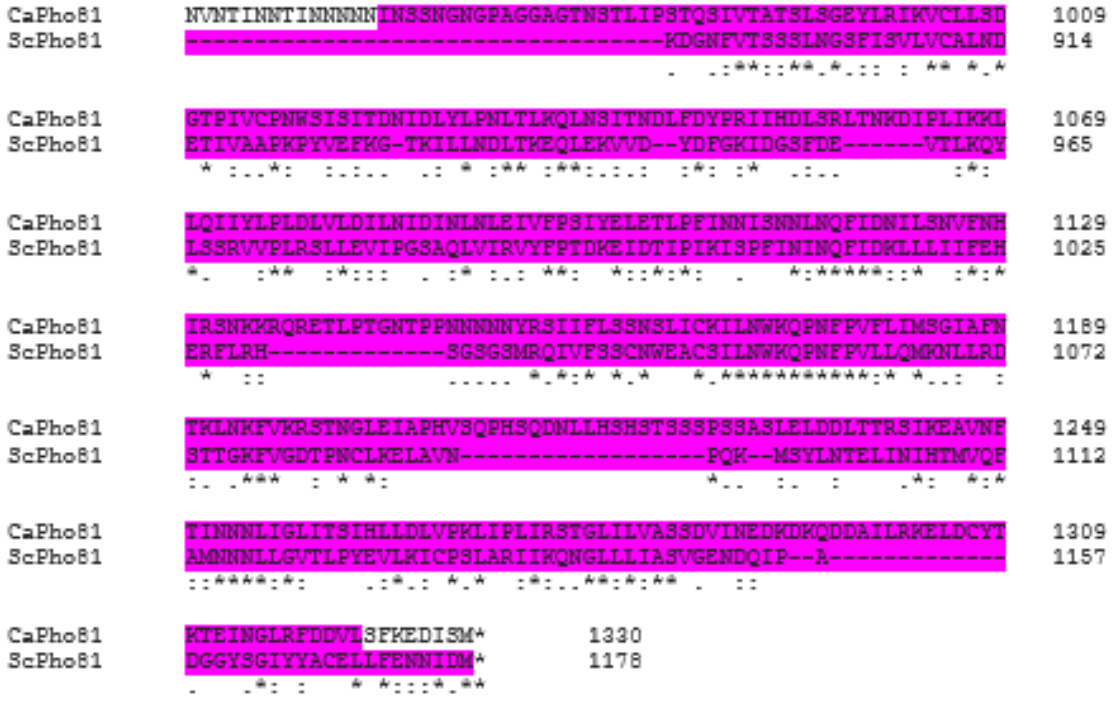

Figure 3.1. Alignment of *C. albicans* and *S. cerevisiae* Pho81 reveals sequence divergence. Sequences of *C. albicans* (Ca) Pho81 and *S. cerevisiae* (Sc) Pho81 were aligned using ClustalW. Identical nucleotides found in both sequences are annotated with *. Gaps were introduced to maximise alignment these are indicated by dashes. SPX domain is shown in green, Ankyrin rich repeat region is shown in blue and GP-PDE domain is shown in pink.

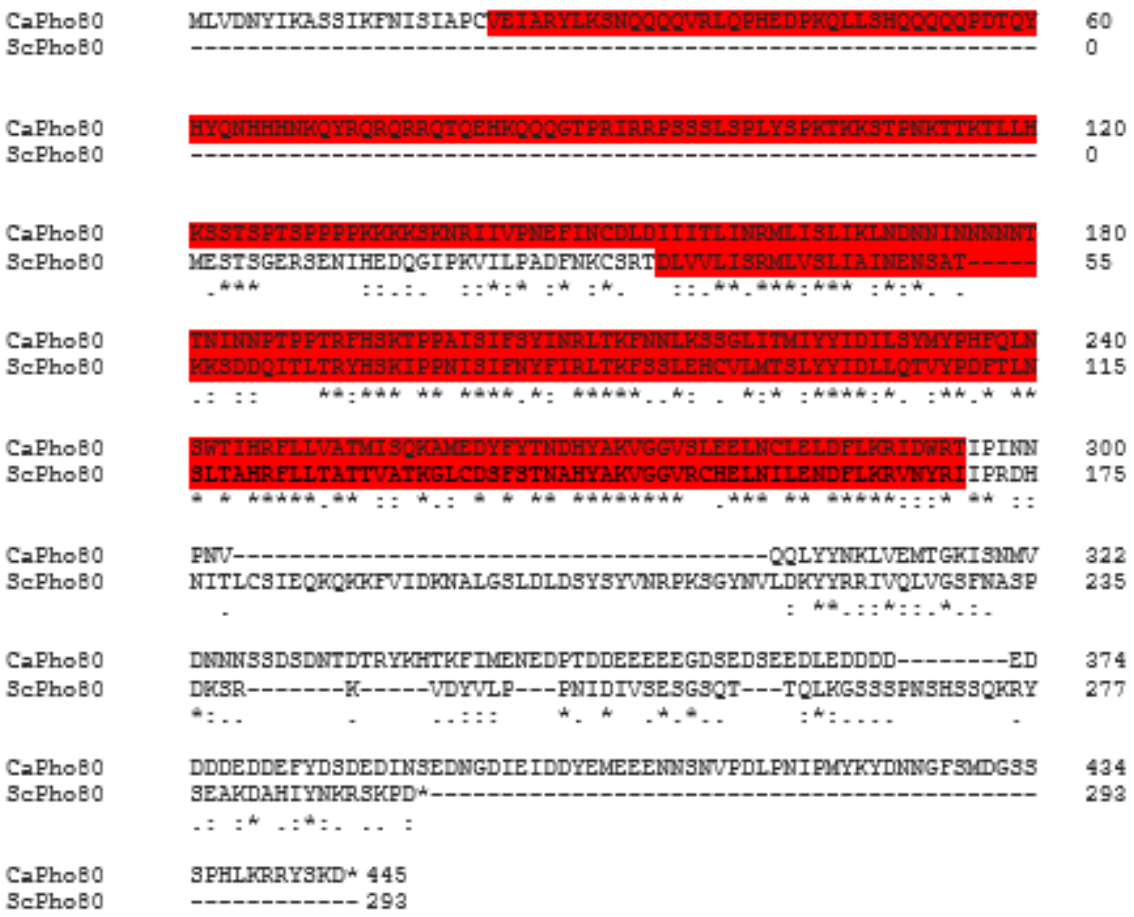

Figure 3.2. Alignment of *C. albicans* and *S. cerevisiae* Pho80 reveals sequence divergence. Sequences of *C. albicans* (Ca) Pho80 and *S. cerevisiae* (Sc) Pho80 were aligned using ClustalW. Identical nucleotides found in both sequences are annotated with *. Gaps were introduced to maximise alignment these are indicated by dashes. The cyclin domain is shown in red.

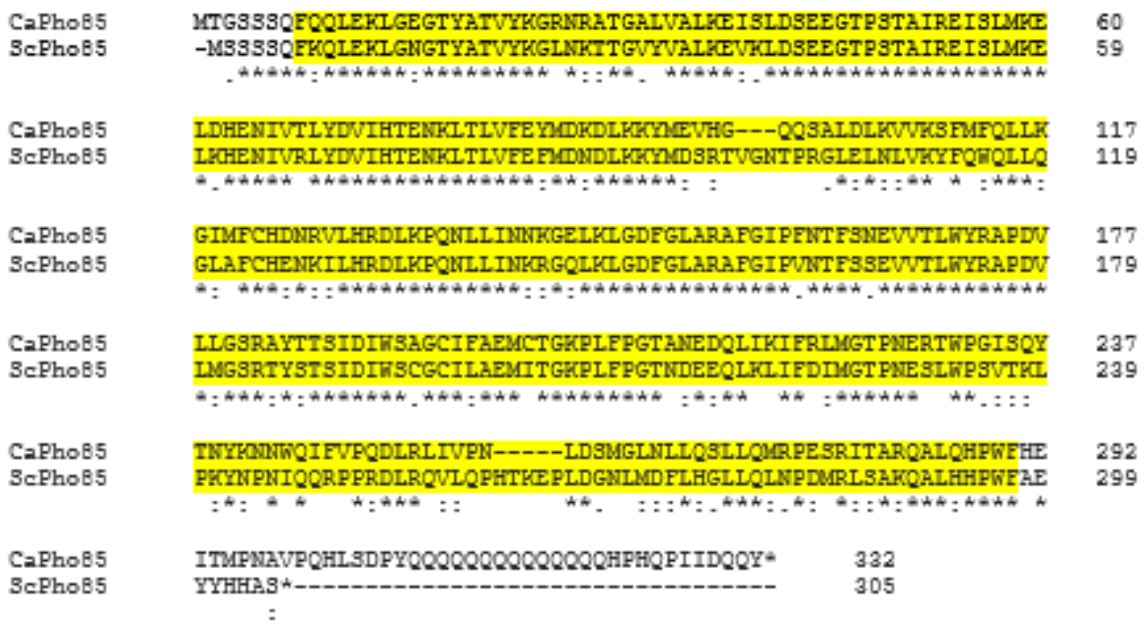

Figure 3.3. Alignment of *C. albicans* and *S. cerevisiae* Pho85.
Sequences of *C. albicans* (Ca) Pho85 and *S. cerevisiae* (Sc) Pho85 were aligned using ClustalW. Identical nucleotides found in both sequences are annotated with *. Gaps were introduced to maximise alignment these are indicated by dashes. The protein kinase domain is shown in yellow.

The *pho81Δ* and *pho80Δ* mutant strains were constructed in different, yet related wild type strain backgrounds, and hence respective wild type strains were used in all subsequent experiments. Cells lacking Pho4 have a significant growth defect in both Pi replete and depleted conditions. Thus, initial experiments aimed to characterise the growth rates of *pho80Δ* and *pho81Δ* cells (Figure 3.4.a, b). The wild type strains for both mutant backgrounds grew almost identically (Figure 3.4.a, b). However, deletion of the CDK inhibitor Pho81 resulted in faster growth than that exhibited by wild type cells, whereas cells lacking the cyclin Pho80 grew considerably slower than wild type cells. Notably, *pho80Δ* cells were slower growing than cells lacking Pho4 (Figure 3.4.a). The reintroduction of *PHO*80 and *PHO81* into *pho80Δ* and *pho81Δ* mutants respectively, restored wild type growth (Figure 3.4.a, b). Cell morphology was also investigated, however none of the mutant strains had an observable morphological defect when grown to mid-logarithmic phase in YPD (Figure 3.4.c).

The ability of *C. albicans* to switch from yeast to hyphae is a key morphological trait as well as virulence determinant. Cells lacking *PHO4* have a delay in the switch from yeast to hyphae (Ikeh *et al*., 2016). A similar delay is seen with another component of the PHO pathway; Pho84, a high affinity Pi transporter (Liu *et al*., 2018). Thus, it was investigated whether loss

of *PHO80* or *PHO81* had any impact on the ability of *C. albicans* to switch from yeast to hyphae morphologies. Cells were incubated with 10% fetal calf serum (FCS) at 37^0C for 3 hours. Such conditions are optimal for inducing hyphal formation *in vitro* (Sudbery, 2011). Cells lacking *PHO80* were found to show a delay in hyphal formation when compared to wild type cells at 3 hours (Figure 3.5.a). Reconstitution of *pho80Δ* with *PHO80* reversed the delay in the switch to hyphal formation (Figure 3.5.a). It is noteworthy however, that although the switch is delayed in *pho80Δ* cells, germ tube formation is observed after 2 hours (Figure 3.5.a). As cells lacking *PHO80* have been shown to have a growth defect (Figure 3.4.a) it is highly plausible that this contributes to the delayed hyphal formation. With regard to Pho81, there was no detectable difference in the timing of the switch from yeast to hyphae in cells lacking *PHO81* compared to wild type cells (Figure 3.5.b).

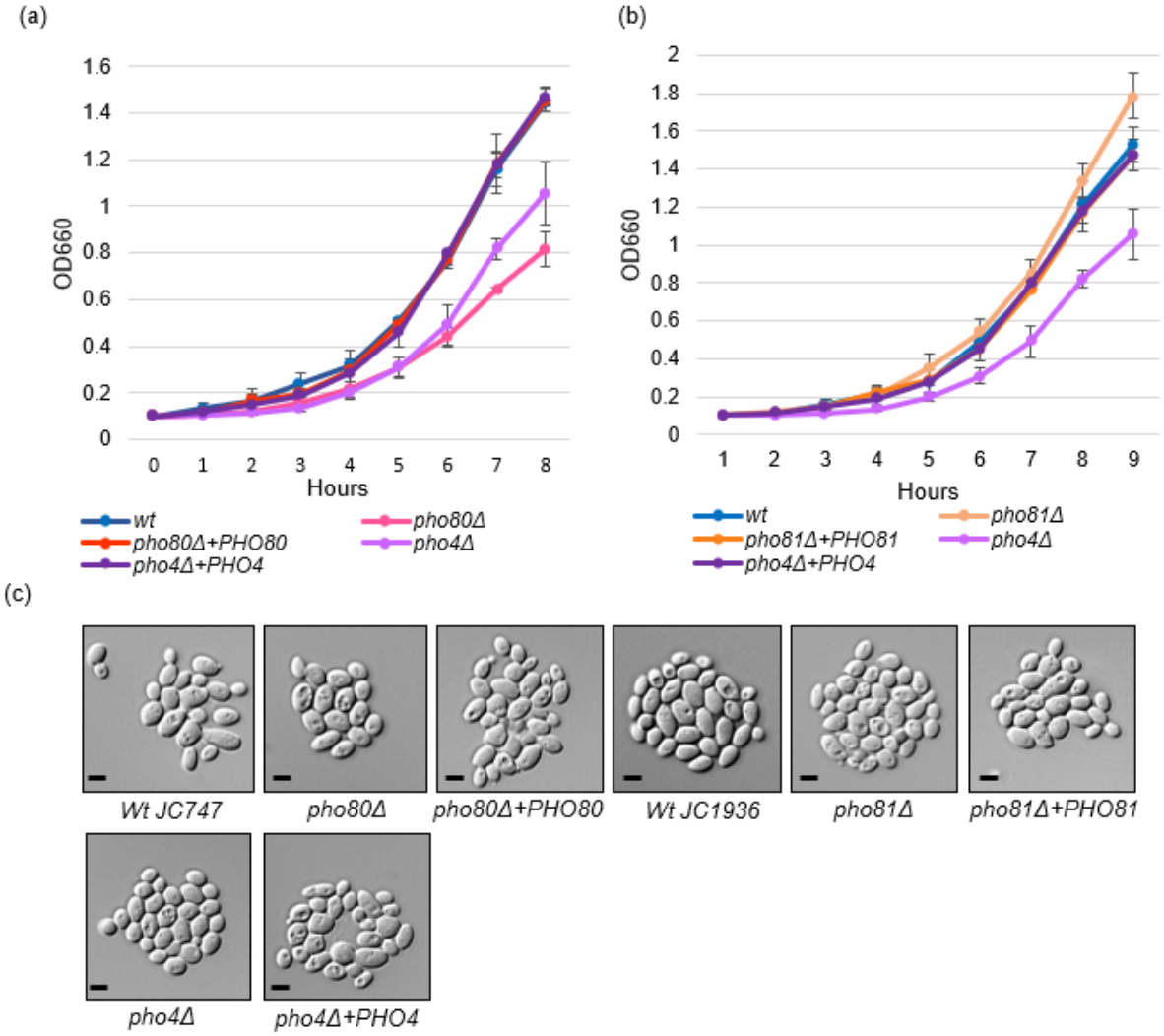

Figure 3.4. Cells lacking *PHO80* have a slow growth phenotype.
(a) Growth curve of *wt* JC747, *pho80Δ*, *pho80Δ+PHO80*, *pho4Δ* and *pho4Δ+PHO4* grown in YPD for 8 hours. N=3. Error bars show SEM. **(b)** Growth curve of *wt* JC1936 *pho81Δ*, *pho81Δ+PHO81, pho4Δ* and *pho4Δ+PHO4* grown in YPD for 8 hours. N=3. Error bars show SEM. **(c)** Cells were grown to mid-log phase before being fixed with paraformaldehyde. DIC images using a 63X objective were taken on a Zeiss Axio microscope. Scale bar = 10 µM. N=3.

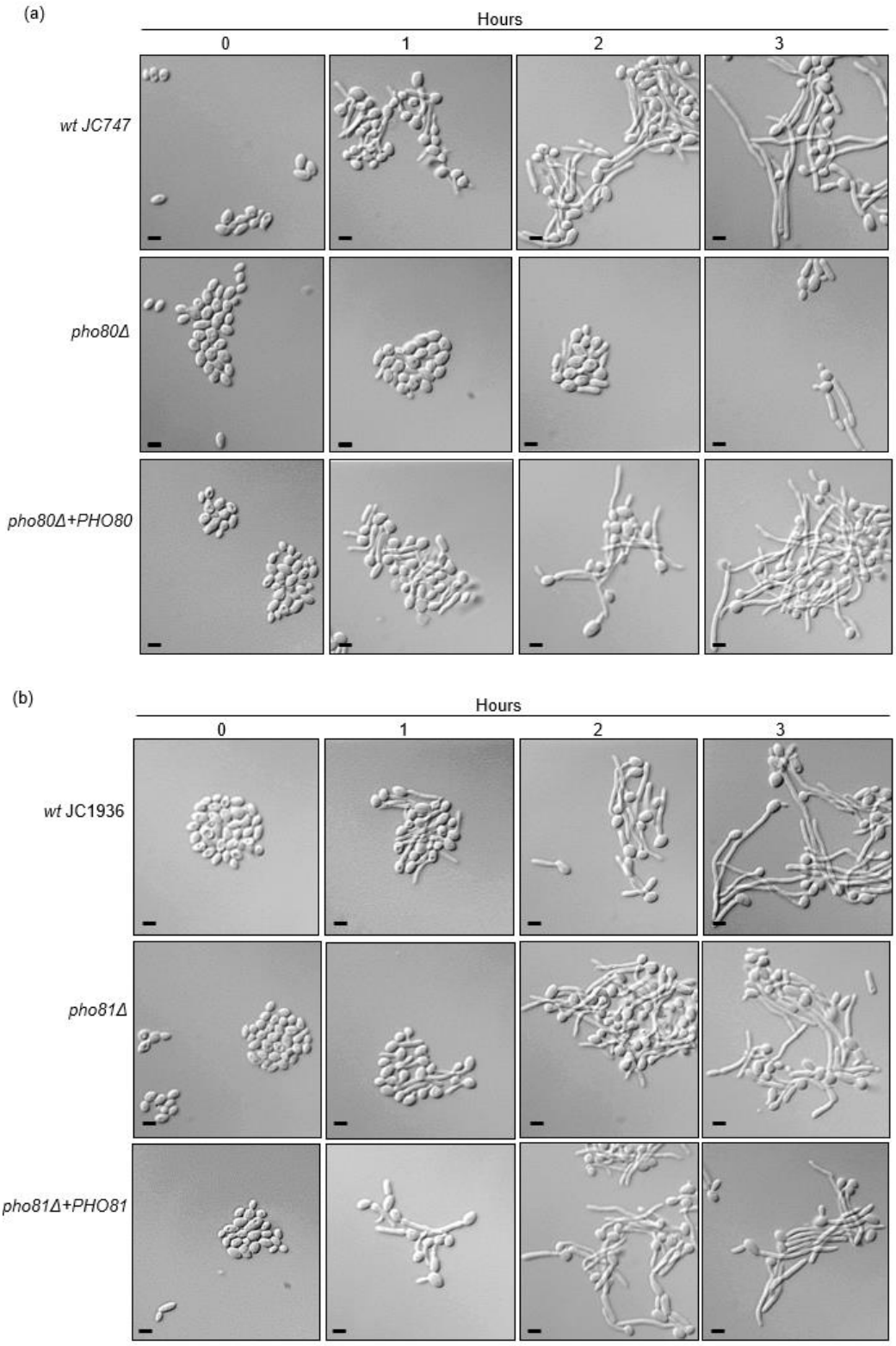

Figure 3.5. Investigating the yeast-hyphae switch in cells lacking *PHO80* and *PHO81*.
(a)(b) Overnight cultures were diluted back 1/10 into YPD supplemented with 10% FCS and incubated for 3 hours at 180 rpm at 37^0C. At each hourly time point, samples were taken, and cells were fixed with paraformaldehyde. DIC images were captured at 63X objective on a Zeiss Axio microscope. Scale bar = 10 µM. N =3.

3.2.1.2 PHO pathway regulation is impacted by the deletion of PHO80 or PHO81

In *S. cerevisiae,* under low Pi conditions, the CDK inhibitor Pho81 inhibits the Pho85-Pho80 CDK complex, allowing for an accumulation of unphosphorylated Pho4 which can accumulate in the nucleus and up-regulate genes involved in Pi acquisition such as secreted acid phosphatases. A colorimetric assay to detect secreted acid phosphatase production (To *et al*., 1973), has been used successfully in *C. albicans* as a readout of PHO pathway activation (Ikeh *et al*., 2016). Briefly, strains are spotted onto Pi limiting PNMC (Peptone, NaCl, $MgSO_4$, $CaCl_2$) media, supplemented or not with 10 mM Pi. Colonies are allowed to grow overnight, then the plates were subjected to an overlay of soft agar containing a Pi substrate and dye. The presence of secreted acid phosphatase activity is confirmed if the colonies stain a dark red. Consistent with previous findings (Ikeh *et al*., 2016), wild type cells produce secreted acid phosphatases following Pi starvation and this is dependent on Pho4 (Figure 3.6.a).

If, as seen in *S. cerevisiae*, Pho80 functions to inhibit Pho4 in *C. albicans* via promoting CDK-mediated phosphorylation, then constitutive activation of Pho4 is predicted in cells lacking *PHO80.* Consistent with this, *C. albicans* cells lacking *PHO80* stained dark red under both Pi replete and limiting conditions which is indicative of the constitutive production of secreted acid phosphatases (Figure 3.6.a). Thus, this indicates that Pho80 functions to negatively regulate Pho4 in *C. albicans*. With regard to the CDK inhibitor Pho81, if this positively regulates Pho4 by inhibiting the Pho85-Pho80 CDK complex, as in *S. cerevisiae,* then the opposite result is expected. Specifically, *C. albicans* cells lacking *PHO81* would be predicted to have no detectable secreted phosphatase activity and thus behave similarly to the *pho4Δ* mutant. Surprisingly, however, cells lacking *PHO81* were also observed to constitutively produce secreted acid phosphatases in both Pi replete and depleted conditions (Figure 3.6.a). This suggest that, rather than preventing Pho4 activation, loss of *PHO81* results in the constitution activation of Pho4, albeit not to the same extent as that seen upon loss of *PHO80*. This indicates that Pho81 differentially regulates the PHO pathway in *S. cerevisiae* and *C. albicans,* in that it functions as an activator of Pho4 in *S. cerevisiae* but an inhibitor of Pho4 activation in *C. albicans*.

To further investigate the role played by Pho80 and Pho81 in PHO pathway regulation *in C. albicans*, Pho4 nuclear accumulation was investigated in cells lacking *PHO80* and *PHO81*. Strains were constructed in which cells lacking *PHO80* or *PHO81* expressed a Pho4-GFP

fusion protein. Cells were fixed following 16 hours Pi starvation and following an additional 2 hours grown in the presence of 10 mM Pi, and the nuclear accumulation of Pho4-GFP determined by fluorescence microscopy. In wild type cells, Pho4 accumulates in the nucleus following 16 hours Pi starvation, as previously described (Ikeh *et al*., 2016) (Figure 3.6.b). In wild type cells following 16 hours Pi starvation there appears to be more Pho4 in the nucleus compared to elsewhere in the cell where lower levels of Pho4-GFP can still be observed (Figure 3.6.b). This will be referred to as nuclear accumulation throughout. Cells lacking *PHO80* appear to have diminished levels of Pho4-GFP, and thus the exposure time was doubled to allow visualisation of Pho4-GFP. However, despite the constitutive production of secreted acid phosphatases, Pho4 localisation in this strain appeared similar to that seen in wild type cells, in that nuclear accumulation was evident under Pi starvation but not Pi replete conditions (Figure 3.6.b). This is unlike the reported in *S. cerevisiae* where Pho4 in *pho80Δ* cells was shown to be constitutively nuclear (Kaffman *et al*., 1994). Thus, why there is secreted acid phosphatase activity in *pho80Δ* cells under Pi replete conditions is unclear. For cells lacking *PHO81*, Pho4 nuclear accumulation was evident following Pi starvation (Figure 3.6.b). However, unlike wild type and *pho80Δ* cells during Pi replete conditions, some Pho4 accumulation in the nucleus is evident in *pho81Δ* cells, in addition to some distinct puncta outside of the nucleus (Figure 3.6.b). This is consistent with the expression of secreted acid phosphatases under Pi replete conditions, that is further increased following Pi starvation (Fig. 3.6.a)

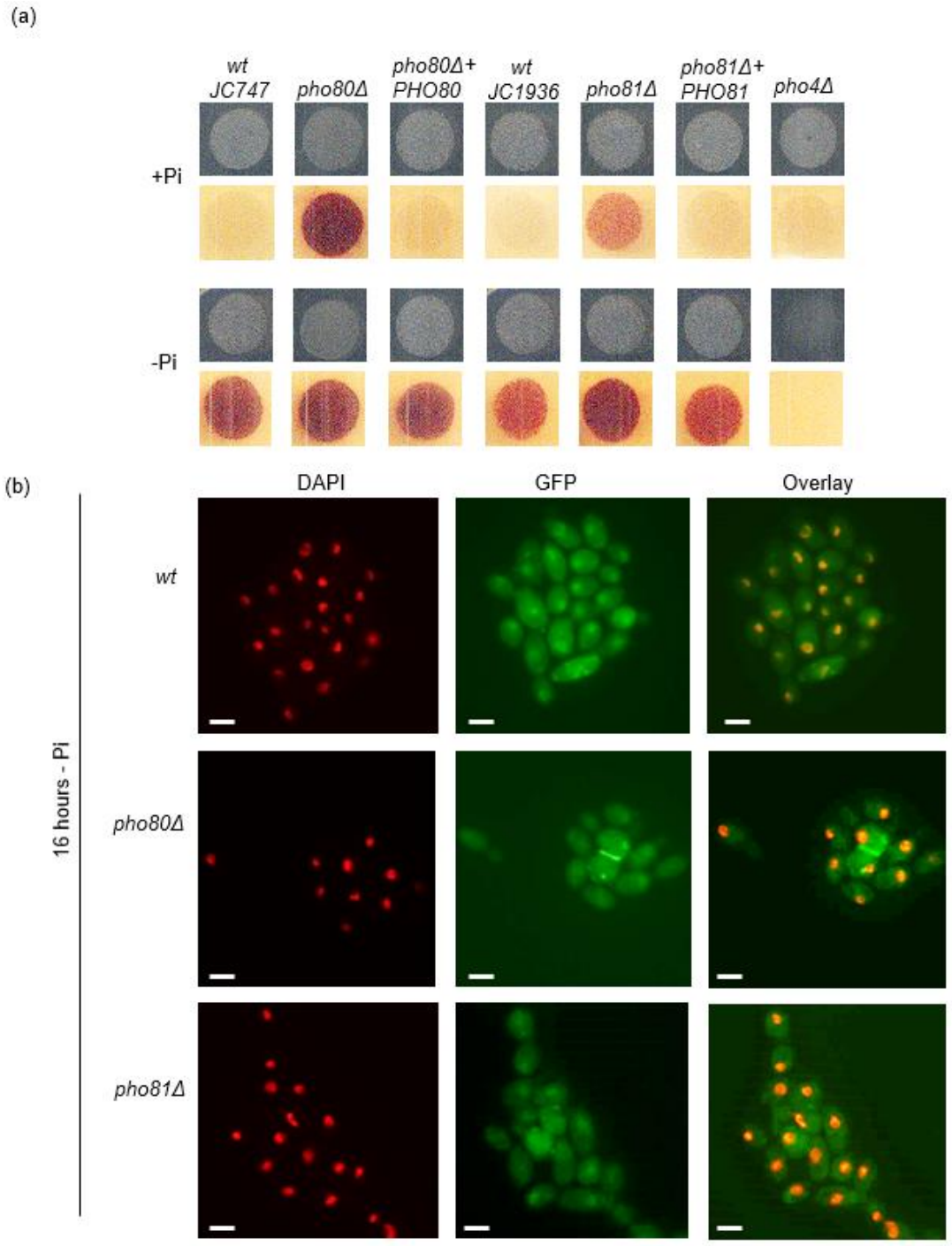
(a)
wt JC747
pho80Δ
pho80Δ+ PHO80
wt JC1936
pho81Δ
pho81Δ+ PHO81
pho4Δ
+Pi
-Pi
(b)
DAPI
GFP
Overlay
16 hours - Pi
wt
pho80Δ
pho81Δ

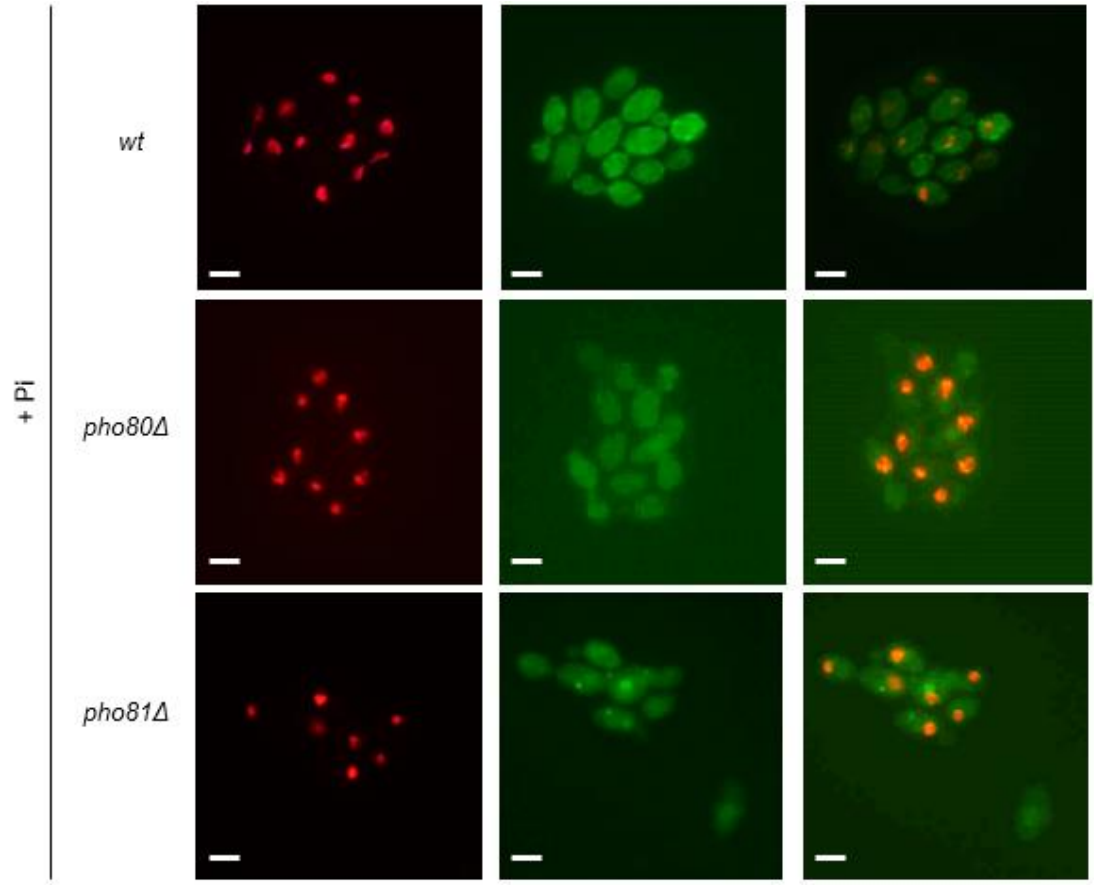

Figure 3.6. Deletion of *PHO80* or *PHO81* impacts on PHO pathway regulation.
(a) Cells were grown to mid-log before being diluted back to an OD660=0.5 and spotted onto PNMC plates (**P**eptone, **N**aCl, **M**gSO_4, **C**aCl_2) with plus or minus 10 mM Pi. Plates were then incubated for 24 hours at 30^0C. Soft agar containing I-napthyl-phosphate and Fast blue salt was poured over plates and incubated at 30^0C for 30 minutes. Red staining of colonies indicates presence of secreted acid phosphatase activity. N=3. **(b)** *wt*, *pho80Δ* and *pho81Δ* cells expressing Pho4-GFP were grown in YPD-Pi for 16 hours before being fixed with paraformaldehyde (-Pi), or for a further 2 hours in the presence of 10 mM Pi (+Pi) before being fixed. Images were captured on a fluorescent microscope with a 63X objective. Nuclear staining by DAPI is represented by the colour red and GFP by the colour green. Scale bar = 10 µM. N=2.

3.2.1.3 Deletion of PHO80 or PHO81 disrupts Pi homeostasis

Intracellular Pi is stored as polyphosphate (polyP), linear chains of inorganic Pi molecules joined with high energy phosphoanhydride bonds (Moreno and Docampo, 2013). Previously, it had been reported that deletion of Pho4 in *C. albicans* significantly impairs Pi homeostasis in the cell, hallmarked by no detectable polyP and low intracellular Pi levels (Ikeh *et al*., 2016). To examine if Pho80 and Pho81 regulate Pi homeostasis, the levels of polyP in cells lacking *PHO80* and *PHO81* were investigated. PolyP was extracted, subjected to electrophoresis on urea-polyacrylamide gels, and visualised with the metachromatic dye

toluidine blue (Smith and Morrissey, 2007). Loss of either *PHO80* or *PHO81* was found to lead to higher levels of polyP compared to wild type cells as indicated by the darker staining (Figure 3.7.a). Loss of Pho81 in particular resulted in increased levels of polyP (Figure 3.7.a.)

To address whether total cellular Pi levels were impacted in *pho80Δ* or *pho81Δ* cells, whole cell digests were analysed by inductively coupled mass spectrometry (ICP-MS) to measure intracellular Pi levels. Complementary to the increase in polyP levels (Figure 3.7.a), a significant increase in intracellular Pi was seen in both *pho80Δ* and *pho81Δ* mutants (Figure 3.7.b). Taken together, these results indicate that deletion of *PHO80* or *PHO81* positively impacts on the PHO pathway, resulting in increased total cellular Pi and polyP levels and the constitutive production of secreted acid phosphatases (Figure 3.6.a). In *S. cerevisiae*, *PHO80* loss has similarly been shown to lead to higher cellular Pi levels (Rosenfeld *et al*., 2010).

C. albicans cells lacking Pho4 also have significantly reduced levels of magnesium (Ikeh *et al*., 2016). The opposite was found for cells lacking Pho80 and Pho81 with both having increased levels of magnesium compared to wild type cells (Figure 3.7.c). The increase in magnesium in *pho80Δ* and *pho81Δ* cells could be underpinned by the high levels of Pi in these strains as Pi and magnesium are commonly found in complexes together (Pontes and Groisman, 2018). It has also been shown previously, that Pho4 mediated production of polyP regulates manganese levels as polyP function as a manganese storage reservoir in *C. albicans* (Ikeh *et al*., 2016). As cells lacking Pho80 or Pho81 have more polyP than wild type cells (Figure 3.7.a), it could be speculated that *pho80Δ* or *pho81Δ* cells may have higher levels of manganese. However, this was not found to be the case with *pho81Δ* and *pho8OΔ* cells displaying very small differences compared to wild type cells (Figure 3.7.c).

Collectively, the results of figures 3.6 and 3.7 are consistent with the hypothesis that Pho81 regulation of the Pho80-Pho85 CDK complex differs between *S. cerevisiae* and *C. albicans*. A key question is why does loss of the CDK inhibitor Pho81 result in activation of the PHO pathway in *C. albicans*?

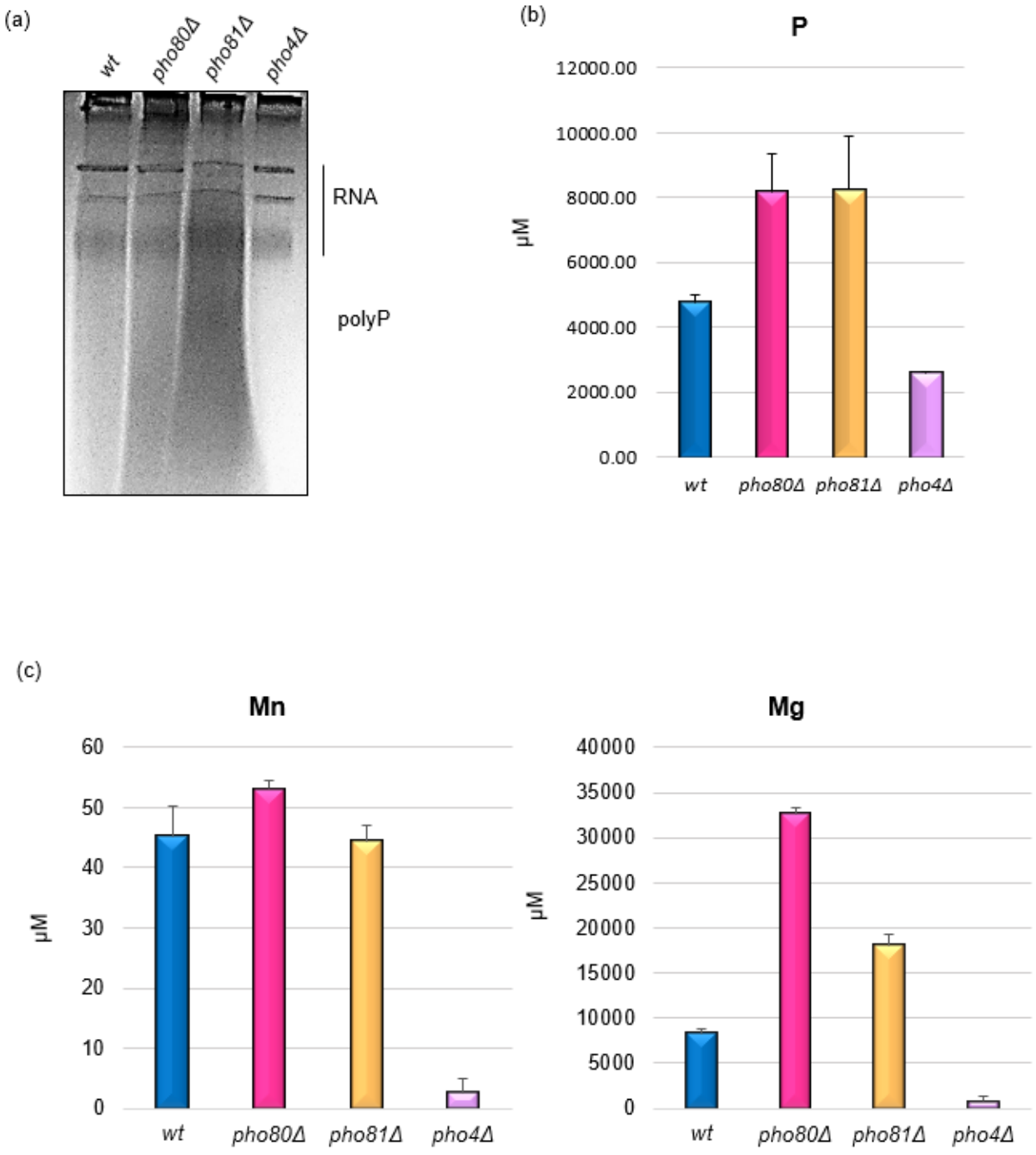

Figure 3.7. Phosphate homeostasis is affected in *pho80Δ and pho81Δ* cells.
(a) 15% UREA-Page gel of RNA extracts from *wt, pho80Δ, pho81Δ* and *pho4* cells, 20µg of RNA was loaded per sample. Gels were stained with 0.05% toluidine blue. N=2. **(b)(c)** Whole cell extracts of *wt, pho80Δ, pho81Δ* and *pho4* cells grown to mid-log in YPD. Extracts were digested in triplicate with nitric acid and analysed by ICP-MS. Errors bars represent SEM. N=3.

3.2.1.4 Investigating whether cells lacking PHO80 or PHO81 are resistant to Pho4 mediated stress responses

In *C. albicans*, Pho4 has been shown to be essential for resistance to a pleiotropy of stress-inducing agents alongside its role in mediating growth under Pi limiting conditions (Ikeh *et al*., 2016; Urrialde *et al*., 2016). In contrast, *S. cerevisiae* Pho4 has only been reported to mediate the response to Pi starvation and alkaline stress. Given the impact of *PHO80* and *PHO81* loss on PHO pathway regulation and increase in intracellular Pi levels, stress resistant phenotypes of *pho80Δ* and *pho81Δ* cells were examined. To investigate this, spot tests were performed on plates containing alkaline, cationic, superoxide and metal stresses. Cells lacking *PHO81* showed slightly increased levels of resistance compared to wild type cells to alkaline, cationic and superoxide stress, imposed pH8, NaCl and menadione, respectively (Figure 3.8). This further illustrates the divergence between Pho4 regulation in *S. cerevisiae* and *C. albicans* as cells lacking *PHO81* in *S. cerevisiae* are sensitive to alkaline stress similar to cells lacking *PHO4* (Serrano *et al*., 2002). It has been suggested that the sensitivity of *C. albicans pho4Δ* cells to alkaline, cationic and superoxide stress could be underpinned by lower intracellular Pi levels in these cells (Ikeh *et al*., 2016). Therefore, the slight increase in resistance of cells lacking *PHO81* to stresses shown in figure 3.8 may be due to higher levels of intracellular Pi in this strain. Although cells lacking *PHO80* also have high levels of intracellular Pi, the strain did not grow very well on any of the spot test plates (Figure 3.8). However, given the dramatic growth defect in cells lacking *PHO80* (Figure 3.8), it is unclear whether this strain differs in its relative sensitivity to cationic, alkaline, metal and superoxide stress.

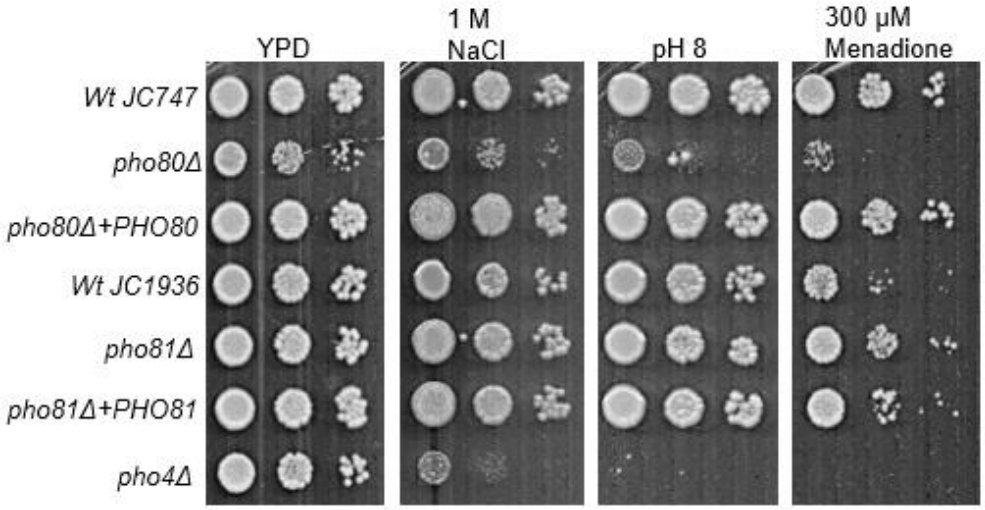

Figure 3.8. The effect of deleting PHO pathway components on *C. albicans* Pho4 mediated stress responses. Mid-log cells were spotted in serial dilutions onto YPD plates containing 1 M NaCL, 300 µM menadione, as well as onto YPD adjusted to pH 8. Plates were incubated at 30^0C for 24 hours. N=3.

3.2.1.5 Investigating Pho4 levels in cells lacking PHO80 and PHO81

The aforementioned results indicate a role for both the cyclin Pho80 and the cyclin dependent kinase inhibitor Pho81 in PHO pathway regulation in *C. albicans.* Thus, Pho4 phosphorylation in cells lacking *PHO80* and *PHO81* compared to wild type cells was investigated. This was achieved by generating *pho80Δ* and *pho81Δ* strains expressing Pho4 tagged with two myc epitopes (Pho4-MH). Whole cell extracts were collected, and subjected to western blotting, to determine Pho4 levels and mobility in *pho80Δ* and *pho81Δ* strains. Interestingly, when grown to mid-logarithmic phase in YPD, in cells lacking *PHO80* Pho4 was found to have a slower mobility than in wild type cells under Pi replete conditions (Figure 3.9.a). If Pho80 functions with Pho85 to phosphorylate Pho4 in Pi replete conditions, as in *S. cerevisiae*, it would be expected that Pho4 would be less phosphorylated and have a faster mobility in *pho80Δ* cells compared to wild type cells. Therefore, the result shown in figure 3.9.a was unexpected. However, it should be noted that it is not known if the difference in mobilisation here is due to phosphorylation, and Pho4 is subjected to a phosphorylation-independent modification (Ikeh *et al*., 2016). For cells lacking *PHO81*, whilst the mobility of Pho4 looked similar to that in wild type cells, there appeared to be significantly greater levels of Pho4 present in this mutant (Figure 3.9.a,b).

To determine whether the mobility or levels of Pho4 changed upon Pi starvation, strains were grown in YPD-Pi for 16 hours, pellets were then collected and to the remaining culture

10 mM Pi was added and cells were grown for a further 2 hours prior to harvesting. In wild type cells, the mobility of Pho4-MH appears to be greater in Pi starvation conditions than in Pi replete (Figure 3.9.c). Surprisingly, levels of Pho4 in *pho80Δ* cells appeared to be almost abolished in minus Pi conditions (Figure 3.9.c). This may underlie the weaker fluorescence exhibited by Pho4-GFP in *pho80Δ* cells (Figure 3.6). It is also noteworthy that the mobility of Pho4-MH in wild type cells after Pi starvation is the same as *pho80Δ* cells under Pi replete conditions (Figure 3.9.c). In cells lacking *PHO81*, a double band was observed under Pi starvation conditions, although a reduction in Pho4 levels was again evident (as in *pho80Δ* cells) compared to wild type cells. However, the reduction in Pho4 levels in *pho81Δ* cells compared to wild type was not found to be significant (Figure 3.6.d). Similar to that shown in Figure 3.9.a, there was a significant increase in Pho4 under Pi replete conditions in *pho81Δ* cells compared to wild type cells (Figure 3.9.c,d). This increased amount of Pho4 in *pho81Δ* cells may drive Pho4-mediated responses under Pi replete conditions, possibly explaining the constitutive production of secreted acid phosphatases (Figure 3.6.a). However, this is not seen in cells lacking Pho80 which also have constitutive production of secreted acid phosphatases in cells lacking Pho80 (Figure 3.6.) yet have no increase in Pho4 levels (Figure 3.9).

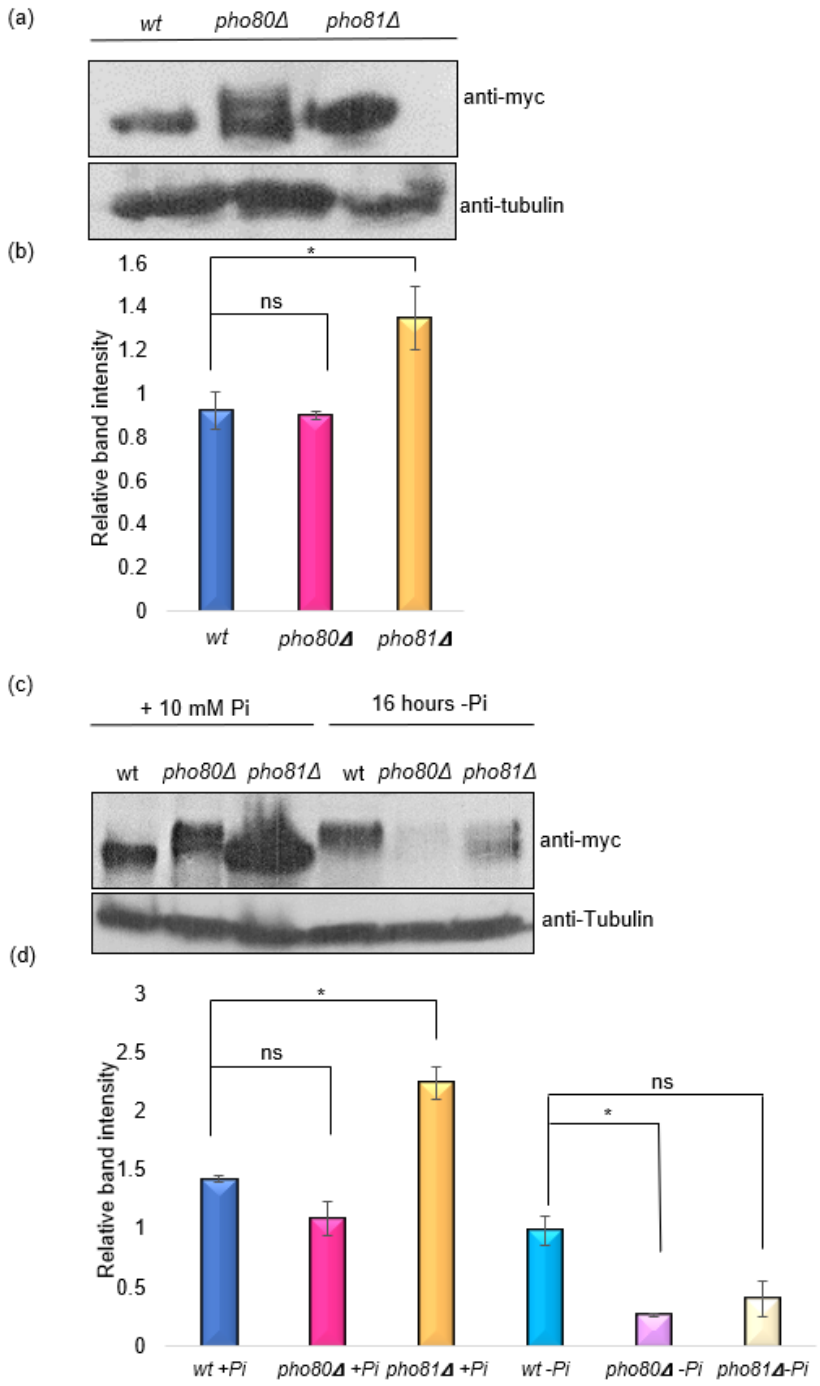

Figure 3.9. Pho4 mobility and protein levels in *pho80Δ* and *pho81Δ* cells in Pi +/- conditions compared to wild type cells.
(a) Whole cell extracts were collected for *wt*, *pho80Δ*, and *pho81Δ* cells all expressing Pho4-MH and analysed by western blotting with an anti-Myc antibody. An anti-tubulin antibody was used as a loading control. **(b)** The band intensity of Pho4-MH was quantified using ImageJ and normalised to the loading control. Errors bars represent SEM. N=3. Statistical analysis was performed using student's two sample t-test: *, P<0.05. **(C)** Whole cell extracts were collected following 16 hours Pi starvation and after a further 2 hours in the presence of 10 mM Pi before whole cell extracts were collected and analysed by western blotting as in **(a)**. **(d)** The band intensity of Pho4-MH was quantified using ImageJ and normalised to the loading control. Errors bars represent SEM. N=3. Statistical analysis was performed using student's two sample t-test: *, P<0.05; ns, not significant.

3.2.1.6 Investigation into whether Pho80 and Pho81 are required for virulence

To investigate the role of Pho80 and Pho81 in *C. albicans* virulence, a *Galleria mellonella* larvae systemic infection model was used. This model has been employed successfully to test the virulence of several different fungal species (Borman *et al*., 2016; Jemel *et al*., 2020). Previous work has shown the Pho4 is needed for virulence in both a *Caenorhabditis elegans* and a systemic murine model (Ikeh *et al*., 2016). However, whether Pi homeostasis mediated by Pho4 is required for virulence in G. mellonella had not been tested. Thus, this was investigated first. Briefly, for each strain n=15 larvae were assigned, these were of similar size and considered healthy due to an absence of melanisation. Larvae were injected in the left hind-limb with a cell suspension of mid-log 5 x 10^5 *C. albicans* cells in PBS. A control group of n=15 larvae were injected with PBS only. Infected larvae were then incubated at 37^0C with daily checks for survival. Larvae were considered deceased when no movement was observed, this usually occurred in conjunction with melanisation. Cells lacking *PHO4* were found to be avirulent in this infection model as no larvae injected with *pho4Δ* cells died, in contrast to wild type cells in which all larvae were deceased by day 2 of infection ($p<0.001$) (Figure 3.10.a). The reconstitution of *pho4Δ* cells with *PHO4* led to no significant difference in survival times when compared to wild type cells (figure 3.10.a). This illustrates that Pho4 is important for virulence in this model of infection.

Cells lacking *PHO80* were similarly observed to cause no infection in *G. mellonella*, compared to wild type cells, in which all larvae were deceased by day 2 of infection ($p<0.001$) (Figure 3.10.c). There was no significant difference observed between wild type and *pho80Δ+PHO80* (Figure 3.10.c). There was also no significant difference in the ability to establish an infection between wild type and *pho81Δ* cells (Figure 3.10.b). Nor was there any difference observed between either wild type strain background JC747 and JC1936 with both leading to 100% fatality by day 2 (Figure 3.10). Collectively, these data indicate that loss of Pho81 does not impact on *C. albicans* virulence in this infection model, in contrast to Pho80. However, the data indicating a role for Pho80 in virulence may be related to the extremely impaired growth of the *pho80Δ* mutant.

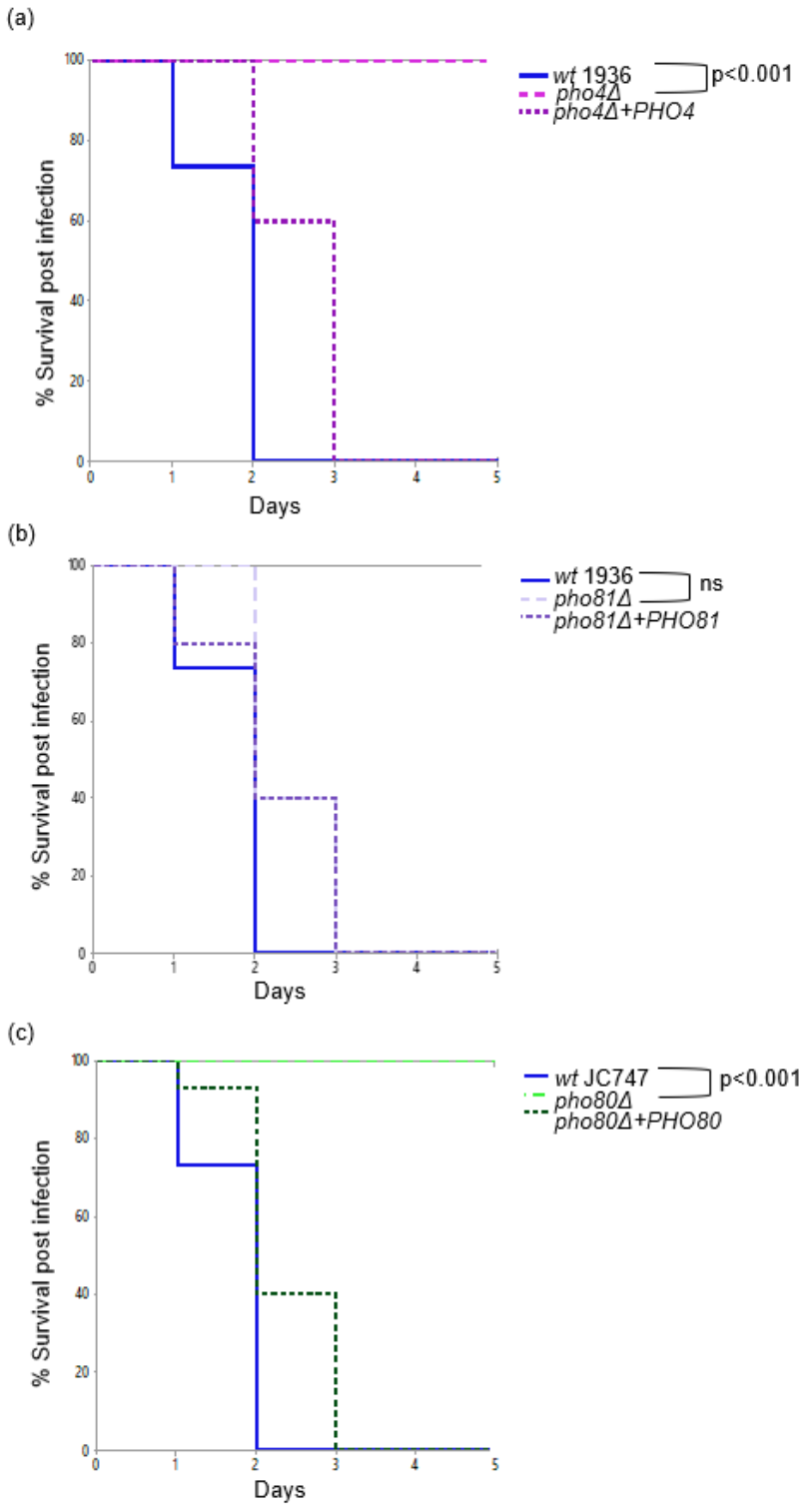

Figure 3.10. Virulence analysis of *pho4Δ*, *pho80Δ* and *pho81Δ* strains in *G. mellonella*. **(a)(b)(c)** For each indicated strain, the left hind leg of 15 larvae was injected with 5 X 10^5 *C. albican*s cells in PBS. An additional 15 larvae were injected with only PBS as a control. Survival was monitored daily. Analysis was performed using a log-rank test with a P value <0.05 considered significant. The graph is a representative of one of three biological repeats.

3.2.2 Investigation into Pho4 regulation by the Ubp3 deubiquitinating enzyme

Previous work found the presence of an uncharacterised PTM on Pho4 which is present in Pi replete conditions but absent following Pi starvation (Ikeh, 2015). This raises the possibility that such a modification must be lost for the nuclear accumulation and activation of Pho4 to occur. Interestingly, in *S. cerevisiae* it has been reported that the deubiquitinating enzyme Ubp3 plays a role in regulating the PHO pathway (Isasa *et al*., 2015), and over-expression of Ubp3 results in the constitutive nuclear accumulation of Pho4 (Isasa *et al*., 2015). Collectively, these results suggest that ubiquitin could be a potential candidate for the uncharacterised PTM seen on *C. albicans* Pho4 in Pi replete conditions with Ubp3 playing a key role in regulating the ubiquitylation status of Pho4. To investigate this, a strain lacking *UBP3* was required. A putative homologue was identified in *C. albicans* (C6_00170C-A) which has 34.4% homology to *UBP3* in *S. cerevisiae*. A homozygous *ubp3Δ* strain was created by replacing the *UBP3* ORF with the auxotrophic markers *ARG4* and *HIS1*.

To begin investigating whether Upb3 was playing a role in PHO pathway regulation, cells lacking *UBP3* were spotted onto plates containing stresses that require Pho4 for resistance. It was rationalised that if Ubp3 was regulating the removal of ubiquitin from Pho4, allowing it to accumulate in the nucleus, then deletion of *UBP3* may prevent Pho4 activation leading to similar stress sensitivities as *pho4Δ* cells. However, *ubp3Δ* cells were found to share none of the *pho4Δ* sensitivities to cationic, alkaline or superoxide stresses (Figure 3.11.a). Furthermore, cells lacking Ubp3 were able to grow similar to wild type on plates lacking Pi (Figure 3.11.a).

Pho4 levels in *ubp3Δ* cells were also investigated by generating a *ubp3Δ* mutant expressing myc-tagged Pho4. Cells were grown to mid-logarithmic phase prior to being harvested. Whole cell extracts were then prepared and underwent western blotting to examine Pho4 levels. As components of the PHO pathway, including Pho4, were shown to be down-regulated in *S. cerevisiae* cells lacking *UBP3* (Isasa *et al*., 2015), it was predicted that *ubp3Δ* cells in *C. albicans* would have lower Pho4 levels than wild type cells. Cells lacking *HOG1* expressing myc-tagged Pho4 were used as a control, as Pho4 levels have previously been shown to be significantly reduced in *hog1Δ* cells (Ikeh, 2015). However, there were no differences seen in Pho4 levels or mobility between wild type and *ubp3Δ* cells (Figure 3.9.b). Taken together, the results suggest that Ubp3 is not playing a significant role in PHO pathway regulation in *C. albicans*.

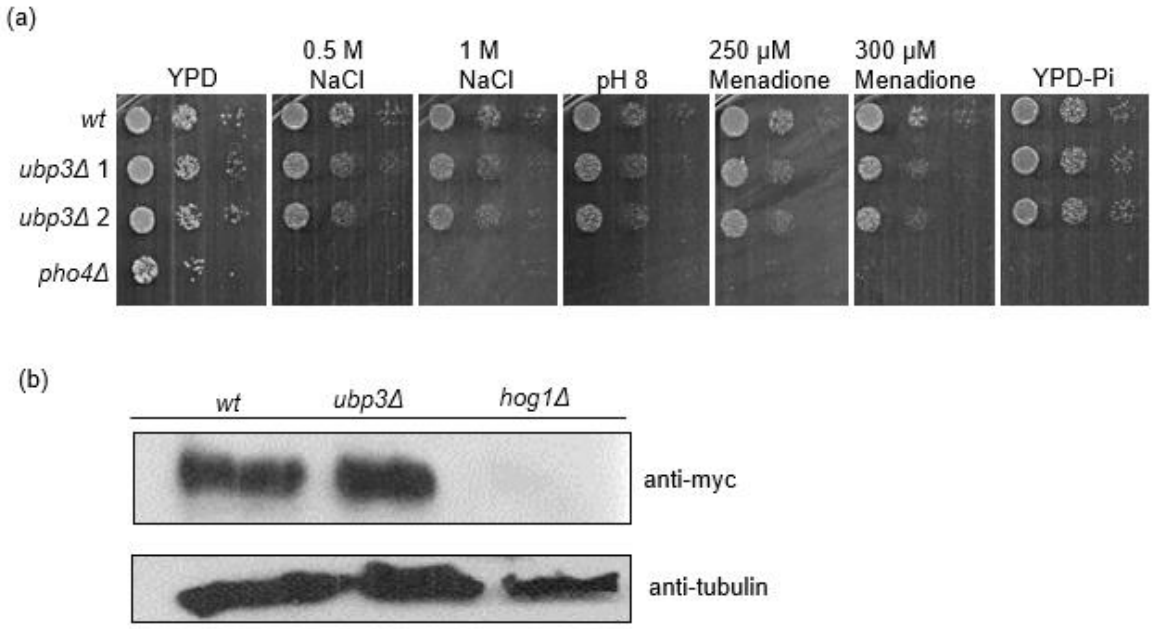

Figure 3.11. Stress phenotypes and Pho4 levels in cells lacking *UBP3*.
(a) Mid-log cells were spotted in serial dilutions onto YPD plates containing 0.5 M NaCl, 1 M NaCl, 250 µM menadione and 300 µM menadione as well as onto YPD pH 8 and YPD-Pi media. Plates were incubated at 30^0C for 24 hours. N=3. **(b)** Whole cell extracts were prepared from *wt*, *ubp3Δ* and *hog1Δ* cells all expressing Pho4-MH and analysed by western blotting with an anti-Myc antibody to detect Pho4-MH, and an anti-tubulin antibody was used as a loading control. N=2.

3.2.3 Investigating the role of inositol polyphosphates in PHO pathway regulation in C. albicans

3.2.3.1 PHO pathway activation in strains lacking KCS1 and VIP1

As described in the introduction (Section 1.9), IP_7 inositol polyphosphate molecules have been shown to bind to SPX domains located on key PHO pathway components, such as Pho81 and Vtc4 (Wild *et al*., 2016). This has led to the hypothesis that IP_7 molecules are the sentinels of cellular Pi levels and play a central role in regulating Pi homeostasis. Furthermore, in *S. cerevisiae* and *C. neoformans*, depletion of IP_7 levels impact on a range of cellular process and lead to a variety of stress sensitivities (Dubois *et al*., 2002; Lev *et al*., 2015). IP_7 can be synthesised from IP_6 and is carried out by either Vip1 or Kcs1 enzymes, generating 1-IP_7 or 5-IP_7 respectively (Lonetti *et al*., 2011).

To identify Vip1 and Kcs1 in *C. albicans,* the amino acid sequences of the *S. cerevisiae* proteins were used to BLAST against the *C. albicans* genome database. This identified Vip1

(C5_00180W_A) and Kcs1 (CR_05260C_A) in *C. albicans,* with 41.4% and 12.7% identity to the respective *S. cerevisiae* proteins. However, sequence alignment indicated that C*. albicans* Vip1 lacked the diphosphoinositol pentakisphosphate kinase 2 N-terminal (PPI5K2_N) domain and a truncated RimK ATP-grasp (RimK) domain at its amino terminus, unlike Vip1 in *S. cerevisiae*. Subsequent analysis of the sequence 1 Kb upstream of the predicted Vip1 start site revealed that the start codon had been misannotated in the *C. albicans* genome database. Consequently, the re-annotated Vip1 sequence with a new start codon location revealed both a full RimK domain and PPI5K2_N domain (Figure 3.12). Moreover, there was a high degree of conservation between the three domains in Vip1 in *C. albicans* and *S. cerevisiae* (Figure 3.12). The identity between the full Vip1 protein in *C. albicans* and *S. cerevisiae* is 65%.

In contrast, there is very little conservation found between the sequences of Kcs1 in *C. albicans* and *S. cerevisiae* (Figure 3.13). However, this is largely due to an amino terminal extension in the *S. cerevisiae* protein of approximately 700 amino acids that is absent in *C. albicans* Kcs1, and there is a good degree of conservation in the inositol polyphosphate kinase (IPK) domain (Figure 3.13). Homozygous *vip1Δ* and *kcs1Δ* strains were made by replacing the *VIP1* or *KCS1* ORFs with the auxotrophic markers *ARG4* and *HIS1*.

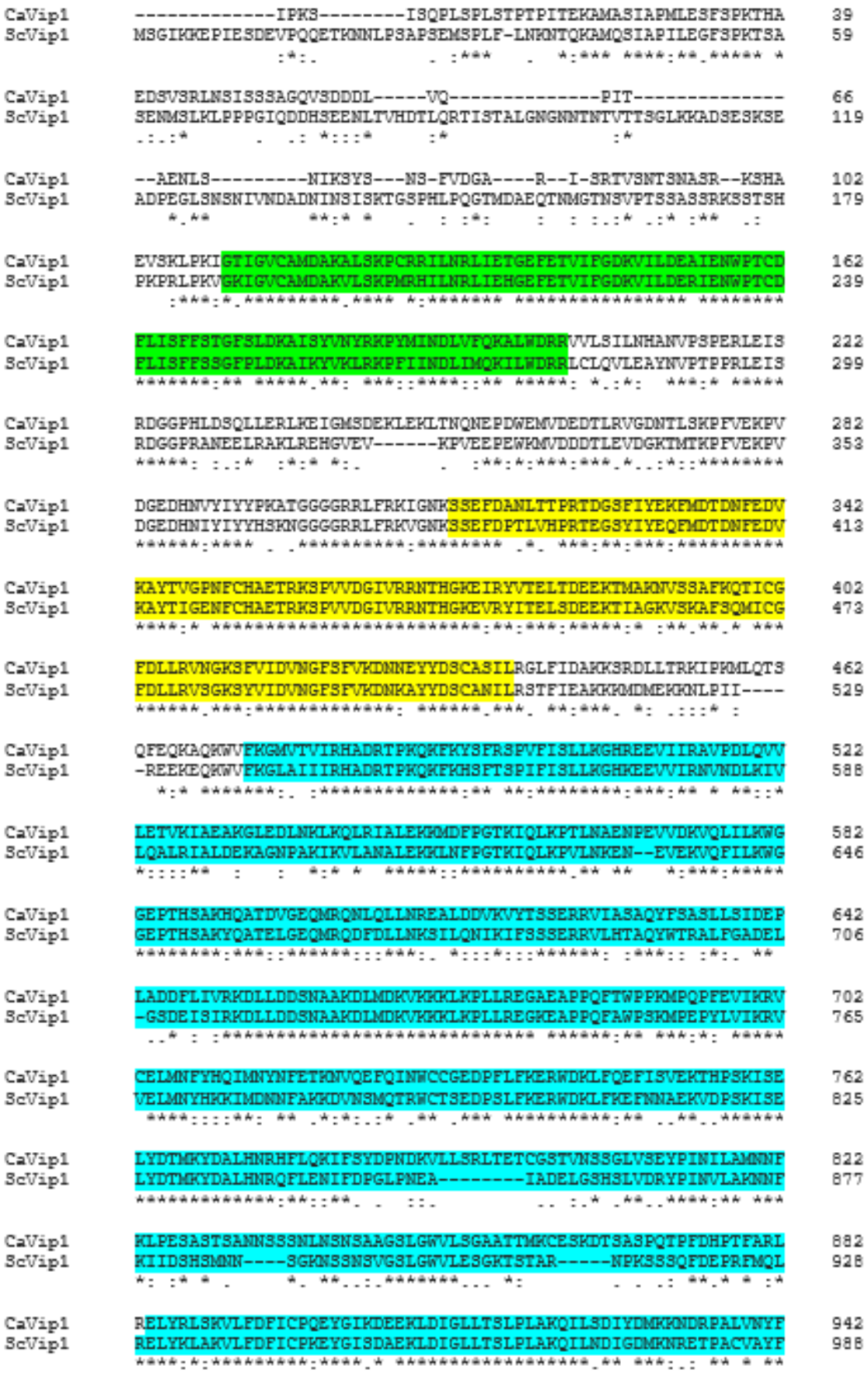

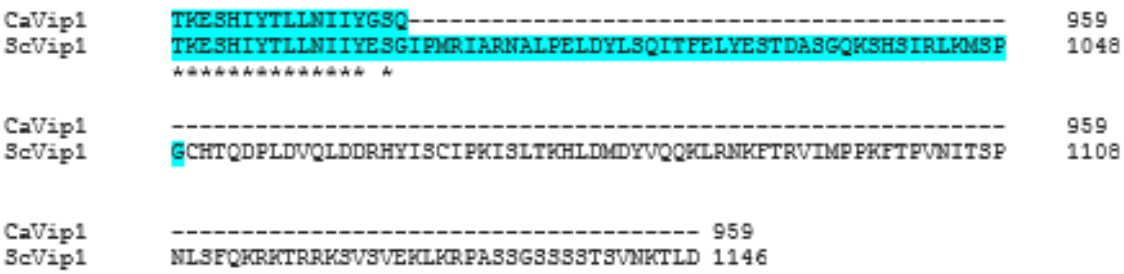

Figure 3.12. Alignment of *C. albicans* and *S. cerevisia*e Vip1 sequences.
Sequences of *C. albicans* (Ca) Vip1 and *S. cerevisiae* (Sc) Vip1 were aligned using ClustalW. Identical nucleotides found in both sequences are annotated with *. Gaps were introduced to maximise alignment these are indicated by dashes. PPIP5K_2 domain is shown in green, RimK domain is shown in yellow and His_Phos_2 domain is shown in blue.

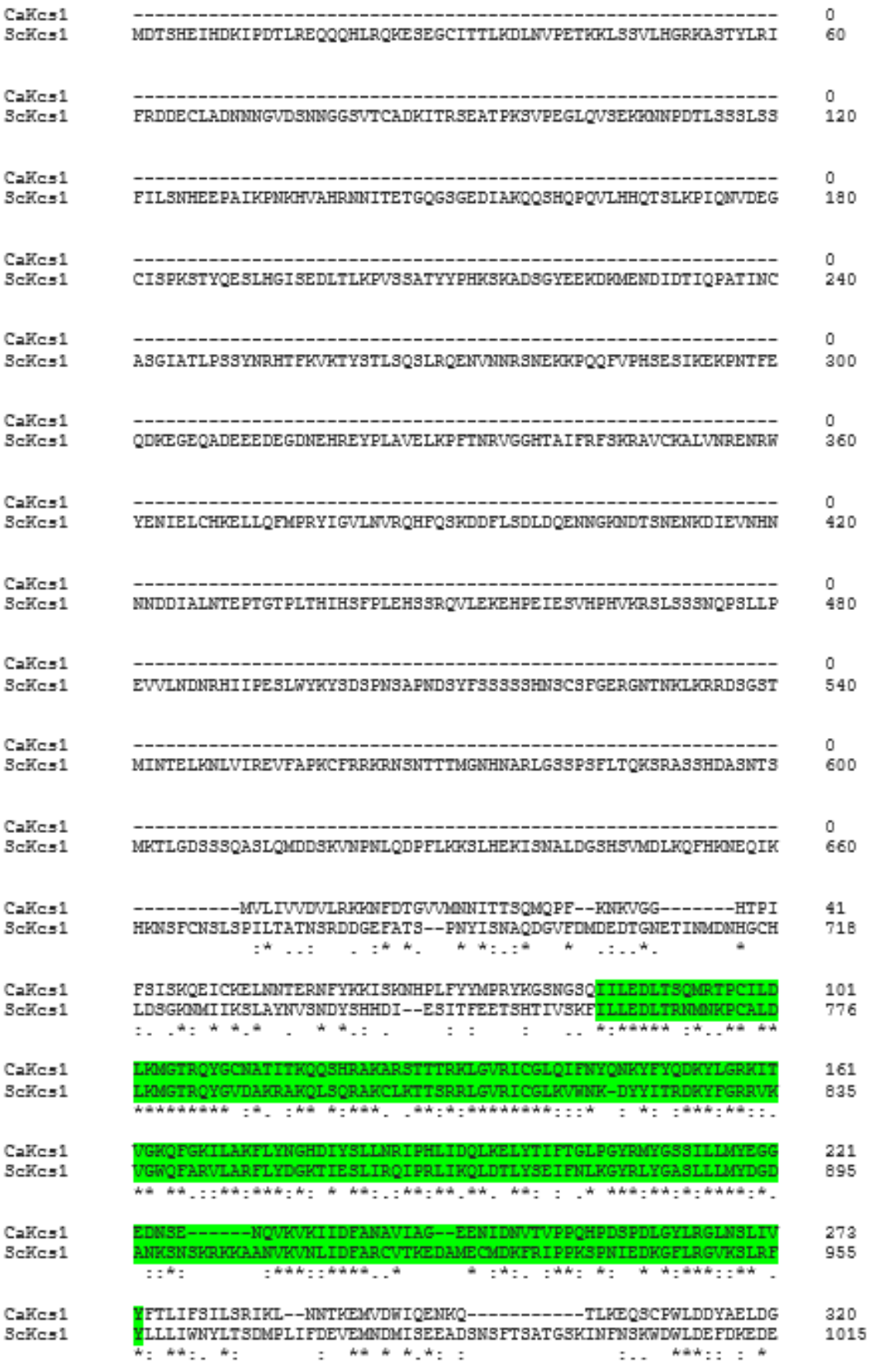

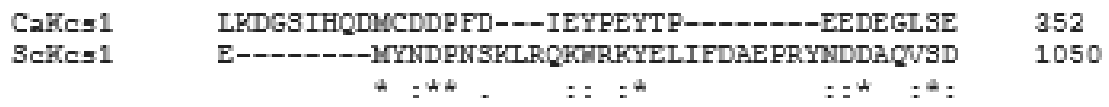

Figure 3.13. Alignment of *C. albicans* and *S. cerevisia*e Kcs1 sequences.
Sequences of *C. albicans* (Ca) Kcs1 and *S. cerevisiae* (Sc) Kcs1 were aligned using ClustalW. Identical nucleotides found in both sequences are annotated with *. Gaps were introduced to maximise alignment these are indicated by dashes. IPK domain is shown in green.

To initially investigate whether Kcs1 or Vip1 were playing a role in PHO pathway regulation in *C. albicans* cells, polyP was extracted from whole cells extracts and electrophoresed on urea-polyacrylamide gels and stained with toluidine blue. If either enzyme were playing a role in PHO pathway regulation, then polyP levels may either be increased compared to wild type cells or diminished as seen with *pho4Δ* cells. There was a modest increase in polyP levels in *kcs1Δ* cells compared to wild type cells (Figure 3.14.a). In cells lacking *VIP1,* a more dramatic increase in polyP levels was observed as well as the presence of longer, higher molecular weight, polyP chains compared to wild type cells (Figure 3.14.a). The reconstitution of either strain led to wild type polyP levels being restored (Figure 3.14.a).

The secreted acid phosphatase assay (To *et al*., 1973), was also employed to investigate whether either IP_7 generating enzyme played a role in PHO pathway regulation *in C. albicans*. As previously described, each strain was spotted onto a PNMC plate containing no Pi or in the presence of 10 mM Pi and then incubated overnight. Following overnight incubation for 16 hours, an overlay of soft agar containing a dye and Pi substrate were added. Secreted acid phosphatase activity was confirmed when colonies stained a dark red. There was no observable difference between either *kcs1Δ* and wild type cells under Pi replete or deplete conditions (Figure 3.14.b). However, in *vip1Δ* cells a decrease in secreted acid phosphatase activity following Pi starvation was seen, which was restored to wild type levels in the *vip1Δ+VIP1* reconstituted strain (Figure 3.14.b). Collectively, these results provide evidence that Kcs1, and in particular Vip1, may play a role Pi homeostasis and PHO pathway regulation in *C. albicans*.

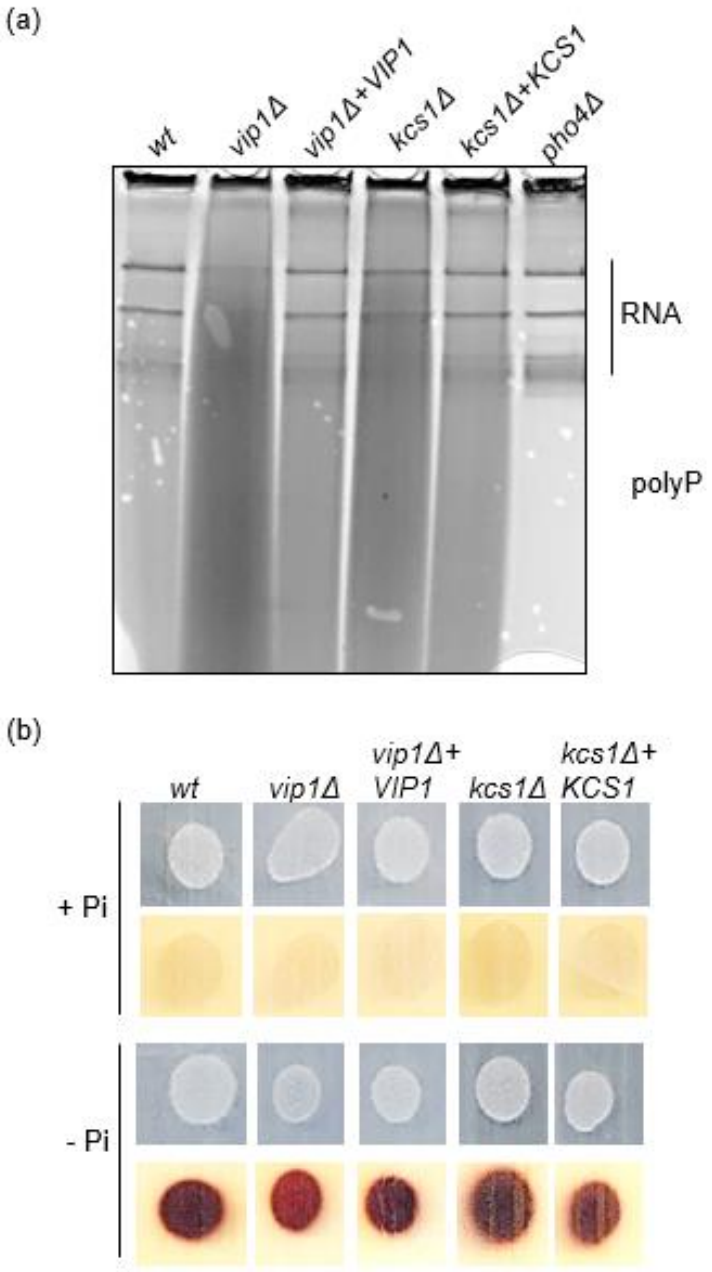

Figure 3.14. Investigating Pi homeostasis in cells lacking *KCS1* or *VIP1*.
(a) Poly P detection. 15% UREA-Page gel of RNA extracts from *wt, kcs1Δ, vip1Δ* and *pho4* cells, 20 μg of RNA was loaded per sample. Gels were stained with 0.05% toluidine blue. N=2
(b) Secreted acid phosphatase activity. Cells were grown to mid-log before being diluted back to an OD660=0.5 and spotted onto PNMC plates (**P**eptone, **N**aCl, **M**gSO_4, **C**aCl_2) with plus or minus 10 mM Pi. Plates were then incubated for 24 hours at 30^0C. Soft agar containing I-napthyl-phosphate and Fast blue salt was poured over plates and incubated at 30^0C for 30 minutes. Red staining of colonies indicates presence of secreted acid phosphatase activity. N=2.

3.2.3.2 Stress phenotypes of cells lacking KCS1 and VIP1

In *S. cerevisiae* and *C. neoformans* IP_7 generating enzymes have been linked to a pleiotropy of stress responses (Dubois *et al*., 2002; Lev *et al*., 2015). As Pho4 promotes resistance to multiple stresses in *C. albicans*, it was investigated whether Kcs1 or Vip1 played a role in mediating resistance to such stresses. In addition, osmotic, cell wall and oxidative stresses were also tested as, in *S. cerevisiae* and *C. neoformans,* cells lacking Kcs1 are sensitive to osmotic and cell wall stresses (Dubois *et al*., 2002; Lev *et al*., 2015), and *S. cerevisiae* cells lacking Kcs1 or Vip1 are resistant to H_2O_2 stress (Onnebo and Saiardi, 2009).

In contrast to *pho4Δ* cells, neither *kcs1Δ* or *vip1Δ* cells were sensitive to NaCl, pH 8 or menadione imposed stresses (Figure 3.15). Nor did either *kcs1Δ* or *vip1Δ* cells struggle to grow on YPD plates lacking Pi (Figure 3.15). However, in the presence of cell wall damaging agents, cells lacking Vip1 were sensitive to sodium dodecyl sulfate (SDS) and to calcofluor white which binds chitin, but not to congo red which binds β-1-3-glucan (Figure 3.15). Cells lacking Kcs1 also showed slight sensitivity to calcofluor white but not to any of the other stresses investigated (Figure 3.15). Reconstitution of *KCS1* and *VIP1* into the respective mutant strains, restored wild type levels of resistance to the cell-wall damaging agents (Figure 3.15). Cells lacking Vip1 appeared to be resistant to the oxidative stress, H_2O_2 compared to wild type cells (Figure 3.15), similar to that reported in *S. cerevisiae*. Taken together, these results suggest that whilst *C. albicans* Kcs1 and Vip1 do not contribute to Pho4 mediated stress resistance, some overlapping stress phenotypes with that reported in analogous *S. cerevisiae* and *C. neoformans* mutants are conserved.

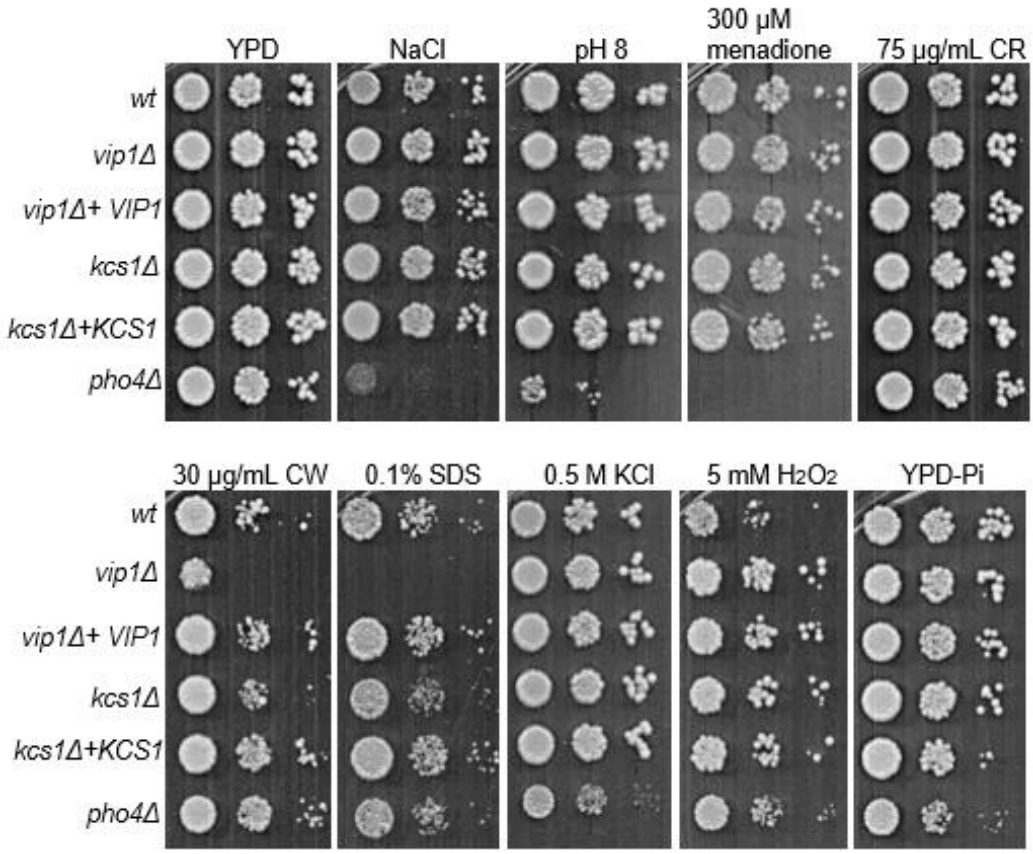

Figure 3.15. Stress phenotypes of cells lacking *KCS1* or *VIP1*.
Mid-log cells were spotted in serial dilutions onto YPD plates containing 1 M NaCl, 300 µM menadione, 0.5 M KCl, 5 mM H_2O2, 30 µg/mL CW, 75 µg/mL CR, 0.1% SDS or 5 mM H_2O_2 as well as onto YPD pH 8 or YPD-Pi media. Plates were incubated at 30^0C for 24 hours. N=3.

3.2.3.3 Cells lacking KCS1 have a morphological defect

In *S. cerevisiae* IPs have been shown to play a role in maintaining cell growth (Dubois *et al*., 2002). Furthermore, as defects in the PHO pathway via deletion of *PHO4* or *PHO80* resulted in slower growing cells, experiments were performed to analyse the growth rates of *vip1Δ* and *kcs1Δ* cells. However, no significant growth differences were found when compared to wild type cells (Figure 3.16.a). An examination of *vip1Δ* and *kcs1Δ* cells did reveal a morphological defect present in cells lacking *KCS1* which was observed as a swollen dot (Figure 3.16.b). There was no difference between the morphology of *vip1Δ* and wild type cells.

It has been reported in *S. cerevisiae* that cells lacking *KCS1* have abnormalities in their vacuolar morphology and fragmentation. Therefore, the vacuolar marker dye, CMAC was employed to investigate whether deletion of *KCS1* had impacted on the vacuole and whether this was underpinning the morphology shown in Figure 3.16.b. However, CMAC

staining revealed that the observed defect of *kcs1⊿* cells was not accounted for by a change in vacuolar morphology (Figure 3.16.c). Recently, it has been shown that deletion of Vip1 or Kcs1 in *C. albicans* can lead to an accumulation of lipid droplets (Ma *et al.,* 2020). Thus, it is plausible that the morphological defect of *kcs1⊿* cells could be lipid droplet accumulation.

In *A. nidulans* and *U. maydis* members of the Vip1 family have been shown to play a role in filamentation (Pöhlmann *et al*., 2014). Furthermore, overexpression of *KCS1* in *S. cerevisiae* has been shown to induce filamentation (Norman *et al*., 2018). Given these links to filamentation it was investigated whether deletion of *VIP1* or *KCS1* in *C. albicans* had an impact on the ability of cells to form hyphae. Cells were incubated for 3 hours at 37^0C in the presence of 10% FCS. There was no difference observed in hyphae formation in cells lacking *VIP1* or cells lacking *KCS1* compared to wild type cells (Figure 3.16.d).

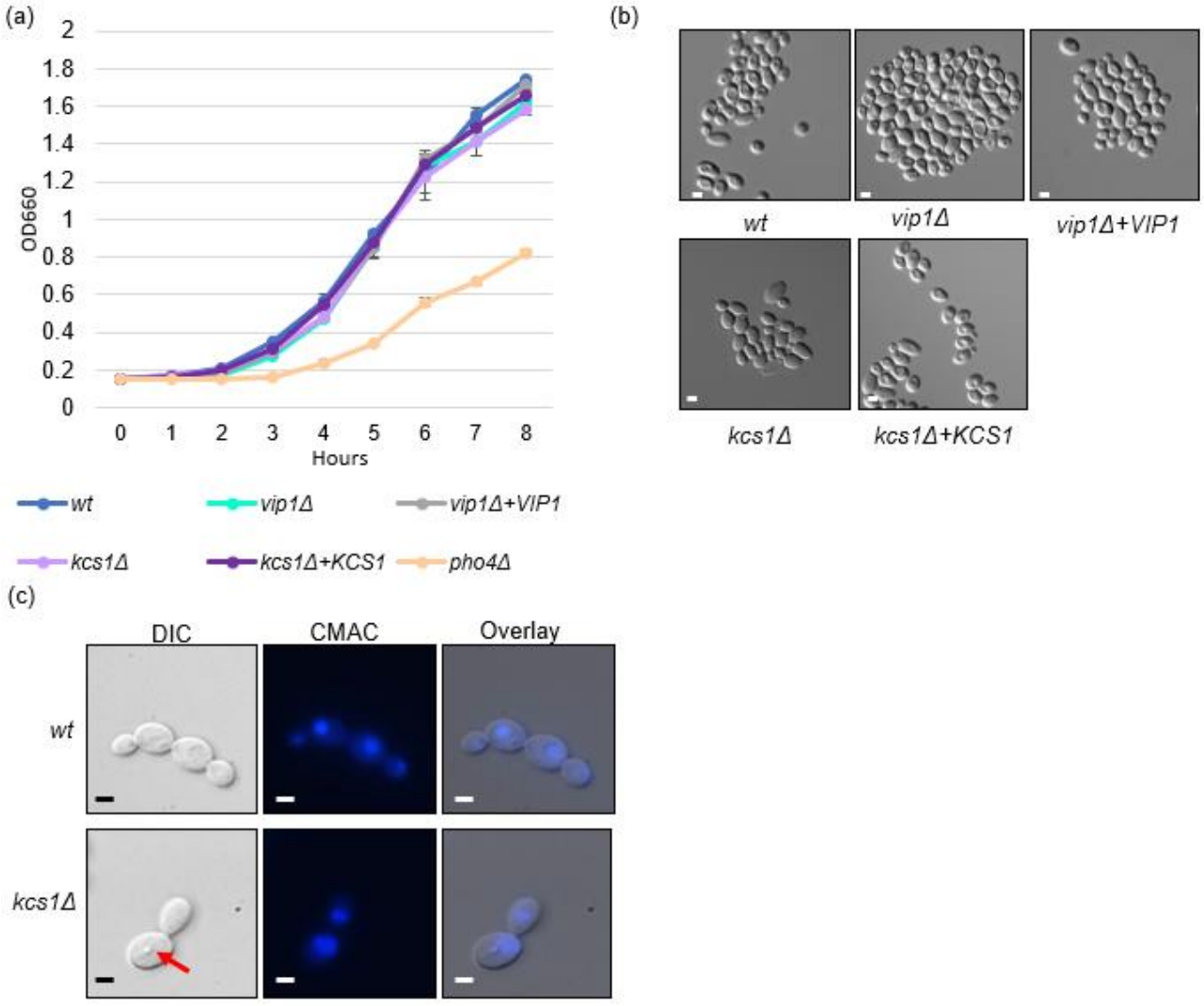
(a)
OD660
Hours
wt
vip1Δ
vip1Δ+VIP1
kcs1Δ
kcs1Δ+KCS1
pho4Δ
(b)
wt
vip1Δ
vip1Δ+VIP1
kcs1Δ
kcs1Δ+KCS1
(c)
DIC
CMAC
Overlay
wt
kcs1Δ

(d)

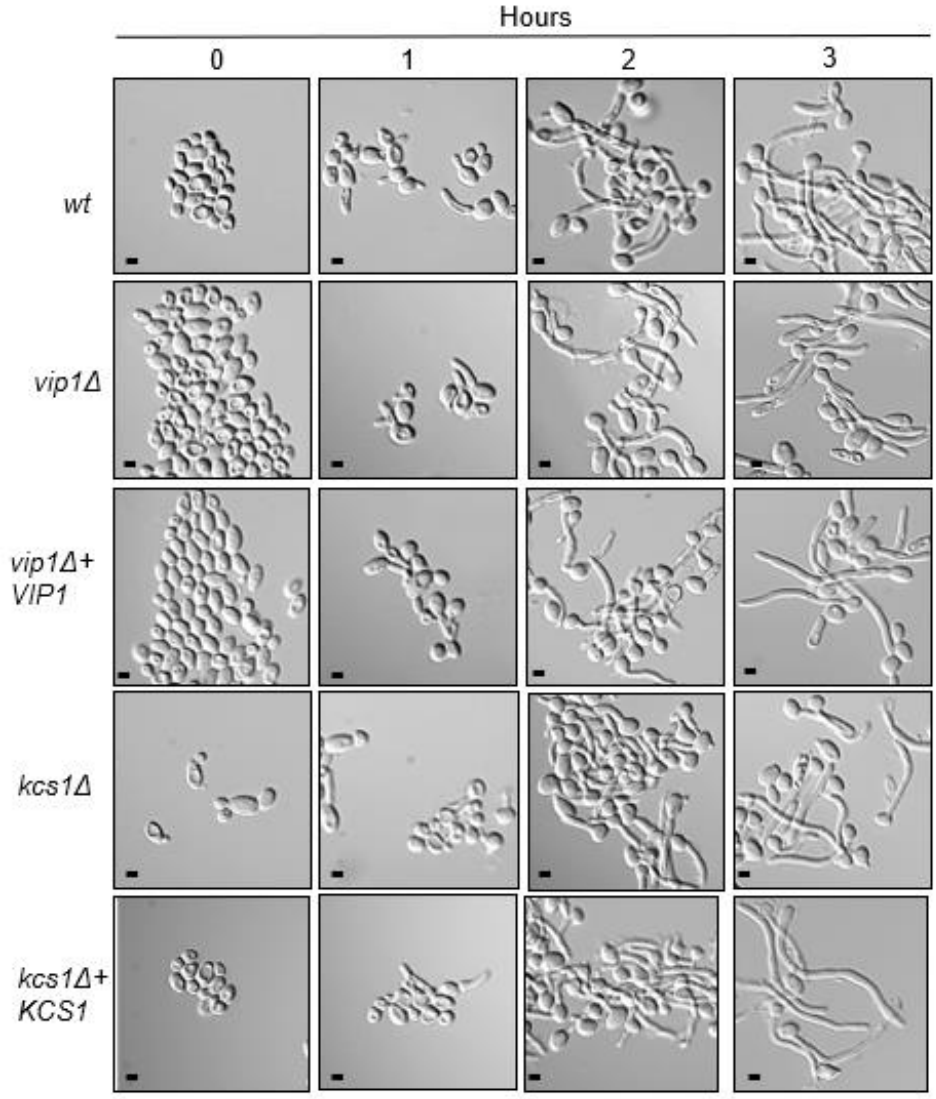

Figure 3.16. Growth and Morphology of Cells lacking Kcs1 or Vip1.
(a) Growth curve of *wt* JC747, *kcs1⊿* and *vip1Δ* cells grown in YPD for 8 hours. N=3, error bars show SEM. **(b)** DIC images of cells grown to mid-log phase before being fixed with Paraformaldehyde. Images, using a 63X objective were taken on a Zeiss Axioscope. N=3. Scale bar = 10 µM. **(c)** Vacuolar staining of *wt* and *kcs1⊿* mid-log cells with 7-amino-4-chloromethylcoumarin (CMAC). Images were taken using a 63X objective on a Zeiss Axioscope. Red arrow indicates morphological defect. Scale bar = 10 µM. **(d)** Yeast to hyphae switching. Overnight cultures were diluted back 1/10 into YPD supplemented with 10% FCS are incubated for 3 hours at 180 rpm at 37^0C. At each hourly time point 10 mL of cells were fixed with paraformaldehyde. DIC images were captured at 63X objective on a Zeiss Axio microscope. N =3.

3.3 Discussion

Most of the current dogma regarding Pi homeostasis in fungi has come from work in *S. cerevisiae*. There are significantly fewer studies investigating Pi regulation in fungal pathogens; however, almost all have reported a link between Pi acquisition, stress resistance and virulence (Lev *et al*., 2017; Kretschmer *et al*., 2014; Ikeh *et al*., 2016). Thus, it is essential that we begin to develop a greater understanding of the mechanisms underpinning Pi homeostasis in these pathogens. This chapter has begun to address the gaps in current knowledge surrounding Pi regulation in the prominent human fungal pathogen *C. albicans*; providing evidence that there is re-wiring of the PHO pathway compared to the model yeast, *S. cerevisiae*.

In *S. cerevisiae* during Pi replete conditions the Pho80-Pho85 CDK complex phosphorylates five key Ser-Pro dipeptides on Pho4 preventing its nuclear accumulation (Komeili and O'Shea, 1999). However, during periods of Pi starvation the inhibitor, Pho81 inhibits the CDK complex. Subsequently, unphosphorylated Pho4 can translocate to the nucleus where it upregulates genes involved in Pi acquisition (Ogawa *et al*., 2000). In this chapter, loss of *PHO80* led to the activation of the secreted acid phosphatases even in Pi replete conditions, suggesting the PHO pathway in *pho80Δ* cells is constitutively active, which replicates that in *S. cerevisiae* (Kaffman *et al*., 1994). In *S. cerevisiae* cells lacking *PHO80* also have reduced growth (Deutschbauer *et al*., 2005), high intracellular levels of Pi (Rosenfeld *et al*., 2010) and sensitivity to cationic and alkaline stress (Ogawa *et al*., 2000). This study has shown that *C. albicans* cells lacking *PHO80* also have a growth defect and high levels of intracellular Pi. However, given the severe growth impairment of cells lacking *PHO80* in *C. albicans*, it was difficult to ascertain any stress sensitive phenotypes. Taken in culmination, this suggests a degree of conservation in the role played by the CDK cyclin Pho80 in PHO pathway regulation of Pho4 in *C. albicans* and *S. cerevisiae*.

There are a limited number of papers addressing PHO pathway regulation in other prominent fungal pathogens. However, cells lacking *PHO80* in *C. neoformans* have detectable levels of secreted acid phosphatases present in Pi replete conditions (Toh-E-A *et al*., 2015), and the same phenotype is observed when the Pho80 homologue in *Aspergillus fumigatus*, PhoB^{PHO80} is deleted (de Gouvéa *et al*., 2008). Taken together, this indicates that the negative regulatory role of the cyclin Pho80 in PHO pathway regulation, first described in *S. cerevisiae*, is conserved across three major human fungal pathogens.

There are, however, a few notable differences in Pho80 regulation between *S. cerevisiae* and *C. albicans* shown in this chapter. For example, in *S. cerevisiae*, loss of *PHO80* leads to the constitutive nuclear accumulation of Pho4 (Kaffman *et al*., 1994); however, this was not the case in *C. albicans pho80Δ* cells as Pho4 nuclear accumulation could only be detected in response to Pi starvation. This seems to conflict with the observation that the Pho4-dependent production of secreted acid phosphatases is evident even under Pi replete conditions. The reason behind this digression remains ambiguous but it is noteworthy here that it is technically difficult to visualise Pho4 nuclear accumulation in wild type cells due to low fluorescent signals. Thus, an inability to detect constitutive Pho4 accumulation in the nucleus in *pho80Δ* cells could be related to observations that Pho4 levels are reduced in this background. However, this requires further investigation.

Based on the PHO pathway in *S. cerevisiae*, the results presented in this chapter regarding the phenotypes of the *pho81Δ* strain were unexpected. In *S. cerevisiae,* deletion of *PHO81* prevents activation of the PHO pathway and the inhibitory function of Pho80-Pho85 cannot be overcome; consequently *pho81Δ* cells mimic the phenotypes of cells lacking *PHO4* (To *et al*., 1973; Sambade *et al*., 2005). Similar findings are seen in *C. glabrata* and *C. neoformans* in which deletion of *PHO81* prevents PHO pathway activation (Kerwin and Wycoff, 2009) (Desmarini *et al*., 2020). However, in *C. albicans,* Pho81 regulates the PHO pathway differently. In stark contrast to a lack of PHO pathway activation in other yeast, *C. albican*s cells lacking *PHO81* show constitutive activation of this pathway as evidenced by the production of secreted acid phosphatases and Pho4 nuclear accumulation even under Pi replete conditions. Moreover, the observations that loss of Pho81 results in increases in intracellular Pi, and detectable increases in resistance to Pho4-dependent stresses, further suggests that Pho81 functions as a negative regulator of Pho4 in *C. albicans*. The apparent increased levels of Pho4 in *pho81Δ* cells during Pi replete conditions may contribute to this role and the constitutive activation of the PHO pathway, but the precise mechanism requires further investigation.

The results of this chapter suggest there could be potential alternative regulatory pathways for Pi acquisition in *C. albicans*. For example, in cells lacking *PHO81* but not *PHO80* there is an increase in levels of Pho4 in Pi replete conditions compared to wild type cells. However, both *pho81Δ* and *pho80Δ* cells have constitutively activated secreted acid phosphatase activity. Thus, it is plausible that there is additional regulation of secreted acid phosphatase

activity in *C. albicans*. For example, it could also be that they are regulated post transcriptionally. Furthermore, an alternative transcription factor could also be regulating PHO pathway components. However, this seems unlikely given that cells lacking Pho4 have low intracellular Pi levels, no polyP and abolished secreted acid phosphatase activity. Furthermore, in *C. albicans* RNA-sequencing analysis showed that Pho4 is required for the expression of genes involved in Pi acquisition (Ikeh *et al*., 2016).

In this chapter cells lacking the cyclin Pho80 appeared to have reduced fitness indicated by a severe growth defect both in liquid media and on spot test plates containing no stresses. Thus, in *C. albicans* Pho80 may be playing a role in alternative processes alongside its role in PHO pathway regulation. For example, Pho80 may play a role in the cell cycle. In *S. cerevisiae*, Pho85 has been shown to target substrates which play roles in the cell cycle (Huang *et al*., 2007). Although, it has been shown to only be required to maintain viability when the activity of Cdc28 is compromised (Huang *et al*., 2007). However, unlike *S. cerevisiae*, in *C. albicans* the CDK Pho85 is essential (Miyakawa *et al*., 2000). Given the phenotype of the Pho80 delete shown in this chapter alongside Pho85 being essential, it is plausible that the Pho85-Pho80 CDK complex is playing an important role in cell cycle progression in *C. albicans*. The results of this chapter also suggest that both Pho80 and Pho81 play a role in negatively regulating Pho4 in *C. albicans*. However, it remains ambiguous how Pho4 is positively regulated in response to Pi starvation in *C. albicans*. Further experiments to gain a greater understanding of the role of Pho80 and Pho81 in the regulation of the PHO pathway are discussed in chapter 6.

In *C. albicans* a PTM independent of phosphorylation is present on Pho4 in Pi replete but not deplete conditions (Ikeh, 2015). This suggests its loss facilitates Pho4 nuclear accumulation. Interestingly, in *S. cerevisiae,* 3 Dubs including Ubp3 were shown to have lower levels of Pho4 regulated targets, linking them to PHO pathway regulation (Isasa *et al*., 2015). Moreover, overexpression of *UBP3* in *S. cerevisiae* leads to Pho4 being constitutively nuclear (Isasa *et al*., 2015). Thus, in this chapter it was investigated whether Ubp3 was playing a PHO pathway regulatory role in *C. albicans*. However, the results of this chapter suggest that unlike in *S. cerevisiae*, Ubp3 does not appear to be playing a significant role in PHO pathway regulation. Potentially this could be due to functional redundancy between Ubp3 and other DUBs in *C. albicans*. Further work therefore needs to be conducted to identify the PTM on *C. albicans* Pho4 such as analysis by mass spectrometry of Pho4 purified

from cells grown under Pi replete and deplete conditions. Furthermore, it could also prove insightful to investigate the overexpression of *UBP3* in *C. albicans* to assess whether it has an impact on PHO pathway regulation.

A recent breakthrough with regard to the regulation of Pi homeostasis is the identification of IP_7 molecules as ligands for SPX domains which are found on a number of proteins involved in Pi homeostasis (Lee *et al*., 2007; Wild *et al*., 2016; Desmarini *et al*., 2020). In *S. cerevisiae*, in cells lacking the IP_7 synthase, *VIP1*, Pho4 was unable to accumulate in the nucleus in response to Pi starvation (Lee *et al*., 2007). Furthermore, cells lacking *VIP1* were unable to inhibit the Pho80-Pho85 CDK complex, as IP_7 interaction with Pho81 is important for this function of Pho81 (Lee *et al*., 2007). In *S. cerevisiae*, Kcs1 has also been linked to Pi homeostasis as *KCS1* lacking cells have depleted polyP levels (Lonetti *et al*., 2011). In *C. neoformans* Kcs1 has been shown to be responsible for synthesising the IP_7 isoform which binds to the SPX domain of Pho81 influencing protein-to-protein interactions within the CDK complex (Desmarini *et al*., 2020). While polyP levels were found to increase in cells lacking Kcs1 this chapter found no other link between Kcs1 and PHO pathway regulation in *C. albicans*. However, deletion of Vip1 led to an increase in polyP levels and a small impairment to secreted acid phosphatase activity under Pi deplete conditions. This suggests that in *C. albicans* Vip1 may be playing a greater role in the regulation of Pi homeostasis that Kcs1. It is plausible however, that a level of functional redundancy exists between the Kcs1 and Vip1 derived IP_7 isoforms in *C. albicans*. Thus, future work could assess whether a strain lacking both *VIP1* and *KCS1* had a greater impact on PHO pathway regulation. Collectively, the results of this chapter indicate differences in PHO pathway regulation in *C. albicans* compared to that reported in other fungi including *S. cerevisiae* and *C. neoformans*.

As well as being linked to Pi homeostasis in eukaryotic cells, IP_7 generating enzymes have also been shown to regulate resistance to a variety of stresses. In *S. cerevisiae*, Kcs1 has been shown to be required for the response to salt stress as well as growth at 37^0C and maintenance of cell wall integrity and cell length (Dubois *et al*., 2002). Furthermore*, S. cerevisiae* cells lacking *KCS1* have also been reported have fragmented vacuoles (Saiardi *et al*., 2002). Moreover, in *C. neoformans,* loss of *KCS1* is associated to phenotypes linked to virulence (Lev *et al*., 2015), drug susceptibility (Lev *et al*., 2015), and growth on alternative carbon sources (Li *et al*., 2016). However, in this chapter the only modest sensitivity attributed to loss of *KCS1* in *C. albicans* was to the cell wall chitin binding dye, calcofluor

white. *C. albicans* cells lacking *VIP1* were found to be acutely sensitive to calcofluor white and SDS as well as being resistant to oxidative stress produced by H_2O_2. Further work is needed to dissect the role of IP_7 molecules in *C. albicans* and this is considered more fully in the final discussion. However, the results presented in this chapter suggest that the IP_7 generating enzymes play different roles in *C. albicans* compared to those described in *S. cerevisiae* and *C. neoformans*.

Chapter 4: The Role of PolyP Mobilisation in the Pathobiology of *C. albicans*

4.1 Introduction

Within cells Pi is stored as polyphosphate (polyP), a linear polymer composed of inorganic Pi molecules joined together with high-energy phosphoanhydride bonds (Moreno and Docampo, 2013). Within yeast, the synthesis of polyP is mediated by a vacuolar membrane protein assembly, known as the vacuolar transporter chaperone (VTC) complex. Expression of components of the VTC complex is under control of the PHO pathway. The VTC complex is composed of the synthetase Vtc4 along with the subunits Vtc1 and either Vtc2 or Vtc3 which are functionally redundant (Desfougeres *et al*., 2016). Components of the VTC complex contain SPX domains that exclusively bind the inositol polyphosphates, IP_6 and IP_7, driving polyP synthesis (Wild *et al*., 2016). Following activation of the PHO pathway in response to Pi starvation, initial Pi demands are met by the mobilisation of polyP by polyphosphatases, including Ppn1 and Ppx1. Ppn1 is an endopolyphosphatase which cleaves long chains of polyP. Ppx1 functions dually as an endo- and exo-polyphosphatase that splits the orthophosphate from the ends of polyP (Jimenez *et al*., 2016). Following hydrolysation of polyP, Pi molecules are thought to leave the vacuole via the intracellular low affinity Na/Pi symporter, Pho91 which is localised to the vacuolar membrane and which also has an SPX domain (Potapenko *et al*., 2018). The vast majority of polyP in fungal cells is stored in the vacuole to prevent cytotoxicity (Lonetti *et al*., 2011). However, the presence of low levels of polyP has also been reported in the cytoplasm, mitochondria, and nucleus (Moreno and Docampo, 2013). There is significantly more polyP in yeast than in mammalian cells with approximately 10% of the dry weight of *S. cerevisiae* being attributed to polyP (Lonetti *et al*., 2011).

Previously deemed a molecular relic, there has been a recent surge into investigating the roles of polyP outside its role as a Pi storage molecule. In particular, polyP has been extensively studied in bacteria. The pioneering work of Arthur Kornberg and colleagues provided evidence for roles of polyP in bacterial biofilm development, growth, stress responses, virulence, and quorum sensing (reviewed in Rao *et al*., 2009). More recently, polyP has been implicated in an additional array of processes including; antioxidant protection (Gray and Jakob, 2015), protein chaperoning (Gray *et al*., 2014), signalling (Azevedo *et al*., 2015), and poly3-hydroxybutyrate production (Tumlirsch *et al*., 2015).

Although extensive work has been carried out investigating the role of polyP in prokaryotic cells, comparatively less is known for eukaryotes. In *S. cerevisiae*, polyP has been shown to play a role in cell cycle progression and the response to genotoxic stress (Bru *et al*., 2016), and a novel post-translational modification of protein lysines by polyphosphate addition (polyphosphorylation) has recently been discovered (Azevedo *et al*., 2015). Intriguingly, in *Trypanosoma cruzi* in response to hyperosmotic stress polyP levels dramatically increase, whereas hyposmotic stress triggers the rapid mobilization of polyP stores (Ruiz *et al*., 2001). Interestingly, in *C. neoformans*, cells which either have no polyP or impairment in polyP mobilisation display sensitivity to zinc (Kretschmer *et al*., 2014). Finally, in higher eukaryotic cells, polyP is a potent modulator of inflammation (Muller et al., 2009) and blood coagulation in mammalian cells (Smith *et al*., 2006).

In *C. albicans,* the Pho4 transcription factor has been shown to be required for a pleiotropy of stress responses (Ikeh *et al*., 2016). Cells lacking Pho4 are sensitive to alkaline pH, cationic stress and superoxide stress (Ikeh *et al*., 2016). Moreover, in wild type cells the activation of Pho4 in response to Pi limiting conditions and alkaline pH stress co-incides with polyP mobilization (Ikeh *et al*., 2016). However, an analysis of *vtc1Δ* and *vtc4Δ* cells, lacking polyP, revealed that the stress sensitivities of cells lacking *PHO4* were not due to polyP absence (Ikeh *et al*., 2016). However, as polyP is rapidly mobilised following Pi limitation and a range of stress conditions (Ikeh *et al*., 2016), the aim of this chapter is to investigate the physiological relevance of polyP mobilisation in the pathobiology of *C. albicans*.

4.2 Results

4.2.1 Cells lacking PPN1 and PPX1 have increased levels of polyP

To provide insight into the impact of polyP mobilisation on Pho4 regulation and stress resistance, putative polyphosphatase enzymes in *C. albicans* were identified. The amino acid sequences of the *S. cerevisiae* Ppx1 exopolyphosphatase and the Ppn1 endo/exopolyphosphatase were BLASTed against the *C. albicans* genome database. This identified both Ppx1 (C2_06110W_A) and Ppn1 (C7_00980W_A) homologues in *C. albicans* with 32.8% and 41% identity to the respective *S. cerevisiae* proteins. To explore functional conservation, *C. albicans* strains lacking *PPX1* and *PPN1* homologues were generated and polyP levels, and the size of polyP chains, was examined. Interestingly, unpublished data from the Quinn lab revealed that deletion of either *PPN1* or *PPX1* had no obvious impact on

polyP levels or on the size of the polyP chains (Ikeh, 2015). Hence, in this study, potential functional redundancy between Ppn1 and Ppx1 in *C. albicans* was explored, which necessitated the creation of a strain lacking both Ppn1 and Ppx1.

In order to assess whether *ppn1Δ/ppx1Δ* cells had an increase in polyP levels compared to wild type cells a whole cell staining procedure was employed. Neisser staining is a technique routinely performed on prokaryotic cells in which the dye methylene blue undergoes a metachromatic shift when staining polyP granules resulting in a dark brown/black colour (Gurr, 1965). In addition, to gain a more quantitative measure of polyP levels and length of polyP chains, polyP was extracted from in *ppn1Δ/ppx1Δ* cells and subjected to electrophoresis on urea-polyacrylamide gels followed by toluidine blue staining (Smith and Morrissey, 2007). Toluidine blue staining of the urea-polyacrylamide gels metachromatically stains the polyP a pink/purple colour. The procedure to extract samples for urea-polyacrylamide gels extracts both RNA and polyP but the two resolve differently on gels, enabling the use of RNA as a loading control.

PolyP levels were examined in the single and double polyphosphatase mutants and compared to those in wild type and *pho4Δ* cells. Previous published work has shown that cells lacking Pho4 have no polyP present (Ikeh *et al*., 2016). Both Neisser staining and urea-polyacrylamide gels confirmed there was no detectable increase in polyP levels in the single *ppn1Δ* or *ppx1Δ* mutant cells as previously observed in the Quinn lab (Figure 4.1a, b). However, deletion of both polyphosphatase genes *PPN1* and *PPX1* resulted in more intense Neisser staining of cells (Figure 4.1a), and an accumulation of higher molecular weight polyP chains as revealed by toluidine blue staining of urea-polyacrylamide gels (Figure 4.1b). Due to the abundance of higher chain polyP in cells lacking both polyphosphatases which ran with a similar mobility as RNA, the RNA was unable to be used to quantify the amount of polyP present (Figure 4.1.b). To validate that the accumulation of longer polyP chains in *ppn1Δ/ppx1Δ* cells was due to the deletion of both genes, reconstituted strains were made in which either *PPN1* or *PPX1* were reintegrated. Taken together, the Neisser staining and urea-polyacrylamide gel show that reconstitution of either Ppn1 or Ppx1 polyP levels and length of polyP chains in *ppn1Δ/ppx1Δ* to those seen in wild type cells (Figure 4.1). Collectively, these results confirm a level of functional redundancy exists between the two polyphosphatases Ppn1 and Ppx1 and that both genes need to be deleted before cells accumulate longer length polyP.

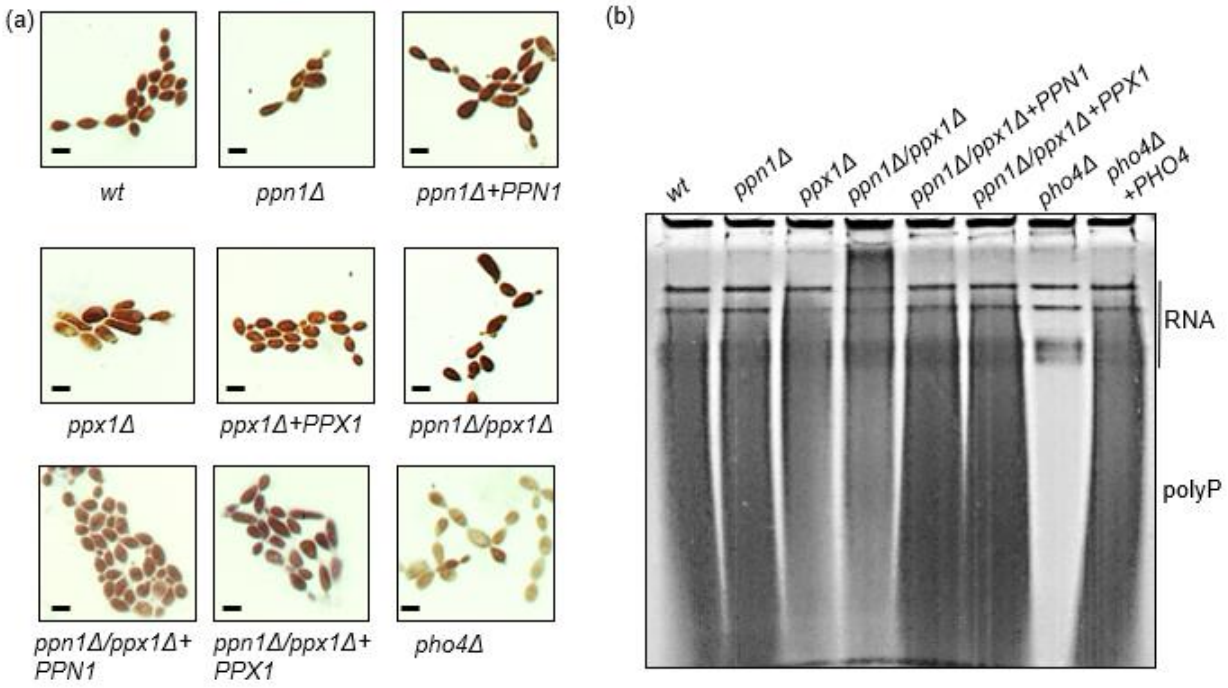

Figure 4.1. Cells lacking both polyphosphatases have increased levels of polyP.
(a) Neisser staining of polyP in *wt, ppn1Δ, ppn1Δ+PPN1, ppx1Δ, ppx1Δ+PPX1, ppn1Δ/ppx1Δ, ppn1Δ/ppx1Δ+PPN1, ppn1Δ/ppx1Δ+PPX1* and *pho4Δ* cells. N=3. **(b)** UREA-Page gel of polyP extracted from *wt, ppn1Δ, ppx1, ppn1Δ/ppx1Δ, pho4Δ, ppn1Δ/ppx1Δ +PPN1* and *ppn1Δ/ppx1Δ+PPX1*, 20 µg of RNA was loaded per sample. Gels were stained with 0.05% toluidine blue. Scale bar = 10 µM. N=3.

4.2.2 PolyP mobilisation in response to Pi starvation

Having established that cells lacking both Ppn1 and Ppx1 exhibit longer chains of polyP, it was next examined whether mobilisation of Pi from polyP was abolished in this strain. To explore this via Neisser staining, cells were collected before and after 16 hours growth in Pi limiting media. PolyP stores in response to Pi starvation have been shown to be fully mobilised by 16 hours in *C. albicans* (Ikeh *et al*., 2016). Neisser staining revealed polyP mobilisation was almost completely abolished in *ppn1Δ/ppx1Δ* cells following Pi starvation (Figure 4.2.a). Whereas, in wild type, single deletion strains and reconstitute strains polyP stores were fully mobilised as indicated by the weak Neisser staining (Figure 4.2.a).

To further explore mobilisation in cells lacking both polyphosphatases, samples were collected following 16 hours Pi starvation and then a further two hours following the addition of 10 mM KH_2PO_4. Samples were then subjected to fractionation and

electrophoresis by urea-PAGE, revealing Pi starvation triggered full liberation of polyP stores in wild type cells and in the reintegrated *ppn1Δ/ppx1Δ* + *PPN1* and *ppn1Δ/ppx1Δ* + *PPX1* cells (Figure 4.2.b). In stark contrast, cells lacking both polyphosphatases still retained an intense degree of toluidine blue staining of polyP (Figure 4.2.b). However, some of the higher molecular weight polyP chains characteristic of *ppn1Δ/ppx1Δ* cells, were resolved to slightly shorter chains, similar to that seen in wild type cells under Pi replete conditions (Figure 4.2. b). Taken together these results demonstrate that Ppn1 and Ppx1 function redundantly to mobilise polyP in response to Pi starvation.

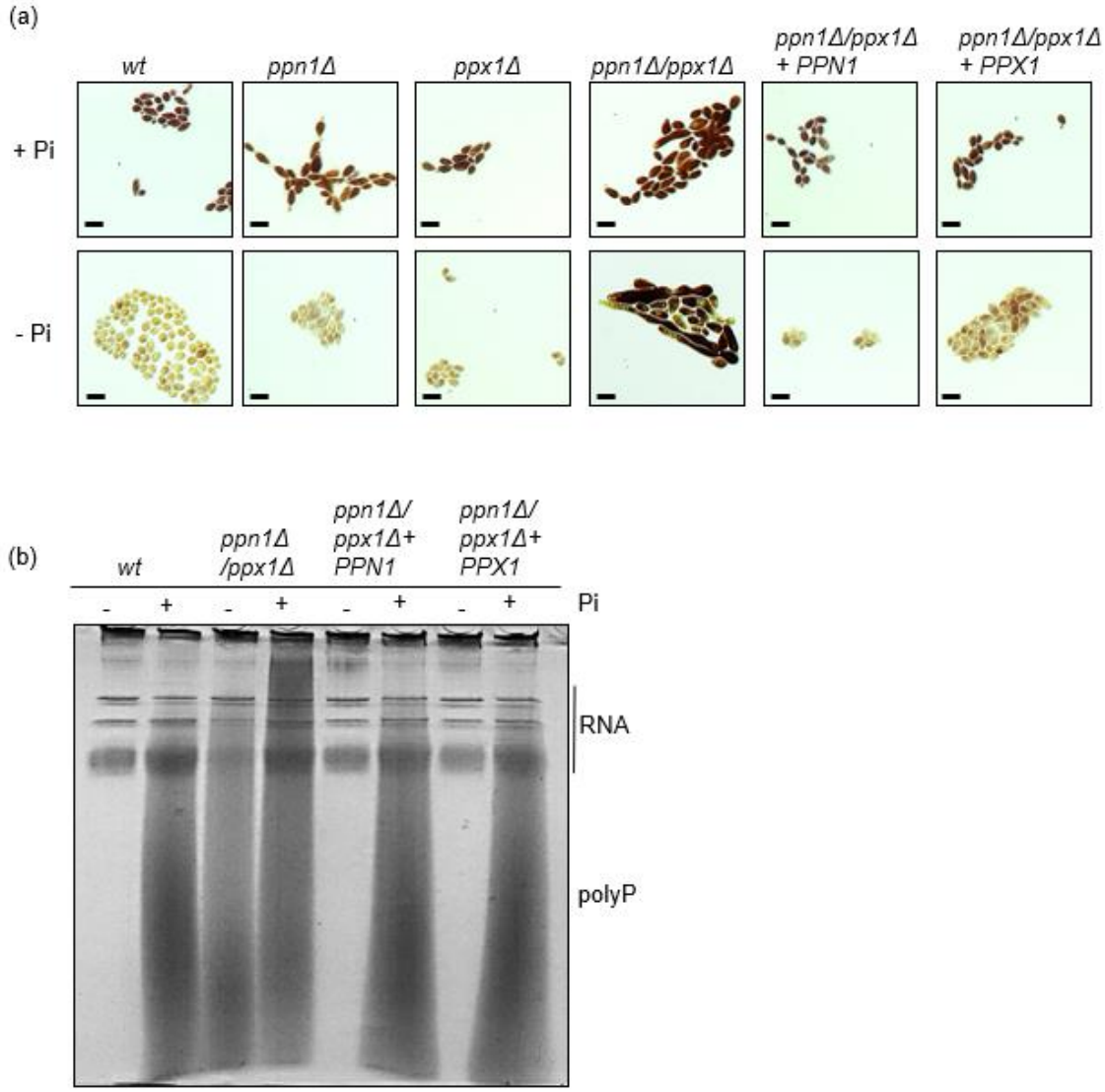

Figure 4.2. PolyP mobilisation in response to Pi starvation.
(a) The indicated strains were grown in YPD-Pi (16 h) then fixed with paraformaldehyde before undergoing Neisser staining for the presence of polyP. N=3. **(b)** UREA-Page gel of RNA and polyP extracted from the indicated strains following 16 hours Pi starvation (- Pi) and then a further 2 hours growth in the presence of 10 mM Pi (+Pi)., 20µg of RNA was loaded per sample. Gels were stained with 0.05% toluidine blue. N=3.

4.2.3 PolyP mobilisation is required for Pho4 mediated stress resistance under phosphate limiting but not phosphate replete conditions

Previous work has shown that cells deficient in polyP via deletion of the VTC synthetase, Vtc4 do not share the stress-sensitivities of *pho4Δ* cells, illustrating that Pho4-mediated production of polyP is not the mechanism underlying the stress-protective roles of this transcription factor (Ikeh *et al*., 2016). However, as polyP is mobilised following Pi limitation and exposure to cationic and alkaline stresses (Ikeh *et al*., 2016), the stress sensitivities of

cells lacking both polyphosphatases was examined. Spot tests were performed on media containing stresses which require Pho4 for resistance (Ikeh *et al*., 2016). Both Pi replete and deplete conditions were used as it was hypothesised that polyP mobilisation may only be crucial when external sources of Pi are limited. Indeed, it has been suggested that cells are able to overcome lack of polyP by regulating Pi uptake when grown in Pi abundant media such as YPD (Thomas and O'Shea, 2005).

When tested under Pi replete conditions, cells lacking *PPN1* or *PPX1* did not display significantly impaired growth to any of the stresses tested (Figure 4.3.a). Cells lacking both polyphosphatases exhibited marginal sensitivity to cationic and superoxide stress (Figure 4.3.a). There was also a marginal growth defect for *ppn1Δ/ppx1Δ* when spotted on alkaline stress containing plates (Figure 4.3.a). Consistent with previous results, cells lacking Pho4 were sensitive to all of the stresses tested.

Under Pi limiting conditions when cells must mobilise their polyP stores to maintain cellular Pi demands more striking sensitivities were observed. It is noteworthy that all strains appear more sensitive to pH 8 and menadione stress in Pi limiting conditions than in Pi replete media(Figure 4.3.b). Cells lacking the polyphosphatase Ppn1 were slightly sensitive to cationic stress imposed by NaCl alongside alkaline and superoxide stress (Figure 4.3.b). However, cells lacking the exo-polyphosphatase, Ppx1 showed slight sensitivity to alkaline , superoxide stress and cationic stress. Cells lacking both polyphosphatases displayed greater sensitivity to cationic, alkaline and superoxide stresses than the single *ppn1Δ* and *ppx1Δ* mutants (Figure 4.3.b). These results indicate that polyP mobilisation does play a role in Pho4 mediated responses to superoxide, cationic and alkaline stress under Pi limiting conditions. The reconstitution of either *PPN1* or *PPX1* was shown to at least partially rescue stress sensitivities (Figure 4.3.b).

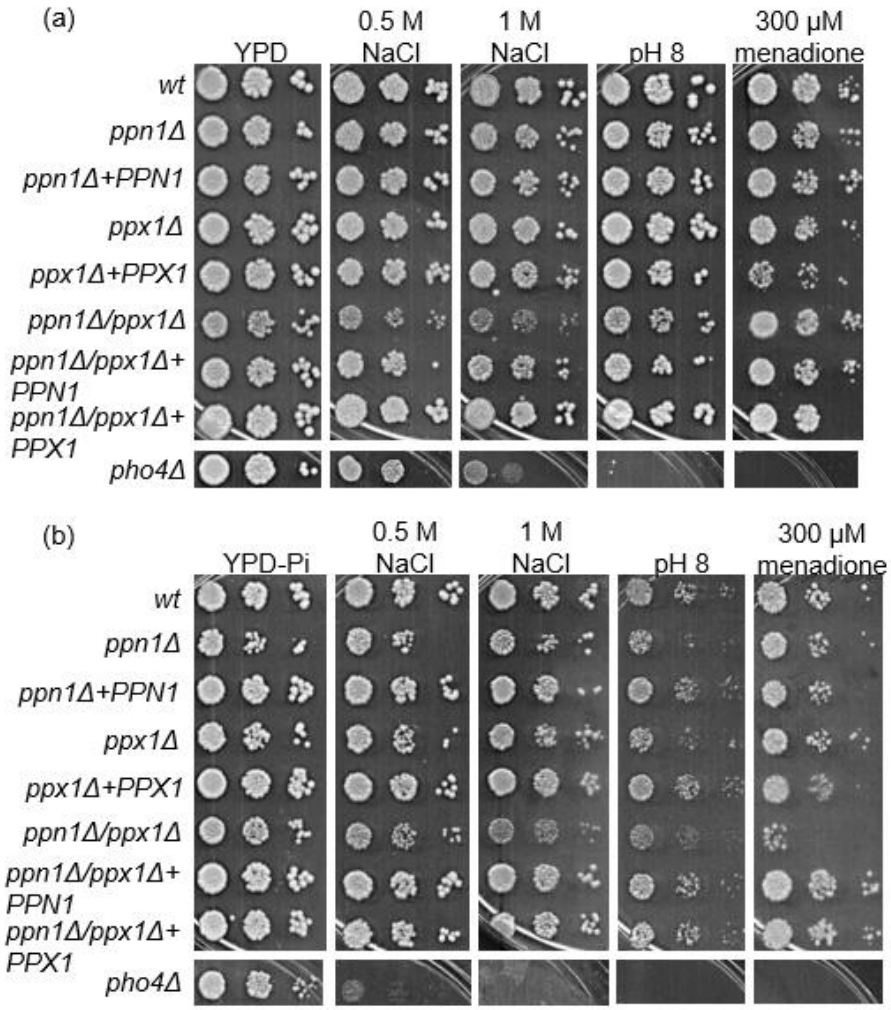

Figure 4.3. The effect of blocking polyP mobilisation on Pho4 mediated stress resistance. (a) Mid-log cells were spotted in serial dilutions onto YPD or **(b)** YPD – Pi plates containing 0.5 M NaCl, 1 M NaCL, 300 µM menadione, or where the pH was raised to pH 8. Plates were incubated at 30^0C for 24 hours. All strains were spotted on the same plate. N=3.

4.2.3.1 PolyP mobilisation in response to alkaline pH

Previous work on Pho4 revealed that polyP is rapidly mobilised in response to alkaline pH, and that this mobilisation precedes Pho4 nuclear accumulation (Ikeh *et al*., 2016). As *ppx1Δ/ppn1Δ* cells displayed impaired resistance to alkaline stress it was examined whether polyp mobilisation in response to this condition was blocked, similar to that seen following Pi starvation. Neisser staining of cells, and toluidine blue staining of polyP resolved by electrophoresis on urea-page cells, was used to explore polyP levels in *ppn1Δ/ppx1Δ* cells in response to alkaline stress. The results of both Neisser staining and urea-page illustrate the mobilisation of polyP in wild type cells following 30 minutes exposure to alkaline stress

(Figure 4.4). Furthermore, the urea-page gel analysis shows a further depletion of polyP levels after 60 minutes exposure to alkaline stress (Figure 4.4.b). These results are consistent with previous findings (Ikeh *et al*., 2016). In contrast, after 30 minutes alkaline stress Neisser staining showed a considerable degree of polyP staining in *ppn1Δ/ppx1Δ* cells that was reduced upon reintegration of either *PPN1* or *PPX1* (Figure 4.4.a). Furthermore, when assayed via urea-PAGE, it can be seen that polyP levels in *ppn1Δ/ppx1Δ* cells do not significantly alter following exposure to alkaline stress (Figure 4.4.b). As *ppn1Δ/ppx1Δ* cells are sensitive to alkaline stress, this indicates that polyP mobilisation by Ppn1 and Ppx1 is important to promote the resistance of *C. albicans* cells to alkaline stress.

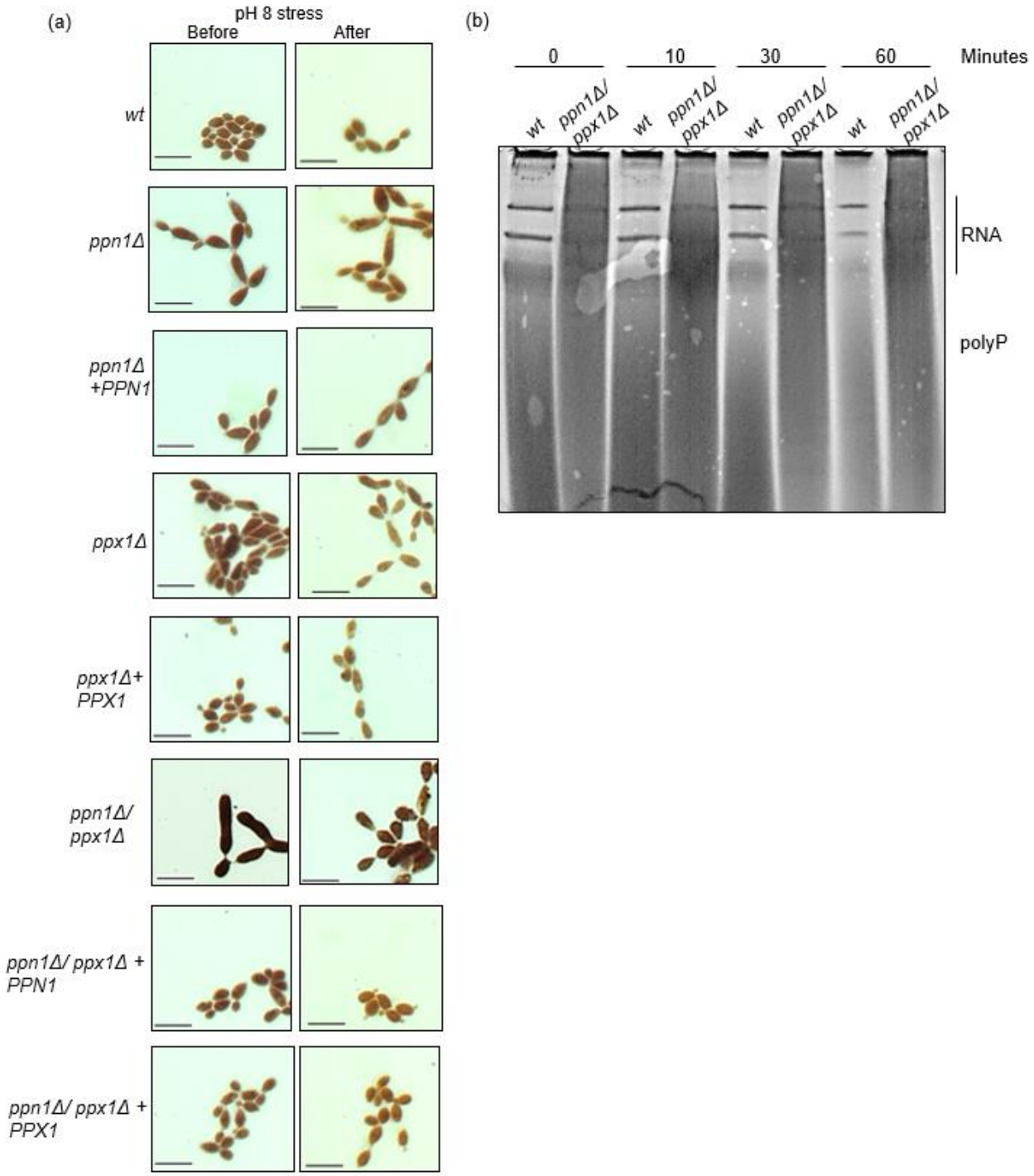

Figure 4.4. PolyP levels in response to alkaline stress.
(a) Neisser staining for the presence of polyP in the indicated strains before and following 30 minutes exposure to pH 8 stress. Scale bar = 20 microns. N=3 **(b)** UREA-Page gel of RNA and polyP extracted from the indicated strains taken at 0-, 10-, 30- and 60-minutes following pH 8 stress. 20ug of RNA was loaded per sample. Gels were stained with 0.05% toluidine blue.

4.2.4 Prevention of polyP mobilisation impacts on Pho4 accumulation and PHO pathway activation

In previous work it was shown that mobilisation of Pi stores from polyP precedes the nuclear accumulation of Pho4 and the induction of Pi acquisition genes (Ikeh *et al*., 2016). The results in this chapter have shown that there is a clear decrease in polyP mobilisation in cells lacking *PPN1* and *PPX1* together with an increase in stress sensitivity to conditions known to require Pho4 for resistance. Therefore, it was examined whether Pho4 activation was impaired in *ppn1Δ/ppx1Δ* cells due to an inability to mobilise polyP. To begin addressing whether polyP mobilisation was required for PHO pathway activation a strain was constructed in which *ppn1Δ/ppx1Δ* cells express a Pho4-GFP fusion protein. This allowed the use of fluorescence microscopy to determine whether the nuclear accumulation of Pho4 in response to Pi starvation was impaired in cells lacking *PPN1* and *PPX1*. In wild type cells following 16 hours Pi starvation there appears to be more Pho4 in the nucleus compared to elsewhere in the cell where lower levels of Pho4-GFP can still be observed (Figure 4.5.a). This will be referred to as nuclear accumulation throughout this chapter. Furthermore, as Pho4 nuclear accumulation was observed in the majority of wild type cells in focus it is referred to in this chapter as uniform.

To investigate whether preventing polyP mobilisation led to a delay in PHO pathway activation, we looked at Pho4-GFP nuclear accumulation up until 22 hours Pi starvation. However, whilst in *ppn1Δ/ppx1Δ* cells there was accumulation of Pho4, this was not uniform (Figure 4.5.a.b). Furthermore, there appeared to be a greater intensity of Pho4-GFP following 16 hours Pi starvation in some *ppn1Δ/ppx1Δ* cells (Figure 4.5.a). However, whether the greater intensity of Pho4-GFP reflects Pho4 levels within the cell requires further investigation. Furthermore, an additional non-tagged GFP strain is needed to ascertain that the greater intensity of Pho4-GFP is not background. Unlike wild type cells, under Pi replete conditions there appears to be a small degree of Pho4 nuclear accumulation in *ppn1Δ/ppx1Δ* cells (Figure 4.5.a).

Given that preventing polyP mobilisation impacted the uniform nuclear accumulation of Pho4 in response to Pi starvation, it was investigated what impact blocking polyP mobilisation had on PHO pathway activity. When Pho4 accumulates in the nucleus in response to Pi starvation it up regulates Pi acquisition genes including the high affinity Pi symporter *PHO84* and the secreted acid phosphatase *PHO100* (Ikeh *et al*., 2016). qPCR

confirmed that both *PHO84* and *PHO100* were highly expressed in wild type cells grown under Pi-limiting conditions (Fig. 4.6a). However, in response to Pi starvation the expression of the secreted acid phosphatase, *PHO100* and the high affinity symporter, *PHO84* was reduced compared to wild type cells (Figure 4.6.a). Reconstitution of *ppn1Δ/ppx1Δ* cells with either *PPN1* or *PPX1* at least partially restored wild type transcript levels of *PHO84* and *PHO100* under Pi replete and deplete conditions (figure 4.5.a). Taken together, the differences in Pho4 nuclear accumulation between wild type and *ppn1Δ/ppx1Δ* cells following Pi starvation (figure 4.5) and the expression levels of *PHO84* and *PHO100* suggests that preventing polyP mobilisation may cause deregulation of the *PHO* pathway.

The presence of secreted acid phosphatase activity can also be examined via a colorimetric agar overlay assay , in which colonies on plates stain red/brown if secreted phosphatases are present (To *et al*., 1973). Wild type cells, and cells lacking either *PPN1* or *PPX1*, secrete acid phosphatases following growth in Pi depleted media, but not under Pi replete conditions, and this is dependent on Pho4 (Fig. 4.6b). However, there was a slight decrease in secreted acid phosphatase production in *ppn1Δ/ppx1Δ* cells following Pi (Figure 4.d.b). The discrepancy between the expression level of *PHO100* by qPCR and the secreted acid phosphatase activity assay shown by the colorimetric overly assay could potentially be explained by the lack of sensitivity of the latter.

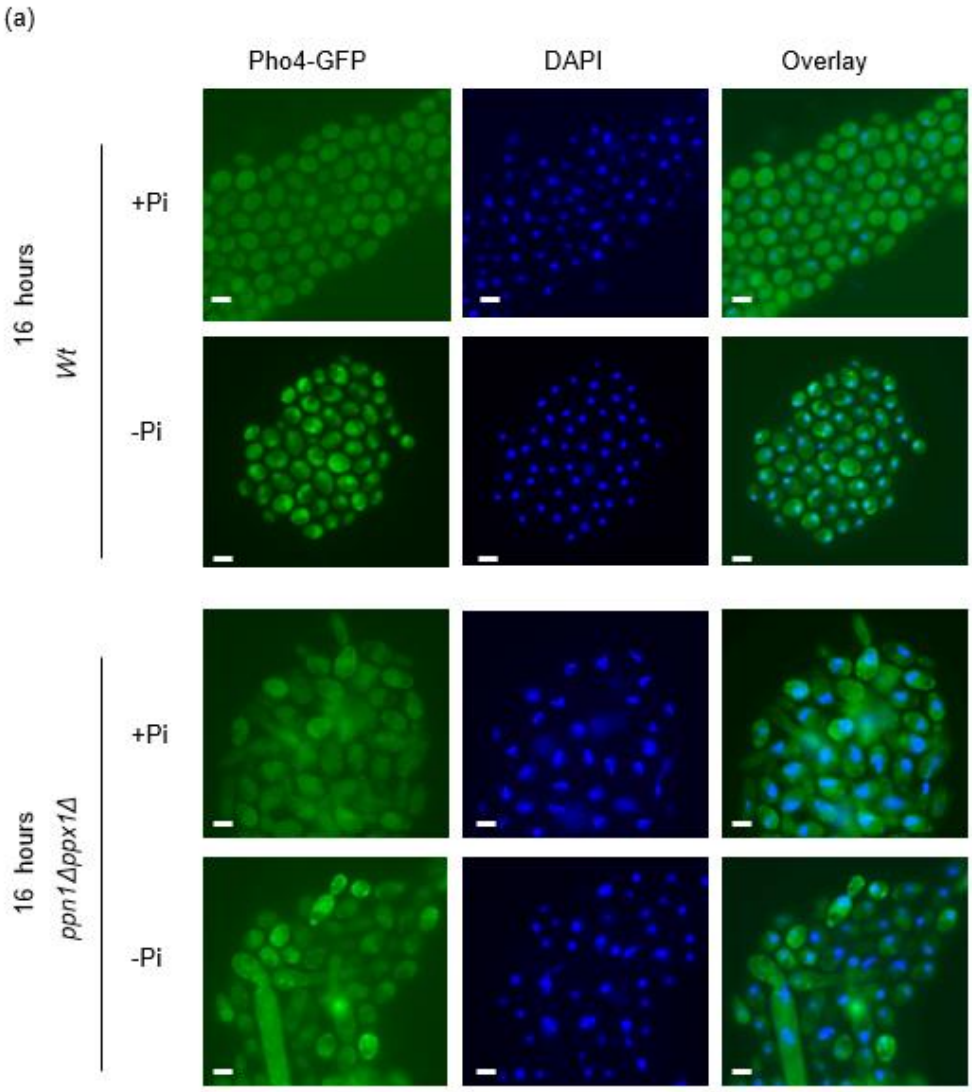
(a)
Pho4-GFP
DAPI
Overlay
16 hours
Wt
+Pi
-Pi
16 hours
ppn1Δppx1Δ
+Pi
-Pi

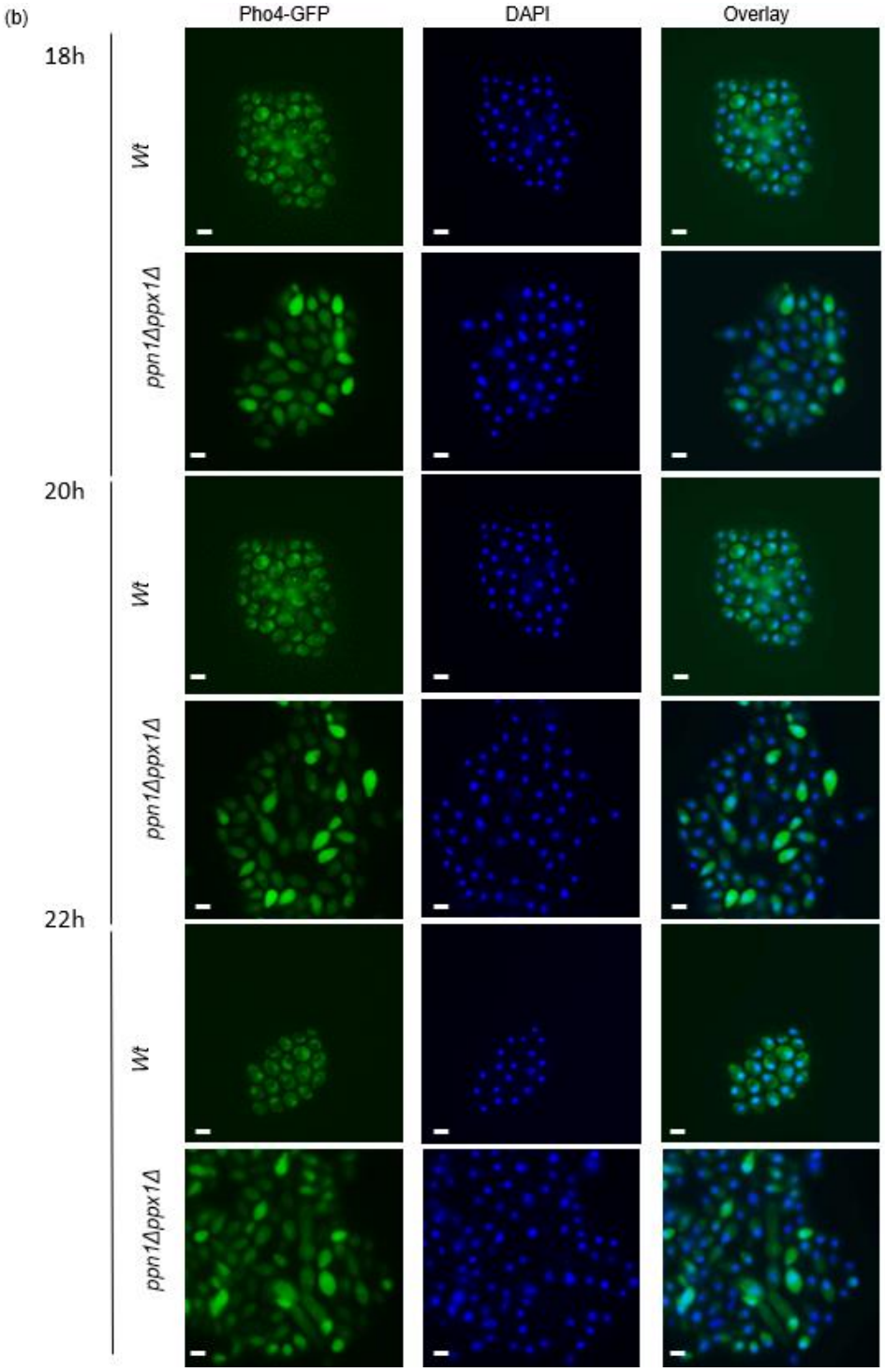

Figure 4.5 Prevention of polyP mobilisation impacts on Pho4 nuclear accumulation in response to Pi starvation. (a)(b) *wt* and *ppn1Δ/*ppx1*Δ* cells expressing Pho4-GFP were grown in YPD-Pi for 22 hours with samples taken every 2 hours from 16 hours, an additional sample was also taken at 16 hours in which 10 mM Pi was added and grown for a further 2 hours before being fixed with paraformaldehyde and images on a fluorescent microscope with a 63X objective. Nuclear staining by DAPI is represent by the colour blue and GFP by the colour green. Scale bar = 10 µM. N=3.

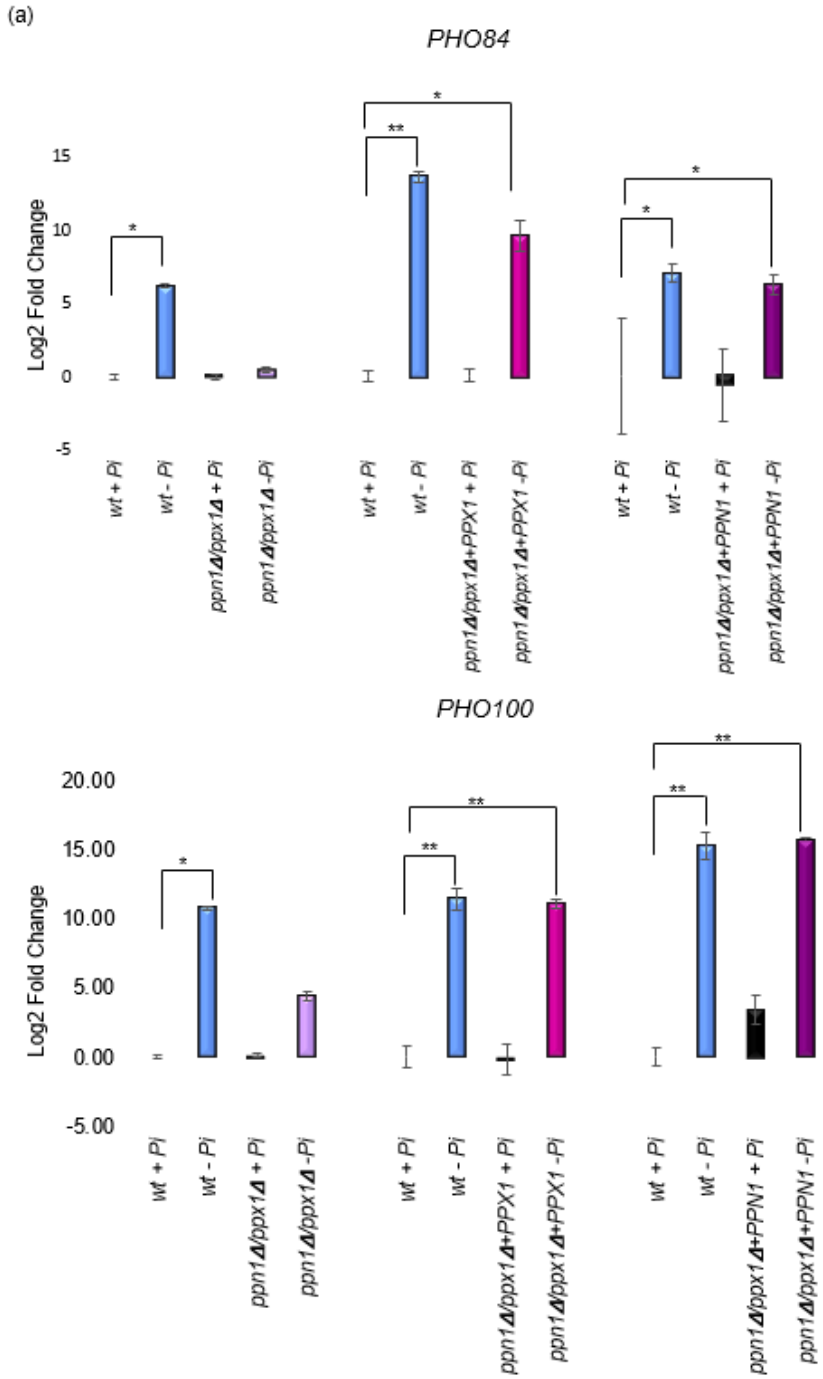
(a)
PHO84
Log2 Fold Change
15
10
5
0
-5
wt + Pi
wt - Pi
ppn1Δ/ppx1Δ + Pi
ppn1Δ/ppx1Δ -Pi
ppn1Δ/ppx1Δ+PPX1 + Pi
ppn1Δ/ppx1Δ+PPX1 -Pi
ppn1Δ/ppx1Δ+PPN1 + Pi
ppn1Δ/ppx1Δ+PPN1 -Pi
PHO100
Log2 Fold Change
20.00
15.00
10.00
5.00
0.00
-5.00

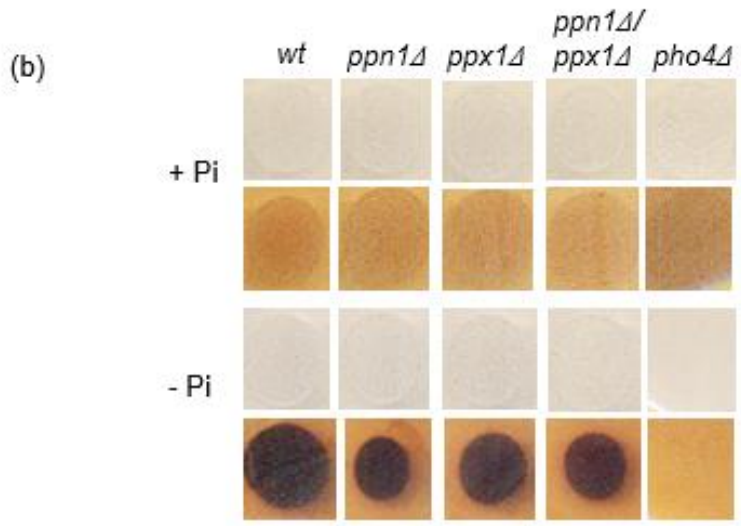

Figure 4.6. Prevention of polyP mobilisation impacts on PHO pathway activation.
(a) RT-qPCR analysis showing fold induction of Pho4 target genes *PHO84* and *PHO100* following growth in YPD – Pi for 16 h (-Pi), compared to cells after 10 mM Pi was added and grown for a further 2 h (+Pi). Transcript levels were measured relative to the internal *ACT1* mRNA control and normalized to the level of transcript in Wt cells +Pi. Means and standard deviations are shown for three biological replicates. The data were analysed statistically using ANOVA with post-Dunnett's test for multiple comparisons: *, $P < 0.05$; **, $P < 0.01$. **(b)** Secreted acid phosphatase assay. Cells were grown to mid-log before being diluted back to an OD660=0.5 and spotted onto PNMC plates (**P**eptone, **N**aCl, **M**gSO_4, **C**aCl_2) with plus or minus 10 mM Pi. Plates were then incubated for 24 hours at 30^0C. Soft agar containing I-napthyl-phosphate and Fast blue salt was poured over plates and incubated at 30^0C for 30 minutes. Red staining of colonies indicates presence of secreted acid phosphatase activity. N=3.

4.2.5 Cells lacking both polyphosphatases have a severe morphological defect

During the investigation into polyP mobilisation in *C. albicans*, morphological defects were observed especially in cells lacking both Ppn1 and Ppx1 (Figure 4.7a). Cells lacking the polyphosphatases appear larger than wild type cells, with *ppn1Δ/ppx1Δ* cells also often forming swollen pseudohyphae like cells. The reintegration of either *PPN1* or *PPX1* into the double *ppn1Δ/ppx1Δ* mutant partially rescued the cellular morphology defects (Figure 4.7.a). These morphological defects can also be seen in earlier images; in the Neisser stained cells in Figures 4.2 and 4.4, and in the fluorescent microscopy images in Figure 4.5. To gain a more quantitative measure of the larger size of the polyphosphatase deletion mutants compared to wild type cells, cell volume was measured using a coulter counter. Cells were sonicated prior to analysis to negate the possible artefacts that cells clumping together may produce.

Loss of *PPN1* or *PPX1* led to a significant increase in cell volume ($p<0.05$) (Figure 4.7.b). Notably, this was dramatically exacerbated when cells lacked both enzymes. ($p<0.001$) (Figure 4.7.b).

Furthermore, cells lacking both polyphosphatases also had a slight growth defect compared to wild type cells (Figure 4.7.c); this slow growth defect was reverted to wild type by the reconstitution of either gene (Figure 4.7.c). As the majority of polyP is stored in the vacuole, it was investigated whether prevention of polyP mobilisation would result in altered vacuolar morphology. Using the vacuolar marker dye CMAC, microscopy revealed that a proportion of *ppn1Δ/ppx1Δ* cells had highly expanded vacuoles (Figure 4.7.d). Such expanded vacuoles tended to be associated with those cells displaying highly abnormal morphologies (Figure 4.7d). Vacuole volume is implicated in cell cycle control in *C. albicans* (Barelle *et al*., 2003), and therefore the expanded vacuoles seen in some *ppn1Δ/ppx1Δ* cells may contribute to their morphological defects, and slower growth rate.

Recently, work in *S. cerevisiae* has shown that polyP levels dip during the S phase of the cell cycle. Furthermore, loss of Ppn1 and Ppx1 leads to a delay in progression through the G1/S phase of the cell cycle which correlates with impaired deoxyribonucleotide (dNTP) production (Bru *et al*., 2016). These findings support a model whereby the synthesis of dNTPs required for DNA replication is supported by the liberation of Pi from polyP stores. However, the morphological defects of *ppn1Δ/ppx1Δ* cells prevented obtaining a synchronous population (via centrifugal elutriation) to investigate whether cells unable to mobilise polyP had an S phase delay. Hence, it was alternatively asked whether *ppn1Δ/ppx1Δ* cells were sensitive to the DNA replication stress. This was investigated by using hydroxyurea (HU) which inhibits ribonucleotide reductase (RNR) which synthesises the dNTPs necessary for replication (Koç *et al*., 2004). Cells lacking both polyphosphatases were extremely sensitive to HU and this sensitivity was rescued by reintegration of either *PPN1* or *PPX1* (Figure 4.8.a). Notably, this was under Pi replete conditions. Furthermore, the sensitivity of *ppn1Δ/ppx1Δ* cells was only observed in response to HU-mediated replication stress as oppose to other genotoxic stresses the DNA alkylating agent methyl methanesulfonate (MMS) or UV light (Figure 4.8.a). It was next explored whether cells lacking polyP would also show sensitivity to DNA stress. However, no sensitivity to HU was observed in *vtc4Δ* cells (Figure 4.8.a). Thus, suggesting that an inability to liberate Pi from polyP, rather than synthesise, polyP, results in replication stress sensitivity. It is noteworthy,

that in *C. albicans* it has been reported that a variety of genotoxic stresses including replication stress induce filamentous growth via the significant elongation of the daughter bud (Bachewich *et al*., 2005; Shi *et al*., 2007). Thus, it was examined whether in *ppn1Δ/ppx1Δ* cells HU-induced hyperpolarised bud growth was impacted. Consistent with previous results (Bachewich *et al*., 2005; Shi *et al*., 2007), following HU exposure, wild type cells formed extensive filaments (Figure 4.8.b). However, in response to HU, compared to wild type cells, *ppn1Δ/ppx1Δ* cells displayed significantly longer filaments demonstrating a heightened response (Figure 4.8.b,c). Significantly longer filaments in *ppn1Δ/ppx1Δ* cells may be linked to acute sensitivity of such cells to HU, attributed to a delay in S phase progression.

Dependent upon environmental cues *C. albicans* can exist as yeast, pseudohyphal or hyphal cells. Of particular interest is the switch from yeast to hyphae as it has been shown to be a key virulence determinant (Carlisle *et al*., 2009). Given the dramatic morphological defects of the polyphosphatase mutants it was investigated whether this impacted on serum-induced filamentation. Cells lacking either *PPN1* or *PPX1* were found to switch from yeast to hyphae, akin to wild type cells, with germ tube formation clearly evident following a one hour incubation at 37^0C in the presence of 10% serum, with hyphae formation after two hours (Figure 4.9.a). Strikingly, serum-induced filamentation was impaired in cells lacking both *PPN1* and *PPX1* (Figure 4.9.a). Whilst there is the presence of some pseudo-hyphal and hyphal cells in *ppn1Δ/ppx1Δ* cells, these cell types are present irrespective of the amount of time incubated with 10 % serum at 37^oC (Figure 4.9.a). The reconstitution of *ppn1Δ/ppx1Δ* cells with either *PPN1* or *PPX1* completely reversed the defect in morphological switching (Figure 4.9.a). Next it was explored whether polyP mobilisation was required for serum induced filamentation as this could explain the impairment in *ppn1Δ/ppx1Δ* cells. However, in wild type cells polyP was not found to be significantly mobilised in response to incubation at 37^0C in the presence of 10% serum (Figure 4.9.b).

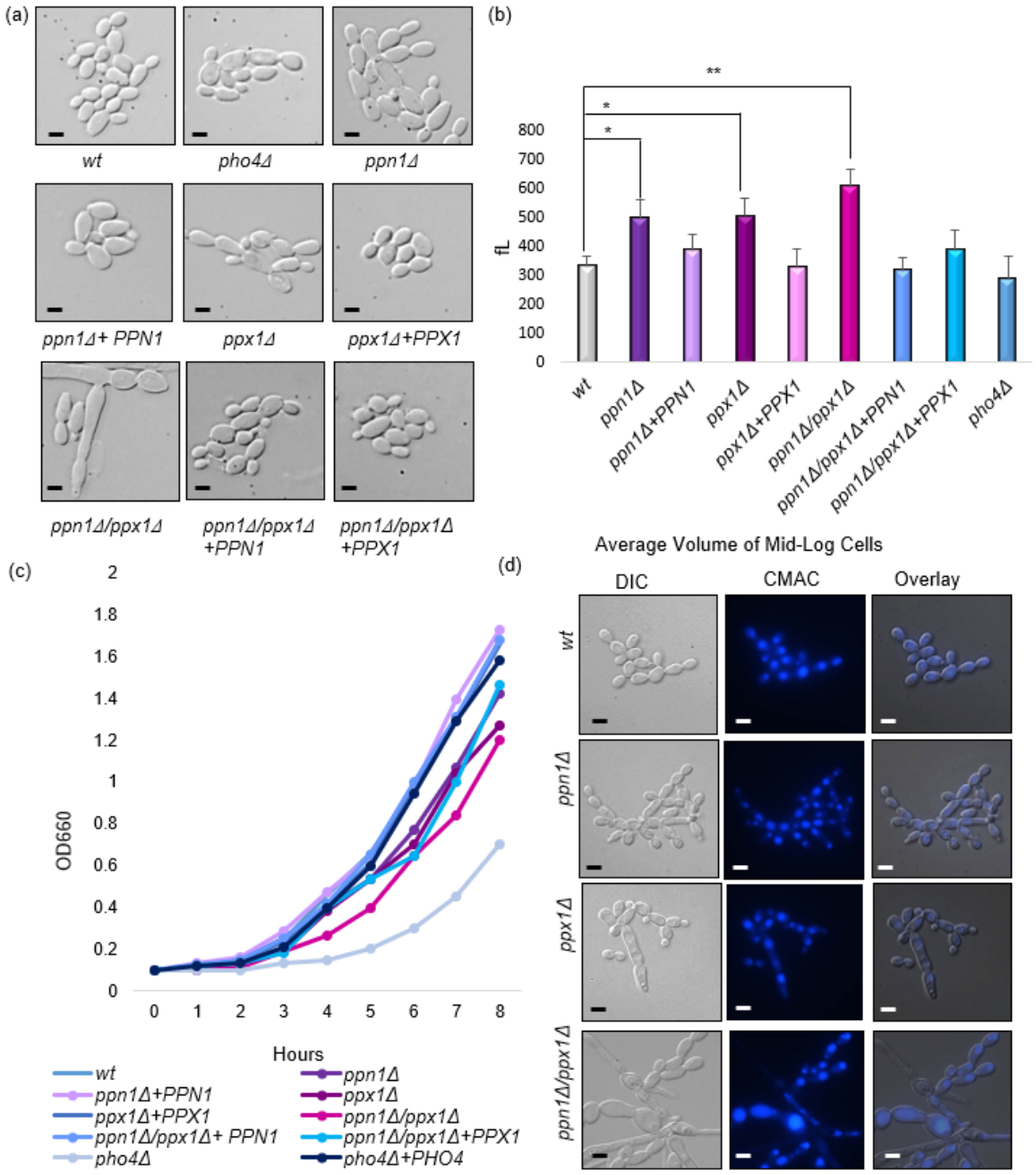

Figure 4.7. Cells lacking both polyphosphatases have a severe morphological defect. **(a)** Cells were grown to mid-log phase before being fixed with Paraformaldehyde. DIC images at 63X objective were taken on a Zeiss microscope. Scale bar is 10 microns. N=3. **(b)** Cells were grown to mid-log phase before being sonicated for 5 seconds and undergoing analysis on a coulter counter. Analysis showing the mean ± SD. Statistical analysis was performed using the student's two sample t-test: *, $P < 0.05$; **, $P < 0.01$. N=3. **(c)** Growth curve of wt, ppn1*Δ, ppn1Δ+PPN1, ppx1Δ, ppx1Δ+PPX1, ppn1Δ/ppx1Δ, ppn1Δ/ppx1Δ+PPN1, ppn1Δ/ppx1Δ+PPX1, pho4Δ* and *pho4Δ+PHO4* grown for 8 hours in YPD. Graph is representative of n=2. **(d)** Vacuolar staining of *wt, ppn1Δ, ppx1Δ* and *ppn1Δ/ppx1Δ* mid-log cells with 10 mM 7-amino-4-chloromethylcoumarin (CMAC). Images were taken using a 63X objective on a Zeiss microscope. Scale bar is 10 microns.

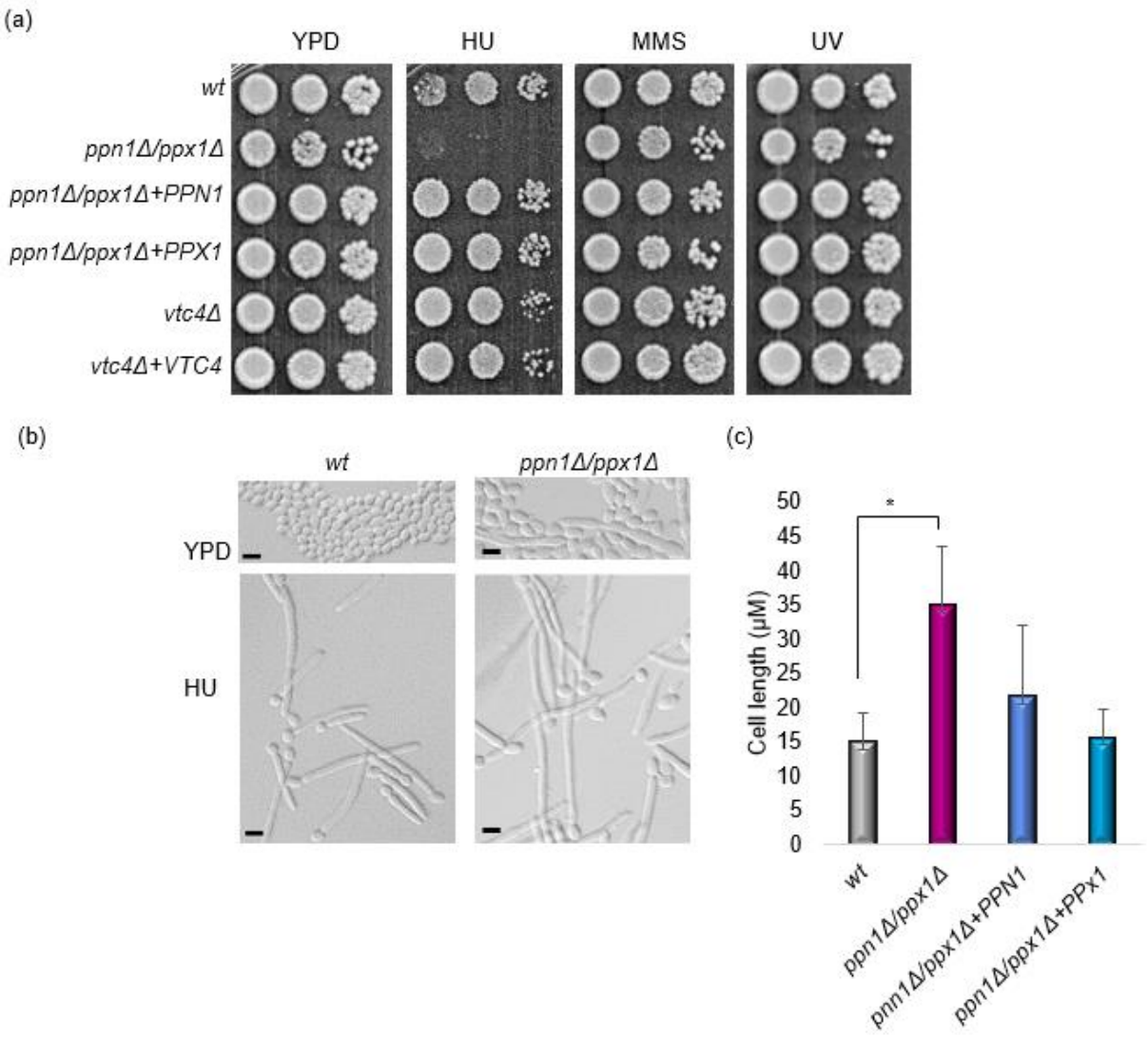

Figure 4.8. PolyP mobilisation is required for the response to replication stress.
(a) Mid-log cells were spotted in serial dilutions onto YPD plates containing 30 mM HU, 0.02% MMS and 75 J/m^2 UV and incubated for 24-48 hours. N=3. **(b)** Cells were grown in YPD prior to the addition of 40 mM HU for 4 hours. Cells were fixed with paraformaldehyde and images were taken using a 63X objective on a Zeiss microscope. Scale bar is representative of 10 μM and is the same for each image. **(c)** 200 cells for each strain were measured using Zeiss Imaging software. Analysis showing the mean ± SD. Statistical analysis was performed using the student's two sample t-test: *, $P < 0.05$. N=3.

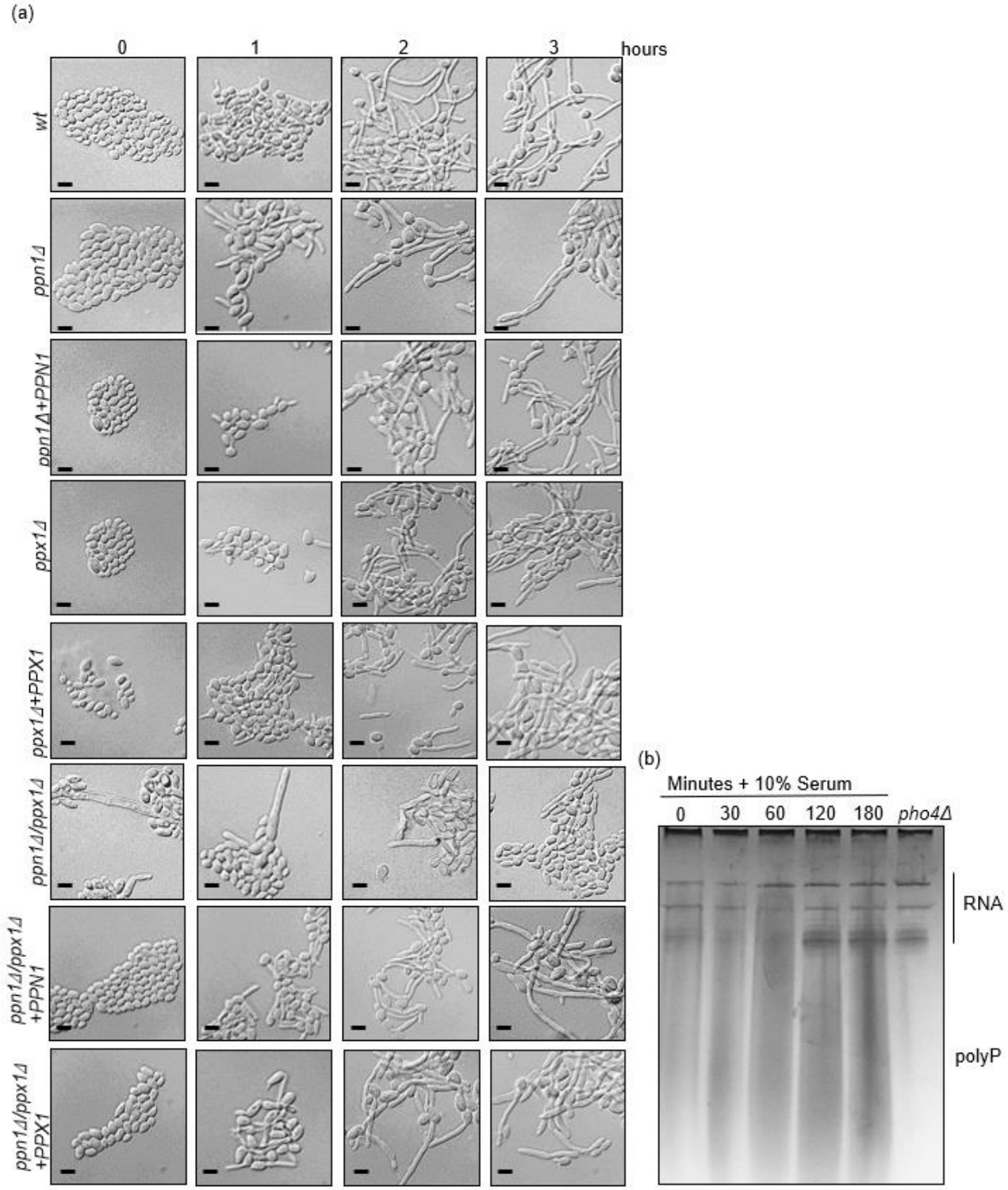

Figure 4.9. The formation of hyphae is impaired in cells lacking both polyphosphatases. **(a)** Overnight cultures were diluted back 1/10 into YPD supplemented with 10% FCS are incubated for 3 hours at 180 rpm at 37^0C. At each hourly time point 10 mL of cells were fixed with paraformaldehyde. DIC images were captured at 63X objective on a Zeiss microscope. N=3. **(b)** UREA-Page gel of RNA and polyP extracted from the indicated strains taken at 0, 30, 60, 120 and 180 minutes following incubation at 37^0C in the presence of 10% FCS. 20ug of RNA was loaded per sample. Gels were stained with 0.05% toluidine blue. N=2.

4.2.6 PolyP mobilisation is required for virulence

4.2.6.1 PolyP plays a role in virulence in Caenorhabditis elegans

Given that preventing polyP mobilisation led to a defect in the yeast to hyphae switch and a level of sensitivity to cationic and superoxide stresses, both of which are encountered during phagocytosis; the effect of preventing polyP mobilisation on *C. albicans* virulence was investigated. To begin addressing this, the invertebrate model host *Caenorhabditis elegans* was used. Previous studies have successfully used the *C. elegans* model to investigate *C. albicans* virulence, based on results showing that strains which are less successful in establishing an infection in *C. elegans* also have attenuated virulence in a murine model (Pukkila-Worely *et al*., 2011). Furthermore, when fed live *C. albicans* versus heat-killed *C. albicans*, *C. elegans* rapidly succumbs to infection (Pukkila-Worely *et al*., 2011). Strikingly, the survival of *C. elegans* was significantly extended when fed with *ppn1Δ/ppx1Δ* cells as opposed to wild type cells ($p<0.0001$) (Figure 4.10). The reconstitution of *ppn1Δ/ppx1Δ* cells with either *PPN1* or *PPX1* led to a partial restoration of infectivity (Figure 4.10). This is interesting as despite the redundancy displayed by Ppn1 and Ppx1 in previous experiments these results indicate that Ppn1 and Ppx1 both contribute to *C. albicans* virulence in this model.

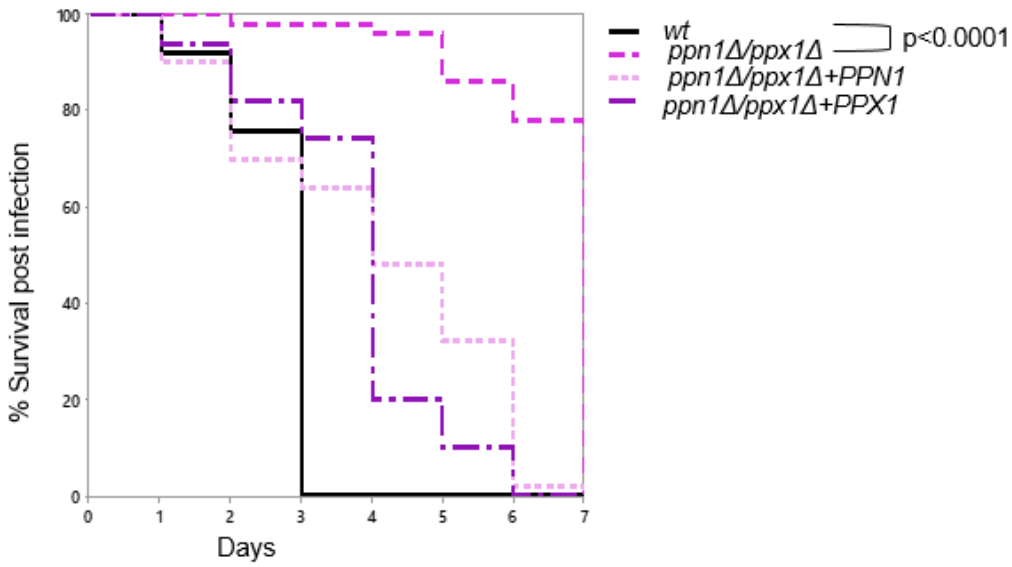

Figure 4.10. PolyP mobilisation is required for virulence in *C. elegans*.
Nematodes (3 x25 per *C. albicans* strain) were plated onto BHI plates containing either *wt, ppn1Δ/ppx1Δ*, *ppn1Δ/ppx1Δ+PPN1* and *ppn1Δ/ppx1Δ+PPX1* colonies. Survival was monitored daily. Analysis was performed using a log-rank test with a P value <0.05 considered significant. The graph is a representative of one of three biological repeats.

4.2.6.2 PolyP plays a role in virulence in Galleria mellonella

Following the *C. elegans* infection experiments, a second invertebrate mini-host was employed, the greater wax moth (*Galleria mellonella*) larvae model. This has some advantages over the *C. elegans* model, as the *G. mellonella* larvae can be incubated at 37°C, allowing virulence to be studied at a physiologically relevant temperature, and the primitive innate immune system in *G. mellonella* show similarities with the innate immune response of mammals (Chamilos *et al*., 2007). Injecting *G. mellonella* with *ppn1Δ/ppx1Δ* cells led to significantly longer survival compared to wild type cells (p<0.001) (Figure 4.11.a). All of the larvae were dead 2 days post infection with wild type *C. albicans* cells whereas no larvae had died 5 days post infection with *ppn1Δ/ppx1Δ* cells. This avirulence seen with *ppn1Δ/ppx1Δ* cells is akin to that observed with cells lacking the Pho4 transcription factor reported in chapter 3 (Figure 3.8.). Thus, both Pi acquisition (via Pho4) and mobilisation (by Ppn1 and Ppx1) promote the virulence of *C. albicans* in *G. mellonella*. Reconstitution of *ppn1Δ/ppx1Δ* with either *PPN1* or *PPX1* only partially restored infectivity to that of wild type cells (Figure 4.11.a). Thus, as seen in the *C. elegans* infection model (Figure 4.10), it appears that Ppn1 and Ppx1 function non-redundantly in promoting virulence in the *G. mellonella* infection

model. This was verified following testing of the *ppn1Δ* and *ppx1Δ* single mutants in *G. mellonella*, where loss of either *PPN1* or *PPX1* had an impact on virulence ($p<0.01$) (Figure 4.11.b).

To conclude this series of experiments, we explored the importance of polyP synthesis in mediating *C. albicans* virulence. Deletion of the polyP synthase Vtc4 did impair *C. albicans* virulence in the *G. mellonella* model ($p<0.01$), although not to the same level as that seen for *pho4Δ* and *ppn1Δ/ppx1Δ* cells (Figure 4.11c). Nonetheless, although *in vitro* experiments have not yet uncovered the roles of polyP in *C. albicans*, its presence does promote the virulence of this important human fungal pathogen.

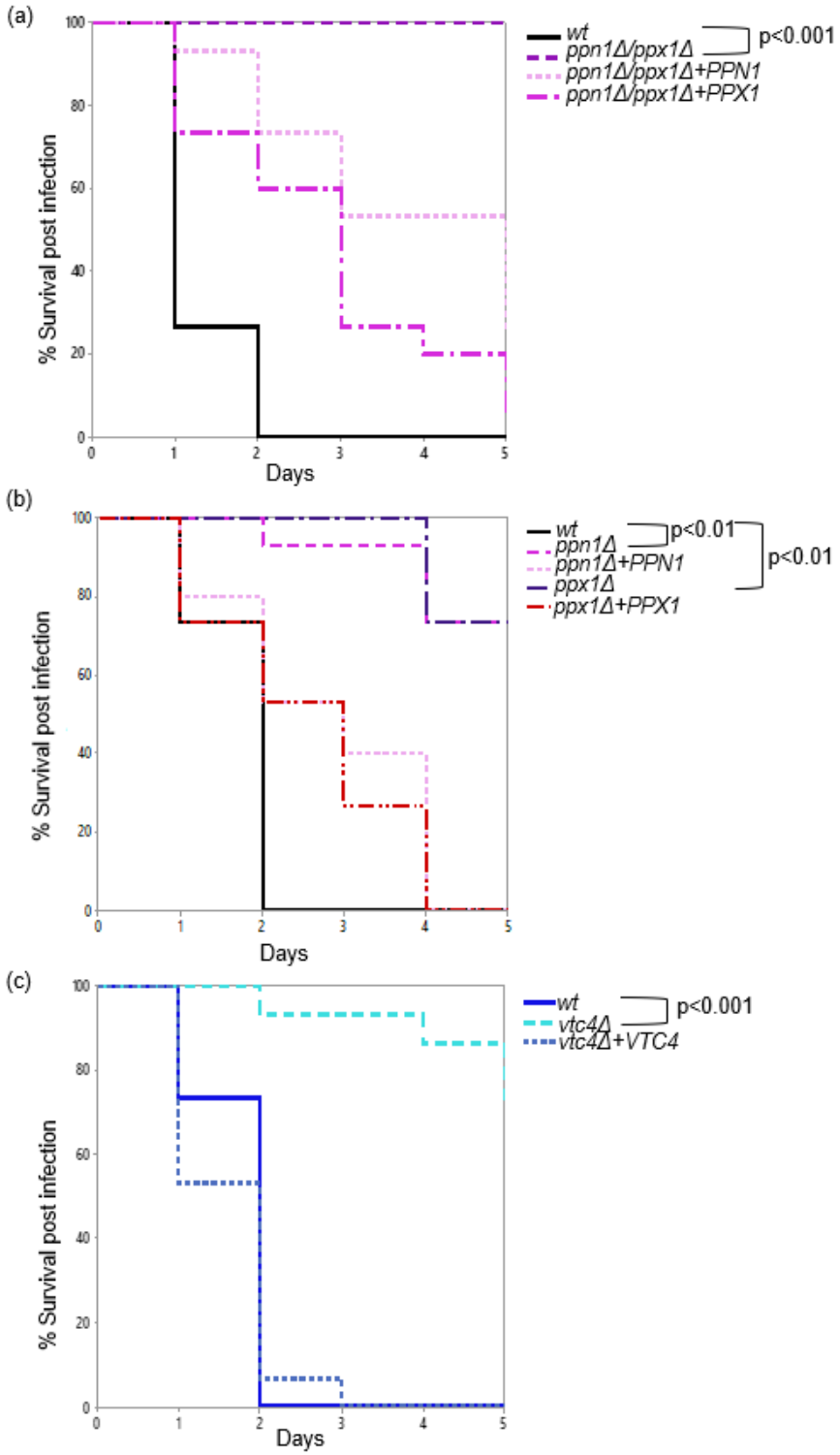

Figure 4.11. PolyP mobilisation and synthesis is required for virulence in *G. mellonella.* For each indicated strain, the left hind leg of 15 larvae was injected with 5 X 10^5 *C. albicans* cells in PBS. An additional 15 larvae were injected with only PBS as a control. Survival was monitored daily. Analysis was performed using a log-rank test with a P value <0.05 considered significant. Each graph is representative of one of three biological repeats.

4.3 Discussion

In yeast there is significantly more polyP in than in bacterial or mammalian cells (Moreno and Docampo, 2013). Yet, whilst there has been extensive work investigating polyP function in prokaryotic cells, significantly less is known about the role of polyP outside its role as a Pi storage molecule in eukaryotic cells. Indeed, very little is known regarding the role of polyP in fungal pathogens. The previous chapter provided evidence that there were some similarities in the regulation of Pi homeostasis in *C. albicans*, but also several significant deviations, when compared to *S. cerevisiae*. In this chapter, experiments have revealed that two polyphosphatase enzymes, Ppn1 and Ppx1, function redundantly to regulate polyP mobilisation in *C. albicans.* This again seems different to that in the model yeast *S. cerevisiae* (as descried below). Moreover, an extensive phenotypic characterisation of the double *ppn1Δ/ppx1Δ* mutant revealed for the first time that polyP mobilisation is needed for PHO pathway activation, and additional key roles including DNA replication, morphogenesis, and stress resistance. Consistent with these traits being important for the virulence of *C. albicans*, preventing polyP mobilisation resulted in significantly diminished virulence in two invertebrate models of infection.

The functional redundancy that exists between Ppn1 and Ppx1 in *C. albicans* was unexpected as, in *S. cerevisiae*, deletion of Ppn1 alone results in the accumulation of longer-chain polyP molecules compared to wild type cells (Azavedo *et al*., 2020). However, in *C. albicans* both Ppn1 and Ppx1 need to be deleted before an increase in polyP chain length and defects in mobilisation of polyP are seen. Although deletion of Ppn1 and Ppx1 in *C. albicans* largely prevents polyP mobilisation, there is a small amount of mobilisation seen in *ppn1Δ/ppx1Δ* cells following Pi starvation (Figure 4.2). So, what enzymes could be responsible for this? A total of four enzymes exhibiting polyphosphatase activity have been identified In *S. cerevisiae that* include Ppn2 (Gerasimaitė *et al*., 2017), and Ddp1 (Lonetti *et al*., 2011), in addition to Ppn1 and Ppx1. The *C. albicans* genome also contains homologues of Ppn2 (C7_03500W) and Ddp1 (C5_02220C), which share 29% and 49% identity to their respective *S. cerevisiae* homologues. Nonetheless, the functional redundancy that exists between Ppn1 and Ppx1 in *C. albicans* is clear; reintroduction of either *PPX1* or *PPN1* into *ppx1Δ/ppn1Δ* cells rescues the majority of phenotypes exhibited by the double mutant. As Ppx1 is predicted to be a cytoplasmic enzyme, this is particularly intriguing as the majority of polyP is stored in the vacuole.

The finding presented in this chapter that blocking polyP mobilisation impairs activation of the PHO pathway is, to the best of knowledge, a novel finding. In previous studies it had been documented that polyP mobilisation coincided with the nuclear accumulation of the Pho4 transcription factor following Pi starvation (Ikeh *et al*., 2016). It makes sense that a cell would use its Pi stores before activating acquisition pathways. However, even following sustained growth under Pi limiting conditions, no uniform nuclear accumulation of Pho4 is seen in *ppn1Δ/ppx1Δ* cells and consistent with this there appears to be a degree of impairment in the induction of Pho4-dependent genes. This indicates that polyP presence (including polyP that cannot be mobilised) may inhibit the activation of the PHO pathway. The mechanism underlying this is unknown and requires further investigation. Notably, activation of Pho4-dependent genes occurs more rapidly in cells lacking polyP in *S. cerevisiae* (Neef *et al*., 2003; Thomas *et al*., 2005), which is consistent with the overall concept that polyP presence impacts on the activation of the PHO pathway.

PolyP has been implicated in stress resistance in many prokaryotic pathogens (reviewed in Rao *et al*., 2009). Thus, it was suggested that the stress sensitive phenotypes exhibited by *pho4Δ* cells in *C. albicans* was possibly due to the absence of polyP in these cells. However, phenotypic analysis of *C. albicans vtc4Δ* cells, lacking polyP, showed essentially no overlap with the acute stress phenotypes exhibited by *pho4Δ* cells (Ikeh *et al*., 2016). The only overlapping phenotype was increased sensitivity to manganese, suggesting a function of polyP as a manganese storage reservoir. However, there is a body of literature supporting a link between polyP mobilisation and stress resistance. For example, in *Trypanosoma cruzi* polyP stores have been shown to be mobilised in response to hyper- and hyposmotic stress (Ruiz *et al*., 2001). Furthermore, in *S. cerevisiae*, it has been shown that an increase in pH triggers the rapid utilisation of intracellular polyP stores (Castro *et al*., 1995). Relevant to this work, it was also reported that in *C. albicans* polyP stores are also rapidly mobilised in response to alkaline stress, and following cationic stress (Ikeh *et al*., 2016). Furthermore, as work in this chapter has also found that blocking polyP mobilisation impairs Pho4 activation, this would also indicate that Ppn1 and Ppx1 have stress protective roles. Indeed, the results presented in this chapter show that during Pi limiting conditions, cells lacking both polyphosphatases Ppn1 and Ppx1 are sensitive to a number of Pho4-dependent stresses, perhaps most notably alkaline stress. However, *pho4Δ* cells are much more stress-sensitive than *ppn1Δ/ppx1Δ* cells. This could be due to the fact that *pho4Δ* cells have significantly

lower Pi levels than wild type cells (Ikeh *et al*., 2016), whereas the residual polyphosphatase activity in *ppn1Δ/ppx1Δ* cells will release some Pi. This, together with the observation that there is a very low level of induction of Pho4-dependent genes in *ppn1Δ/ppx1Δ* cells, may explain why *pho4Δ* cells are more acutely sensitive to stress. With regard to alkaline stress, there is strong evidence in *S. cerevisiae* and *C. albicans* that this stress triggers a Pi starvation response resulting in the nuclear accumulation of Pho4 (Serreno *et al*., 2002; Ikeh *et al*., 2016). It has been suggested that this could be due to the fact that the major high-affinity Pi transporter, Pho84, is a H+/Pi symporter, and is therefore barely active at alkaline pH (Serra-Cardona *et al*., 2015).

In this chapter it was also found that cells unable to mobilise their polyP have an inherent morphological defect. Both single *ppx1Δ* and *ppn1Δ* mutants are larger than wild type cells, which is intensified in the double mutant where large swollen pseudohyphal cells are often observed. Such morphological defects may be due in part to delays in cell cycle progression. In *S. cerevisiae*, PHO pathway genes have been shown to be specifically induced during M phase coinciding with a decrease in intracellular polyP levels in *S. cerevisiae* (Neef and Clade, 2003). More recently it was shown that polyP mobilisation mediated by the polyphosphatases, Ppn1 and Ppx1 is important for the Pi demanding process of dNTP synthesis and normal S-phase progression in *S. cerevisiae* (Bru *et al*., 2016). It is noteworthy, that in *S. cerevisiae*, cells lacking the endopolyphosphatase Ppn1 have a growth defect due to a cell cycle defect (Ogawa *et al*., 2000). Complimentary to this, in *C. albicans* cells lacking the Pho4 transcription factor have an up-regulation in genes involved in the cell cycle as well as DNA damage, metabolism and repair (Ikeh *et al*., 2016). Thus, it is plausible that the morphological defects exhibited in *C. albicans* cells lacking *PPN1* and *PPX1* is due to a cell cycle defect. Possibly the strongest evidence supporting this is the acute sensitivity of *ppn1Δ/ppx1Δ* cells to grow on HU which blocks dNTP synthesis. However, unlike a recent study in *S. cerevisiae* which demonstrated that the enzymes, Ppn1 and Ppx1 were needed for the DNA damage response (Bru *et al*., 2017), cells lacking both these polyphosphatases in *C. albicans* were exclusively sensitive to HU and not the other tested cell cycle and genotoxic stresses. A further morphological defect exhibited by *ppn1Δ/ppx1Δ* cells was the inability of the strain to switch from yeast to hyphae, one of the key virulence determinants of *C. albicans;* suggesting polyP plays a role in this process. PolyP mobilisation does not appear to be stimulated during the yeast to hyphae transition thus the inability of *ppn1Δ/ppx1Δ* cells

to form true hyphae may, instead, be linked to the cell cycle/morphological defects characteristic of this mutant. It is noteworthy, that in the fungal pathogen of maize, *Ustilago maydis* its ability to grow as a filament has been attributed to polyP (Boyce *et al*., 2006).

Regarding polyP and microbial virulence, polyP has been extensively linked to virulence in a variety of bacterial human pathogens (Rashid *et al*., 2000; Candon *et al*., 2008; Grillo-Puertas *et al*., 2012; Varas *et al*., 2018). In eukaryotic pathogens, whether polyP plays a role in virulence is more ambiguous. Although there is a significant reduction in disease in wheat infected with *U. maydis* cells lacking *VTC4* compared to wild type cells (Boyce *et al*., 2006). Similarly, work presented in this chapter shows that *VTC4* is needed to establish wild type levels of infection in *G. mellonella*. However, in the human fungal pathogen, *C. neoformans*, whereas Pi acquisition via Pho4 is important for virulence, cells lacking *VTC4* were no different than wild type in their ability to survive or colonise a murine model of Cryptococcosis (Kretschmer *et al*., 2014). Similarly, mutation of the polyphosphatase orthologues of Ppn1 and Ppx1 in *C. neoformans*, Eep1 and Xpp1, did not impact on macrophage uptake or survival (Kretschmer *et al*., 2014). However, this study shows that in *C. albicans,* cells lacking *PPN1* and *PPX1* were severely impacted in their ability to establish an infection in *C. elegans* and *G. mellonella.* This is consistent with the findings described above of how preventing polyP mobilisation significantly impairs important pathogenesis traits in this important fungal pathogen, including PHO pathway activation and the yeast to hyphal switch, which likely contribute to the virulence defect in *ppn1Δ/ppx1Δ* cells. Indeed, the PHO pathway targets, *PHO84* and *PHO100,* which are down-regulated in *ppn1Δ/ppx1Δ* cells both contribute to *C. albicans* virulence (Liu *et al*., 2018; MacCallum *et al*., 2009). Thus, this chapter adds to a growing body of evidence that Pi homeostasis is important for the pathogenesis of *C. albicans*, a major fungal pathogen of humans.

Chapter 5: Exploiting our Knowledge of the PHO pathway in the Quest for New Antifungals

5.1 Introduction

Invasive candidiasis is a global health issue, with an estimated ~700,000 infections per year (Bongomin *et al*., 2017). Moreover, infections caused by *C. albicans* are now recorded as the main hospital acquired fungal infection accounting for ~15% of all recorded sepsis cases (Nobile and Johnson, 2015). However, there is a limited arsenal of effective antifungals and little interest in the development of new drugs from pharmaceutical companies (Lee *et al*., 2020).

Currently there are only three classes of antifungals licensed for the treatment of systemic fungal infections; azoles, echinocandins and polyenes (Odds *et al*., 2003; Brown *et al*., 2012). There are issues with all three of these classes, for example the nephrotoxicity associated with polyenes, the species-dependent efficacy of the echinocandins, and the growing emergence of azole resistant isolates (Sharpio *et al*., 2011). In addition, the recent emergence of the multi-drug resistant *Candida auris* pathogen in 2009 poses a serious threat (Jeffery-Smith *et al*., 2018). Clearly there is an unmet clinical need for new antifungals. However, a major constraint in antifungal drug development is the limited number of druggable targets due the evolutionary relationship between host and fungal pathogen (Fuentefria *et al*., 2017). A further hurdle is the length of time drug development takes. For example, the development of echinocandins took 30 years from discovery to licence, highlighting the time and challenges it takes to bring novel antifungal compounds to the clinic (Roemer and Krysan, 2014).

Traditional antifungal drug screens rely on the screening of compounds for those which prevent fungal growth using OD based methods (Roemer and Krysan, 2014). The speed and efficiency of this method has been facilitated by the development of high-throughput screening (Lee *et al*., 2020). A recent approach taken to improve antifungal therapies is a combinational approach, in which compounds are identified that act synergistically with existing antifungals. For example, the fluconazole resistance of clinical *C. albicans* isolates is reported to be overcome when co-treated with an indole derivative (Youngsaye *et al*., 2012). The targeting of fungal virulence factors has also been proposed as an attractive antifungal

strategy which could be used in combination with traditional antifungal drugs (Lee *et al*., 2020).

Pi homeostasis has been identified as an important virulence determinant in both *C. albicans* and *C. neoformans* (Ikeh *et al*., 2016; Lev *et al*., 2017; Kretschmer *et al*., 2014). Previous work in *C. albicans* found that the Pho4 transcription factor, a key regulator of Pi acquisition, promotes virulence in a range of infection models (Ikeh *et al*., 2016). In response to Pi limitation, Pho4 accumulates in the nucleus where it regulates the induction of a suite of genes involved in Pi acquisition such as secreted acid phosphatases including Pho100, and the high affinity Pi transporter Pho84. Notably, such targets of Pho4 have also been found to contribute to the virulence of *C. albicans* (Liu *et al*., 2017; MacCallum *et al*., 2009). Cells lacking Pho4 also display a range of stress sensitive phenotypes, to stresses encountered following phagocytosis such as superoxide and cationic stresses, and in other host niches such as alkaline pH stress (Ikeh *et al*., 2016).

The aim of this chapter is to use our knowledge of the cellular processes regulated by Pho4, to design assays amenable to high through-put screening, to allow for the screening of compound libraries to identify small molecules that prevent activation of the PHO pathway. The identification of such compounds would be an important first step in determining whether Pi acquisition can be targeted as a potential future antifungal therapy.

5.2 Results

5.2.1 Assay Development

Pi starvation triggers the Pho4-dependent secretion of acid phosphatases which scavenge extracellular Pi. It was reasoned that, as these enzymes are secreted into the media, that these should be able to be detected in cell cultures grown in Pi limiting media. Furthermore, by employing the chromogenic acid phosphatase substrate, p-nitrophenyl phosphate (pNPP), a colorimetric assay could be developed to detect secreted acid phosphatase activity. Specifically, hydrolysis of pNPP by acid phosphatases releases p-nitrophenyl (pNP), a yellow compound which can be measured spectrophotometrically at 405 nm (Figure 5.1.a). To validate the use of this assay, wild type and *pho4Δ* mutant cells were grown to logarithmic phase in phosphate replete media (PNMC + 2 mM), before being washed 3 times in Pi starvation media (PNMC-Pi). Following this, cells were seeded into 384 well plates and grown overnight in Pi starvation media. Secreted acid phosphatase production was then

detected by adding the p-nitrophenyl phosphate substrate and allowing the reaction to proceed for 20 minutes at 37^0C. The reaction was stopped by the addition of 0.2 M NaOH and readings taken at Abs 405nm.

Wild type cells grown under Pi starvation conditions secrete acid phosphatases as indicated by the yellow colour (Figure 5.1.b). This does not occur in wild type cells grown under Pi replete conditions (Figure 5.1.b). Importantly the secreted acid phosphatase seen in wild type cells following Pi starvation is entirely dependent upon the Pho4 transcription factor, as no yellow coloration is seen in the wells containing *pho4Δ* mutant cells grown under Pi limiting conditions (Figure 5.1.b).

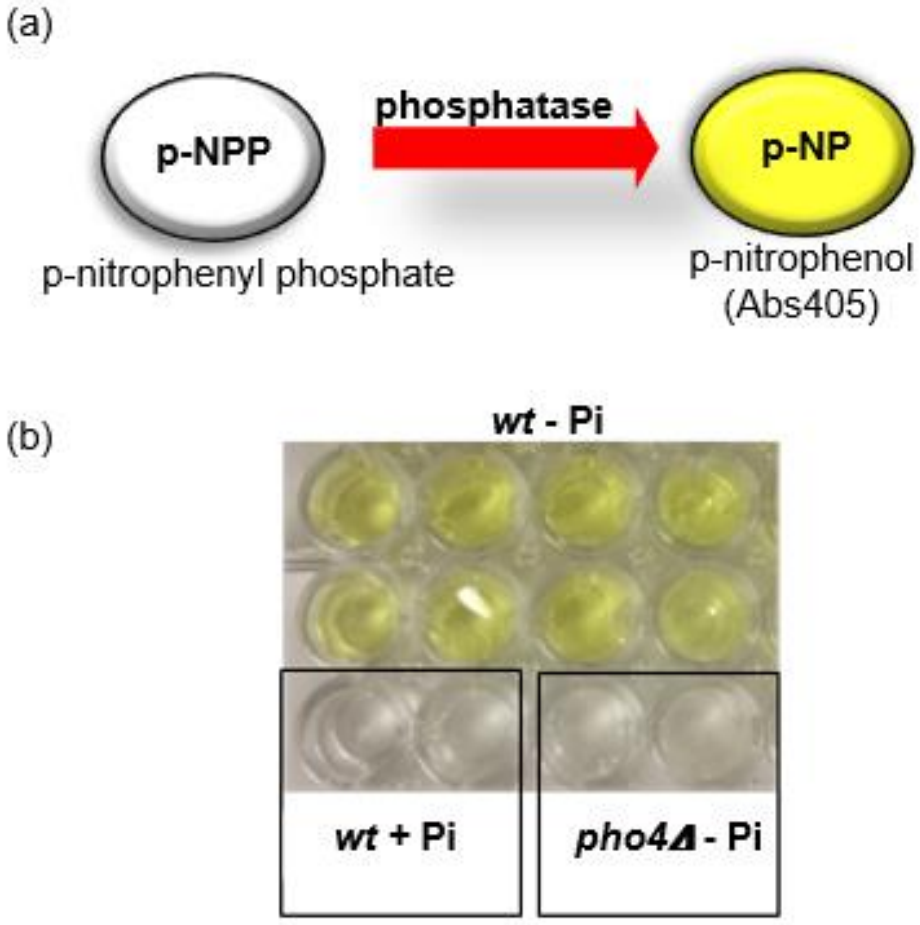

Figure 5.1. Screen of LifeArc Index Collection.
(a) The release of p-NP (yellow) from the chromogenic p-NPP substrate is used to measure acid phosphatase activity measured at an absorbance of 405 nm. **(b)** Following 16 hours Pi starvation *wt* cells secrete acid phosphatases which cleave phosphate from p-NPP releasing p-NP. This only occurs once cells are Pi starved and is dependent on Pho4.

5.2.2 Initial Compound Screen

This colorimetric assay, which allows for the detection of secreted acid phosphatases, was amenable to a high-throughput screen for compounds that inhibit this Pho4-dependent response. From LifeArc, approximately 12,000 compounds were supplied from their Index Collection which is the core subset of their largest collection (Birchall *et al*., 2018). Furthermore, approximately 5000 compounds were supplied by LifeArc from their Kinase Collection (Birchall *et al*., 2018). Both compound libraries were screened together using the secreted acid phosphatase assay shown in Figure 5.1 and described in section 5.2.1.

The purpose of this screen was to identify compounds which potentially inhibited Pi acquisition using secreted acid phosphatase production as a read-out. The criteria for successful hits were those which prevented secreted acid phosphatase activity, but which did not impact significantly upon growth. The rationale behind this was that previous screens of the Index collection will have focused on identifying compounds which are fungicidal. The concept here is to identify compounds that prevent processes necessary for virulence (in this case Pi acquisition) but not growth *in vitro,* and thus will not have been identified in previous screens.

Wild type cells were prepared as described in section 5.2.1 and added to 384 well plates, each well of which was seeded with a compound at 100 µM concentration. Following incubation overnight, production of pNP was recorded at 405 nm and cell growth was recorded by measuring the OD_{600}. Abs_{405} and OD_{600} measurements were compared to those obtained with wild type cells treated with DMSO, the carrier used for the compounds. Screening of the compound libraries was repeated four times.

From the 17,000-compound screen, hits which successfully matched the criteria of inhibiting secreted acid phosphatase activity, but not growth, are highlighted in green (Figure 5.2). The majority of compounds had no impact on growth or secreted phosphates activity and are indicated as black spots (Figure 5.2). A small number of compounds which impacted growth, but not secreted acid phosphatase activity are shown in blue, and those which impacted both growth and secreted acid phosphatase are shown in red (Figure 5.2). To select which compounds to take forward, two lists were created; one of compounds in the lowest 6% for growth, and one of compounds in the lowest 6% for secreted acid phosphatase activity. Compounds were selected which were identified in the bottom 2.5% of Abs_{405} but which

were not in the bottom 6% for growth. From this, 296 compounds that inhibited secreted acid phosphatase activity, but not growth, were taken forward for further analysis (shown in green in Figure 5.2).

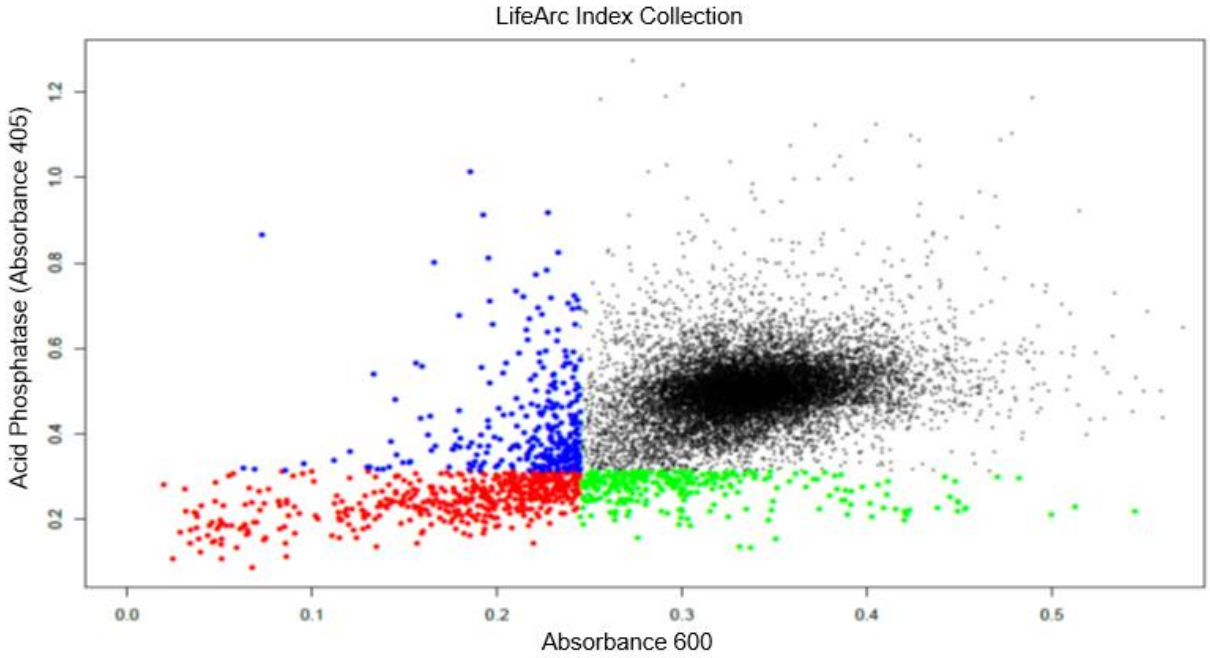

Figure 5.2. Screen of the 17,000 LifeArc Index Collection.
The screen of the compound library is plotted OD_{600} vs. OD_{405}. Most compounds did not impact on growth or secreted acid phosphatase activity and are shown as black spots. Red hits represent compounds that inhibit growth or are fungicidal. Blue hits represent those which affected growth but not secreted acid phosphatase activity. Green hits represent the compounds which did not affect growth but inhibited secreted acid phosphatase activity.

5.2.3 Concentration validation screen

As the original screen was performed using 100 µM of each drug, the next stage was to investigate their potency, and the ability of the selected 296 compounds to impact on secreted acid phosphatase activity at lower concentrations was measured. LifeArc supplied fresh samples of the 296 compounds to facilitate the rescreening across a range of concentrations. Validation, based on the original high-throughput screen assay, was carried out at 100 µM, 25 µM, 6.25 µM and 1.5625 µM concentrations (Figure 5.3). As no information was available for the compounds on the likely best dose, 4-fold dilutions were used. The rationale of using 4-fold dilutions, as opposed to say 10-fold, is that this gave a narrower concentration range.

Analysis of the validation screen was performed by t-test to identify compounds which resulted in a statistically significant reduction in secreted acid phosphatase activity compared to the no drug control. These compounds are shown in red in Figure 5.3. At a concentration of 100 µM, 240 compounds were identified indicating that 56 of the 296 potential hits from the original screen were not reproducible in the second screen. At a concentration of 25 µM, 204 compounds were identified as causing a significant reduction in secreted acid phosphatase activity, with 125 and 56 identified at 6.25 µM and 1.5625 µM respectively.

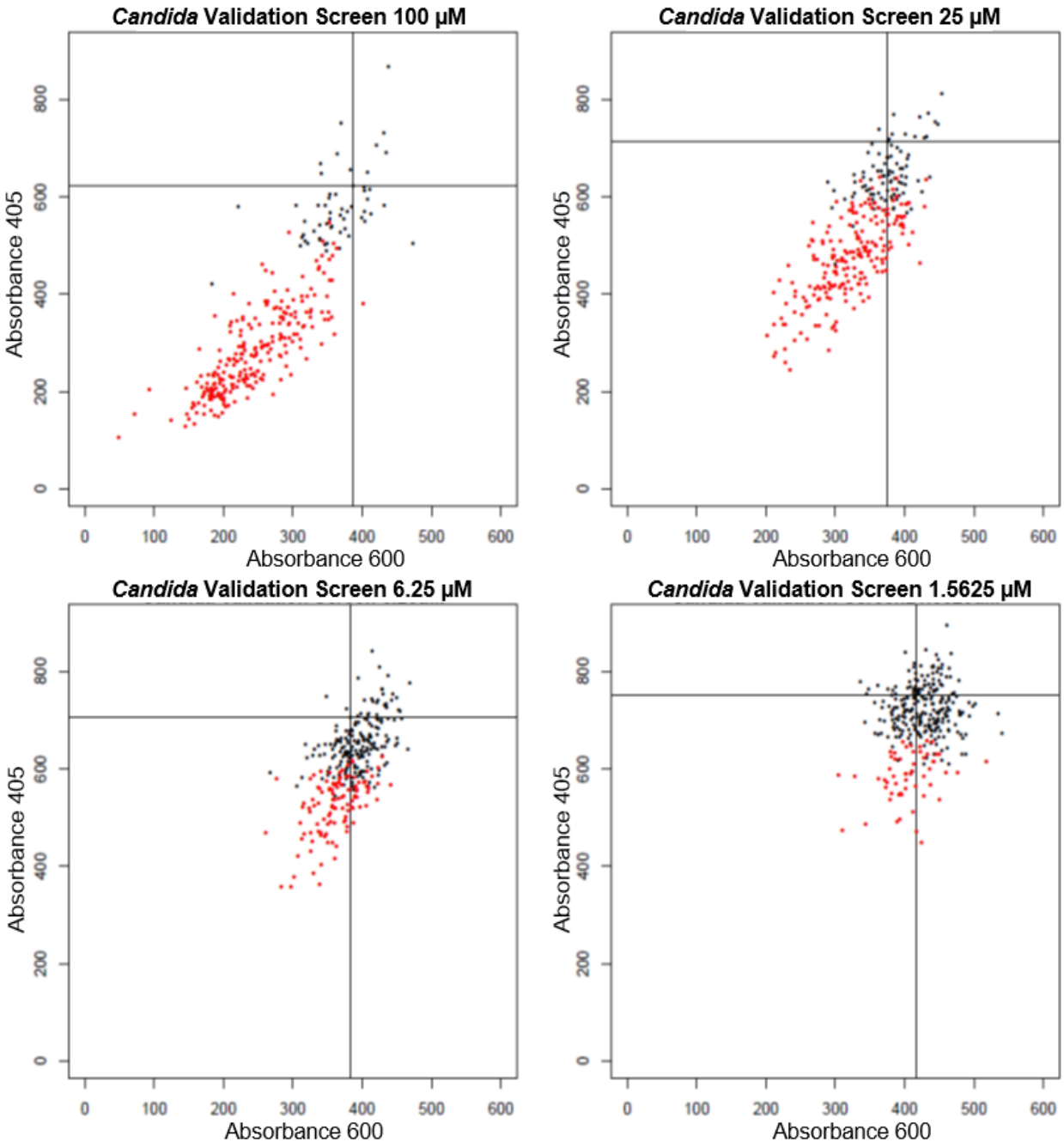

Figure 5.3. Validation of 296 prospective hits from screening the LifeArc Index Collection. Compounds found to prevent secreted acid phosphatase activity were retested at four drug concentrations;100 µM, 25 µM, 6.25 µM and 1.5625 µM using the colorimetric secreted acid phosphatase assay. Compounds which reduced the OD_{405} secreted acid phosphatase reading compared to the no drug control are represented by red hits. Black lines represent the reference readings of wild type cells treated with no compound.

5.2.4 Cluster Analysis

Following repetition of the primary screen with the selected compounds over a range of concentrations, LifeArc undertook a cluster analysis of compounds. This was carried out for those compounds that displaying reduced secreted acid phosphatase activity over at least 3 concentrations. From this, it was found many of the identified compounds were associated with reasonable size clusters – 97 actives fell into 29 clusters sized 2-9 (Table 5.1). This provides a level of confidence in the findings as multiple compounds from the same chemical cluster inhibit secreted acid phosphatase activity. However, although LifeArc provided a cluster analysis, detailing which cluster each active belongs to, there is no information given regarding the chemical structure or known activities of each cluster.

Cluster, No of actives
1, 9
2, 7
3, 7
4, 6
5, 5
6, 5
7, 4
8, 4
9, 4
10, 3
11, 3
12, 3
13, 3
14, 3
15, 3
16, 2
17, 2
18, 2
19, 2
20, 2
21, 2
22, 2
23, 2
24, 2
25, 2
26, 2
27, 2
28, 2
29, 2

Table 5.1. Analysis of clusters which have more than one compound that inhibits secreted acid phosphatase activity.

5.2.5 Secondary screen; impaired growth at alkaline pH

In *C. albicans*, cells unable to acquire Pi due to inactivation of Pho4 are sensitive to a pleiotropy of stresses including alkaline pH (Ikeh *et al*., 2016). The aim here was to perform a secondary screen on validated compounds found to inhibit secreted acid phosphatase activity (Figure 5.3), to see if they also prevented growth under alkaline pH conditions. The expectation was that if the compounds prevented acid phosphatases secretion, by inhibiting Pho4 function, then such compounds would also inhibit growth under alkaline pH conditions. Briefly, cells were grown to logarithmic phase in YPD before being washed 3

times in YPD pH 8 media, diluted, and then seeded into a 384 well plate containing either 100 µM, 25 µM, or 6.25 µM of compound. Plates were incubated for 16 hours then growth was recorded at OD_{600}. Wild type cells grown at pH 8 was used as a control. Screening was carried out on all of the 240 compounds found to be impacting secreted acid phosphatase activity but not growth validated at a compound concentration of 100 µM (Figure 5.3). This was conducted whilst awaiting the cluster analysis from LifeArc. Screening was repeated four times.

To analyse the high-throughput alkaline pH growth screen, the effect of compounds on the growth of wild type cells when grown at pH 8 was plotted against the growth of wild type cells under alkaline conditions with no compounds and a regression line fitted. A regression line was also fitted for wild type growth at OD_{600} versus secreted acid phosphatase activity OD_{405}. The distance from these regression lines was used as a measure of the effect of the compound on either secreted phosphatase activity or growth at pH 8. The same analysis was then carried out for 25 µM and 6.25 µM of compound. Figure 5.4 shows the validation screen plotted of growth of wild type cells at pH8 (OD_{600}) versus secreted acid phosphatase activity (OD_{405}) for a compound concentration of 100 µM. Highlighted in red are the compounds which were found to have an impact across 100 µM, 25 µM and 6.25 µM of compound. Graphs showing how compounds in each cluster behave are presented in the appendix.

This analysis yielded 22 top hits which did not impact on growth in unbuffered YPD and had the most potent impact on secreted acid phosphatase activity and growth at pH 8 across three concentrations. From this, 13 compounds (Table 5.2.) were taken forward based on compound availability. It is noteworthy that of the 13 compounds two belong to cluster 2 and three belong to cluster 8 both of which appear as promising clusters as have multiple active hits present. MRT00222573 from cluster 51 and MRT00233511 from cluster 114 were not identified by LifeArc as multiple active compound hit clusters (Table 5.1). However, as both were identified by the analysis as being in the 22 top hits they were included.

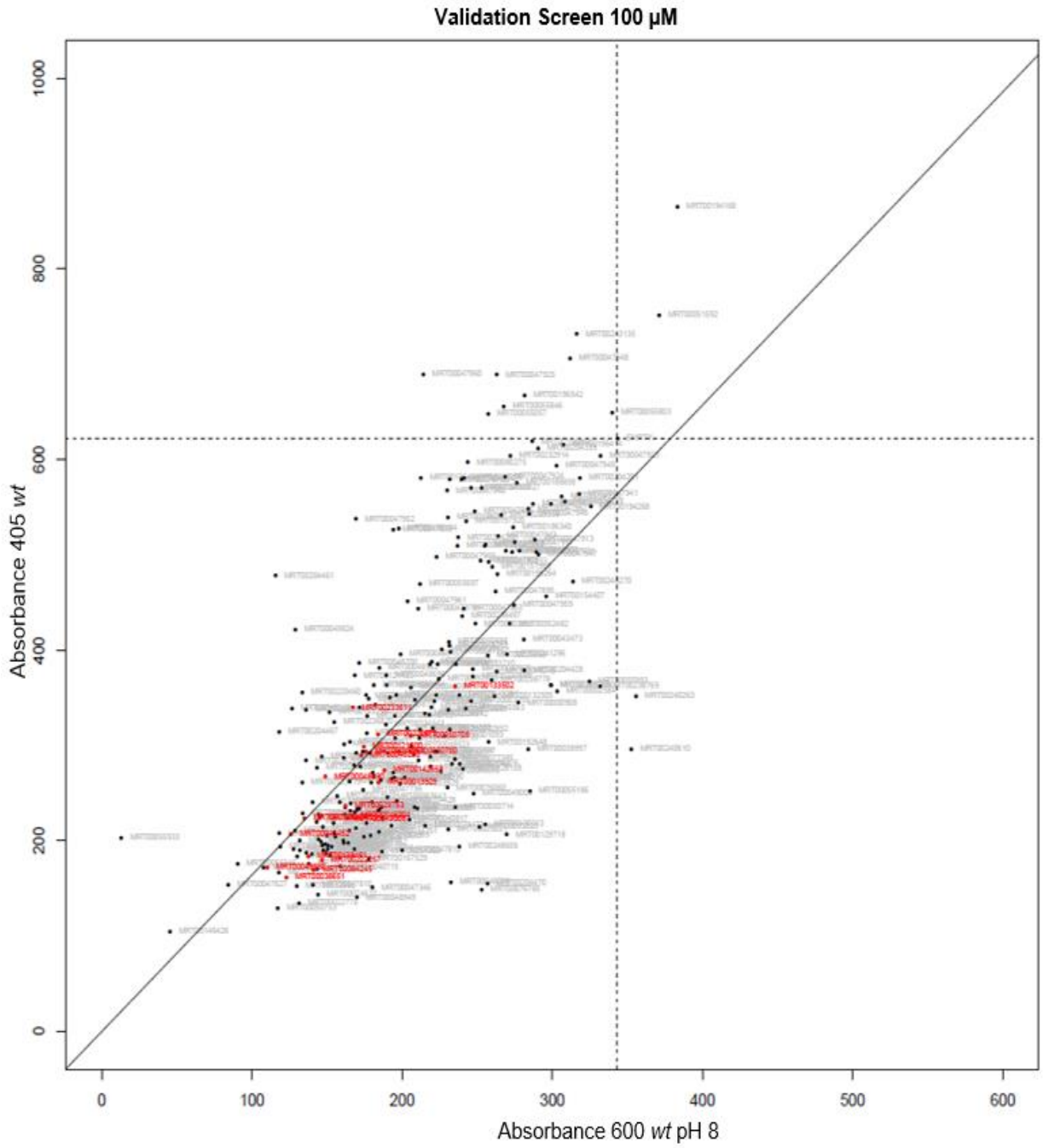

Figure 5.4. 100 µM Secondary Screen: pH8 as a readout for PHO Pathway activity.
Plot of OD_{600} *wt* cells grown in pH 8 vs. OD_{405} of *wt* cells. Cells were grown to log phase in YPD before being washed 3 times in pH8 media and diluted back to OD_{600} = 0.05 then seeded into 384 well plates containing 100 µM of compound. Absorbance of 600 nm is used for growth at pH and 405 for secreted acid phosphatase activity. Red hits represent those which, following analysis, displayed a reduction in secreted acid phosphatase activity and impaired growth at pH8 over multiple concentrations.

Compound Name	Cluster
MRT00048290	1
MRT00049860	2
MRT00050700	2
MRT00048690	4
MRT00043452	7
MRT00048264	8
MRT00049008	8
MRT00050708	8
MRT00046004	11
MTR00038651	15
MRT00015946	21
MRT00222573	51
MRT00233511	114

Table 5.2. Top Drug Hits.

5.2.6 Investigating whether the top screen hits prevent Pho4 nuclear accumulation

To explore further whether the top 13 compounds identified by the pH 8 screen were directly targeting the PHO pathway, the impact of the compounds on Pho4 nuclear accumulation was investigated. Following Pi starvation, Pho4 translocates to the nucleus where it up-regulates genes involved in Pi acquisition (Ikeh *et al*., 2016). Wild type cells expressing Pho4-GFP were grown to mid-log then diluted back to OD_{600}= 0.1, or washed 3 times in -Pi media and diluted back in OD600= 0.1 in -Pi media. Cells were then grown for 16 hours in the presence of 100 µM compound in dimethyl sulfoxide (DMSO), or DMSO as a no-drug control, before being fixed and imaged. An additional control was provided by the inclusion of a drug which had been shown in the initial compound screen to have no effect on either growth or secreted acid phosphatase activity (Figure 5.5).

Uniform nuclear Pho4 accumulation was observed in cells which were starved of Pi for 16 hours, without a compound present and in the presence of DMSO (Figure 5.5). Thus, the response of Pho4 to 16 hours Pi starvation was the same as previously reported (Ikeh *et al*., 2016) and none of the effects seen in the presence of a compound can be attributed to DMSO. Furthermore, growing cells in presence of the control compound MRT00057949 led to no impairment in Pho4 nuclear accumulation following Pi starvation (Figure 5.5).

For the compounds tested in cluster 8, nuclear accumulation of Pho4 in response to Pi starvation was prevented in cells treated with MRT00048264 but not MRT00049008 or

MRT00050708 (Figure 5.6). Moreover, treatment with MRT00048264 impacted upon cellular morphology irrespective of Pi condition (Figure 5.6). The levels of Pho4 also appeared to be increased in cells treated with MRT00048264 and MRT00049008 (Figure 5.6). For the two compounds investigated belonging to cluster 2, neither of these prevented Pho4 nuclear accumulation in response to Pi starvation (Figure 5.7). Although, in cells treated with MRT00049860 the level if Pho4 in cells appeared to be increased (Figure 5.7).

All of the other compounds investigated belong to discrete clusters. As shown in Figure 5.8, treating cells with MRT00048290 (cluster 1) did not impact upon Pho4 nuclear accumulation in response to Pi starvation. However, cells treated with this compound did display an increase in Pho4-GFP intensity and an abnormal morphology (Figure 5.8). The other compound shown in Figure 5.8, MRT00233511 (cluster 114) did not prevent Pho4 nuclear accumulation in cells in response to Pi starvation. Neither did treating cells with a cluster 4 compound MRT00048690 (Figure 5.9). However, treating cells with MRT00043452 (cluster 7) prevented Pho4 nuclear accumulation. Furthermore, it also impacted on the level of Pho4 and morphology, both irrespective of Pi condition (Figure 5.9). Cells treated with MRT00046004 (cluster 11) or MTR00038651 (cluster 15) prevented Pho4 nuclear accumulation as well as impacting upon the level of Pho4 and morphology of the cell (Figure 5.10). Treating cells with MRT00015946 (cluster 21) prevented Pho4 nuclear accumulation in response to Pi starvation as well as impacting morphology and level of Pho4 within the cell (Figure 5.11). However, treating cells with MRT00222573 (cluster 51) had no impact (Figure 5.11). From Pho4 localisation analysis, 5 compounds were found to inhibit Pho4 nuclear accumulation in response to Pi starvation (Table 5.3) and match all of the hit criteria (Figure 5.12). Taken together, the results suggest that five of the compounds may directly target the PHO pathway and thus warrant further investigation.

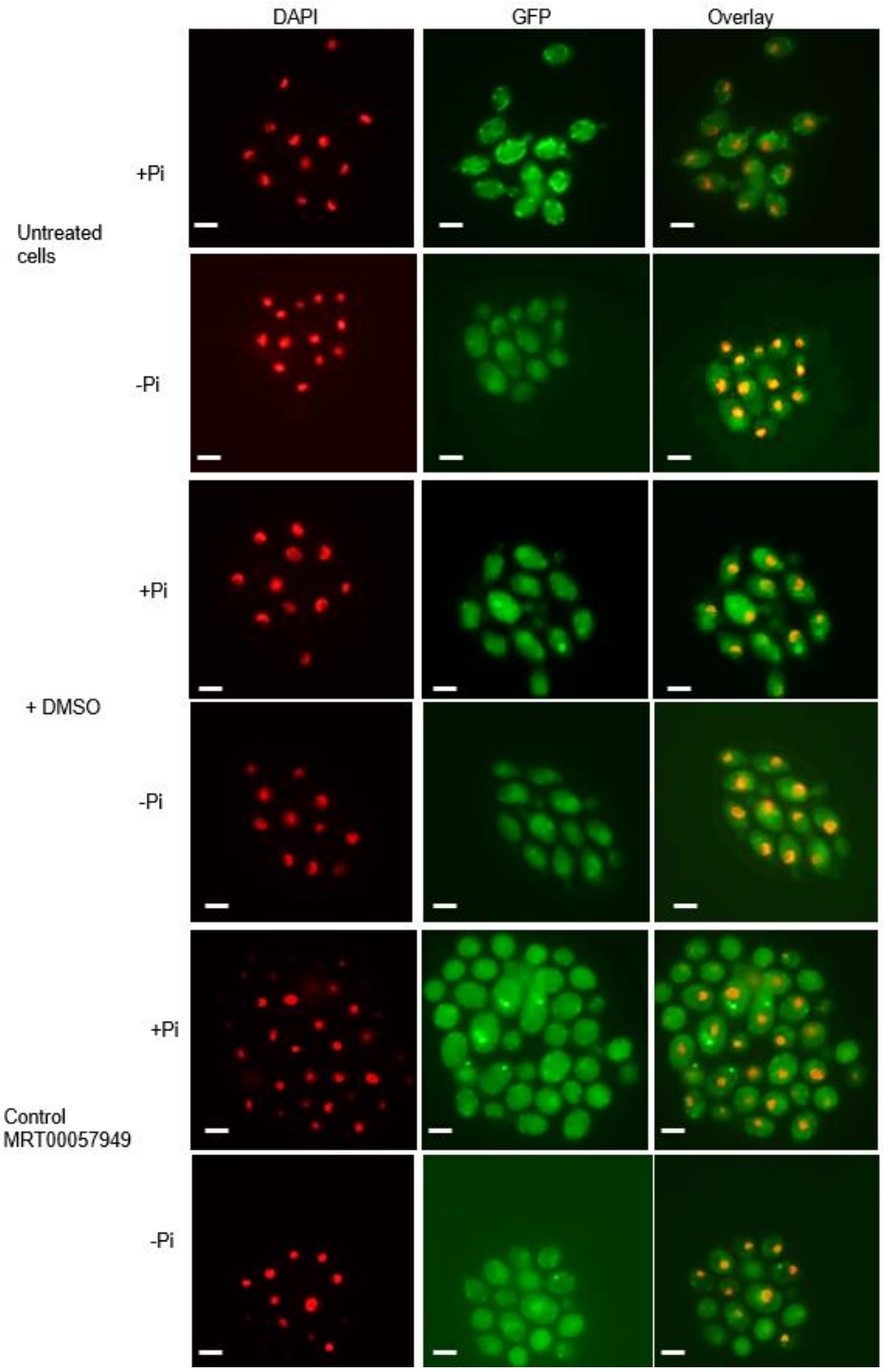

Figure 5.5. Controls for investigating whether the top drug hits are preventing PHO pathway activation.

Cells expressing Pho4-GFP were grown in YPD-Pi for 16 hours in the presence of 100 µM of the indicated compounds before being fixed with paraformaldehyde. Images were captured on a fluorescent microscope with a 63X objective. Nuclear staining by DAPI is represented by the colour red and GFP by the colour green. Scale bar = 10 µM. N=2.

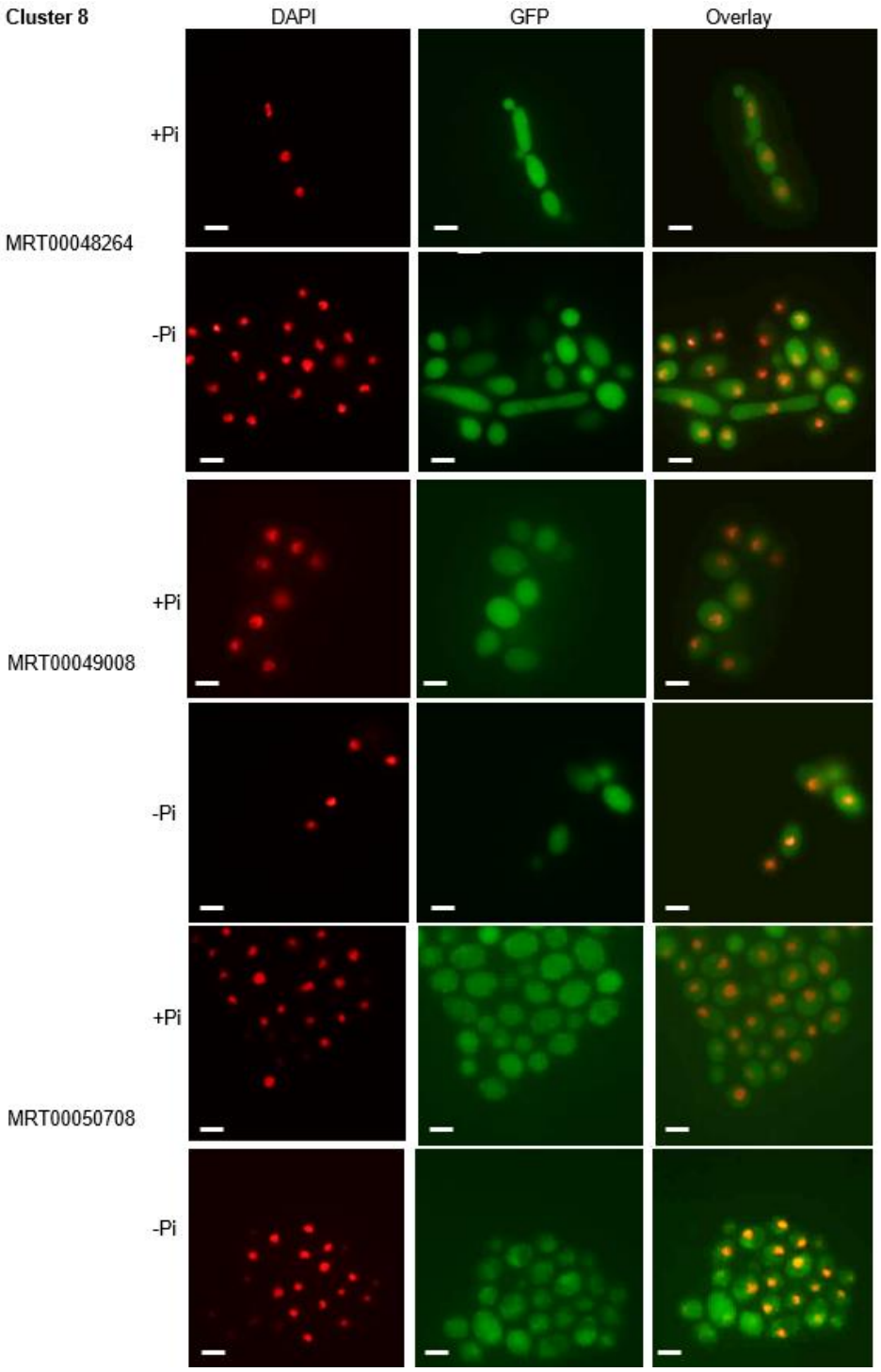

Figure 5.6. Investigating whether the top drug hits from cluster 8 are preventing PHO pathway activation.

Cells expressing Pho4-GFP were grown in YPD-Pi for 16 hours in the presence of 100 µM of the indicated compounds before being fixed with paraformaldehyde. Images were captured on a fluorescent microscope with a 63X objective. Nuclear staining by DAPI is represented by the colour red and GFP by the colour green. Scale bar = 10 µM. N=2.

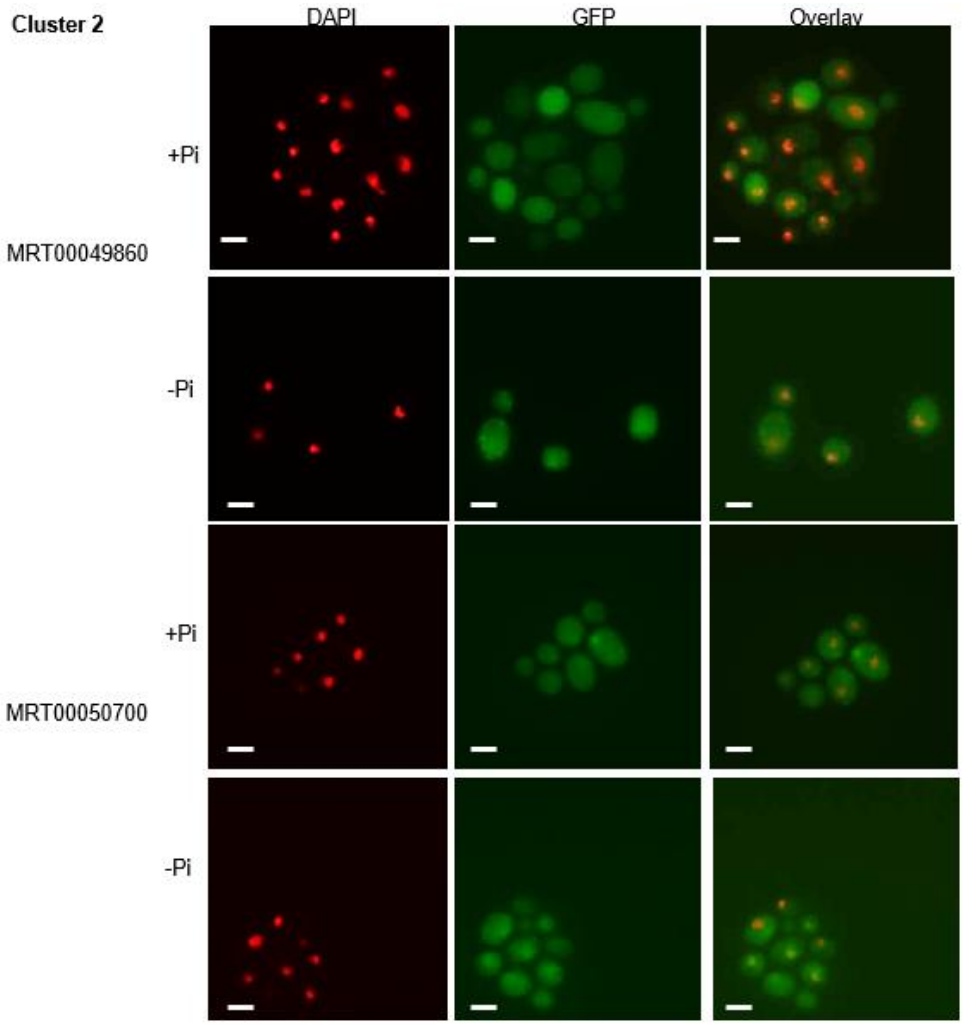

Figure 5.7. Investigating whether the top drug hits from cluster 2 are preventing PHO pathway activation.

Cells expressing Pho4-GFP were grown in YPD-Pi for 16 hours in the presence of 100 µM of the indicated compounds before being fixed with paraformaldehyde. Images were captured on a fluorescent microscope with a 63X objective. Nuclear staining by DAPI is represented by the colour red and GFP by the colour green. Scale bar = 10 µM. N=2.

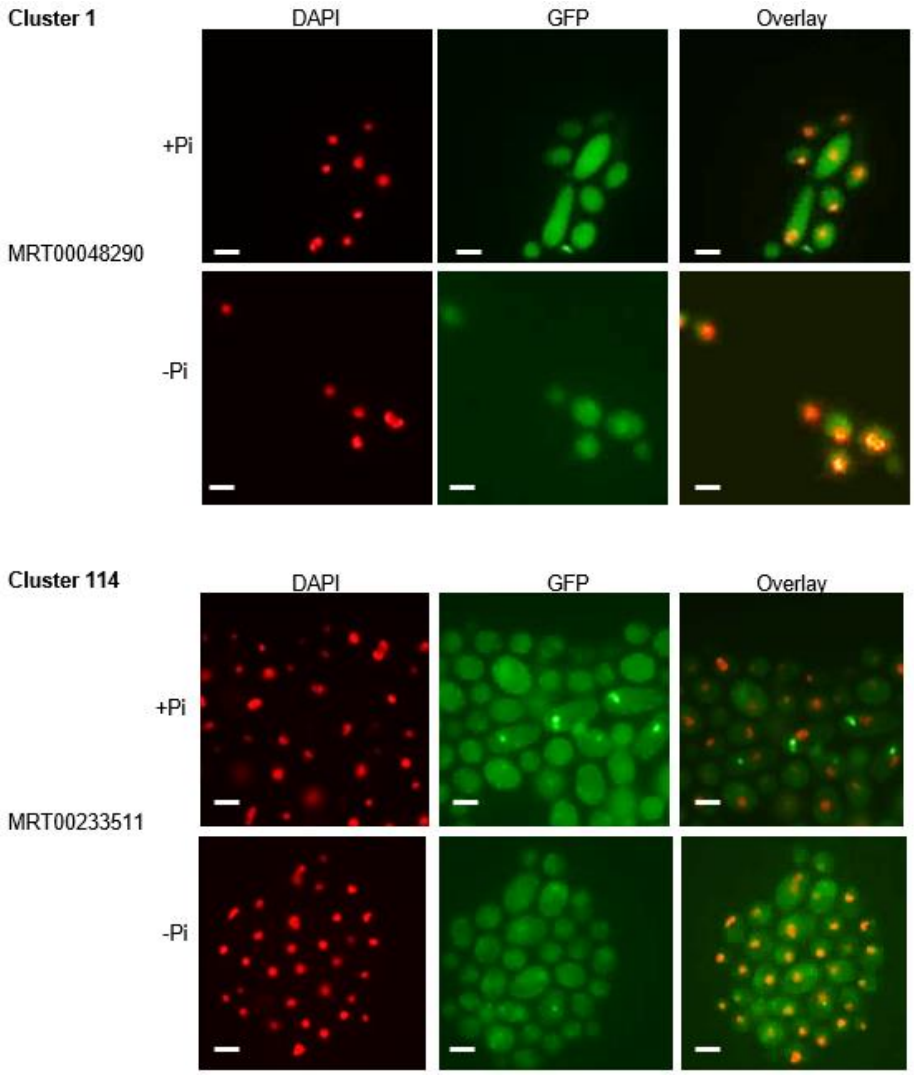

Figure 5.8. Investigating whether the top drug hits from clusters 1 and 114 are preventing PHO pathway activation.

Cells expressing Pho4-GFP were grown in YPD-Pi for 16 hours in the presence of 100 µM of the indicated compounds before being fixed with paraformaldehyde. Images were captured on a fluorescent microscope with a 63X objective. Nuclear staining by DAPI is represented by the colour red and GFP by the colour green. Scale bar = 10 µM. N=2.

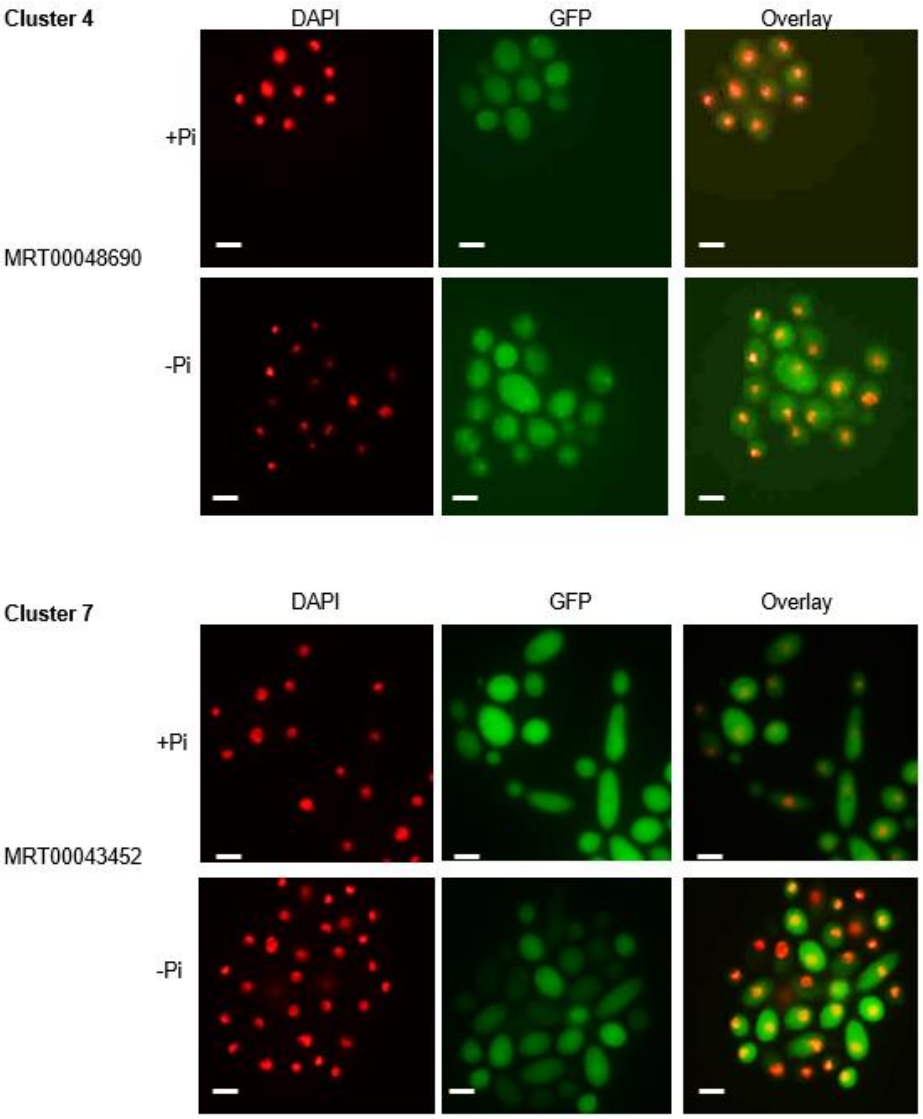

Figure 5.9. Investigating whether the top drug hits from clusters 4 and 7 are preventing PHO pathway activation.

Cells expressing Pho4-GFP were grown in YPD-Pi for 16 hours in the presence of 100 µM of the indicated compounds before being fixed with paraformaldehyde. Images were captured on a fluorescent microscope with a 63X objective. Nuclear staining by DAPI is represented by the colour red and GFP by the colour green. Scale bar = 10 µM. N=2.

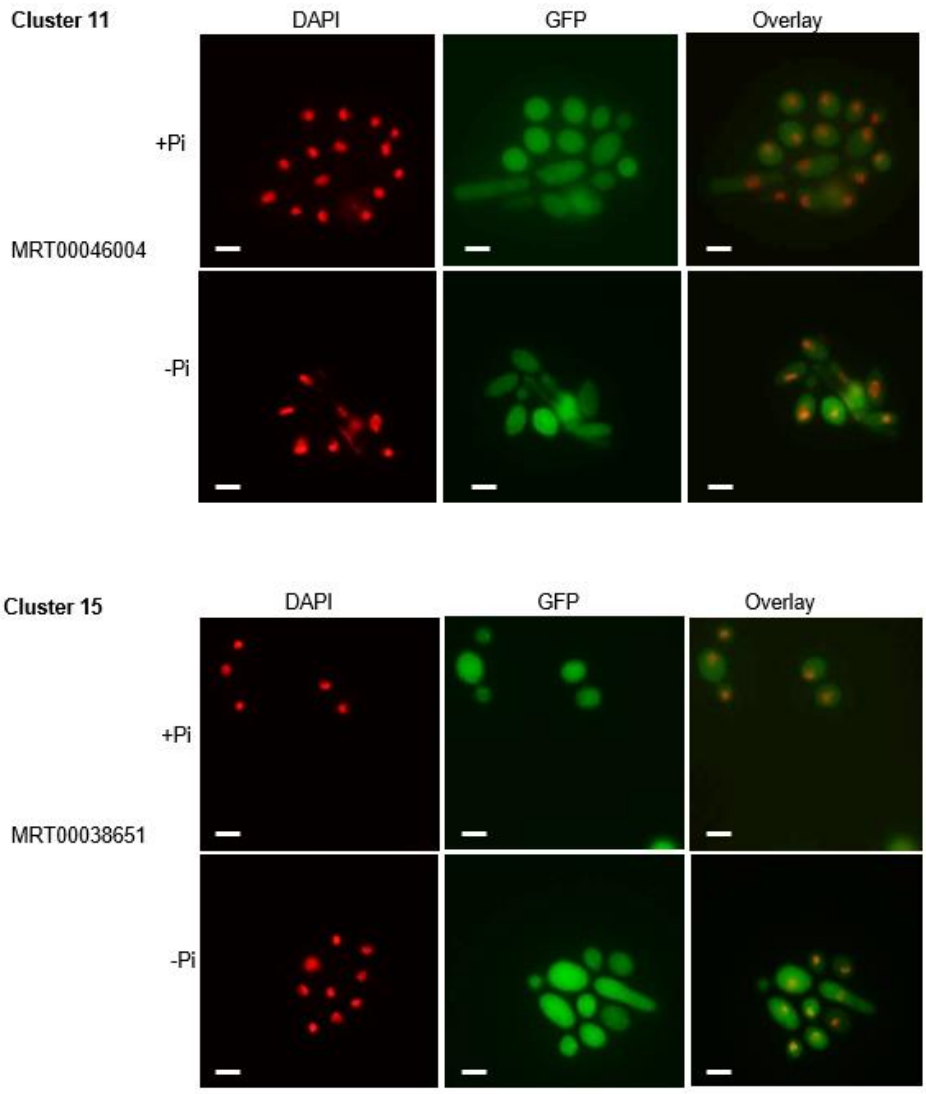

Figure 5.10. Investigating whether the top drug hits from clusters 11 and 15 are preventing PHO pathway activation.

Cells expressing Pho4-GFP were grown in YPD-Pi for 16 hours in the presence of 100 µM of the indicated compounds before being fixed with paraformaldehyde. Images were captured on a fluorescent microscope with a 63X objective. Nuclear staining by DAPI is represented by the colour red and GFP by the colour green. Scale bar = 10 µM. N=2.

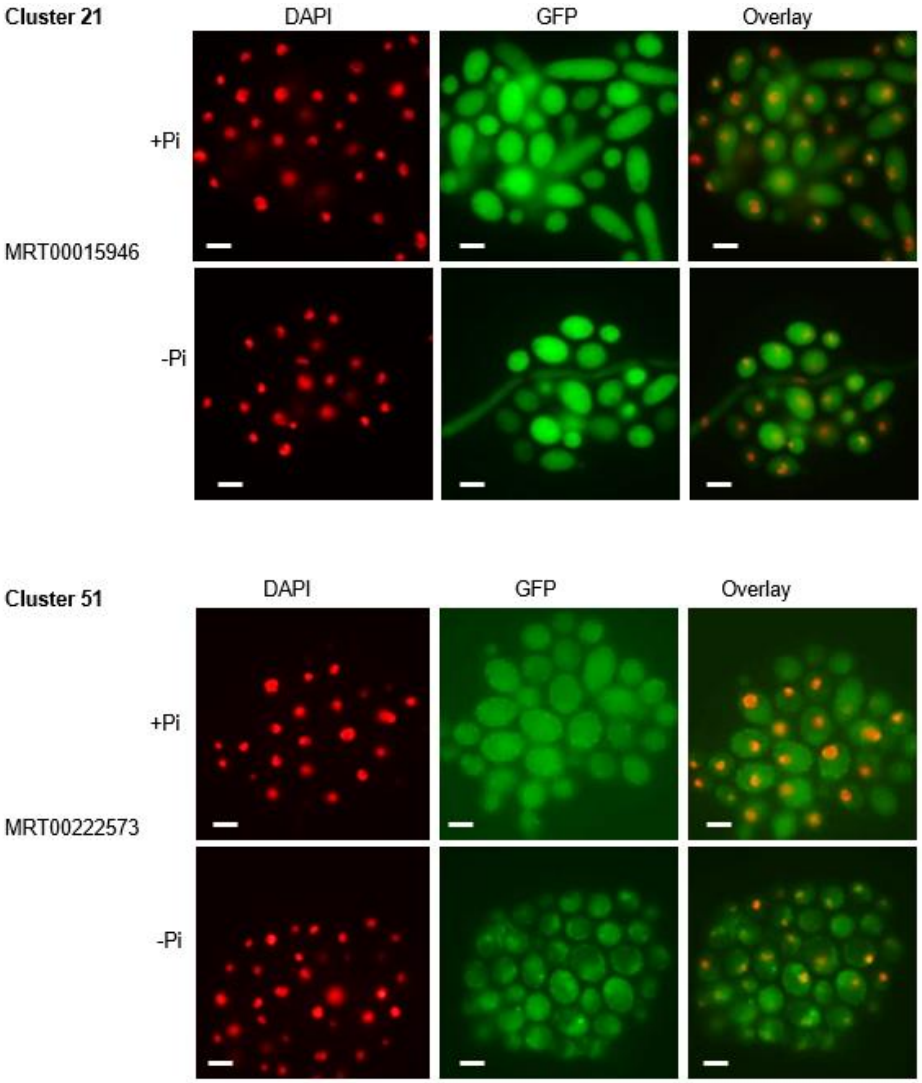

Figure 5.11. Investigating whether the top drug hits from clusters 21 and 51 are preventing PHO pathway activation.

Cells expressing Pho4-GFP were grown in YPD-Pi for 16 hours in the presence of 100 µM of the indicated compounds before being fixed with paraformaldehyde. Images were captured on a fluorescent microscope with a 63X objective. Nuclear staining by DAPI is represented by the colour red and GFP by the colour green. Scale bar = 10 µM. N=2.

Compound Name	Cluster	Pho4 Nuclear Accumulation in Response to Pi Starvation	Cell Morphology	Pho4 Levels
MRT00048290	1	Yes	Impacted	Increased
MRT00049860	2	Yes	No impact	Varied
MRT00050700	2	Yes	No impact	No impact
MRT00048690	4	Yes	No impact	No impact
MRT00043452	7	No	Impacted	Increased
MRT00048264	8	No	Impacted	Increased
MRT00049008	8	Yes	No impact	Varied
MRT00050708	8	Yes	No impact	No impact
MRT00046004	11	No	Impacted	Increased
MTR00038651	15	No	Impacted	Increased
MRT00015946	21	No	Impacted	Increased
MRT00222573	51	Yes	No impact	No impact
MRT00233511	114	Yes	No impact	No impact

Table 5.3. The impact of compounds on Pho4 localisation.

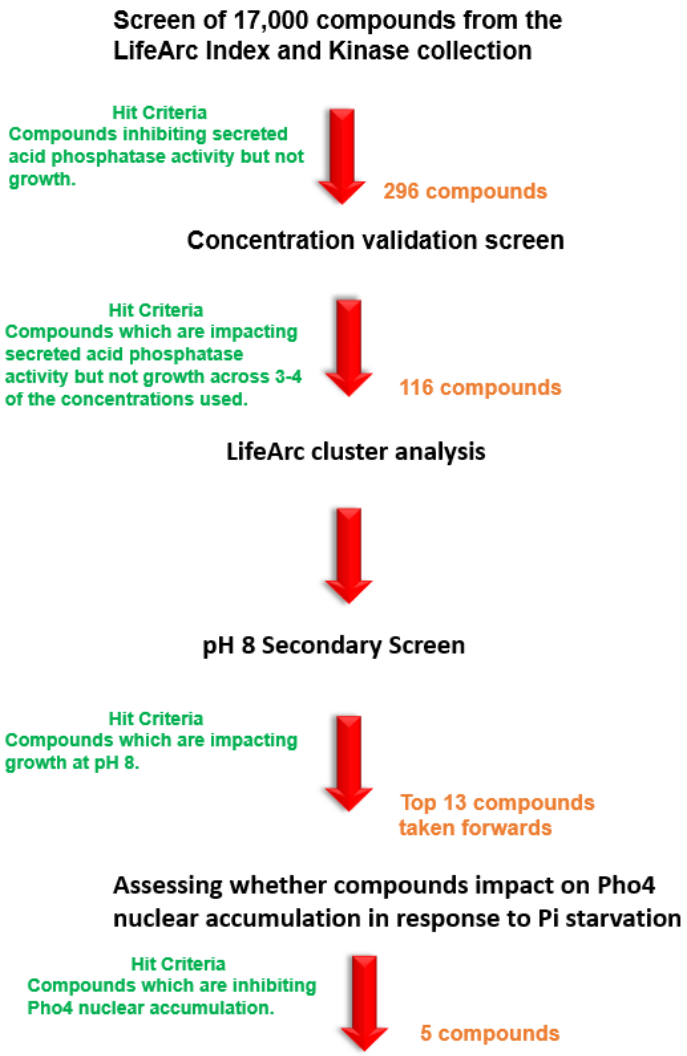

Figure 5.12. Flow Chart of Drug Screen Stages.

5.3 Discussion

There is a huge social and economic cost of treating invasive fungal diseases (Benedict *et al*., 2019). Furthermore, there is a limited antifungal drug arsenal available with varying levels of side effects. Woefully, the increase in drug resistance is set to exacerbate the situation further. Moreover, the current repertoire of antifungals focuses on a small number of cellular targets, mainly the cell wall and membrane (Roemer and Krysan, 2014). Given the current situation, new approaches are being investigated to identify novel antifungal compounds. Furthermore, there is a growing body of work focusing on re-purposing current drugs as antifungals as well as high throughput screening to identify compounds which can work in synergy with current antifungals.

Pi is essential for ATP, nucleic acids, membrane phospholipids and signal transduction (Jimenez *et al*., 2016). Furthermore, in fungal pathogens it has been shown that preventing a variety of Pi acquisition mechanisms impacts on virulence. For example, in *C. albicans* deletion of the genes encoding the PHO pathway transcription factor *PHO4* (Ikeh *et al*., 2016), the secreted acid phosphatase, *PHO100* (MacCallum *et al*., 2009) or the high affinity Pi transporter *PHO84* attenuates virulence (Liu *et al*., 2017). In *C. neoformans* deletion of the genes encoding the three high affinity Pi transporters (Kretschmer *et al*., 2014) or *PHO4* (Lev *et al*., 2017) lead to a reduction in virulence. This suggests that pharmacological compounds inhibiting Pi acquisition may provide novel antifungal treatments.

In humans many key aspects of the PHO pathway are not conserved. There are no human homologues of Pho4, Pho84 or the polyP synthase Vtc4 (Ikeh *et al*., 2016; Liu *et al*., 2017). It has been shown that FDA-approved drugs, phosphonoformic acid and phosphonoacetic acid can inhibit Pho84 in *C. albicans* and thus consequently indirectly inhibit TORC-1 signalling (Liu *et al*., 2017). Furthermore, both these compounds worked synergistically with the existing antifungals, micafungin, and amphotericin B (Liu *et al.*, 2017). Taken together, this suggests that the PHO pathway in *C. albicans* is an attractive druggable target.

From an initial screen of 17,000 compounds, a number were found to target secreted acid phosphatase activity. Those which were fungicidal were discarded on the basis that decreased secreted acid phosphatase activity was due to the fact cells are dead. Furthermore, screens will likely have already been conducted directly looking for fungicidal compounds from the LifeArc Index Collection and Kinase Collection (Birchall *et al*., 2018). Of the 296 compounds found to be preventing secreted acid phosphatase activity, only 204

were found to be more potent at lower concentrations. Investigating efficacy at lower concentrations is important to negate any toxic side effects more likely at higher drug levels. Future work investigating the efficacy of promising compounds as antifungals in animal models, will require compound concentration to be as low as possible. This may prove challenging given that only 56 of the identified potential compounds significantly impacted secreted acid phosphatase activity at the lowest concentration tested. Furthermore, the physiochemical properties of the compounds could lead to issues with solubility and permeability.

Compounds were further shortlisted by their ability to prevent growth at an alkaline pH and by preventing Pho4 nuclear localisation, both of which are hallmarks of PHO pathway activation (Ikeh *et al*., 2016). The secondary screen uncovered compounds which impacted on both secreted acid phosphatase activity and growth at pH 8. Analysis generated a list of 22 compounds found to have the most impact on secreted acid phosphatase activity and growth at pH 8 across all three concentrations tested (100 µM, 25 µM and 6.25 µM). Furthermore, some of the compounds initially identified as preventing secreted acid activity, were found to have no impact on a second Pho4-dependent trait examined - growth under alkaline conditions. This could be because some of these compounds may directly target secreted acid phosphatases as opposed to the PHO pathway. Furthermore, it is plausible that some of these compounds are targeting other cellular processes important for this particular read-out, such as the secretory pathway. It is, however, possible that compounds which inhibit secreted acid phosphatase, without targeting the PHO pathway, may still prove fruitful given that deletion of *PHO100* impaired *C. albicans* virulence (MacCallum et *al*., 2009).

Exploring whether the top compounds identified prevented Pho4 nuclear accumulation in response to Pi starvation yielded 5 compounds which came from different clusters. Moreover, for cluster 8, 3 compounds were identified as having the biggest impact on secreted acid phosphatase activity and growth at pH8, yet only one was found to prevent Pho4 nuclear accumulation in response to Pi starvation. Interestingly, all 5 compounds found to prevent Pho4 nuclear accumulation also impacted on morphology of the cell and level of Pho4 in cells. This was irrespective of Pi condition. It is noteworthy that there is a degree of similarity between the Pho4-GFP profiles of cells treated with these 5 compounds and the one shown in chapter 4 for *ppn1Δ/ppx1Δ* mutant cells. Perhaps this could be an adaptive

strategy of the cell in response to impairment of the PHO pathway? Although, a further 2 compounds which did not prevent Pho4 nuclear accumulation had an impact on morphology. All of the compounds identified as having an impact on morphology came from different clusters. The impact of compounds on morphology may prove interesting given the link between being able to reversibly switch between different morphologies is vital for *C. albicans* to successfully establish an infection (Saville *et al*., 2003).

Pho4 nuclear accumulation in response to Pi starvation was found to be unaffected in 8 of the 13 compounds tested. However, these 8 compounds had a significant impact on secreted acid phosphatase activity and growth at an alkaline pH, both of which are readouts of PHO pathway activity. Thus, it is plausible that these compounds could be impacting on the PHO pathway independent of Pho4 nuclear accumulation. For example, some of the compounds could be targeting transcription. Furthermore, in *S. cerevisiae*, Pho4 has been shown to require chromatin remodelling complexes (Zhou and O'Shea, 2011) therefore compounds may be directly inhibiting these.

In this chapter a total of 5 compounds were found to stringently match the criteria of targeting Pi acquisition via preventing Pho4 nuclear accumulation and thus, warrant biochemical analysis. To being addressing this, compounds could be used to treat cells expressing Pho4-MH to investigate the impact the compounds are having on Pho4 levels in Pi replete and deplete conditions. Furthermore, investigating the efficacy of these compounds as antifungals in animal models would be worthwhile. However, due to time constraints these 5 compounds have not been investigated further.

Chapter 6: Final Discussion

6.1 Summary

This thesis set out to investigate Pi homeostasis mechanisms in the major human fungal pathogen, *C. albicans,* to ascertain roles in stress resistance and virulence and whether the PHO pathway could be targeted as a novel antifungal strategy. These aims were initially addressed by characterising the regulators of Pho4 and the role which they play within the PHO pathway. Whilst *C. albicans* has homologues of the main Pho4 regulators in *S. cerevisiae* this study found that there was key differences. Unexpectedly, Pho81 was found to behave as a negative regulator of Pho4 in *C. albicans* unlike *S. cerevisiae* and *C. neoformans*. Further insights into the regulation of Pi acquisition in *C. albicans* were gained through investigating the role of IP_7 generating enzymes, Vip1 and Kcs1. These are an interesting area for future investigation as this work found there were key differences in their role in Pi homeostasis compared to *S. cerevisiae*. Alongside addressing putative regulators of the PHO pathway, the enigmatic Pi storage molecule, polyP, was also investigated. PolyP mobilisation was found to contribute to Pho4 mediated stress under Pi limiting conditions, as well as virulence in two invertebrate models. Importantly, this study also provides the first report linking polyP mobilisation to PHO pathway activation. Finally, high throughput screening of compound libraries uncovered compounds which appear to target Pho4 mediated processes, and in some cases Pho4 nuclear localisation. As Pho4 is an important virulence determinant, these compounds provide an exciting avenue for future work.

6.2 PHO pathway regulation differs in *C. albicans* from *S. cerevisiae*

In *S. cerevisiae*, following Pi starvation, Pho81 inhibits the Pho85-Pho80 CDK complex thus allowing unphosphorylated Pho4 to accumulate in the nucleus where it up-regulates genes involved in Pi acquisition (Figure 6.1). However, a comprehensive characterisation of strains lacking Pho80 and Pho81 revealed that Pho81 behaves differently in *C. albicans* (Figure 6.1). Indeed, analysis of *pho81Δ* using PHO pathway activity readouts including; secreted acid phosphatase assay and polyP analysis, all suggest that Pho81 negatively regulates Pho4 in *C. albicans*. This poses the question of why Pho81 a negative regulator of Pho4 in *C. albicans* but a positive regulator in *S. cerevisiae*? A plausible explanation could be that Pho81 is acting as a scaffolding protein for the Pho85-Pho80 CDK complex in *C. albicans*. Attempts were initiated to address this by epitope tagging Pho80 and Pho85 in wild type and *pho81Δ cells,*

to investigate for co-immunoprecipitation of the kinase-cyclin pair and whether this is Pho81 dependent. However, detection of tagged Pho80 was not possible so the use of alternative or multiple epitopes may be necessary. An analysis of Pho4 phosphorylation sites in *C. albicans* may also prove insightful for understanding regulation of the transcription factor in this organism. Moreover, it has been observed that Pho4 has a phosphorylation independent PTM under Pi replete, but not Pi limiting, conditions (Ikeh, 2015). Thus, suggesting the PTM must be lost to allow for Pho4 nuclear accumulation/activation. Identification of this PTM by mass spectrometry analysis would further inform how Pho4 is regulated in *C. albicans*. Future work could also investigate expression levels of PHO pathway targets in *pho80Δ* and *pho81Δ* cells to gain a more quantitative understanding of PHO pathway deregulation in these cells.

In relation to the emerging finding that inositol polyphosphate (IP) molecules play key roles in sensing cellular Pi levels, there are very few studies addressing the role of IP signalling molecules in *C. albicans*. Two papers have investigated the role of the enzyme generating IP_4/IP_5, Ipk2 (Li *et al*., 2017) and the IP_6 generating enzyme, Ipk1 (Zhu *et al*., 2020). Recently, a study showed that Vip1 played a role in autophagy in *C. albicans* and was required for virulence (Ma *et al*., 2020). This thesis set out to characterise the role of the IP_7 generating enzymes, Vip1 and Kcs1, in regulating *C. albicans* Pi homeostasis. Previous reports in *S. cerevisiae* have linked Vip1-derived IP_7 molecules to Pi regulation within the cell (Lee *et al*., 2007). Furthermore, SPX domain-containing proteins including Vtc4 have been shown to be regulated via the binding of IP_6 and IP_7 molecules (Wild *et al*., 2016). Moreover, recent work in *C. neoformans* has shown the Kcs1 IP_7 derivative to play an important role in promoting the association of Pho81 with Pho80-Pho85 during Pi starvation (Desmarini *et al*., 2020). In this thesis, it was found that deletion of *VIP1* but not *KCS1* impacted on Pi homeostasis in the cell. This was demonstrated by increased levels of polyP in *vip1Δ* cells compared to wild type cells and lower levels of secreted acid phosphatase activity in response to Pi starvation. The observation that Kcs1 is largely dispensable for Pi homeostasis was unexpected due to previous studies revealing that Kcs1-derived IP_7 molecules activate the *C. albicans* Vtc4 polyP polymerase (Wild *et al*., 2016). It may be possible that Kc1 and Vip1 function redundantly in *C. albicans*. To begin addressing this, how/if IP_7 levels change in the face of Pi starvation is *C. albicans* is necessary, followed by an analysis of IP levels in cells lacking either Vip1 or Kcs1,

to ascertain whether they are the key IP_7 generating enzymes in *C. albicans*.

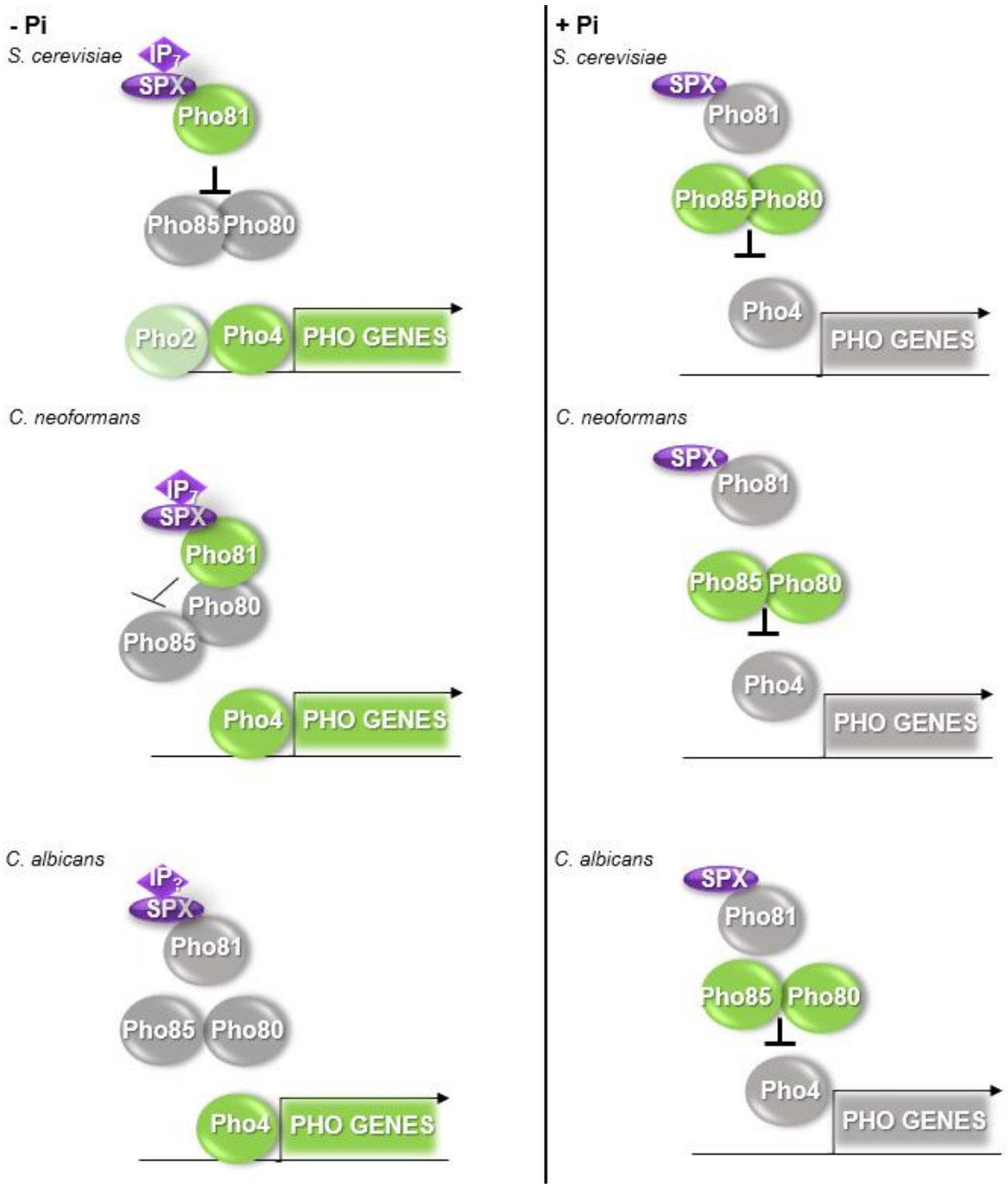

Figure 6.1.PHO pathway model in *S. cerevisiae*, *C. neoformans* and *C. albicans*.
Under Pi starvation conditions in *S. cerevisiae* IP_7 is bound to the SPX domain of Pho81 which inhibits the CDK complex composed of the kinase Pho85 and the cyclin Pho80, allowing Pho4 to accumulate in the nucleus where it works cooperatively with Pho2 to up-regulate genes involved in Pi acquisition. In *C. neoformans* during Pi starvation Pho81 inhibits the CDK complex allowing Pho4 nuclear accumulation. The binding of IP_7 to the SPX domain of Pho81 promotes association with the CDK complex. In *C. albicans* Pho81 as well as Pho80 appears to be negatively regulating Pho4. The role of IP signalling in Pho pathway regulation in *C. albicans* remains unknown.

6.3 The importance of polyP mobilisation

In this study polyP mobilisation was investigated as previous work revealed polyP stores were mobilised in response to Pi starvation, alkaline pH and NaCl. Moreover, in response to alkaline stress and Pi limitation polyP mobilisation preludes Pho4 nuclear accumulation and thus, PHO pathway activation (Ikeh *et al*., 2016). This study provided a comprehensive characterisation of polyP mobilisation in *C. albicans* (Figure 6.2). Firstly, it demonstrated that unlike *S. cerevisiae*, functional redundancy exists between the two major polyphosphatases Ppn1 and Ppx1. In *S. cerevisiae* solo deletion of Ppn1 leads to an increase in polyP chain length (Ogawa *et al*., 2000; Lonetti *et al*., 2011; Azevedo *et al*., 2020). However, in *C. albicans* both enzymes need to be deleted to observe higher molecular weight chains of polyP. In *S. cerevisiae*, Ppn1 is found within the vacuole where the majority of polyP is stored within the cell (Gerasimaitė and Mayer, 2016). In contrast, Ppx1 is mainly found in the cytoplasm with low levels in the nucleus and mitochondrial matrix (Gerasimaitė and Mayer, 2016). As the majority of polyP is described as being in the vacuole it is perplexing why the other main polyphosphatase in the cell Ppx1 is excluded from the vacuole. Given, that both enzymes must be deleted in *C. albicans* before any notable difference in polyP length and mobilisation is observed it may prove insightful to investigate their localisation in *C. albicans*. This could be addressed in future work by fluorescently tagging either enzyme and investigating their cellular localisation under Pi replete and deplete conditions given that Ppn1 in *S. cerevisiae* is only active during Pi starvation (Ogawa *et al*., 2000). Furthermore, it could be that the cellular localisation of polyP is more cytoplasmic in *C. albicans* than in *S. cerevisiae*. Indeed, Neisser did not appear to be localised to one particular area within the cell. The functional redundancy between Ppn1 and Ppx1 in *C. albicans* was also highlighted by the fact that both needed to be deleted an impact was observed to Pho4-mediated stress responses under Pi limiting conditions (Figure 6.2).

One of the most interesting aspects of this study was uncovering a role of polyP mobilisation in Pho4 activation. This was demonstrated by a degree of impairment in the induction of key Pi acquisition genes, *PHO84* and *PHO100,* and a lack of uniform Pho4 nuclear accumulation in response to Pi starvation in cells lacking both polyphosphatases. How polyP mobilisation regulates Pho4 activation remains ambiguous. Although not found in Ppn1 and Ppx1, many components of the PHO pathway including Pho81, Vtc4 and the vacuolar Na/Pi symporter Pho91 have SPX domains. Furthermore, it has been shown that IP_7

binds to the SPX domain of Vtc4 to stimulate polyP synthesis (Wild *et al*., 2016).Thus, an attractive hypothesis could be polyP levels influence IP_7 levels within the cell. It is plausible that as cells unable to mobilise polyP and therefore have high polyP may be sensing that their polyP reserves are plentiful even though they cannot be appropriately utilised and therefore the Pi starvation response is not being activated. Complimentary to this hypothesis Pho4 dependent gene in *S. cerevisiae* are activated more quickly in polyP deficient cells (Neef *et al*., 2003; Thomas and O'Shea, 2005). If polyP levels impact upon IP_7 levels it could be speculated that *ppn1Δ/ ppx1Δ* cells prevent Vip1 activity thus lowering IP_7 levels reducing activation of the PHO pathway. This would fit with the results of this thesis which show high levels of polyP and impacted secreted acid phosphatase activity in *vip1Δ.* However, this model conflicts with what has been shown in *S. cerevisiae* and *C. neoformans*. It also raises questions over why IP_7 derived from Kcs1 was shown to activate Vtc4 in *C. albicans* (Wild *et al.*, 2016). Although no significant impact on the PHO pathway was seen in cells lacking Kcs1 in chapter 3. Future work could begin addressing whether there is a link between IP signalling and polyP levels by measuring IP levels in cells lacking both polyphosphatases.

Under Pi deplete conditions, similar to cells lacking Pho4, preventing polyP mobilisation led to sensitivity to alkaline, cationic and superoxide stress (Figure 6.2). However, unlike cells lacking Pho4, preventing polyP mobilisation rendered cells exquisitely sensitive to DNA replication stress posed by HU (Figure 6.2). The sensitivity to replication stress could underpin the morphological defect of *ppn1Δ /ppx1Δ* cells (Figure 6.2).

Preventing polyP synthesis via deletion of VTC4 has been shown to reduce virulence in *U. maydis* (Boyce *et al*., 2006) but not in *C. neoformans* (Kretschmer *et al*., 2014). Similarly, in *C. neoformans* cells lacking the polyphosphatases Eep1 and Xpp1 had no impact on macrophage uptake or survival (Kretschmer *et al*., 2014). In chapter four, preventing polyP mobilisation was found to have a significant impact on the ability to establish an infection in *C. elegans* and *G. mellonella* (Figure 6.2). Moreover, using the *G. mellonella* infection model, deletion of either Ppn1 or Ppx1 led to a virulence impairment and explains the partial restoration of wild type virulence levels with either *ppn1Δ /ppx1Δ+PPN1* or *ppn1Δ/ppx1Δ+PPX1*. This suggests that functional redundancy does not exist for Ppn1 and Ppx1 for *C. albicans* virulence. In mammalian cells there is an exopolyphosphatase homologue (Tammenkoski *et al*., 2008) with 26% identity to Ppx1 in *C. albicans*. However, whilst enzymes with endopolyphosphatase activity have been described (Kumble and

Kronber, 1996; Lonetti *et al*., 2011), BLAST searches against the Ppn1 amino acid sequence do not return any mammalian proteins. In mammalian cells there is no vacuolar chaperone complex synthesising polyP (Lonetti *et al*., 2011). Thus, as preventing polyP synthesis in *C. albican*s was found to have a significant impact on the ability to establish infection in *G. mellonella* future work could explore the importance of Vtc4 in other infection models. Moreover, if *vtc4Δ* cells have impaired ability to cause infection in other virulence models then it could be an attractive druggable target.

Future work investigating the importance of polyP mobilisation in PHO pathway regulation could focus on transcript profiling studies to assess the extent of de-regulation of Pho4 targets in cells lacking both polyphosphatases. As there appeared to be higher levels of Pho4 in *ppn1Δ /ppx1Δ* cells in the Pho4-GFP images it may prove insightful to investigate Pho4 levels and mobilisation in these cells. It would also be interesting to investigate the localisation of Pho4 and the activation of PHO pathway targets in cells lacking Ppn1 and Ppx1 following alkaline stress.

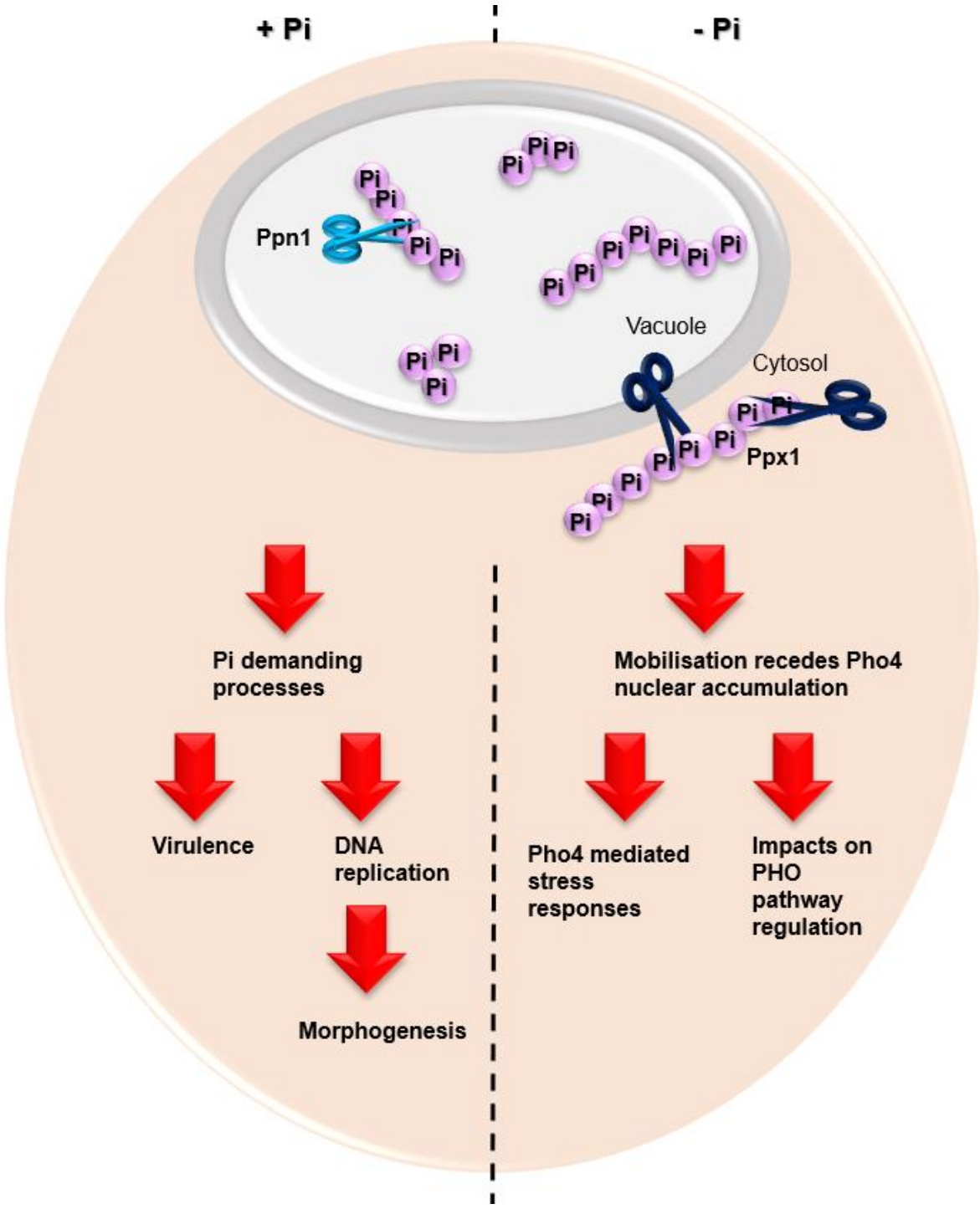

Figure 6.2. Model of proposed roles of polyP mobilisation in *C. albicans*.
Under Pi starvation, polyP mobilisation precedes Pho4 nuclear accumulation and play a role in PHO pathway activation and in Pho4 mediated stress resistance. Under Pi replete conditions polyP mobilisation is needed to meet the Pi demands of processes including DNA replication, morphogenesis, and virulence.

6.4 Is the PHO pathway a druggable target?

Dysregulation of Pi homeostasis in the cell has been linked to virulence in several prominent fungal pathogens (Boyce *et al*., 2006; Ikeh *et al*., 2016; Urrialde *et al*., 2016; Lev *et al*., 2017; Liu *et al*., 2018). Moreover, in *C. albicans* loss of the *PHO4*, *PHO100* , *PHO84*, *GDE1* and *GIT3* have all been shown to attenuate virulence in systemic infection models (Ikeh *et al*., 2016; MaCallum *et al*., 2009; Liu *et al*., 2018; Bishop *et al*., 2013). Furthermore, this thesis has shown that impairing polyP mobilisation or synthesis and deletion of the CDK cyclin Pho80 all impair the ability of *C. albicans* to establish an infection in *G. mellonella*. In culmination, this suggests that the PHO pathway may prove a promising target for the development of novel antifungals.

Given the link between preventing Pi acquisition and reduced virulence, compound libraries were screened for compounds preventing secreted acid phosphatase activity. Compounds were then selected which inhibited growth at pH 8 and which were found to directly prevent Pho4 nuclear accumulation and therefore PHO pathway activation.

This thesis found compounds which directly target the PHO pathway as demonstrated by the prevention of Pho4 nuclear accumulation during Pi starvation. Future work is needed to assess toxicity and thus inform suitability. Furthermore, to assess efficacy as an antifungal, compounds need to be administered to virulence models to determine antifungal ability. To being addressing this, future work could begin by testing potential compounds in *G. mellonella* and infecting with wild type cells to assess efficacy as an antifungal. Additionally, it could be investigated whether any antifungal activity found is Pho4 dependent by repeating testing of potential compounds in *G. mellonella* but with *pho4Δ cells.* Furthermore, as Pho4 has also been shown to be required for virulence in *C. neoformans* (Lev *et al*., 2017), there is scope that targeting this pathway could general broad-acting antifungals. This is dependent on future work deciphering the precise mode of action of selected compounds.

6.5 Concluding remarks

Taken together, the results of this thesis have made progress in advancing knowledge of Pi homeostasis in *C. albicans*. Particularly, it has highlighted key differences in PHO pathway regulation in *C. albicans* compared to *S. cerevisiae*. Moreover, it has provided insight into the role of polyP mobilisation for PHO pathway activation and Pho4 mediated stress responses

following Pi starvation. Furthermore, it has uncovered functions for poly mobilisation under Pi replete conditions such as DNA replication and morphogenesis. This study has also furthered knowledge linking Pi homeostasis and *C. albicans* virulence and identified promising lead compounds that inhibit PHO activation which provide an interesting avenue for future work.

Chapter 7: References

Aiking, H., Stijnman, A., van Garderen, C., van Heerikhuizen, H. and van 't Riet, J. (1984) 'Inorganic phosphate accumulation and cadmium detoxification in Klebsiella aerogenes NCTC 418 growing in continuous culture', *Appl Environ Microbiol*, 47(2), pp. 374-7.

Alarco, A.M. and Raymond, M. (1999) 'The bZip transcription factor Cap1p is involved in multidrug resistance and oxidative stress response in Candida albicans', *J Bacteriol*, 181(3), pp. 700-8.

Albi, T. and Serrano, A. (2016) 'Inorganic polyphosphate in the microbial world. Emerging roles for a multifaceted biopolymer', *World J Microbiol Biotechnol*, 32(2), p. 27.

Allert, S., Förster, T.M., Svensson, C.M., Richardson, J.P., Pawlik, T., Hebecker, B., Rudolphi, S., Juraschitz, M., Schaller, M., Blagojevic, M., Morschhäuser, J., Figge, M.T., Jacobsen, I.D., Naglik, J.R., Kasper, L., Mogavero, S. and Hube, B. (2018) 'Candida albicans-Induced Epithelial Damage Mediates Translocation through Intestinal Barriers', *mBio*, 9(3).

Almaguer, C., Mantella, D., Perez, E. and Patton-Vogt, J. (2003) 'Inositol and phosphate regulate GIT1 transcription and glycerophosphoinositol incorporation in Saccharomyces cerevisiae', *Eukaryot Cell*, 2(4), pp. 729-36.

Almeida, R.S., Wilson, D. and Hube, B. (2009) 'Candida albicans iron acquisition within the host', *FEMS Yeast Res*, 9(7), pp. 1000-12.

Alonso-Monge, R., Navarro-García, F., Molero, G., Diez-Orejas, R., Gustin, M., Pla, J., Sánchez, M. and Nombela, C. (1999) 'Role of the mitogen-activated protein kinase Hog1p in morphogenesis and virulence of Candida albicans', *J Bacteriol*, 181(10), pp. 3058-68.

Alonso-Monge, R., Navarro-García, F., Román, E., Negredo, A.I., Eisman, B., Nombela, C. and Pla, J. (2003) 'The Hog1 mitogen-activated protein kinase is essential in the oxidative stress response and chlamydospore formation in Candida albicans', *Eukaryot Cell*, 2(2), pp. 351-61.

Alvarez-Peral, F.J., Zaragoza, O., Pedreno, Y. and Argüelles, J.C. (2002) 'Protective role of trehalose during severe oxidative stress caused by hydrogen peroxide and the adaptive oxidative stress response in Candida albicans', *Microbiology (Reading)*, 148(Pt 8), pp. 2599-2606.

Alves, R., Barata-Antunes, C., Casal, M., Brown, A.J.P., Van Dijck, P. and Paiva, S. (2020) 'Adapting to survive: How Candida overcomes host-imposed constraints during human colonization', *PLoS Pathog*, 16(5), p. e1008478.

Anderson, T.M., Clay, M.C., Cioffi, A.G., Diaz, K.A., Hisao, G.S., Tuttle, M.D., Nieuwkoop, A.J., Comellas, G., Maryum, N., Wang, S., Uno, B.E., Wildeman, E.L., Gonen, T., Rienstra, C.M. and Burke, M.D. (2014) 'Amphotericin forms an extramembranous and fungicidal sterol sponge', *Nat Chem Biol*, 10(5), pp. 400-6.

Arana, D.M., Alonso-Monge, R., Du, C., Calderone, R. and Pla, J. (2007) 'Differential susceptibility of mitogen-activated protein kinase pathway mutants to oxidative-mediated killing by phagocytes in the fungal pathogen Candida albicans', *Cell Microbiol*, 9(7), pp. 1647-59.

Armstrong-James, D., Brown, G.D., Netea, M.G., Zelante, T., Gresnigt, M.S., van de Veerdonk, F.L. and Levitz, S.M. (2017) 'Immunotherapeutic approaches to treatment of fungal diseases', *Lancet Infect Dis*, 17(12), pp. e393-e402.

Asleson, C.M., Bensen, E.S., Gale, C.A., Melms, A.S., Kurischko, C. and Berman, J. (2001) 'Candida albicans INT1-induced filamentation in Saccharomyces cerevisiae depends on Sla2p', *Mol Cell Biol*, 21(4), pp. 1272-84.

Auesukaree, C., Tochio, H., Shirakawa, M., Kaneko, Y. and Harashima, S. (2005) 'Plc1p, Arg82p, and Kcs1p, enzymes involved in inositol pyrophosphate synthesis, are essential for phosphate regulation and polyphosphate accumulation in Saccharomyces cerevisiae', *J Biol Chem*, 280(26), pp. 25127-33.

Austin, S. and Mayer, A. (2020) 'Phosphate Homeostasis - A Vital Metabolic Equilibrium Maintained Through the INPHORS Signaling Pathway', *Front Microbiol*, 11, p. 1367.

Azevedo, C., Desfougères, Y., Jiramongkol, Y., Partington, H., Trakansuebkul, S., Singh, J., Steck, N., Jessen, H.J. and Saiardi, A. (2020) 'Development of a yeast model to study the contribution of vacuolar polyphosphate metabolism to lysine polyphosphorylation', *J Biol Chem*, 295(6), pp. 1439-1451.

Azevedo, C., Livermore, T. and Saiardi, A. (2015) 'Protein polyphosphorylation of lysine residues by inorganic polyphosphate', *Mol Cell*, 58(1), pp. 71-82.

Azevedo, C., Livermore, T. and Saiardi, A. (2015) 'Protein polyphosphorylation of lysine residues by inorganic polyphosphate', *Mol Cell*, 58(1), pp. 71-82.

Bachewich, C., Nantel, A. and Whiteway, M. (2005) 'Cell cycle arrest during S or M phase generates polarized growth via distinct signals in Candida albicans', *Mol Microbiol*, 57(4), pp. 942-59.

Barelle, C.J., Priest, C.L., Maccallum, D.M., Gow, N.A., Odds, F.C. and Brown, A.J. (2006) 'Niche-specific regulation of central metabolic pathways in a fungal pathogen', *Cell Microbiol*, 8(6), pp. 961-71.

Basso, V., d'Enfert, C., Znaidi, S. and Bachellier-Bassi, S. (2019) 'From Genes to Networks: The Regulatory Circuitry Controlling Candida albicans Morphogenesis', *Curr Top Microbiol Immunol*, 422, pp. 61-99.

Beach, D., Durkacz, B. and Nurse, P. (1982) 'Functionally homologous cell cycle control genes in budding and fission yeast', *Nature*, 300(5894), pp. 706-9.

Benedict, K., Jackson, B.R., Chiller, T. and Beer, K.D. (2019) 'Estimation of Direct Healthcare Costs of Fungal Diseases in the United States', *Clin Infect Dis*, 68(11), pp. 1791-1797.

Bennett, M., Onnebo, S.M., Azevedo, C. and Saiardi, A. (2006) 'Inositol pyrophosphates: metabolism and signaling', *Cell Mol Life Sci*, 63(5), pp. 552-64.

Bensen, E.S., Martin, S.J., Li, M., Berman, J. and Davis, D.A. (2004) 'Transcriptional profiling in Candida albicans reveals new adaptive responses to extracellular pH and functions for Rim101p', *Mol Microbiol*, 54(5), pp. 1335-51.

Berman, J. (2006) 'Morphogenesis and cell cycle progression in Candida albicans', *Curr Opin Microbiol*, 9(6), pp. 595-601.

Berman, J. and Sudbery, P.E. (2002) 'Candida Albicans: a molecular revolution built on lessons from budding yeast', *Nat Rev Genet*, 3(12), pp. 918-30.

Bhat, K.P. and Greer, S.F. (2011) 'Proteolytic and non-proteolytic roles of ubiquitin and the ubiquitin proteasome system in transcriptional regulation', *Biochim Biophys Acta*, 1809(2), pp. 150-5.

Birchall, K., Merritt, A., Sattikar, A., Kettleborough, C. and Saxty, B. (2019) 'Design of the LifeArc Index Set and Retrospective Review of Its Performance: A Collection for Sharing', *SLAS Discov*, 24(3), pp. 332-345.

Birnboim, H.C. and Doly, J. (1979) 'A rapid alkaline extraction procedure for screening recombinant plasmid DNA', *Nucleic Acids Res*, 7(6), pp. 1513-23.

Bishop, A.C., Ganguly, S., Solis, N.V., Cooley, B.M., Jensen-Seaman, M.I., Filler, S.G., Mitchell, A.P. and Patton-Vogt, J. (2013) 'Glycerophosphocholine utilization by Candida albicans: role of the Git3 transporter in virulence', *J Biol Chem*, 288(47), pp. 33939-52.

Biswas, S., Van Dijck, P. and Datta, A. (2007) 'Environmental sensing and signal transduction pathways regulating morphopathogenic determinants of Candida albicans', *Microbiol Mol Biol Rev*, 71(2), pp. 348-76.

Bongomin, F., Gago, S., Oladele, R.O. and Denning, D.W. (2017) 'Global and Multi-National Prevalence of Fungal Diseases-Estimate Precision', *J Fungi (Basel)*, 3(4).
Borman, A.M., Szekely, A. and Johnson, E.M. (2016) 'Comparative Pathogenicity of United Kingdom Isolates of the Emerging Pathogen Candida auris and Other Key Pathogenic Candida Species', *mSphere*, 1(4).
Boyce, K.J., Kretschmer, M. and Kronstad, J.W. (2006) 'The vtc4 gene influences polyphosphate storage, morphogenesis, and virulence in the maize pathogen Ustilago maydis', *Eukaryot Cell*, 5(8), pp. 1399-409.
Brand, A. (2012) 'Hyphal growth in human fungal pathogens and its role in virulence', *Int J Microbiol*, 2012, p. 517529.
Brown, A.J., Budge, S., Kaloriti, D., Tillmann, A., Jacobsen, M.D., Yin, Z., Ene, I.V., Bohovych, I., Sandai, D., Kastora, S., Potrykus, J., Ballou, E.R., Childers, D.S., Shahana, S. and Leach, M.D. (2014) 'Stress adaptation in a pathogenic fungus', *J Exp Biol*, 217(Pt 1), pp. 144-55.
Brown, A.J., Haynes, K. and Quinn, J. (2009) 'Nitrosative and oxidative stress responses in fungal pathogenicity', *Curr Opin Microbiol*, 12(4), pp. 384-91.
Brown, A.J., Odds, F.C. and Gow, N.A. (2007) 'Infection-related gene expression in Candida albicans', *Curr Opin Microbiol*, 10(4), pp. 307-13.
Brown, A.J.P., Cowen, L.E., di Pietro, A. and Quinn, J. (2017) 'Stress Adaptation', *Microbiol Spectr*, 5(4).
Brown, G.D., Denning, D.W., Gow, N.A., Levitz, S.M., Netea, M.G. and White, T.C. (2012) 'Hidden killers: human fungal infections', *Sci Transl Med*, 4(165), p. 165rv13.
Broxton, C.N. and Culotta, V.C. (2016) 'SOD Enzymes and Microbial Pathogens: Surviving the Oxidative Storm of Infection', *PLoS Pathog*, 12(1), p. e1005295.
Bru, S., Martínez-Laínez, J.M., Hernández-Ortega, S., Quandt, E., Torres-Torronteras, J., Martí, R., Canadell, D., Ariño, J., Sharma, S., Jiménez, J. and Clotet, J. (2016) 'Polyphosphate is involved in cell cycle progression and genomic stability in Saccharomyces cerevisiae', *Mol Microbiol*, 101(3), pp. 367-80.
Bru, S., Samper-Martín, B., Quandt, E., Hernández-Ortega, S., Martínez-Laínez, J.M., Garí, E., Rafel, M., Torres-Torronteras, J., Martí, R., Ribeiro, M.P.C., Jiménez, J. and Clotet, J. (2017) 'Polyphosphate is a key factor for cell survival after DNA damage in eukaryotic cells', *DNA Repair (Amst)*, 57, pp. 171-178.

Byrne, M., Miller, N., Springer, M. and O'Shea, E.K. (2004) 'A distal, high-affinity binding site on the cyclin-CDK substrate Pho4 is important for its phosphorylation and regulation', *J Mol Biol*, 335(1), pp. 57-70.
Byrne, M., Miller, N., Springer, M. and O'Shea, E.K. (2004) 'A distal, high-affinity binding site on the cyclin-CDK substrate Pho4 is important for its phosphorylation and regulation', *J Mol Biol*, 335(1), pp. 57-70.
Caffrey, J.J., Safrany, S.T., Yang, X. and Shears, S.B. (2000) 'Discovery of molecular and catalytic diversity among human diphosphoinositol-polyphosphate phosphohydrolases. An expanding Nudt family', *J Biol Chem*, 275(17), pp. 12730-6.

Calderone, R.A. and Clancy, C.J. (2012) *Candida and candidiasis*. Washington: ASM Press.

Calderone, R.A. and Fonzi, W.A. (2001) 'Virulence factors of Candida albicans', *Trends Microbiol*, 9(7), pp. 327-35.

Candon, H.L., Allan, B.J., Fraley, C.D. and Gaynor, E.C. (2007) 'Polyphosphate kinase 1 is a pathogenesis determinant in Campylobacter jejuni', *J Bacteriol*, 189(22), pp. 8099-108.

Carlisle, P.L., Banerjee, M., Lazzell, A., Monteagudo, C., López-Ribot, J.L. and Kadosh, D. (2009) 'Expression levels of a filament-specific transcriptional regulator are sufficient to determine Candida albicans morphology and virulence', *Proc Natl Acad Sci U S A*, 106(2), pp. 599-604.

Carroll, A.S. and O'Shea, E.K. (2002) 'Pho85 and signaling environmental conditions', *Trends Biochem Sci*, 27(2), pp. 87-93.

Castro, C.D., Meehan, A.J., Koretsky, A.P. and Domach, M.M. (1995) 'In situ 31P nuclear magnetic resonance for observation of polyphosphate and catabolite responses of chemostat-cultivated Saccharomyces cerevisiae after alkalinization', *Appl Environ Microbiol*, 61(12), pp. 4448-53.

Chakraborty, A. (2018) 'The inositol pyrophosphate pathway in health and diseases', *Biol Rev Camb Philos Soc*, 93(2), pp. 1203-1227.

Chakraborty, S., Sivaraman, J., Leung, K.Y. and Mok, Y.K. (2011) 'Two-component PhoB-PhoR regulatory system and ferric uptake regulator sense phosphate and iron to control virulence genes in type III and VI secretion systems of Edwardsiella tarda', *J Biol Chem*, 286(45), pp. 39417-30.

Chamilos, G., Lionakis, M.S., Lewis, R.E. and Kontoyiannis, D.P. (2007) 'Role of mini-host models in the study of medically important fungi', *Lancet Infect Dis*, 7(1), pp. 42-55.

Chandra, J., Kuhn, D.M., Mukherjee, P.K., Hoyer, L.L., McCormick, T. and Ghannoum, M.A. (2001) 'Biofilm formation by the fungal pathogen Candida albicans: development, architecture, and drug resistance', *J Bacteriol*, 183(18), pp. 5385-94.

Chandrasekar, P. (2011) 'Management of invasive fungal infections: a role for polyenes', *J Antimicrob Chemother*, 66(3), pp. 457-65.

Chauhan, N., Inglis, D., Roman, E., Pla, J., Li, D., Calera, J.A. and Calderone, R. (2003) 'Candida albicans response regulator gene SSK1 regulates a subset of genes whose functions are associated with cell wall biosynthesis and adaptation to oxidative stress', *Eukaryot Cell*, 2(5), pp. 1018-24.

Chaves, G.M., Bates, S., Maccallum, D.M. and Odds, F.C. (2007) 'Candida albicans GRX2, encoding a putative glutaredoxin, is required for virulence in a murine model', *Genet Mol Res*, 6(4), pp. 1051-63.

Cheetham, J., MacCallum, D.M., Doris, K.S., da Silva Dantas, A., Scorfield, S., Odds, F., Smith, D.A. and Quinn, J. (2011) 'MAPKKK-independent regulation of the Hog1 stress-activated protein kinase in Candida albicans', *J Biol Chem*, 286(49), pp. 42002-16.

Chekabab, S.M., Harel, J. and Dozois, C.M. (2014) 'Interplay between genetic regulation of phosphate homeostasis and bacterial virulence', *Virulence*, 5(8), pp. 786-93.

Childers, D.S., Raziunaite, I., Mol Avelar, G., Mackie, J., Budge, S., Stead, D., Gow, N.A., Lenardon, M.D., Ballou, E.R., MacCallum, D.M. and Brown, A.J. (2016) 'The Rewiring of Ubiquitination Targets in a Pathogenic Yeast Promotes Metabolic Flexibility, Host Colonization and Virulence', *PLoS Pathog*, 12(4), p. e1005566.

Citiulo, F., Jacobsen, I.D., Miramón, P., Schild, L., Brunke, S., Zipfel, P., Brock, M., Hube, B. and Wilson, D. (2012) 'Candida albicans scavenges host zinc via Pra1 during endothelial invasion', *PLoS Pathog*, 8(6), p. e1002777.

Citiulo, F., Jacobsen, I.D., Miramón, P., Schild, L., Brunke, S., Zipfel, P., Brock, M., Hube, B. and Wilson, D. (2012) 'Candida albicans scavenges host zinc via Pra1 during endothelial invasion', *PLoS Pathog*, 8(6), p. e1002777.

Cleary, I.A., Lazzell, A.L., Monteagudo, C., Thomas, D.P. and Saville, S.P. (2012) 'BRG1 and NRG1 form a novel feedback circuit regulating Candida albicans hypha formation and virulence', *Mol Microbiol*, 85(3), pp. 557-73.

Cohen, A., Perzov, N., Nelson, H. and Nelson, N. (1999) 'A novel family of yeast chaperons involved in the distribution of V-ATPase and other membrane proteins', *J Biol Chem*, 274(38), pp. 26885-93.

Collins, J.F., Prohaska, J.R. and Knutson, M.D. (2010) 'Metabolic crossroads of iron and copper', *Nutr Rev*, 68(3), pp. 133-47.

Coste, A., Selmecki, A., Forche, A., Diogo, D., Bougnoux, M.E., d'Enfert, C., Berman, J. and Sanglard, D. (2007) 'Genotypic evolution of azole resistance mechanisms in sequential Candida albicans isolates', *Eukaryot Cell*, 6(10), pp. 1889-904.

da Silva Dantas, A., Patterson, M.J., Smith, D.A., Maccallum, D.M., Erwig, L.P., Morgan, B.A. and Quinn, J. (2010) 'Thioredoxin regulates multiple hydrogen peroxide-induced signaling pathways in Candida albicans', *Mol Cell Biol*, 30(19), pp. 4550-63.

Dantas Ada, S., Day, A., Ikeh, M., Kos, I., Achan, B. and Quinn, J. (2015) 'Oxidative stress responses in the human fungal pathogen, Candida albicans', *Biomolecules*, 5(1), pp. 142-65.

Davis, D. (2003) 'Adaptation to environmental pH in Candida albicans and its relation to pathogenesis', *Curr Genet*, 44(1), pp. 1-7.

Day, A.M., Herrero-de-Dios, C.M., MacCallum, D.M., Brown, A.J.P. and Quinn, J. (2017) 'Stress-induced nuclear accumulation is dispensable for Hog1-dependent gene expression and virulence in a fungal pathogen', *Sci Rep*, 7(1), p. 14340.

Day, A.M. and Quinn, J. (2019) 'Stress-Activated Protein Kinases in Human Fungal Pathogens', *Front Cell Infect Microbiol*, 9, p. 261.

De Bernardis, F., Mühlschlegel, F.A., Cassone, A. and Fonzi, W.A. (1998) 'The pH of the host niche controls gene expression in and virulence of Candida albicans', *Infect Immun*, 66(7), pp. 3317-25.

de Gouvêa, P.F., Soriani, F.M., Malavazi, I., Savoldi, M., Goldman, M.H., Loss, O., Bignell, E., da Silva Ferreira, M.E. and Goldman, G.H. (2008) 'Functional characterization of the Aspergillus fumigatusPHO80 homologue', *Fungal Genet Biol*, 45(7), pp. 1135-46.

de Repentigny, L., Lewandowski, D. and Jolicoeur, P. (2004) 'Immunopathogenesis of oropharyngeal candidiasis in human immunodeficiency virus infection', *Clin Microbiol Rev*, 17(4), pp. 729-59, table of contents.

Delattin, N., Cammue, B.P. and Thevissen, K. (2014) 'Reactive oxygen species-inducing antifungal agents and their activity against fungal biofilms', *Future Med Chem*, 6(1), pp. 77-90.

Deng, J., Yang, C., Wang, Y., Yang, M., Chen, H., Ning, H., Wang, C., Liu, Y., Zhang, Z. and Hu, T. (2019) 'Inositol pyrophosphates mediated the apoptosis induced by hypoxic injury in bone marrow-derived mesenchymal stem cells by autophagy', *Stem Cell Res Ther*, 10(1), p. 159.

Dennison, P.M., Ramsdale, M., Manson, C.L. and Brown, A.J. (2005) 'Gene disruption in Candida albicans using a synthetic, codon-optimised Cre-loxP system', *Fungal Genet Biol*, 42(9), pp. 737-48.

Desfougères, Y., Gerasimaitė, R.U., Jessen, H.J. and Mayer, A. (2016) 'Vtc5, a Novel Subunit of the Vacuolar Transporter Chaperone Complex, Regulates Polyphosphate Synthesis and Phosphate Homeostasis in Yeast', *J Biol Chem*, 291(42), pp. 22262-22275.

Desmarini, D., Lev, S., Furkert, D., Crossett, B., Saiardi, A., Kaufman-Francis, K., Li, C., Sorrell, T.C., Wilkinson-White, L., Matthews, J., Fiedler, D. and Djordjevic, J.T. (2020) 'IP(7)-SPX Domain Interaction Controls Fungal Virulence by Stabilizing Phosphate Signaling Machinery', *mBio*, 11(5).

Deutschbauer, A.M., Jaramillo, D.F., Proctor, M., Kumm, J., Hillenmeyer, M.E., Davis, R.W., Nislow, C. and Giaever, G. (2005) 'Mechanisms of haploinsufficiency revealed by genome-wide profiling in yeast', *Genetics*, 169(4), pp. 1915-25.

Dhar, R., Sägesser, R., Weikert, C. and Wagner, A. (2013) 'Yeast adapts to a changing stressful environment by evolving cross-protection and anticipatory gene regulation', *Mol Biol Evol*, 30(3), pp. 573-88.

Douglas, L.M. and Konopka, J.B. (2019) 'Plasma membrane architecture protects Candida albicans from killing by copper', *PLoS Genet*, 15(1), p. e1007911.

Du, H. and Huang, G. (2016) 'Environmental pH adaption and morphological transitions in Candida albicans', *Curr Genet*, 62(2), pp. 283-6.

Dubois, E., Scherens, B., Vierendeels, F., Ho, M.M., Messenguy, F. and Shears, S.B. (2002) 'In Saccharomyces cerevisiae, the inositol polyphosphate kinase activity of Kcs1p is required for resistance to salt stress, cell wall integrity, and vacuolar morphogenesis', *J Biol Chem*, 277(26), pp. 23755-63.

Dutton, L.C., Paszkiewicz, K.H., Silverman, R.J., Splatt, P.R., Shaw, S., Nobbs, A.H., Lamont, R.J., Jenkinson, H.F. and Ramsdale, M. (2016) 'Transcriptional landscape of trans-kingdom communication between Candida albicans and Streptococcus gordonii', *Mol Oral Microbiol*, 31(2), pp. 136-61.

Eck, R., Hundt, S., Härtl, A., Roemer, E. and Künkel, W. (1999) 'A multicopper oxidase gene from Candida albicans: cloning, characterization and disruption', *Microbiology (Reading)*, 145 (Pt 9), pp. 2415-2422.

Ehrensberger, K.M. and Bird, A.J. (2011) 'Hammering out details: regulating metal levels in eukaryotes', *Trends Biochem Sci*, 36(10), pp. 524-31.

Ene, I.V., Brunke, S., Brown, A.J. and Hube, B. (2014) 'Metabolism in fungal pathogenesis', *Cold Spring Harb Perspect Med*, 4(12), p. a019695.

Enjalbert, B., MacCallum, D.M., Odds, F.C. and Brown, A.J. (2007) 'Niche-specific activation of the oxidative stress response by the pathogenic fungus Candida albicans', *Infect Immun*, 75(5), pp. 2143-51.

Enjalbert, B., Nantel, A. and Whiteway, M. (2003) 'Stress-induced gene expression in Candida albicans: absence of a general stress response', *Mol Biol Cell*, 14(4), pp. 1460-7.

Enjalbert, B., Smith, D.A., Cornell, M.J., Alam, I., Nicholls, S., Brown, A.J. and Quinn, J. (2006) 'Role of the Hog1 stress-activated protein kinase in the global transcriptional response to stress in the fungal pathogen Candida albicans', *Mol Biol Cell*, 17(2), pp. 1018-32.

Fan, J., Whiteway, M. and Shen, S.H. (2005) 'Disruption of a gene encoding glycerol 3-phosphatase from Candida albicans impairs intracellular glycerol accumulation-mediated salt-tolerance', *FEMS Microbiol Lett*, 245(1), pp. 107-16.

Fan, W., Kraus, P.R., Boily, M.J. and Heitman, J. (2005) 'Cryptococcus neoformans gene expression during murine macrophage infection', *Eukaryot Cell*, 4(8), pp. 1420-33.

Finkel, J.S. and Mitchell, A.P. (2011) 'Genetic control of Candida albicans biofilm development', *Nat Rev Microbiol*, 9(2), pp. 109-18.

Finley, D., Ulrich, H.D., Sommer, T. and Kaiser, P. (2012) 'The ubiquitin-proteasome system of Saccharomyces cerevisiae', *Genetics*, 192(2), pp. 319-60.

Fisher, E., Almaguer, C., Holic, R., Griac, P. and Patton-Vogt, J. (2005) 'Glycerophosphocholine-dependent growth requires Gde1p (YPL110c) and Git1p in Saccharomyces cerevisiae', *J Biol Chem*, 280(43), pp. 36110-7.

Fisher, M.C., Gurr, S.J., Cuomo, C.A., Blehert, D.S., Jin, H., Stukenbrock, E.H., Stajich, J.E., Kahmann, R., Boone, C., Denning, D.W., Gow, N.A.R., Klein, B.S., Kronstad, J.W., Sheppard, D.C., Taylor, J.W., Wright, G.D., Heitman, J., Casadevall, A. and Cowen, L.E. (2020) 'Threats Posed by the Fungal Kingdom to Humans, Wildlife, and Agriculture', *mBio*, 11(3).

Forche, A., Alby, K., Schaefer, D., Johnson, A.D., Berman, J. and Bennett, R.J. (2008) 'The parasexual cycle in Candida albicans provides an alternative pathway to meiosis for the formation of recombinant strains', *PLoS Biol*, 6(5), p. e110.

Fourie, R., Kuloyo, O.O., Mochochoko, B.M., Albertyn, J. and Pohl, C.H. (2018) 'Iron at the Centre of Candida albicans Interactions', *Front Cell Infect Microbiol*, 8, p. 185.

Fradin, C., De Groot, P., MacCallum, D., Schaller, M., Klis, F., Odds, F.C. and Hube, B. (2005) 'Granulocytes govern the transcriptional response, morphology and proliferation of Candida albicans in human blood', *Mol Microbiol*, 56(2), pp. 397-415.
Fradin, C., De Groot, P., MacCallum, D., Schaller, M., Klis, F., Odds, F.C. and Hube, B. (2005) 'Granulocytes govern the transcriptional response, morphology and proliferation of Candida albicans in human blood', *Mol Microbiol*, 56(2), pp. 397-415.
Fradin, C., Kretschmar, M., Nichterlein, T., Gaillardin, C., d'Enfert, C. and Hube, B. (2003) 'Stage-specific gene expression of Candida albicans in human blood', *Mol Microbiol*, 47(6), pp. 1523-43.

François, I., Cammue, B., Borgers, M., Ausma, J., Dispersyn, G. and Thevissen, K. (2006) 'Azoles: Mode of Antifungal Action and Resistance Development. Effect of Miconazole on Endogenous Reactive Oxygen Species Production in Candida albicans', *Anti-Infective Agents in Medicinal Chemistry (Formerly Current Medicinal Chemistry - Anti-Infective Agents)*, 5, pp. 3-13.

Frohner, I.E., Bourgeois, C., Yatsyk, K., Majer, O. and Kuchler, K. (2009) 'Candida albicans cell surface superoxide dismutases degrade host-derived reactive oxygen species to escape innate immune surveillance', *Mol Microbiol*, 71(1), pp. 240-52.
Frohner, I.E., Bourgeois, C., Yatsyk, K., Majer, O. and Kuchler, K. (2009) 'Candida albicans cell surface superoxide dismutases degrade host-derived reactive oxygen species to escape innate immune surveillance', *Mol Microbiol*, 71(1), pp. 240-52.
Fuentefria, A.M., Pippi, B., Dalla Lana, D.F., Donato, K.K. and de Andrade, S.F. (2018) 'Antifungals discovery: an insight into new strategies to combat antifungal resistance', *Lett Appl Microbiol*, 66(1), pp. 2-13.

Gauwerky, K., Borelli, C. and Korting, H.C. (2009) 'Targeting virulence: a new paradigm for antifungals', *Drug Discov Today*, 14(3-4), pp. 214-22.

Gerasimaitė, R. and Mayer, A. (2016) 'Enzymes of yeast polyphosphate metabolism: structure, enzymology and biological roles', *Biochem Soc Trans*, 44(1), pp. 234-9.

Gerasimaitė, R. and Mayer, A. (2017) 'Ppn2, a novel Zn(2+)-dependent polyphosphatase in the acidocalcisome-like yeast vacuole', *J Cell Sci*, 130(9), pp. 1625-1636.

Gerasimaitė, R., Sharma, S., Desfougères, Y., Schmidt, A. and Mayer, A. (2014) 'Coupled synthesis and translocation restrains polyphosphate to acidocalcisome-like vacuoles and prevents its toxicity', *J Cell Sci*, 127(Pt 23), pp. 5093-104.

Ghannoum, M.A. (1998) 'Extracellular phospholipases as universal virulence factor in pathogenic fungi', *Nihon Ishinkin Gakkai Zasshi*, 39(2), pp. 55-9.
Girmenia, C. (2009) 'New generation azole antifungals in clinical investigation', *Expert Opin Investig Drugs*, 18(9), pp. 1279-95.
Glöckner, A., Steinbach, A., Vehreschild, J.J. and Cornely, O.A. (2009) 'Treatment of invasive candidiasis with echinocandins', *Mycoses*, 52(6), pp. 476-86.
Gray, M.J. and Jakob, U. (2015) 'Oxidative stress protection by polyphosphate--new roles for an old player', *Curr Opin Microbiol*, 24, pp. 1-6.
Gray, M.J., Wholey, W.Y., Wagner, N.O., Cremers, C.M., Mueller-Schickert, A., Hock, N.T., Krieger, A.G., Smith, E.M., Bender, R.A., Bardwell, J.C. and Jakob, U. (2014) 'Polyphosphate is a primordial chaperone', *Mol Cell*, 53(5), pp. 689-99.
Greenfield, N.J., Hussain, M. and Lenard, J. (1987) 'Effects of growth state and amines on cytoplasmic and vacuolar pH, phosphate and polyphosphate levels in Saccharomyces cerevisiae: a 31P-nuclear magnetic resonance study', *Biochim Biophys Acta*, 926(3), pp. 205-14.
Grela, E., Piet, M., Luchowski, R., Grudzinski, W., Paduch, R. and Gruszecki, W.I. (2018) 'Imaging of human cells exposed to an antifungal antibiotic amphotericin B reveals the mechanisms associated with the drug toxicity and cell defence', *Sci Rep*, 8(1), p. 14067.
Griffiths, E.J., Hu, G., Fries, B., Caza, M., Wang, J., Gsponer, J., Gates-Hollingsworth, M.A., Kozel, T.R., De Repentigny, L. and Kronstad, J.W. (2012) 'A defect in ATP-citrate lyase links acetyl-CoA production, virulence factor elaboration and virulence in Cryptococcus neoformans', *Mol Microbiol*, 86(6), pp. 1404-23.
Grillo-Puertas, M., Villegas, J.M., Rintoul, M.R. and Rapisarda, V.A. (2012) 'Polyphosphate degradation in stationary phase triggers biofilm formation via LuxS quorum sensing system in Escherichia coli', *PLoS One*, 7(11), p. e50368.
Grubb, S.E., Murdoch, C., Sudbery, P.E., Saville, S.P., Lopez-Ribot, J.L. and Thornhill, M.H. (2009) 'Adhesion of Candida albicans to endothelial cells under physiological conditions of flow', *Infect Immun*, 77(9), pp. 3872-8.
Gu, C., Wilson, M.S., Jessen, H.J., Saiardi, A. and Shears, S.B. (2016) 'Inositol Pyrophosphate Profiling of Two HCT116 Cell Lines Uncovers Variation in InsP8 Levels', *PLoS One*, 11(10), p. e0165286.
Gurr, E. (1965) *The rational use of dyes in biology and general staining methods*. London: Leonard Hill.

He, B.Z., Zhou, X. and O'Shea, E.K. (2017) 'Evolution of reduced co-activator dependence led to target expansion of a starvation response pathway', *Elife*, 6.
He, F. (2011) 'Synchronization of Worm', *Bio-protocol*, 1(7), p. e56.
Hebecker, B., Vlaic, S., Conrad, T., Bauer, M., Brunke, S., Kapitan, M., Linde, J., Hube, B. and Jacobsen, I.D. (2016) 'Dual-species transcriptional profiling during systemic candidiasis reveals organ-specific host-pathogen interactions', *Sci Rep*, 6, p. 36055.
Heckman, D.S., Geiser, D.M., Eidell, B.R., Stauffer, R.L., Kardos, N.L. and Hedges, S.B. (2001) 'Molecular evidence for the early colonization of land by fungi and plants', *Science*, 293(5532), pp. 1129-33.
Heckman, D.S., Geiser, D.M., Eidell, B.R., Stauffer, R.L., Kardos, N.L. and Hedges, S.B. (2001) 'Molecular evidence for the early colonization of land by fungi and plants', *Science*, 293(5532), pp. 1129-33.
Hertzberger, R., Arents, J., Dekker, H.L., Pridmore, R.D., Gysler, C., Kleerebezem, M. and de Mattos, M.J. (2014) 'H(2)O(2) production in species of the Lactobacillus acidophilus group: a central role for a novel NADH-dependent flavin reductase', *Appl Environ Microbiol*, 80(7), pp. 2229-39.
Hickman, M.A., Zeng, G., Forche, A., Hirakawa, M.P., Abbey, D., Harrison, B.D., Wang, Y.M., Su, C.H., Bennett, R.J., Wang, Y. and Berman, J. (2013) 'The 'obligate diploid' Candida albicans forms mating-competent haploids', *Nature*, 494(7435), pp. 55-9.
Hidaka, K., Caffrey, J.J., Hua, L., Zhang, T., Falck, J.R., Nickel, G.C., Carrel, L., Barnes, L.D. and Shears, S.B. (2002) 'An adjacent pair of human NUDT genes on chromosome X are preferentially expressed in testis and encode two new isoforms of diphosphoinositol polyphosphate phosphohydrolase', *J Biol Chem*, 277(36), pp. 32730-8.
Ho, J., Yang, X., Nikou, S.A., Kichik, N., Donkin, A., Ponde, N.O., Richardson, J.P., Gratacap, R.L., Archambault, L.S., Zwirner, C.P., Murciano, C., Henley-Smith, R., Thavaraj, S., Tynan, C.J., Gaffen, S.L., Hube, B., Wheeler, R.T., Moyes, D.L. and Naglik, J.R. (2019) 'Candidalysin activates innate epithelial immune responses via epidermal growth factor receptor', *Nat Commun*, 10(1), p. 2297.
Homann, O.R., Dea, J., Noble, S.M. and Johnson, A.D. (2009) 'A phenotypic profile of the Candida albicans regulatory network', *PLoS Genet*, 5(12), p. e1000783.
Homann, O.R., Dea, J., Noble, S.M. and Johnson, A.D. (2009) 'A phenotypic profile of the Candida albicans regulatory network', *PLoS Genet*, 5(12), p. e1000783.

Hood, M.I. and Skaar, E.P. (2012) 'Nutritional immunity: transition metals at the pathogen-host interface', *Nat Rev Microbiol*, 10(8), pp. 525-37.

Hothorn, M., Neumann, H., Lenherr, E.D., Wehner, M., Rybin, V., Hassa, P.O., Uttenweiler, A., Reinhardt, M., Schmidt, A., Seiler, J., Ladurner, A.G., Herrmann, C., Scheffzek, K. and Mayer, A. (2009) 'Catalytic core of a membrane-associated eukaryotic polyphosphate polymerase', *Science*, 324(5926), pp. 513-6.

Hoyer, L.L., Green, C.B., Oh, S.H. and Zhao, X. (2008) 'Discovering the secrets of the Candida albicans agglutinin-like sequence (ALS) gene family--a sticky pursuit', *Med Mycol*, 46(1), pp. 1-15.

Hoyer, L.L., Green, C.B., Oh, S.H. and Zhao, X. (2008) 'Discovering the secrets of the Candida albicans agglutinin-like sequence (ALS) gene family--a sticky pursuit', *Med Mycol*, 46(1), pp. 1-15.

Hromatka, B.S., Noble, S.M. and Johnson, A.D. (2005) 'Transcriptional response of Candida albicans to nitric oxide and the role of the YHB1 gene in nitrosative stress and virulence', *Mol Biol Cell*, 16(10), pp. 4814-26.

Hsieh, Y.J. and Wanner, B.L. (2010) 'Global regulation by the seven-component Pi signaling system', *Curr Opin Microbiol*, 13(2), pp. 198-203.

Huang, D., Friesen, H. and Andrews, B. (2007) 'Pho85, a multifunctional cyclin-dependent protein kinase in budding yeast', *Molecular Microbiology*, 66(2), pp. 303-314.

Huang, K., Ferrin-O'Connell, I., Zhang, W., Leonard, G.A., O'Shea, E.K. and Quiocho, F.A. (2007) 'Structure of the Pho85-Pho80 CDK-cyclin complex of the phosphate-responsive signal transduction pathway', *Mol Cell*, 28(4), pp. 614-23.

Hube, B. (2004) 'From commensal to pathogen: stage- and tissue-specific gene expression of Candida albicans', *Curr Opin Microbiol*, 7(4), pp. 336-41.

Hube, B., Stehr, F., Bossenz, M., Mazur, A., Kretschmar, M. and Schäfer, W. (2000) 'Secreted lipases of Candida albicans: cloning, characterisation and expression analysis of a new gene family with at least ten members', *Arch Microbiol*, 174(5), pp. 362-74.

Hürlimann, H.C., Pinson, B., Stadler-Waibel, M., Zeeman, S.C. and Freimoser, F.M. (2009) 'The SPX domain of the yeast low-affinity phosphate transporter Pho90 regulates transport activity', *EMBO Rep*, 10(9), pp. 1003-8.

Hussein, B., Huang, H., Glory, A., Osmani, A., Kaminskyj, S., Nantel, A. and Bachewich, C. (2011) 'G1/S transcription factor orthologues Swi4p and Swi6p are important but not

essential for cell proliferation and influence hyphal development in the fungal pathogen Candida albicans', *Eukaryot Cell*, 10(3), pp. 384-97.

Huycke, M.M., Moore, D., Joyce, W., Wise, P., Shepard, L., Kotake, Y. and Gilmore, M.S. (2001) 'Extracellular superoxide production by Enterococcus faecalis requires demethylmenaquinone and is attenuated by functional terminal quinol oxidases', *Mol Microbiol*, 42(3), pp. 729-40.

Hwang, C.S., Rhie, G.E., Oh, J.H., Huh, W.K., Yim, H.S. and Kang, S.O. (2002) 'Copper- and zinc-containing superoxide dismutase (Cu/ZnSOD) is required for the protection of Candida albicans against oxidative stresses and the expression of its full virulence', *Microbiology (Reading)*, 148(Pt 11), pp. 3705-3713.

Ibrahim, A.S., Luo, G., Gebremariam, T., Lee, H., Schmidt, C.S., Hennessey, J.P., Jr., French, S.W., Yeaman, M.R., Filler, S.G. and Edwards, J.E., Jr. (2013) 'NDV-3 protects mice from vulvovaginal candidiasis through T- and B-cell immune response', *Vaccine*, 31(47), pp. 5549-56.

Ihmels, J., Bergmann, S., Berman, J. and Barkai, N. (2005) 'Comparative gene expression analysis by differential clustering approach: application to the Candida albicans transcription program', *PLoS Genet*, 1(3), p. e39.

Ikeh, M., Ahmed, Y. and Quinn, J. (2017) 'Phosphate Acquisition and Virulence in Human Fungal Pathogens', *Microorganisms*, 5(3).

Ikeh, M.A., Kastora, S.L., Day, A.M., Herrero-de-Dios, C.M., Tarrant, E., Waldron, K.J., Banks, A.P., Bain, J.M., Lydall, D., Veal, E.A., MacCallum, D.M., Erwig, L.P., Brown, A.J. and Quinn, J. (2016) 'Pho4 mediates phosphate acquisition in Candida albicans and is vital for stress resistance and metal homeostasis', *Mol Biol Cell*, 27(17), pp. 2784-801.

Ikeh, M.A.C. (2015) *An investigation into the stress response mechanisms and virulence of the human fungal pathogen, Candida albicans*. Newcastle Univeristy.

Isasa, M., Rose, C.M., Elsasser, S., Navarrete-Perea, J., Paulo, J.A., Finley, D.J. and Gygi, S.P. (2015) 'Multiplexed, Proteome-Wide Protein Expression Profiling: Yeast Deubiquitylating Enzyme Knockout Strains', *J Proteome Res*, 14(12), pp. 5306-17.

Jain, C., Pastor, K., Gonzalez, A.Y., Lorenz, M.C. and Rao, R.P. (2013) 'The role of Candida albicans AP-1 protein against host derived ROS in in vivo models of infection', *Virulence*, 4(1), pp. 67-76.

Jeffery-Smith, A., Taori, S.K., Schelenz, S., Jeffery, K., Johnson, E.M., Borman, A., Manuel, R. and Brown, C.S. (2018) 'Candida auris: a Review of the Literature', *Clin Microbiol Rev*, 31(1).

Jemel, S., Guillot, J., Kallel, K., Botterel, F. and Dannaoui, E. (2020) 'Galleria mellonella for the Evaluation of Antifungal Efficacy against Medically Important Fungi, a Narrative Review', *Microorganisms*, 8(3), p. 390.

Jiménez, J., Bru, S., Ribeiro, M.P. and Clotet, J. (2017) 'Polyphosphate: popping up from oblivion', *Curr Genet*, 63(1), pp. 15-18.

Kaffman, A., Herskowitz, I., Tjian, R. and O'Shea, E.K. (1994) 'Phosphorylation of the transcription factor PHO4 by a cyclin-CDK complex, PHO80-PHO85', *Science*, 263(5150), pp. 1153-6.

Kaffman, A., Herskowitz, I., Tjian, R. and O'Shea, E.K. (1994) 'Phosphorylation of the transcription factor PHO4 by a cyclin-CDK complex, PHO80-PHO85', *Science*, 263(5150), pp. 1153-6.

Kaloriti, D., Jacobsen, M., Yin, Z., Patterson, M., Tillmann, A., Smith, D.A., Cook, E., You, T., Grimm, M.J., Bohovych, I., Grebogi, C., Segal, B.H., Gow, N.A., Haynes, K., Quinn, J. and Brown, A.J. (2014) 'Mechanisms underlying the exquisite sensitivity of Candida albicans to combinatorial cationic and oxidative stress that enhances the potent fungicidal activity of phagocytes', *mBio*, 5(4), pp. e01334-14.

Kaloriti, D., Jacobsen, M., Yin, Z., Patterson, M., Tillmann, A., Smith, D.A., Cook, E., You, T., Grimm, M.J., Bohovych, I., Grebogi, C., Segal, B.H., Gow, N.A., Haynes, K., Quinn, J. and Brown, A.J. (2014) 'Mechanisms underlying the exquisite sensitivity of Candida albicans to combinatorial cationic and oxidative stress that enhances the potent fungicidal activity of phagocytes', *mBio*, 5(4), pp. e01334-14.

Kantarcioglu, A.S. and Yücel, A. (2002) 'Phospholipase and protease activities in clinical Candida isolates with reference to the sources of strains', *Mycoses*, 45(5-6), pp. 160-5.

Kayingo, G., Martins, A., Andrie, R., Neves, L., Lucas, C. and Wong, B. (2009) 'A permease encoded by STL1 is required for active glycerol uptake by Candida albicans', *Microbiology (Reading)*, 155(Pt 5), pp. 1547-1557.

Keasling, J.D. (1997) 'Regulation of intracellular toxic metals and other cations by hydrolysis of polyphosphate', *Ann N Y Acad Sci*, 829, pp. 242-9.

Kennedy, E.J., Pillus, L. and Ghosh, G. (2005) 'Pho5p and newly identified nucleotide pyrophosphatases/ phosphodiesterases regulate extracellular nucleotide phosphate metabolism in Saccharomyces cerevisiae', *Eukaryot Cell*, 4(11), pp. 1892-901.

Kerwin, C.L. and Wykoff, D.D. (2009) 'Candida glabrata PHO4 is necessary and sufficient for Pho2-independent transcription of phosphate starvation genes', *Genetics*, 182(2), pp. 471-9.

Kerwin, C.L. and Wykoff, D.D. (2009) 'Candida glabrata PHO4 is necessary and sufficient for Pho2-independent transcription of phosphate starvation genes', *Genetics*, 182(2), pp. 471-9.
Keyhani, S., Lopez, J., Clark, D. and Keasling, J. (1996) 'Effect of polyphosphate on cadmium tolerance in the cyanobacterium Anacystis nidulans R2', *Microbios*, 88, pp. 105-114.
Kim, J.H., Chan, K.L., Cheng, L.W., Tell, L.A., Byrne, B.A., Clothier, K. and Land, K.M. (2019) 'High Efficiency Drug Repurposing Design for New Antifungal Agents', *Methods Protoc*, 2(2).
Kim, K.S., Rao, N.N., Fraley, C.D. and Kornberg, A. (2002) 'Inorganic polyphosphate is essential for long-term survival and virulence factors in Shigella and Salmonella spp', *Proc Natl Acad Sci U S A*, 99(11), pp. 7675-80.
Koç, A., Wheeler, L.J., Mathews, C.K. and Merrill, G.F. (2004) 'Hydroxyurea arrests DNA replication by a mechanism that preserves basal dNTP pools', *J Biol Chem*, 279(1), pp. 223-30.
Kofla, G. and Ruhnke, M. (2011) 'Pharmacology and metabolism of anidulafungin, caspofungin and micafungin in the treatment of invasive candidosis: review of the literature', *Eur J Med Res*, 16(4), pp. 159-66.
Köhler, J.R., Acosta-Zaldívar, M. and Qi, W. (2020) 'Phosphate in Virulence of Candida albicans and Candida glabrata', *J Fungi (Basel)*, 6(2).
Köhler, J.R., Hube, B., Puccia, R., Casadevall, A. and Perfect, J.R. (2017) 'Fungi that Infect Humans', *Microbiol Spectr*, 5(3).
Komalapriya, C., Kaloriti, D., Tillmann, A.T., Yin, Z., Herrero-de-Dios, C., Jacobsen, M.D., Belmonte, R.C., Cameron, G., Haynes, K., Grebogi, C., de Moura, A.P., Gow, N.A., Thiel, M., Quinn, J., Brown, A.J. and Romano, M.C. (2015) 'Integrative Model of Oxidative Stress Adaptation in the Fungal Pathogen Candida albicans', *PLoS One*, 10(9), p. e0137750.
Komeili, A. and O'Shea, E.K. (1999) 'Roles of phosphorylation sites in regulating activity of the transcription factor Pho4', *Science*, 284(5416), pp. 977-80.
Kos, I., Patterson, M.J., Znaidi, S., Kaloriti, D., da Silva Dantas, A., Herrero-de-Dios, C.M., d'Enfert, C., Brown, A.J. and Quinn, J. (2016) 'Mechanisms Underlying the Delayed Activation of the Cap1 Transcription Factor in Candida albicans following Combinatorial Oxidative and Cationic Stress Important for Phagocytic Potency', *mBio*, 7(2), p. e00331.
Kretschmer, M., Reiner, E., Hu, G., Tam, N., Oliveira, D.L., Caza, M., Yeon, J.H., Kim, J., Kastrup, C.J., Jung, W.H. and Kronstad, J.W. (2014) 'Defects in phosphate acquisition and storage influence virulence of Cryptococcus neoformans', *Infect Immun*, 82(7), pp. 2697-712.

Kulakovskaya, T.V. (2012) 'Inorganic polyphosphate in industry, agriculture and medicine: Modern state and outlook', *Process biochemistry*, v. 47(no. 1), pp. pp. 1-10-2012 v.47 no.1.
Kumble, K.D. and Kornberg, A. (1996) 'Endopolyphosphatases for long chain inorganic polyphosphate in yeast and mammals', *J Biol Chem*, 271(43), pp. 27146-51.
LaFleur, M.D., Lucumi, E., Napper, A.D., Diamond, S.L. and Lewis, K. (2011) 'Novel high-throughput screen against Candida albicans identifies antifungal potentiators and agents effective against biofilms', *J Antimicrob Chemother*, 66(4), pp. 820-6.
Lagerstedt, J.O., Zvyagilskaya, R., Pratt, J.R., Pattison-Granberg, J., Kruckeberg, A.L., Berden, J.A. and Persson, B.L. (2002) 'Mutagenic and functional analysis of the C-terminus of Saccharomyces cerevisiae Pho84 phosphate transporter', *FEBS Lett*, 526(1-3), pp. 31-7.
Lamarche, M.G., Wanner, B.L., Crépin, S. and Harel, J. (2008) 'The phosphate regulon and bacterial virulence: a regulatory network connecting phosphate homeostasis and pathogenesis', *FEMS Microbiol Rev*, 32(3), pp. 461-73.
Lamarre, C., LeMay, J.D., Deslauriers, N. and Bourbonnais, Y. (2001) 'Candida albicans expresses an unusual cytoplasmic manganese-containing superoxide dismutase (SOD3 gene product) upon the entry and during the stationary phase', *J Biol Chem*, 276(47), pp. 43784-91.
Lander, N., Ulrich, P.N. and Docampo, R. (2013) 'Trypanosoma brucei vacuolar transporter chaperone 4 (TbVtc4) is an acidocalcisome polyphosphate kinase required for in vivo infection', *J Biol Chem*, 288(47), pp. 34205-16.
Lavoie, H., Hogues, H. and Whiteway, M. (2009) 'Rearrangements of the transcriptional regulatory networks of metabolic pathways in fungi', *Curr Opin Microbiol*, 12(6), pp. 655-63.
Lavoie, H., Sellam, A., Askew, C., Nantel, A. and Whiteway, M. (2008) 'A toolbox for epitope-tagging and genome-wide location analysis in Candida albicans', *BMC Genomics*, 9, p. 578.
Lee, Y., Puumala, E., Robbins, N. and Cowen, L.E. (2020) 'Antifungal Drug Resistance: Molecular Mechanisms in Candida albicans and Beyond', *Chem Rev*.
Lee, Y.S., Mulugu, S., York, J.D. and O'Shea, E.K. (2007) 'Regulation of a cyclin-CDK-CDK inhibitor complex by inositol pyrophosphates', *Science*, 316(5821), pp. 109-12.
Lev, S., Crossett, B., Cha, S.Y., Desmarini, D., Li, C., Chayakulkeeree, M., Wilson, C.F., Williamson, P.R., Sorrell, T.C. and Djordjevic, J.T. (2014) 'Identification of Aph1, a phosphate-regulated, secreted, and vacuolar acid phosphatase in Cryptococcus neoformans', *mBio*, 5(5), pp. e01649-14.

Lev, S. and Djordjevic, J.T. (2018) 'Why is a functional PHO pathway required by fungal pathogens to disseminate within a phosphate-rich host: A paradox explained by alkaline pH-simulated nutrient deprivation and expanded PHO pathway function', *PLoS Pathog*, 14(6), p. e1007021.
Lev, S. and Djordjevic, J.T. (2018) 'Why is a functional PHO pathway required by fungal pathogens to disseminate within a phosphate-rich host: A paradox explained by alkaline pH-simulated nutrient deprivation and expanded PHO pathway function', *PLoS Pathog*, 14(6), p. e1007021.
Lev, S., Kaufman-Francis, K., Desmarini, D., Juillard, P.G., Li, C., Stifter, S.A., Feng, C.G., Sorrell, T.C., Grau, G.E., Bahn, Y.S. and Djordjevic, J.T. (2017) 'Pho4 Is Essential for Dissemination of Cryptococcus neoformans to the Host Brain by Promoting Phosphate Uptake and Growth at Alkaline pH', *mSphere*, 2(1).

Lev, S., Li, C., Desmarini, D., Saiardi, A., Fewings, N.L., Schibeci, S.D., Sharma, R., Sorrell, T.C. and Djordjevic, J.T. (2015) 'Fungal Inositol Pyrophosphate IP7 Is Crucial for Metabolic Adaptation to the Host Environment and Pathogenicity', *mBio*, 6(3), pp. e00531-15.

Li, C.X., Gleason, J.E., Zhang, S.X., Bruno, V.M., Cormack, B.P. and Culotta, V.C. (2015) 'Candida albicans adapts to host copper during infection by swapping metal cofactors for superoxide dismutase', *Proc Natl Acad Sci U S A*, 112(38), pp. E5336-42.

Li, J., Zhang, B., Ma, T., Wang, H., Zhang, B., Yu, Q. and Li, M. (2017) 'Role of the Inositol Polyphosphate Multikinase Ipk2 in Regulation of Hyphal Development, Calcium Signaling and Secretion in Candida albicans', *Mycopathologia*, 182(7-8), pp. 609-623.

Lichko, L.P., Kulakovskaya, T.V. and Kulaev, I.S. (2010) 'Properties of partially purified endopolyphosphatase of the yeast Saccharomyces cerevisiae', *Biochemistry (Mosc)*, 75(11), pp. 1404-7.

Lichko, L.P., Kulakovskaya, T.V., Kulakovskaya, E.V. and Kulaev, I.S. (2008) 'Inactivation of PPX1 and PPN1 genes encoding exopolyphosphatases of Saccharomyces cerevisiae does not prevent utilization of polyphosphates as phosphate reserve', *Biochemistry (Mosc)*, 73(9), pp. 985-9.

Lim, S. and Kaldis, P. (2013) 'Cdks, cyclins and CKIs: roles beyond cell cycle regulation', *Development*, 140(15), pp. 3079-3093.

Liu, N.N., Flanagan, P.R., Zeng, J., Jani, N.M., Cardenas, M.E., Moran, G.P. and Köhler, J.R. (2017) 'Phosphate is the third nutrient monitored by TOR in Candida albicans and provides a

target for fungal-specific indirect TOR inhibition', *Proc Natl Acad Sci U S A*, 114(24), pp. 6346-6351.

Liu, N.N., Uppuluri, P., Broggi, A., Besold, A., Ryman, K., Kambara, H., Solis, N., Lorenz, V., Qi, W., Acosta-Zaldívar, M., Emami, S.N., Bao, B., An, D., Bonilla, F.A., Sola-Visner, M., Filler, S.G., Luo, H.R., Engström, Y., Ljungdahl, P.O., Culotta, V.C., Zanoni, I., Lopez-Ribot, J.L. and Köhler, J.R. (2018) 'Intersection of phosphate transport, oxidative stress and TOR signalling in Candida albicans virulence', *PLoS Pathog*, 14(7), p. e1007076.

Liu, Y., Mittal, R., Solis, N.V., Prasadarao, N.V. and Filler, S.G. (2011) 'Mechanisms of Candida albicans trafficking to the brain', *PLoS Pathog*, 7(10), p. e1002305.

Lo, H.J., Köhler, J.R., DiDomenico, B., Loebenberg, D., Cacciapuoti, A. and Fink, G.R. (1997) 'Nonfilamentous C. albicans mutants are avirulent', *Cell*, 90(5), pp. 939-49.

Lohberger, A., Coste, A.T. and Sanglard, D. (2014) 'Distinct roles of Candida albicans drug resistance transcription factors TAC1, MRR1, and UPC2 in virulence', *Eukaryot Cell*, 13(1), pp. 127-42.

Lonetti, A., Szijgyarto, Z., Bosch, D., Loss, O., Azevedo, C. and Saiardi, A. (2011) 'Identification of an evolutionarily conserved family of inorganic polyphosphate endopolyphosphatases', *J Biol Chem*, 286(37), pp. 31966-74.

Lorenz, M.C., Bender, J.A. and Fink, G.R. (2004) 'Transcriptional response of Candida albicans upon internalization by macrophages', *Eukaryot Cell*, 3(5), pp. 1076-87.

Loyse, A., Burry, J., Cohn, J., Ford, N., Chiller, T., Ribeiro, I., Koulla-Shiro, S., Mghamba, J., Ramadhani, A., Nyirenda, R., Aliyu, S.H., Wilson, D., Le, T., Oladele, R., Lesikari, S., Muzoora, C., Kalata, N., Temfack, E., Mapoure, Y., Sini, V., Chanda, D., Shimwela, M., Lakhi, S., Ngoma, J., Gondwe-Chunda, L., Perfect, C., Shroufi, A., Andrieux-Meyer, I., Chan, A., Schutz, C., Hosseinipour, M., Van der Horst, C., Klausner, J.D., Boulware, D.R., Heyderman, R., Lalloo, D., Day, J., Jarvis, J.N., Rodrigues, M., Jaffar, S., Denning, D., Migone, C., Doherty, M., Lortholary, O., Dromer, F., Stack, M., Molloy, S.F., Bicanic, T., van Oosterhout, J., Mwaba, P., Kanyama, C., Kouanfack, C., Mfinanga, S., Govender, N. and Harrison, T.S. (2019) 'Leave no one behind: response to new evidence and guidelines for the management of cryptococcal meningitis in low-income and middle-income countries', *Lancet Infect Dis*, 19(4), pp. e143-e147.

Lu, Y., Su, C., Solis, N.V., Filler, S.G. and Liu, H. (2013) 'Synergistic regulation of hyphal elongation by hypoxia, CO(2), and nutrient conditions controls the virulence of Candida albicans', *Cell Host Microbe*, 14(5), pp. 499-509.

Lu, Y., Su, C., Wang, A. and Liu, H. (2011) 'Hyphal development in Candida albicans requires two temporally linked changes in promoter chromatin for initiation and maintenance', *PLoS Biol*, 9(7), p. e1001105.

Luo, H.R., Saiardi, A., Yu, H., Nagata, E., Ye, K. and Snyder, S.H. (2002) 'Inositol pyrophosphates are required for DNA hyperrecombination in protein kinase c1 mutant yeast', *Biochemistry*, 41(8), pp. 2509-15.

Lushchak, V.I. (2011) 'Adaptive response to oxidative stress: Bacteria, fungi, plants and animals', *Comp Biochem Physiol C Toxicol Pharmacol*, 153(2), pp. 175-90.

Ma, T., Yu, Q., Ma, C., Mao, X., Liu, Y., Peng, X. and Li, M. (2020) 'Role of the inositol polyphosphate kinase Vip1 in autophagy and pathogenesis in Candida albicans', *Future Microbiol*, 15, pp. 1363-1377.

MacCallum, D.M., Castillo, L., Nather, K., Munro, C.A., Brown, A.J., Gow, N.A. and Odds, F.C. (2009) 'Property differences among the four major Candida albicans strain clades', *Eukaryot Cell*, 8(3), pp. 373-87.

Mackie, J., Szabo, E.K., Urgast, D.S., Ballou, E.R., Childers, D.S., MacCallum, D.M., Feldmann, J. and Brown, A.J. (2016) 'Host-Imposed Copper Poisoning Impacts Fungal Micronutrient Acquisition during Systemic Candida albicans Infections', *PLoS One*, 11(6), p. e0158683.

Mallick, E.M., Bergeron, A.C., Jones, S.K., Jr., Newman, Z.R., Brothers, K.M., Creton, R., Wheeler, R.T. and Bennett, R.J. (2016) 'Phenotypic Plasticity Regulates Candida albicans Interactions and Virulence in the Vertebrate Host', *Front Microbiol*, 7, p. 780.

Martchenko, M., Alarco, A.M., Harcus, D. and Whiteway, M. (2004) 'Superoxide dismutases in Candida albicans: transcriptional regulation and functional characterization of the hyphal-induced SOD5 gene', *Mol Biol Cell*, 15(2), pp. 456-67.

Martinez, P., Zvyagilskaya, R., Allard, P. and Persson, B.L. (1998) 'Physiological regulation of the derepressible phosphate transporter in Saccharomyces cerevisiae', *J Bacteriol*, 180(8), pp. 2253-6.

Martínez-Esparza, M., Aguinaga, A., González-Párraga, P., García-Peñarrubia, P., Jouault, T. and Argüelles, J.C. (2007) 'Role of trehalose in resistance to macrophage killing: study with a tps1/tps1 trehalose-deficient mutant of Candida albicans', *Clin Microbiol Infect*, 13(4), pp. 384-94.

Martínez-Esparza, M., Martínez-Vicente, E., González-Párraga, P., Ros, J.M., García-Peñarrubia, P. and Argüelles, J.C. (2009) 'Role of trehalose-6P phosphatase (TPS2) in stress

tolerance and resistance to macrophage killing in Candida albicans', *Int J Med Microbiol*, 299(6), pp. 453-64.

Mast, N., Zheng, W., Stout, C.D. and Pikuleva, I.A. (2013) 'Antifungal Azoles: Structural Insights into Undesired Tight Binding to Cholesterol-Metabolizing CYP46A1', *Mol Pharmacol*, 84(1), pp. 86-94.

Mathew, B.P. and Nath, M. (2009) 'Recent approaches to antifungal therapy for invasive mycoses', *ChemMedChem*, 4(3), pp. 310-23.

Mayer, F.L., Wilson, D., Jacobsen, I.D., Miramón, P., Slesiona, S., Bohovych, I.M., Brown, A.J. and Hube, B. (2012) 'Small but crucial: the novel small heat shock protein Hsp21 mediates stress adaptation and virulence in Candida albicans', *PLoS One*, 7(6), p. e38584.

Measday, V., McBride, H., Moffat, J., Stillman, D. and Andrews, B. (2000) 'Interactions between Pho85 cyclin-dependent kinase complexes and the Swi5 transcription factor in budding yeast', *Mol Microbiol*, 35(4), pp. 825-34.

Menoyo, S., Ricco, N., Bru, S., Hernández-Ortega, S., Escoté, X., Aldea, M. and Clotet, J. (2013) 'Phosphate-activated cyclin-dependent kinase stabilizes G1 cyclin to trigger cell cycle entry', *Mol Cell Biol*, 33(7), pp. 1273-84.

Mesa-Arango, A.C., Trevijano-Contador, N., Román, E., Sánchez-Fresneda, R., Casas, C., Herrero, E., Argüelles, J.C., Pla, J., Cuenca-Estrella, M. and Zaragoza, O. (2014) 'The production of reactive oxygen species is a universal action mechanism of Amphotericin B against pathogenic yeasts and contributes to the fungicidal effect of this drug', *Antimicrob Agents Chemother*, 58(11), pp. 6627-38.

Miramón, P., Dunker, C., Kasper, L., Jacobsen, I.D., Barz, D., Kurzai, O. and Hube, B. (2014) 'A family of glutathione peroxidases contributes to oxidative stress resistance in Candida albicans', *Med Mycol*, 52(3), pp. 223-39.

Miyakawa, Y. (2000) 'Identification of a Candida albicans homologue of the PHO85 gene, a negative regulator of the PHO system in Saccharomyces cerevisiae', *Yeast*, 16(11), pp. 1045-51.

Monod, M. and Borg-von Zepelin, M. (2002) 'Secreted proteinases and other virulence mechanisms of Candida albicans', *Chem Immunol*, 81, pp. 114-28.

Moreno, S.N. and Docampo, R. (2013) 'Polyphosphate and its diverse functions in host cells and pathogens', *PLoS Pathog*, 9(5), p. e1003230.

Morgan, J. (2005) 'Global trends in candidemia: review of reports from 1995-2005', *Curr Infect Dis Rep*, 7(6), pp. 429-39.

Mukherjee, P.K., Chandra, J., Kuhn, D.M. and Ghannoum, M.A. (2003) 'Differential expression of Candida albicans phospholipase B (PLB1) under various environmental and physiological conditions', *Microbiology (Reading)*, 149(Pt 1), pp. 261-7.
Müller, F., Mutch, N.J., Schenk, W.A., Smith, S.A., Esterl, L., Spronk, H.M., Schmidbauer, S., Gahl, W.A., Morrissey, J.H. and Renné, T. (2009) 'Platelet polyphosphates are proinflammatory and procoagulant mediators in vivo', *Cell*, 139(6), pp. 1143-56.
Müller, O., Bayer, M.J., Peters, C., Andersen, J.S., Mann, M. and Mayer, A. (2002) 'The Vtc proteins in vacuole fusion: coupling NSF activity to V(0) trans-complex formation', *Embo j*, 21(3), pp. 259-69.
Muñoz, J.F., Delorey, T., Ford, C.B., Li, B.Y., Thompson, D.A., Rao, R.P. and Cuomo, C.A. (2019) 'Coordinated host-pathogen transcriptional dynamics revealed using sorted subpopulations and single macrophages infected with Candida albicans', *Nat Commun*, 10(1), p. 1607.
Murad, A.M., Leng, P., Straffon, M., Wishart, J., Macaskill, S., MacCallum, D., Schnell, N., Talibi, D., Marechal, D., Tekaia, F., d'Enfert, C., Gaillardin, C., Odds, F.C. and Brown, A.J. (2001) 'NRG1 represses yeast-hypha morphogenesis and hypha-specific gene expression in Candida albicans', *Embo j*, 20(17), pp. 4742-52.
Naglik, J., Albrecht, A., Bader, O. and Hube, B. (2004) 'Candida albicans proteinases and host/pathogen interactions', *Cell Microbiol*, 6(10), pp. 915-26.
Naglik, J.R., Challacombe, S.J. and Hube, B. (2003) 'Candida albicans secreted aspartyl proteinases in virulence and pathogenesis', *Microbiol Mol Biol Rev*, 67(3), pp. 400-28, table of contents.
Naglik, J.R., Fostira, F., Ruprai, J., Staab, J.F., Challacombe, S.J. and Sundstrom, P. (2006) 'Candida albicans HWP1 gene expression and host antibody responses in colonization and disease', *J Med Microbiol*, 55(Pt 10), pp. 1323-1327.
Naglik, J.R., Gaffen, S.L. and Hube, B. (2019) 'Candidalysin: discovery and function in Candida albicans infections', *Curr Opin Microbiol*, 52, pp. 100-109.
Naglik, J.R., König, A., Hube, B. and Gaffen, S.L. (2017) 'Candida albicans-epithelial interactions and induction of mucosal innate immunity', *Curr Opin Microbiol*, 40, pp. 104-112.
Naglik, J.R., Rodgers, C.A., Shirlaw, P.J., Dobbie, J.L., Fernandes-Naglik, L.L., Greenspan, D., Agabian, N. and Challacombe, S.J. (2003) 'Differential expression of Candida albicans

secreted aspartyl proteinase and phospholipase B genes in humans correlates with active oral and vaginal infections', *J Infect Dis*, 188(3), pp. 469-79.
Nakagawa, Y. (2008) 'Catalase gene disruptant of the human pathogenic yeast Candida albicans is defective in hyphal growth, and a catalase-specific inhibitor can suppress hyphal growth of wild-type cells', *Microbiol Immunol*, 52(1), pp. 16-24.
Navarathna, D.H. and Roberts, D.D. (2010) 'Candida albicans heme oxygenase and its product CO contribute to pathogenesis of candidemia and alter systemic chemokine and cytokine expression', *Free Radic Biol Med*, 49(10), pp. 1561-73.
Neef, D.W. and Kladde, M.P. (2003) 'Polyphosphate loss promotes SNF/SWI- and Gcn5-dependent mitotic induction of PHO5', *Mol Cell Biol*, 23(11), pp. 3788-97.
Netea, M.G., Joosten, L.A., van der Meer, J.W., Kullberg, B.J. and van de Veerdonk, F.L. (2015) 'Immune defence against Candida fungal infections', *Nat Rev Immunol*, 15(10), pp. 630-42.
Niimi, K., Monk, B.C., Hirai, A., Hatakenaka, K., Umeyama, T., Lamping, E., Maki, K., Tanabe, K., Kamimura, T., Ikeda, F., Uehara, Y., Kano, R., Hasegawa, A., Cannon, R.D. and Niimi, M. (2010) 'Clinically significant micafungin resistance in Candida albicans involves modification of a glucan synthase catalytic subunit GSC1 (FKS1) allele followed by loss of heterozygosity', *J Antimicrob Chemother*, 65(5), pp. 842-52.
Nishizawa, M., Suzuki, K., Fujino, M., Oguchi, T. and Toh-e, A. (1999) 'The Pho85 kinase, a member of the yeast cyclin-dependent kinase (Cdk) family, has a regulation mechanism different from Cdks functioning throughout the cell cycle', *Genes Cells*, 4(11), pp. 627-42.
Nobbs, A.H., Vickerman, M.M. and Jenkinson, H.F. (2010) 'Heterologous expression of Candida albicans cell wall-associated adhesins in Saccharomyces cerevisiae Reveals differential specificities in adherence and biofilm formation and in binding oral Streptococcus gordonii', *Eukaryot Cell*, 9(10), pp. 1622-34.
Nobile, C.J. and Johnson, A.D. (2015) 'Candida albicans Biofilms and Human Disease', *Annu Rev Microbiol*, 69, pp. 71-92.
Noble, S.M., French, S., Kohn, L.A., Chen, V. and Johnson, A.D. (2010) 'Systematic screens of a Candida albicans homozygous deletion library decouple morphogenetic switching and pathogenicity', *Nat Genet*, 42(7), pp. 590-8.
Nurse, P., Thuriaux, P. and Nasmyth, K. (1976) 'Genetic control of the cell division cycle in the fission yeast Schizosaccharomyces pombe', *Mol Gen Genet*, 146(2), pp. 167-78.

Odds, F.C., Brown, A.J. and Gow, N.A. (2003) 'Antifungal agents: mechanisms of action', *Trends Microbiol*, 11(6), pp. 272-9.
Ohno, A., Müller, E., Fraek, M.L., Thurau, K. and Beck, F. (1997) 'Solute composition and heat shock proteins in rat renal medulla', *Pflugers Arch*, 434(1), pp. 117-22.
O'Neill, E.M., Kaffman, A., Jolly, E.R. and O'Shea, E.K. (1996) 'Regulation of PHO4 nuclear localization by the PHO80-PHO85 cyclin-CDK complex', *Science*, 271(5246), pp. 209-12.
O'Neill, E.M., Kaffman, A., Jolly, E.R. and O'Shea, E.K. (1996) 'Regulation of PHO4 nuclear localization by the PHO80-PHO85 cyclin-CDK complex', *Science*, 271(5246), pp. 209-12.
Owen, D.H. and Katz, D.F. (1999) 'A vaginal fluid simulant', *Contraception*, 59(2), pp. 91-5.
Pappas, P.G., Kauffman, C.A., Andes, D.R., Clancy, C.J., Marr, K.A., Ostrosky-Zeichner, L., Reboli, A.C., Schuster, M.G., Vazquez, J.A., Walsh, T.J., Zaoutis, T.E. and Sobel, J.D. (2016) 'Clinical Practice Guideline for the Management of Candidiasis: 2016 Update by the Infectious Diseases Society of America', *Clin Infect Dis*, 62(4), pp. e1-50.
Patterson, M.J., McKenzie, C.G., Smith, D.A., da Silva Dantas, A., Sherston, S., Veal, E.A., Morgan, B.A., MacCallum, D.M., Erwig, L.P. and Quinn, J. (2013) 'Ybp1 and Gpx3 signaling in Candida albicans govern hydrogen peroxide-induced oxidation of the Cap1 transcription factor and macrophage escape', *Antioxid Redox Signal*, 19(18), pp. 2244-60.
Pemán, J., Cantón, E. and Espinel-Ingroff, A. (2009) 'Antifungal drug resistance mechanisms', *Expert Rev Anti Infect Ther*, 7(4), pp. 453-60.
Pentland, D.R., Stevens, S., Williams, L., Baker, M., McCall, C., Makarovaite, V., Balfour, A., Mühlschlegel, F.A. and Gourlay, C.W. (2020) 'Precision Antifungal Treatment Significantly Extends Voice Prosthesis Lifespan in Patients Following Total Laryngectomy', *Front Microbiol*, 11, p. 975.
Persson, B.L., Lagerstedt, J.O., Pratt, J.R., Pattison-Granberg, J., Lundh, K., Shokrollahzadeh, S. and Lundh, F. (2003) 'Regulation of phosphate acquisition in Saccharomyces cerevisiae', *Curr Genet*, 43(4), pp. 225-44.
Petersson, J., Pattison, J., Kruckeberg, A.L., Berden, J.A. and Persson, B.L. (1999) 'Intracellular localization of an active green fluorescent protein-tagged Pho84 phosphate permease in Saccharomyces cerevisiae', *FEBS Lett*, 462(1-2), pp. 37-42.
PETTERSSON, A., Kunst, L., Bergman, B. and Roomans, G.M. (1985) 'Accumulation of aluminium by Anabaena cylindrica into polyphosphate granules and cell walls: an X-ray energy-dispersive microanalysis study', *Microbiology*, 131(10), pp. 2545-2548.

Pfaller, M.A. and Diekema, D.J. (2007) 'Epidemiology of invasive candidiasis: a persistent public health problem', *Clin Microbiol Rev*, 20(1), pp. 133-63.
Pfaller, M.A. and Diekema, D.J. (2007) 'Epidemiology of invasive candidiasis: a persistent public health problem', *Clin Microbiol Rev*, 20(1), pp. 133-63.
Pfaller, M.A., Diekema, D.J., Andes, D., Arendrup, M.C., Brown, S.D., Lockhart, S.R., Motyl, M. and Perlin, D.S. (2011) 'Clinical breakpoints for the echinocandins and Candida revisited: integration of molecular, clinical, and microbiological data to arrive at species-specific interpretive criteria', *Drug Resist Updat*, 14(3), pp. 164-76.

Phan, Q.T., Myers, C.L., Fu, Y., Sheppard, D.C., Yeaman, M.R., Welch, W.H., Ibrahim, A.S., Edwards, J.E., Jr. and Filler, S.G. (2007) 'Als3 is a Candida albicans invasin that binds to cadherins and induces endocytosis by host cells', *PLoS Biol*, 5(3), p. e64.

Pick, U. and Weiss, M. (1991) 'Polyphosphate Hydrolysis within Acidic Vacuoles in Response to Amine-Induced Alkaline Stress in the Halotolerant Alga Dunaliella salina', *Plant Physiol*, 97(3), pp. 1234-40.

Pierce, C.G. and Lopez-Ribot, J.L. (2013) 'Candidiasis drug discovery and development: new approaches targeting virulence for discovering and identifying new drugs', *Expert Opin Drug Discov*, 8(9), pp. 1117-26.

Pontes, M.H. and Groisman, E.A. (2018) 'Protein synthesis controls phosphate homeostasis', *Genes Dev*, 32(1), pp. 79-92.

Potrykus, J., Stead, D., Maccallum, D.M., Urgast, D.S., Raab, A., van Rooijen, N., Feldmann, J. and Brown, A.J. (2013) 'Fungal iron availability during deep seated candidiasis is defined by a complex interplay involving systemic and local events', *PLoS Pathog*, 9(10), p. e1003676.

Poulain, D. (2015) 'Candida albicans, plasticity and pathogenesis', *Crit Rev Microbiol*, 41(2), pp. 208-17.

Pratt, J.T., Ismail, A.M. and Camilli, A. (2010) 'PhoB regulates both environmental and virulence gene expression in Vibrio cholerae', *Mol Microbiol*, 77(6), pp. 1595-605.

Pukkila-Worley, R., Ausubel, F.M. and Mylonakis, E. (2011) 'Candida albicans infection of Caenorhabditis elegans induces antifungal immune defenses', *PLoS Pathog*, 7(6), p. e1002074.

Ramanan, N. and Wang, Y. (2000) 'A high-affinity iron permease essential for Candida albicans virulence', *Science*, 288(5468), pp. 1062-4.

Ramos, C.L., Gomes, F.M., Girard-Dias, W., Almeida, F.P., Albuquerque, P.C., Kretschmer, M., Kronstad, J.W., Frases, S., de Souza, W., Rodrigues, M.L. and Miranda, K. (2017) 'Phosphorus-

rich structures and capsular architecture in Cryptococcus neoformans', *Future Microbiol*, 12, pp. 227-238.

Rao, N.N., Gómez-García, M.R. and Kornberg, A. (2009) 'Inorganic polyphosphate: essential for growth and survival', *Annu Rev Biochem*, 78, pp. 605-47.

Rashid, M.H., Rumbaugh, K., Passador, L., Davies, D.G., Hamood, A.N., Iglewski, B.H. and Kornberg, A. (2000) 'Polyphosphate kinase is essential for biofilm development, quorum sensing, and virulence of Pseudomonas aeruginosa', *Proc Natl Acad Sci U S A*, 97(17), pp. 9636-41.

Reed, S.I., Ferguson, J. and Groppe, J.C. (1982) 'Preliminary characterization of the transcriptional and translational products of the Saccharomyces cerevisiae cell division cycle gene CDC28', *Molecular and Cellular Biology*, 2(4), pp. 412-425.

Reeves, E.P., Lu, H., Jacobs, H.L., Messina, C.G., Bolsover, S., Gabella, G., Potma, E.O., Warley, A., Roes, J. and Segal, A.W. (2002) 'Killing activity of neutrophils is mediated through activation of proteases by K+ flux', *Nature*, 416(6878), pp. 291-7.

Revie, N.M., Iyer, K.R., Robbins, N. and Cowen, L.E. (2018) 'Antifungal drug resistance: evolution, mechanisms and impact', *Curr Opin Microbiol*, 45, pp. 70-76.

Revie, N.M., Robbins, N., Whitesell, L., Frost, J.R., Appavoo, S.D., Yudin, A.K. and Cowen, L.E. (2020) 'Oxadiazole-Containing Macrocyclic Peptides Potentiate Azole Activity against Pathogenic Candida Species', *mSphere*, 5(2).

Richardson, J.P., Mogavero, S., Moyes, D.L., Blagojevic, M., Krüger, T., Verma, A.H., Coleman, B.M., De La Cruz Diaz, J., Schulz, D., Ponde, N.O., Carrano, G., Kniemeyer, O., Wilson, D., Bader, O., Enoiu, S.I., Ho, J., Kichik, N., Gaffen, S.L., Hube, B. and Naglik, J.R. (2018) 'Processing of Candida albicans Ece1p Is Critical for Candidalysin Maturation and Fungal Virulence', *mBio*, 9(1).

Richardson, J.P., Moyes, D.L., Ho, J. and Naglik, J.R. (2019) 'Candida innate immunity at the mucosa', *Semin Cell Dev Biol*, 89, pp. 58-70.

Rinnerthaler, M., Büttner, S., Laun, P., Heeren, G., Felder, T.K., Klinger, H., Weinberger, M., Stolze, K., Grousl, T., Hasek, J., Benada, O., Frydlova, I., Klocker, A., Simon-Nobbe, B., Jansko, B., Breitenbach-Koller, H., Eisenberg, T., Gourlay, C.W., Madeo, F., Burhans, W.C. and Breitenbach, M. (2012) 'Yno1p/Aim14p, a NADPH-oxidase ortholog, controls extramitochondrial reactive oxygen species generation, apoptosis, and actin cable formation in yeast', *Proc Natl Acad Sci U S A*, 109(22), pp. 8658-63.

Robbins, N., Caplan, T. and Cowen, L.E. (2017) 'Molecular Evolution of Antifungal Drug Resistance', *Annu Rev Microbiol*, 71, pp. 753-775.

Rodaki, A., Bohovych, I.M., Enjalbert, B., Young, T., Odds, F.C., Gow, N.A. and Brown, A.J. (2009) 'Glucose promotes stress resistance in the fungal pathogen Candida albicans', *Mol Biol Cell*, 20(22), pp. 4845-55.

Roemer, T. and Krysan, D.J. (2014) 'Antifungal drug development: challenges, unmet clinical needs, and new approaches', *Cold Spring Harb Perspect Med*, 4(5).

Romanowski, K., Zaborin, A., Valuckaite, V., Rolfes, R.J., Babrowski, T., Bethel, C., Olivas, A., Zaborina, O. and Alverdy, J.C. (2012) 'Candida albicans isolates from the gut of critically ill patients respond to phosphate limitation by expressing filaments and a lethal phenotype', *PLoS One*, 7(1), p. e30119.

Rosenfeld, L., Reddi, A.R., Leung, E., Aranda, K., Jensen, L.T. and Culotta, V.C. (2010) 'The effect of phosphate accumulation on metal ion homeostasis in Saccharomyces cerevisiae', *J Biol Inorg Chem*, 15(7), pp. 1051-62.

Rothstein, A. and Meier, R. (1951) 'The relationship of the cell surface to metabolism. VI. The chemical nature of uranium-complexing groups of the cell surface', *J Cell Comp Physiol*, 38(2), pp. 245-70.

Rubin-Bejerano, I., Fraser, I., Grisafi, P. and Fink, G.R. (2003) 'Phagocytosis by neutrophils induces an amino acid deprivation response in Saccharomyces cerevisiae and Candida albicans', *Proc Natl Acad Sci U S A*, 100(19), pp. 11007-12.

Ruiz, F.A., Rodrigues, C.O. and Docampo, R. (2001) 'Rapid changes in polyphosphate content within acidocalcisomes in response to cell growth, differentiation, and environmental stress in Trypanosoma cruzi', *J Biol Chem*, 276(28), pp. 26114-21.

Safrany, S.T., Caffrey, J.J., Yang, X., Bembenek, M.E., Moyer, M.B., Burkhart, W.A. and Shears, S.B. (1998) 'A novel context for the 'MutT' module, a guardian of cell integrity, in a diphosphoinositol polyphosphate phosphohydrolase', *Embo j*, 17(22), pp. 6599-607.

Saiardi, A., Bhandari, R., Resnick, A.C., Snowman, A.M. and Snyder, S.H. (2004) 'Phosphorylation of proteins by inositol pyrophosphates', *Science*, 306(5704), pp. 2101-5.

Saiardi, A., Caffrey, J.J., Snyder, S.H. and Shears, S.B. (2000) 'The inositol hexakisphosphate kinase family. Catalytic flexibility and function in yeast vacuole biogenesis', *J Biol Chem*, 275(32), pp. 24686-92.

Saiardi, A., Sciambi, C., McCaffery, J.M., Wendland, B. and Snyder, S.H. (2002) 'Inositol pyrophosphates regulate endocytic trafficking', *Proc Natl Acad Sci U S A*, 99(22), pp. 14206-11.

Salgado, P.S., Yan, R., Taylor, J.D., Burchell, L., Jones, R., Hoyer, L.L., Matthews, S.J., Simpson, P.J. and Cota, E. (2011) 'Structural basis for the broad specificity to host-cell ligands by the pathogenic fungus Candida albicans', *Proc Natl Acad Sci U S A*, 108(38), pp. 15775-9.

Sambade, M., Alba, M., Smardon, A.M., West, R.W. and Kane, P.M. (2005) 'A genomic screen for yeast vacuolar membrane ATPase mutants', *Genetics*, 170(4), pp. 1539-51.

Sambade, M., Alba, M., Smardon, A.M., West, R.W. and Kane, P.M. (2005) 'A genomic screen for yeast vacuolar membrane ATPase mutants', *Genetics*, 170(4), pp. 1539-51.

Sanglard, D., Ischer, F., Parkinson, T., Falconer, D. and Bille, J. (2003) 'Candida albicans mutations in the ergosterol biosynthetic pathway and resistance to several antifungal agents', *Antimicrob Agents Chemother*, 47(8), pp. 2404-12.

Sardi Jde, C., Pitangui Nde, S., Rodríguez-Arellanes, G., Taylor, M.L., Fusco-Almeida, A.M. and Mendes-Giannini, M.J. (2014) 'Highlights in pathogenic fungal biofilms', *Rev Iberoam Micol*, 31(1), pp. 22-9.

Saville, S.P., Lazzell, A.L., Bryant, A.P., Fretzen, A., Monreal, A., Solberg, E.O., Monteagudo, C., Lopez-Ribot, J.L. and Milne, G.T. (2006) 'Inhibition of filamentation can be used to treat disseminated candidiasis', *Antimicrob Agents Chemother*, 50(10), pp. 3312-6.

Saville, S.P., Lazzell, A.L., Monteagudo, C. and Lopez-Ribot, J.L. (2003) 'Engineered control of cell morphology in vivo reveals distinct roles for yeast and filamentous forms of Candida albicans during infection', *Eukaryot Cell*, 2(5), pp. 1053-60.

Scaduto, C.M. and Bennett, R.J. (2015) 'Candida albicans the chameleon: transitions and interactions between multiple phenotypic states confer phenotypic plasticity', *Curr Opin Microbiol*, 26, pp. 102-8.

Schaller, M., Borelli, C., Korting, H.C. and Hube, B. (2005) 'Hydrolytic enzymes as virulence factors of Candida albicans', *Mycoses*, 48(6), pp. 365-77.

Schatzman, S.S., Peterson, R.L., Teka, M., He, B., Cabelli, D.E., Cormack, B.P. and Culotta, V.C. (2020) 'Copper-only superoxide dismutase enzymes and iron starvation stress in Candida fungal pathogens', *J Biol Chem*, 295(2), pp. 570-583.

Schiavi, S.C. and Kumar, R. (2004) 'The phosphatonin pathway: new insights in phosphate homeostasis', *Kidney Int*, 65(1), pp. 1-14.

Schneider, K.R., Smith, R.L. and O'Shea, E.K. (1994) 'Phosphate-regulated inactivation of the kinase PHO80-PHO85 by the CDK inhibitor PHO81', *Science*, 266(5182), pp. 122-6.
Schwalfenberg, G.K. (2012) 'The alkaline diet: is there evidence that an alkaline pH diet benefits health?', *J Environ Public Health*, 2012, p. 727630.
Secco, D., Wang, C., Shou, H. and Whelan, J. (2012) 'Phosphate homeostasis in the yeast Saccharomyces cerevisiae, the key role of the SPX domain-containing proteins', *FEBS Lett*, 586(4), pp. 289-95.
Segal, E.S., Gritsenko, V., Levitan, A., Yadav, B., Dror, N., Steenwyk, J.L., Silberberg, Y., Mielich, K., Rokas, A., Gow, N.A.R., Kunze, R., Sharan, R. and Berman, J. (2018) 'Gene Essentiality Analyzed by In Vivo Transposon Mutagenesis and Machine Learning in a Stable Haploid Isolate of Candida albicans', *mBio*, 9(5).
Sellam, A. and Whiteway, M. (2016) 'Recent advances on Candida albicans biology and virulence', *F1000Res*, 5, p. 2582.
Selmecki, A., Forche, A. and Berman, J. (2006) 'Aneuploidy and isochromosome formation in drug-resistant Candida albicans', *Science*, 313(5785), pp. 367-70.
Serra-Cardona, A., Canadell, D. and Ariño, J. (2015) 'Coordinate responses to alkaline pH stress in budding yeast', *Microb Cell*, 2(6), pp. 182-196.
Serra-Cardona, A., Petrezsélyová, S., Canadell, D., Ramos, J. and Ariño, J. (2014) 'Coregulated expression of the Na+/phosphate Pho89 transporter and Ena1 Na+-ATPase allows their functional coupling under high-pH stress', *Mol Cell Biol*, 34(24), pp. 4420-35.
Serrano, R., Ruiz, A., Bernal, D., Chambers, J.R. and Ariño, J. (2002) 'The transcriptional response to alkaline pH in Saccharomyces cerevisiae: evidence for calcium-mediated signalling', *Mol Microbiol*, 46(5), pp. 1319-33.
Serrano, R., Ruiz, A., Bernal, D., Chambers, J.R. and Ariño, J. (2002) 'The transcriptional response to alkaline pH in Saccharomyces cerevisiae: evidence for calcium-mediated signalling', *Mol Microbiol*, 46(5), pp. 1319-33.
Sethuraman, A., Rao, N.N. and Kornberg, A. (2001) 'The endopolyphosphatase gene: essential in Saccharomyces cerevisiae', *Proc Natl Acad Sci U S A*, 98(15), pp. 8542-7.
Shahana, S., Childers, D.S., Ballou, E.R., Bohovych, I., Odds, F.C., Gow, N.A. and Brown, A.J. (2014) 'New Clox Systems for rapid and efficient gene disruption in Candida albicans', *PLoS One*, 9(6), p. e100390.
Shapiro, R.S., Robbins, N. and Cowen, L.E. (2011) 'Regulatory circuitry governing fungal development, drug resistance, and disease', *Microbiol Mol Biol Rev*, 75(2), pp. 213-67.

Shapiro, R.S., Sellam, A., Tebbji, F., Whiteway, M., Nantel, A. and Cowen, L.E. (2012) 'Pho85, Pcl1, and Hms1 signaling governs Candida albicans morphogenesis induced by high temperature or Hsp90 compromise', *Curr Biol*, 22(6), pp. 461-70.

Shears, S.B. (2018) 'Intimate connections: Inositol pyrophosphates at the interface of metabolic regulation and cell signaling', *J Cell Physiol*, 233(3), pp. 1897-1912.

Shemer, R., Meimoun, A., Holtzman, T. and Kornitzer, D. (2002) 'Regulation of the transcription factor Gcn4 by Pho85 cyclin PCL5', *Mol Cell Biol*, 22(15), pp. 5395-404.

Sherlock, G., Bahman, A.M., Mahal, A., Shieh, J.C., Ferreira, M. and Rosamond, J. (1994) 'Molecular cloning and analysis of CDC28 and cyclin homologues from the human fungal pathogen Candida albicans', *Mol Gen Genet*, 245(6), pp. 716-23.

Shi, Q.M., Wang, Y.M., Zheng, X.D., Lee, R.T. and Wang, Y. (2007) 'Critical role of DNA checkpoints in mediating genotoxic-stress-induced filamentous growth in Candida albicans', *Mol Biol Cell*, 18(3), pp. 815-26.

Shi, Q.M., Wang, Y.M., Zheng, X.D., Lee, R.T. and Wang, Y. (2007) 'Critical role of DNA checkpoints in mediating genotoxic-stress-induced filamentous growth in Candida albicans', *Mol Biol Cell*, 18(3), pp. 815-26.

Shi, X. and Kornberg, A. (2005) 'Endopolyphosphatase in Saccharomyces cerevisiae undergoes post-translational activations to produce short-chain polyphosphates', *FEBS Lett*, 579(9), pp. 2014-8.

Sicko-Goad, L. and Lazinsky, D. (1986) 'Quantitative ultrastructural changes associated with lead-coupled luxury phosphate uptake and polyphosphate utilization', *Archives of Environmental Contamination and Toxicology*, 15(6), pp. 617-627.

Singh, P., Chauhan, N., Ghosh, A., Dixon, F. and Calderone, R. (2004) 'SKN7 of Candida albicans: mutant construction and phenotype analysis', *Infect Immun*, 72(4), pp. 2390-4.

Smith, D.A., Morgan, B.A. and Quinn, J. (2010) 'Stress signalling to fungal stress-activated protein kinase pathways', *FEMS Microbiol Lett*, 306(1), pp. 1-8.

Smith, D.A., Nicholls, S., Morgan, B.A., Brown, A.J. and Quinn, J. (2004) 'A conserved stress-activated protein kinase regulates a core stress response in the human pathogen Candida albicans', *Mol Biol Cell*, 15(9), pp. 4179-90.

Smith, S.A. and Morrissey, J.H. (2007) 'Sensitive fluorescence detection of polyphosphate in polyacrylamide gels using 4',6-diamidino-2-phenylindol', *Electrophoresis*, 28(19), pp. 3461-5.

Smith, S.A., Mutch, N.J., Baskar, D., Rohloff, P., Docampo, R. and Morrissey, J.H. (2006) 'Polyphosphate modulates blood coagulation and fibrinolysis', *Proc Natl Acad Sci U S A*, 103(4), pp. 903-8.

Sobel, J.D. (2007) 'Vulvovaginal candidosis', *Lancet*, 369(9577), pp. 1961-71.

Sorgo, A.G., Heilmann, C.J., Brul, S., de Koster, C.G. and Klis, F.M. (2013) 'Beyond the wall: Candida albicans secret(e)s to survive', *FEMS Microbiol Lett*, 338(1), pp. 10-7.

Spitzer, M., Robbins, N. and Wright, G.D. (2017) 'Combinatorial strategies for combating invasive fungal infections', *Virulence*, 8(2), pp. 169-185.

Springer, M., Wykoff, D.D., Miller, N. and O'Shea, E.K. (2003) 'Partially phosphorylated Pho4 activates transcription of a subset of phosphate-responsive genes', *PLoS Biol*, 1(2), p. E28.

Stylianou, M., Kulesskiy, E., Lopes, J.P., Granlund, M., Wennerberg, K. and Urban, C.F. (2014) 'Antifungal application of nonantifungal drugs', *Antimicrob Agents Chemother*, 58(2), pp. 1055-62.

Sudbery, P.E. (2011) 'Growth of Candida albicans hyphae', *Nat Rev Microbiol*, 9(10), pp. 737-48.

Svaren, J. and Hörz, W. (1997) 'Transcription factors vs nucleosomes: regulation of the PHO5 promoter in yeast', *Trends Biochem Sci*, 22(3), pp. 93-7.

Takeda, E., Taketani, Y., Sawada, N., Sato, T. and Yamamoto, H. (2004) 'The regulation and function of phosphate in the human body', *Biofactors*, 21(1-4), pp. 345-55.

Tammenkoski, M., Koivula, K., Cusanelli, E., Zollo, M., Steegborn, C., Baykov, A.A. and Lahti, R. (2008) 'Human metastasis regulator protein H-prune is a short-chain exopolyphosphatase', *Biochemistry*, 47(36), pp. 9707-13.

Tammenkoski, M., Moiseev, V.M., Lahti, M., Ugochukwu, E., Brondijk, T.H., White, S.A., Lahti, R. and Baykov, A.A. (2007) 'Kinetic and mutational analyses of the major cytosolic exopolyphosphatase from Saccharomyces cerevisiae', *J Biol Chem*, 282(13), pp. 9302-11.

Tammenkoski, M., Moiseev, V.M., Lahti, M., Ugochukwu, E., Brondijk, T.H., White, S.A., Lahti, R. and Baykov, A.A. (2007) 'Kinetic and mutational analyses of the major cytosolic exopolyphosphatase from Saccharomyces cerevisiae', *J Biol Chem*, 282(13), pp. 9302-11.

Thewes, S., Kretschmar, M., Park, H., Schaller, M., Filler, S.G. and Hube, B. (2007) 'In vivo and ex vivo comparative transcriptional profiling of invasive and non-invasive Candida albicans isolates identifies genes associated with tissue invasion', *Mol Microbiol*, 63(6), pp. 1606-28.

Thewes, S., Kretschmar, M., Park, H., Schaller, M., Filler, S.G. and Hube, B. (2007) 'In vivo and ex vivo comparative transcriptional profiling of invasive and non-invasive Candida albicans isolates identifies genes associated with tissue invasion', *Mol Microbiol*, 63(6), pp. 1606-28.
Thomas, M.R. and O'Shea, E.K. (2005) 'An intracellular phosphate buffer filters transient fluctuations in extracellular phosphate levels', *Proc Natl Acad Sci U S A*, 102(27), pp. 9565-70.
Thota, S.G., Unnikannan, C.P., Thampatty, S.R., Manorama, R. and Bhandari, R. (2015) 'Inositol pyrophosphates regulate RNA polymerase I-mediated rRNA transcription in Saccharomyces cerevisiae', *Biochem J*, 466(1), pp. 105-14.
Tillmann, A.T., Strijbis, K., Cameron, G., Radmaneshfar, E., Thiel, M., Munro, C.A., MacCallum, D.M., Distel, B., Gow, N.A. and Brown, A.J. (2015) 'Contribution of Fdh3 and Glr1 to Glutathione Redox State, Stress Adaptation and Virulence in Candida albicans', *PLoS One*, 10(6), p. e0126940.
To, E.A., Ueda, Y., Kakimoto, S.I. and Oshima, Y. (1973) 'Isolation and characterization of acid phosphatase mutants in Saccharomyces cerevisiae', *J Bacteriol*, 113(2), pp. 727-38.
Toh, E.A. and Nishizawa, M. (2001) 'Structure and function of cyclin-dependent Pho85 kinase of Saccharomyces cerevisiae', *J Gen Appl Microbiol*, 47(3), pp. 107-117.
Toh-e, A., Ohkusu, M., Li, H.M., Shimizu, K., Takahashi-Nakaguchi, A., Gonoi, T., Kawamoto, S., Kanesaki, Y., Yoshikawa, H. and Nishizawa, M. (2015) 'Identification of genes involved in the phosphate metabolism in Cryptococcus neoformans', *Fungal Genet Biol*, 80, pp. 19-30.
Toh-e, A., Ohkusu, M., Li, H.M., Shimizu, K., Takahashi-Nakaguchi, A., Gonoi, T., Kawamoto, S., Kanesaki, Y., Yoshikawa, H. and Nishizawa, M. (2015) 'Identification of genes involved in the phosphate metabolism in Cryptococcus neoformans', *Fungal Genet Biol*, 80, pp. 19-30.
Tomar, P. and Sinha, H. (2014) 'Conservation of PHO pathway in ascomycetes and the role of Pho84', *J Biosci*, 39(3), pp. 525-36.
Tomashevski, A. and Petrov, V. (2015) '164 Mutations in membrane and extracytosolic domains of the yeast Pma1 ATPase cause different distribution of polyphosphates', *Journal of biomolecular structure & dynamics*, 33, pp. 106-107.
Torosantucci, A., Bromuro, C., Chiani, P., De Bernardis, F., Berti, F., Galli, C., Norelli, F., Bellucci, C., Polonelli, L., Costantino, P., Rappuoli, R. and Cassone, A. (2005) 'A novel glyco-conjugate vaccine against fungal pathogens', *J Exp Med*, 202(5), pp. 597-606.
Tumlirsch, T., Sznajder, A. and Jendrossek, D. (2015) 'Formation of polyphosphate by polyphosphate kinases and its relationship to poly(3-hydroxybutyrate) accumulation in Ralstonia eutropha strain H16', *Appl Environ Microbiol*, 81(24), pp. 8277-93.

Ugochukwu, E., Lovering, A.L., Mather, O.C., Young, T.W. and White, S.A. (2007) 'The crystal structure of the cytosolic exopolyphosphatase from Saccharomyces cerevisiae reveals the basis for substrate specificity', *J Mol Biol*, 371(4), pp. 1007-21.

Urrialde, V., Prieto, D., Pla, J. and Alonso-Monge, R. (2016) 'The Candida albicans Pho4 Transcription Factor Mediates Susceptibility to Stress and Influences Fitness in a Mouse Commensalism Model', *Front Microbiol*, 7, p. 1062.

Uttenweiler, A., Schwarz, H., Neumann, H. and Mayer, A. (2007) 'The vacuolar transporter chaperone (VTC) complex is required for microautophagy', *Mol Biol Cell*, 18(1), pp. 166-75.

Van Daele, R., Spriet, I., Wauters, J., Maertens, J., Mercier, T., Van Hecke, S. and Brüggemann, R. (2019) 'Antifungal drugs: What brings the future?', *Med Mycol*, 57(Supplement_3), pp. S328-s343.

van de Veerdonk, F.L., Gresnigt, M.S., Romani, L., Netea, M.G. and Latgé, J.P. (2017) 'Aspergillus fumigatus morphology and dynamic host interactions', *Nat Rev Microbiol*, 15(11), pp. 661-674.

Varas, M.A., Riquelme-Barrios, S., Valenzuela, C., Marcoleta, A.E., Berríos-Pastén, C., Santiviago, C.A. and Chávez, F.P. (2018) 'Inorganic Polyphosphate Is Essential for Salmonella Typhimurium Virulence and Survival in Dictyostelium discoideum', *Front Cell Infect Microbiol*, 8, p. 8.

Veal, E.A., Findlay, V.J., Day, A.M., Bozonet, S.M., Evans, J.M., Quinn, J. and Morgan, B.A. (2004) 'A 2-Cys peroxiredoxin regulates peroxide-induced oxidation and activation of a stress-activated MAP kinase', *Mol Cell*, 15(1), pp. 129-39.

Verbalis, J.G. (2003) 'Disorders of body water homeostasis', *Best Pract Res Clin Endocrinol Metab*, 17(4), pp. 471-503.

Verweij, P.E., Mellado, E. and Melchers, W.J. (2007) 'Multiple-triazole-resistant aspergillosis', *N Engl J Med*, 356(14), pp. 1481-3.

Veses, V. and Gow, N.A. (2008) 'Vacuolar dynamics during the morphogenetic transition in Candida albicans', *FEMS Yeast Res*, 8(8), pp. 1339-48.

Walker, L.A., Maccallum, D.M., Bertram, G., Gow, N.A., Odds, F.C. and Brown, A.J. (2009) 'Genome-wide analysis of Candida albicans gene expression patterns during infection of the mammalian kidney', *Fungal Genet Biol*, 46(2), pp. 210-9.

Walker, L.A., Maccallum, D.M., Bertram, G., Gow, N.A., Odds, F.C. and Brown, A.J. (2009) 'Genome-wide analysis of Candida albicans gene expression patterns during infection of the mammalian kidney', *Fungal Genet Biol*, 46(2), pp. 210-9.

Warris, A. and Ballou, E.R. (2019) 'Oxidative responses and fungal infection biology', *Semin Cell Dev Biol*, 89, pp. 34-46.
Wild, R., Gerasimaite, R., Jung, J.Y., Truffault, V., Pavlovic, I., Schmidt, A., Saiardi, A., Jessen, H.J., Poirier, Y., Hothorn, M. and Mayer, A. (2016) 'Control of eukaryotic phosphate homeostasis by inositol polyphosphate sensor domains', *Science*, 352(6288), pp. 986-90.
Willinger, B., Berger, A., Li, L., Hirschl, A.M., Aspöck, C., Makristathis, A., Prückl, M. and Rotter, M.L. (1994) 'Epidemiological analysis of Candida yeasts by pulsed-field gel electrophoresis', *Mycoses*, 37(11-12), pp. 401-3.
Wilson, D., Thewes, S., Zakikhany, K., Fradin, C., Albrecht, A., Almeida, R., Brunke, S., Grosse, K., Martin, R., Mayer, F., Leonhardt, I., Schild, L., Seider, K., Skibbe, M., Slesiona, S., Waechtler, B., Jacobsen, I. and Hube, B. (2009) 'Identifying infection-associated genes of Candida albicans in the postgenomic era', *FEMS Yeast Res*, 9(5), pp. 688-700.
Witchley, J.N., Penumetcha, P., Abon, N.V., Woolford, C.A., Mitchell, A.P. and Noble, S.M. (2019) 'Candida albicans Morphogenesis Programs Control the Balance between Gut Commensalism and Invasive Infection', *Cell Host Microbe*, 25(3), pp. 432-443.e6.
Wurst, H. and Kornberg, A. (1994) 'A soluble exopolyphosphatase of Saccharomyces cerevisiae. Purification and characterization', *J Biol Chem*, 269(15), pp. 10996-1001.
Wykoff, D.D., Rizvi, A.H., Raser, J.M., Margolin, B. and O'Shea, E.K. (2007) 'Positive feedback regulates switching of phosphate transporters in S. cerevisiae', *Mol Cell*, 27(6), pp. 1005-13.
Xu, W., Solis, N.V., Ehrlich, R.L., Woolford, C.A., Filler, S.G. and Mitchell, A.P. (2015) 'Activation and alliance of regulatory pathways in C. albicans during mammalian infection', *PLoS Biol*, 13(2), p. e1002076.
Yang, F., Kravets, A., Bethlendy, G., Welle, S. and Rustchenko, E. (2013) 'Chromosome 5 monosomy of Candida albicans controls susceptibility to various toxic agents, including major antifungals', *Antimicrob Agents Chemother*, 57(10), pp. 5026-36.
Yoshida, K., Kuromitsu, Z., Ogawa, N. and Oshima, Y. (1989) 'Mode of expression of the positive regulatory genes PHO2 and PHO4 of the phosphatase regulon in Saccharomyces cerevisiae', *Mol Gen Genet*, 217(1), pp. 31-9.
Zakikhany, K., Naglik, J.R., Schmidt-Westhausen, A., Holland, G., Schaller, M. and Hube, B. (2007) 'In vivo transcript profiling of Candida albicans identifies a gene essential for interepithelial dissemination', *Cell Microbiol*, 9(12), pp. 2938-54.

Zakikhany, K., Naglik, J.R., Schmidt-Westhausen, A., Holland, G., Schaller, M. and Hube, B. (2007) 'In vivo transcript profiling of Candida albicans identifies a gene essential for interepithelial dissemination', *Cellular Microbiology*, 9(12), pp. 2938-2954.

Zaragoza, O., Blazquez, M.A. and Gancedo, C. (1998) 'Disruption of the Candida albicans TPS1 gene encoding trehalose-6-phosphate synthase impairs formation of hyphae and decreases infectivity', *J Bacteriol*, 180(15), pp. 3809-15.

Zeng, Z.R., Tian, G., Ding, Y.H., Yang, K., Liu, J.B. and Deng, J. (2019) 'Surveillance study of the prevalence, species distribution, antifungal susceptibility, risk factors and mortality of invasive candidiasis in a tertiary teaching hospital in Southwest China', *BMC Infect Dis*, 19(1), p. 939.

Zheng, X., Wang, Y. and Wang, Y. (2004) 'Hgc1, a novel hypha-specific G1 cyclin-related protein regulates Candida albicans hyphal morphogenesis', *Embo j*, 23(8), pp. 1845-56.

Zheng, X., Wang, Y. and Wang, Y. (2004) 'Hgc1, a novel hypha-specific G1 cyclin-related protein regulates Candida albicans hyphal morphogenesis', *Embo j*, 23(8), pp. 1845-56.

Zhu, H., Zhu, N., Peng, L., Zhang, B., Yu, Q. and Li, M. (2020) 'The inositol polyphosphate kinase Ipk1 transcriptionally regulates mitochondrial functions in Candida albicans', *FEMS Yeast Res*, 20(6).

Zhu, W. and Filler, S.G. (2010) 'Interactions of Candida albicans with epithelial cells', *Cell Microbiol*, 12(3), pp. 273-82.

Appendix

Cluster 1

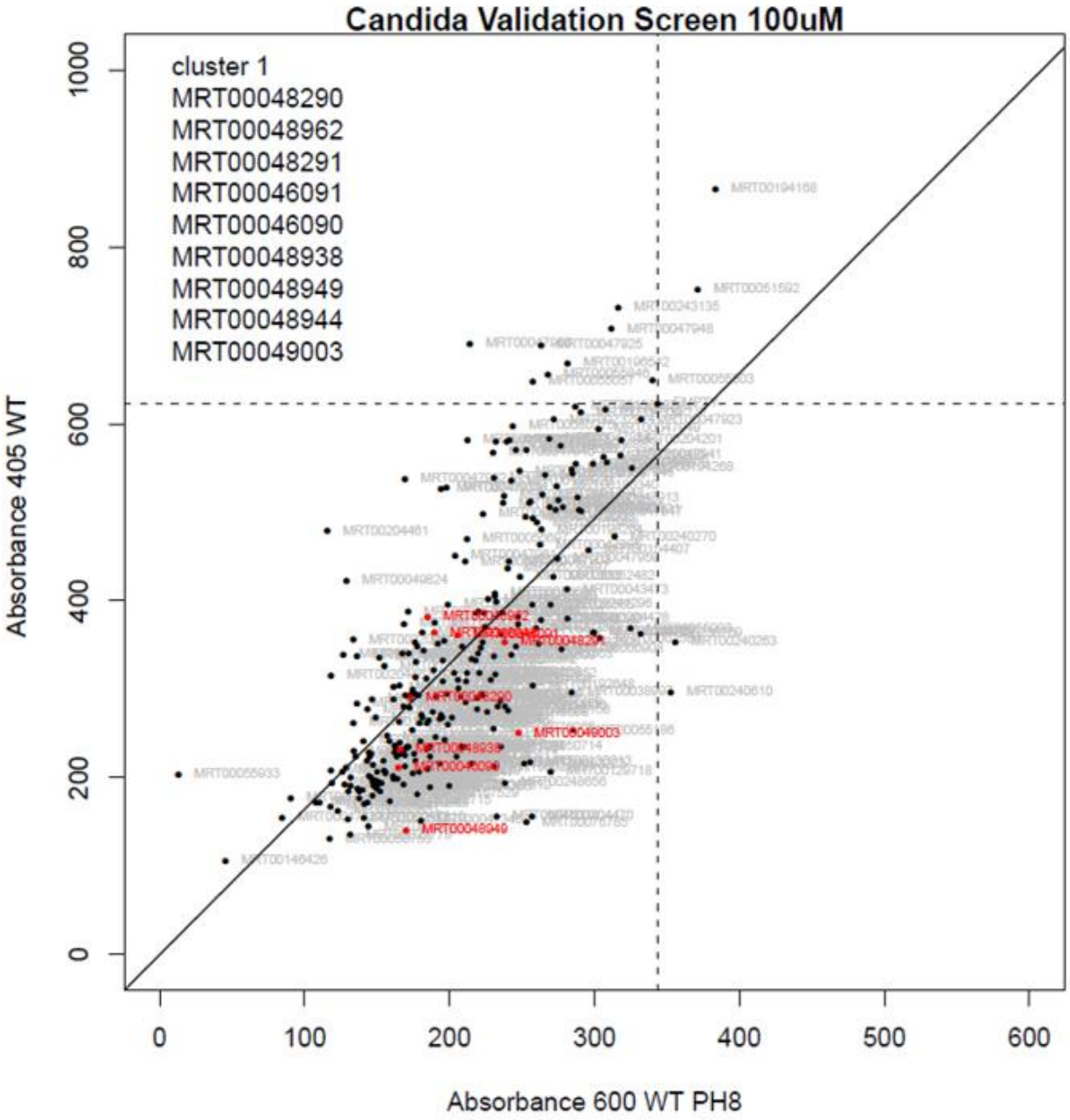

Cluster 1: 100 µM Secondary Screen: pH8 as a readout for PHO Pathway activity.
Plot of OD_{600} *wt* cells grown in pH 8 vs. OD_{405} of *wt* cells. Cells were grown to log phase in YPD before being washed 3 times in pH8 media and diluted back to OD_{600} = 0.05 then seeded into 384 well plates containing 100 µM of compound. Absorbance of 600 nm is used for growth at pH and 405 for secreted acid phosphatase activity. Red hits represent those from cluster 1.

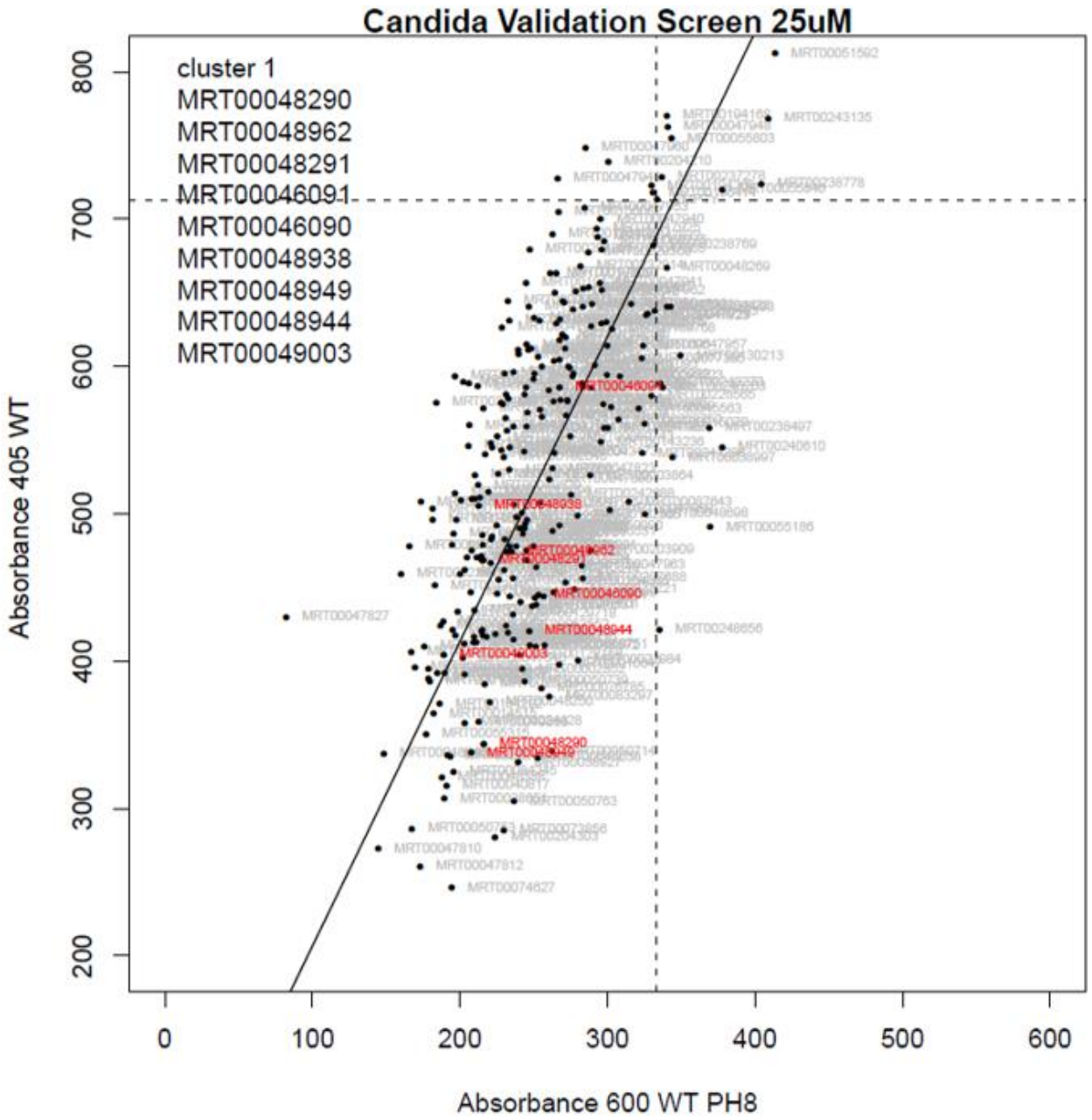

Cluster 1: 25 µM Secondary Screen: pH8 as a readout for PHO Pathway activity.
Plot of OD_{600} *wt* cells grown in pH 8 vs. OD_{405} of *wt* cells. Cells were grown to log phase in YPD before being washed 3 times in pH8 media and diluted back to OD_{600} = 0.05 then seeded into 384 well plates containing 25 µM of compound. Absorbance of 600 nm is used for growth at pH and 405 for secreted acid phosphatase activity. Red hits represent those from cluster 1.

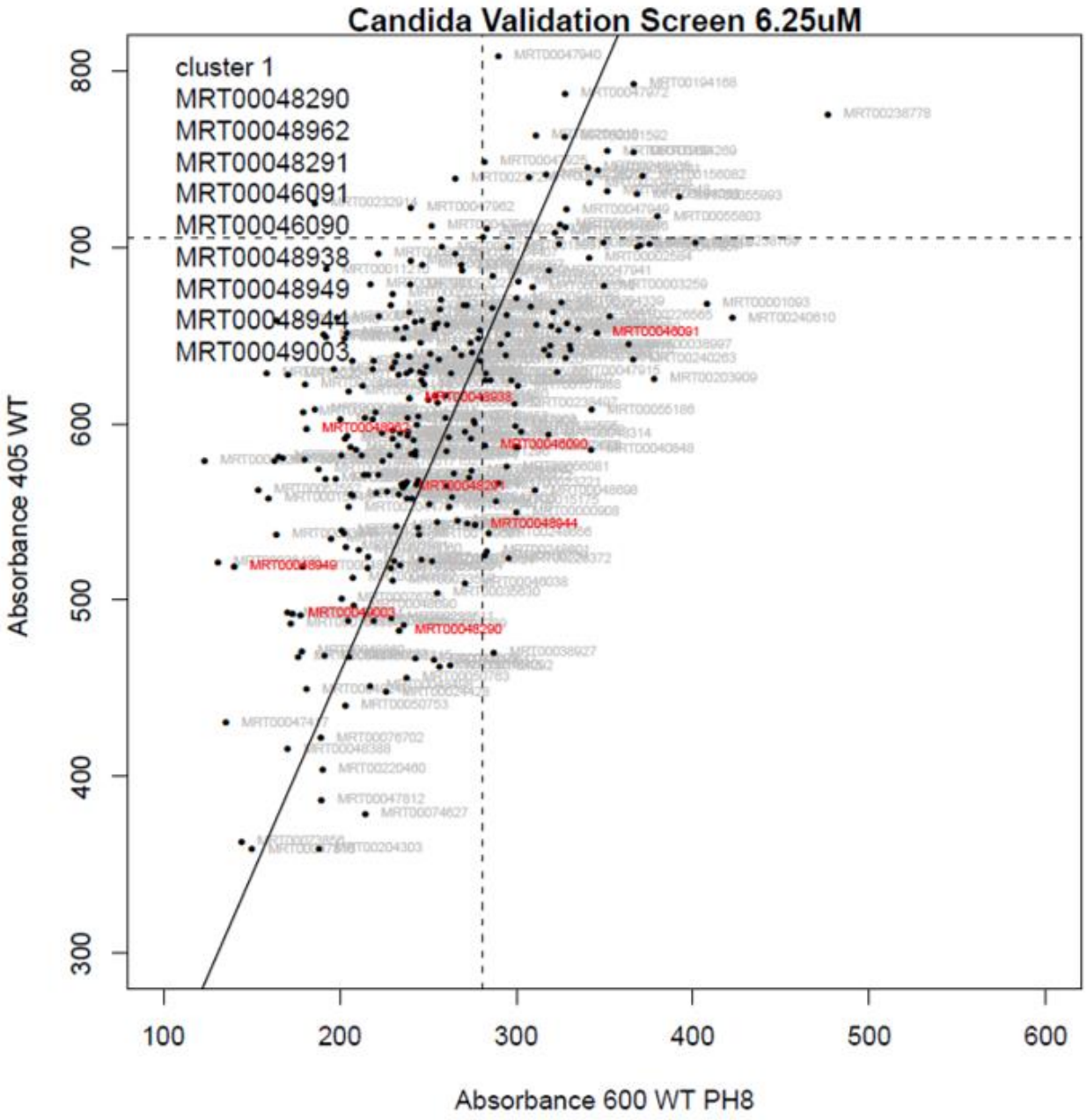

Cluster 1: 6.25 µM Secondary Screen: pH8 as a readout for PHO Pathway activity.
Plot of OD_{600} *wt* cells grown in pH 8 vs. OD_{405} of *wt* cells. Cells were grown to log phase in YPD before being washed 3 times in pH8 media and diluted back to OD_{600} = 0.05 then seeded into 384 well plates containing 6.25 µM of compound. Absorbance of 600 nm is used for growth at pH and 405 for secreted acid phosphatase activity. Red hits represent those from cluster 1.

Cluster 2

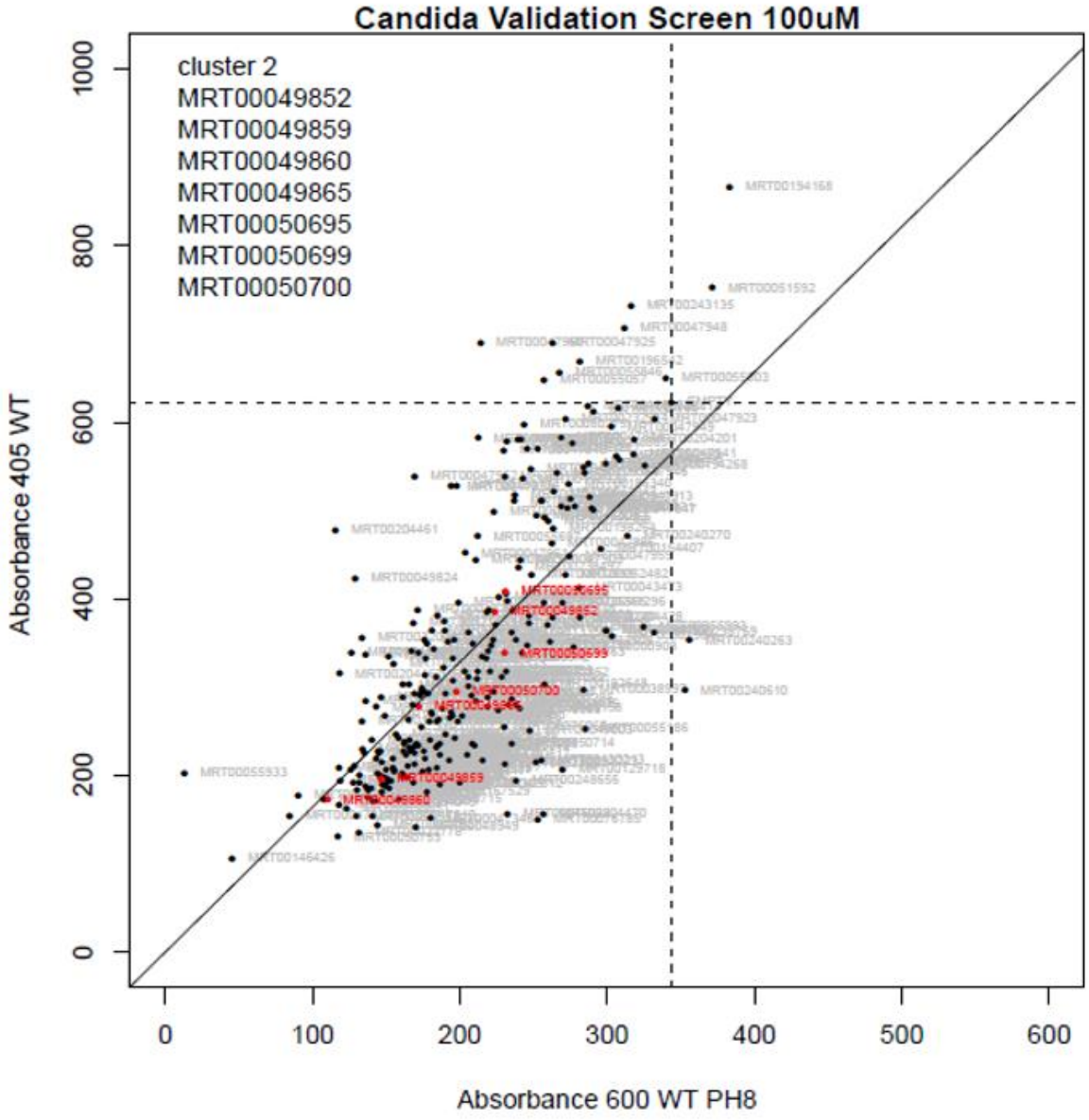

Cluster 2: 100 µM Secondary Screen: pH8 as a readout for PHO Pathway activity.
Plot of OD_{600} *wt* cells grown in pH 8 vs. OD_{405} of *wt* cells. Cells were grown to log phase in YPD before being washed 3 times in pH8 media and diluted back to OD_{600} = 0.05 then seeded into 384 well plates containing 100 µM of compound. Absorbance of 600 nm is used for growth at pH and 405 for secreted acid phosphatase activity. Red hits represent those from cluster 2.

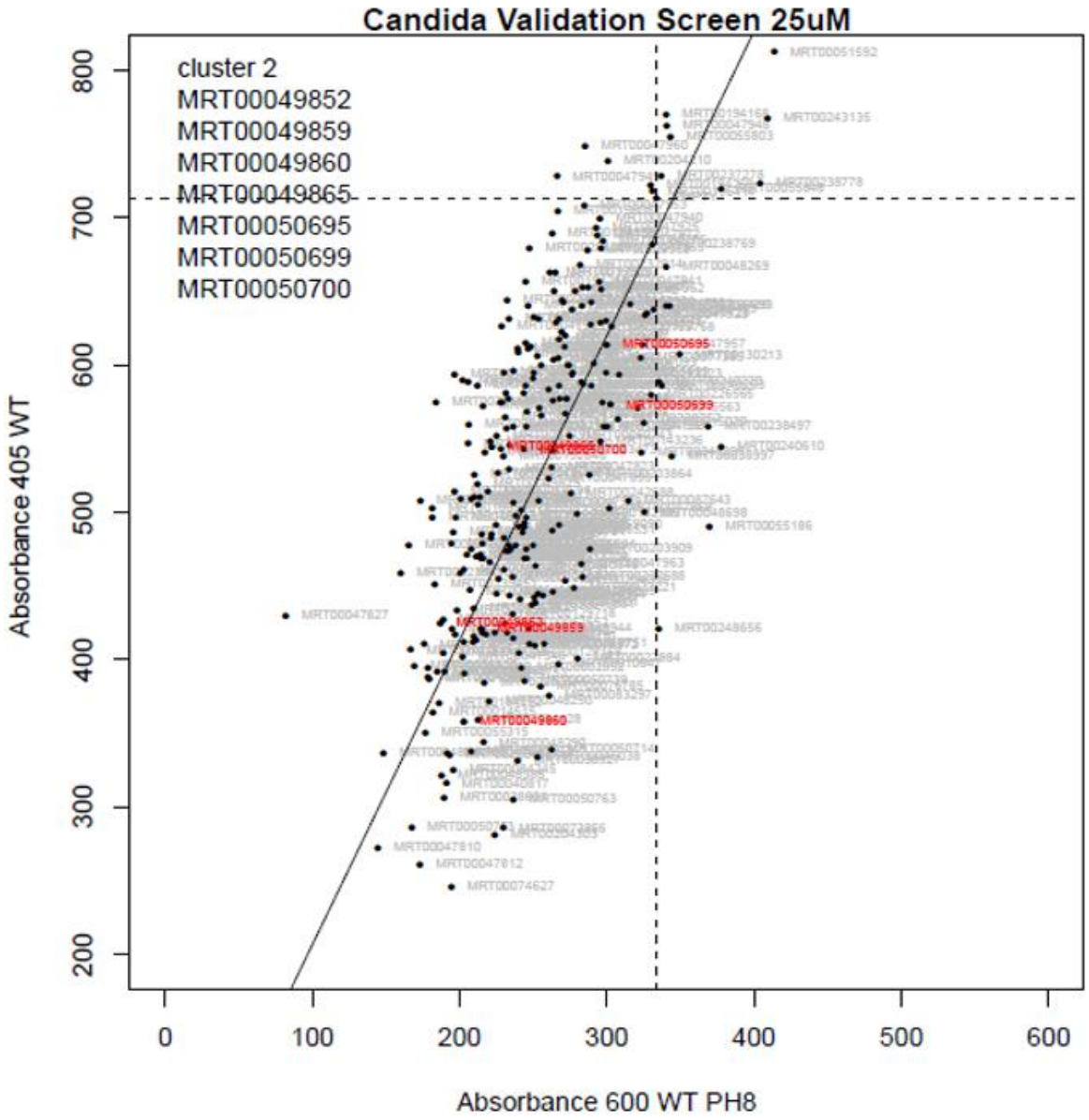

Cluster 2: 25 µM Secondary Screen: pH8 as a readout for PHO Pathway activity.
Plot of OD_{600} *wt* cells grown in pH 8 vs. OD_{405} of *wt* cells. Cells were grown to log phase in YPD before being washed 3 times in pH8 media and diluted back to OD_{600} = 0.05 then seeded into 384 well plates containing 25 µM of compound. Absorbance of 600 nm is used for growth at pH and 405 for secreted acid phosphatase activity. Red hits represent those from cluster 2.

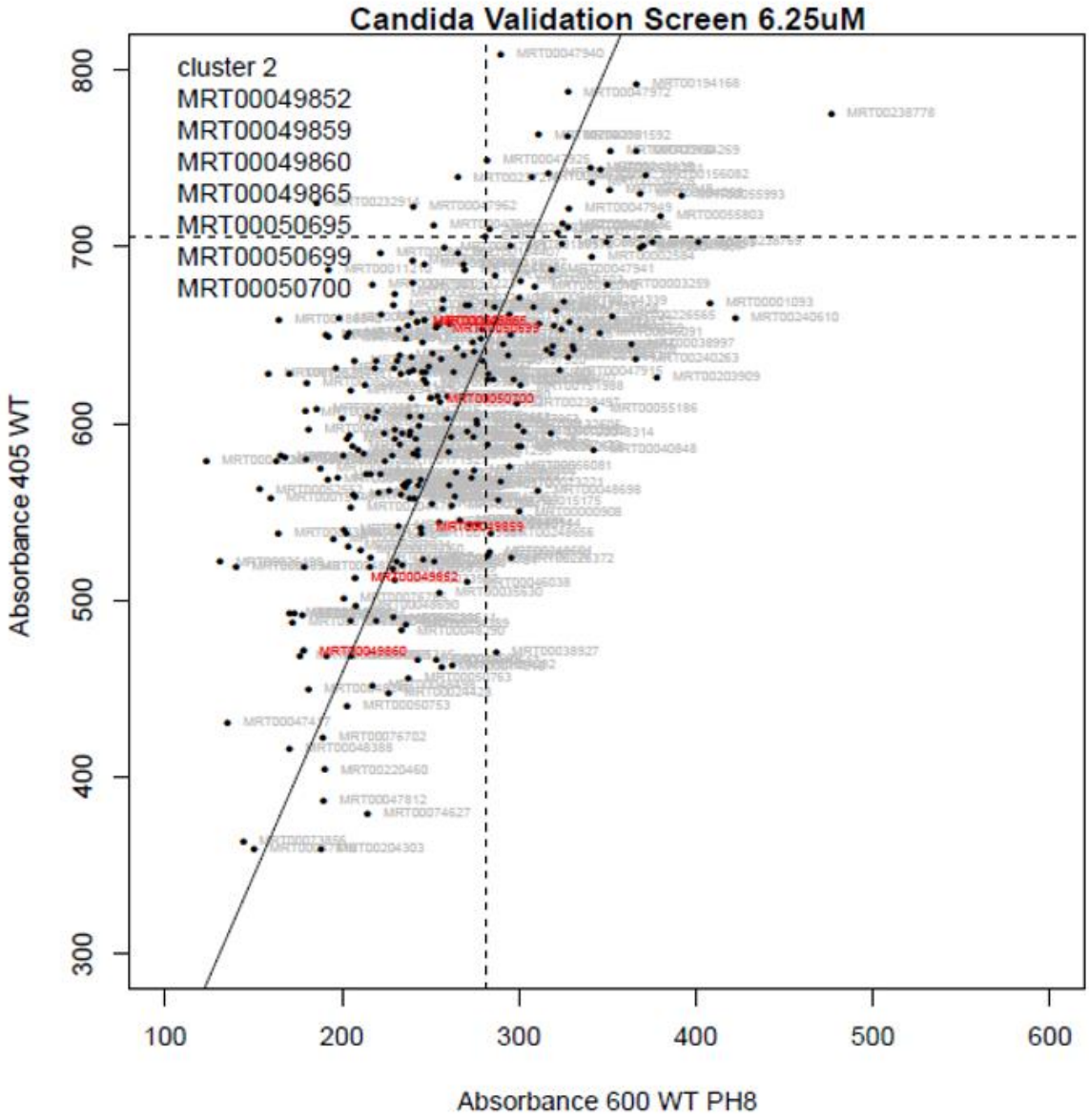

Cluster 2: 6.25 µM Secondary Screen: pH8 as a readout for PHO Pathway activity.
Plot of OD_{600} *wt* cells grown in pH 8 vs. OD_{405} of *wt* cells. Cells were grown to log phase in YPD before being washed 3 times in pH8 media and diluted back to OD_{600} = 0.05 then seeded into 384 well plates containing 6.25 µM of compound. Absorbance of 600 nm is used for growth at pH and 405 for secreted acid phosphatase activity. Red hits represent those from cluster 2.

Cluster 3

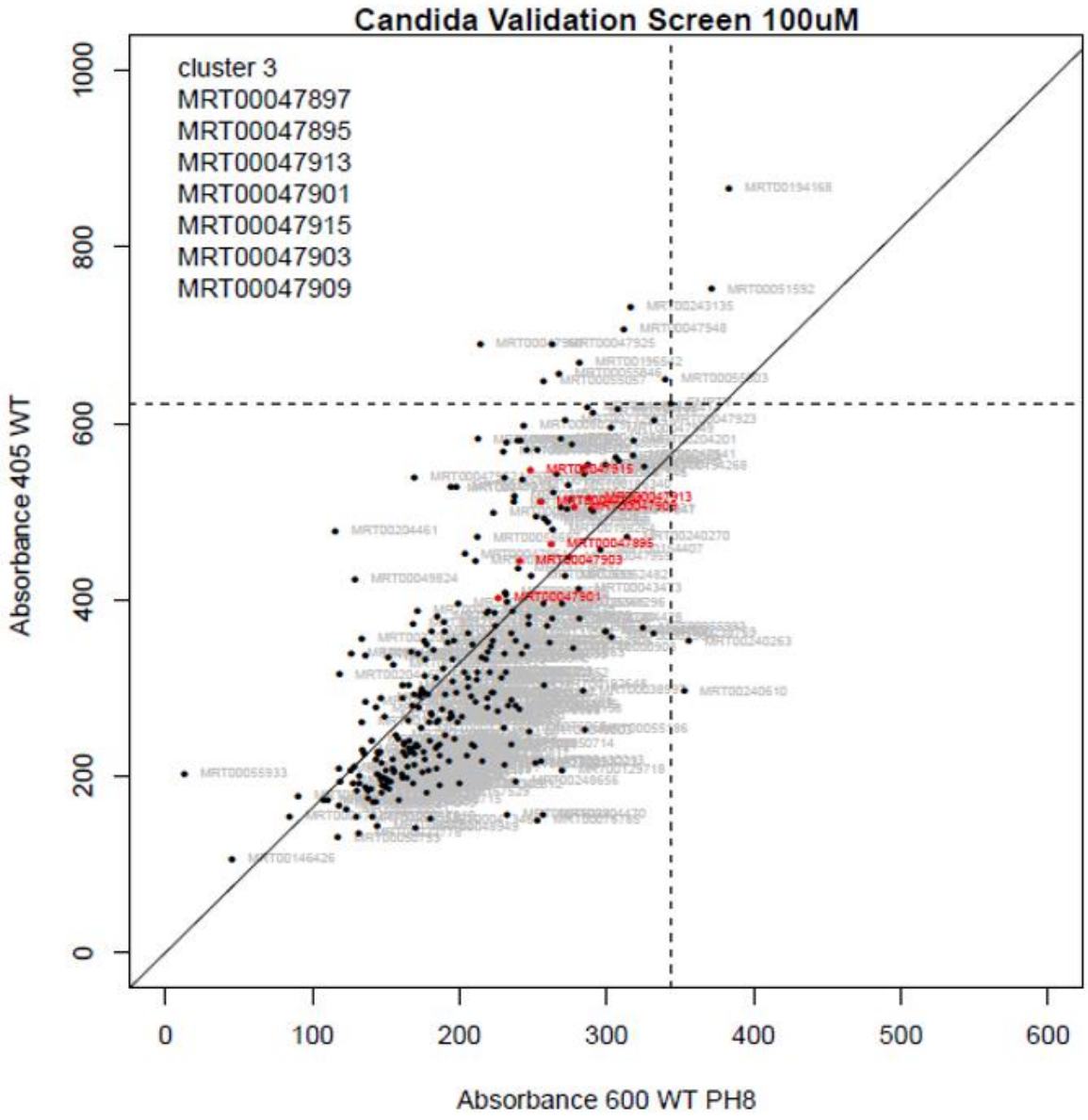

Cluster 3: 100 µM Secondary Screen: pH8 as a readout for PHO Pathway activity.
Plot of OD_{600} *wt* cells grown in pH 8 vs. OD_{405} of *wt* cells. Cells were grown to log phase in YPD before being washed 3 times in pH8 media and diluted back to OD_{600} = 0.05 then seeded into 384 well plates containing 100 µM of compound. Absorbance of 600 nm is used for growth at pH and 405 for secreted acid phosphatase activity. Red hits represent those from cluster 3.

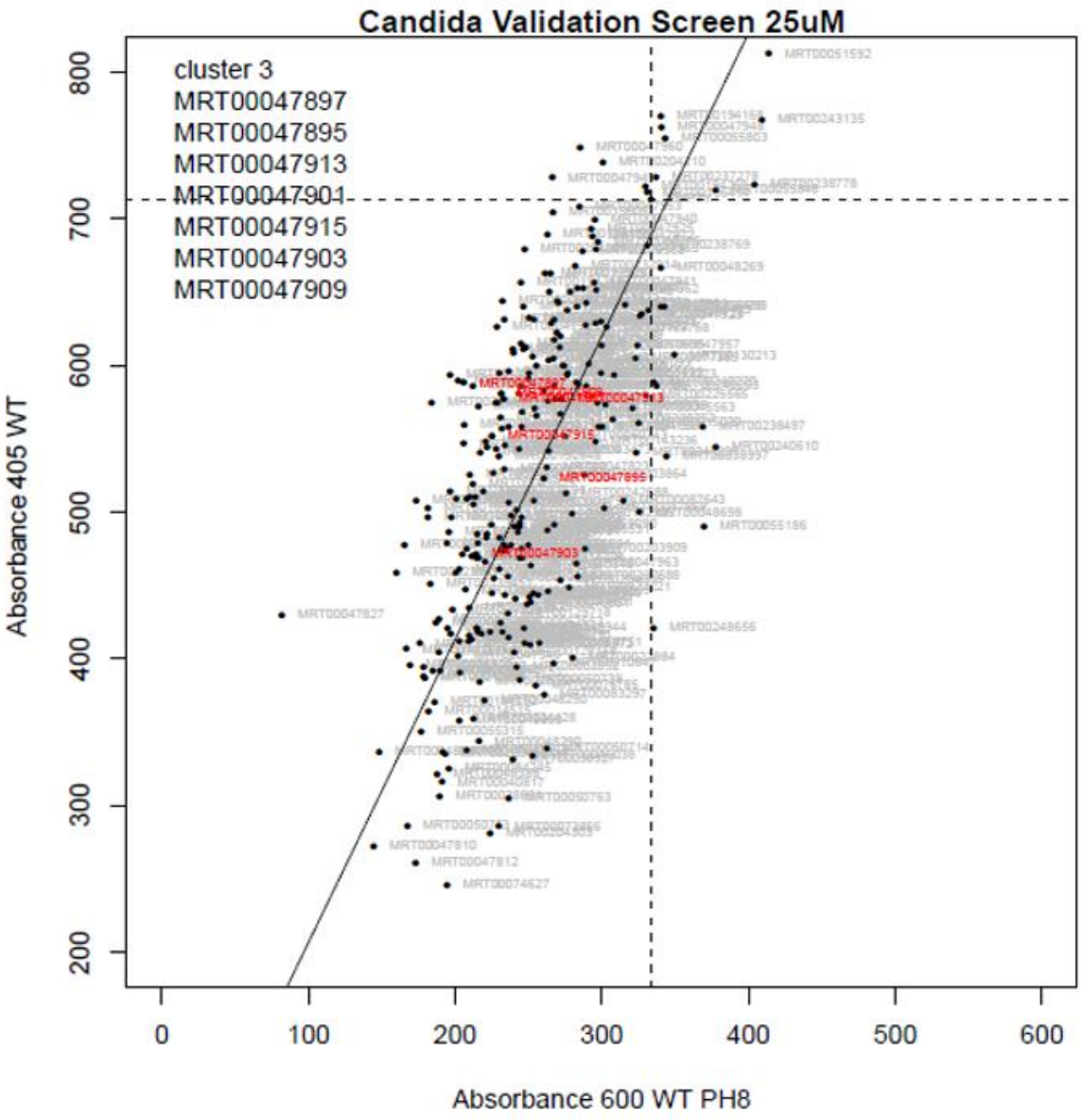

Cluster 3: 25 µM Secondary Screen: pH8 as a readout for PHO Pathway activity.
Plot of OD_{600} *wt* cells grown in pH 8 vs. OD_{405} of *wt* cells. Cells were grown to log phase in YPD before being washed 3 times in pH8 media and diluted back to OD_{600} = 0.05 then seeded into 384 well plates containing 25 µM of compound. Absorbance of 600 nm is used for growth at pH and 405 for secreted acid phosphatase activity. Red hits represent those from cluster 3.

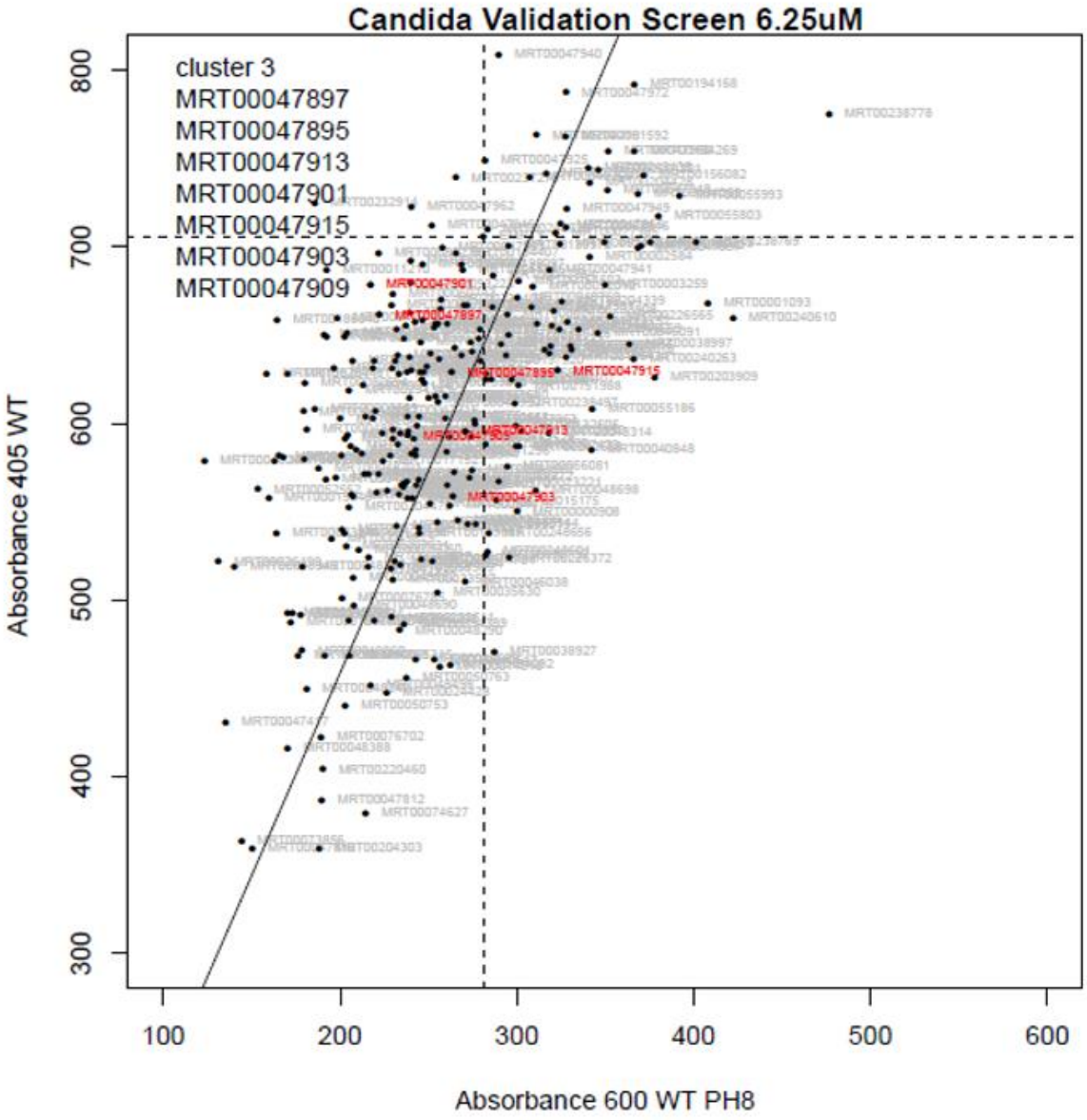

Cluster 3: 6.25 µM Secondary Screen: pH8 as a readout for PHO Pathway activity.
Plot of OD_{600} *wt* cells grown in pH 8 vs. OD_{405} of *wt* cells. Cells were grown to log phase in YPD before being washed 3 times in pH8 media and diluted back to OD_{600} = 0.05 then seeded into 384 well plates containing 6.25 µM of compound. Absorbance of 600 nm is used for growth at pH and 405 for secreted acid phosphatase activity. Red hits represent those from cluster 3.

Cluster 4

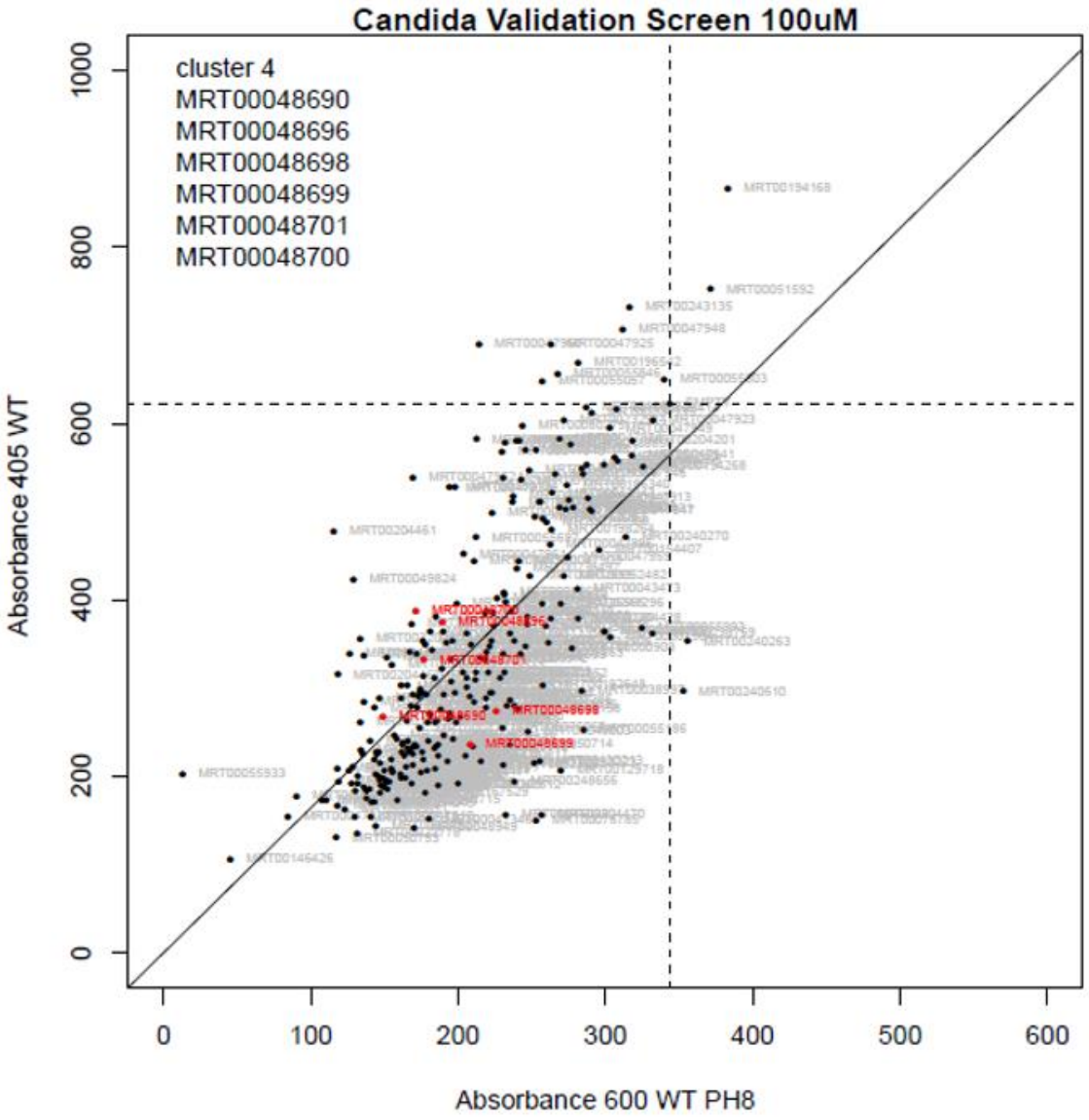

Cluster 4: 100 µM Secondary Screen: pH8 as a readout for PHO Pathway activity.
Plot of OD_{600} *wt* cells grown in pH 8 vs. OD_{405} of *wt* cells. Cells were grown to log phase in YPD before being washed 3 times in pH8 media and diluted back to OD_{600} = 0.05 then seeded into 384 well plates containing 100 µM of compound. Absorbance of 600 nm is used for growth at pH and 405 for secreted acid phosphatase activity. Red hits represent those from cluster 4.

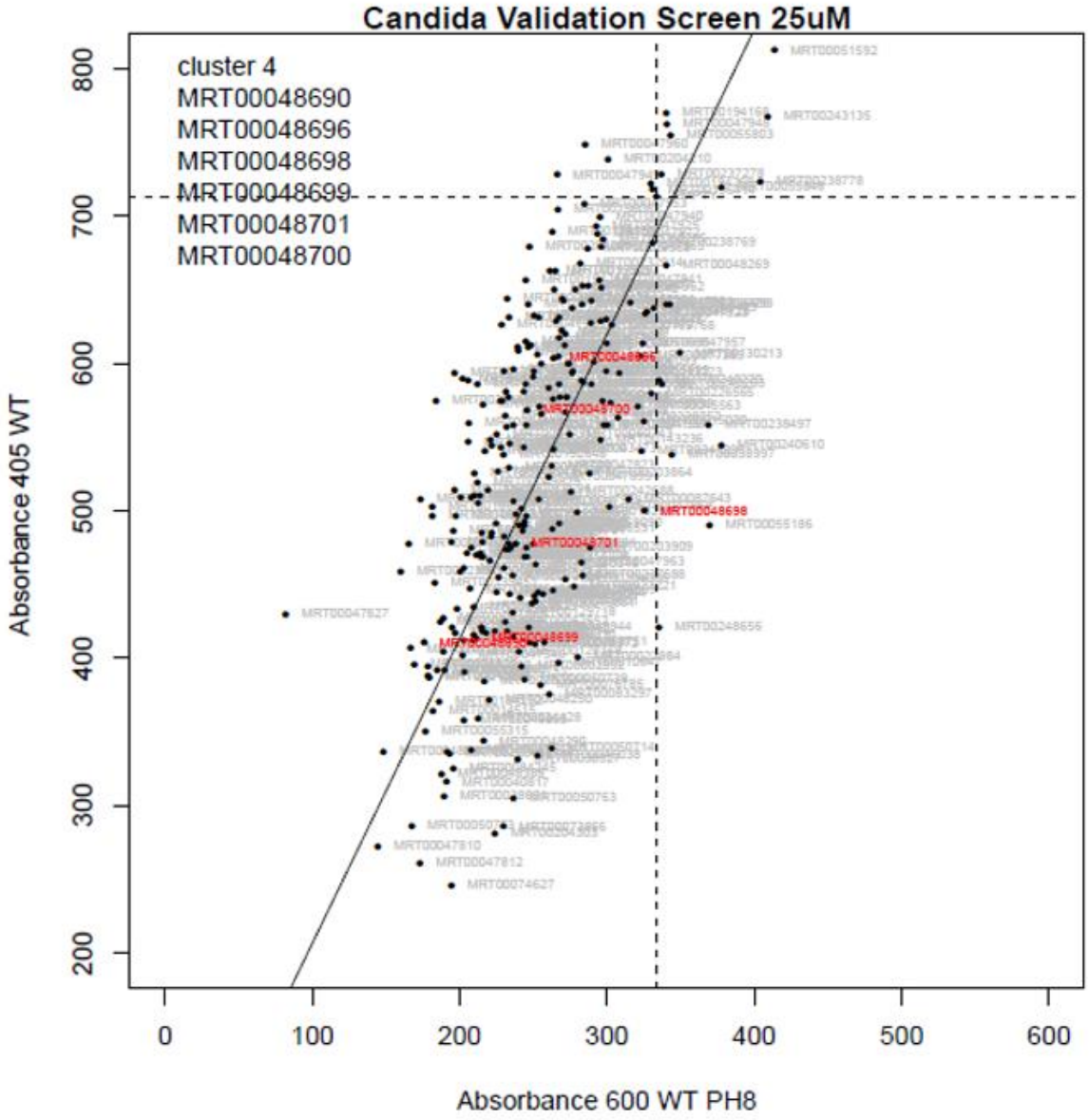

Cluster 4: 25 µM Secondary Screen: pH8 as a readout for PHO Pathway activity.
Plot of OD_{600} *wt* cells grown in pH 8 vs. OD_{405} of *wt* cells. Cells were grown to log phase in YPD before being washed 3 times in pH8 media and diluted back to OD_{600} = 0.05 then seeded into 384 well plates containing 25 µM of compound. Absorbance of 600 nm is used for growth at pH and 405 for secreted acid phosphatase activity. Red hits represent those from cluster 4.

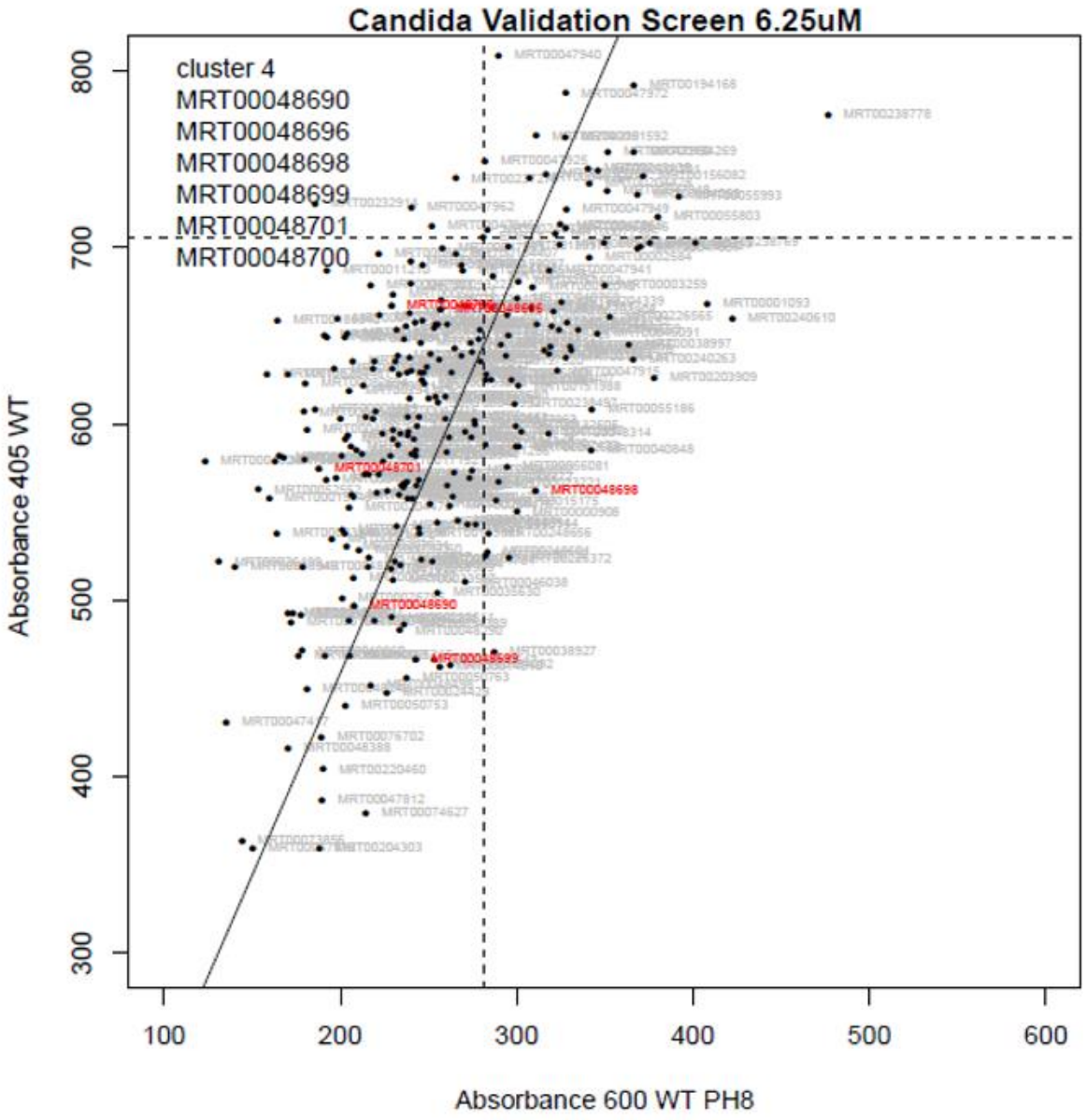

Cluster 4: 6.25 µM Secondary Screen: pH8 as a readout for PHO Pathway activity.
Plot of OD_{600} *wt* cells grown in pH 8 vs. OD_{405} of *wt* cells. Cells were grown to log phase in YPD before being washed 3 times in pH8 media and diluted back to OD_{600} = 0.05 then seeded into 384 well plates containing 6.25 µM of compound. Absorbance of 600 nm is used for growth at pH and 405 for secreted acid phosphatase activity. Red hits represent those from cluster 4.

Cluster 5

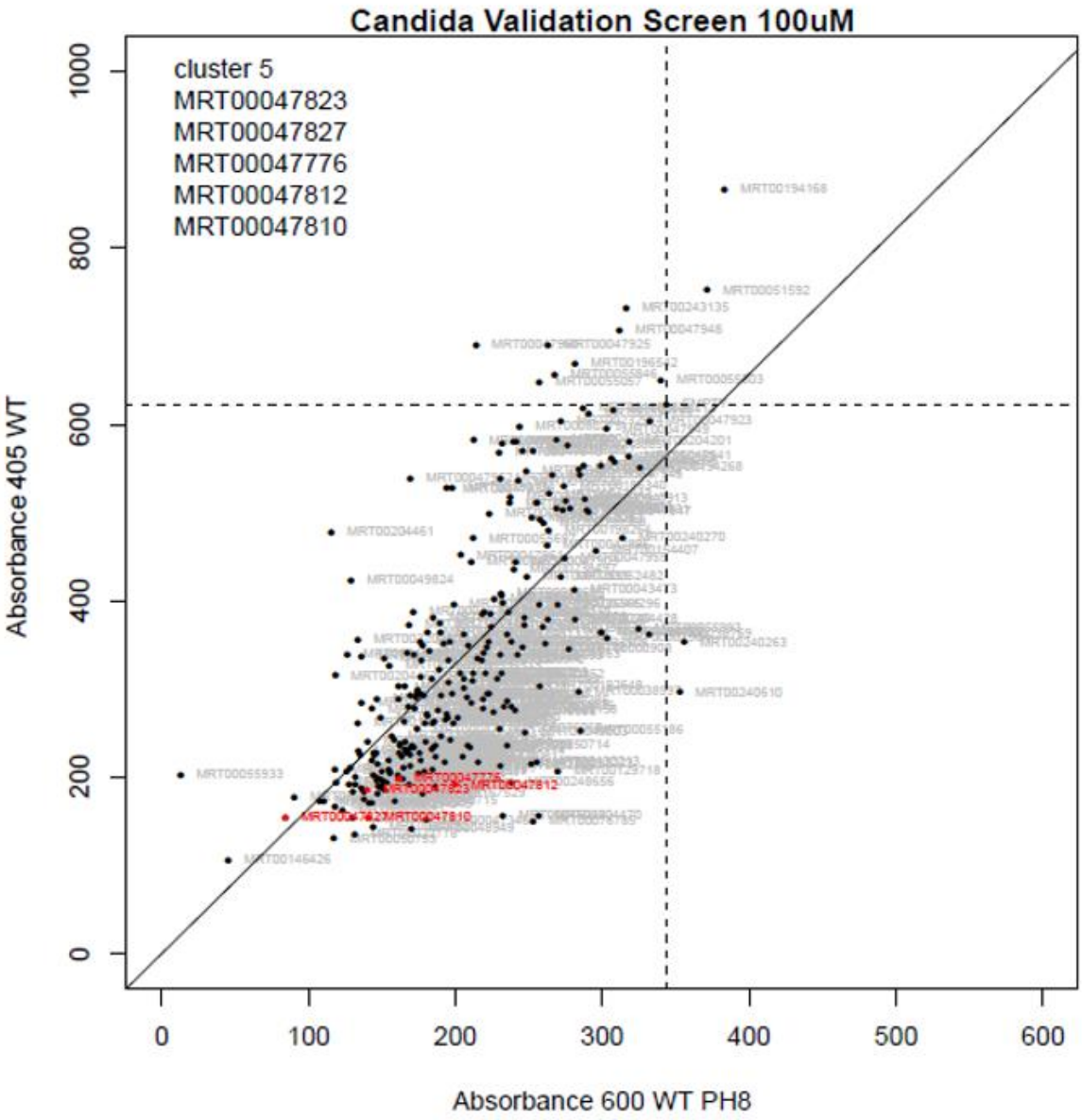

Cluster 5: 100 µM Secondary Screen: pH8 as a readout for PHO Pathway activity.
Plot of OD_{600} *wt* cells grown in pH 8 vs. OD_{405} of *wt* cells. Cells were grown to log phase in YPD before being washed 3 times in pH8 media and diluted back to OD_{600} = 0.05 then seeded into 384 well plates containing 100 µM of compound. Absorbance of 600 nm is used for growth at pH and 405 for secreted acid phosphatase activity. Red hits represent those from cluster 5.

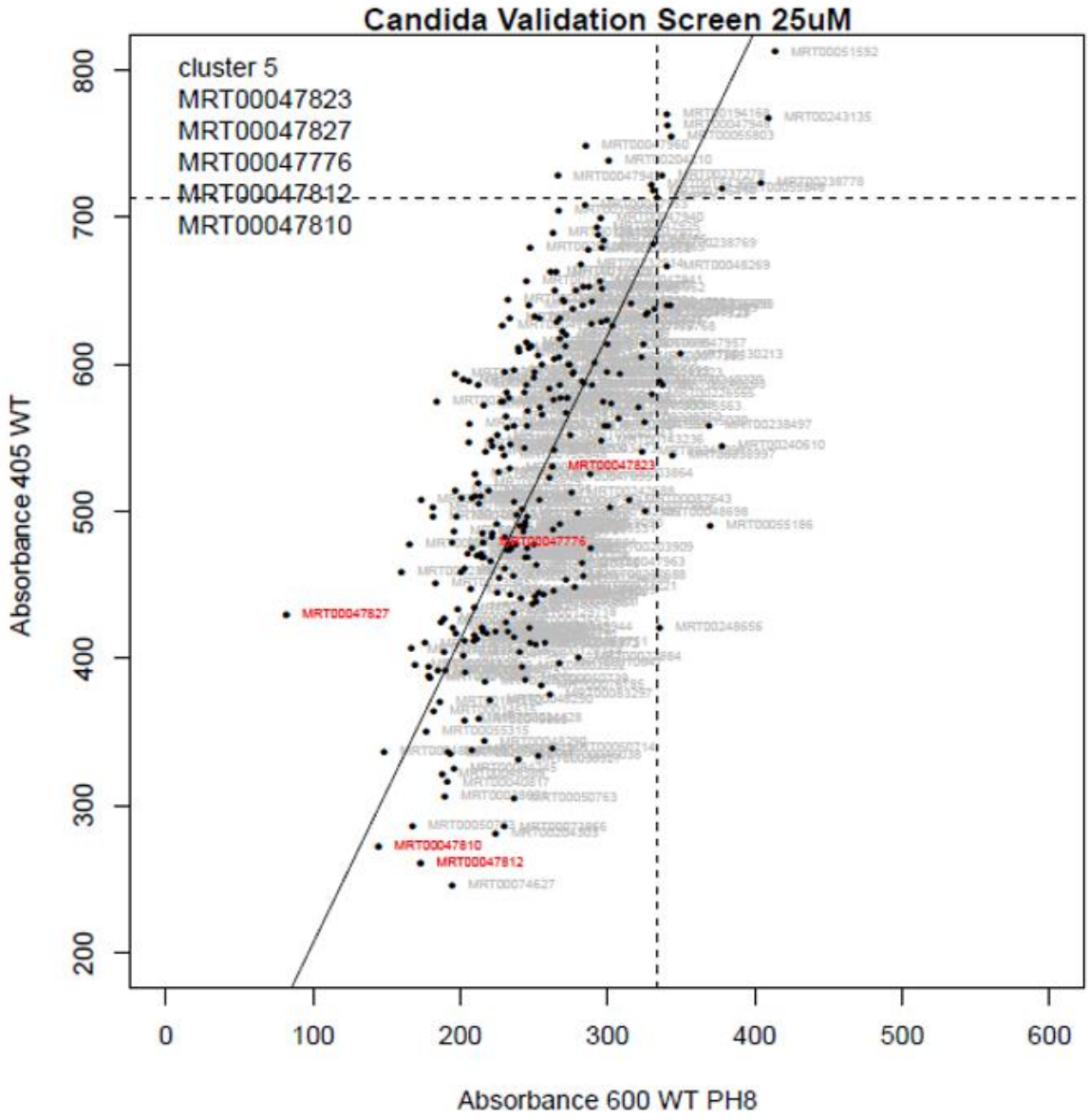

Cluster 4: 25 µM Secondary Screen: pH8 as a readout for PHO Pathway activity.
Plot of OD_{600} *wt* cells grown in pH 8 vs. OD_{405} of *wt* cells. Cells were grown to log phase in YPD before being washed 3 times in pH8 media and diluted back to OD_{600} = 0.05 then seeded into 384 well plates containing 25 µM of compound. Absorbance of 600 nm is used for growth at pH and 405 for secreted acid phosphatase activity. Red hits represent those from cluster 5.

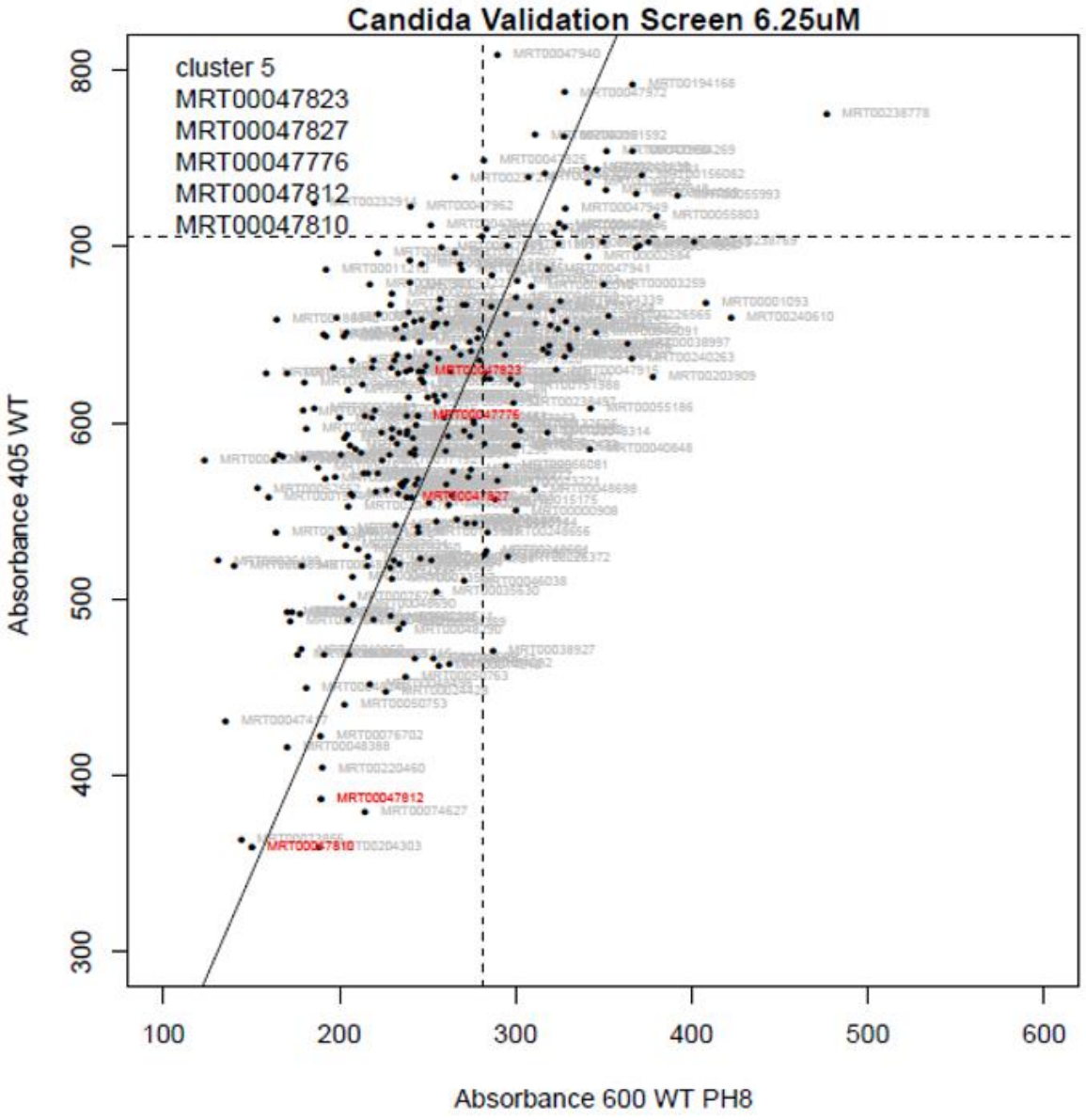

Cluster 4: 6.25 µM Secondary Screen: pH8 as a readout for PHO Pathway activity.
Plot of OD_{600} *wt* cells grown in pH 8 vs. OD_{405} of *wt* cells. Cells were grown to log phase in YPD before being washed 3 times in pH8 media and diluted back to OD_{600} = 0.05 then seeded into 384 well plates containing 6.25 µM of compound. Absorbance of 600 nm is used for growth at pH and 405 for secreted acid phosphatase activity. Red hits represent those from cluster 5.

Cluster 6

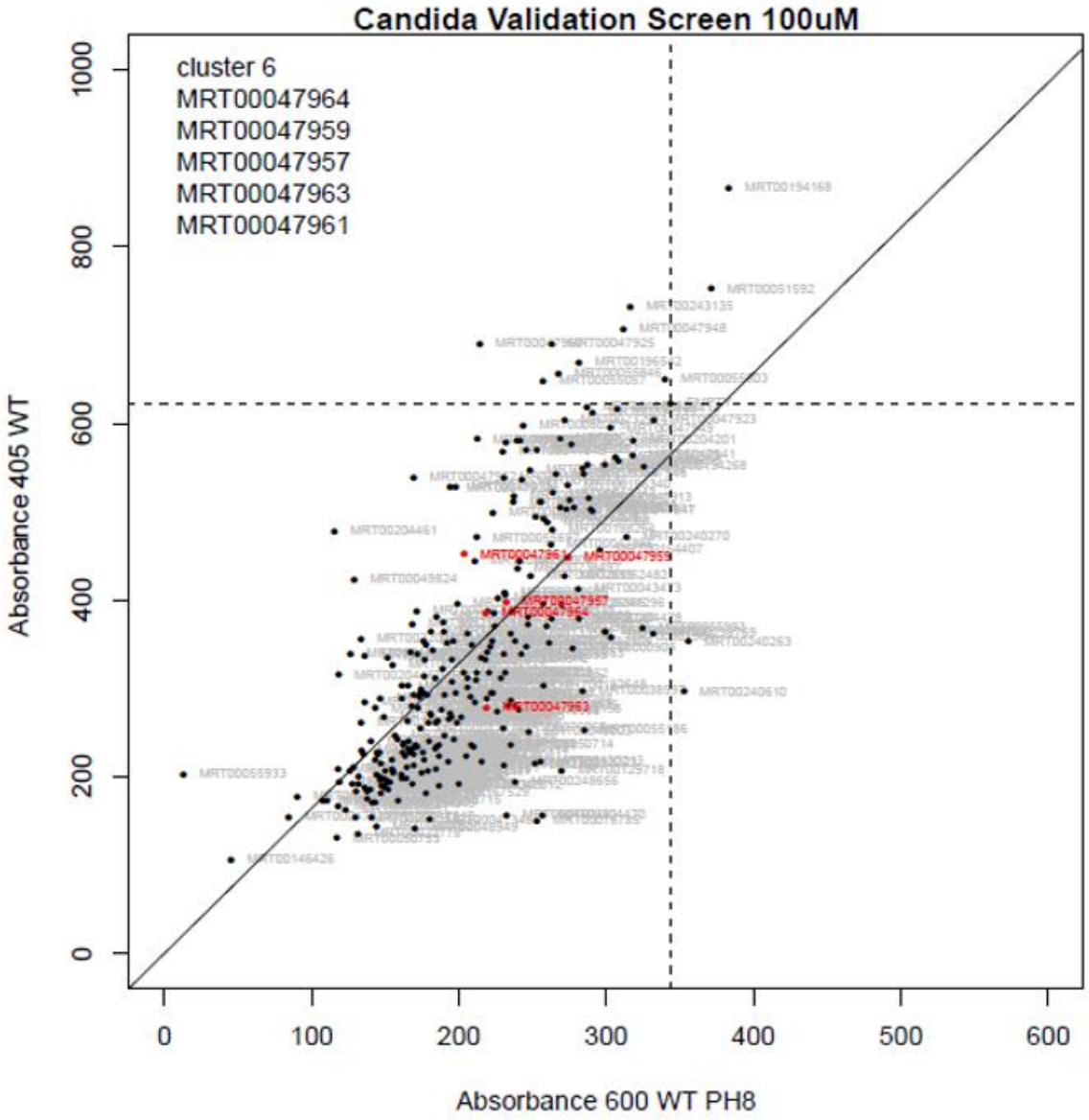

Cluster 6: 100 µM Secondary Screen: pH8 as a readout for PHO Pathway activity.
Plot of OD_{600} *wt* cells grown in pH 8 vs. OD_{405} of *wt* cells. Cells were grown to log phase in YPD before being washed 3 times in pH8 media and diluted back to OD_{600} = 0.05 then seeded into 384 well plates containing 100 µM of compound. Absorbance of 600 nm is used for growth at pH and 405 for secreted acid phosphatase activity. Red hits represent those from cluster 6.

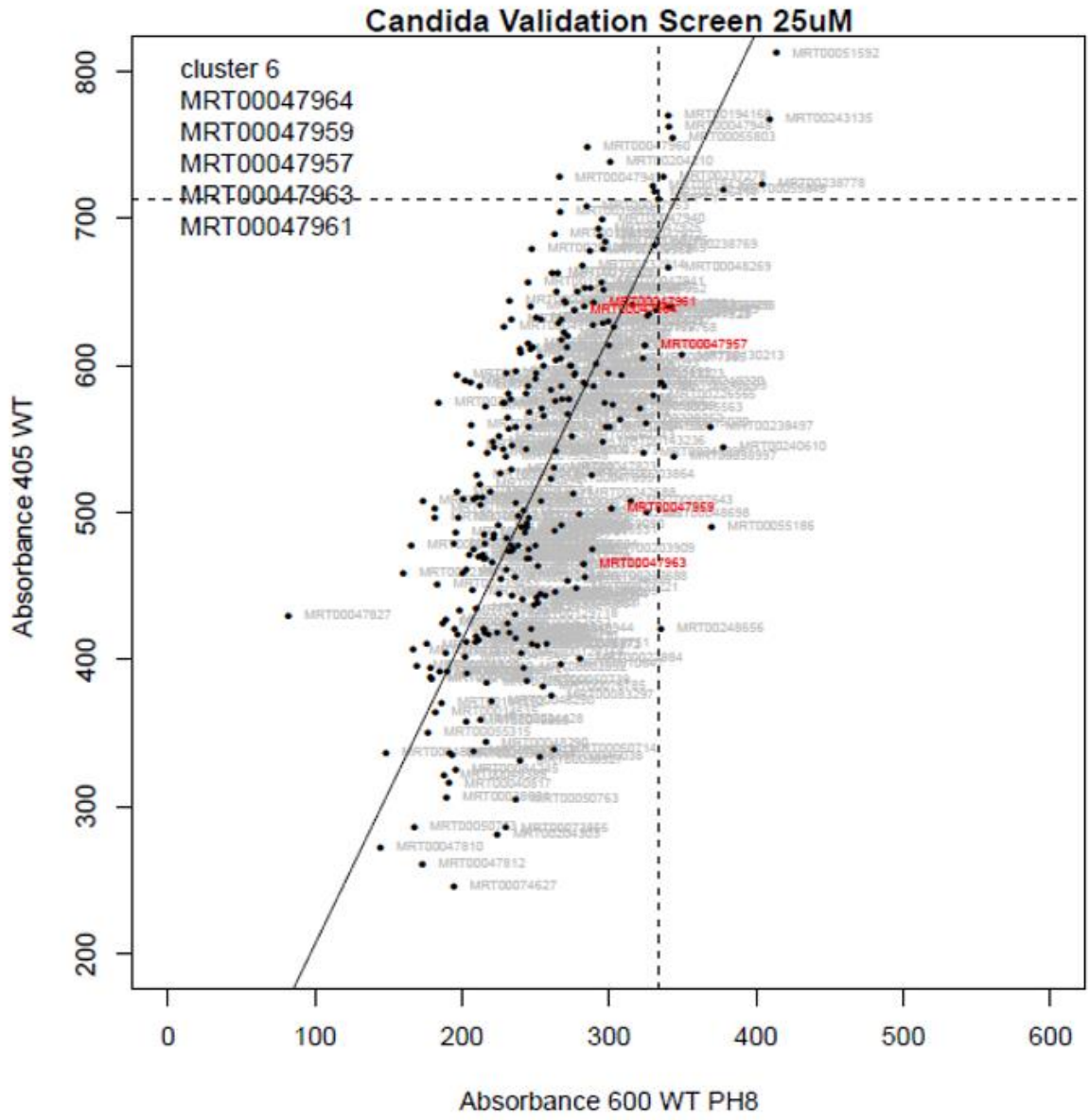

Cluster 6: 25 µM Secondary Screen: pH8 as a readout for PHO Pathway activity.
Plot of OD_{600} *wt* cells grown in pH 8 vs. OD_{405} of *wt* cells. Cells were grown to log phase in YPD before being washed 3 times in pH8 media and diluted back to OD_{600} = 0.05 then seeded into 384 well plates containing 25 µM of compound. Absorbance of 600 nm is used for growth at pH and 405 for secreted acid phosphatase activity. Red hits represent those from cluster 6.

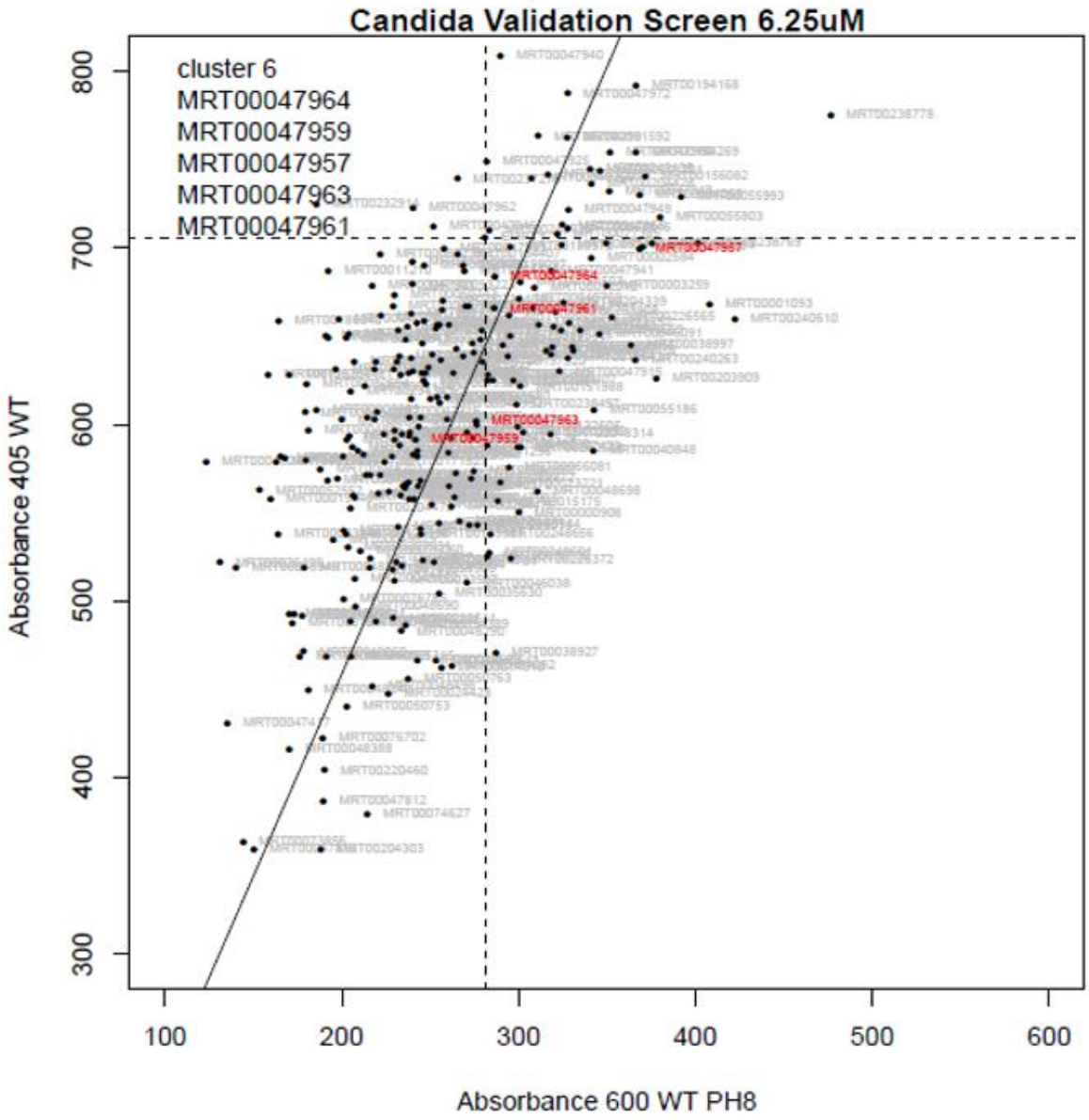

Cluster 6: 6.25 µM Secondary Screen: pH8 as a readout for PHO Pathway activity.
Plot of OD_{600} *wt* cells grown in pH 8 vs. OD_{405} of *wt* cells. Cells were grown to log phase in YPD before being washed 3 times in pH8 media and diluted back to OD_{600} = 0.05 then seeded into 384 well plates containing 6.25 µM of compound. Absorbance of 600 nm is used for growth at pH and 405 for secreted acid phosphatase activity. Red hits represent those from cluster 6.

Cluster 7

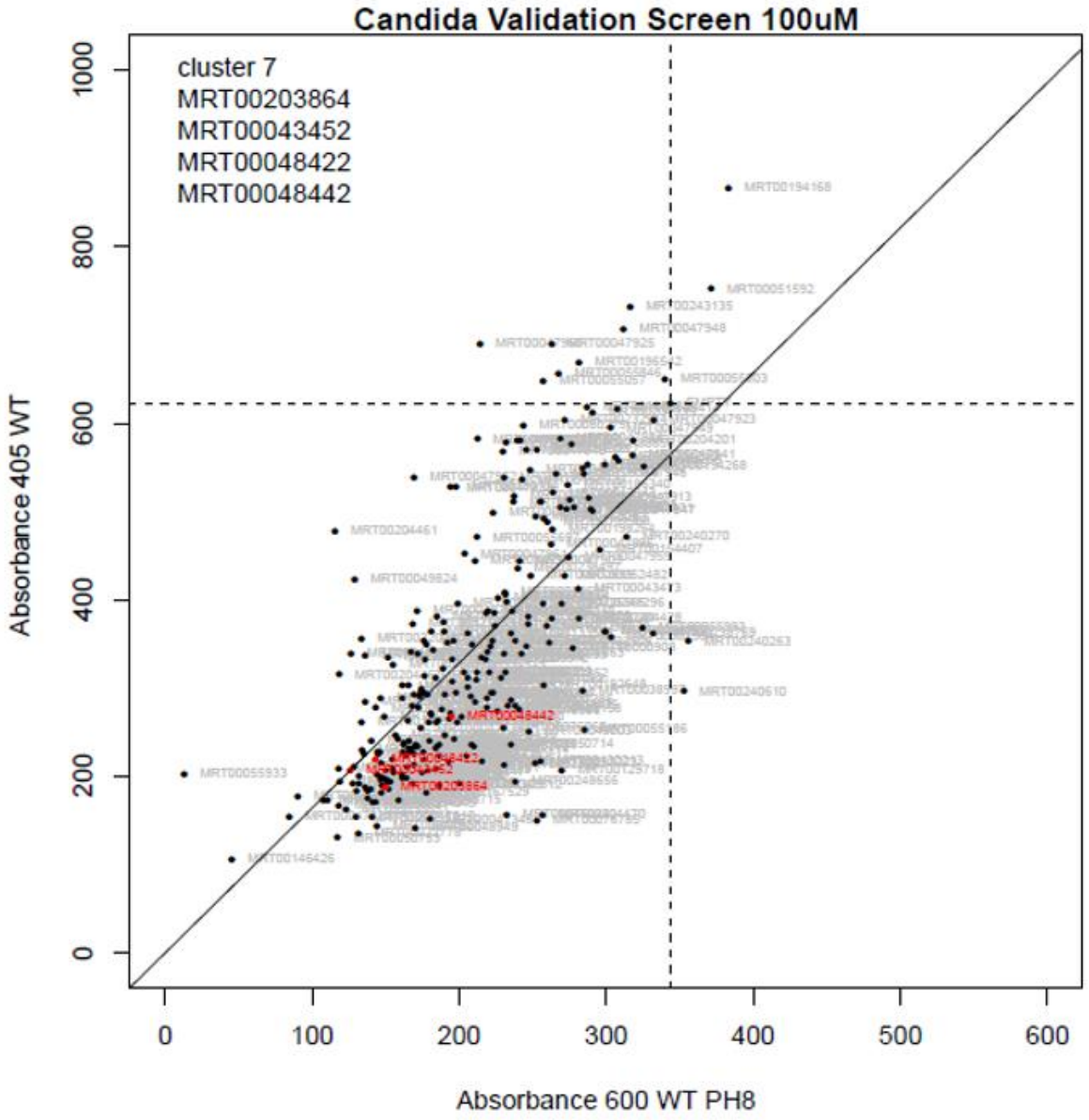

Cluster 7: 100 µM Secondary Screen: pH8 as a readout for PHO Pathway activity.
Plot of OD_{600} *wt* cells grown in pH 8 vs. OD_{405} of *wt* cells. Cells were grown to log phase in YPD before being washed 3 times in pH8 media and diluted back to OD_{600} = 0.05 then seeded into 384 well plates containing 100 µM of compound. Absorbance of 600 nm is used for growth at pH and 405 for secreted acid phosphatase activity. Red hits represent those from cluster 7.

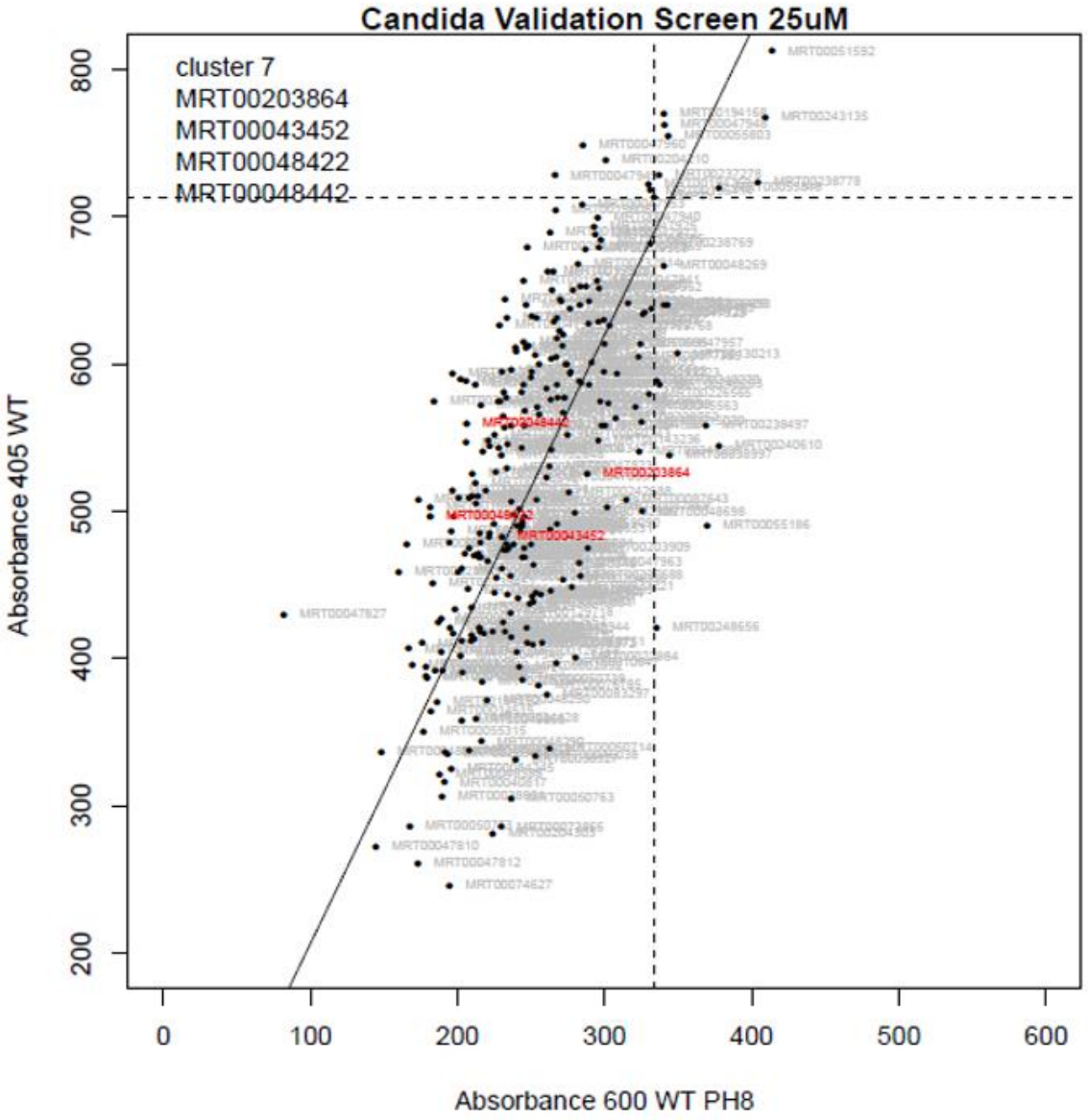

Cluster 7: 25 µM Secondary Screen: pH8 as a readout for PHO Pathway activity.
Plot of OD_{600} *wt* cells grown in pH 8 vs. OD_{405} of *wt* cells. Cells were grown to log phase in YPD before being washed 3 times in pH8 media and diluted back to OD_{600} = 0.05 then seeded into 384 well plates containing 25 µM of compound. Absorbance of 600 nm is used for growth at pH and 405 for secreted acid phosphatase activity. Red hits represent those from cluster 7.

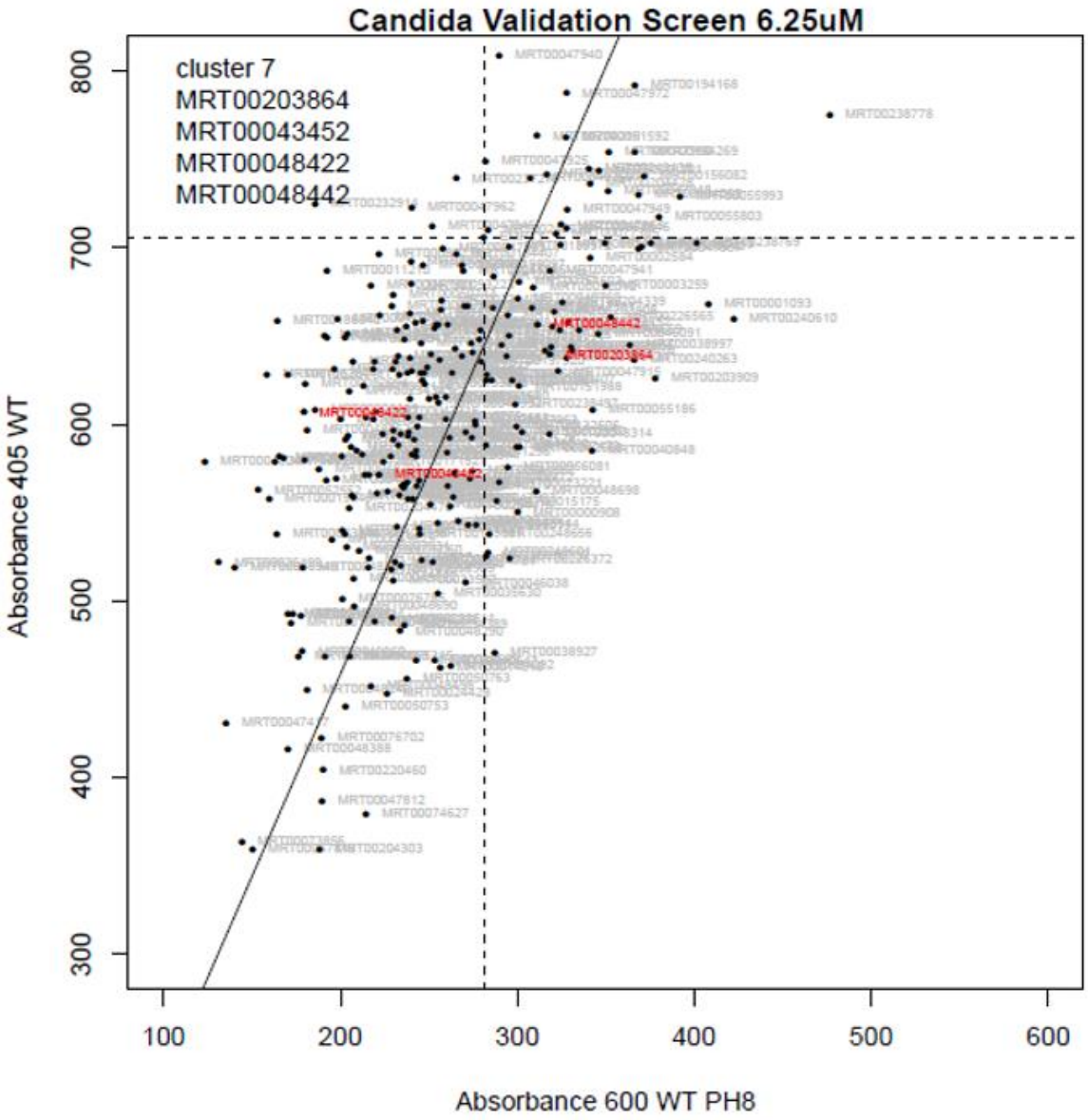

Cluster 7: 6.25 µM Secondary Screen: pH8 as a readout for PHO Pathway activity.
Plot of OD_{600} *wt* cells grown in pH 8 vs. OD_{405} of *wt* cells. Cells were grown to log phase in YPD before being washed 3 times in pH8 media and diluted back to OD_{600} = 0.05 then seeded into 384 well plates containing 6.25 µM of compound. Absorbance of 600 nm is used for growth at pH and 405 for secreted acid phosphatase activity. Red hits represent those from cluster 7.

Cluster 8

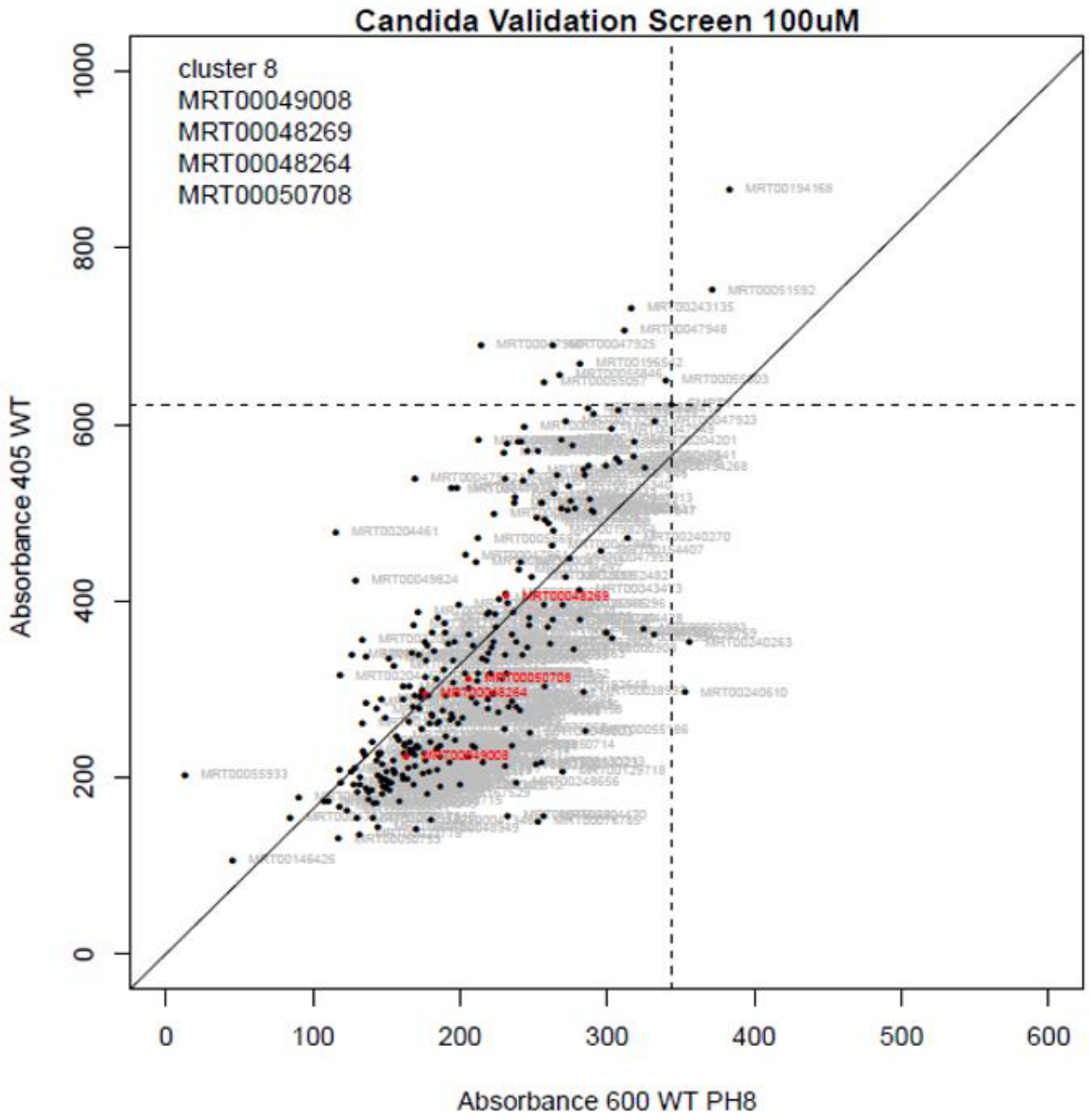

Cluster 8: 100 µM Secondary Screen: pH8 as a readout for PHO Pathway activity.
Plot of OD_{600} *wt* cells grown in pH 8 vs. OD_{405} of *wt* cells. Cells were grown to log phase in YPD before being washed 3 times in pH8 media and diluted back to OD_{600} = 0.05 then seeded into 384 well plates containing 100 µM of compound. Absorbance of 600 nm is used for growth at pH and 405 for secreted acid phosphatase activity. Red hits represent those from cluster 8.

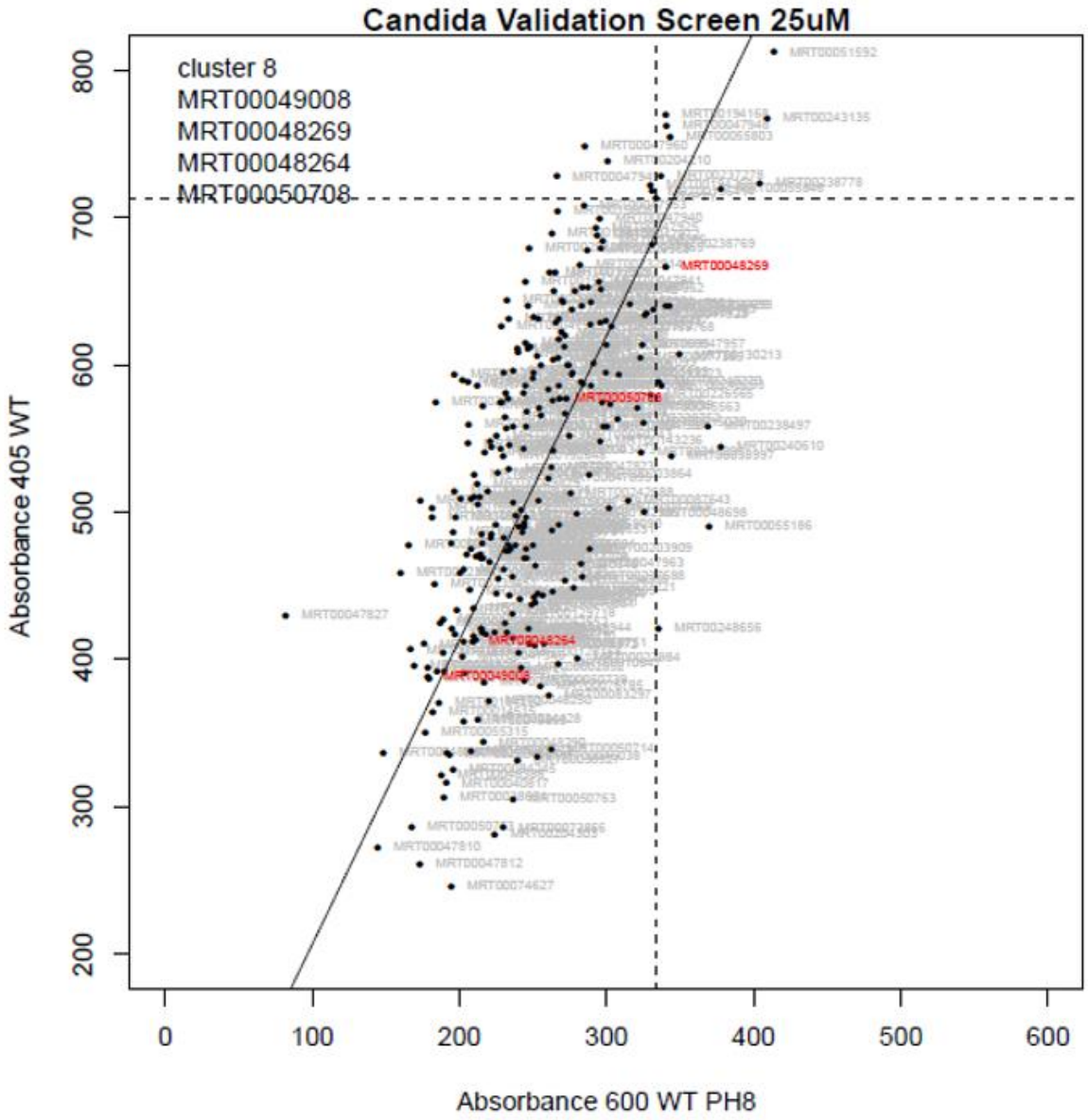

Cluster 8: 25 µM Secondary Screen: pH8 as a readout for PHO Pathway activity.
Plot of OD_{600} *wt* cells grown in pH 8 vs. OD_{405} of *wt* cells. Cells were grown to log phase in YPD before being washed 3 times in pH8 media and diluted back to OD_{600} = 0.05 then seeded into 384 well plates containing 25 µM of compound. Absorbance of 600 nm is used for growth at pH and 405 for secreted acid phosphatase activity. Red hits represent those from cluster 8.

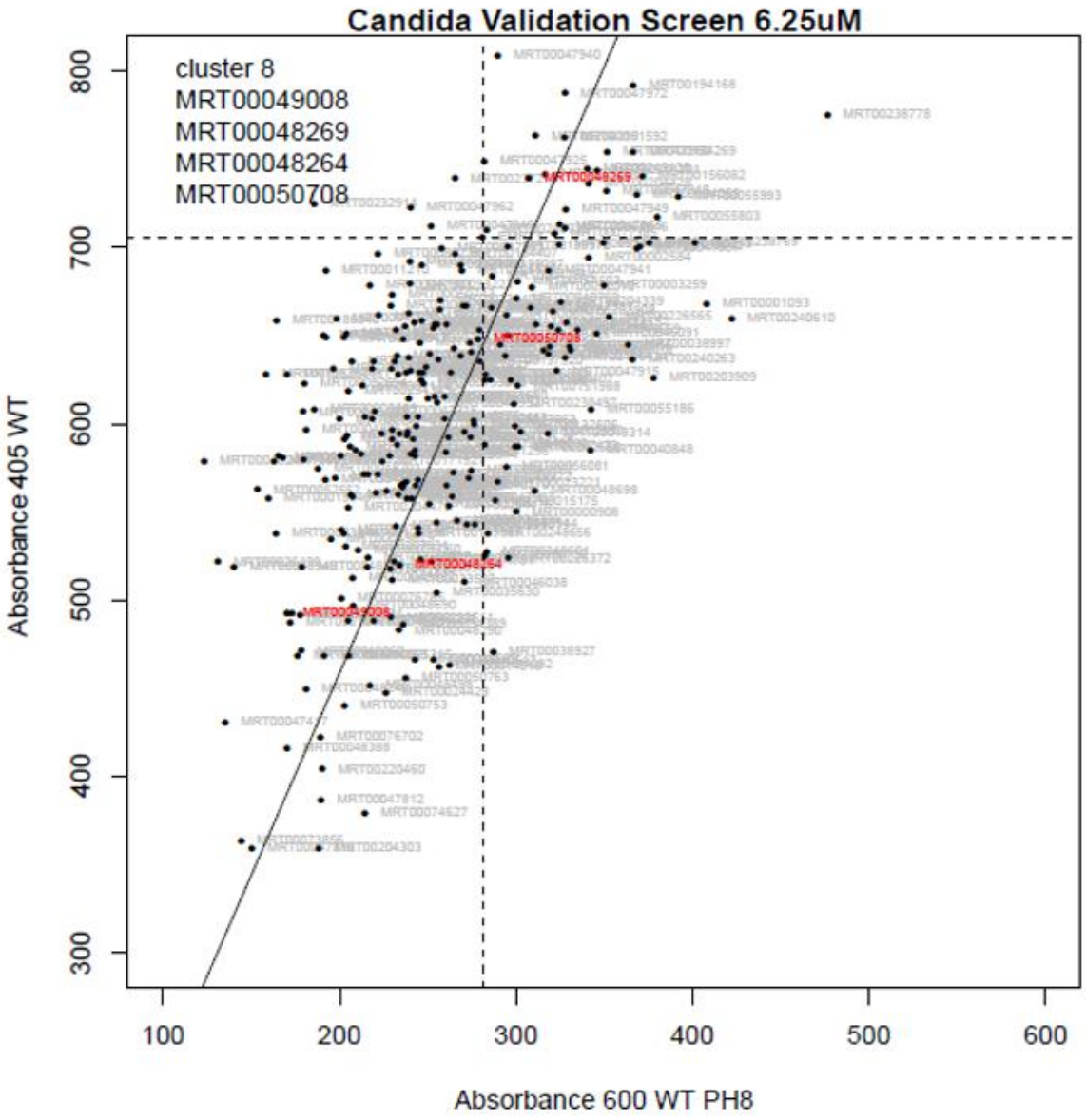

Cluster 8: 6.25 µM Secondary Screen: pH8 as a readout for PHO Pathway activity.
Plot of OD_{600} *wt* cells grown in pH 8 vs. OD_{405} of *wt* cells. Cells were grown to log phase in YPD before being washed 3 times in pH8 media and diluted back to OD_{600} = 0.05 then seeded into 384 well plates containing 6.25 µM of compound. Absorbance of 600 nm is used for growth at pH and 405 for secreted acid phosphatase activity. Red hits represent those from cluster 8.

Cluster 9

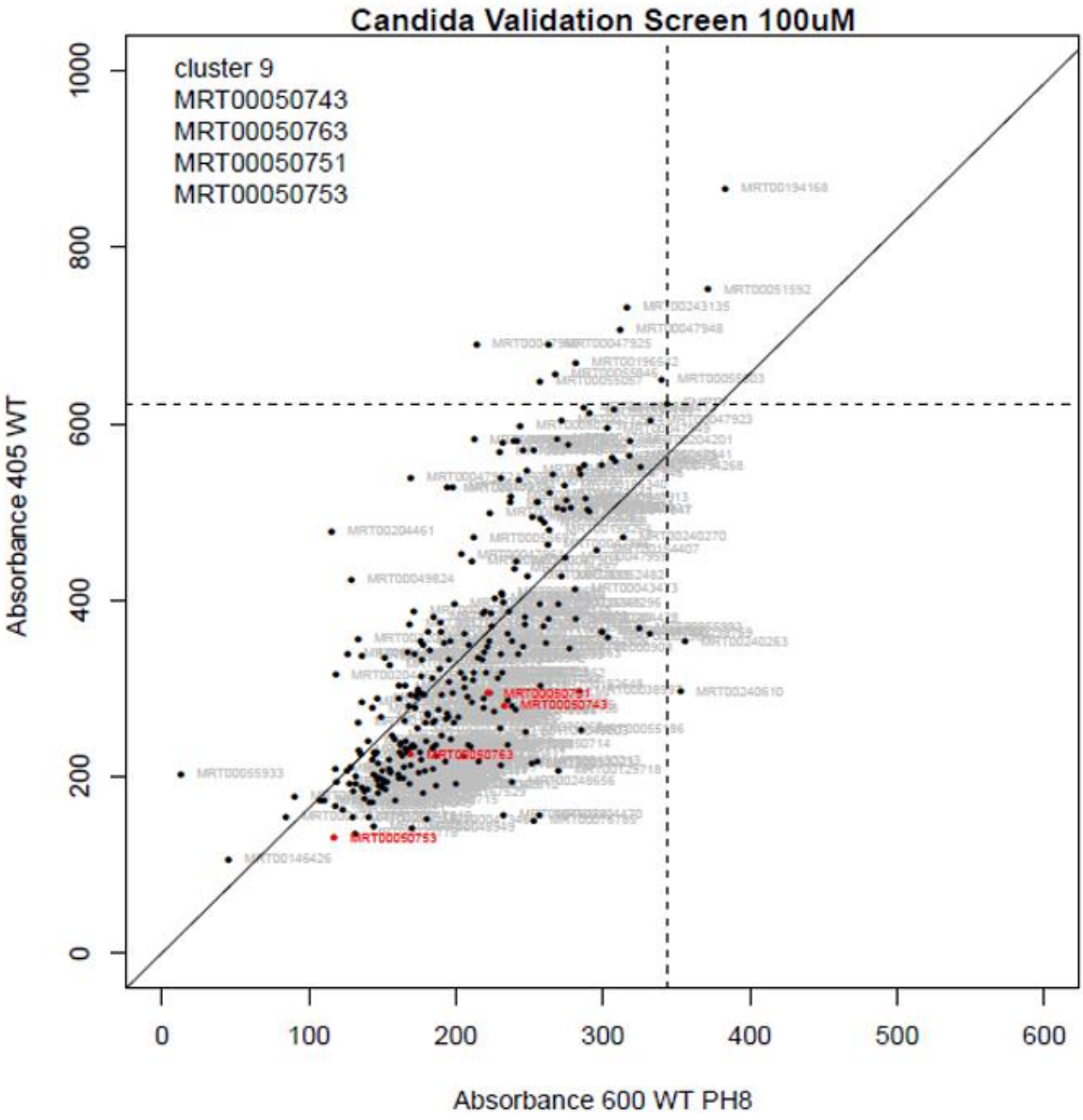

Cluster 9: 100 µM Secondary Screen: pH8 as a readout for PHO Pathway activity.
Plot of OD_{600} *wt* cells grown in pH 8 vs. OD_{405} of *wt* cells. Cells were grown to log phase in YPD before being washed 3 times in pH8 media and diluted back to OD_{600} = 0.05 then seeded into 384 well plates containing 100 µM of compound. Absorbance of 600 nm is used for growth at pH and 405 for secreted acid phosphatase activity. Red hits represent those from cluster 9.

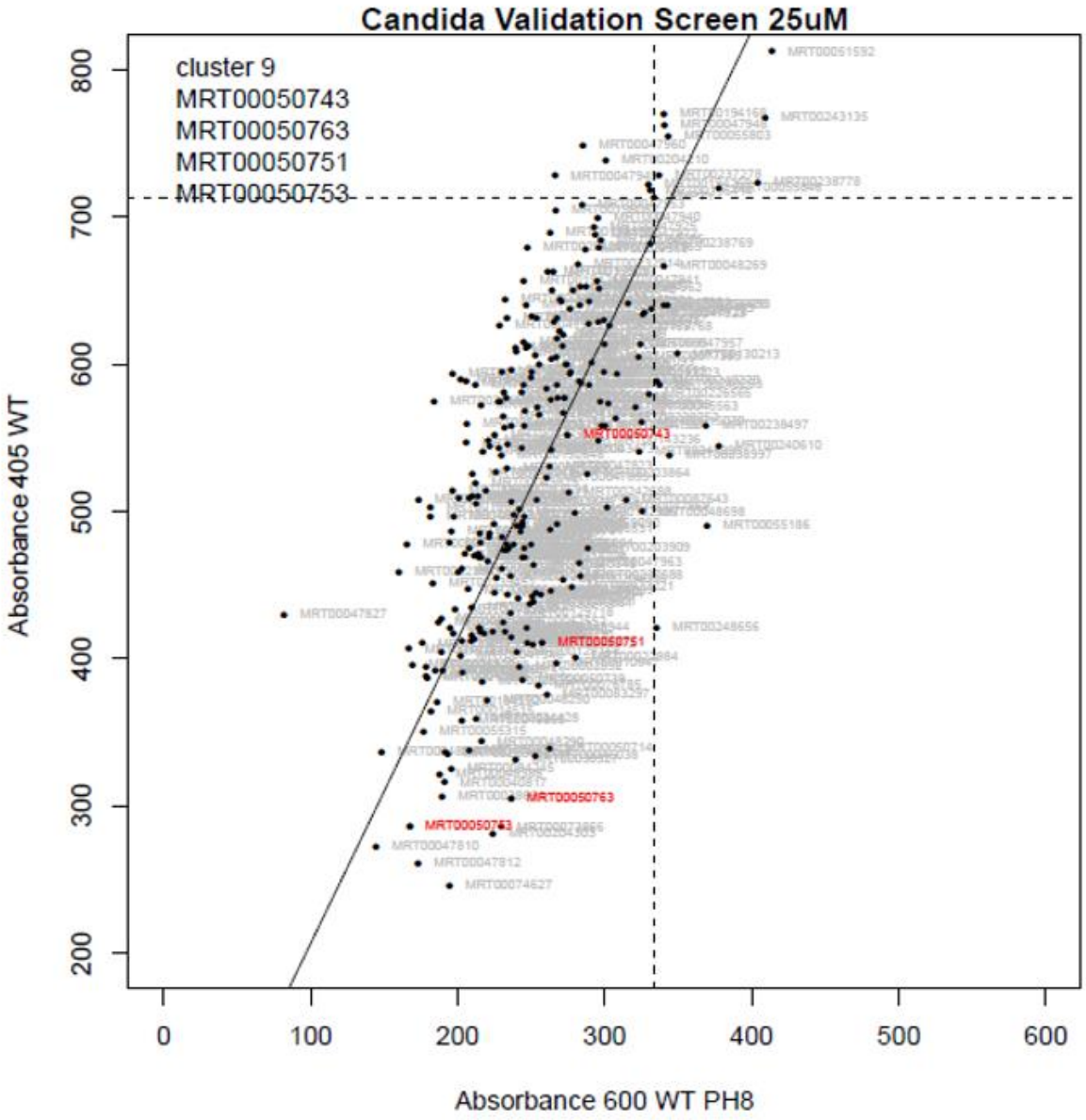

Cluster 9: 25 µM Secondary Screen: pH8 as a readout for PHO Pathway activity.
Plot of OD_{600} *wt* cells grown in pH 8 vs. OD_{405} of *wt* cells. Cells were grown to log phase in YPD before being washed 3 times in pH8 media and diluted back to OD_{600} = 0.05 then seeded into 384 well plates containing 25 µM of compound. Absorbance of 600 nm is used for growth at pH and 405 for secreted acid phosphatase activity. Red hits represent those from cluster 9.

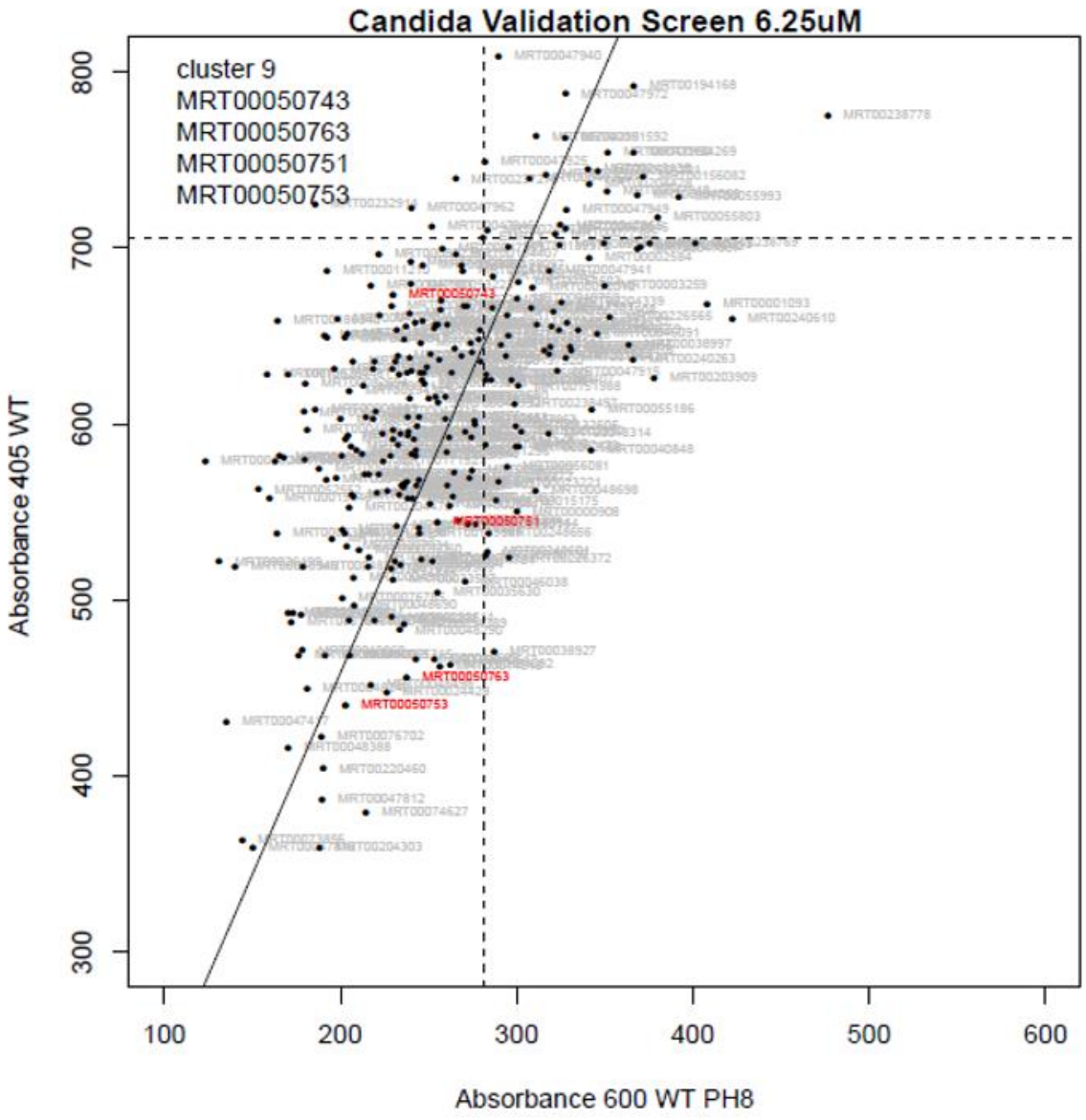

Cluster 9: 6.25 µM Secondary Screen: pH8 as a readout for PHO Pathway activity.
Plot of OD_{600} *wt* cells grown in pH 8 vs. OD_{405} of *wt* cells. Cells were grown to log phase in YPD before being washed 3 times in pH8 media and diluted back to OD_{600} = 0.05 then seeded into 384 well plates containing 6.25 µM of compound. Absorbance of 600 nm is used for growth at pH and 405 for secreted acid phosphatase activity. Red hits represent those from cluster 9.

Cluster 10

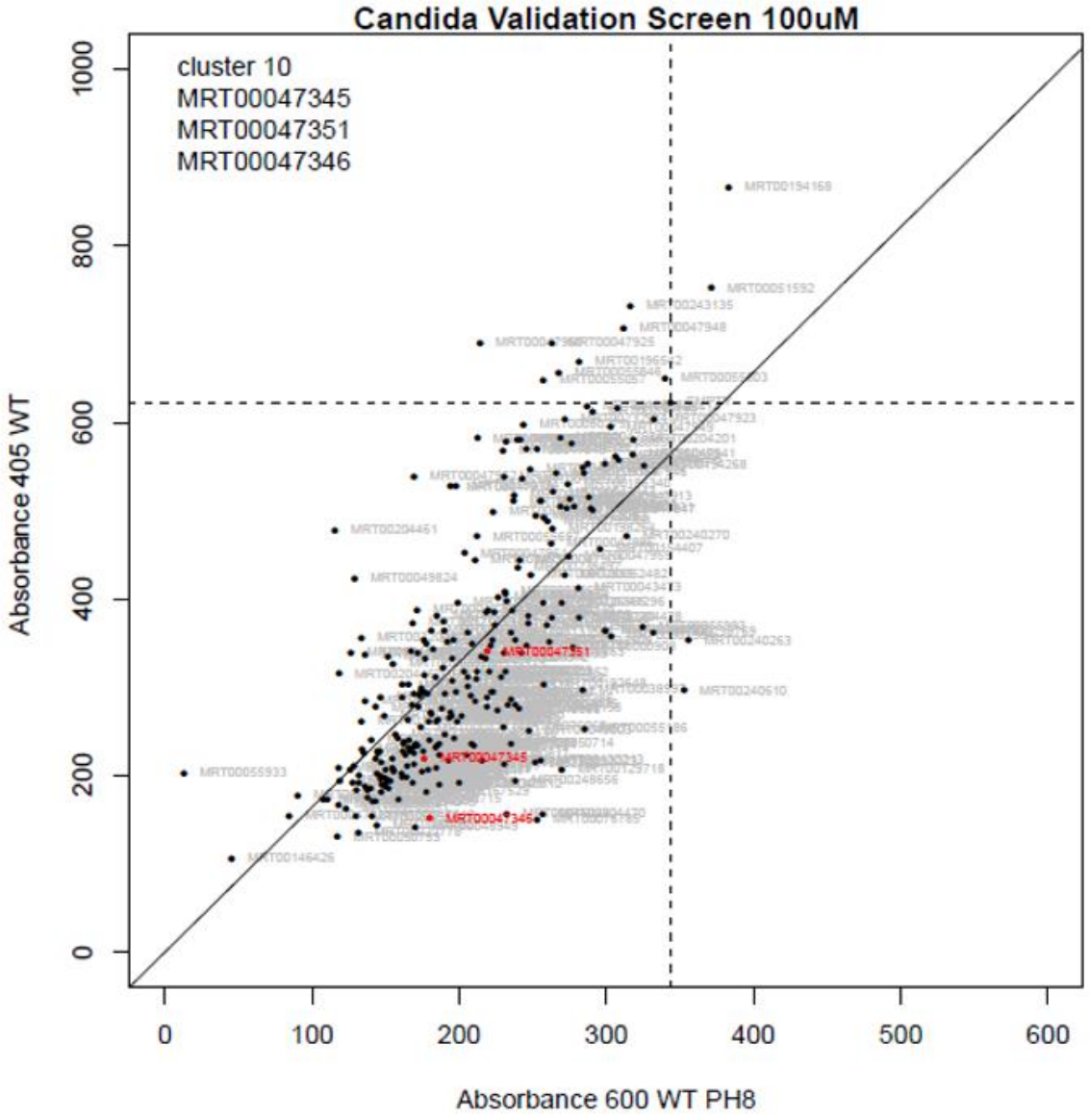

Cluster 10: 100 µM Secondary Screen: pH8 as a readout for PHO Pathway activity.
Plot of OD_{600} *wt* cells grown in pH 8 vs. OD_{405} of *wt* cells. Cells were grown to log phase in YPD before being washed 3 times in pH8 media and diluted back to OD_{600} = 0.05 then seeded into 384 well plates containing 100 µM of compound. Absorbance of 600 nm is used for growth at pH and 405 for secreted acid phosphatase activity. Red hits represent those from cluster 10.

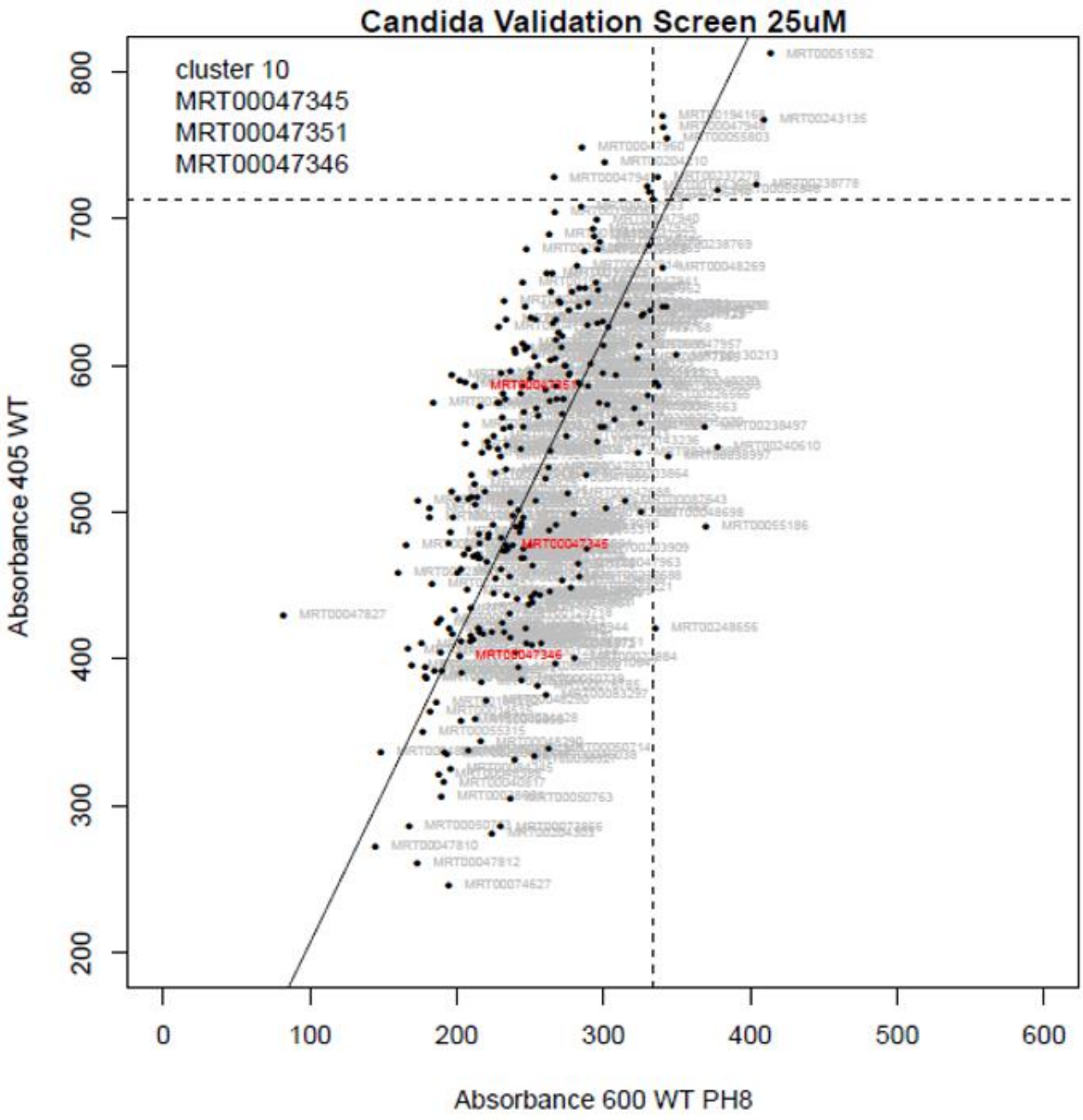

Cluster 10: 25 µM Secondary Screen: pH8 as a readout for PHO Pathway activity.
Plot of OD_{600} *wt* cells grown in pH 8 vs. OD_{405} of *wt* cells. Cells were grown to log phase in YPD before being washed 3 times in pH8 media and diluted back to OD_{600} = 0.05 then seeded into 384 well plates containing 25 µM of compound. Absorbance of 600 nm is used for growth at pH and 405 for secreted acid phosphatase activity. Red hits represent those from cluster 10.

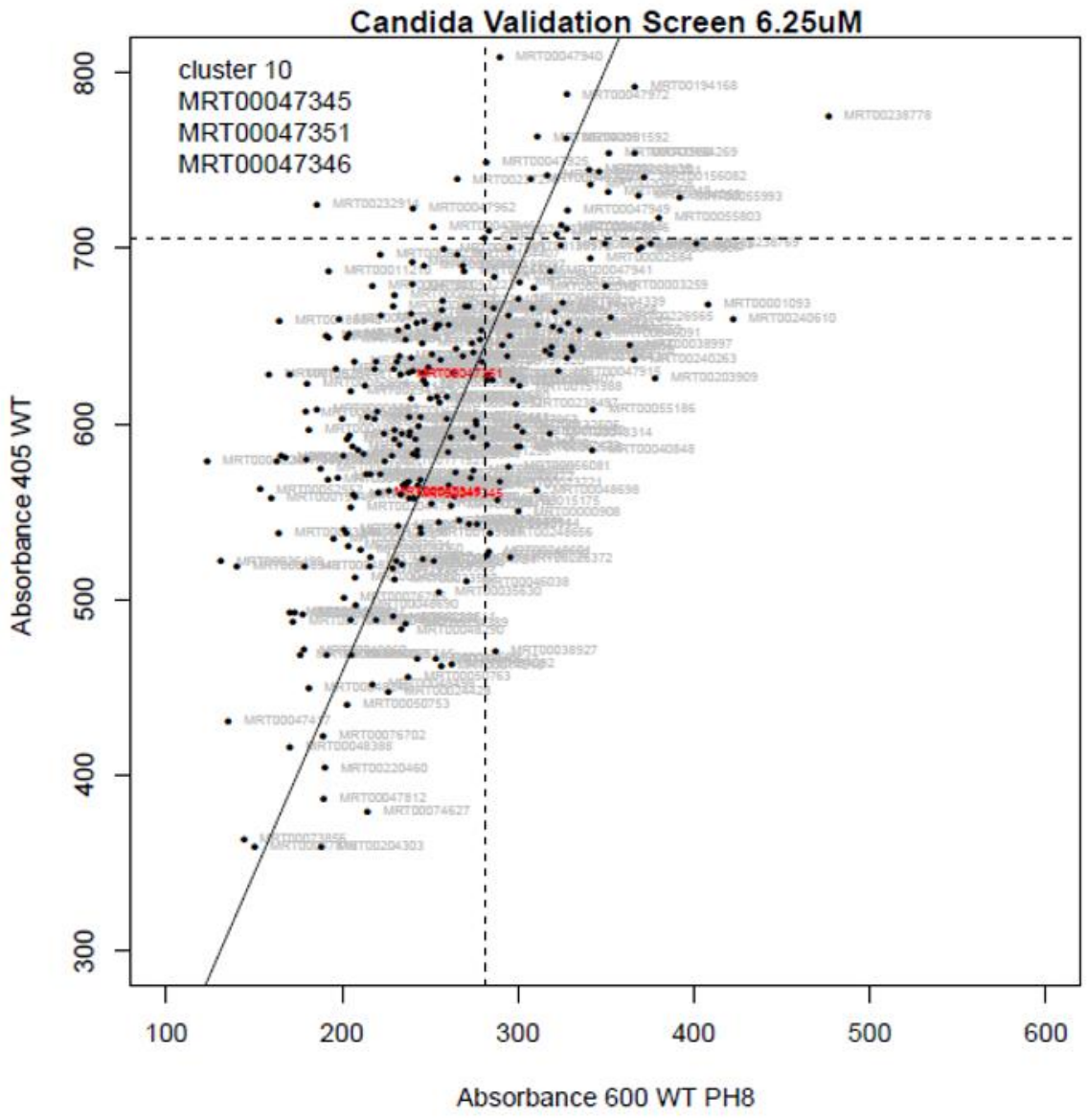

Cluster 10: 6.25 µM Secondary Screen: pH8 as a readout for PHO Pathway activity.
Plot of OD_{600} *wt* cells grown in pH 8 vs. OD_{405} of *wt* cells. Cells were grown to log phase in YPD before being washed 3 times in pH8 media and diluted back to OD_{600} = 0.05 then seeded into 384 well plates containing 6.25 µM of compound. Absorbance of 600 nm is used for growth at pH and 405 for secreted acid phosphatase activity. Red hits represent those from cluster 10.

Cluster 11

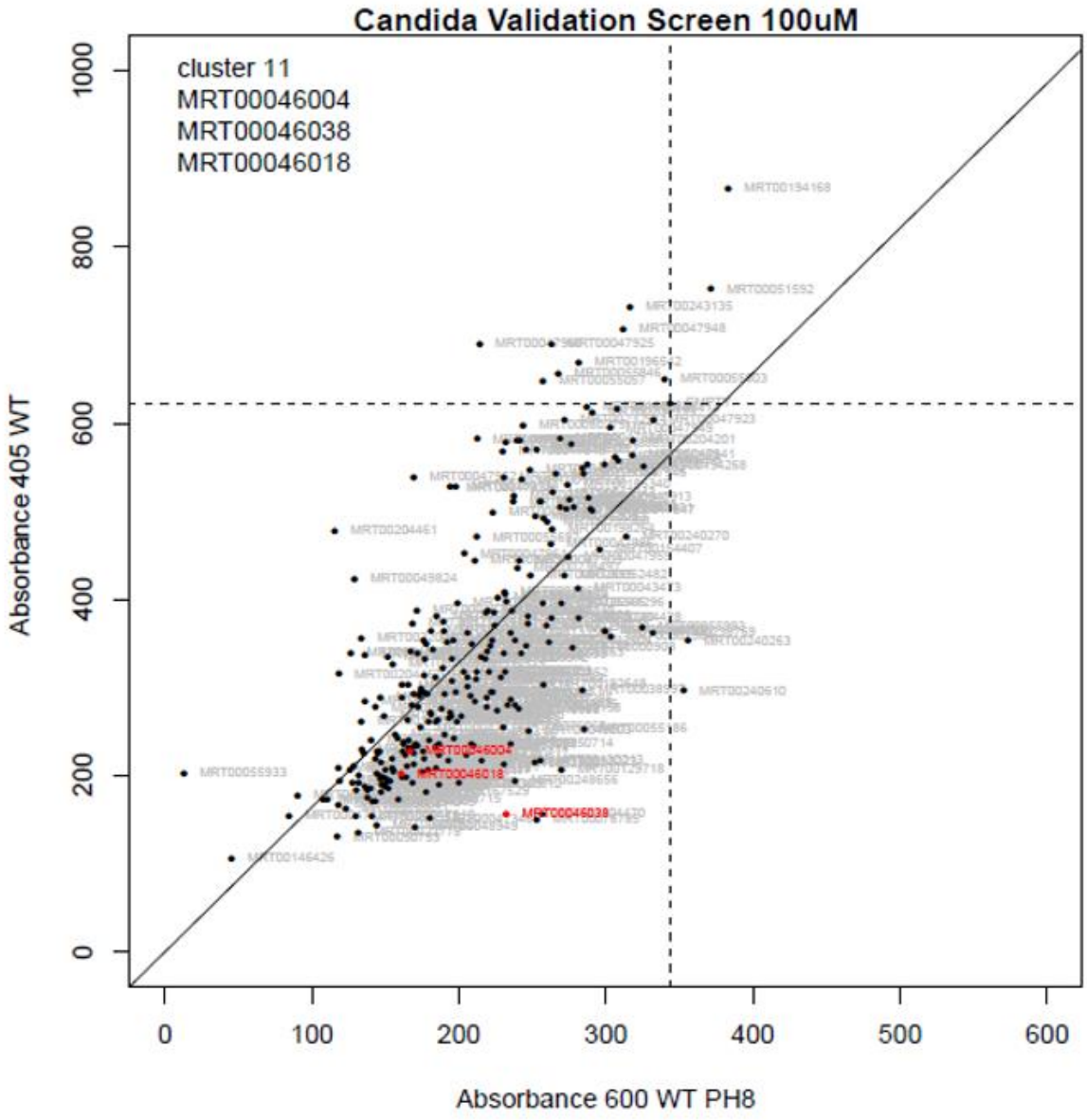

Cluster 11: 100 µM Secondary Screen: pH8 as a readout for PHO Pathway activity.
Plot of OD_{600} *wt* cells grown in pH 8 vs. OD_{405} of *wt* cells. Cells were grown to log phase in YPD before being washed 3 times in pH8 media and diluted back to OD_{600} = 0.05 then seeded into 384 well plates containing 100 µM of compound. Absorbance of 600 nm is used for growth at pH and 405 for secreted acid phosphatase activity. Red hits represent those from cluster 11.

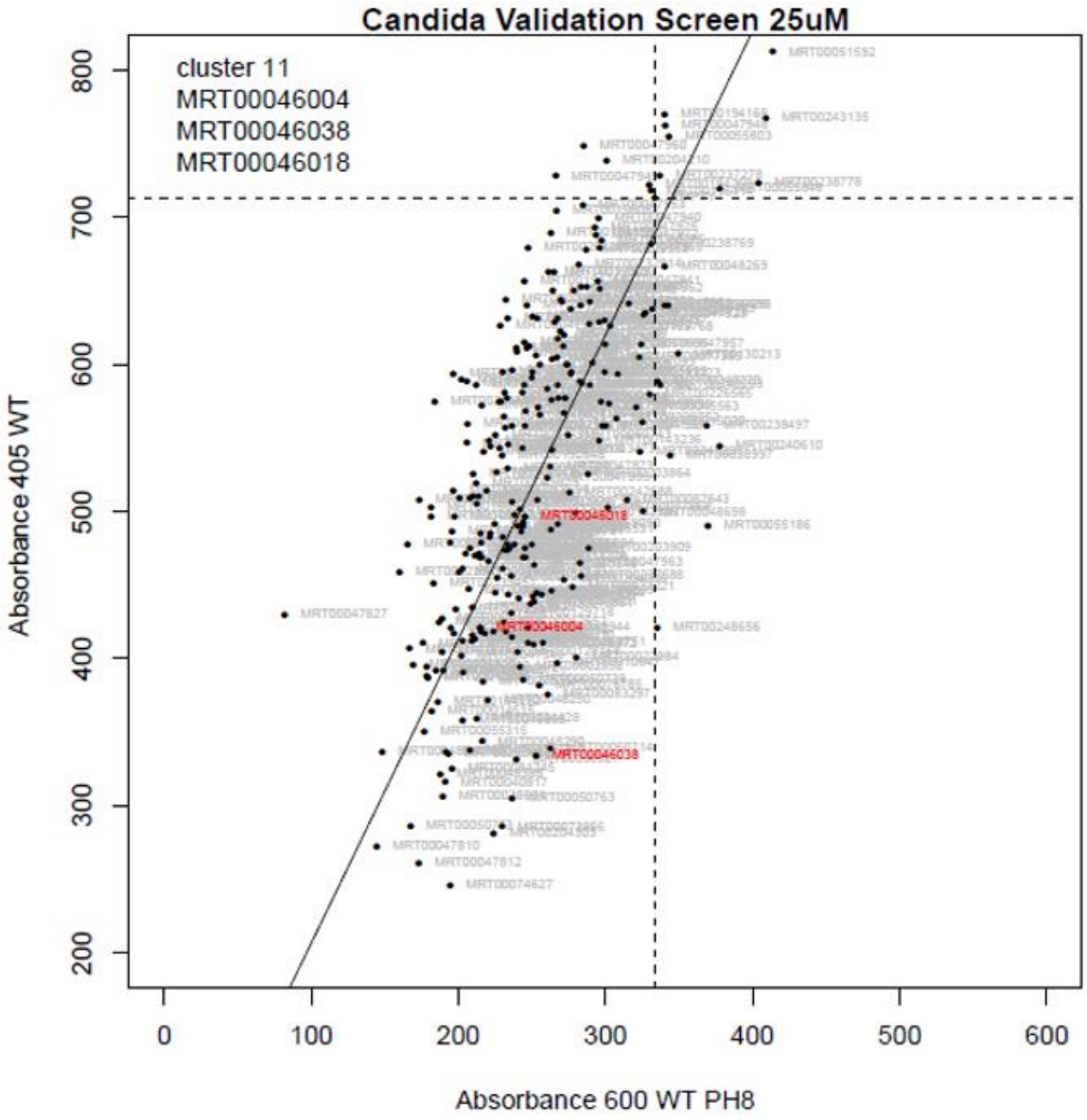

Cluster 11: 25 µM Secondary Screen: pH8 as a readout for PHO Pathway activity.
Plot of OD_{600} *wt* cells grown in pH 8 vs. OD_{405} of *wt* cells. Cells were grown to log phase in YPD before being washed 3 times in pH8 media and diluted back to OD_{600} = 0.05 then seeded into 384 well plates containing 25 µM of compound. Absorbance of 600 nm is used for growth at pH and 405 for secreted acid phosphatase activity. Red hits represent those from cluster 11.

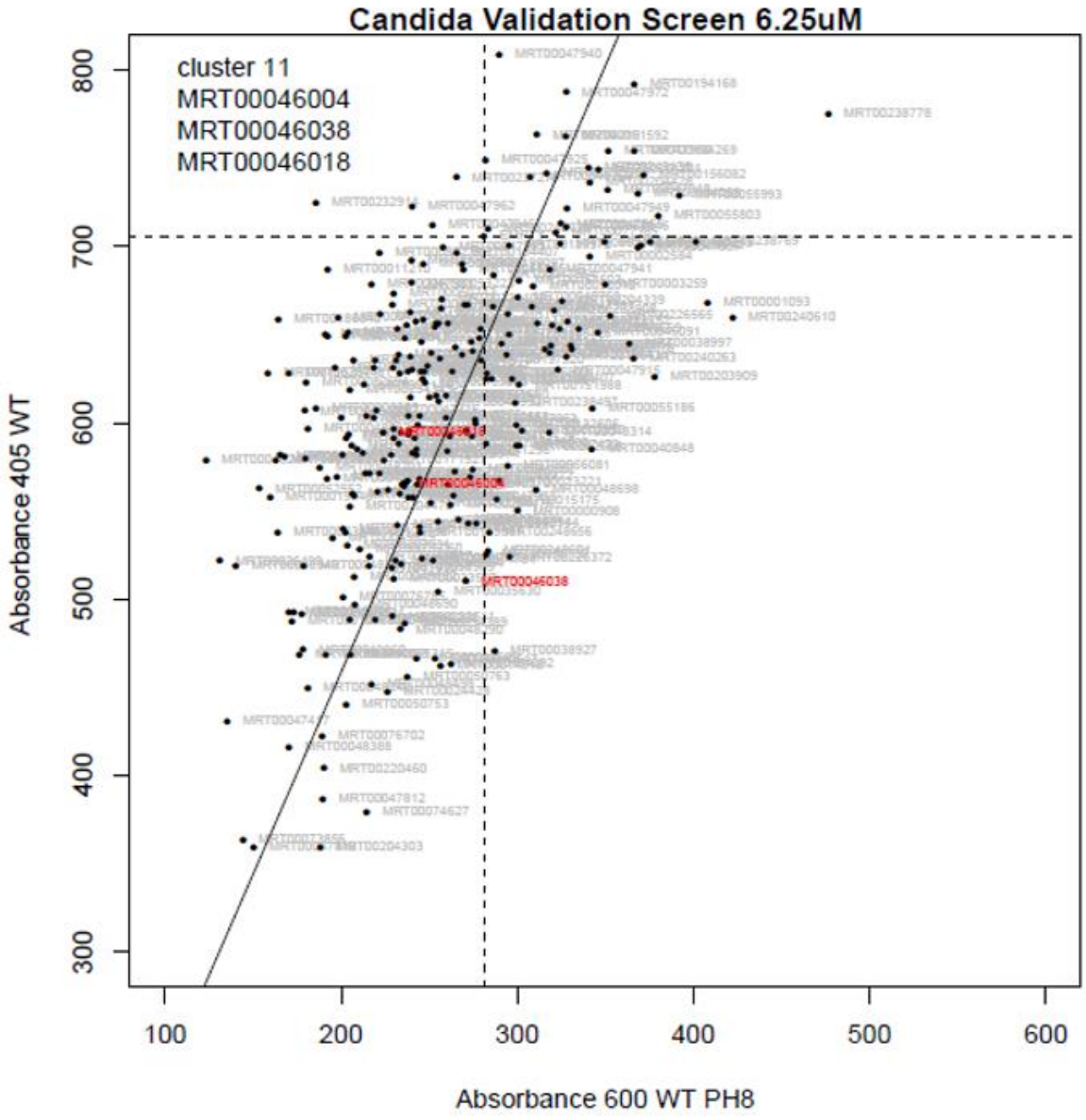

Cluster 11: 6.25 µM Secondary Screen: pH8 as a readout for PHO Pathway activity.
Plot of OD_{600} *wt* cells grown in pH 8 vs. OD_{405} of *wt* cells. Cells were grown to log phase in YPD before being washed 3 times in pH8 media and diluted back to OD_{600} = 0.05 then seeded into 384 well plates containing 6.25 µM of compound. Absorbance of 600 nm is used for growth at pH and 405 for secreted acid phosphatase activity. Red hits represent those from cluster 11.

Cluster 12

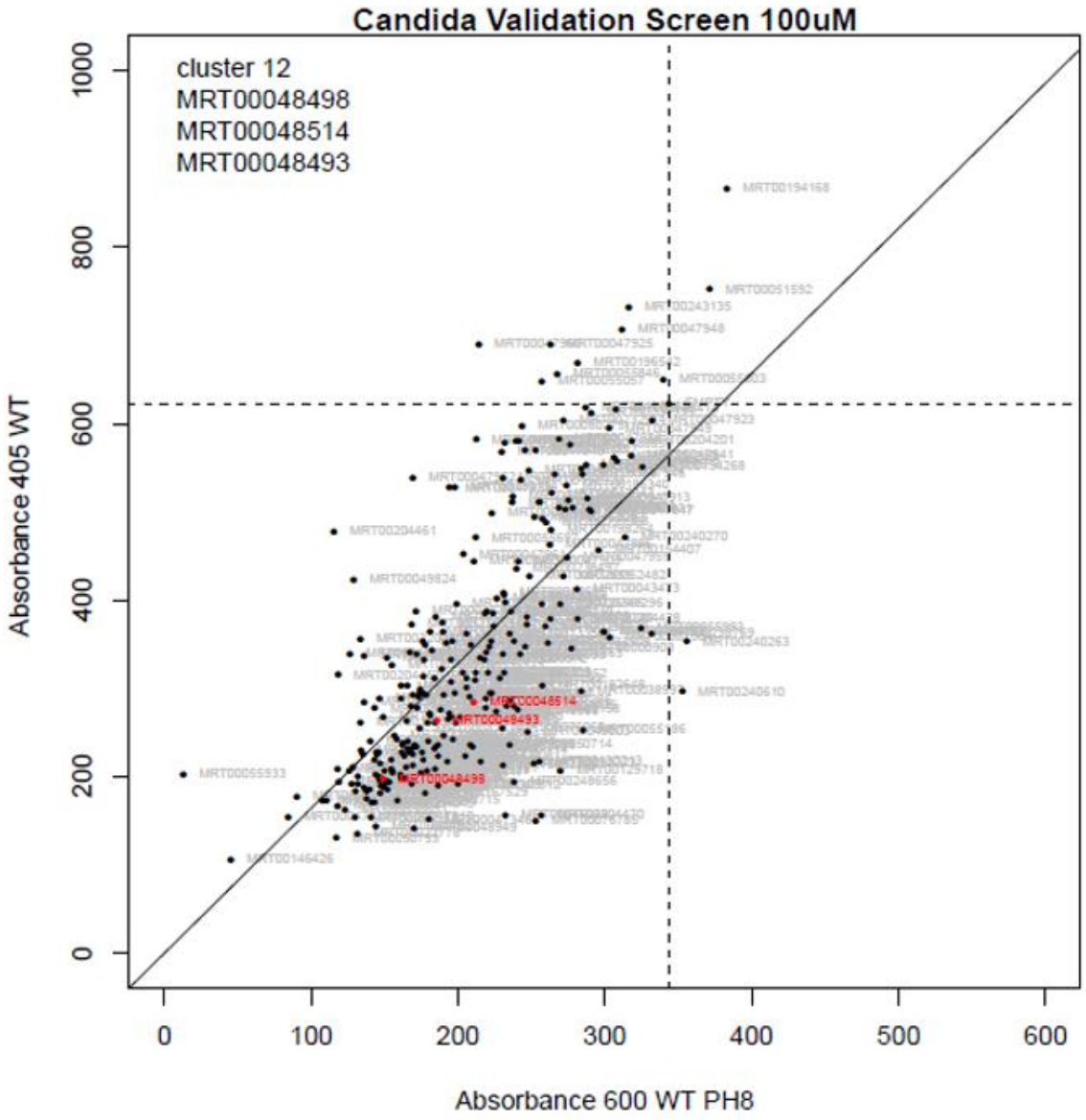

Cluster 12: 100 µM Secondary Screen: pH8 as a readout for PHO Pathway activity.
Plot of OD_{600} *wt* cells grown in pH 8 vs. OD_{405} of *wt* cells. Cells were grown to log phase in YPD before being washed 3 times in pH8 media and diluted back to OD_{600} = 0.05 then seeded into 384 well plates containing 100 µM of compound. Absorbance of 600 nm is used for growth at pH and 405 for secreted acid phosphatase activity. Red hits represent those from cluster 12.

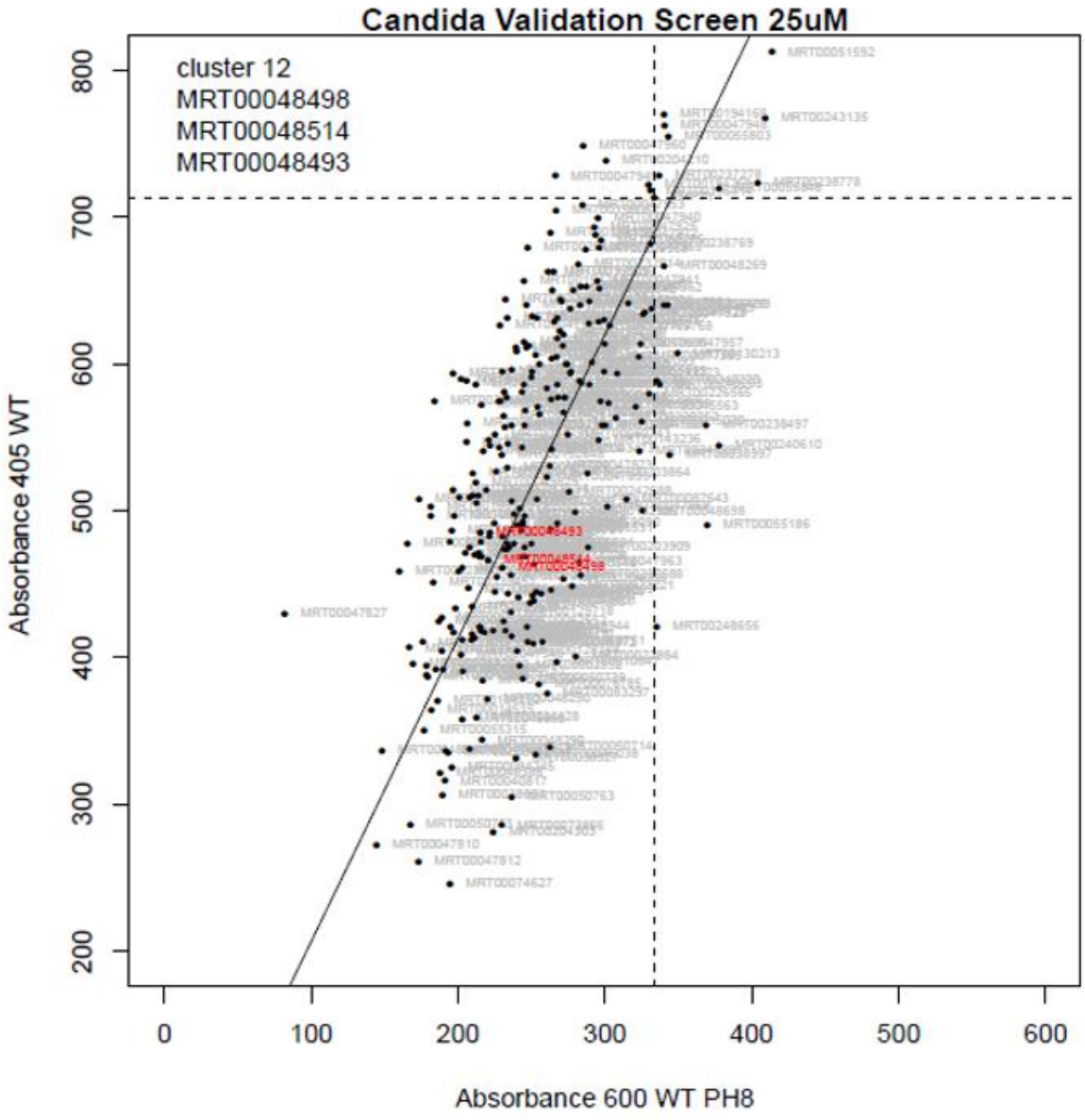

Cluster 12: 25 µM Secondary Screen: pH8 as a readout for PHO Pathway activity.
Plot of OD_{600} *wt* cells grown in pH 8 vs. OD_{405} of *wt* cells. Cells were grown to log phase in YPD before being washed 3 times in pH8 media and diluted back to OD_{600} = 0.05 then seeded into 384 well plates containing 25 µM of compound. Absorbance of 600 nm is used for growth at pH and 405 for secreted acid phosphatase activity. Red hits represent those from cluster 12.

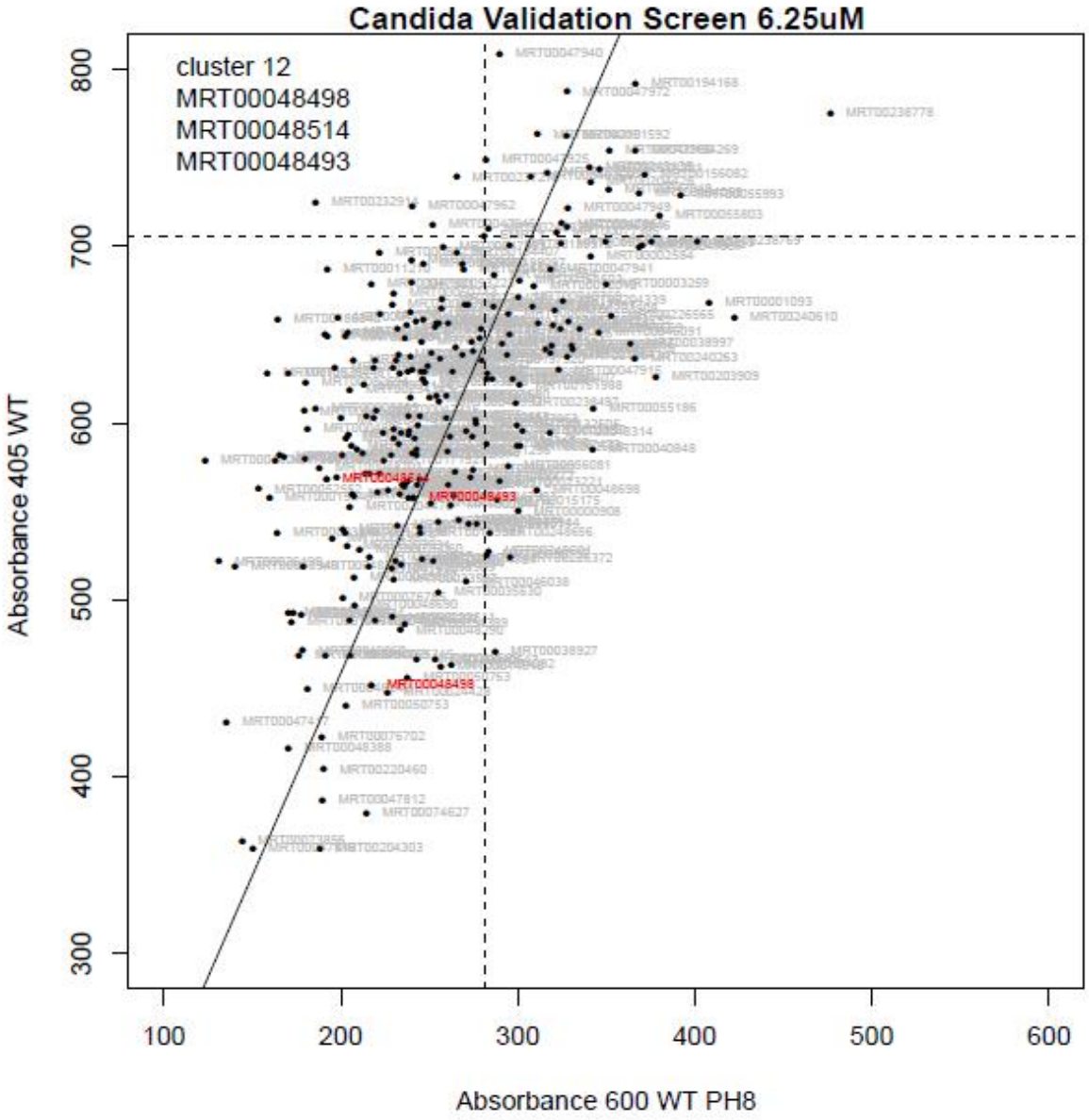

Cluster 12: 6.25 µM Secondary Screen: pH8 as a readout for PHO Pathway activity.
Plot of OD_{600} *wt* cells grown in pH 8 vs. OD_{405} of *wt* cells. Cells were grown to log phase in YPD before being washed 3 times in pH8 media and diluted back to OD_{600} = 0.05 then seeded into 384 well plates containing 6.25 µM of compound. Absorbance of 600 nm is used for growth at pH and 405 for secreted acid phosphatase activity. Red hits represent those from cluster 12.

Cluster 13

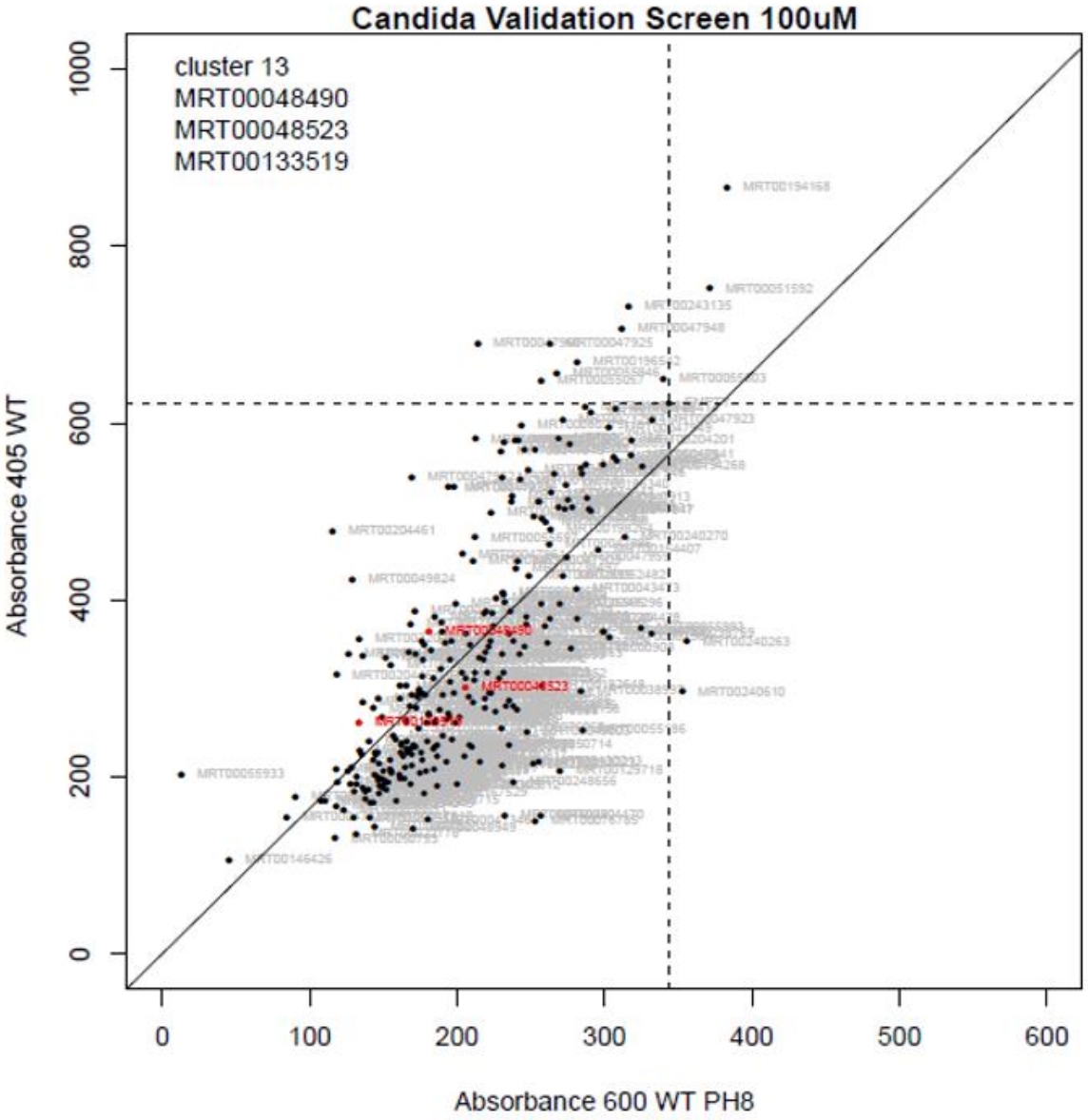

Cluster 13: 100 µM Secondary Screen: pH8 as a readout for PHO Pathway activity.
Plot of OD_{600} *wt* cells grown in pH 8 vs. OD_{405} of *wt* cells. Cells were grown to log phase in YPD before being washed 3 times in pH8 media and diluted back to OD_{600} = 0.05 then seeded into 384 well plates containing 100 µM of compound. Absorbance of 600 nm is used for growth at pH and 405 for secreted acid phosphatase activity. Red hits represent those from cluster 13.

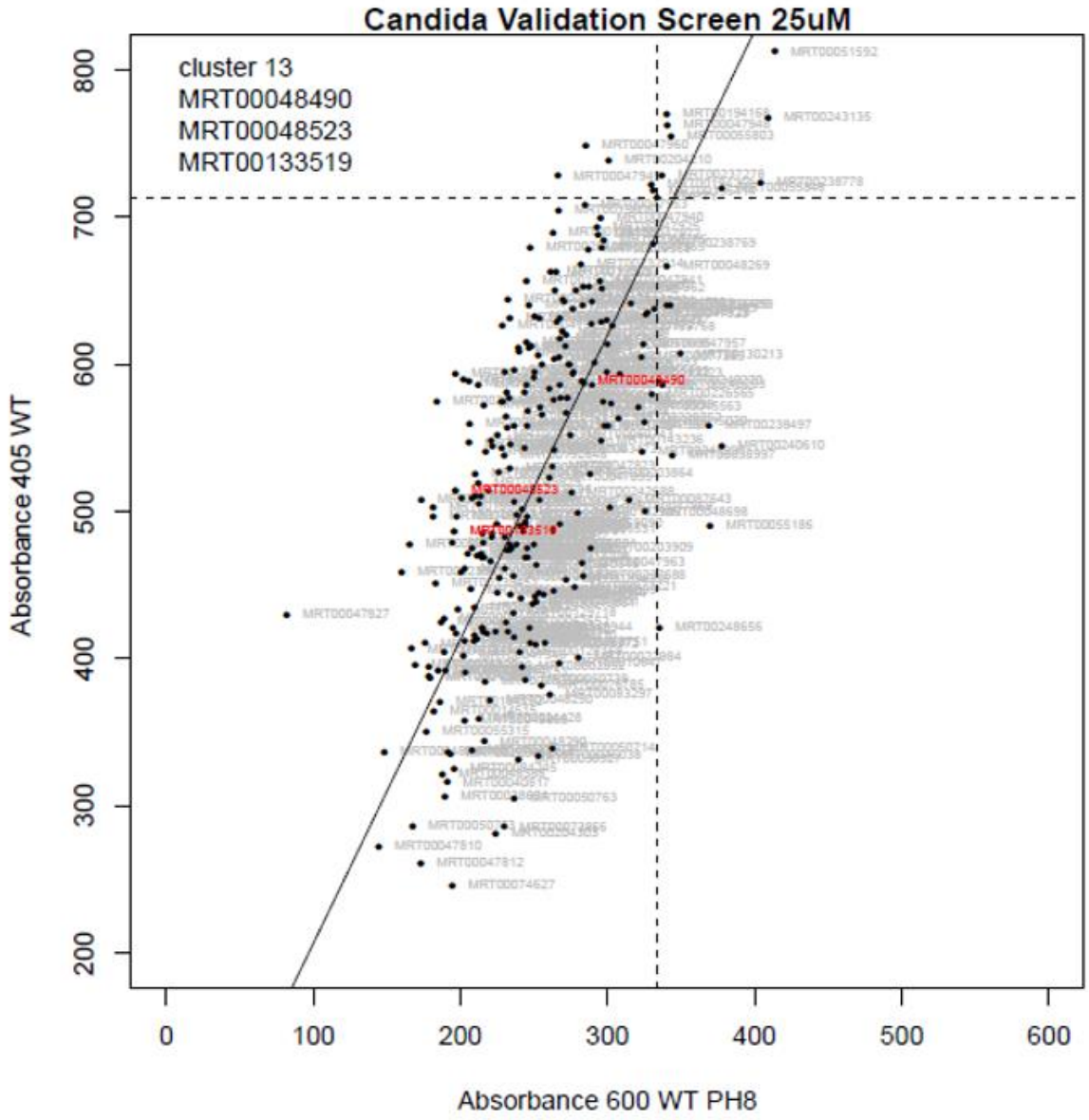

Cluster 13: 25 µM Secondary Screen: pH8 as a readout for PHO Pathway activity.
Plot of OD_{600} *wt* cells grown in pH 8 vs. OD_{405} of *wt* cells. Cells were grown to log phase in YPD before being washed 3 times in pH8 media and diluted back to OD_{600} = 0.05 then seeded into 384 well plates containing 25 µM of compound. Absorbance of 600 nm is used for growth at pH and 405 for secreted acid phosphatase activity. Red hits represent those from cluster 13.

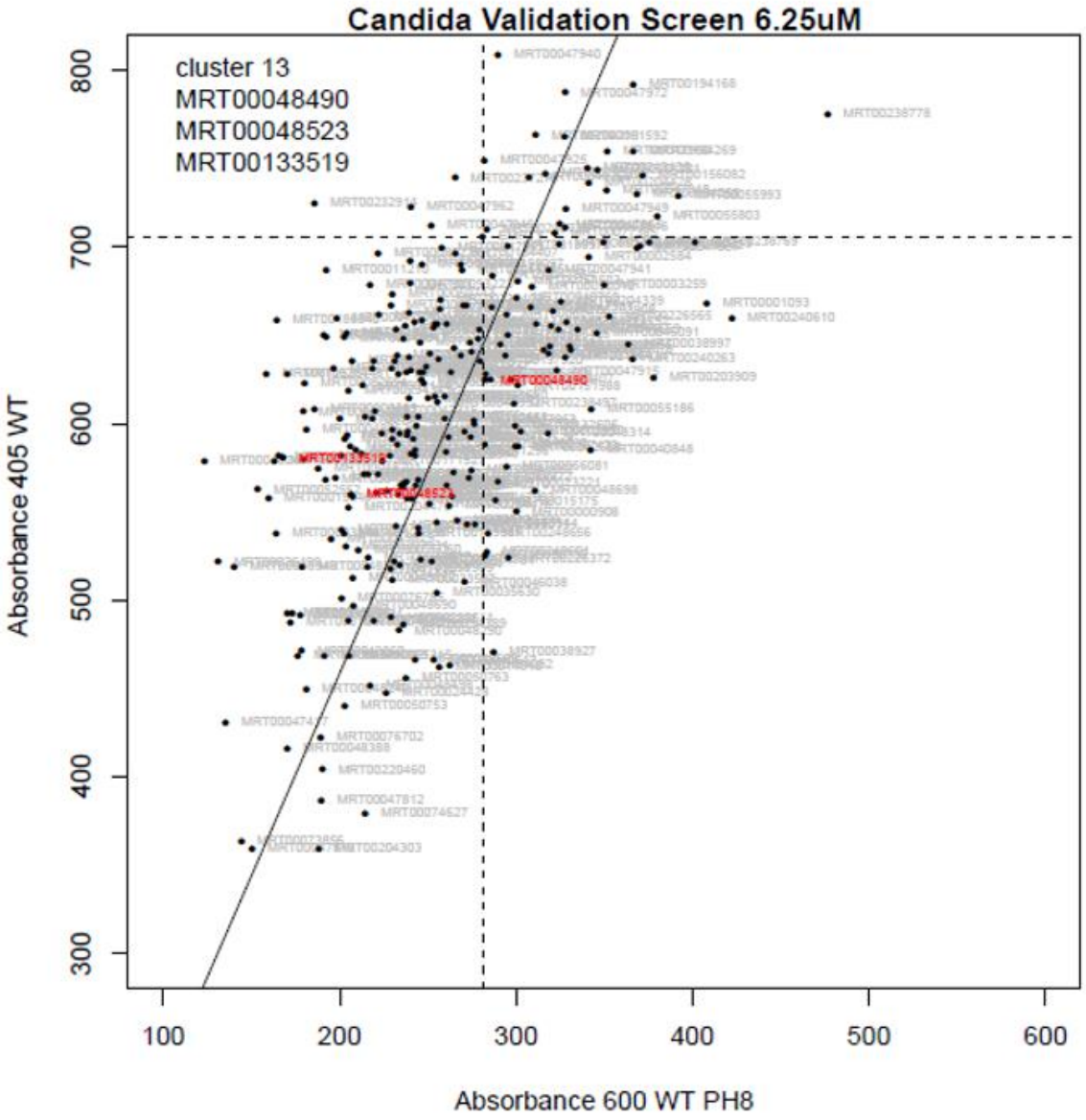

Cluster 13: 6.25 µM Secondary Screen: pH8 as a readout for PHO Pathway activity.
Plot of OD_{600} *wt* cells grown in pH 8 vs. OD_{405} of *wt* cells. Cells were grown to log phase in YPD before being washed 3 times in pH8 media and diluted back to OD_{600} = 0.05 then seeded into 384 well plates containing 6.25 µM of compound. Absorbance of 600 nm is used for growth at pH and 405 for secreted acid phosphatase activity. Red hits represent those from cluster 13.

Cluster 14

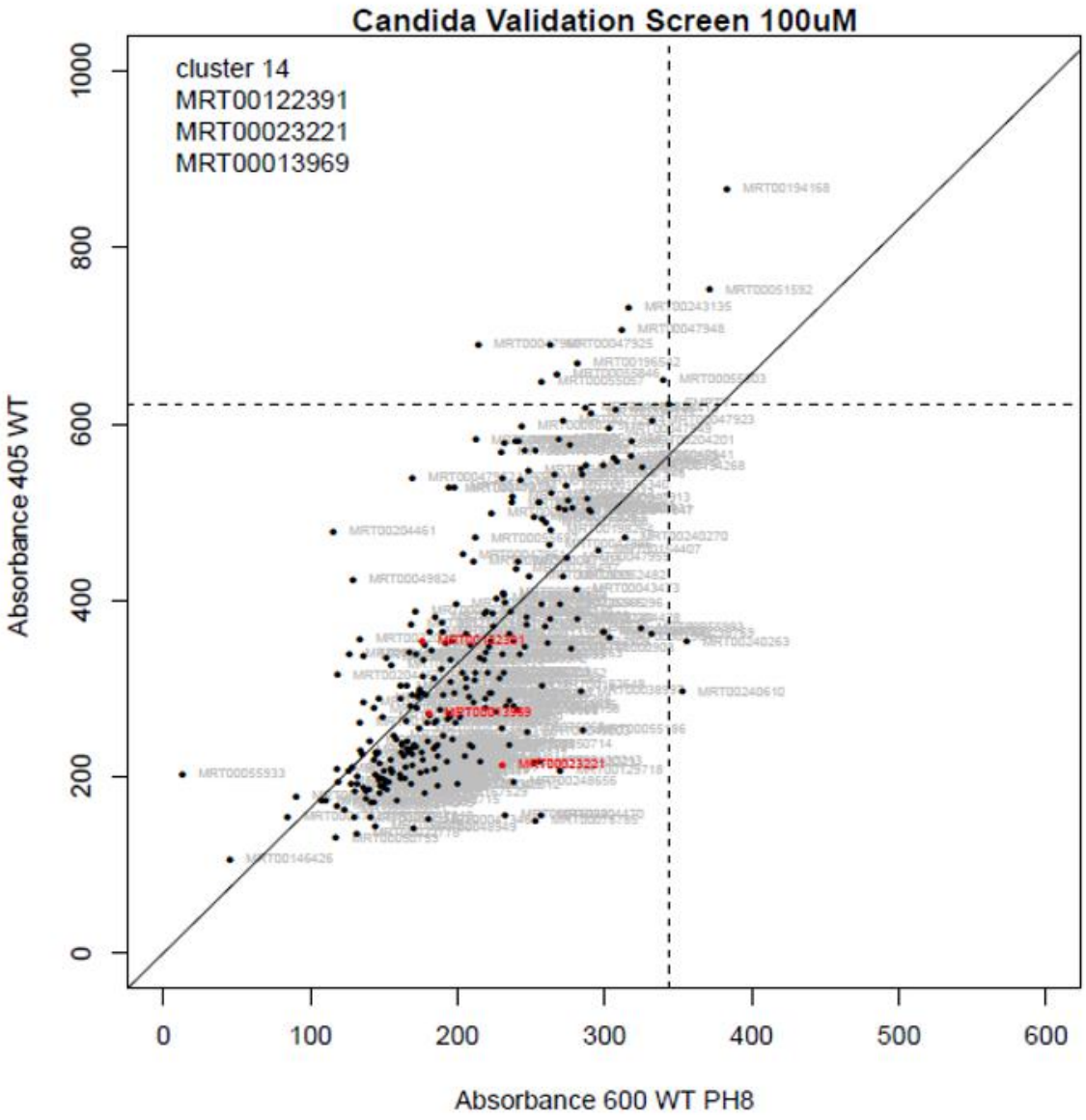

Cluster 14: 100 µM Secondary Screen: pH8 as a readout for PHO Pathway activity.
Plot of OD_{600} *wt* cells grown in pH 8 vs. OD_{405} of *wt* cells. Cells were grown to log phase in YPD before being washed 3 times in pH8 media and diluted back to OD_{600} = 0.05 then seeded into 384 well plates containing 100 µM of compound. Absorbance of 600 nm is used for growth at pH and 405 for secreted acid phosphatase activity. Red hits represent those from cluster 14.

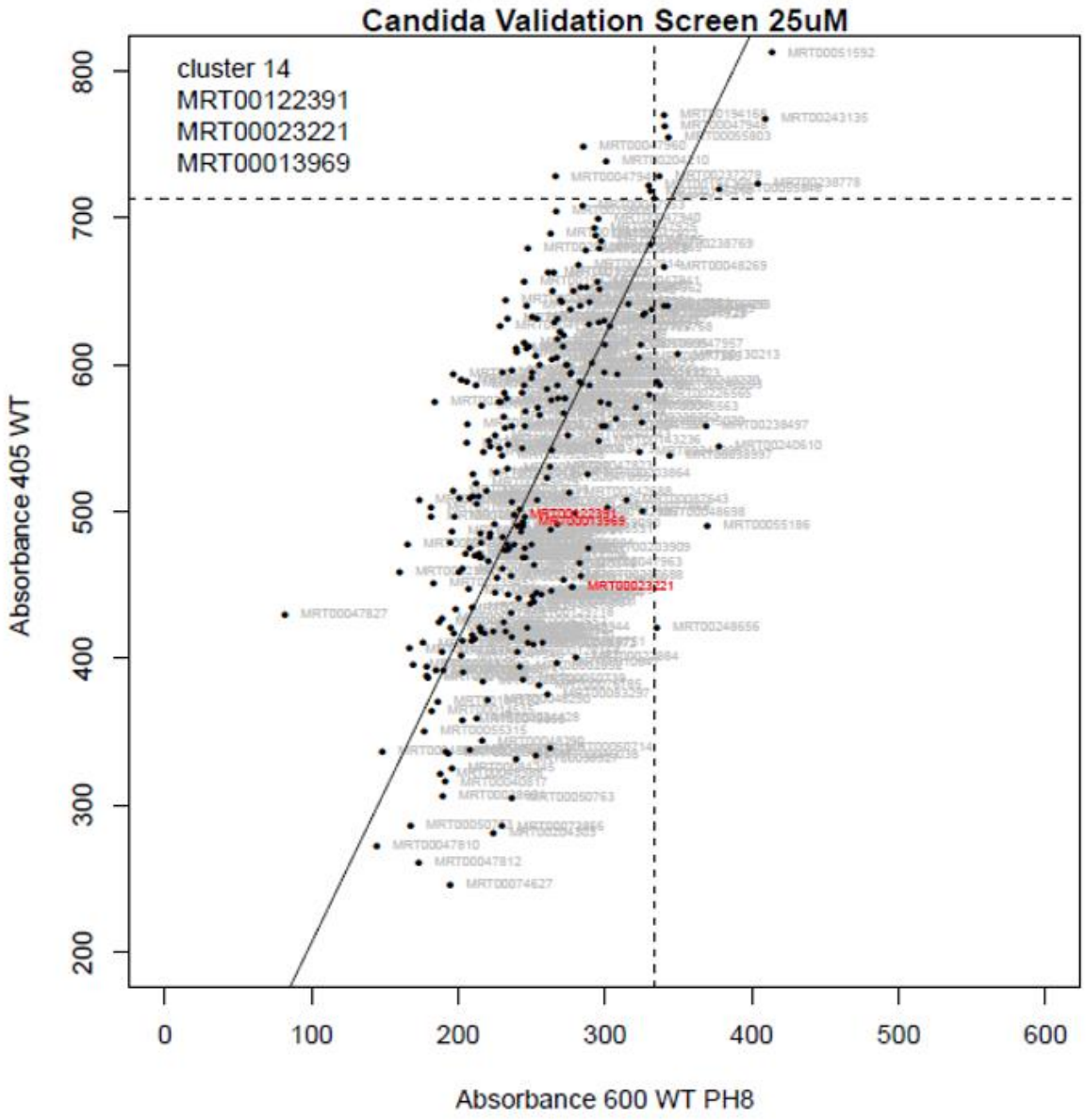

Cluster 14: 25 µM Secondary Screen: pH8 as a readout for PHO Pathway activity.
Plot of OD_{600} *wt* cells grown in pH 8 vs. OD_{405} of *wt* cells. Cells were grown to log phase in YPD before being washed 3 times in pH8 media and diluted back to OD_{600} = 0.05 then seeded into 384 well plates containing 25 µM of compound. Absorbance of 600 nm is used for growth at pH and 405 for secreted acid phosphatase activity. Red hits represent those from cluster 13.

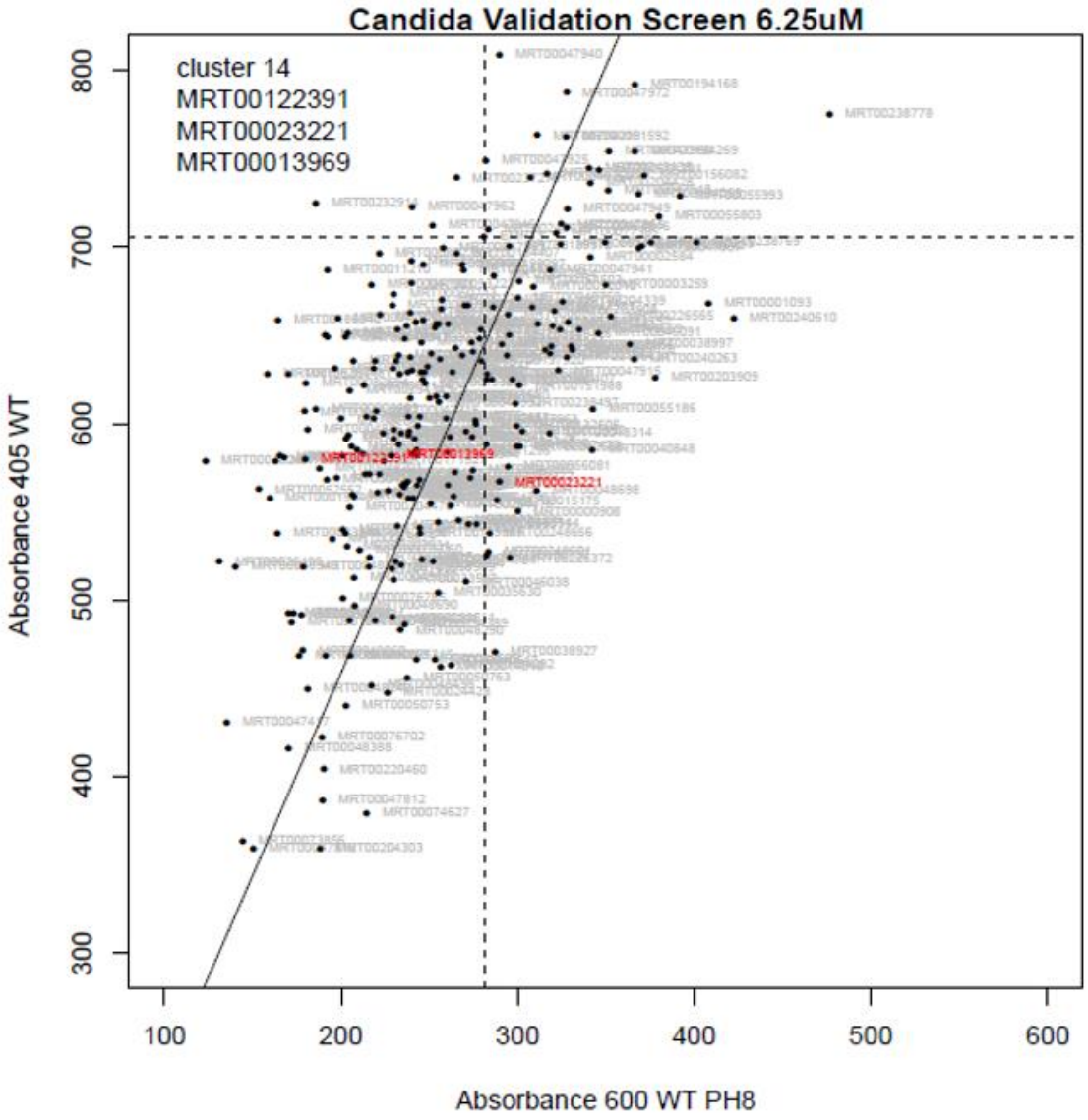

Cluster 13: 6.25 µM Secondary Screen: pH8 as a readout for PHO Pathway activity.
Plot of OD_{600} *wt* cells grown in pH 8 vs. OD_{405} of *wt* cells. Cells were grown to log phase in YPD before being washed 3 times in pH8 media and diluted back to OD_{600} = 0.05 then seeded into 384 well plates containing 6.25 µM of compound. Absorbance of 600 nm is used for growth at pH and 405 for secreted acid phosphatase activity. Red hits represent those from cluster 13.

Cluster 15

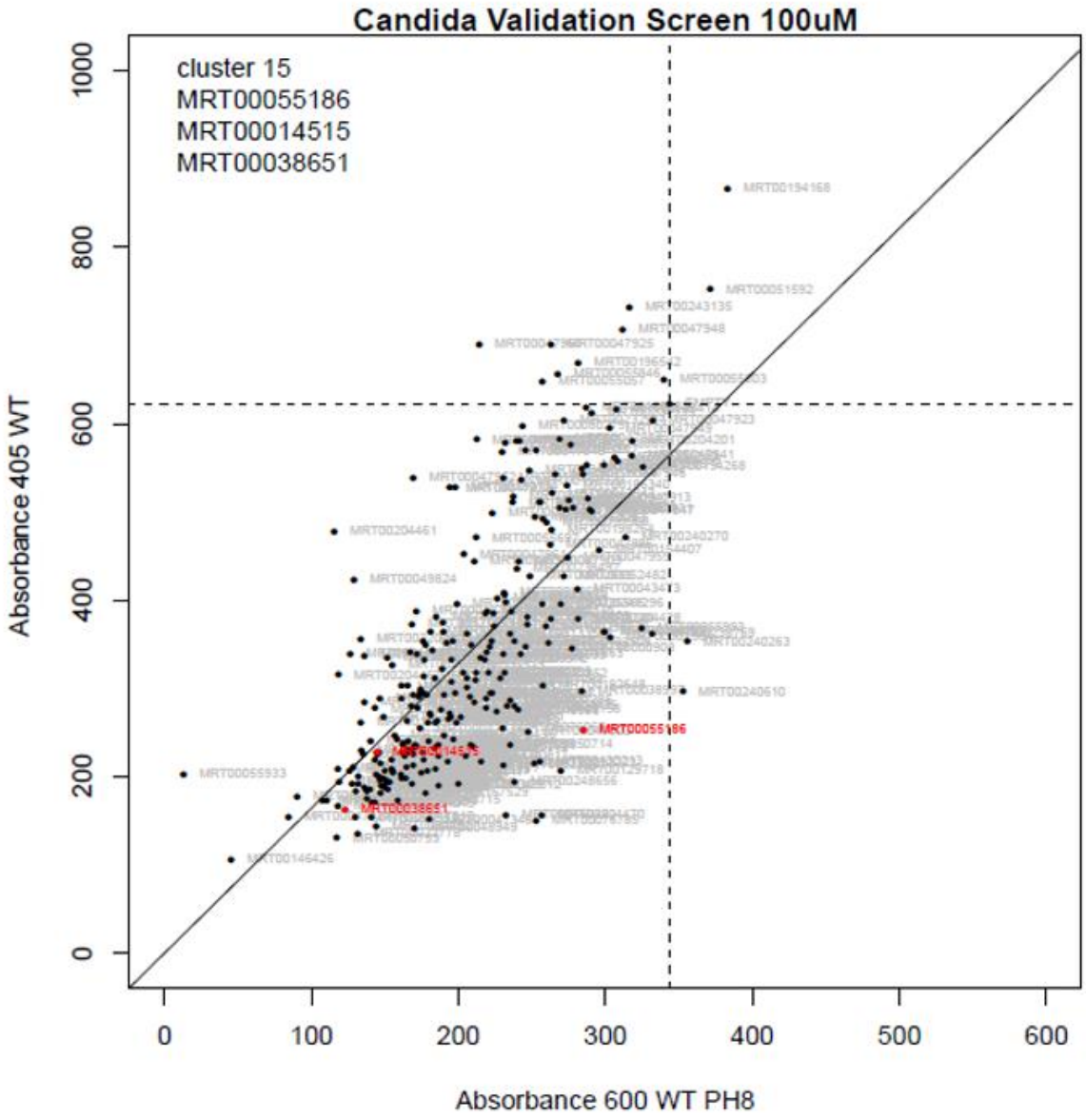

Cluster 15: 100 µM Secondary Screen: pH8 as a readout for PHO Pathway activity.
Plot of OD_{600} *wt* cells grown in pH 8 vs. OD_{405} of *wt* cells. Cells were grown to log phase in YPD before being washed 3 times in pH8 media and diluted back to OD_{600} = 0.05 then seeded into 384 well plates containing 100 µM of compound. Absorbance of 600 nm is used for growth at pH and 405 for secreted acid phosphatase activity. Red hits represent those from cluster 13.

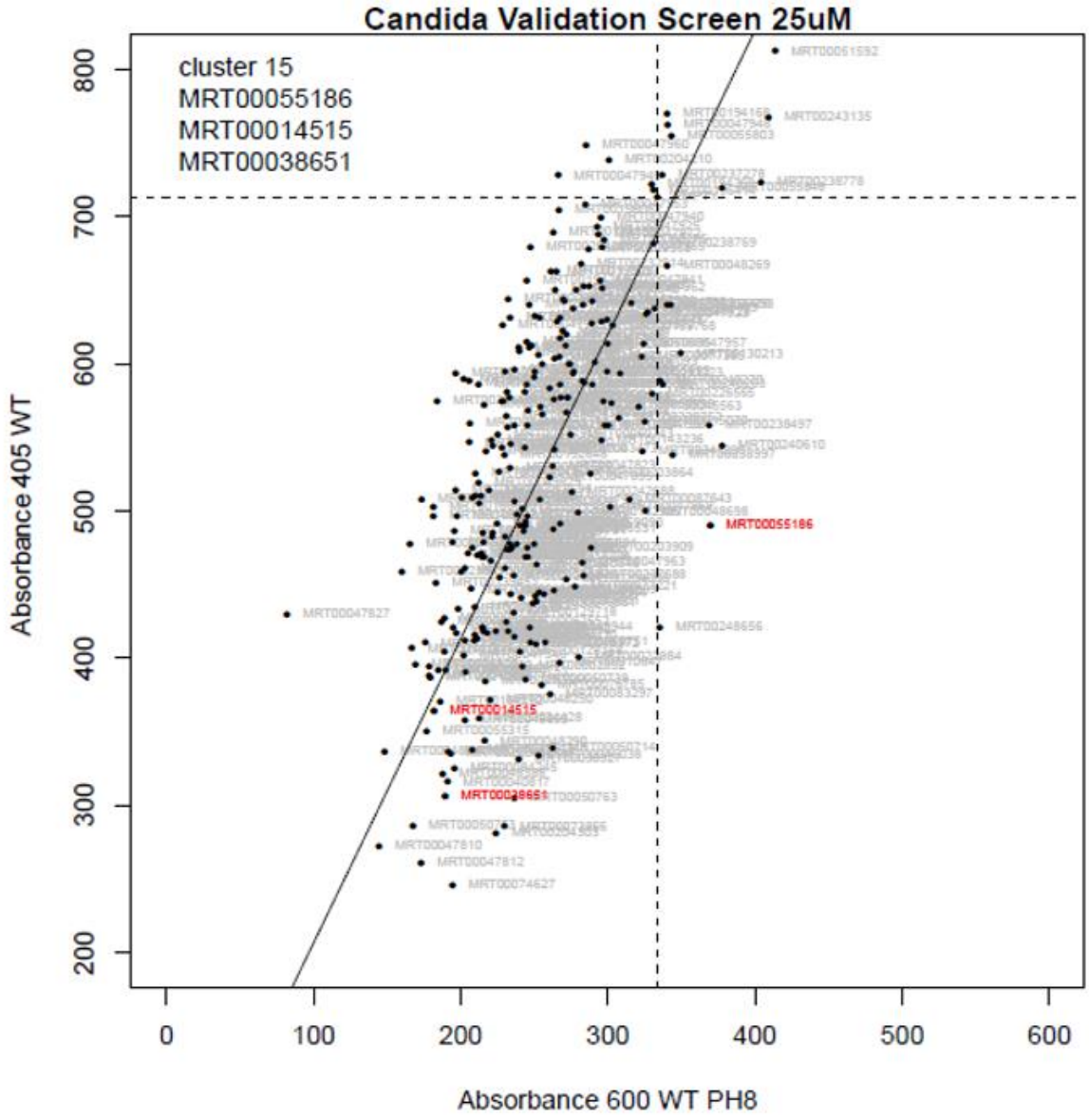

Cluster 13: 100 µM Secondary Screen: pH8 as a readout for PHO Pathway activity.
Plot of OD_{600} *wt* cells grown in pH 8 vs. OD_{405} of *wt* cells. Cells were grown to log phase in YPD before being washed 3 times in pH8 media and diluted back to OD_{600} = 0.05 then seeded into 384 well plates containing 100 µM of compound. Absorbance of 600 nm is used for growth at pH and 405 for secreted acid phosphatase activity. Red hits represent those from cluster 13.

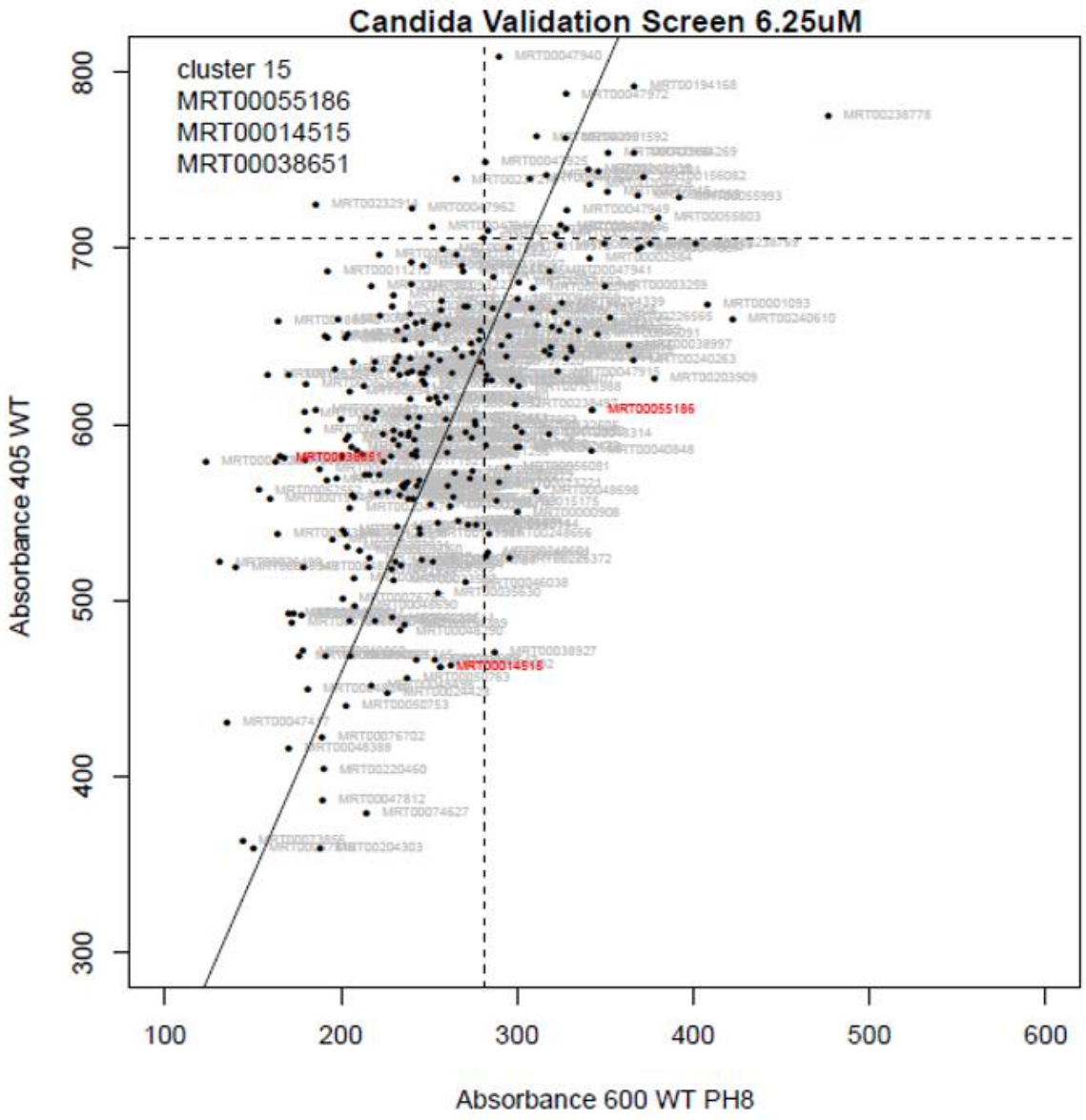

Cluster 13: 6.25 µM Secondary Screen: pH8 as a readout for PHO Pathway activity.
Plot of OD_{600} *wt* cells grown in pH 8 vs. OD_{405} of *wt* cells. Cells were grown to log phase in YPD before being washed 3 times in pH8 media and diluted back to OD_{600} = 0.05 then seeded into 384 well plates containing 6.25 µM of compound. Absorbance of 600 nm is used for growth at pH and 405 for secreted acid phosphatase activity. Red hits represent those from cluster 13.

Cluster 16

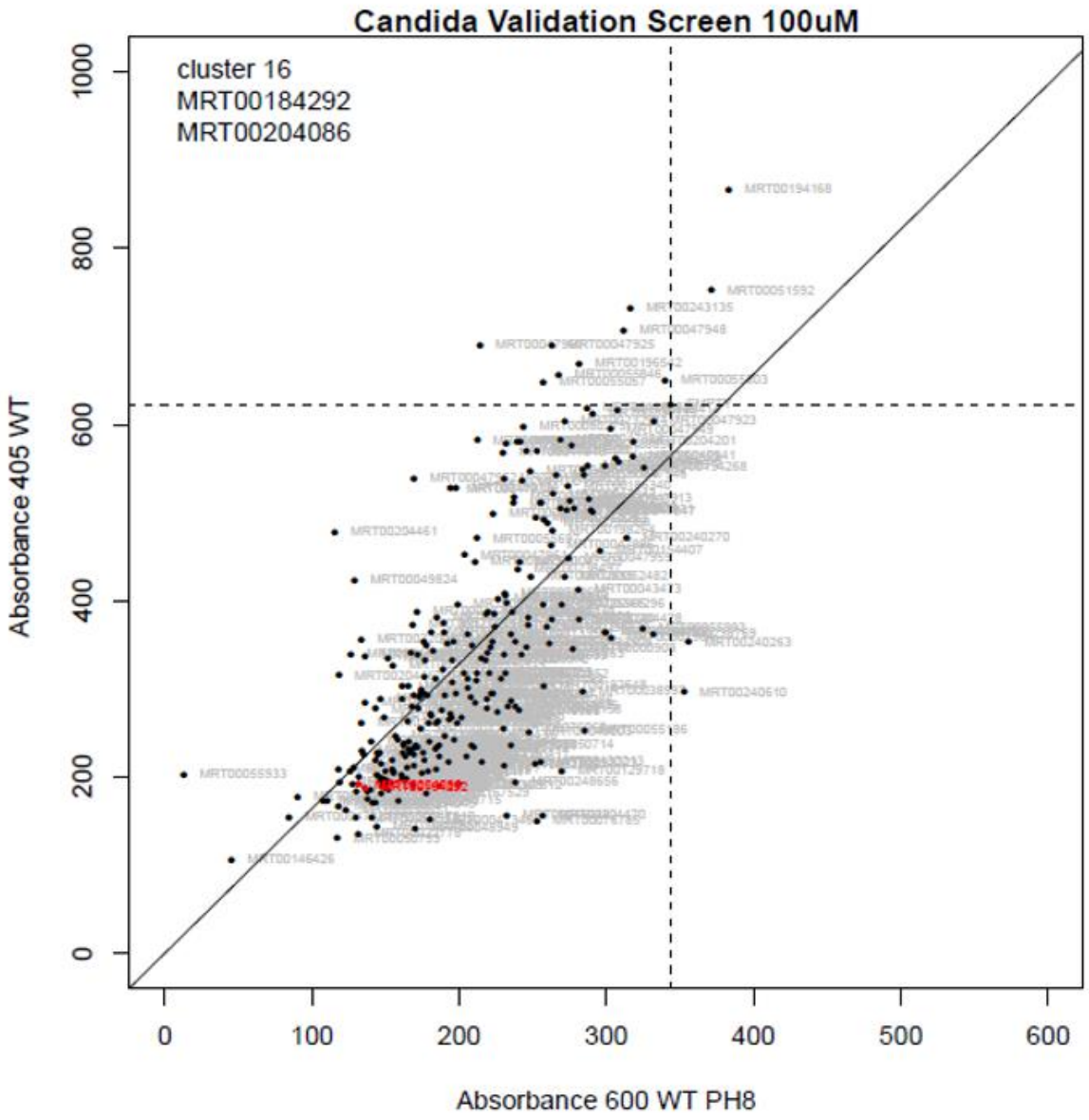

Cluster 16: 100 µM Secondary Screen: pH8 as a readout for PHO Pathway activity.
Plot of OD_{600} *wt* cells grown in pH 8 vs. OD_{405} of *wt* cells. Cells were grown to log phase in YPD before being washed 3 times in pH8 media and diluted back to OD_{600} = 0.05 then seeded into 384 well plates containing 100 µM of compound. Absorbance of 600 nm is used for growth at pH and 405 for secreted acid phosphatase activity. Red hits represent those from cluster 16.

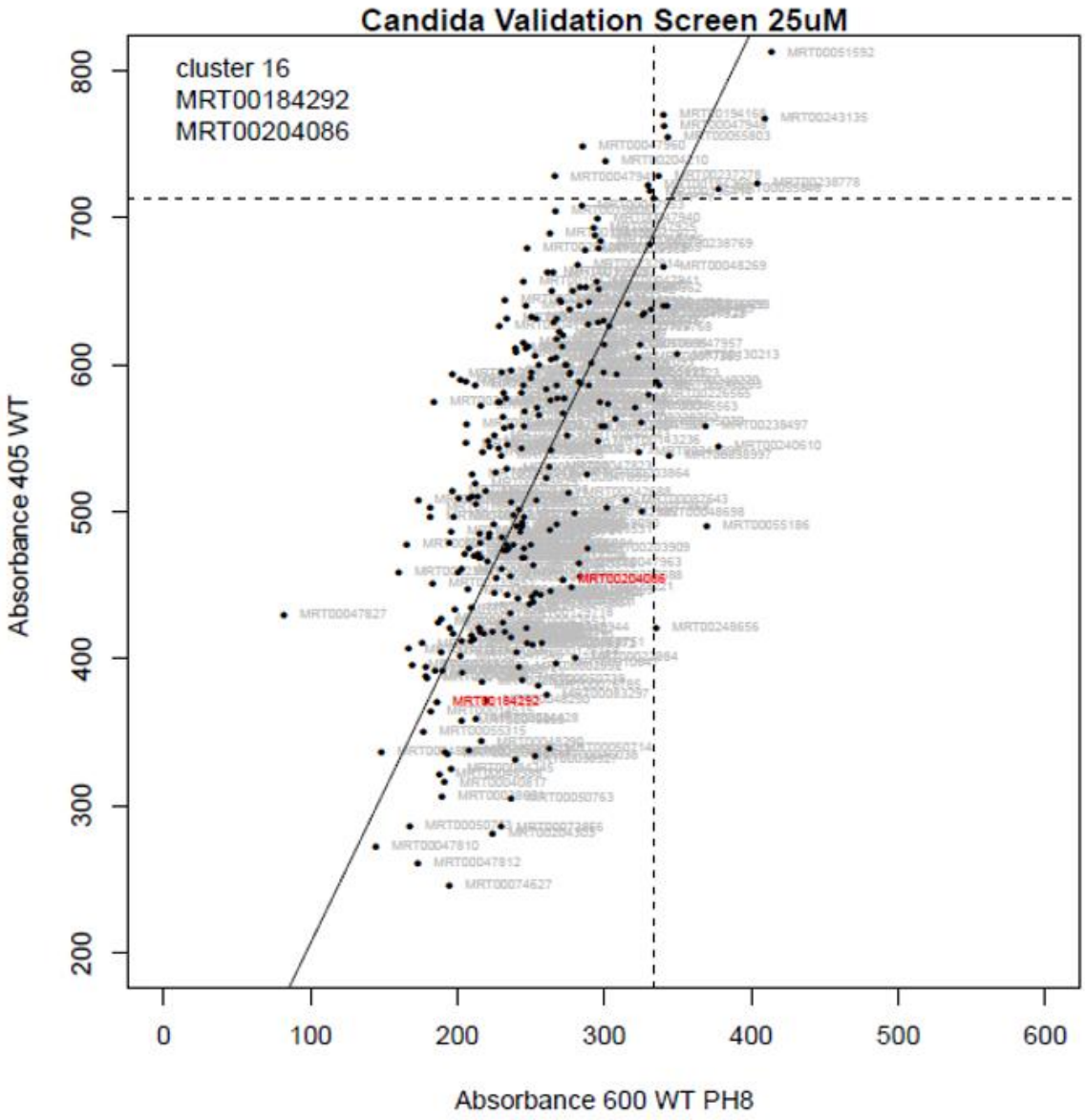

Cluster 16: 25 µM Secondary Screen: pH8 as a readout for PHO Pathway activity.
Plot of OD_{600} *wt* cells grown in pH 8 vs. OD_{405} of *wt* cells. Cells were grown to log phase in YPD before being washed 3 times in pH8 media and diluted back to OD_{600} = 0.05 then seeded into 384 well plates containing 25 µM of compound. Absorbance of 600 nm is used for growth at pH and 405 for secreted acid phosphatase activity. Red hits represent those from cluster 16.

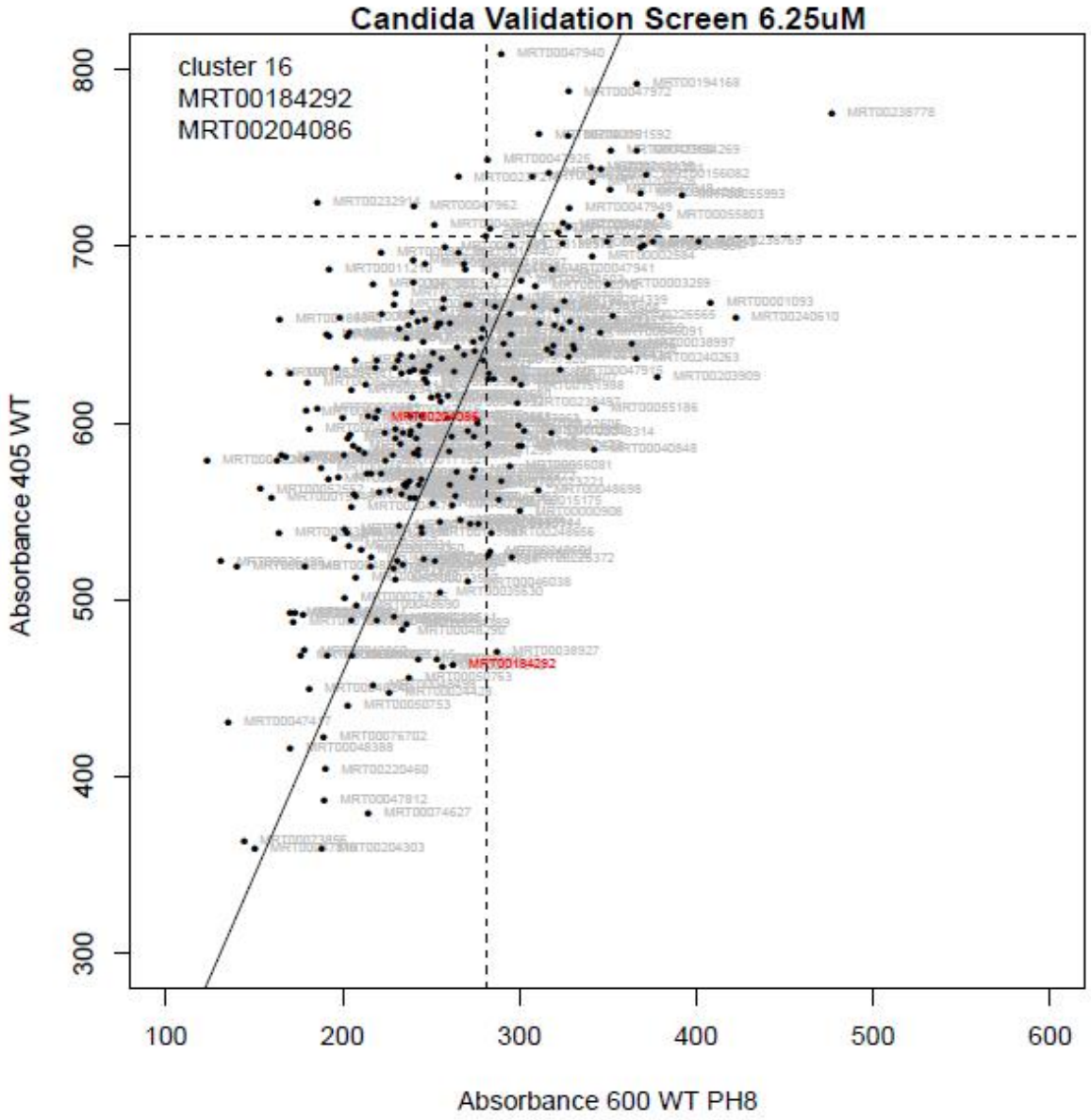

Cluster 16: 6.25 µM Secondary Screen: pH8 as a readout for PHO Pathway activity.
Plot of OD_{600} *wt* cells grown in pH 8 vs. OD_{405} of *wt* cells. Cells were grown to log phase in YPD before being washed 3 times in pH8 media and diluted back to OD_{600} = 0.05 then seeded into 384 well plates containing 6.25 µM of compound. Absorbance of 600 nm is used for growth at pH and 405 for secreted acid phosphatase activity. Red hits represent those from cluster 16.

Cluster 17

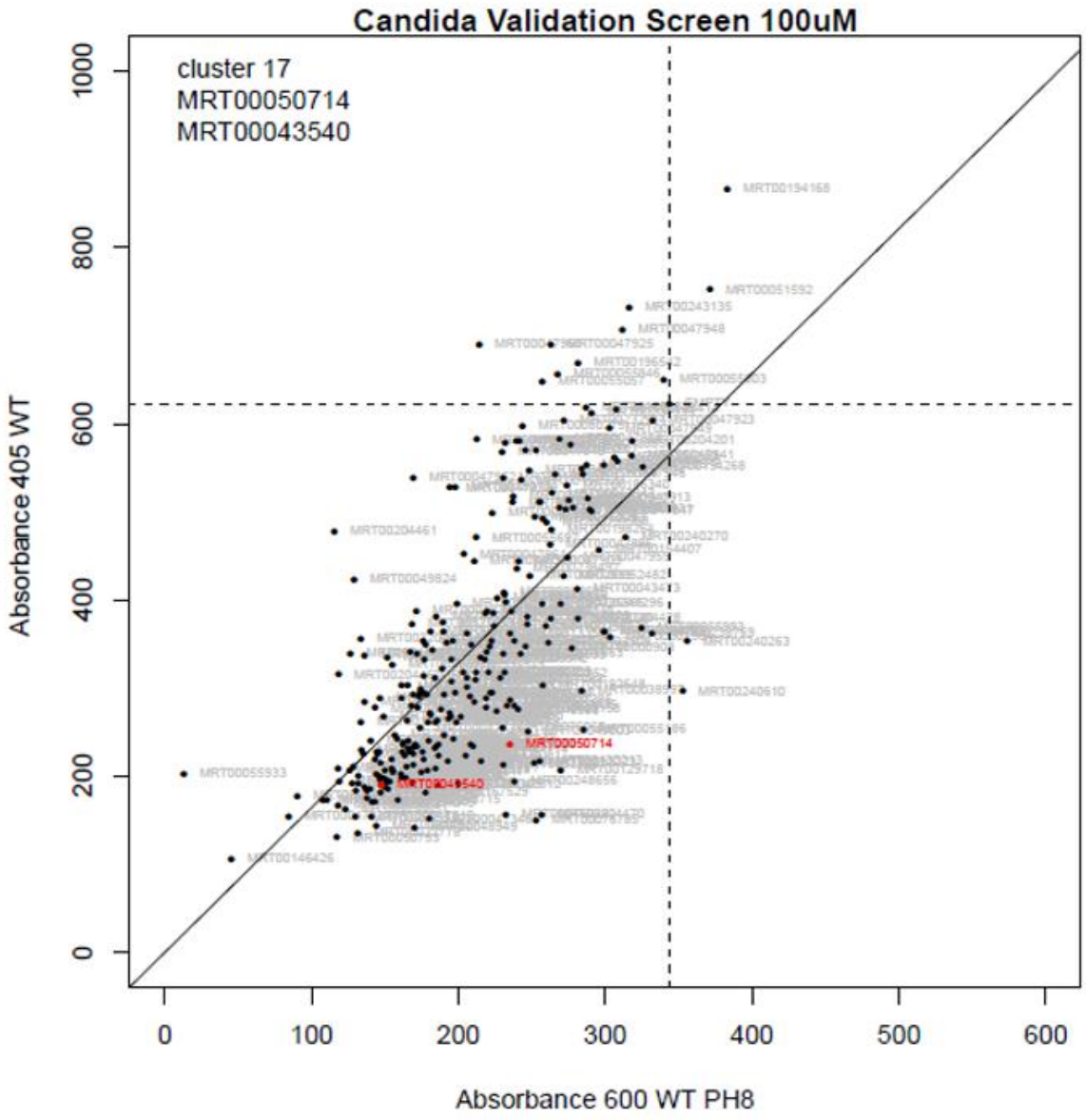

Cluster 17: 100 µM Secondary Screen: pH8 as a readout for PHO Pathway activity.
Plot of OD_{600} *wt* cells grown in pH 8 vs. OD_{405} of *wt* cells. Cells were grown to log phase in YPD before being washed 3 times in pH8 media and diluted back to OD_{600} = 0.05 then seeded into 384 well plates containing 100 µM of compound. Absorbance of 600 nm is used for growth at pH and 405 for secreted acid phosphatase activity. Red hits represent those from cluster 17.

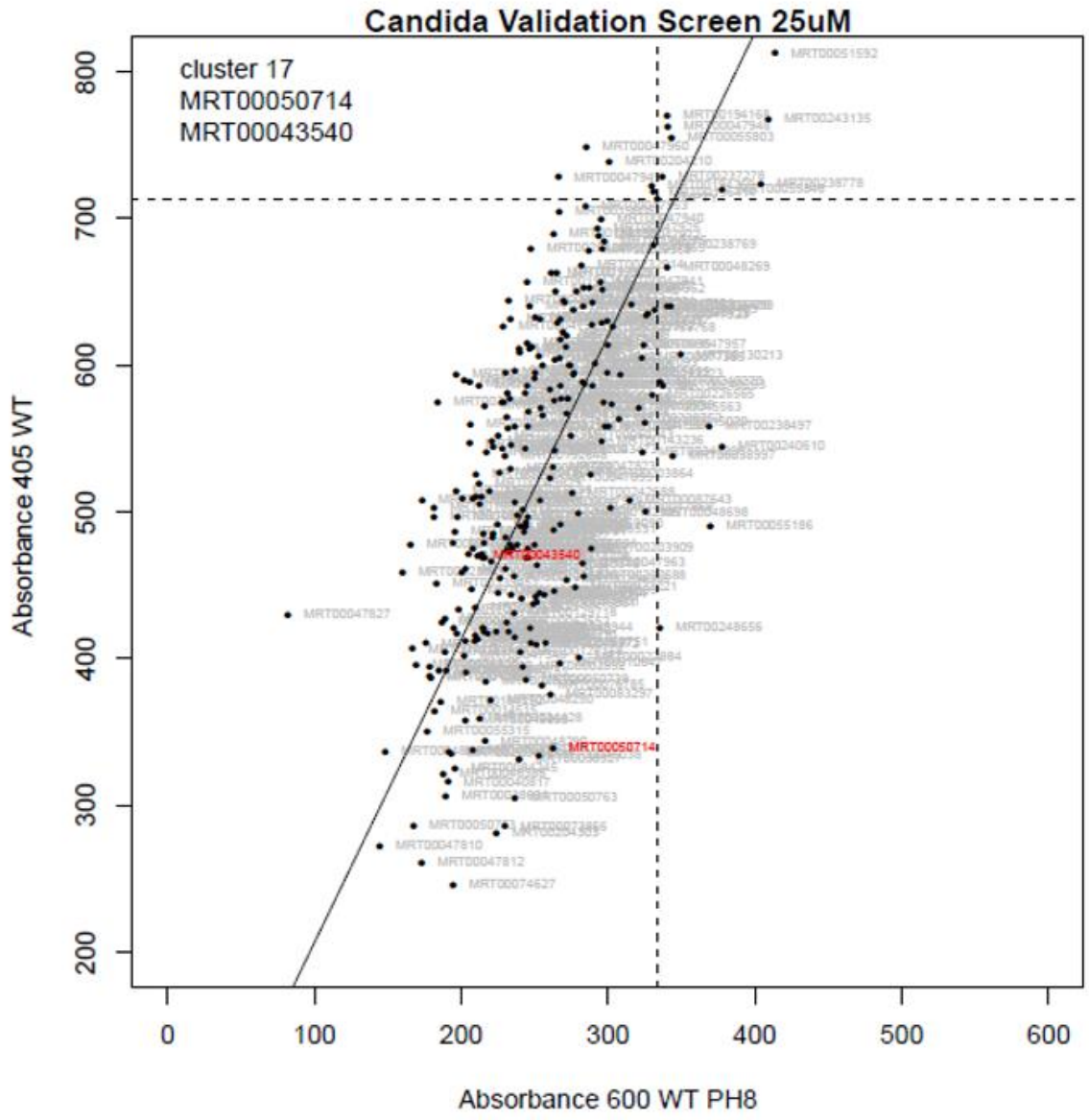

Cluster 17: 25 µM Secondary Screen: pH8 as a readout for PHO Pathway activity.
Plot of OD_{600} *wt* cells grown in pH 8 vs. OD_{405} of *wt* cells. Cells were grown to log phase in YPD before being washed 3 times in pH8 media and diluted back to OD_{600} = 0.05 then seeded into 384 well plates containing 25 µM of compound. Absorbance of 600 nm is used for growth at pH and 405 for secreted acid phosphatase activity. Red hits represent those from cluster 17.

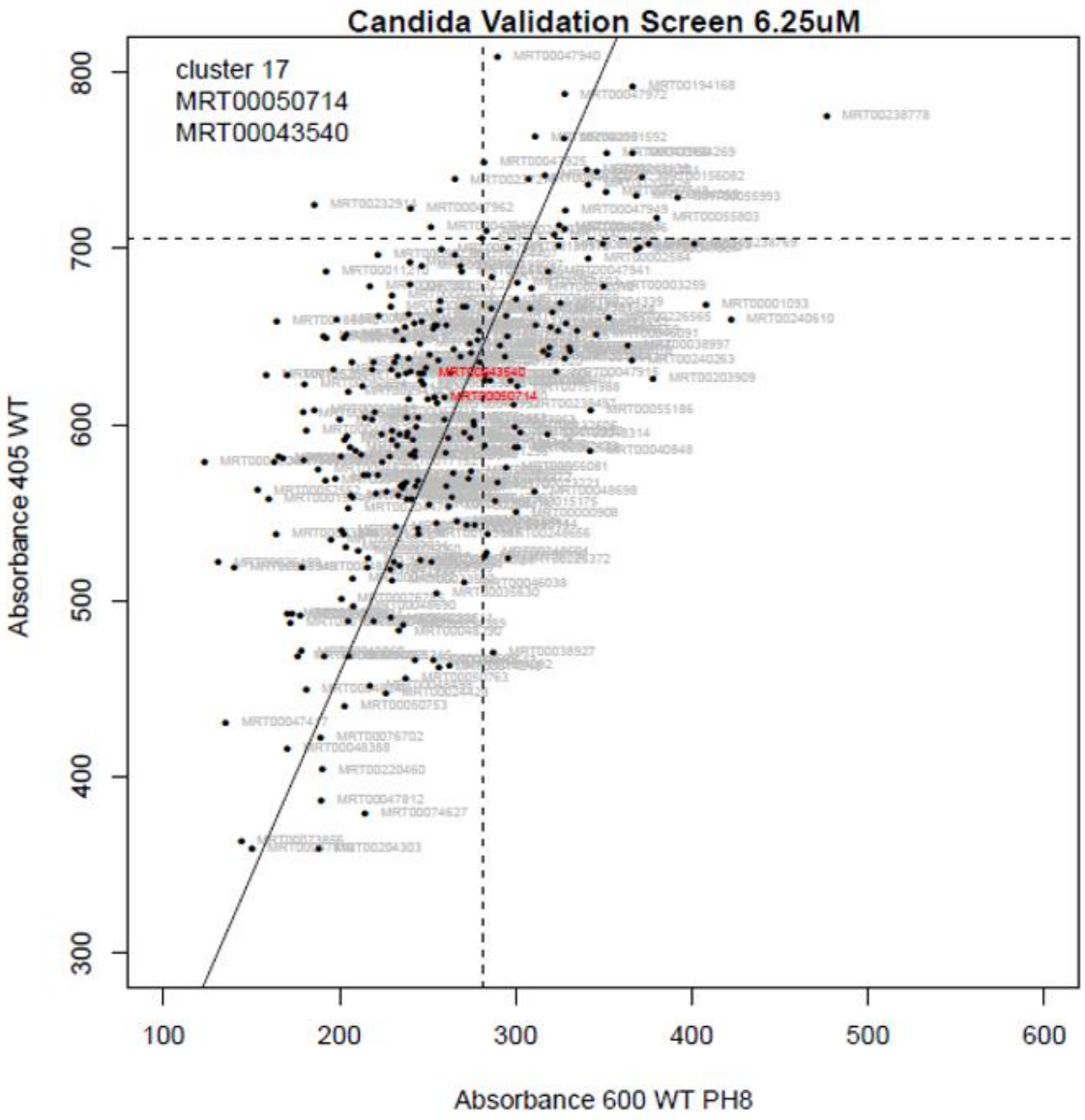

Cluster 17: 6.25 µM Secondary Screen: pH8 as a readout for PHO Pathway activity.
Plot of OD_{600} *wt* cells grown in pH 8 vs. OD_{405} of *wt* cells. Cells were grown to log phase in YPD before being washed 3 times in pH8 media and diluted back to OD_{600} = 0.05 then seeded into 384 well plates containing 6.25 µM of compound. Absorbance of 600 nm is used for growth at pH and 405 for secreted acid phosphatase activity. Red hits represent those from cluster 17.

Cluster 18

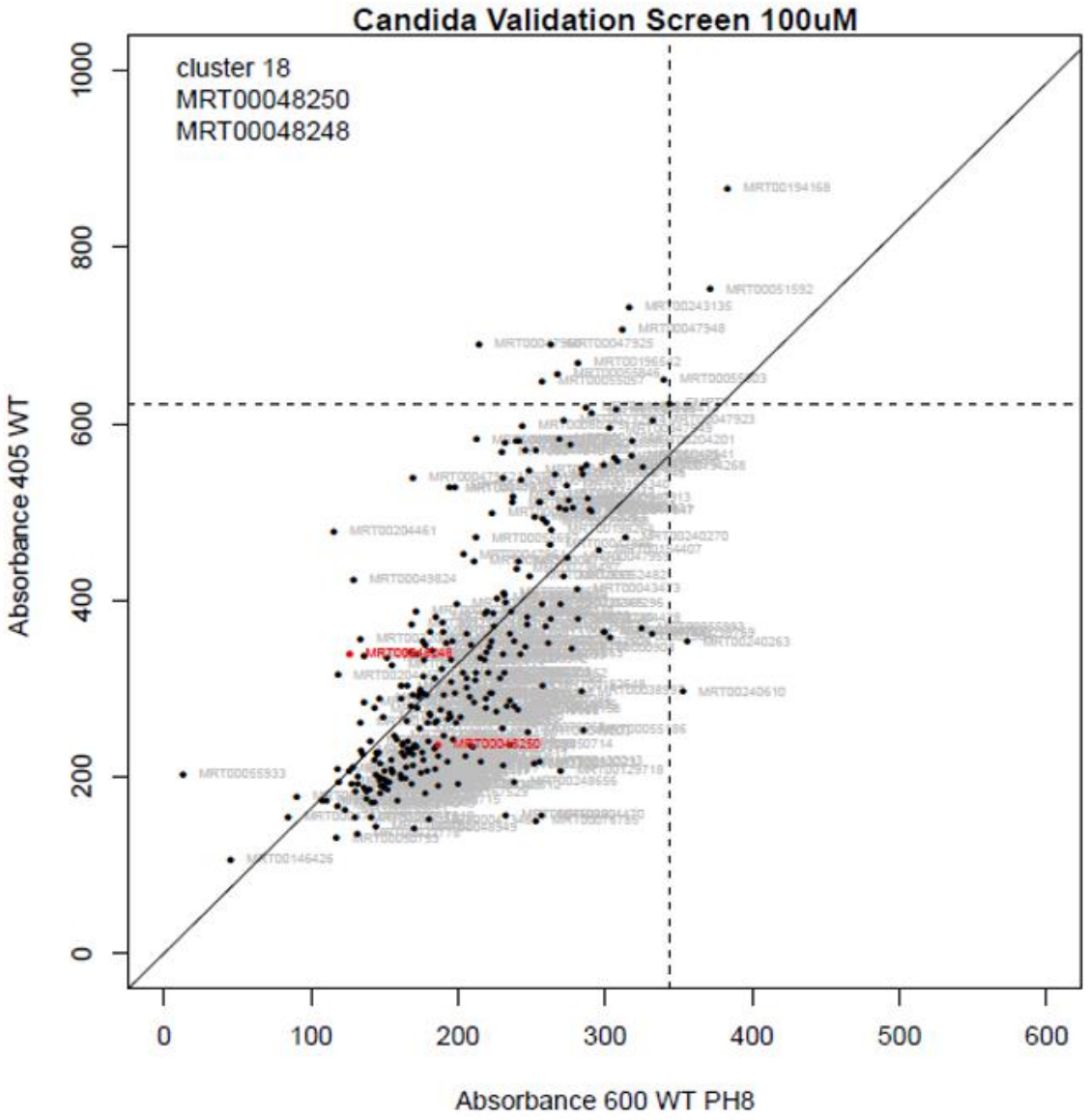

Cluster 18: 100 µM Secondary Screen: pH8 as a readout for PHO Pathway activity.
Plot of OD_{600} *wt* cells grown in pH 8 vs. OD_{405} of *wt* cells. Cells were grown to log phase in YPD before being washed 3 times in pH8 media and diluted back to OD_{600} = 0.05 then seeded into 384 well plates containing 100 µM of compound. Absorbance of 600 nm is used for growth at pH and 405 for secreted acid phosphatase activity. Red hits represent those from cluster 18.

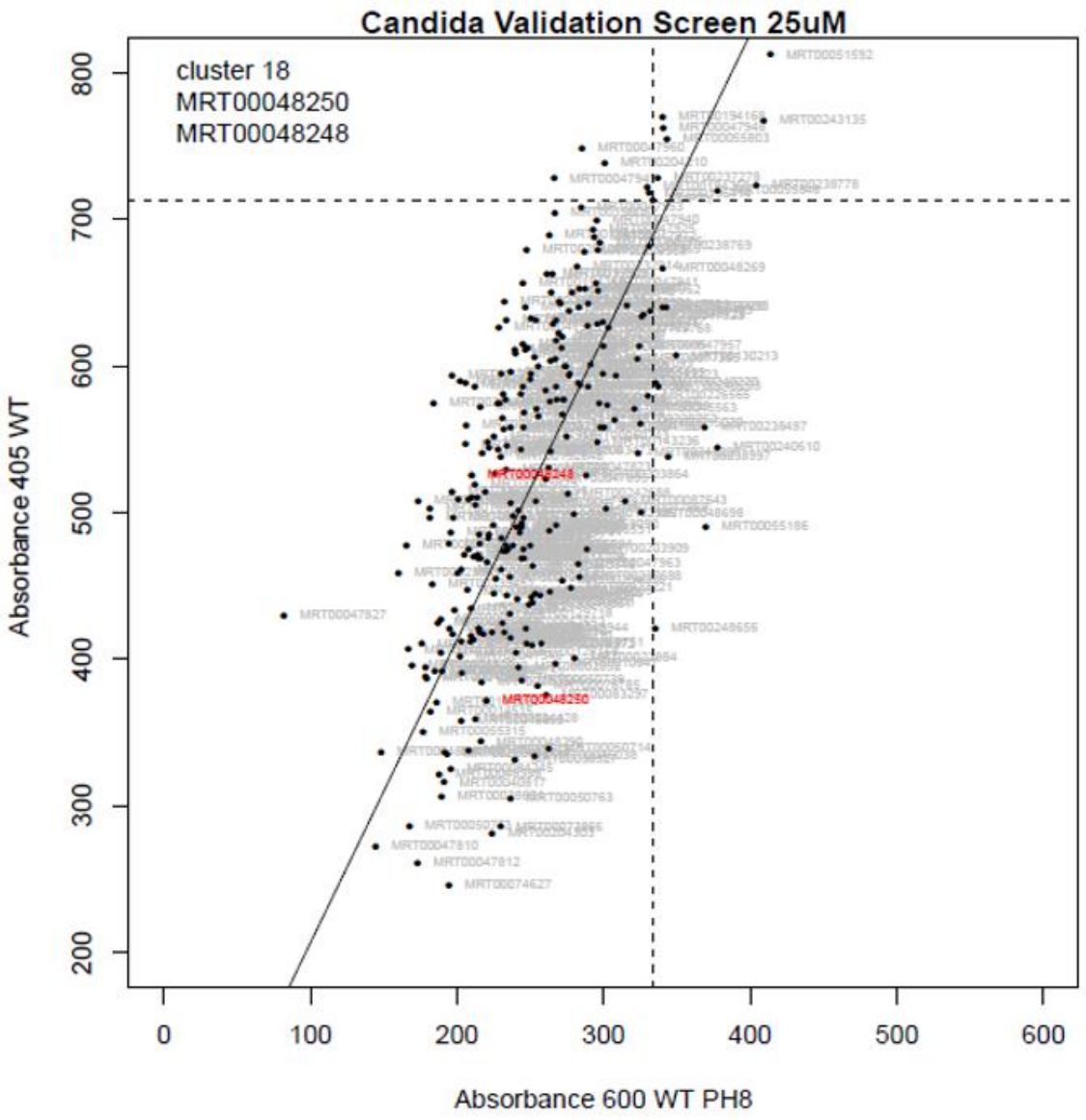

Cluster 18: 25 µM Secondary Screen: pH8 as a readout for PHO Pathway activity.
Plot of OD_{600} *wt* cells grown in pH 8 vs. OD_{405} of *wt* cells. Cells were grown to log phase in YPD before being washed 3 times in pH8 media and diluted back to OD_{600} = 0.05 then seeded into 384 well plates containing 25 µM of compound. Absorbance of 600 nm is used for growth at pH and 405 for secreted acid phosphatase activity. Red hits represent those from cluster 18.

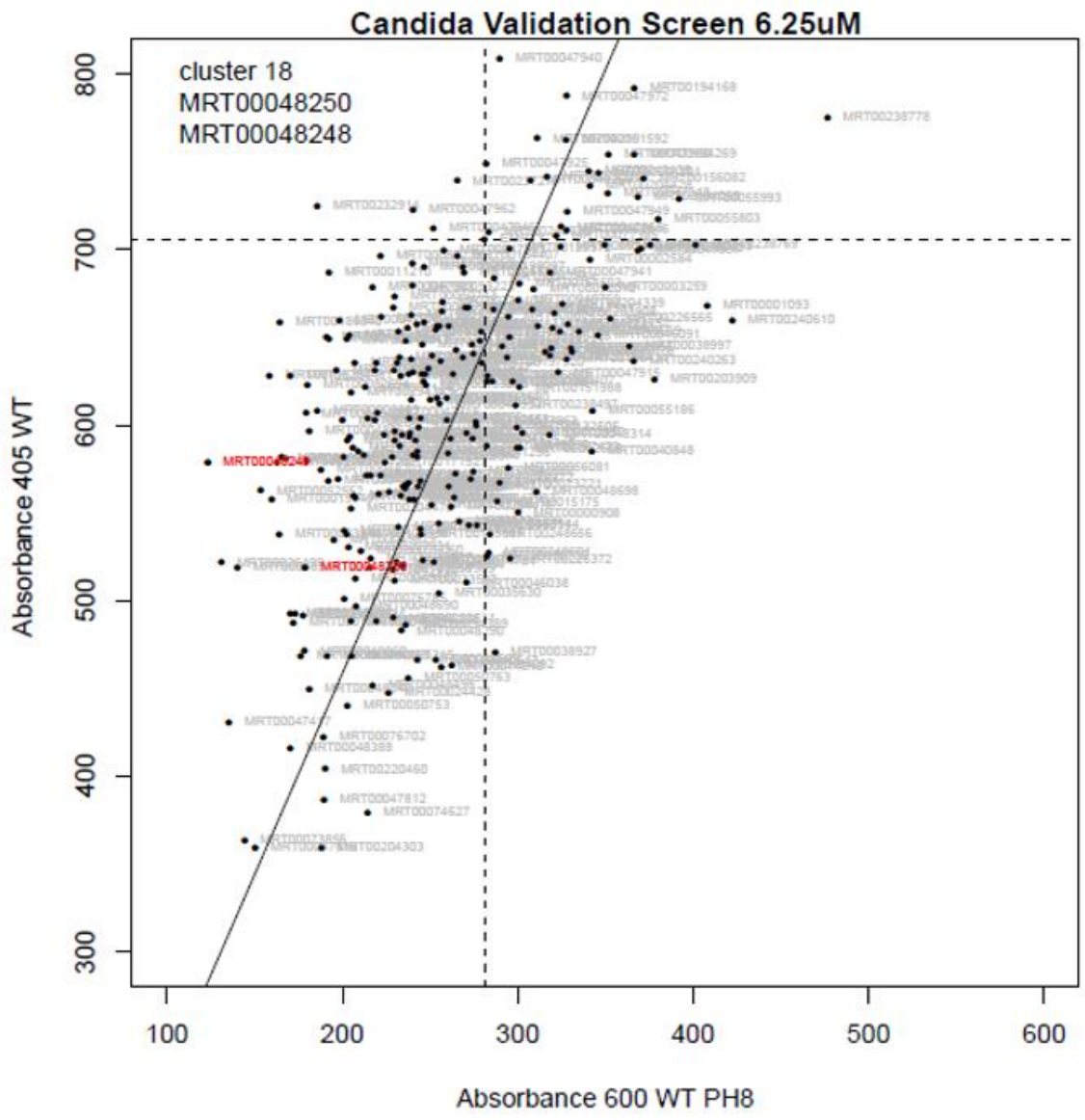

Cluster 18: 6.25 µM Secondary Screen: pH8 as a readout for PHO Pathway activity.
Plot of OD_{600} *wt* cells grown in pH 8 vs. OD_{405} of *wt* cells. Cells were grown to log phase in YPD before being washed 3 times in pH8 media and diluted back to OD_{600} = 0.05 then seeded into 384 well plates containing 6.25 µM of compound. Absorbance of 600 nm is used for growth at pH and 405 for secreted acid phosphatase activity. Red hits represent those from cluster 18.

Cluster 19

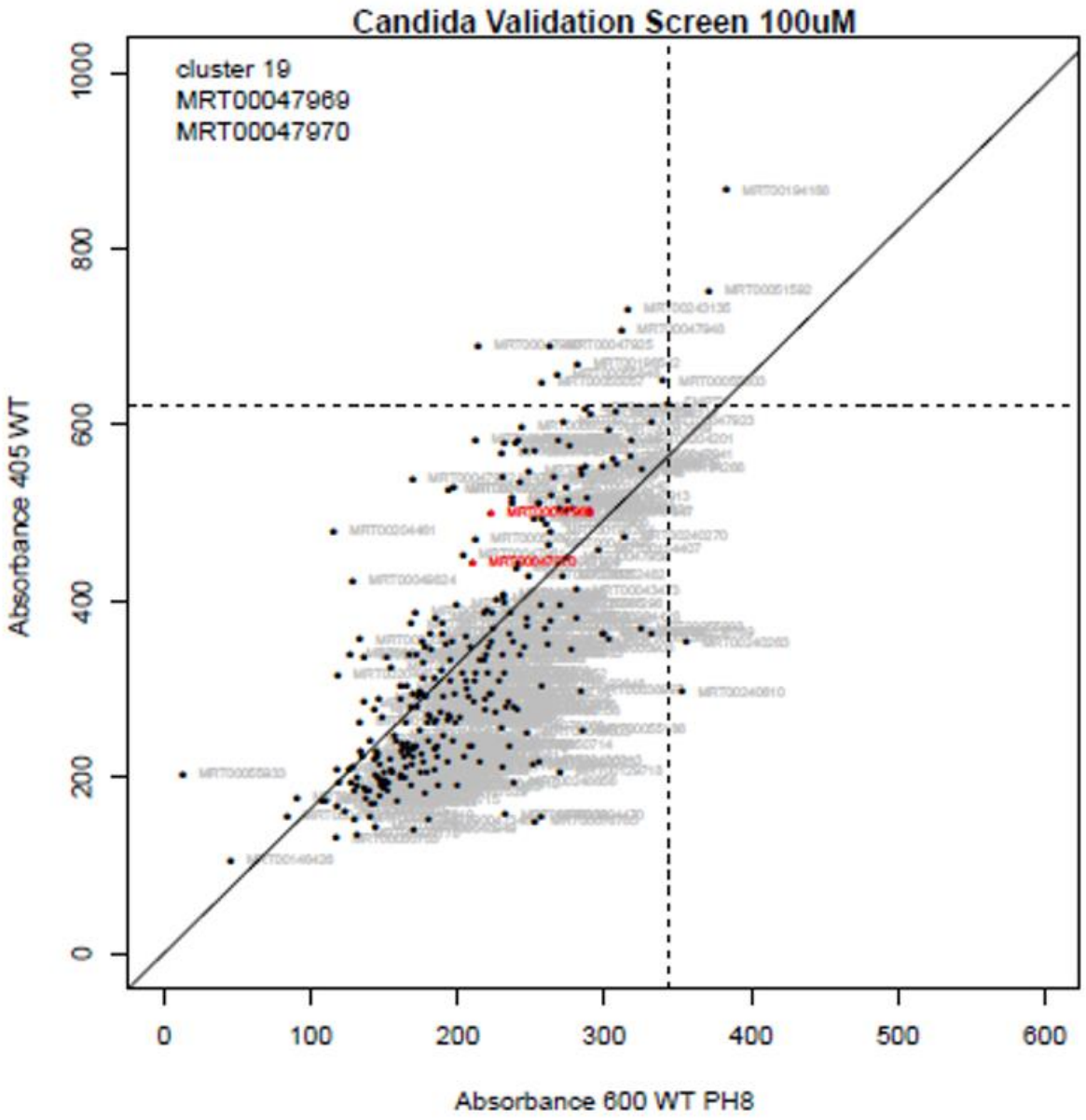

Cluster 19: 100 µM Secondary Screen: pH8 as a readout for PHO Pathway activity.
Plot of OD_{600} *wt* cells grown in pH 8 vs. OD_{405} of *wt* cells. Cells were grown to log phase in YPD before being washed 3 times in pH8 media and diluted back to OD_{600} = 0.05 then seeded into 384 well plates containing 100 µM of compound. Absorbance of 600 nm is used for growth at pH and 405 for secreted acid phosphatase activity. Red hits represent those from cluster 19.

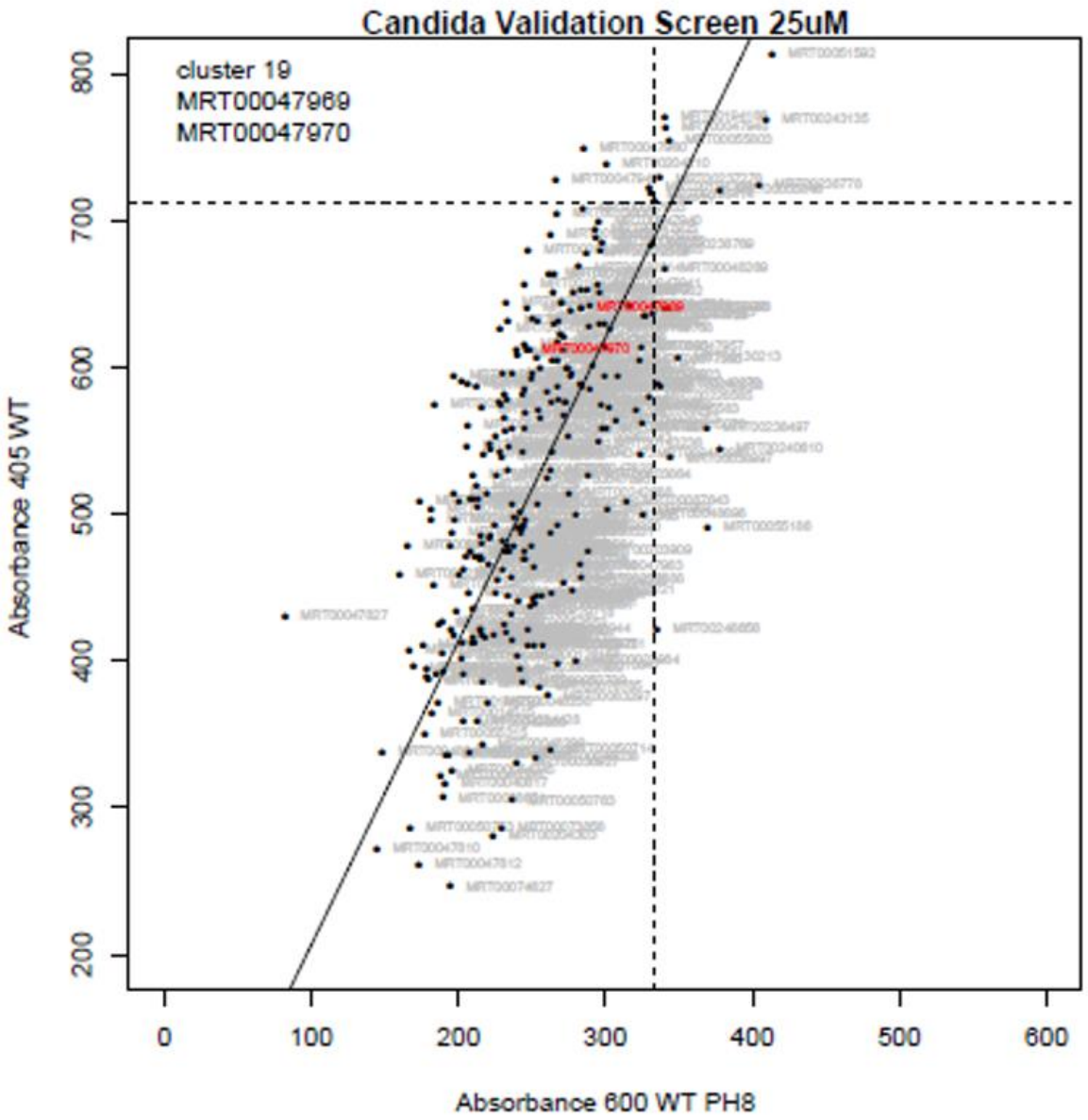

Cluster 19: 25 µM Secondary Screen: pH8 as a readout for PHO Pathway activity.
Plot of OD_{600} *wt* cells grown in pH 8 vs. OD_{405} of *wt* cells. Cells were grown to log phase in YPD before being washed 3 times in pH8 media and diluted back to OD_{600} = 0.05 then seeded into 384 well plates containing 25 µM of compound. Absorbance of 600 nm is used for growth at pH and 405 for secreted acid phosphatase activity. Red hits represent those from cluster 19.

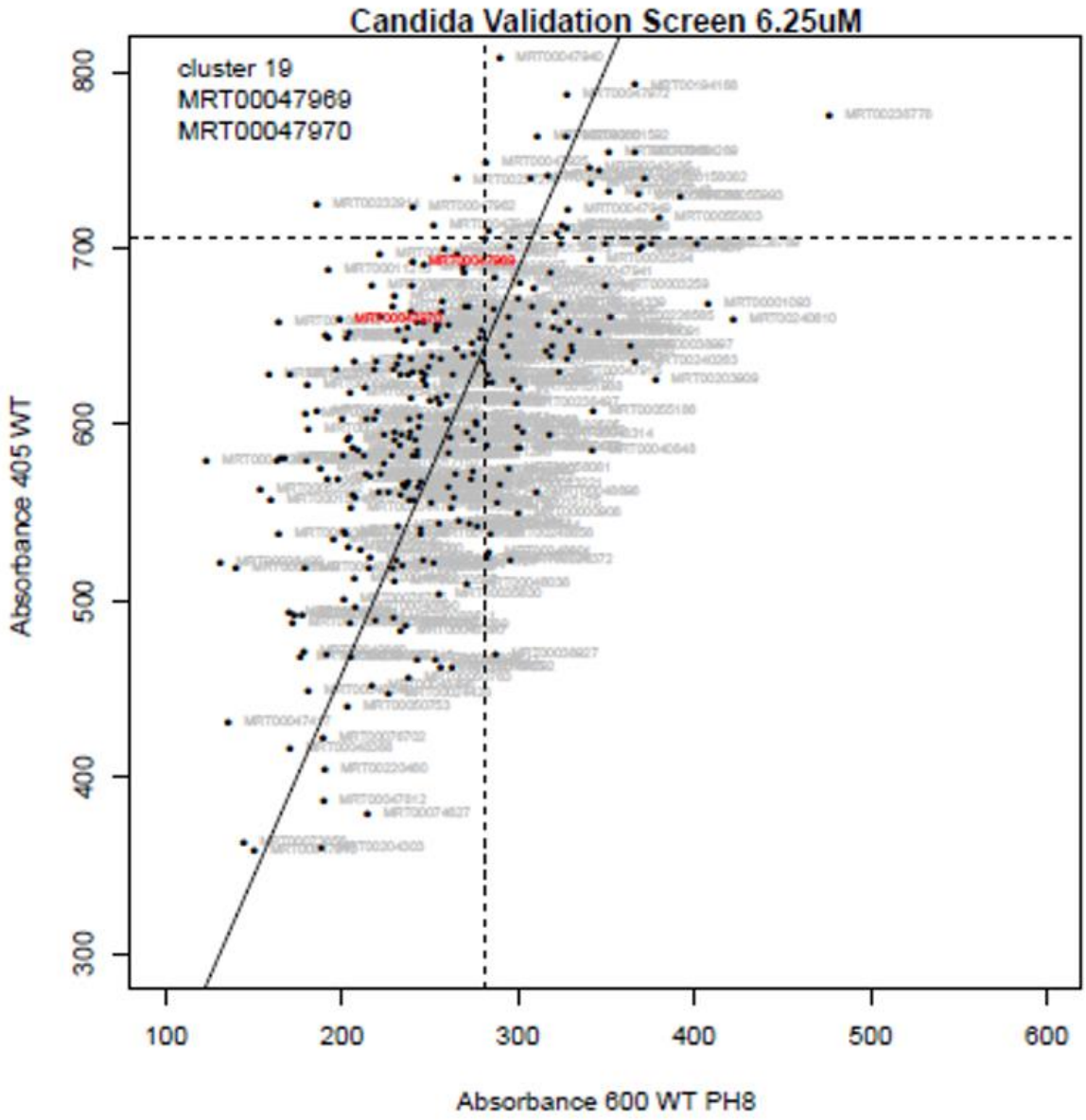

Cluster 19: 6.25 µM Secondary Screen: pH8 as a readout for PHO Pathway activity.
Plot of OD_{600} *wt* cells grown in pH 8 vs. OD_{405} of *wt* cells. Cells were grown to log phase in YPD before being washed 3 times in pH8 media and diluted back to OD_{600} = 0.05 then seeded into 384 well plates containing 6.25 µM of compound. Absorbance of 600 nm is used for growth at pH and 405 for secreted acid phosphatase activity. Red hits represent those from cluster 19.

Cluster 20

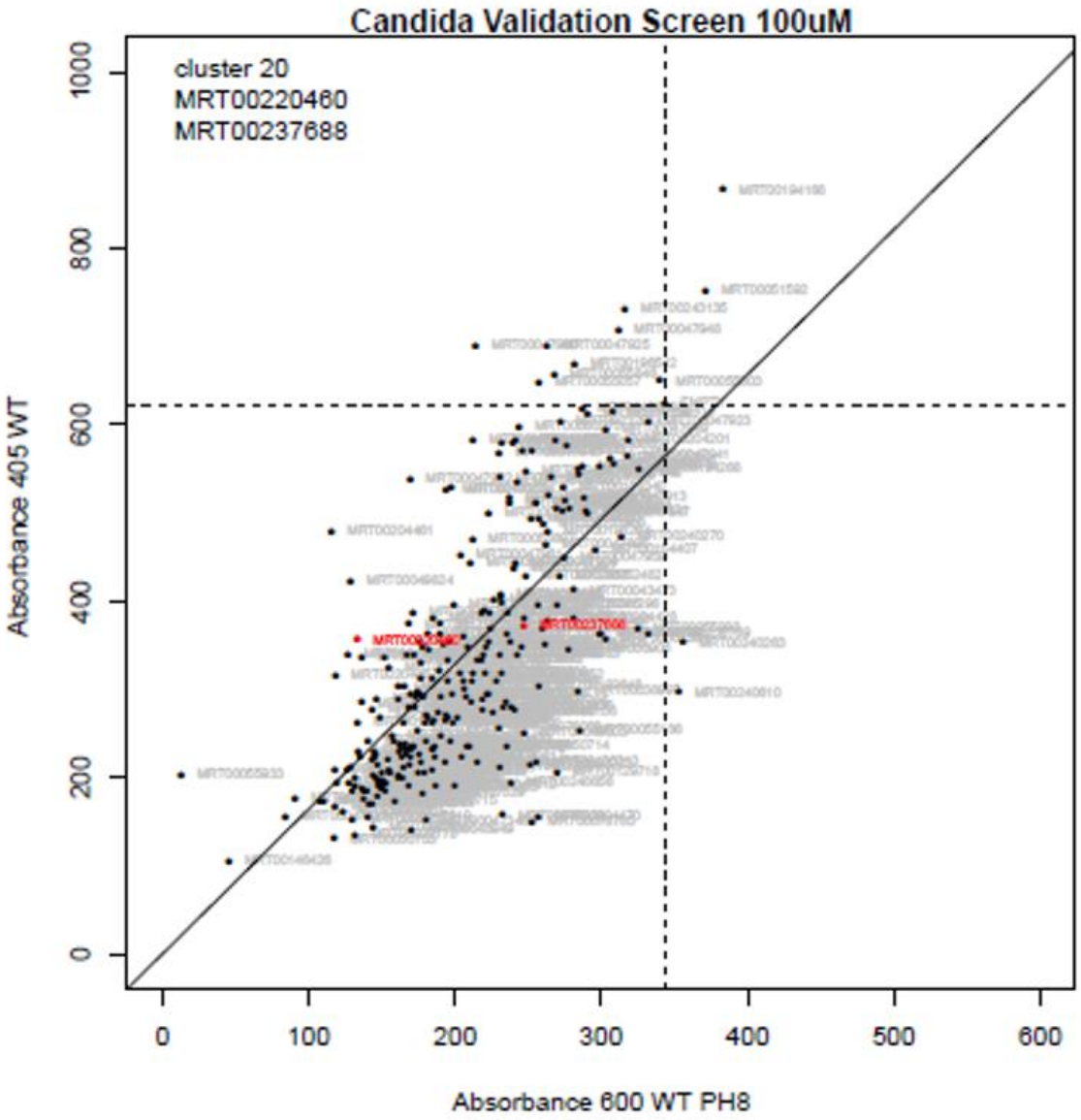

Cluster 20: 100 µM Secondary Screen: pH8 as a readout for PHO Pathway activity.
Plot of OD_{600} *wt* cells grown in pH 8 vs. OD_{405} of *wt* cells. Cells were grown to log phase in YPD before being washed 3 times in pH8 media and diluted back to OD_{600} = 0.05 then seeded into 384 well plates containing 100 µM of compound. Absorbance of 600 nm is used for growth at pH and 405 for secreted acid phosphatase activity. Red hits represent those from cluster 20.

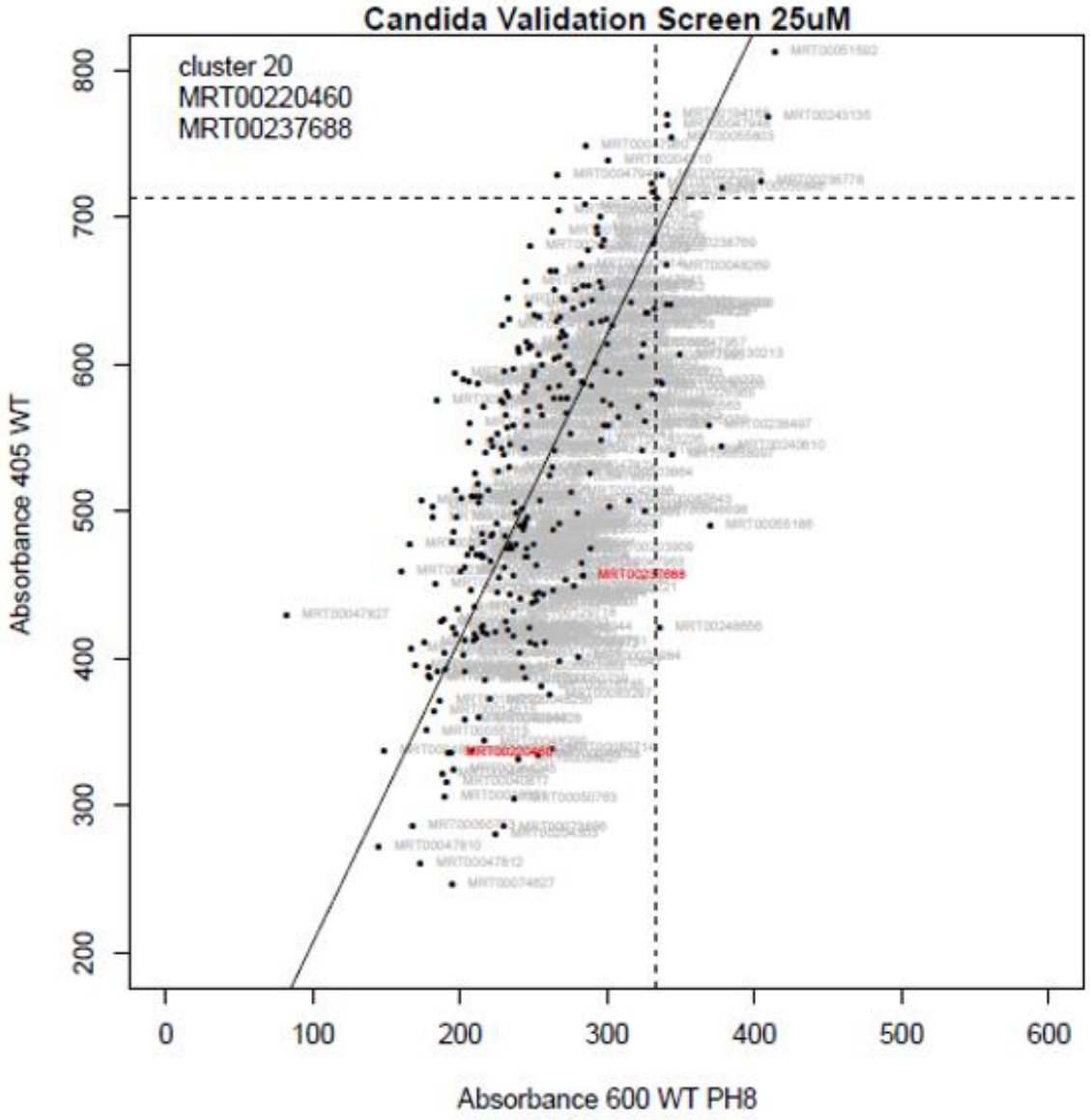

Cluster 20: 25 µM Secondary Screen: pH8 as a readout for PHO Pathway activity.
Plot of OD_{600} *wt* cells grown in pH 8 vs. OD_{405} of *wt* cells. Cells were grown to log phase in YPD before being washed 3 times in pH8 media and diluted back to OD_{600} = 0.05 then seeded into 384 well plates containing 25 µM of compound. Absorbance of 600 nm is used for growth at pH and 405 for secreted acid phosphatase activity. Red hits represent those from cluster 20.

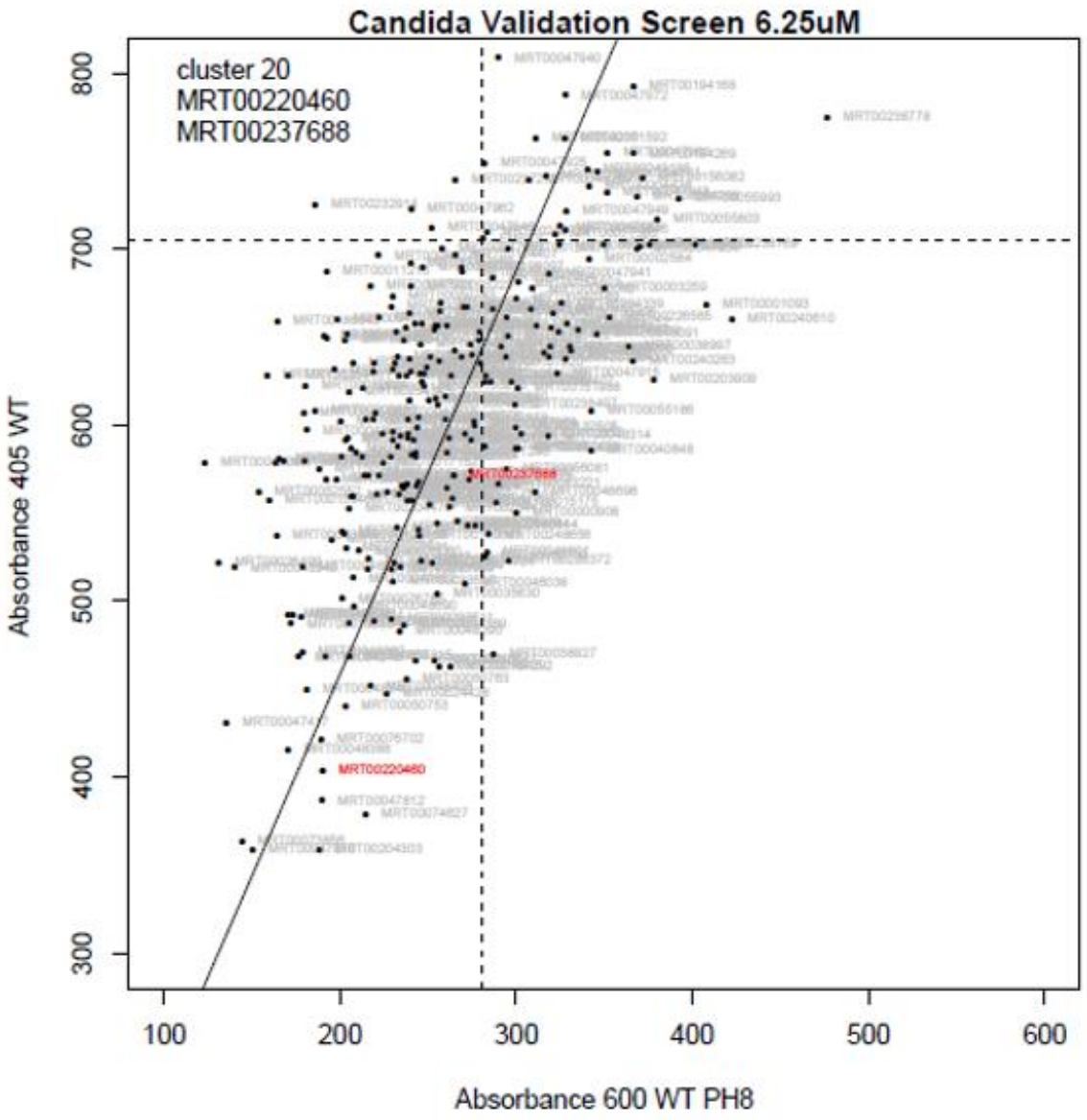

Cluster 20: 6.25 µM Secondary Screen: pH8 as a readout for PHO Pathway activity.
Plot of OD_{600} *wt* cells grown in pH 8 vs. OD_{405} of *wt* cells. Cells were grown to log phase in YPD before being washed 3 times in pH8 media and diluted back to OD_{600} = 0.05 then seeded into 384 well plates containing 6.25 µM of compound. Absorbance of 600 nm is used for growth at pH and 405 for secreted acid phosphatase activity. Red hits represent those from cluster 20.

Cluster 21

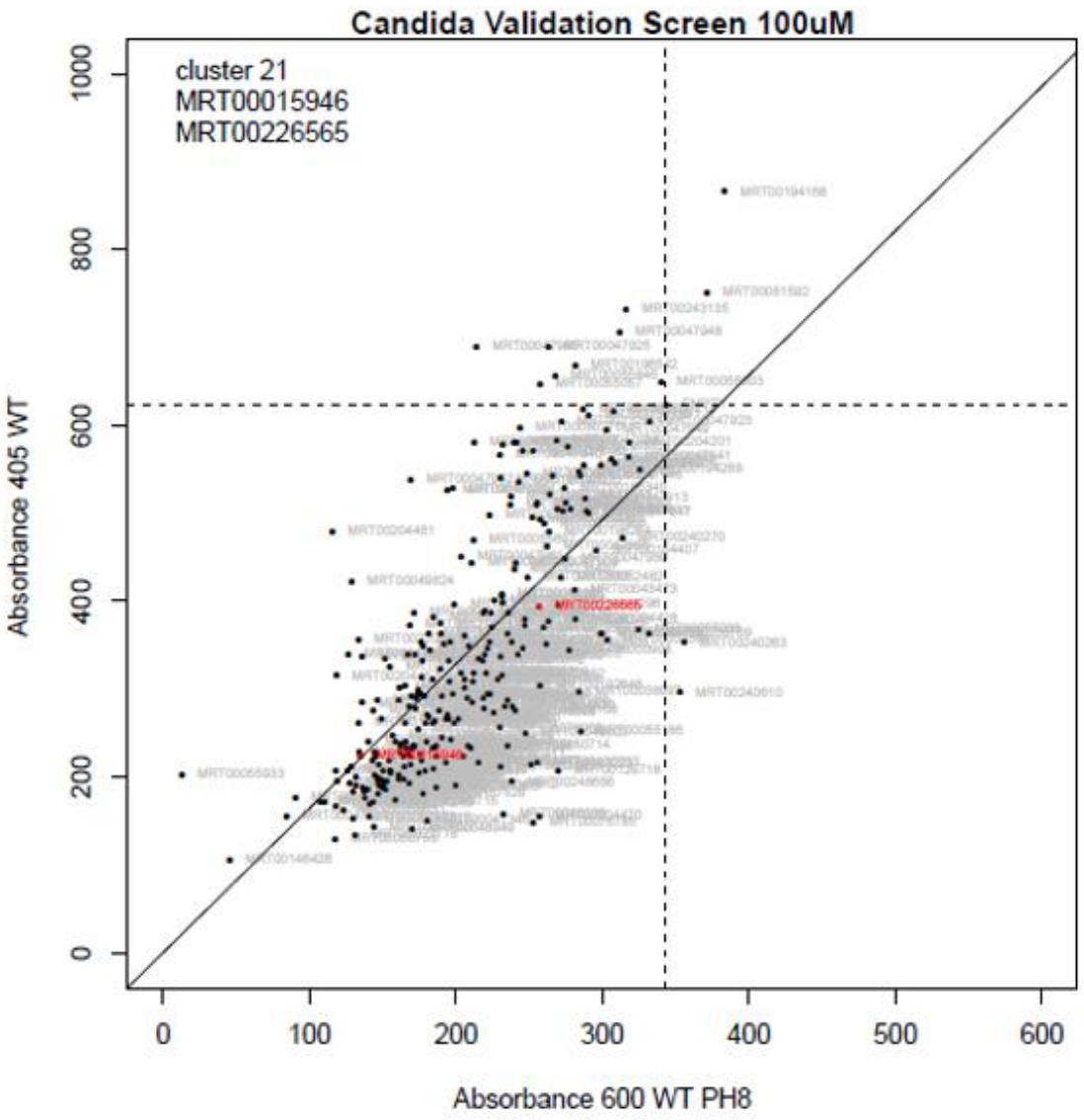

Cluster 21: 100 µM Secondary Screen: pH8 as a readout for PHO Pathway activity.
Plot of OD_{600} *wt* cells grown in pH 8 vs. OD_{405} of *wt* cells. Cells were grown to log phase in YPD before being washed 3 times in pH8 media and diluted back to OD_{600} = 0.05 then seeded into 384 well plates containing 100 µM of compound. Absorbance of 600 nm is used for growth at pH and 405 for secreted acid phosphatase activity. Red hits represent those from cluster 21.

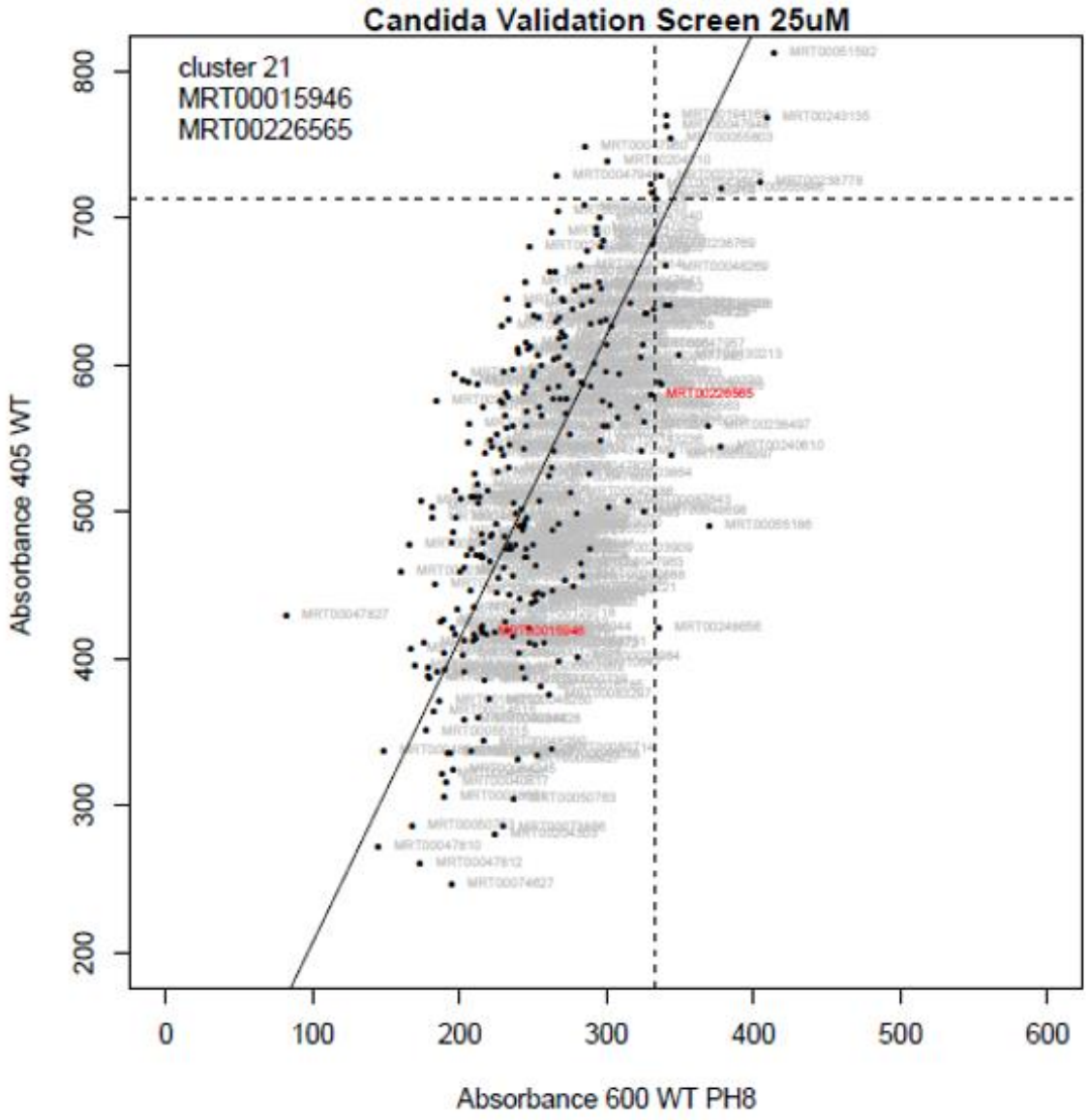

Cluster 21: 25 µM Secondary Screen: pH8 as a readout for PHO Pathway activity.
Plot of OD_{600} *wt* cells grown in pH 8 vs. OD_{405} of *wt* cells. Cells were grown to log phase in YPD before being washed 3 times in pH8 media and diluted back to OD_{600} = 0.05 then seeded into 384 well plates containing 25 µM of compound. Absorbance of 600 nm is used for growth at pH and 405 for secreted acid phosphatase activity. Red hits represent those from cluster 21.

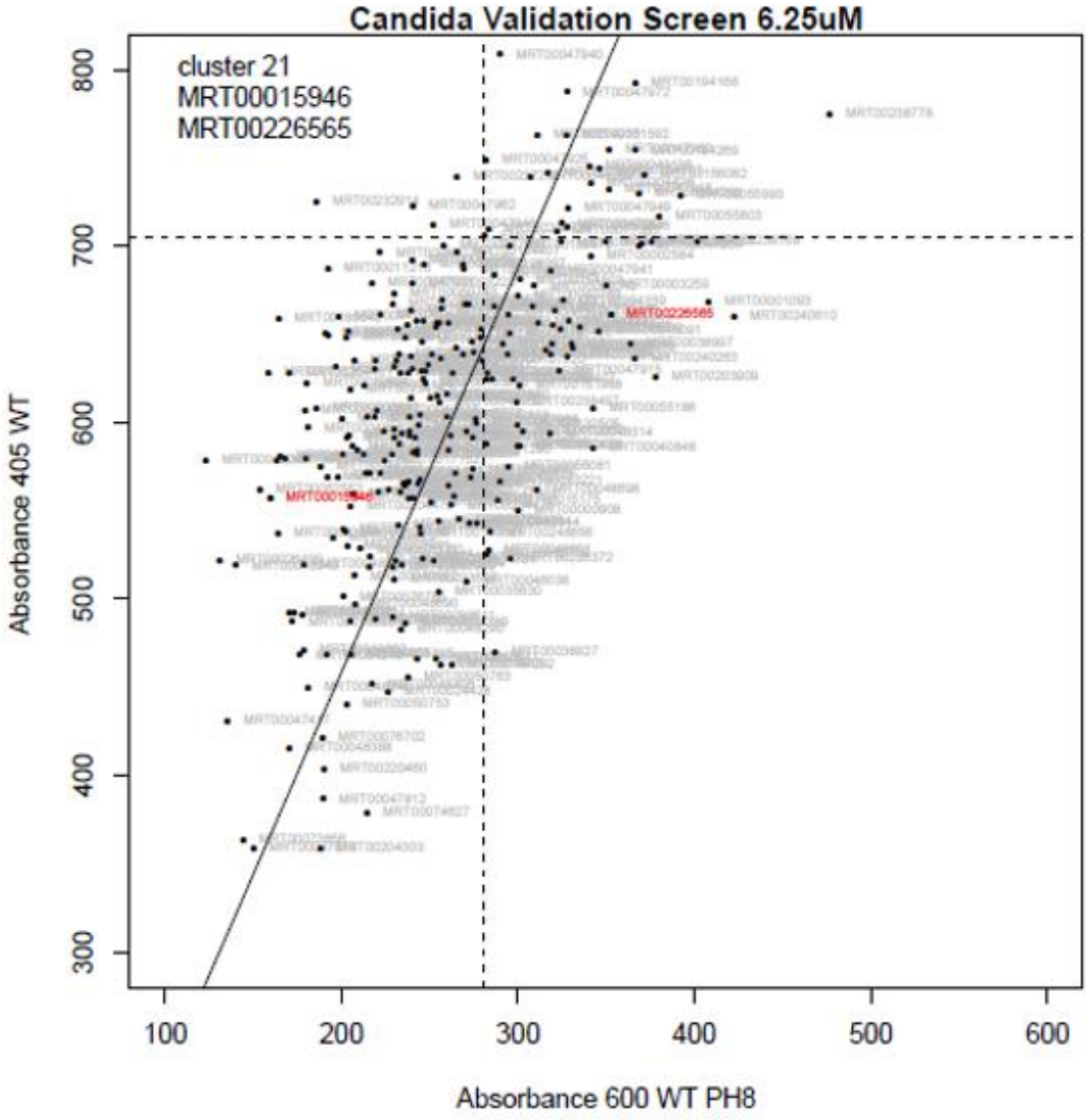

Cluster 21: 6.25 µM Secondary Screen: pH8 as a readout for PHO Pathway activity.
Plot of OD_{600} *wt* cells grown in pH 8 vs. OD_{405} of *wt* cells. Cells were grown to log phase in YPD before being washed 3 times in pH8 media and diluted back to OD_{600} = 0.05 then seeded into 384 well plates containing 6.25 µM of compound. Absorbance of 600 nm is used for growth at pH and 405 for secreted acid phosphatase activity. Red hits represent those from cluster 21.

Cluster 22

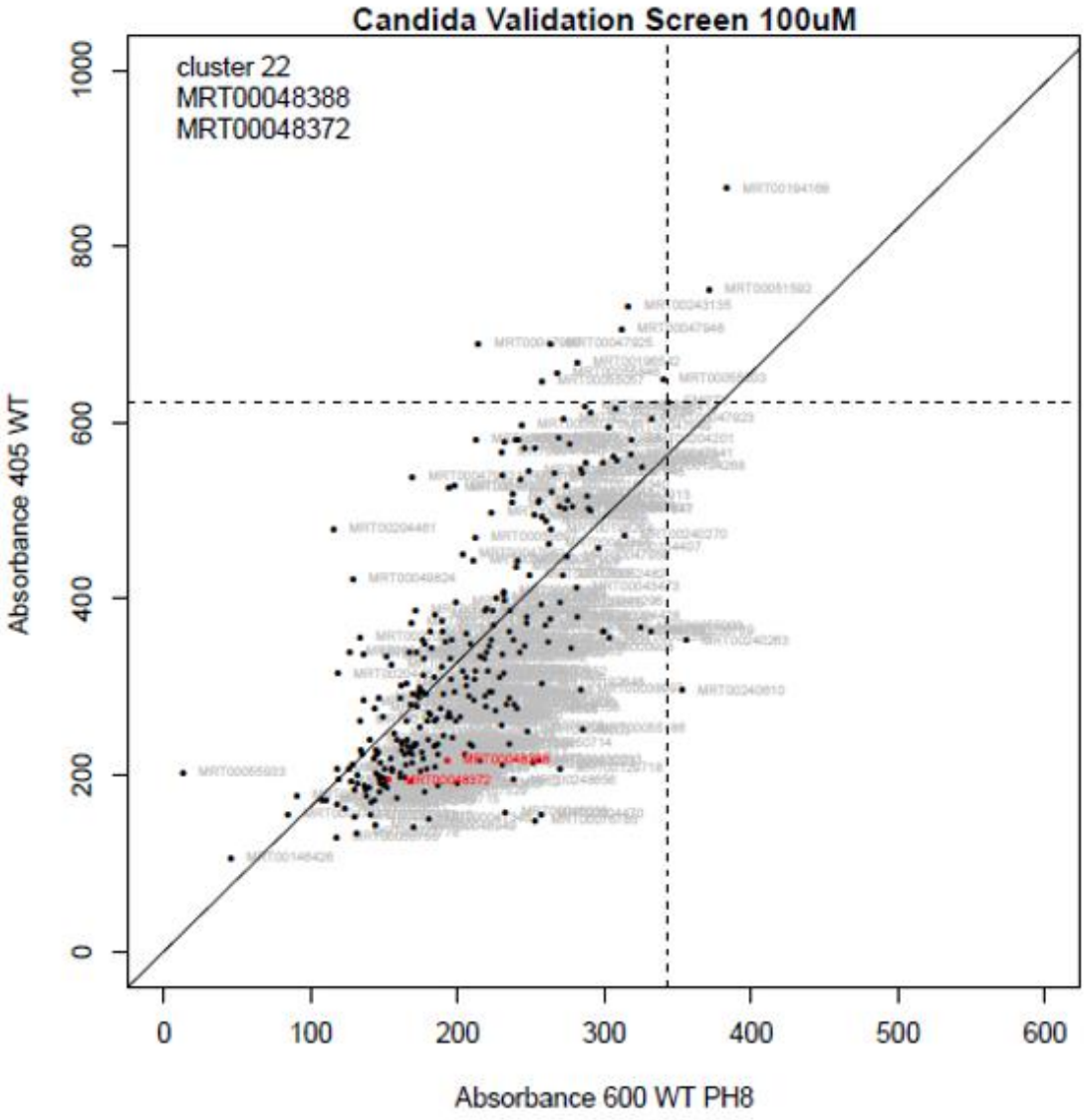

Cluster 22: 100 µM Secondary Screen: pH8 as a readout for PHO Pathway activity.
Plot of OD_{600} *wt* cells grown in pH 8 vs. OD_{405} of *wt* cells. Cells were grown to log phase in YPD before being washed 3 times in pH8 media and diluted back to OD_{600} = 0.05 then seeded into 384 well plates containing 100 µM of compound. Absorbance of 600 nm is used for growth at pH and 405 for secreted acid phosphatase activity. Red hits represent those from cluster 22.

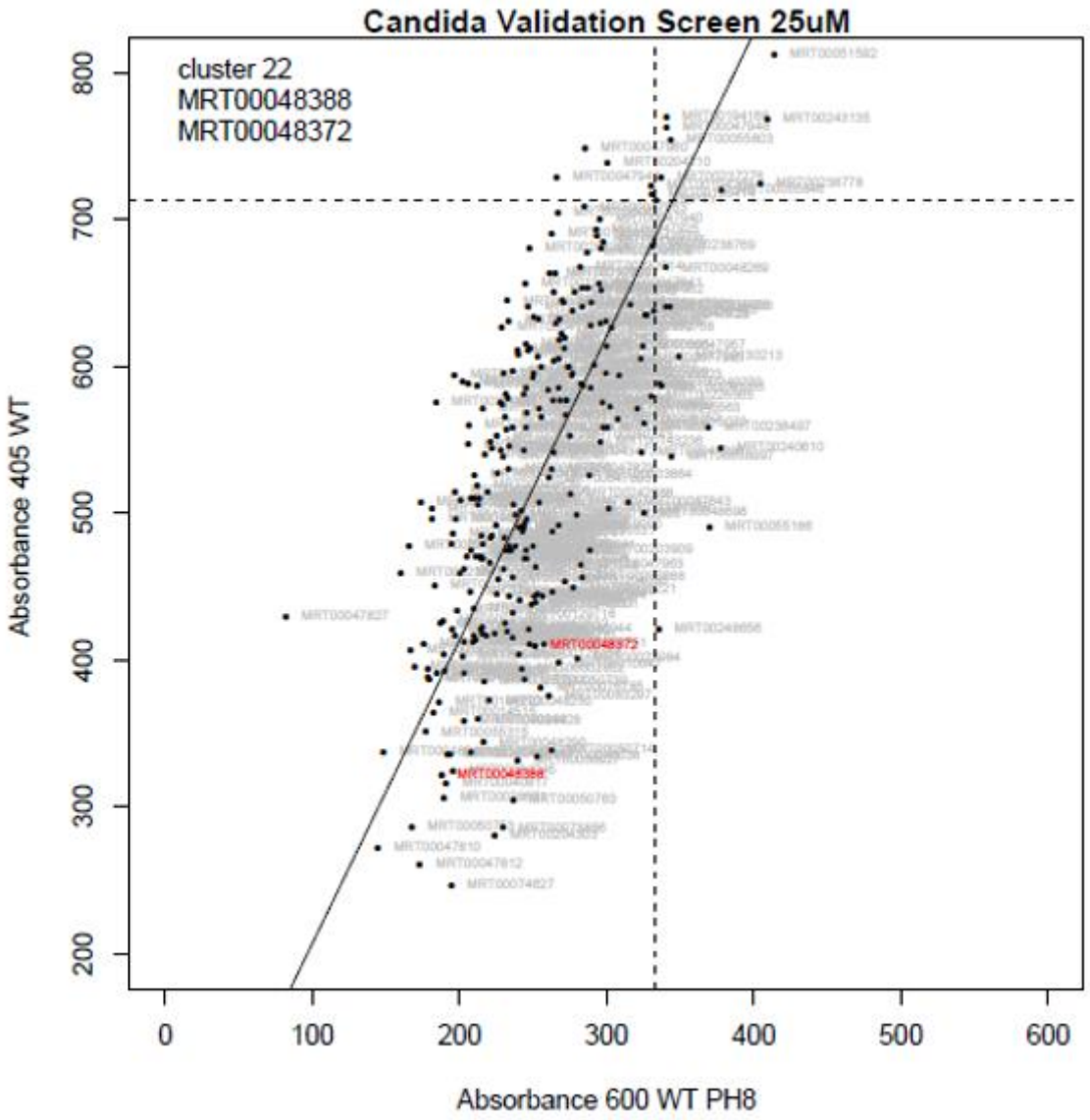

Cluster 22: 25 µM Secondary Screen: pH8 as a readout for PHO Pathway activity.
Plot of OD_{600} *wt* cells grown in pH 8 vs. OD_{405} of *wt* cells. Cells were grown to log phase in YPD before being washed 3 times in pH8 media and diluted back to OD_{600} = 0.05 then seeded into 384 well plates containing 25 µM of compound. Absorbance of 600 nm is used for growth at pH and 405 for secreted acid phosphatase activity. Red hits represent those from cluster 22.

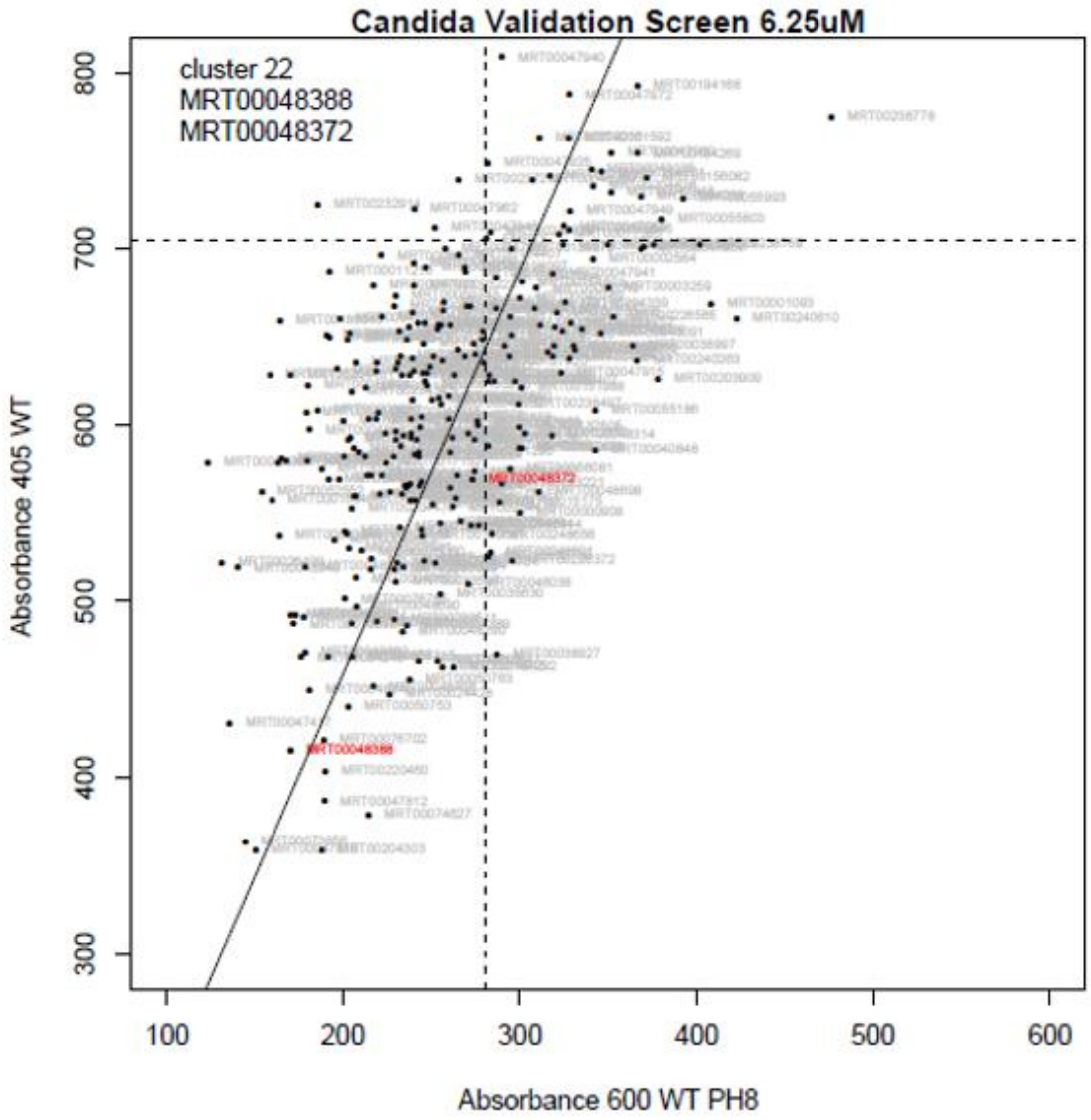

Cluster 22: 6.25 µM Secondary Screen: pH8 as a readout for PHO Pathway activity.
Plot of OD_{600} *wt* cells grown in pH 8 vs. OD_{405} of *wt* cells. Cells were grown to log phase in YPD before being washed 3 times in pH8 media and diluted back to OD_{600} = 0.05 then seeded into 384 well plates containing 6.25 µM of compound. Absorbance of 600 nm is used for growth at pH and 405 for secreted acid phosphatase activity. Red hits represent those from cluster 22.

Cluster 23

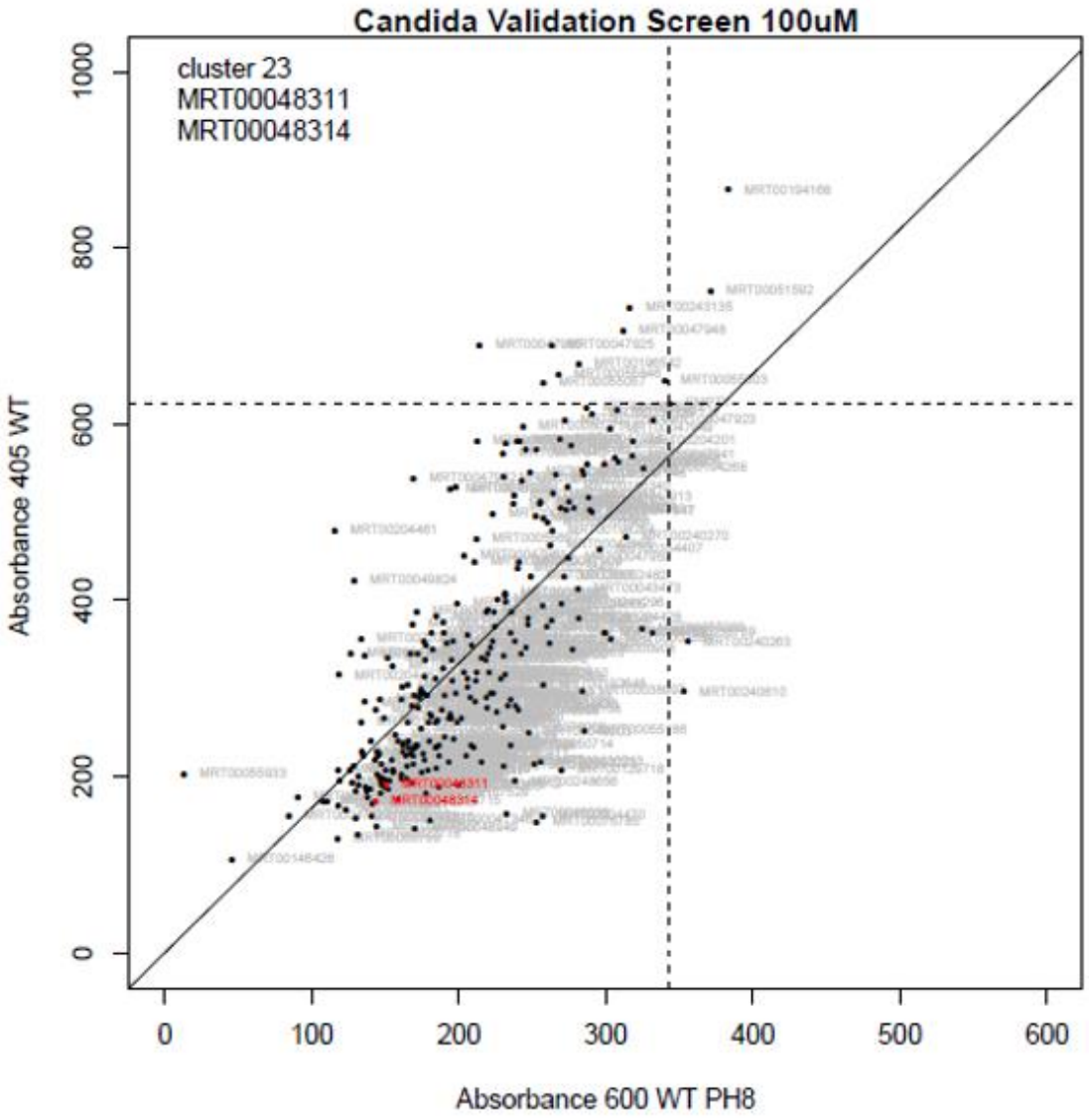

Cluster 23: 100 µM Secondary Screen: pH8 as a readout for PHO Pathway activity.
Plot of OD_{600} *wt* cells grown in pH 8 vs. OD_{405} of *wt* cells. Cells were grown to log phase in YPD before being washed 3 times in pH8 media and diluted back to OD_{600} = 0.05 then seeded into 384 well plates containing 100 µM of compound. Absorbance of 600 nm is used for growth at pH and 405 for secreted acid phosphatase activity. Red hits represent those from cluster 23.

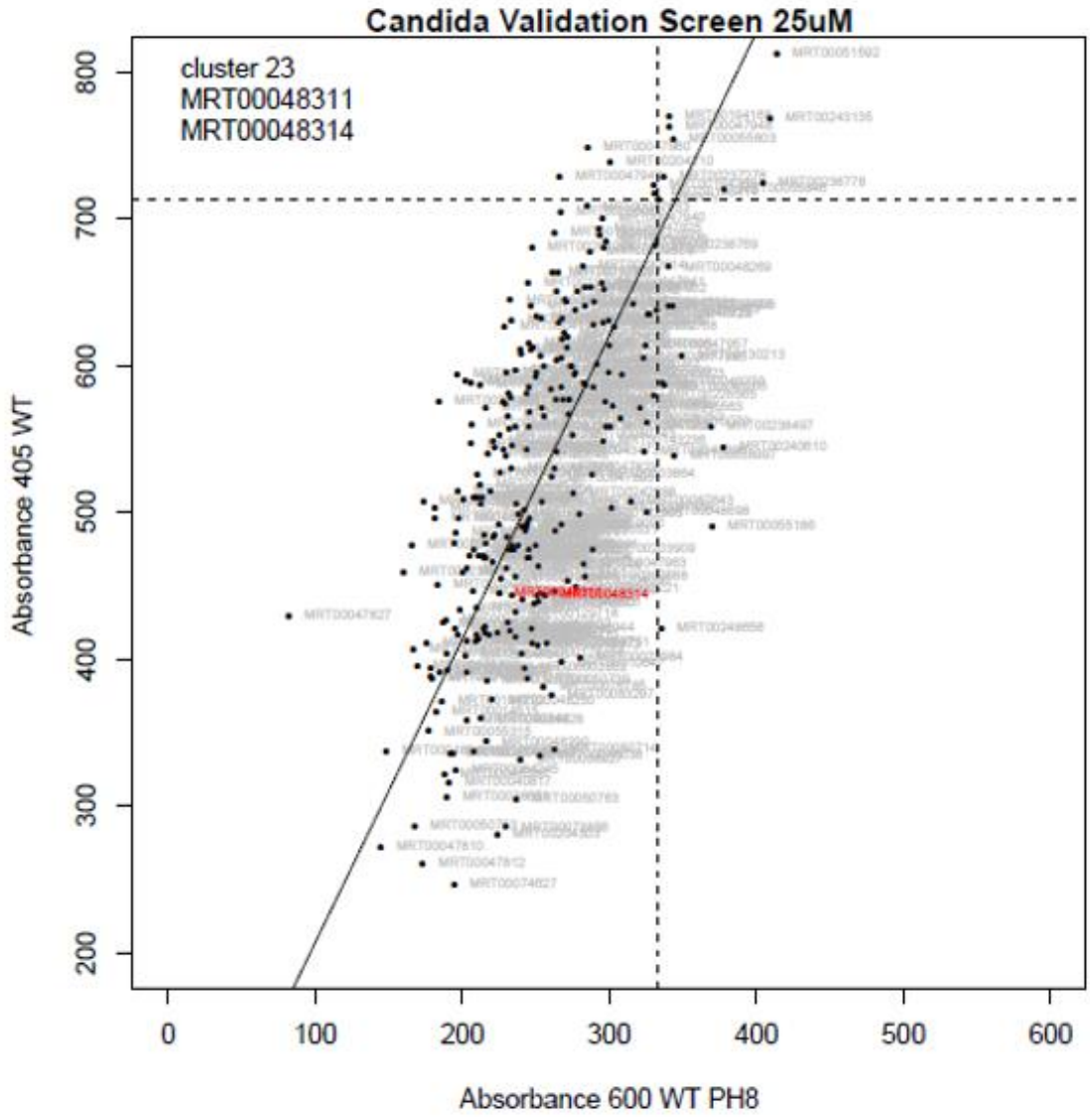

Cluster 23: 25 µM Secondary Screen: pH8 as a readout for PHO Pathway activity.
Plot of OD_{600} *wt* cells grown in pH 8 vs. OD_{405} of *wt* cells. Cells were grown to log phase in YPD before being washed 3 times in pH8 media and diluted back to OD_{600} = 0.05 then seeded into 384 well plates containing 25 µM of compound. Absorbance of 600 nm is used for growth at pH and 405 for secreted acid phosphatase activity. Red hits represent those from cluster 23.

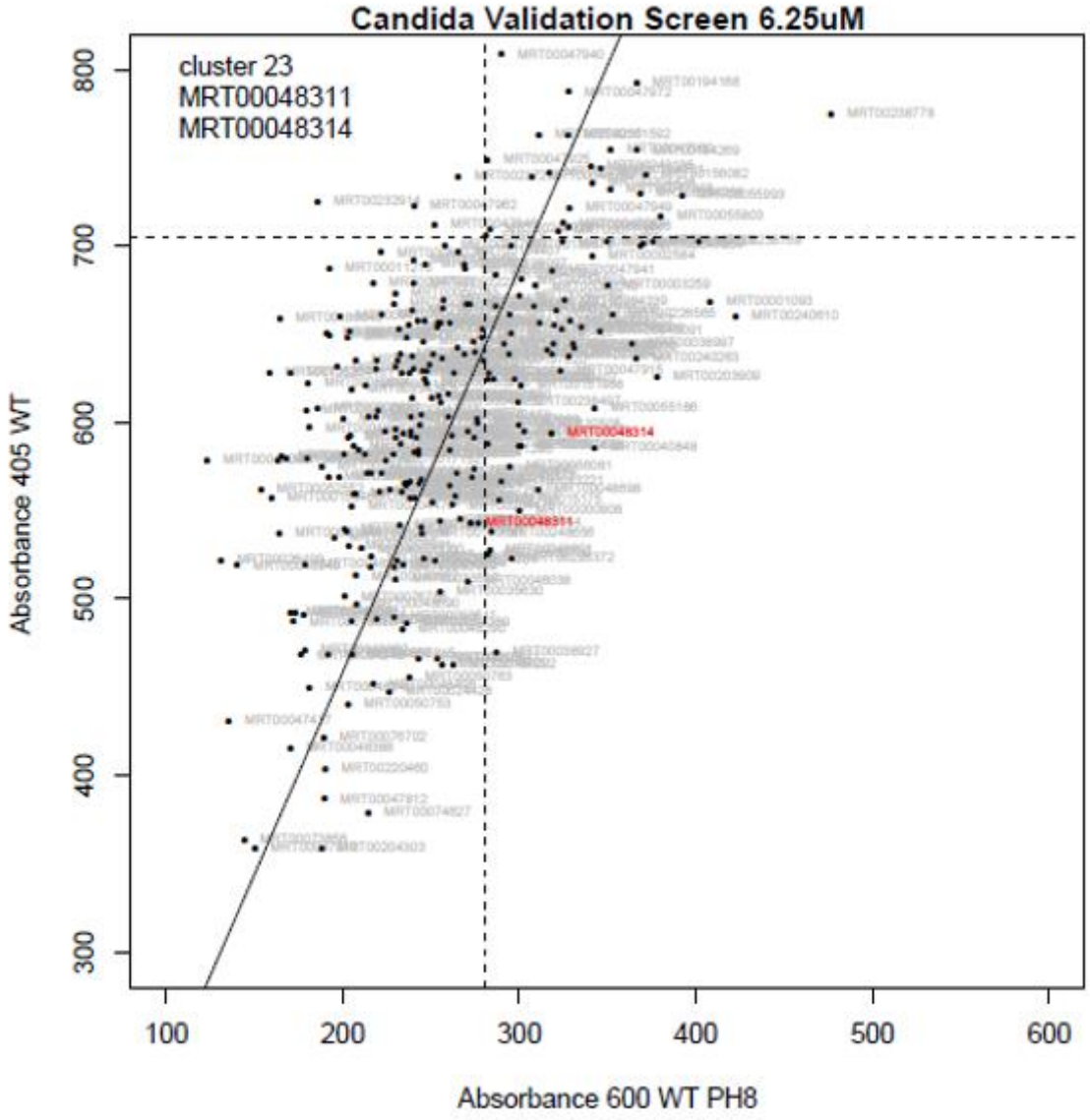

Cluster 23: 6.25 µM Secondary Screen: pH8 as a readout for PHO Pathway activity.
Plot of OD_{600} *wt* cells grown in pH 8 vs. OD_{405} of *wt* cells. Cells were grown to log phase in YPD before being washed 3 times in pH8 media and diluted back to OD_{600} = 0.05 then seeded into 384 well plates containing 6.25 µM of compound. Absorbance of 600 nm is used for growth at pH and 405 for secreted acid phosphatase activity. Red hits represent those from cluster 23.

Cluster 24

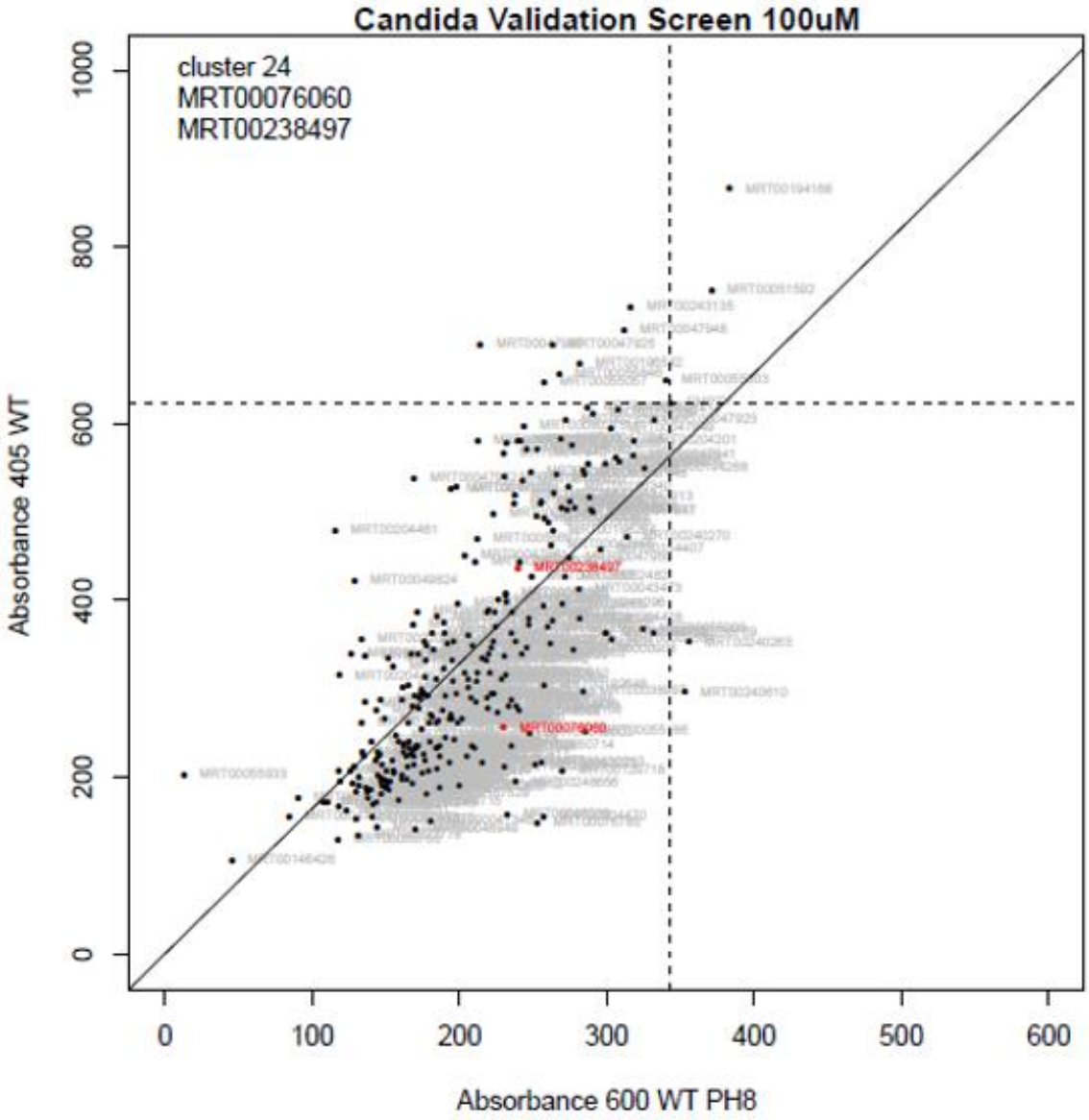

Cluster 24: 100 µM Secondary Screen: pH8 as a readout for PHO Pathway activity.
Plot of OD_{600} *wt* cells grown in pH 8 vs. OD_{405} of *wt* cells. Cells were grown to log phase in YPD before being washed 3 times in pH8 media and diluted back to OD_{600} = 0.05 then seeded into 384 well plates containing 100 µM of compound. Absorbance of 600 nm is used for growth at pH and 405 for secreted acid phosphatase activity. Red hits represent those from cluster 24.

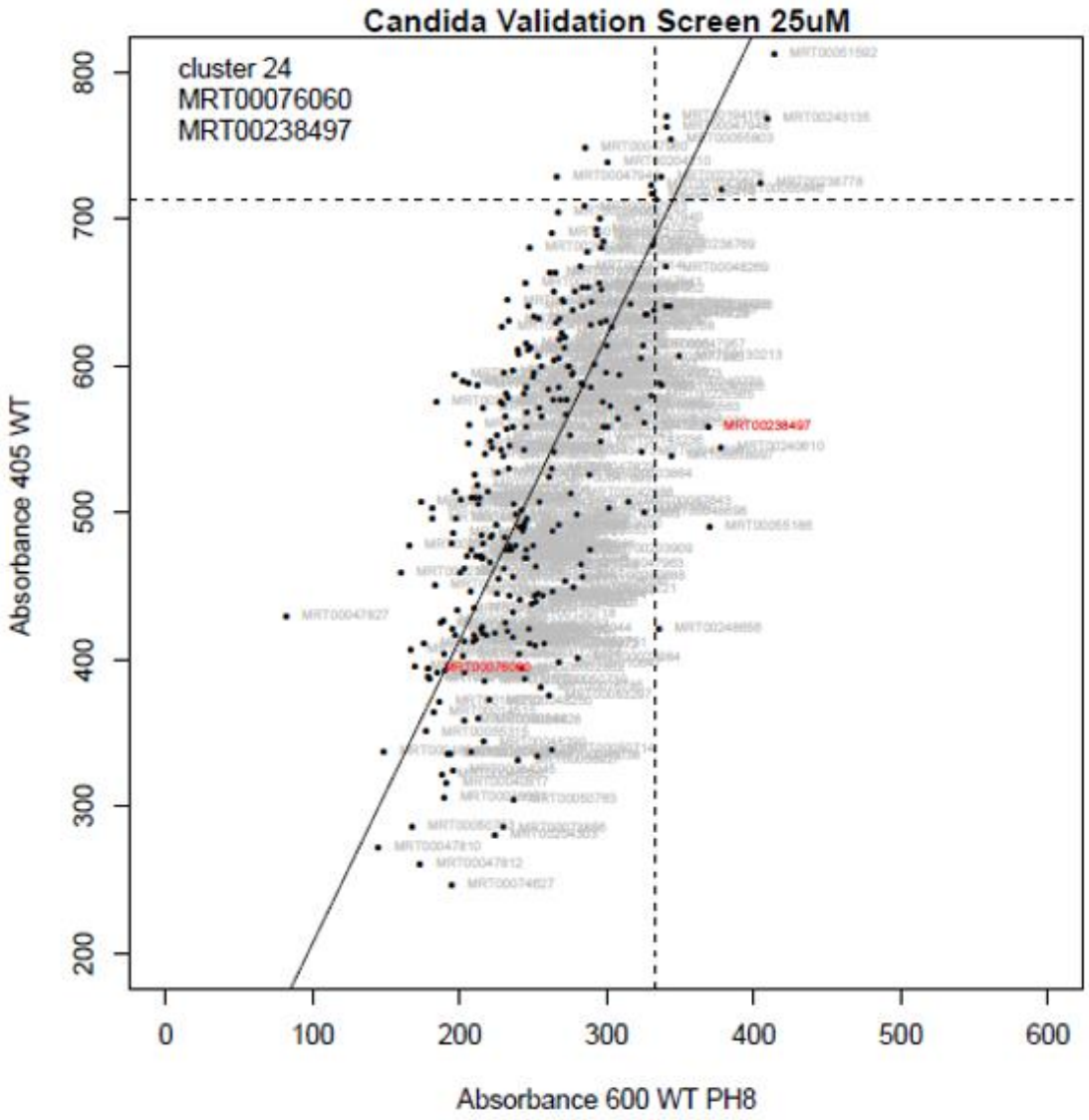

Cluster 24: 25 µM Secondary Screen: pH8 as a readout for PHO Pathway activity.
Plot of OD_{600} *wt* cells grown in pH 8 vs. OD_{405} of *wt* cells. Cells were grown to log phase in YPD before being washed 3 times in pH8 media and diluted back to OD_{600} = 0.05 then seeded into 384 well plates containing 25 µM of compound. Absorbance of 600 nm is used for growth at pH and 405 for secreted acid phosphatase activity. Red hits represent those from cluster 24.

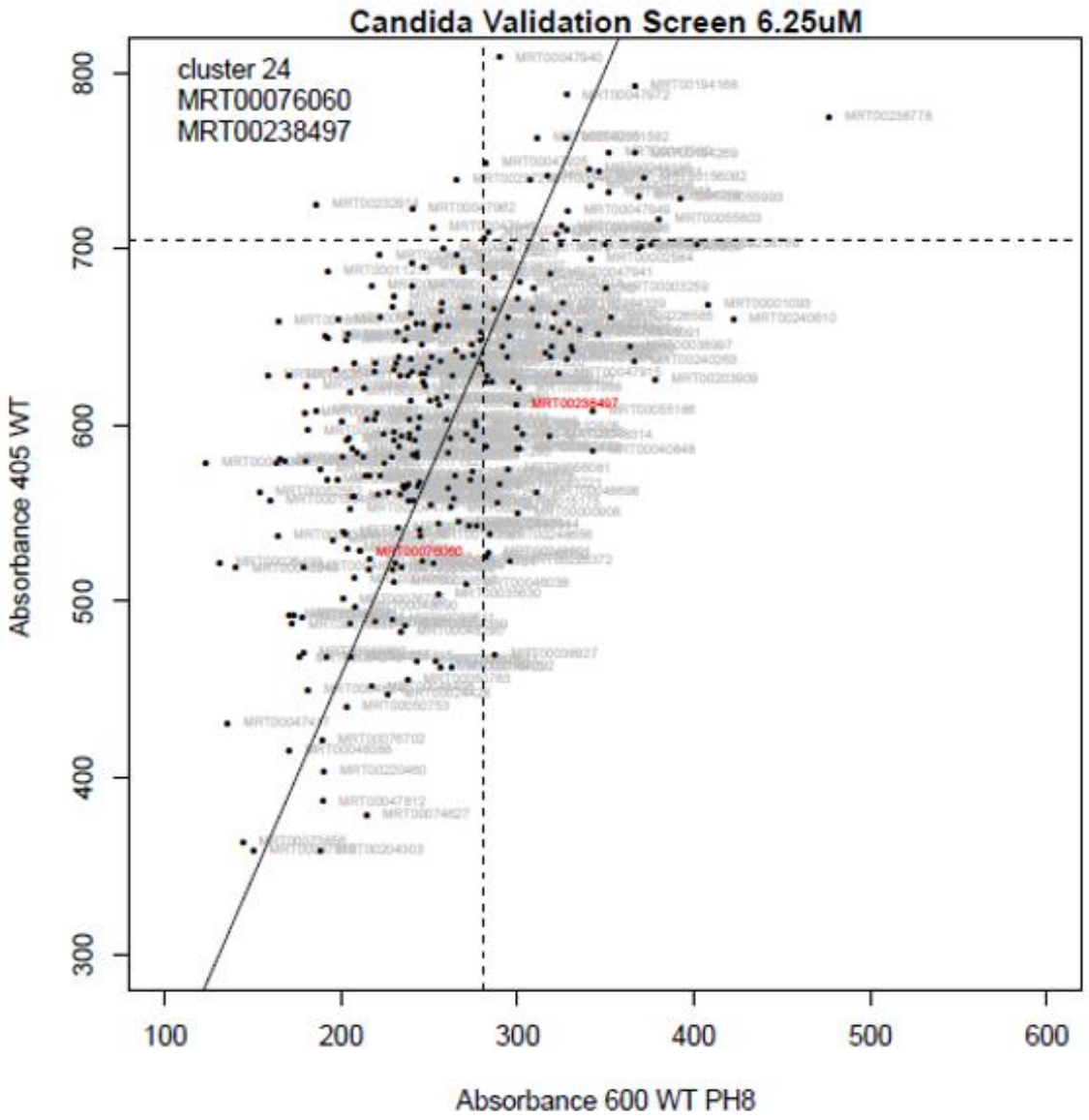

Cluster 24: 6.25 µM Secondary Screen: pH8 as a readout for PHO Pathway activity.
Plot of OD_{600} *wt* cells grown in pH 8 vs. OD_{405} of *wt* cells. Cells were grown to log phase in YPD before being washed 3 times in pH8 media and diluted back to OD_{600} = 0.05 then seeded into 384 well plates containing 6.25 µM of compound. Absorbance of 600 nm is used for growth at pH and 405 for secreted acid phosphatase activity. Red hits represent those from cluster 24.

Cluster 25

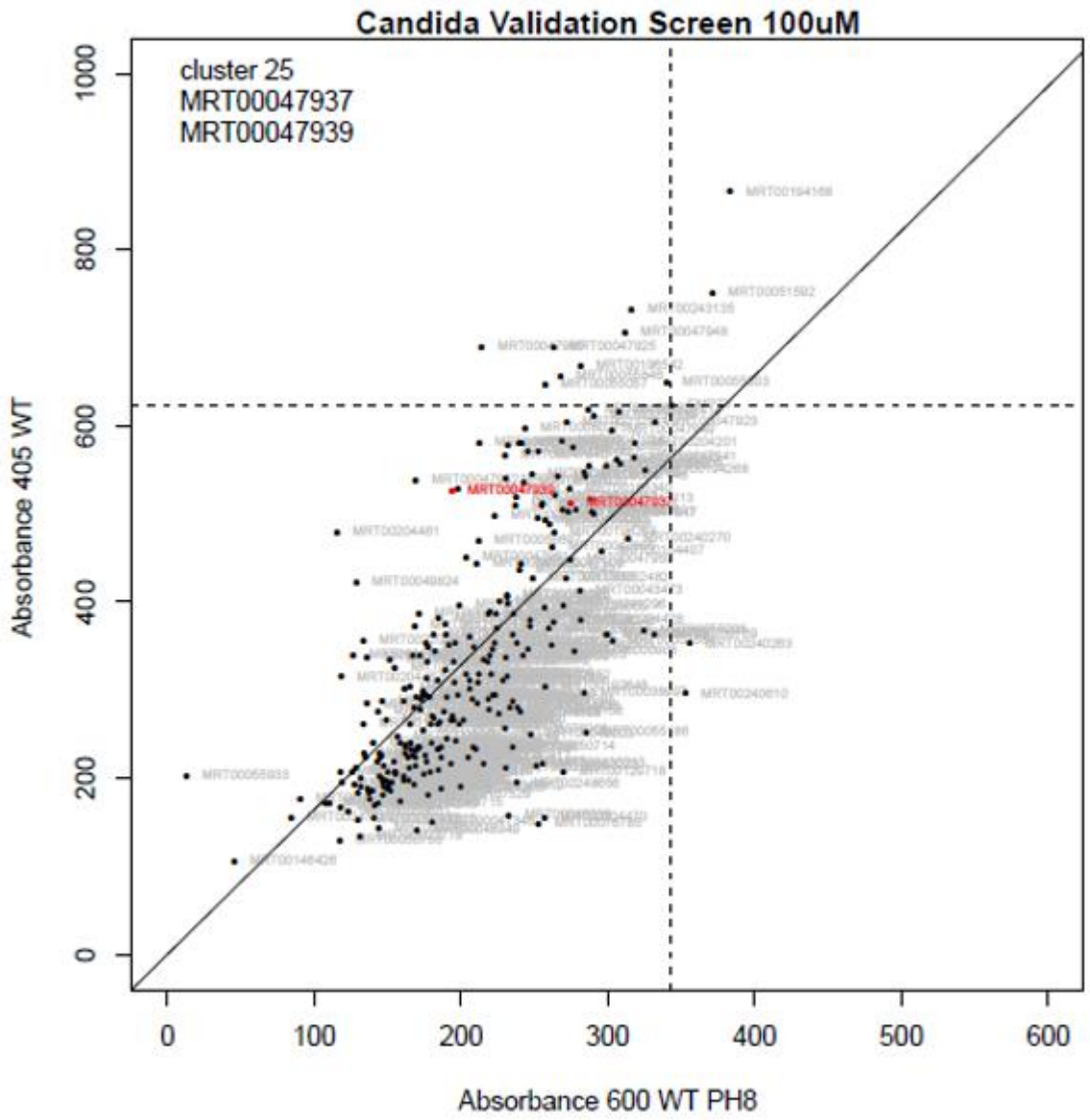

Cluster 25: 100 µM Secondary Screen: pH8 as a readout for PHO Pathway activity.
Plot of OD_{600} *wt* cells grown in pH 8 vs. OD_{405} of *wt* cells. Cells were grown to log phase in YPD before being washed 3 times in pH8 media and diluted back to OD_{600} = 0.05 then seeded into 384 well plates containing 100 µM of compound. Absorbance of 600 nm is used for growth at pH and 405 for secreted acid phosphatase activity. Red hits represent those from cluster 25.

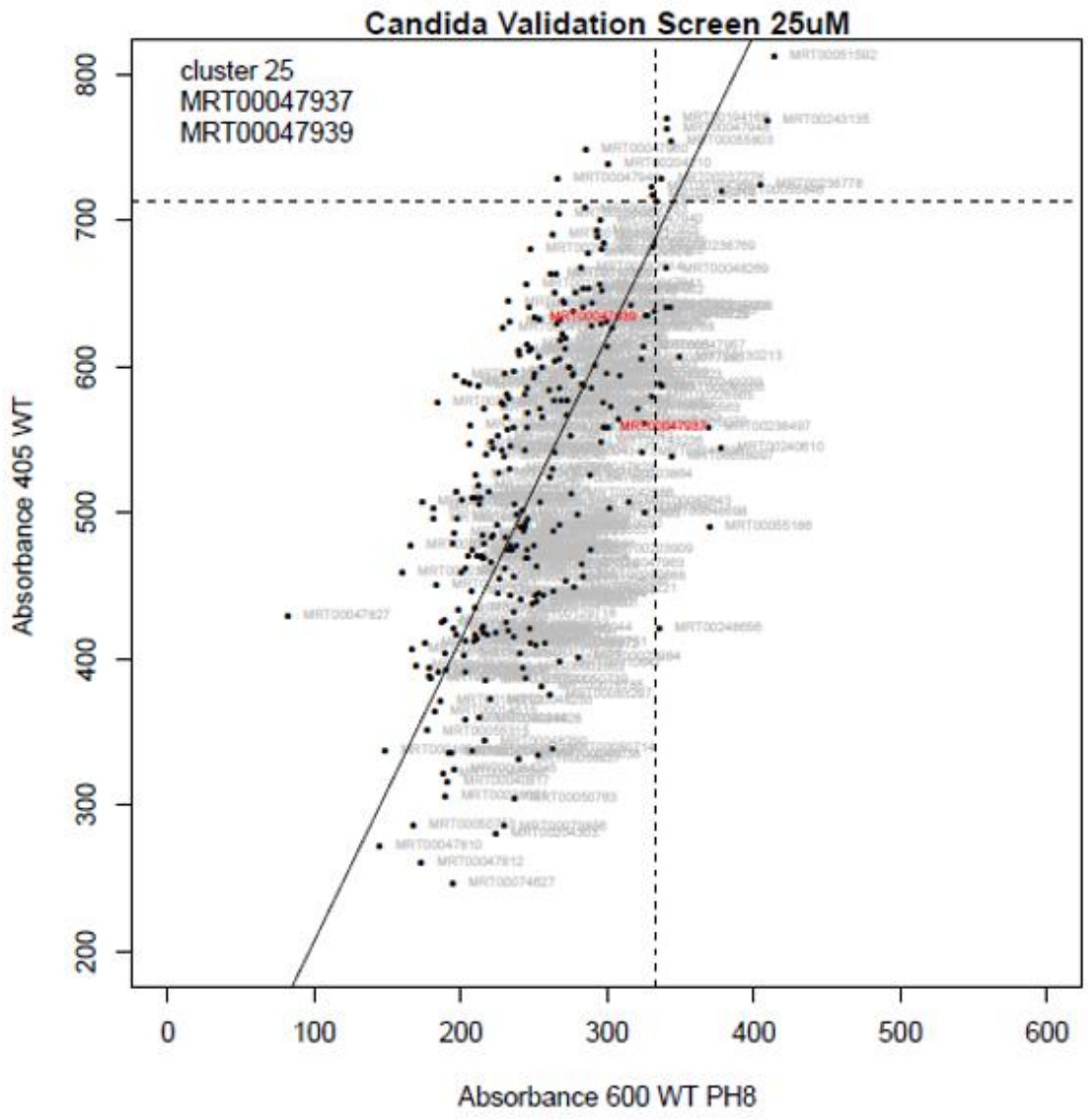

Cluster 25: 25 µM Secondary Screen: pH8 as a readout for PHO Pathway activity.
Plot of OD_{600} *wt* cells grown in pH 8 vs. OD_{405} of *wt* cells. Cells were grown to log phase in YPD before being washed 3 times in pH8 media and diluted back to OD_{600} = 0.05 then seeded into 384 well plates containing 25 µM of compound. Absorbance of 600 nm is used for growth at pH and 405 for secreted acid phosphatase activity. Red hits represent those from cluster 25.

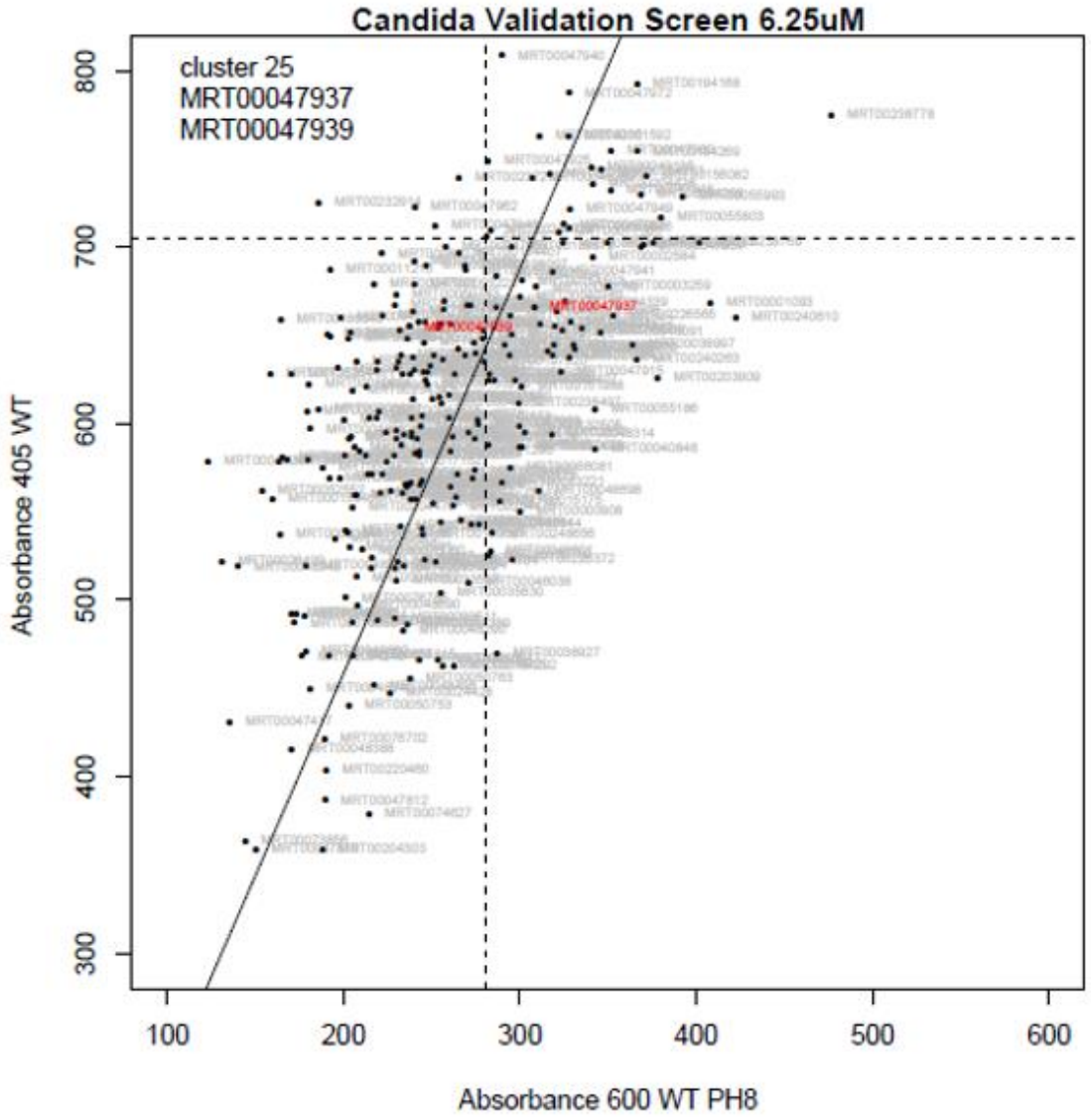

Cluster 25: 6.25 µM Secondary Screen: pH8 as a readout for PHO Pathway activity.
Plot of OD_{600} *wt* cells grown in pH 8 vs. OD_{405} of *wt* cells. Cells were grown to log phase in YPD before being washed 3 times in pH8 media and diluted back to OD_{600} = 0.05 then seeded into 384 well plates containing 6.25 µM of compound. Absorbance of 600 nm is used for growth at pH and 405 for secreted acid phosphatase activity. Red hits represent those from cluster 25.

Cluster 26

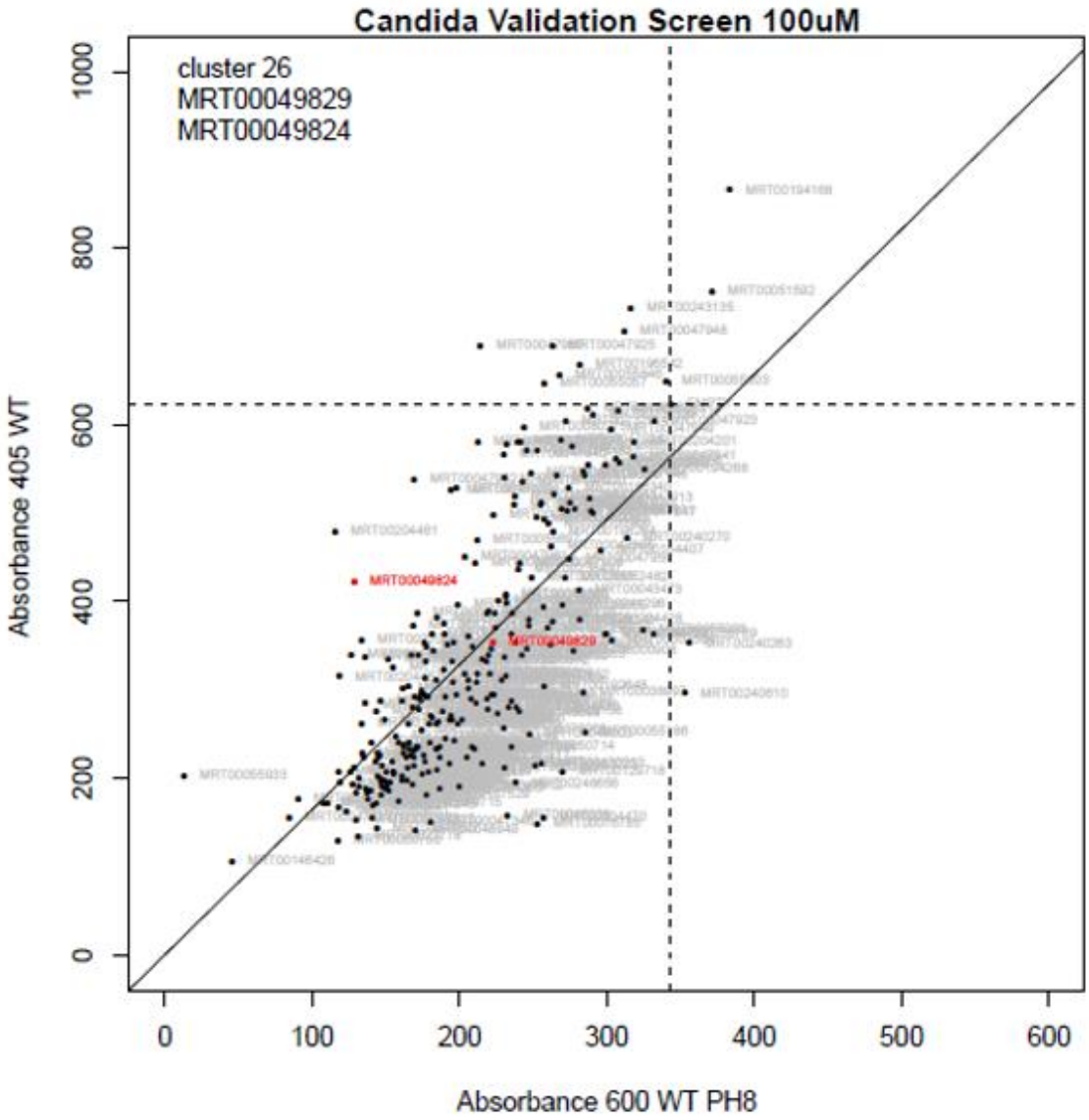

Cluster 26: 100 µM Secondary Screen: pH8 as a readout for PHO Pathway activity.
Plot of OD_{600} *wt* cells grown in pH 8 vs. OD_{405} of *wt* cells. Cells were grown to log phase in YPD before being washed 3 times in pH8 media and diluted back to OD_{600} = 0.05 then seeded into 384 well plates containing 100 µM of compound. Absorbance of 600 nm is used for growth at pH and 405 for secreted acid phosphatase activity. Red hits represent those from cluster 26.

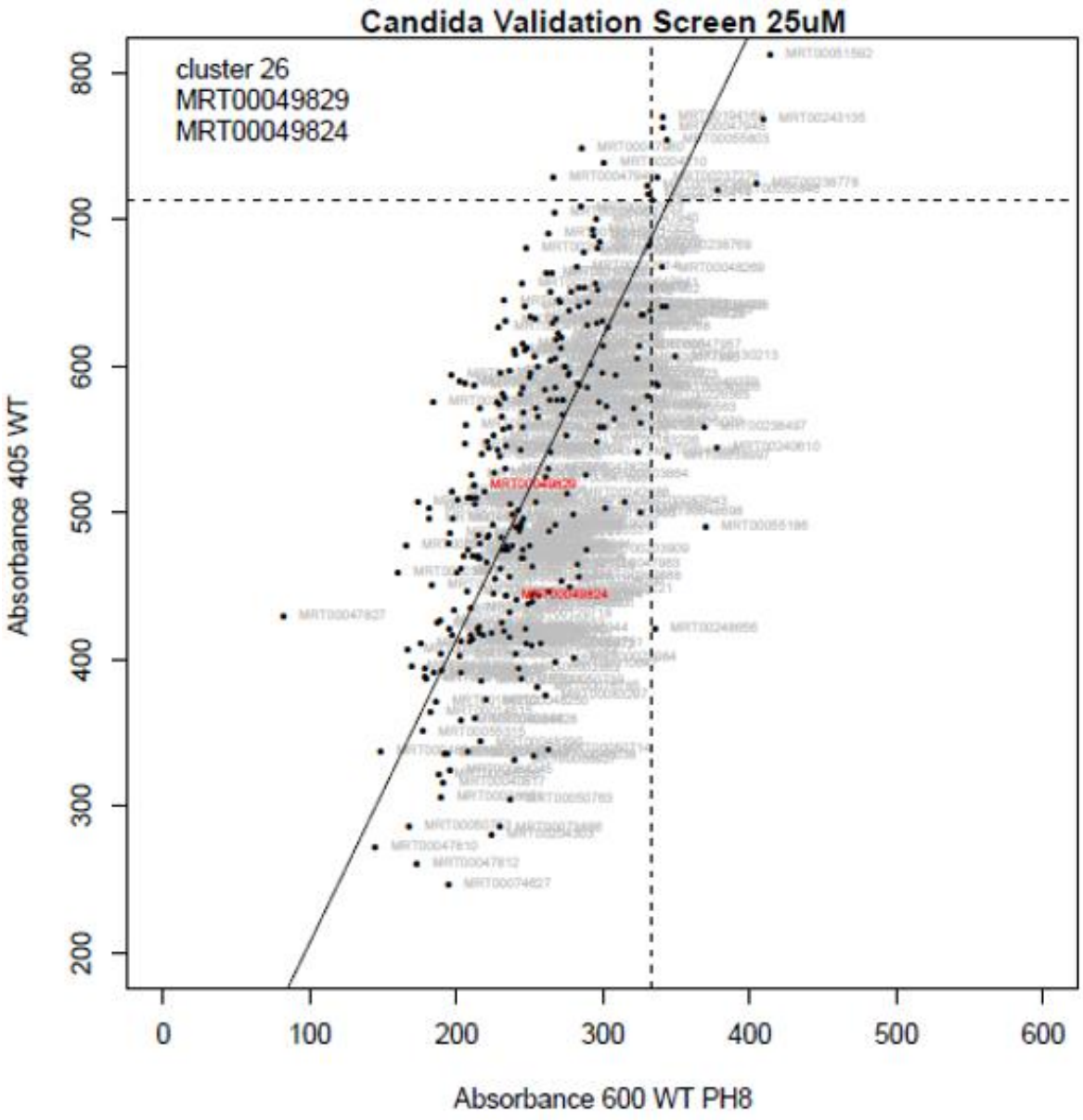

Cluster 26: 25 µM Secondary Screen: pH8 as a readout for PHO Pathway activity.
Plot of OD_{600} *wt* cells grown in pH 8 vs. OD_{405} of *wt* cells. Cells were grown to log phase in YPD before being washed 3 times in pH8 media and diluted back to OD_{600} = 0.05 then seeded into 384 well plates containing 25 µM of compound. Absorbance of 600 nm is used for growth at pH and 405 for secreted acid phosphatase activity. Red hits represent those from cluster 26.

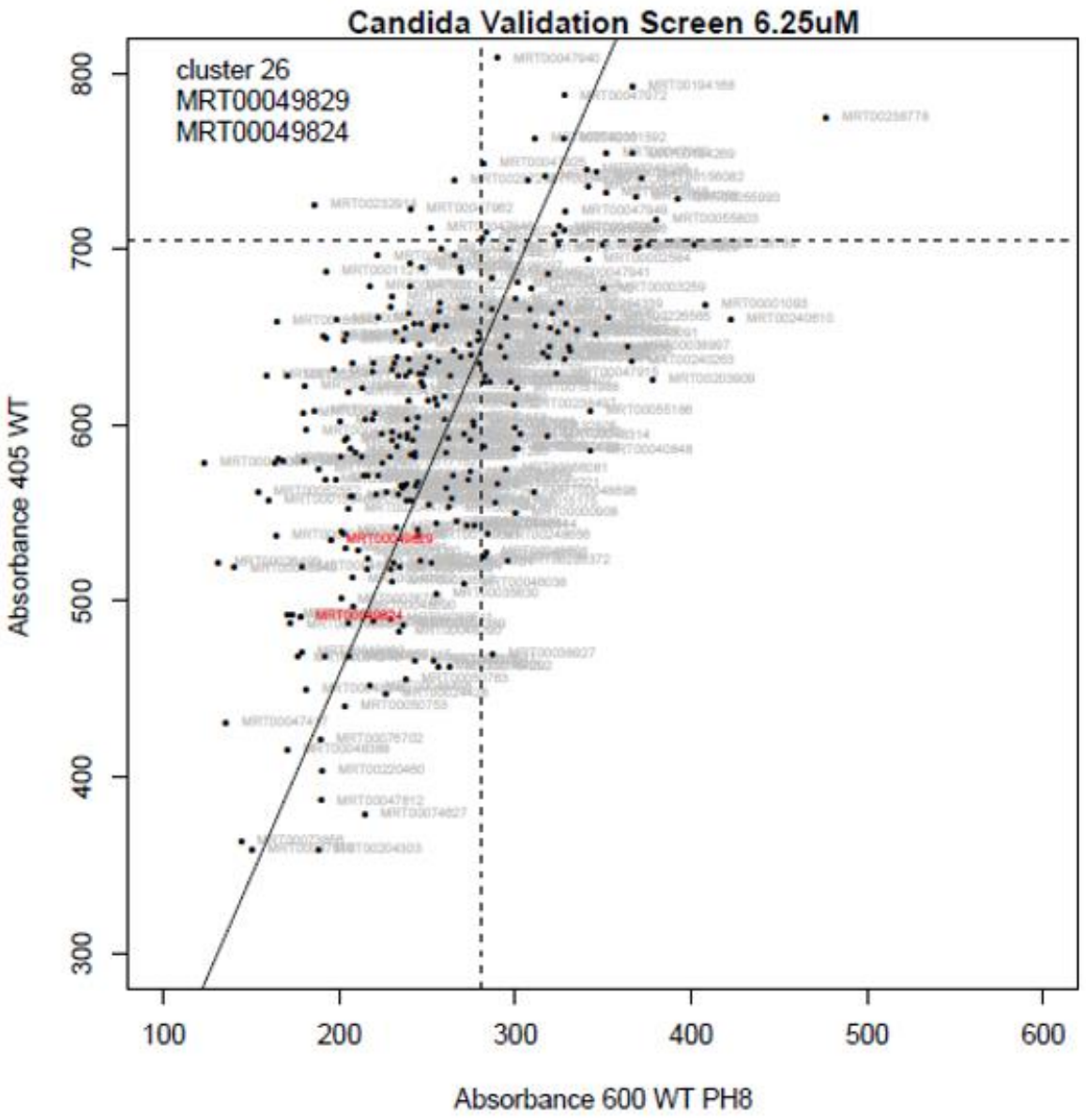

Cluster 26: 6.25 µM Secondary Screen: pH8 as a readout for PHO Pathway activity.
Plot of OD_{600} *wt* cells grown in pH 8 vs. OD_{405} of *wt* cells. Cells were grown to log phase in YPD before being washed 3 times in pH8 media and diluted back to OD_{600} = 0.05 then seeded into 384 well plates containing 6.25 µM of compound. Absorbance of 600 nm is used for growth at pH and 405 for secreted acid phosphatase activity. Red hits represent those from cluster 26.

Cluster 27

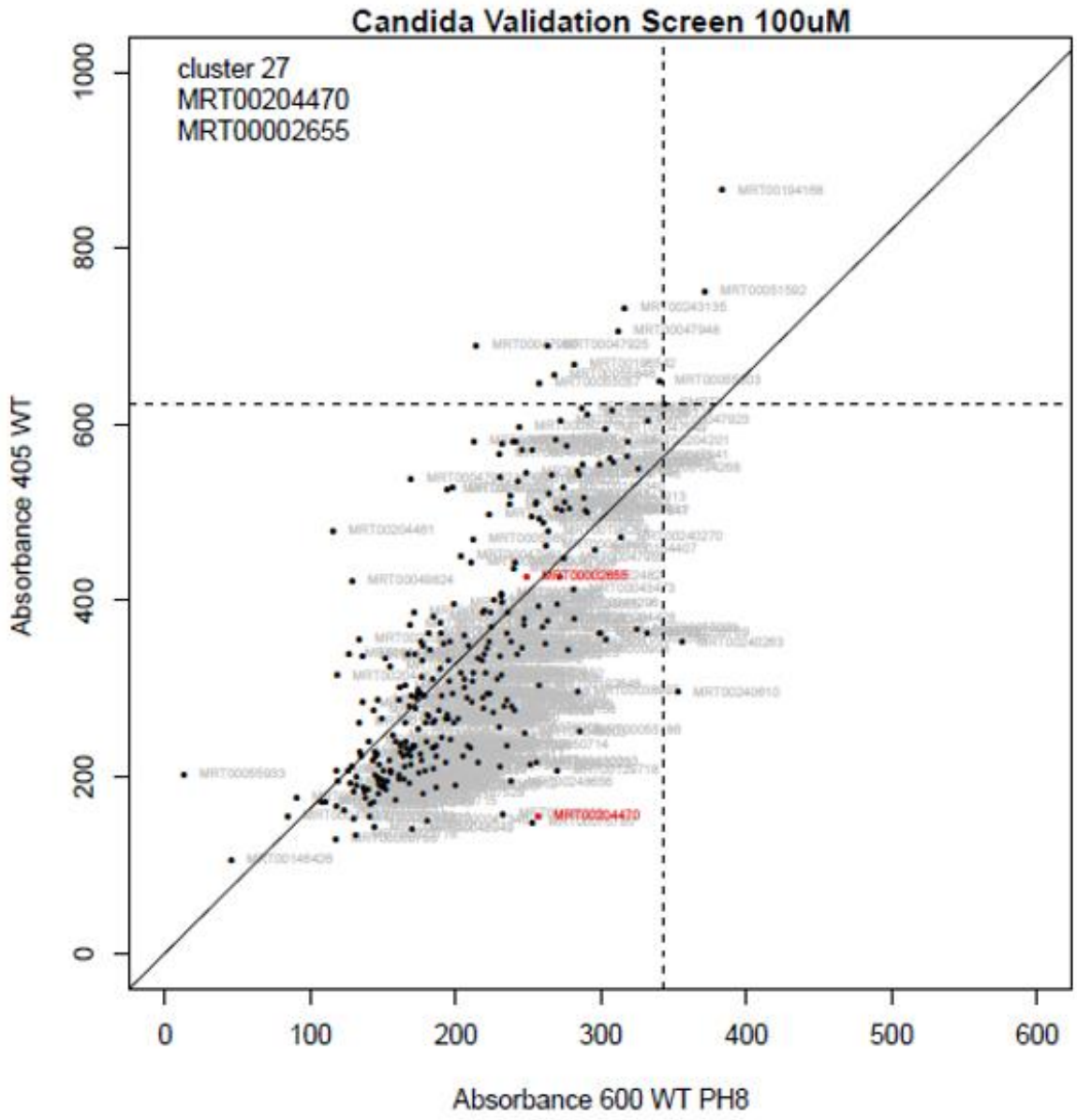

Cluster 27: 100 µM Secondary Screen: pH8 as a readout for PHO Pathway activity.
Plot of OD_{600} *wt* cells grown in pH 8 vs. OD_{405} of *wt* cells. Cells were grown to log phase in YPD before being washed 3 times in pH8 media and diluted back to OD_{600} = 0.05 then seeded into 384 well plates containing 100 µM of compound. Absorbance of 600 nm is used for growth at pH and 405 for secreted acid phosphatase activity. Red hits represent those from cluster 27.

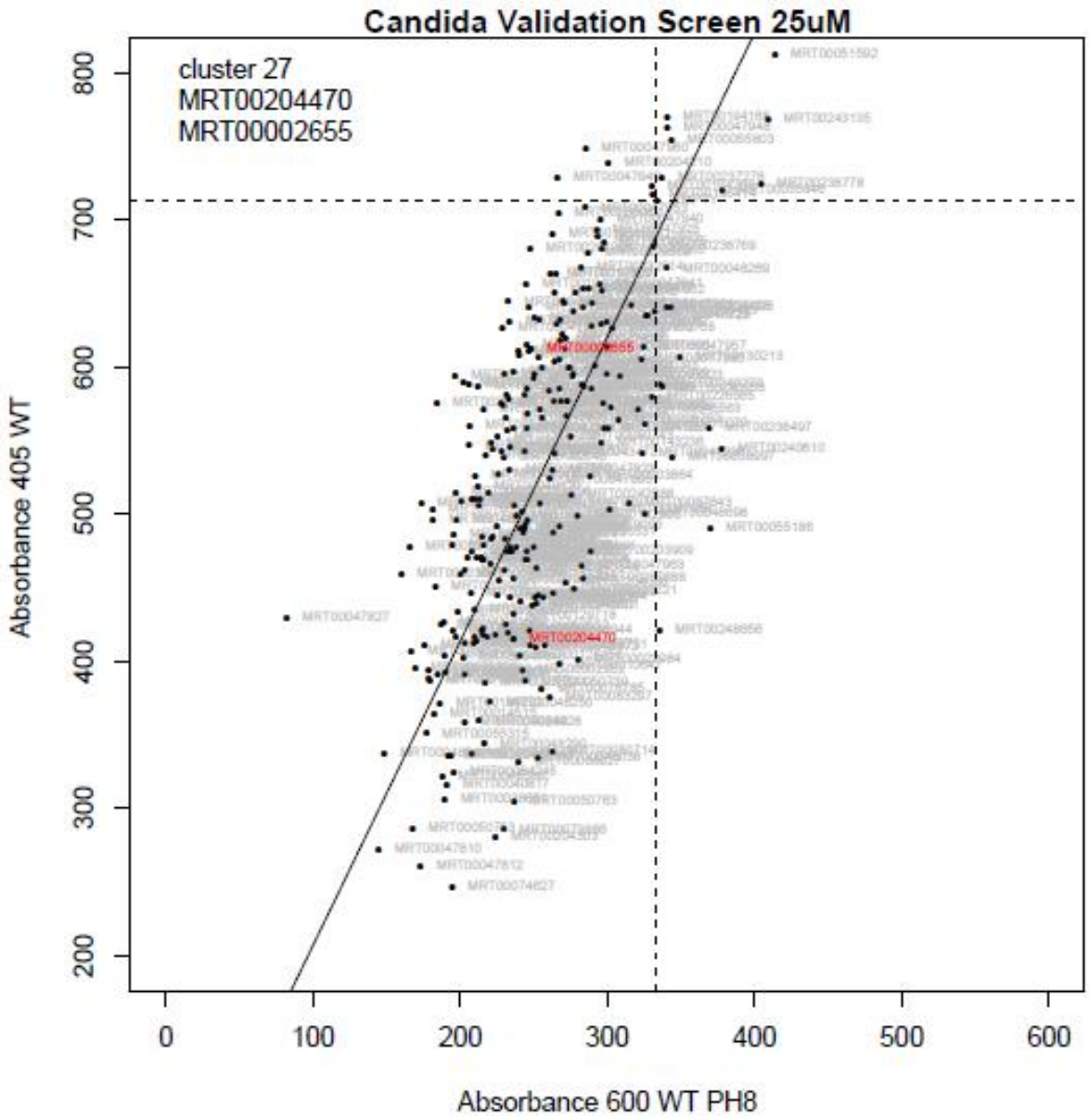

Cluster 27: 25 µM Secondary Screen: pH8 as a readout for PHO Pathway activity.
Plot of OD_{600} *wt* cells grown in pH 8 vs. OD_{405} of *wt* cells. Cells were grown to log phase in YPD before being washed 3 times in pH8 media and diluted back to OD_{600} = 0.05 then seeded into 384 well plates containing 25 µM of compound. Absorbance of 600 nm is used for growth at pH and 405 for secreted acid phosphatase activity. Red hits represent those from cluster 27.

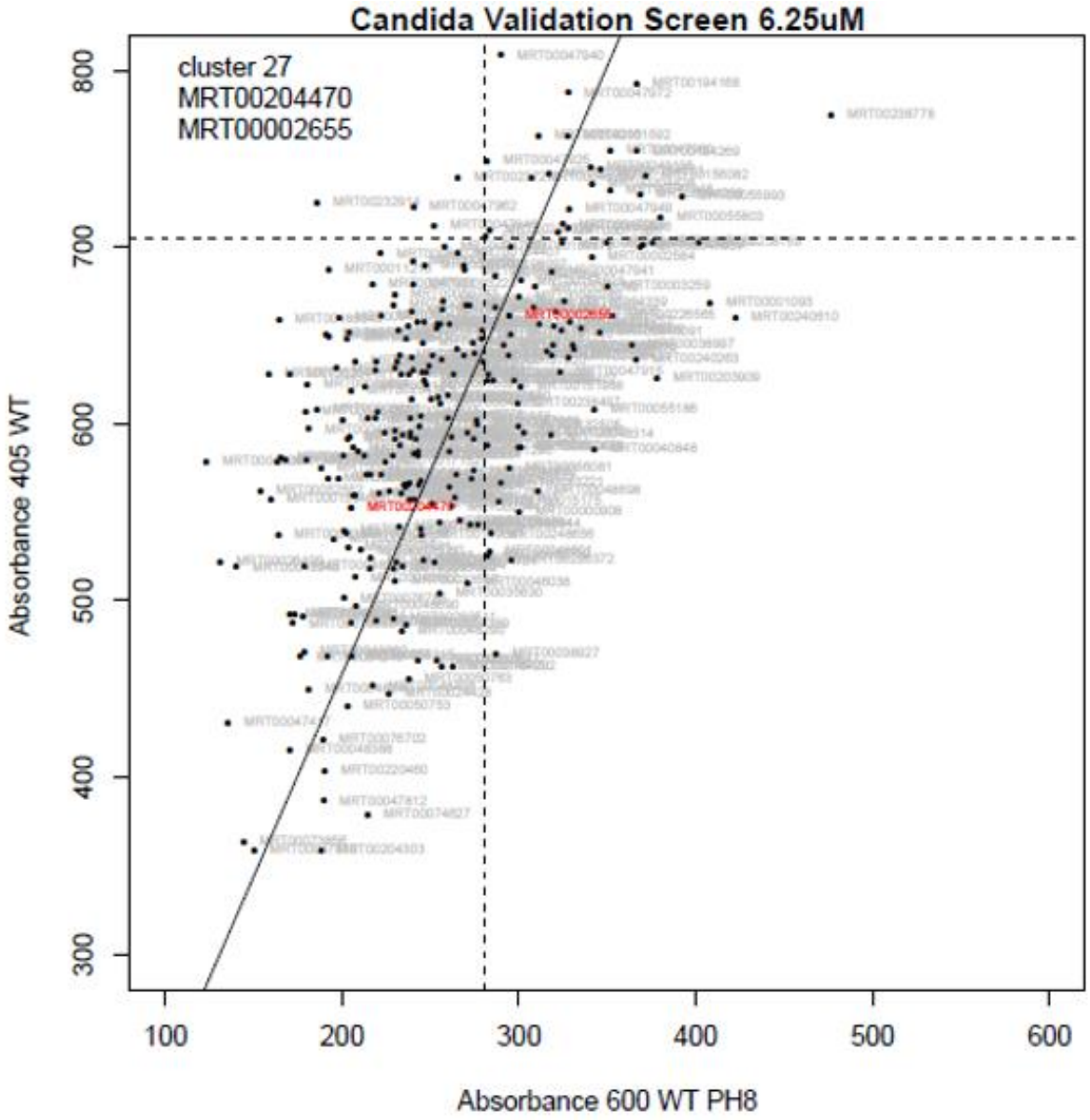

Cluster 27: 6.25 µM Secondary Screen: pH8 as a readout for PHO Pathway activity.
Plot of OD_{600} *wt* cells grown in pH 8 vs. OD_{405} of *wt* cells. Cells were grown to log phase in YPD before being washed 3 times in pH8 media and diluted back to OD_{600} = 0.05 then seeded into 384 well plates containing 6.25 µM of compound. Absorbance of 600 nm is used for growth at pH and 405 for secreted acid phosphatase activity. Red hits represent those from cluster 27.

Cluster 28

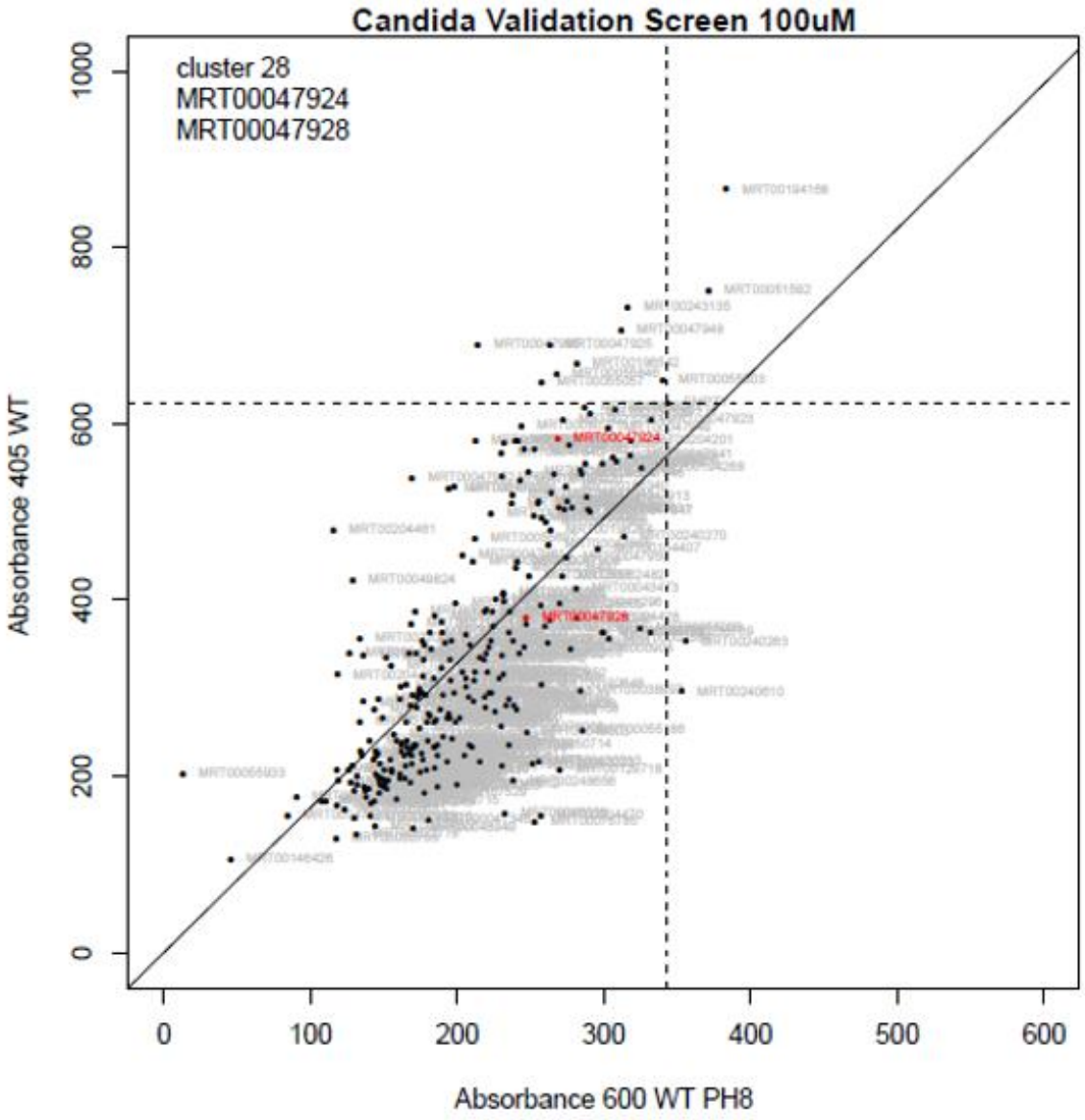

Cluster 28: 100 µM Secondary Screen: pH8 as a readout for PHO Pathway activity.
Plot of OD_{600} *wt* cells grown in pH 8 vs. OD_{405} of *wt* cells. Cells were grown to log phase in YPD before being washed 3 times in pH8 media and diluted back to OD_{600} = 0.05 then seeded into 384 well plates containing 100 µM of compound. Absorbance of 600 nm is used for growth at pH and 405 for secreted acid phosphatase activity. Red hits represent those from cluster 28.

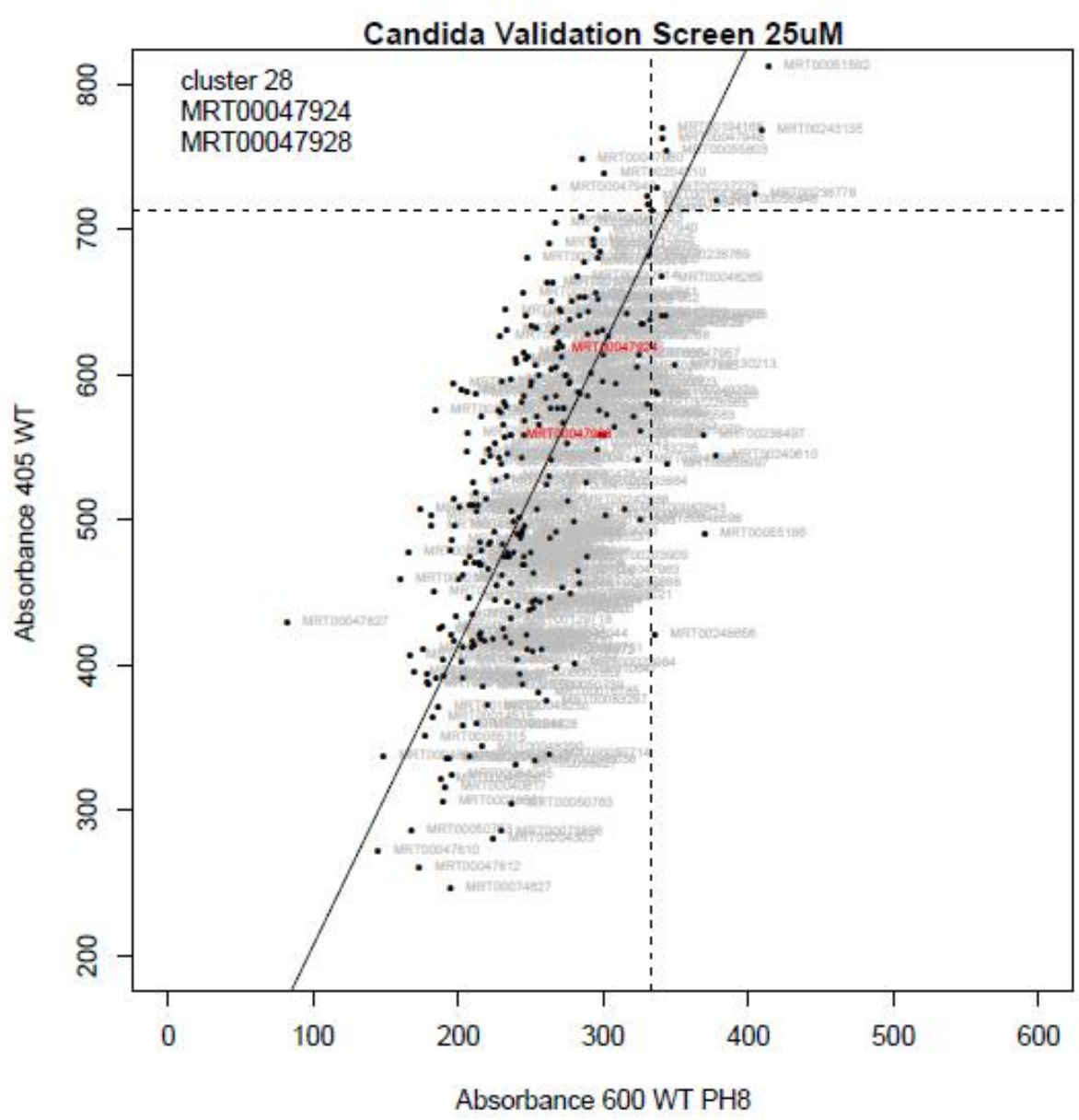

Cluster 28: 25 µM Secondary Screen: pH8 as a readout for PHO Pathway activity.
Plot of OD_{600} *wt* cells grown in pH 8 vs. OD_{405} of *wt* cells. Cells were grown to log phase in YPD before being washed 3 times in pH8 media and diluted back to OD_{600} = 0.05 then seeded into 384 well plates containing 25 µM of compound. Absorbance of 600 nm is used for growth at pH and 405 for secreted acid phosphatase activity. Red hits represent those from cluster 28.

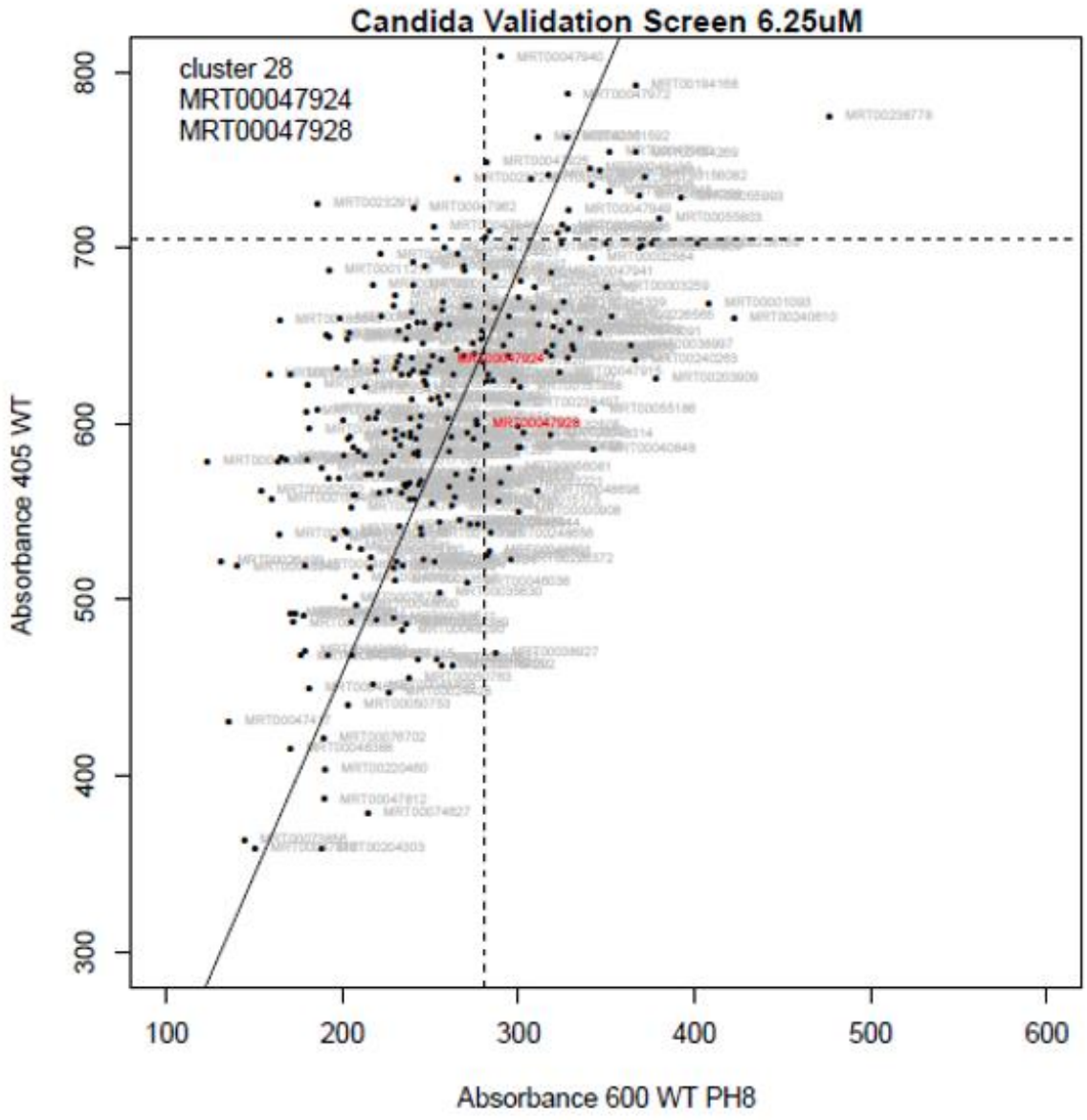

Cluster 28: 6.25 µM Secondary Screen: pH8 as a readout for PHO Pathway activity.
Plot of OD_{600} *wt* cells grown in pH 8 vs. OD_{405} of *wt* cells. Cells were grown to log phase in YPD before being washed 3 times in pH8 media and diluted back to OD_{600} = 0.05 then seeded into 384 well plates containing 6.25 µM of compound. Absorbance of 600 nm is used for growth at pH and 405 for secreted acid phosphatase activity. Red hits represent those from cluster 28.

Cluster 29

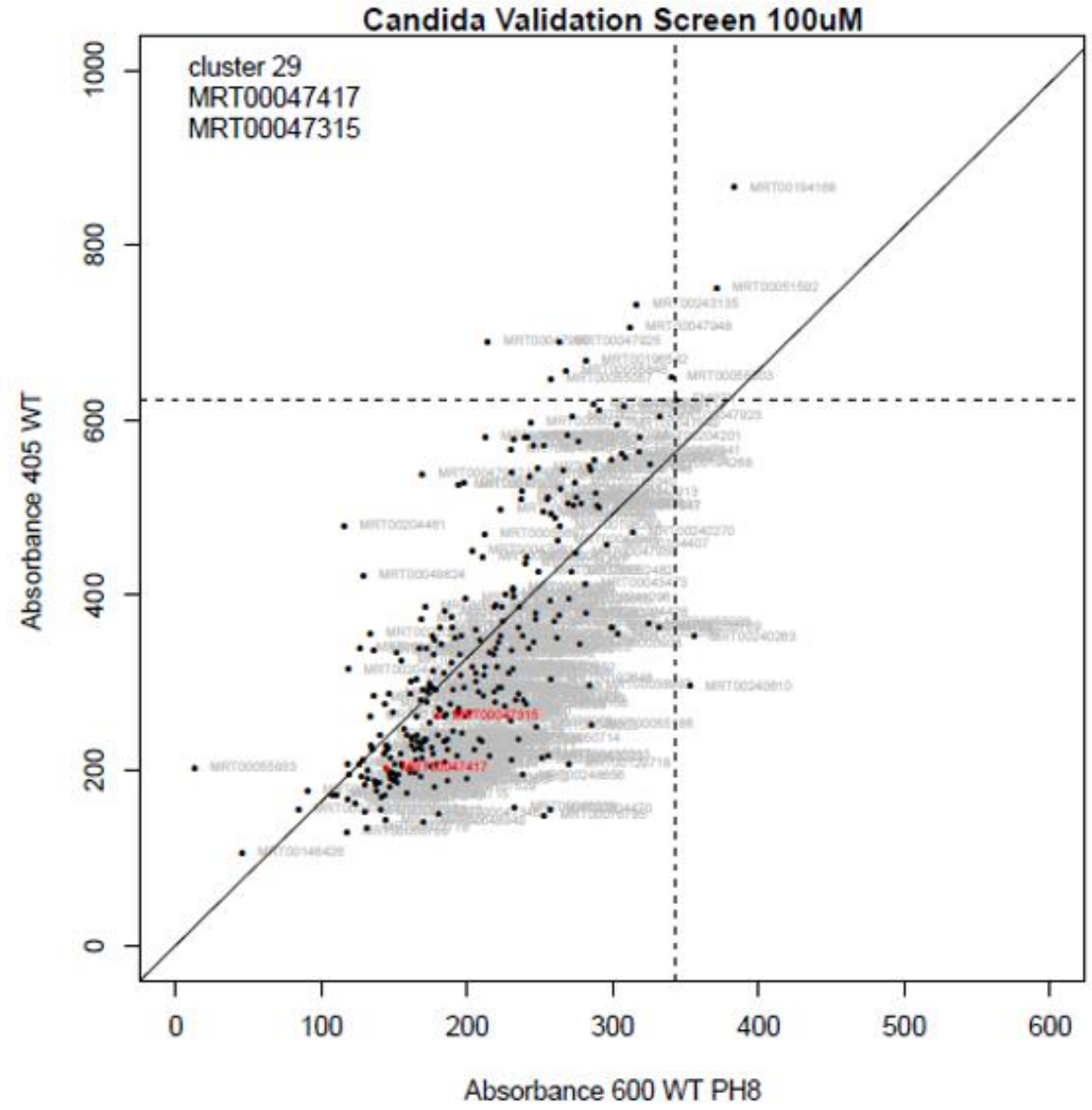

Cluster 29: 100 µM Secondary Screen: pH8 as a readout for PHO Pathway activity.
Plot of OD_{600} *wt* cells grown in pH 8 vs. OD_{405} of *wt* cells. Cells were grown to log phase in YPD before being washed 3 times in pH8 media and diluted back to OD_{600} = 0.05 then seeded into 384 well plates containing 100 µM of compound. Absorbance of 600 nm is used for growth at pH and 405 for secreted acid phosphatase activity. Red hits represent those from cluster 29.

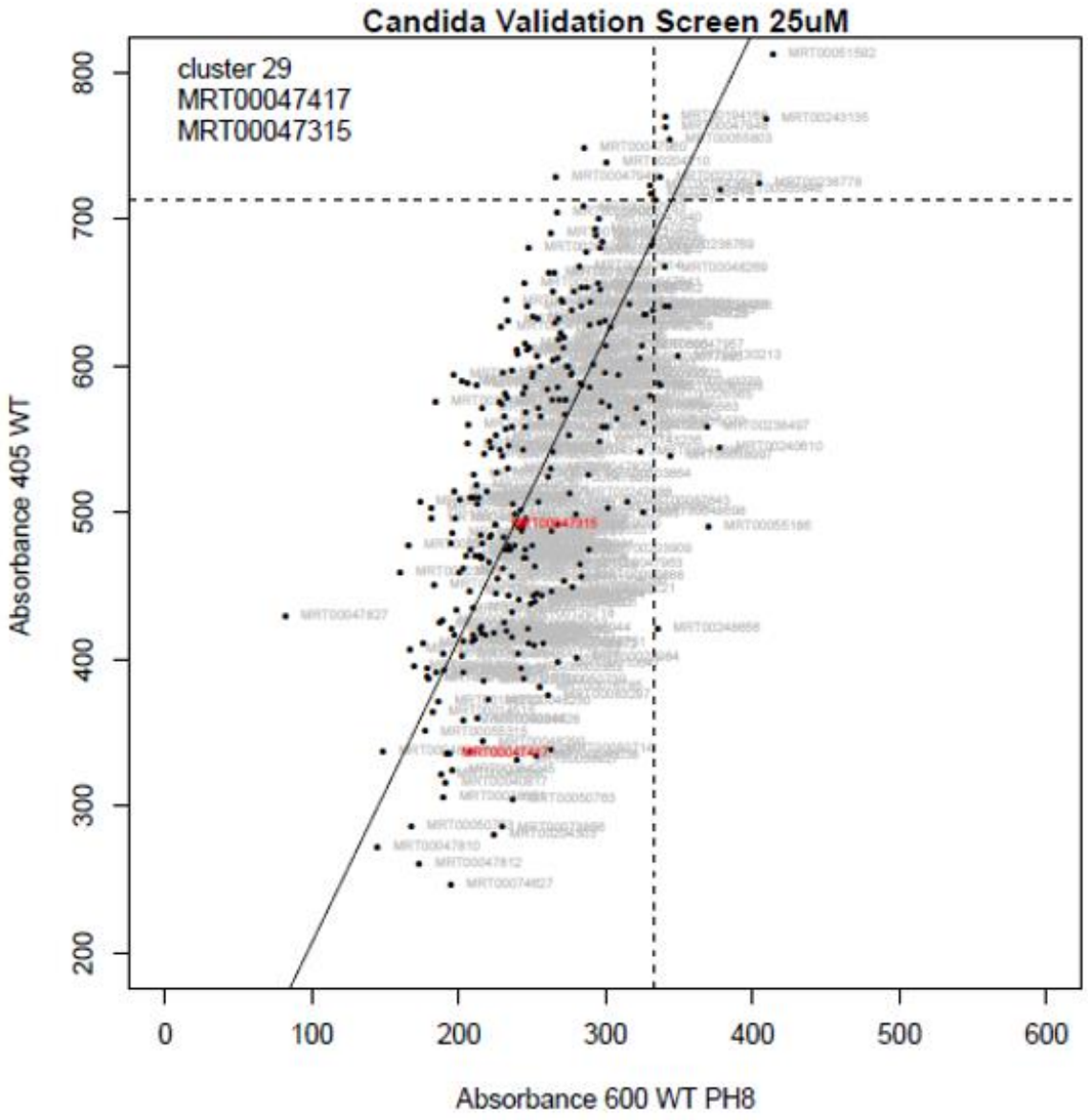

Cluster 29: 25 µM Secondary Screen: pH8 as a readout for PHO Pathway activity.
Plot of OD_{600} *wt* cells grown in pH 8 vs. OD_{405} of *wt* cells. Cells were grown to log phase in YPD before being washed 3 times in pH8 media and diluted back to OD_{600} = 0.05 then seeded into 384 well plates containing 25 µM of compound. Absorbance of 600 nm is used for growth at pH and 405 for secreted acid phosphatase activity. Red hits represent those from cluster 29.

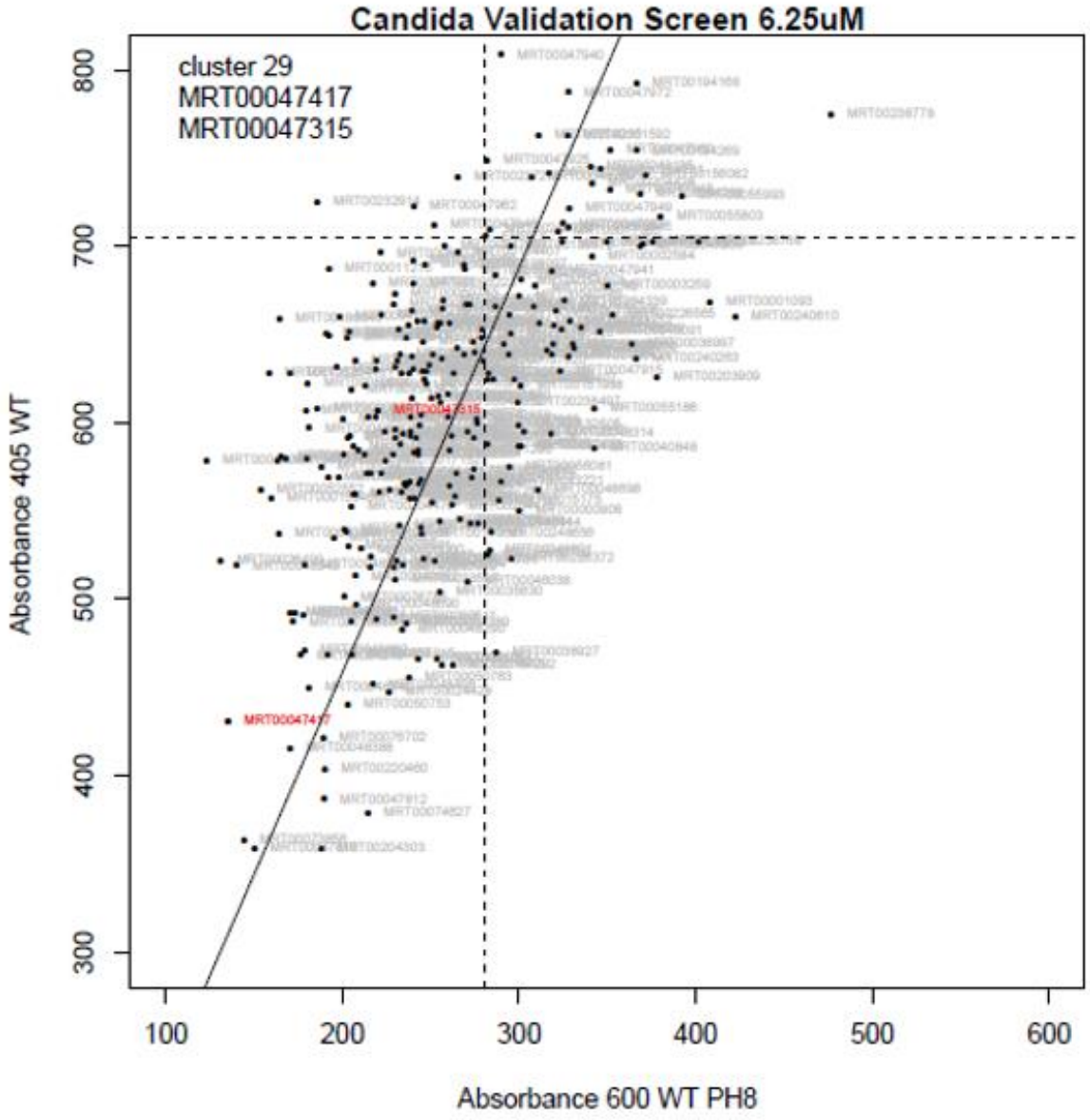

Cluster 29: 6.25 µM Secondary Screen: pH8 as a readout for PHO Pathway activity.
Plot of OD_{600} *wt* cells grown in pH 8 vs. OD_{405} of *wt* cells. Cells were grown to log phase in YPD before being washed 3 times in pH8 media and diluted back to OD_{600} = 0.05 then seeded into 384 well plates containing 6.25 µM of compound. Absorbance of 600 nm is used for growth at pH and 405 for secreted acid phosphatase activity. Red hits represent those from cluster 29.

Cluster 33

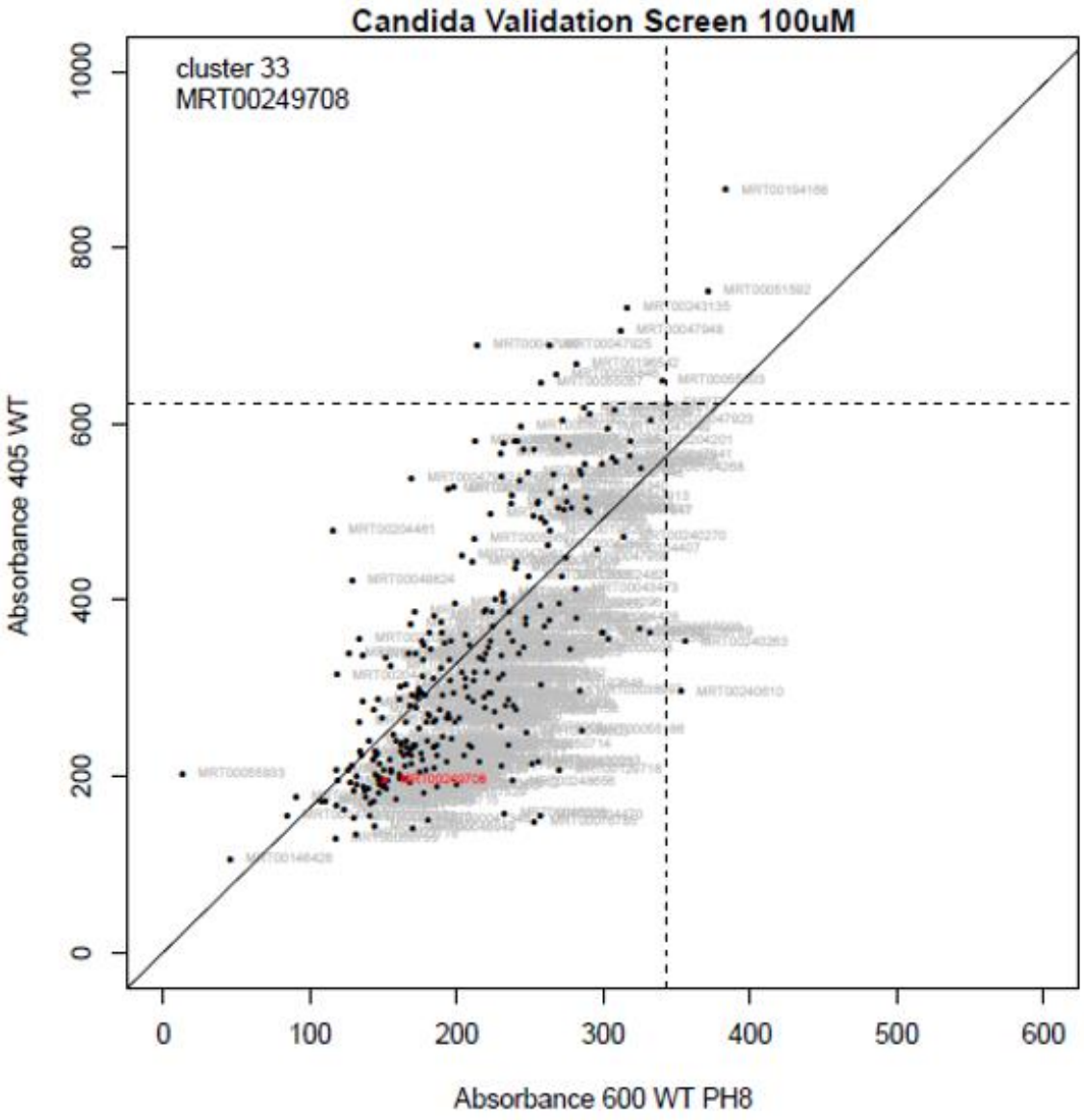

Cluster 33: 100 µM Secondary Screen: pH8 as a readout for PHO Pathway activity.
Plot of OD_{600} *wt* cells grown in pH 8 vs. OD_{405} of *wt* cells. Cells were grown to log phase in YPD before being washed 3 times in pH8 media and diluted back to OD_{600} = 0.05 then seeded into 384 well plates containing 100 µM of compound. Absorbance of 600 nm is used for growth at pH and 405 for secreted acid phosphatase activity. Red hits represent those from cluster 33.

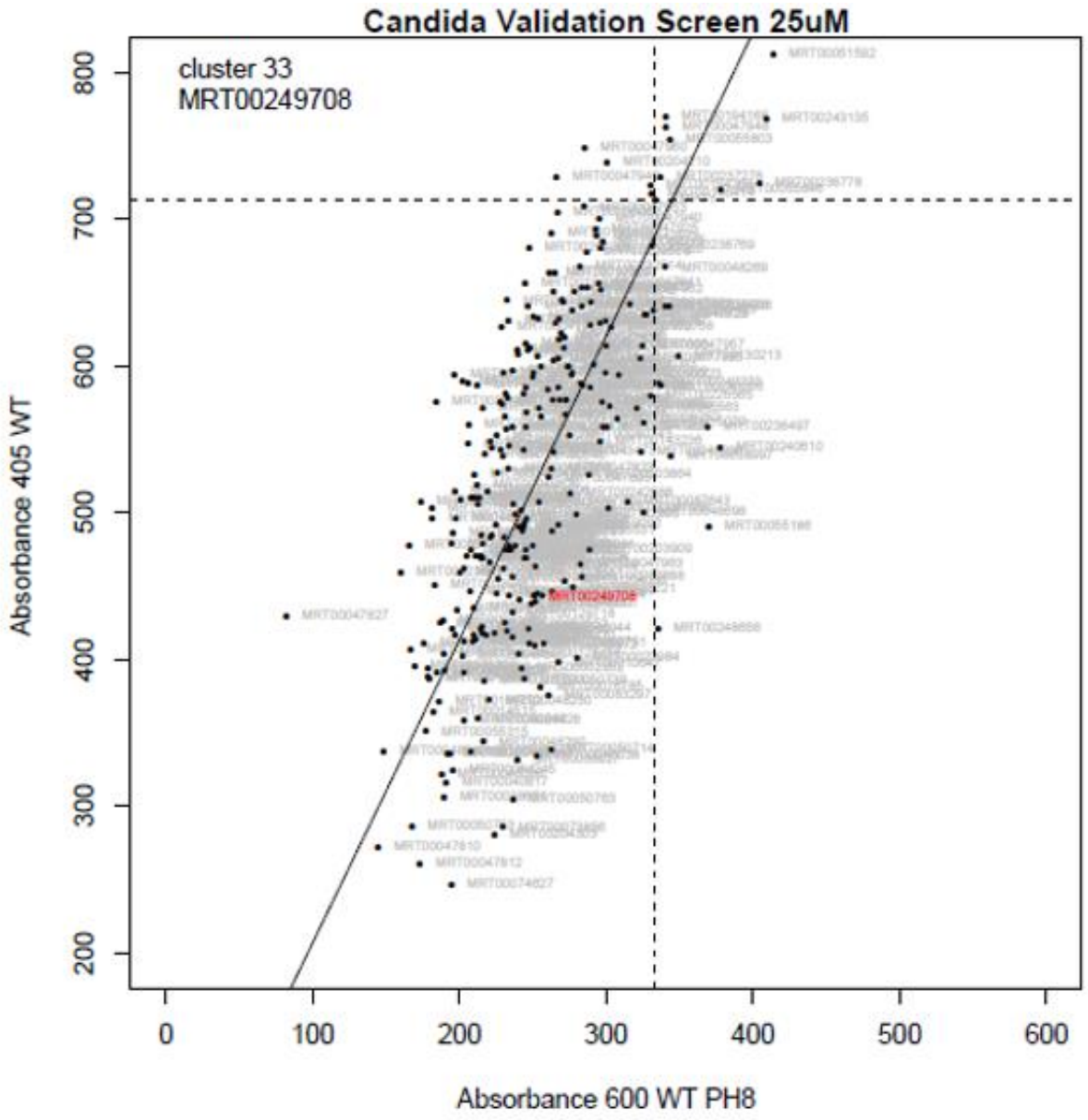

Cluster 33: 25 µM Secondary Screen: pH8 as a readout for PHO Pathway activity.
Plot of OD_{600} *wt* cells grown in pH 8 vs. OD_{405} of *wt* cells. Cells were grown to log phase in YPD before being washed 3 times in pH8 media and diluted back to OD_{600} = 0.05 then seeded into 384 well plates containing 25 µM of compound. Absorbance of 600 nm is used for growth at pH and 405 for secreted acid phosphatase activity. Red hits represent those from cluster 33.

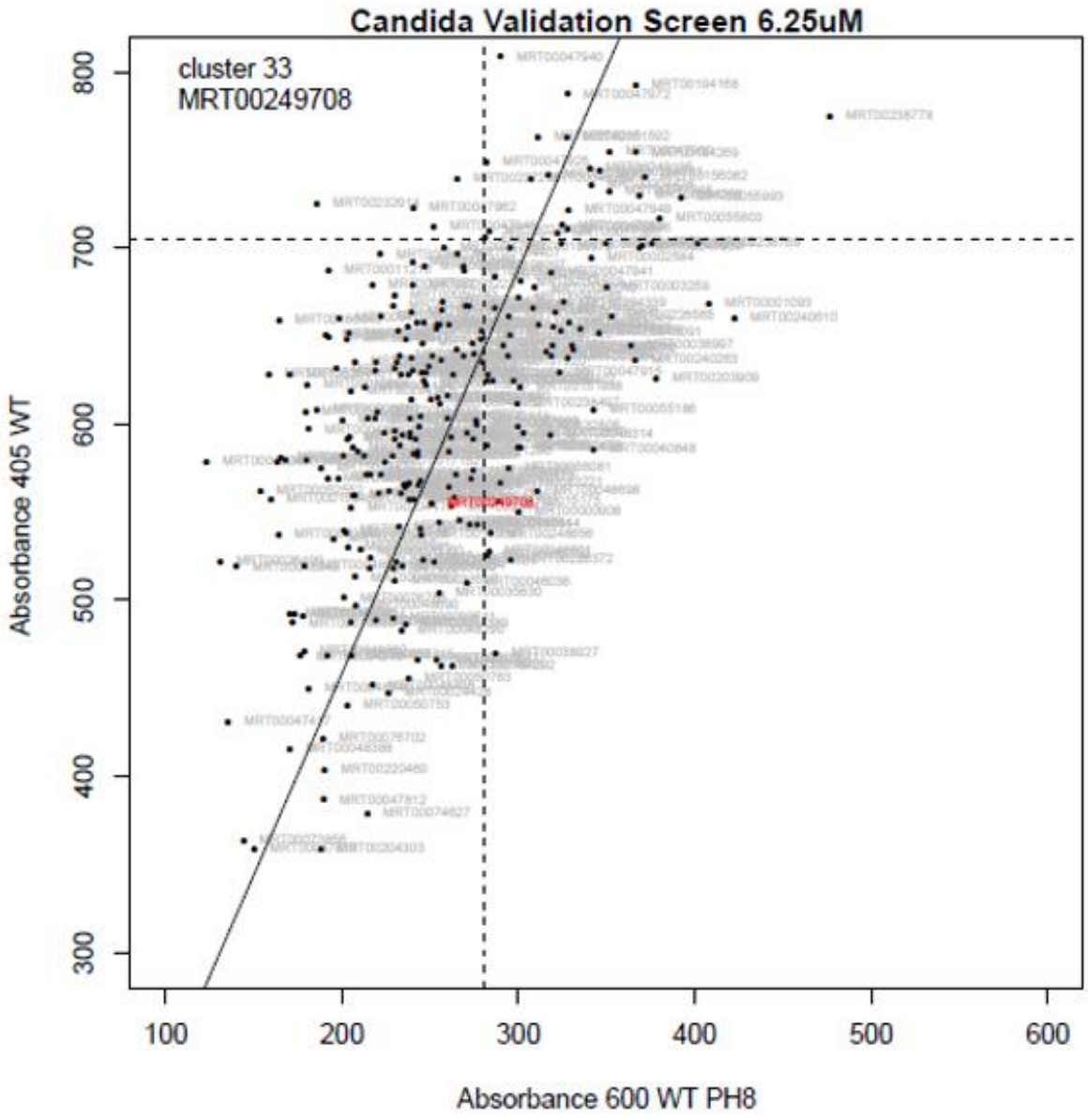

Cluster 33: 6.25 µM Secondary Screen: pH8 as a readout for PHO Pathway activity.
Plot of OD_{600} *wt* cells grown in pH 8 vs. OD_{405} of *wt* cells. Cells were grown to log phase in YPD before being washed 3 times in pH8 media and diluted back to OD_{600} = 0.05 then seeded into 384 well plates containing 6.25 µM of compound. Absorbance of 600 nm is used for growth at pH and 405 for secreted acid phosphatase activity. Red hits represent those from cluster 33.

Cluster 39

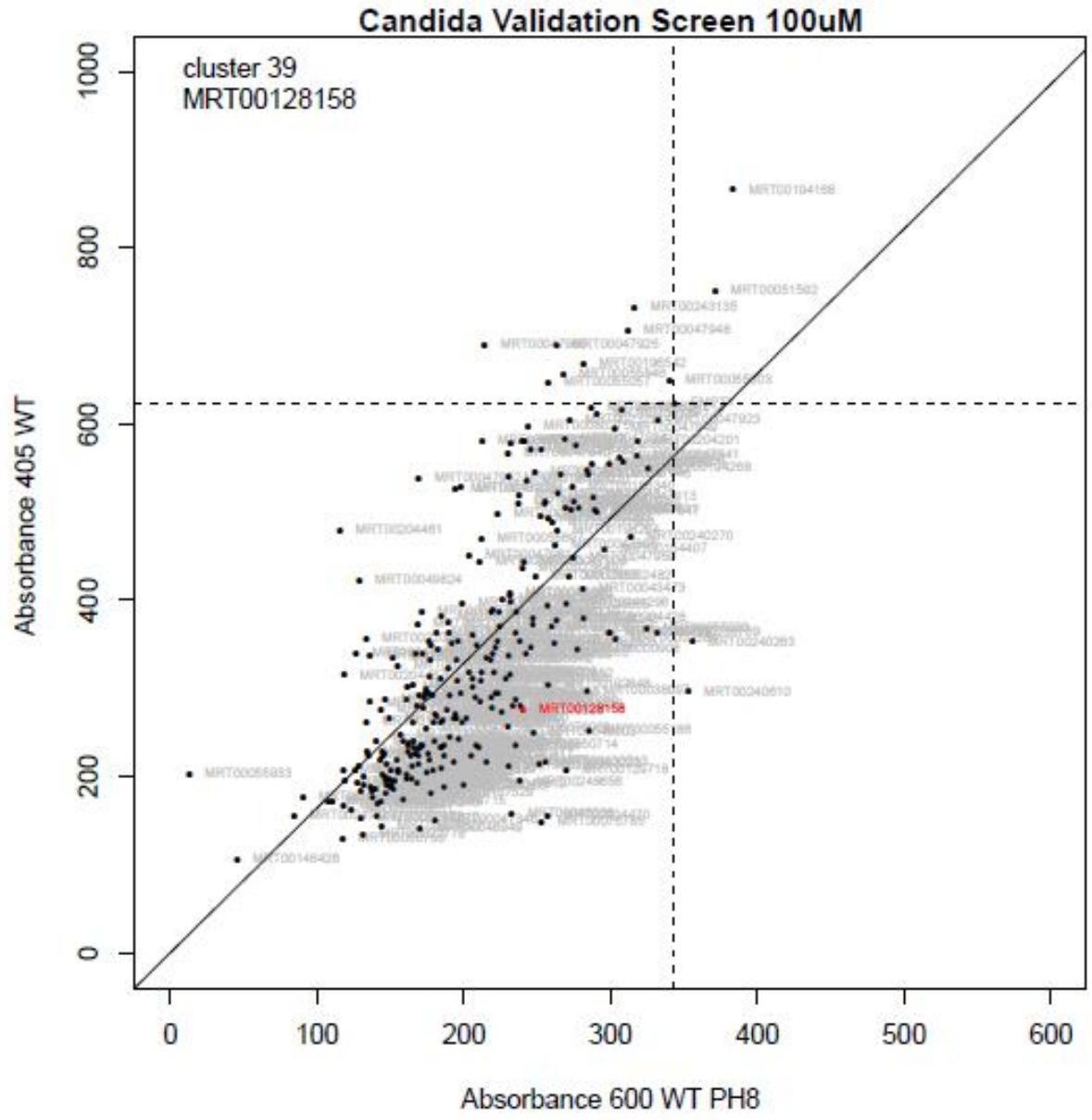

Cluster 39: 100 µM Secondary Screen: pH8 as a readout for PHO Pathway activity.
Plot of OD_{600} *wt* cells grown in pH 8 vs. OD_{405} of *wt* cells. Cells were grown to log phase in YPD before being washed 3 times in pH8 media and diluted back to OD_{600} = 0.05 then seeded into 384 well plates containing 100 µM of compound. Absorbance of 600 nm is used for growth at pH and 405 for secreted acid phosphatase activity. Red hits represent those from cluster 39.

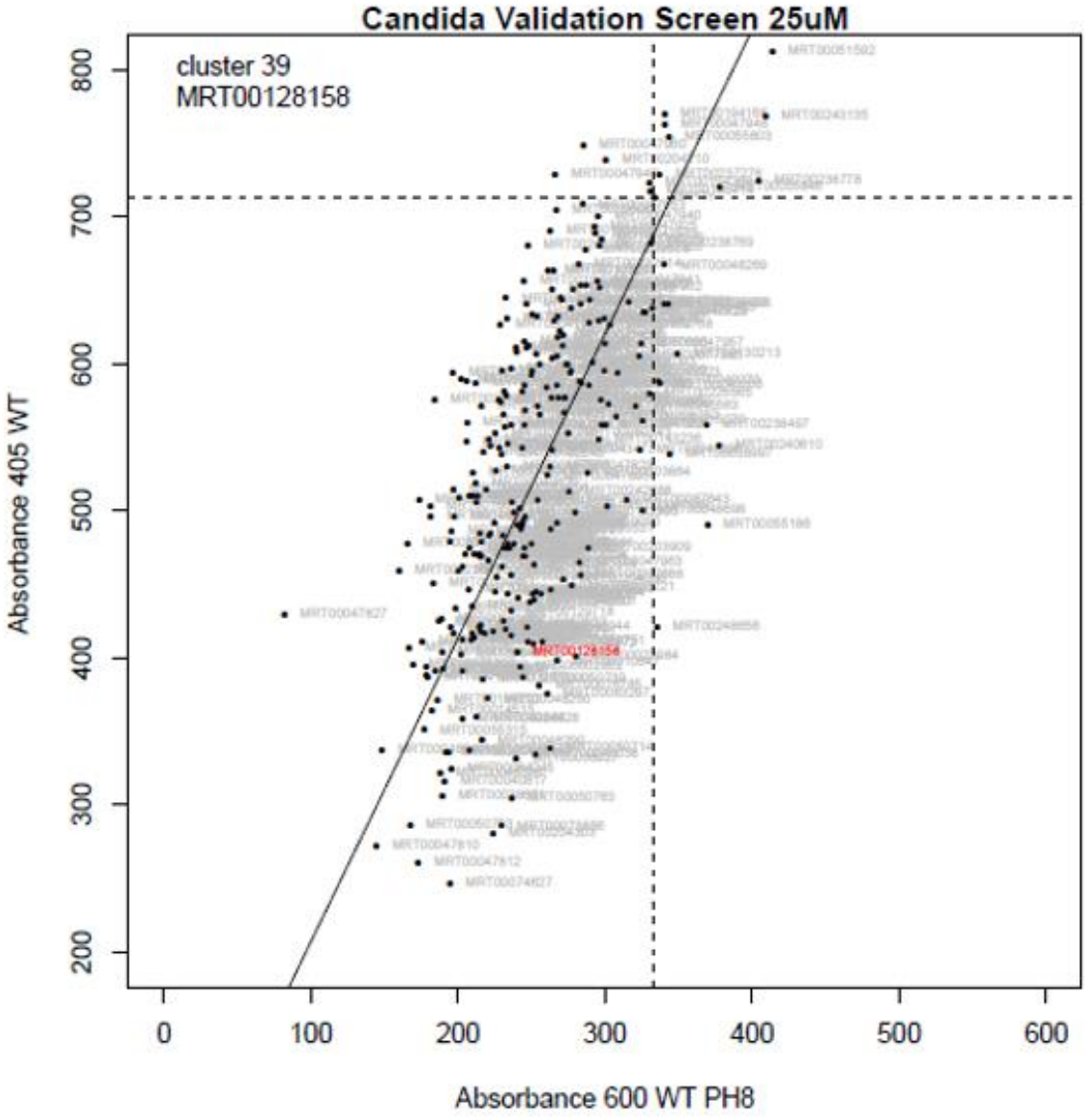

Cluster 39: 25 µM Secondary Screen: pH8 as a readout for PHO Pathway activity.
Plot of OD_{600} *wt* cells grown in pH 8 vs. OD_{405} of *wt* cells. Cells were grown to log phase in YPD before being washed 3 times in pH8 media and diluted back to OD_{600} = 0.05 then seeded into 384 well plates containing 25 µM of compound. Absorbance of 600 nm is used for growth at pH and 405 for secreted acid phosphatase activity. Red hits represent those from cluster 39.

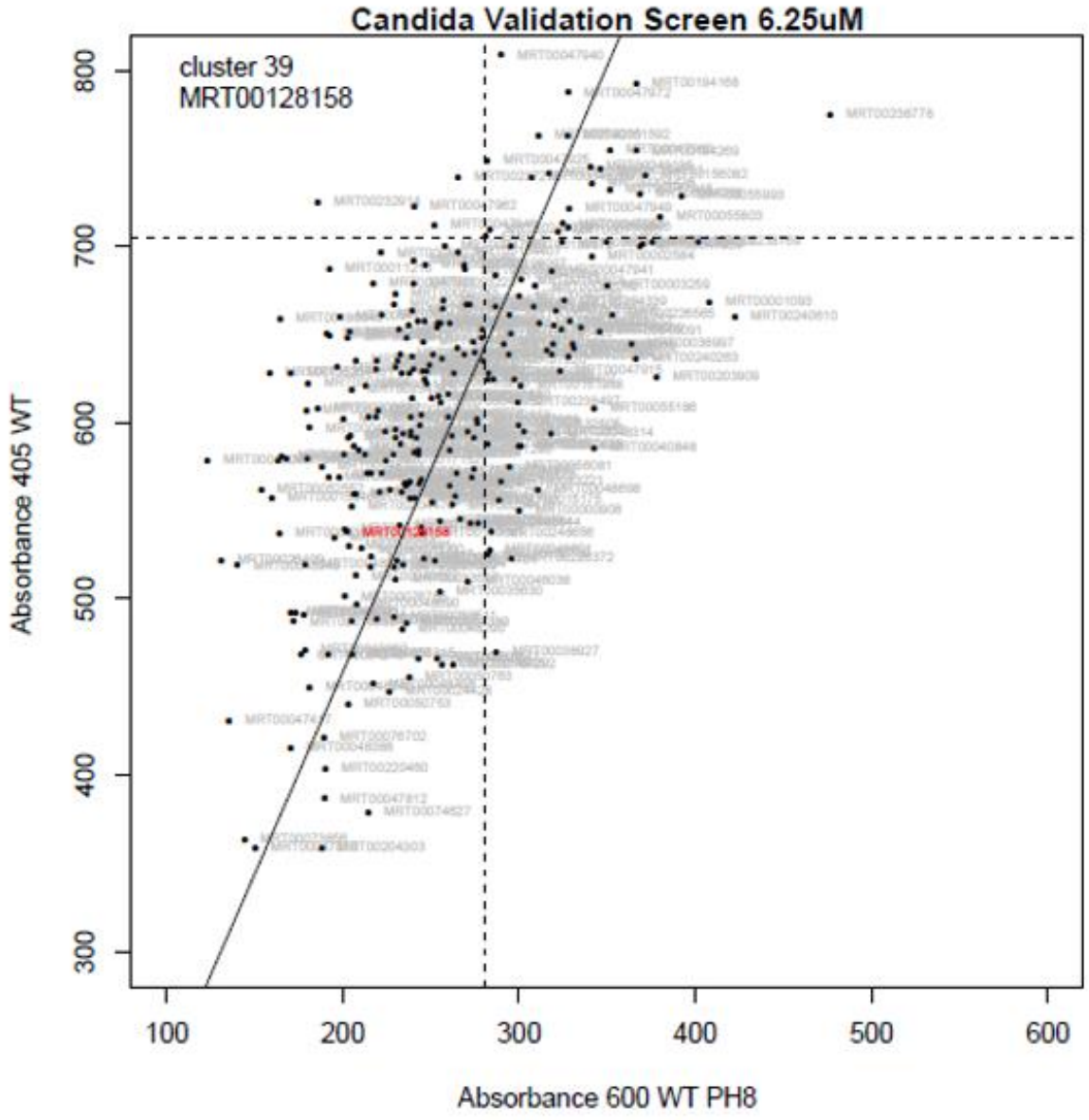

Cluster 39: 6.25 µM Secondary Screen: pH8 as a readout for PHO Pathway activity.
Plot of OD_{600} *wt* cells grown in pH 8 vs. OD_{405} of *wt* cells. Cells were grown to log phase in YPD before being washed 3 times in pH8 media and diluted back to OD_{600} = 0.05 then seeded into 384 well plates containing 6.25 µM of compound. Absorbance of 600 nm is used for growth at pH and 405 for secreted acid phosphatase activity. Red hits represent those from cluster 39.

Cluster 44

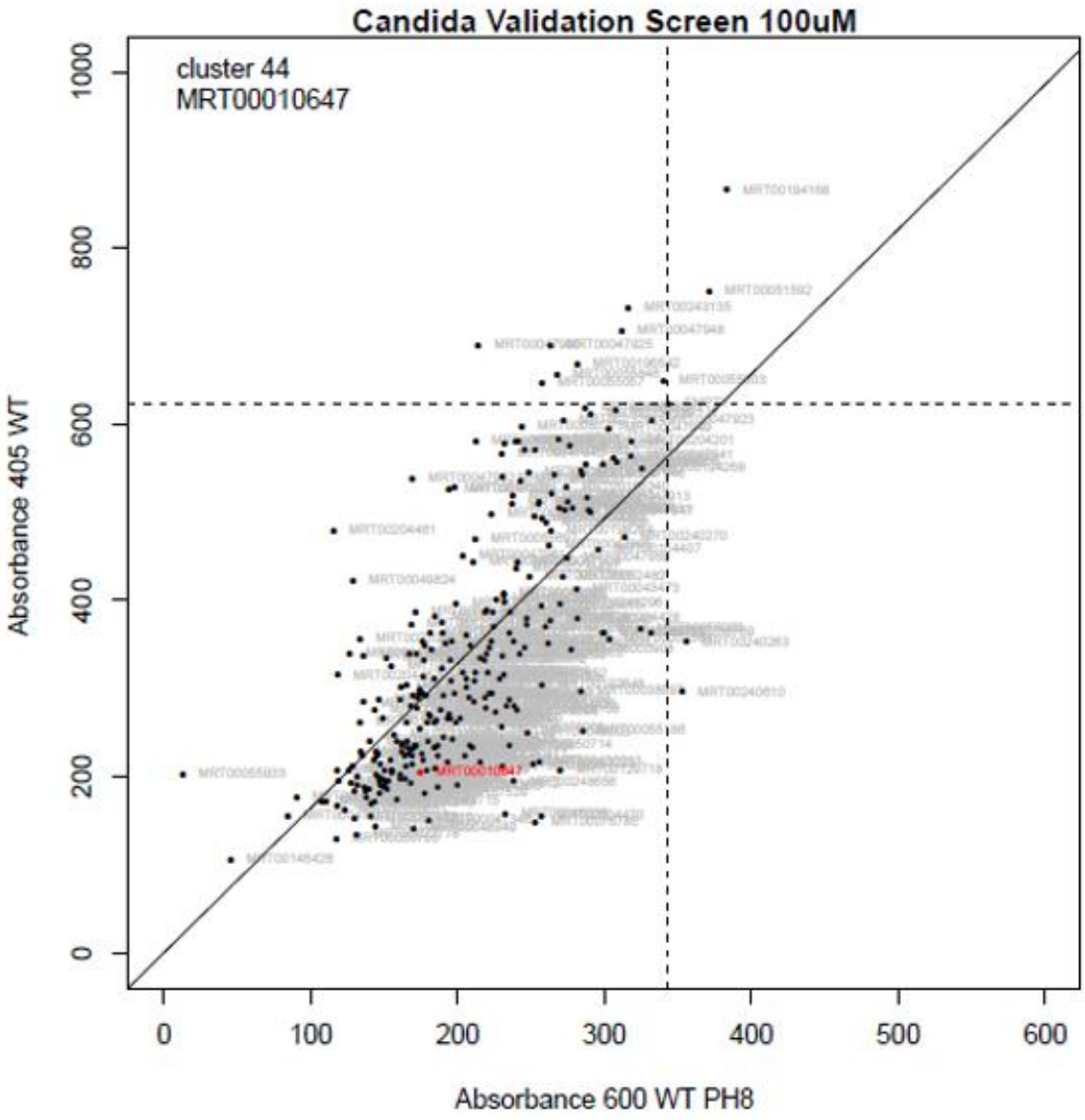

Cluster 44: 100 µM Secondary Screen: pH8 as a readout for PHO Pathway activity.
Plot of OD_{600} *wt* cells grown in pH 8 vs. OD_{405} of *wt* cells. Cells were grown to log phase in YPD before being washed 3 times in pH8 media and diluted back to OD_{600} = 0.05 then seeded into 384 well plates containing 100 µM of compound. Absorbance of 600 nm is used for growth at pH and 405 for secreted acid phosphatase activity. Red hits represent those from cluster 44.

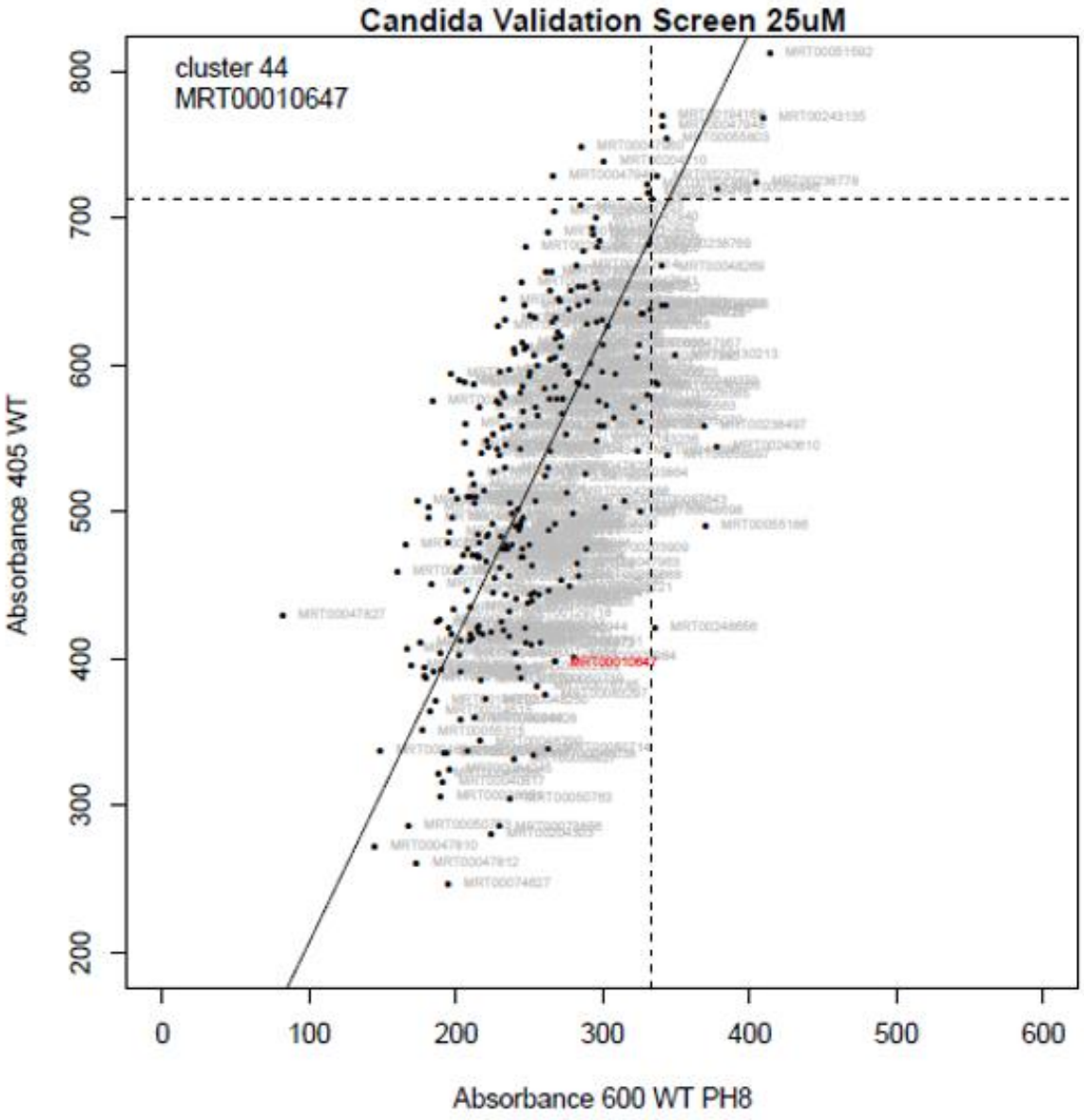

Cluster 44: 25 µM Secondary Screen: pH8 as a readout for PHO Pathway activity.
Plot of OD_{600} *wt* cells grown in pH 8 vs. OD_{405} of *wt* cells. Cells were grown to log phase in YPD before being washed 3 times in pH8 media and diluted back to OD_{600} = 0.05 then seeded into 384 well plates containing 25 µM of compound. Absorbance of 600 nm is used for growth at pH and 405 for secreted acid phosphatase activity. Red hits represent those from cluster 44.

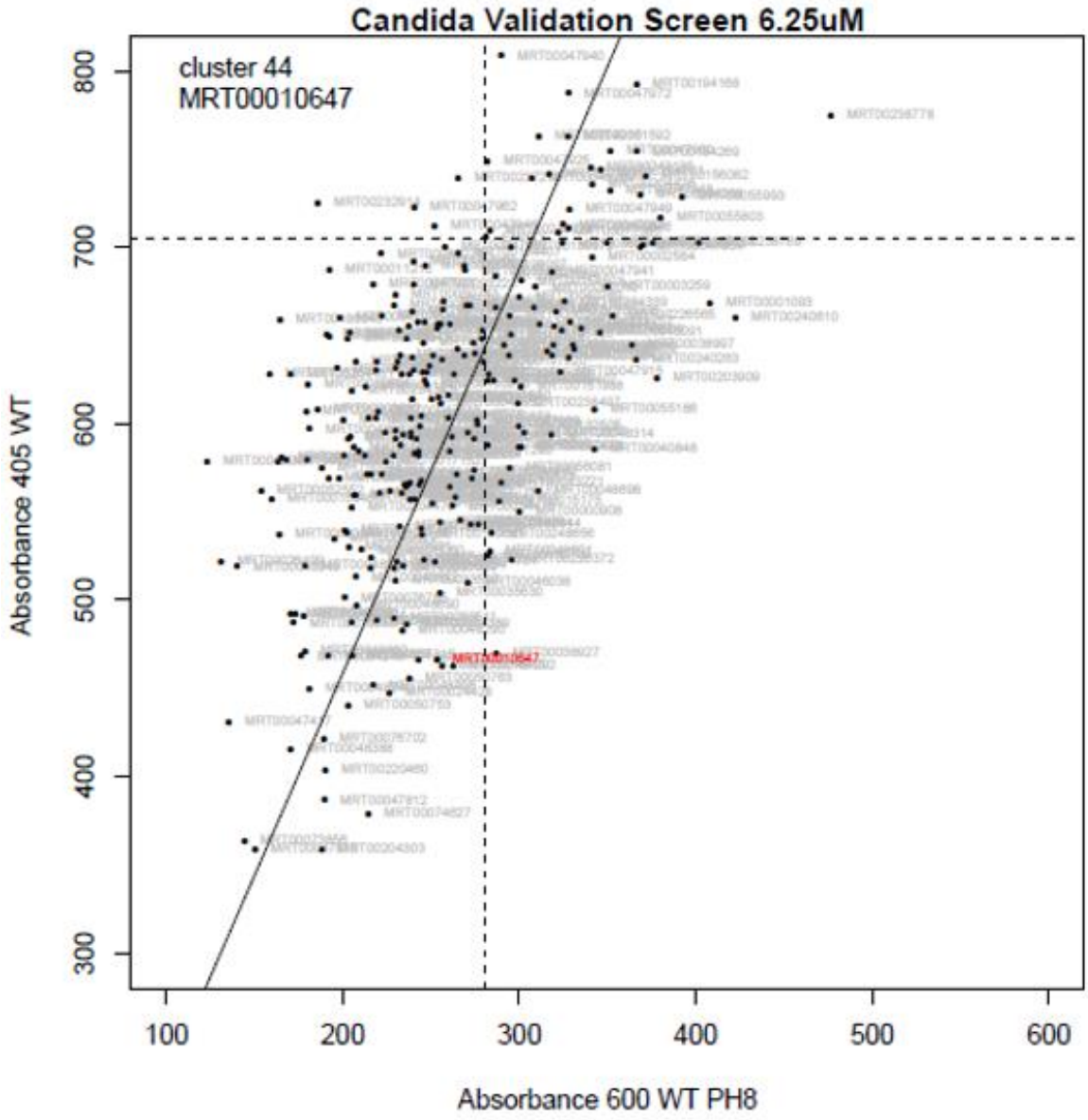

Cluster 44: 6.25 µM Secondary Screen: pH8 as a readout for PHO Pathway activity.
Plot of OD_{600} *wt* cells grown in pH 8 vs. OD_{405} of *wt* cells. Cells were grown to log phase in YPD before being washed 3 times in pH8 media and diluted back to OD_{600} = 0.05 then seeded into 384 well plates containing 6.25 µM of compound. Absorbance of 600 nm is used for growth at pH and 405 for secreted acid phosphatase activity. Red hits represent those from cluster 44.

Cluster 51

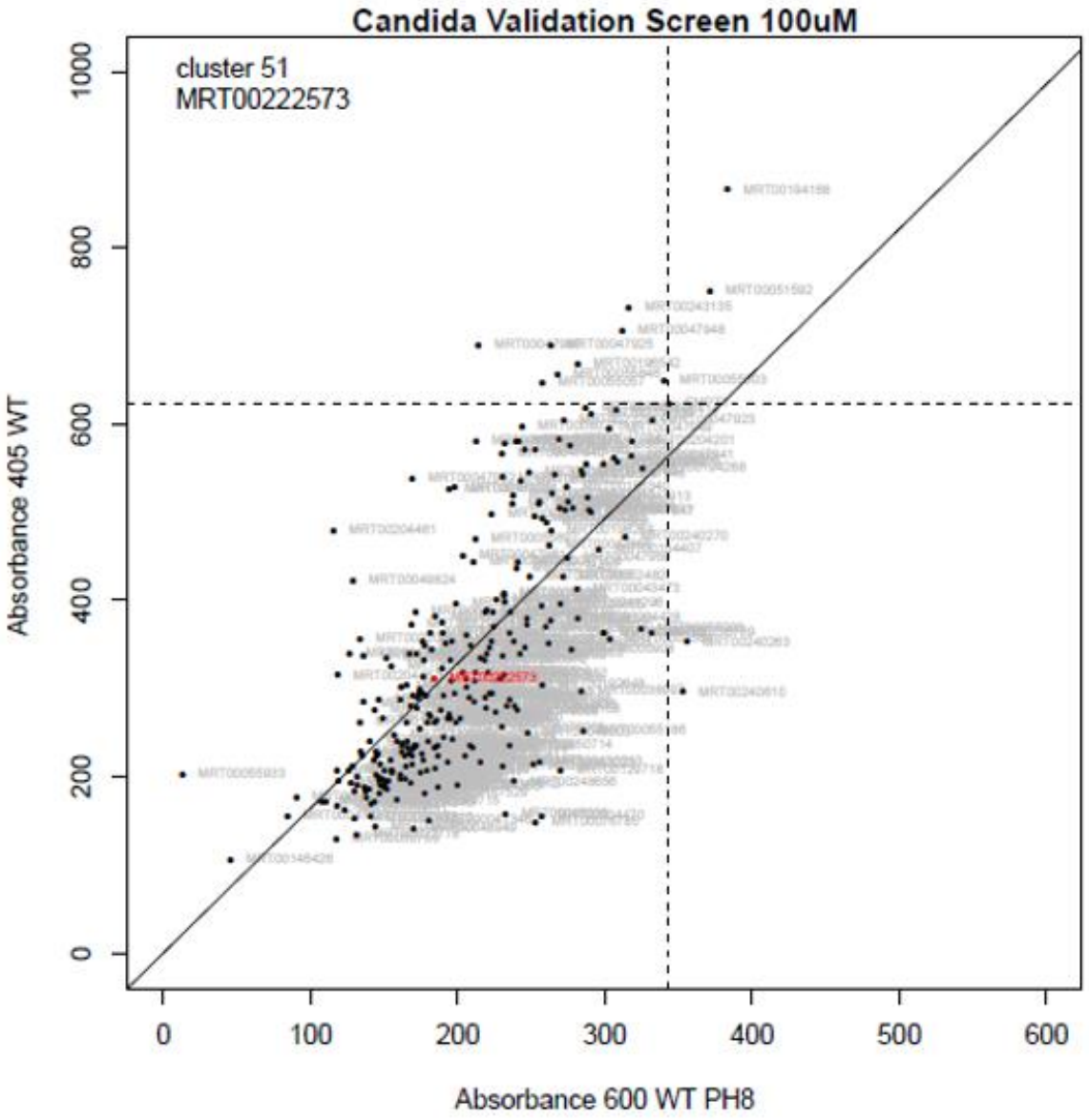

Cluster 51: 100 µM Secondary Screen: pH8 as a readout for PHO Pathway activity.
Plot of OD_{600} *wt* cells grown in pH 8 vs. OD_{405} of *wt* cells. Cells were grown to log phase in YPD before being washed 3 times in pH8 media and diluted back to OD_{600} = 0.05 then seeded into 384 well plates containing 100 µM of compound. Absorbance of 600 nm is used for growth at pH and 405 for secreted acid phosphatase activity. Red hits represent those from cluster 51.

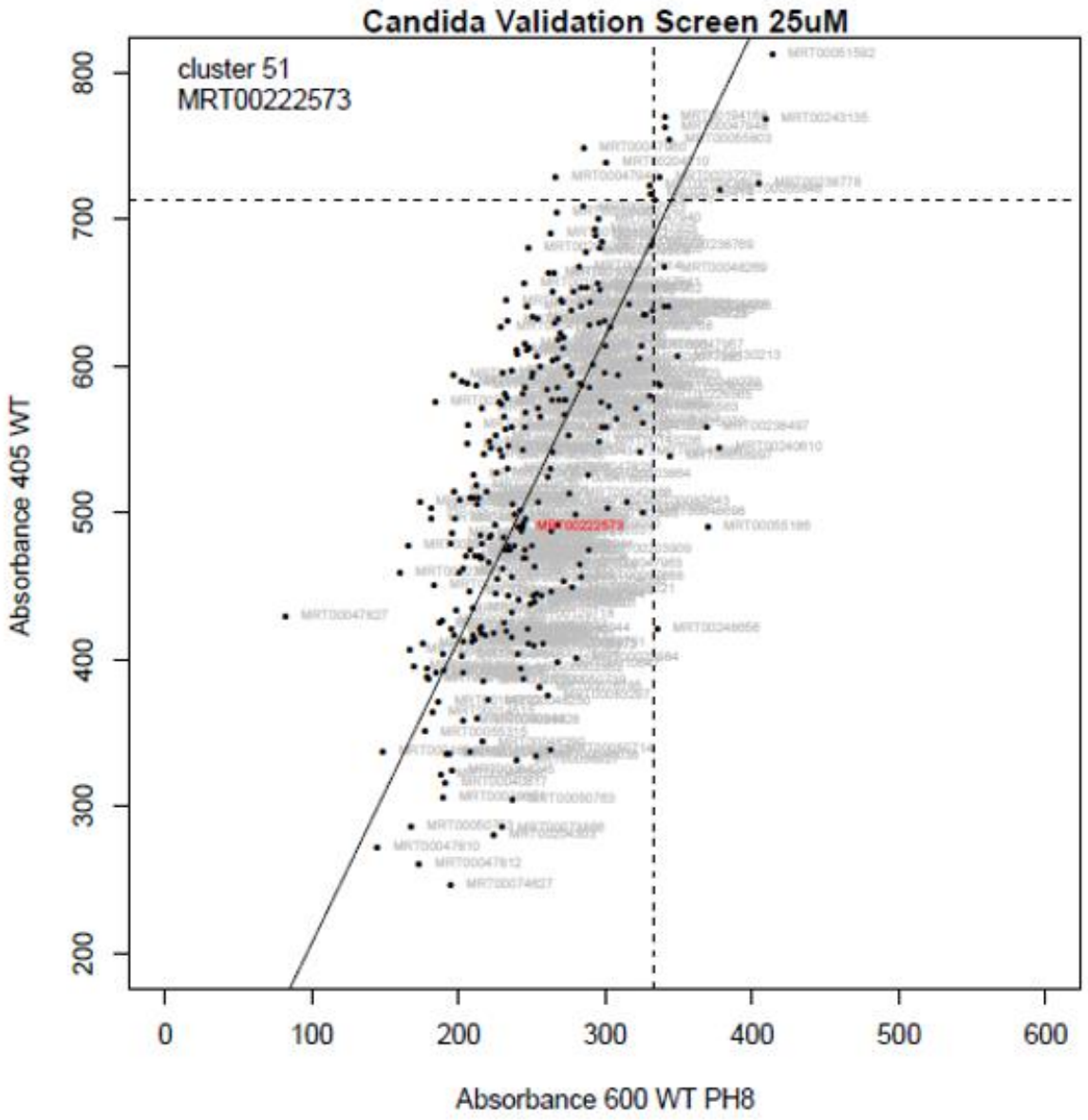

Cluster 51: 25 µM Secondary Screen: pH8 as a readout for PHO Pathway activity.
Plot of OD_{600} *wt* cells grown in pH 8 vs. OD_{405} of *wt* cells. Cells were grown to log phase in YPD before being washed 3 times in pH8 media and diluted back to OD_{600} = 0.05 then seeded into 384 well plates containing 25 µM of compound. Absorbance of 600 nm is used for growth at pH and 405 for secreted acid phosphatase activity. Red hits represent those from cluster 51.

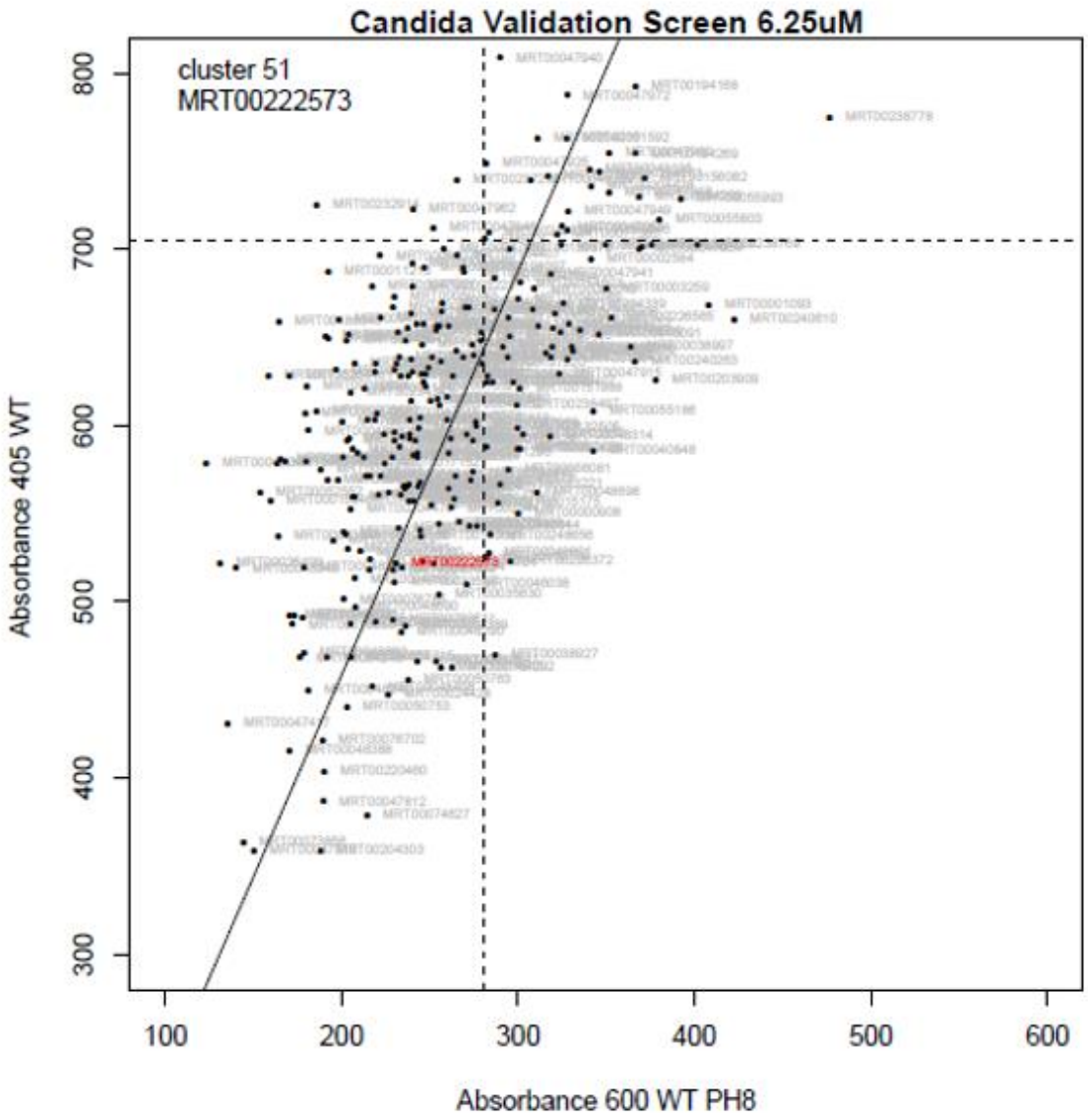

Cluster 51: 6.25 µM Secondary Screen: pH8 as a readout for PHO Pathway activity.
Plot of OD_{600} *wt* cells grown in pH 8 vs. OD_{405} of *wt* cells. Cells were grown to log phase in YPD before being washed 3 times in pH8 media and diluted back to OD_{600} = 0.05 then seeded into 384 well plates containing 6.25 µM of compound. Absorbance of 600 nm is used for growth at pH and 405 for secreted acid phosphatase activity. Red hits represent those from cluster 51.

Cluster 58

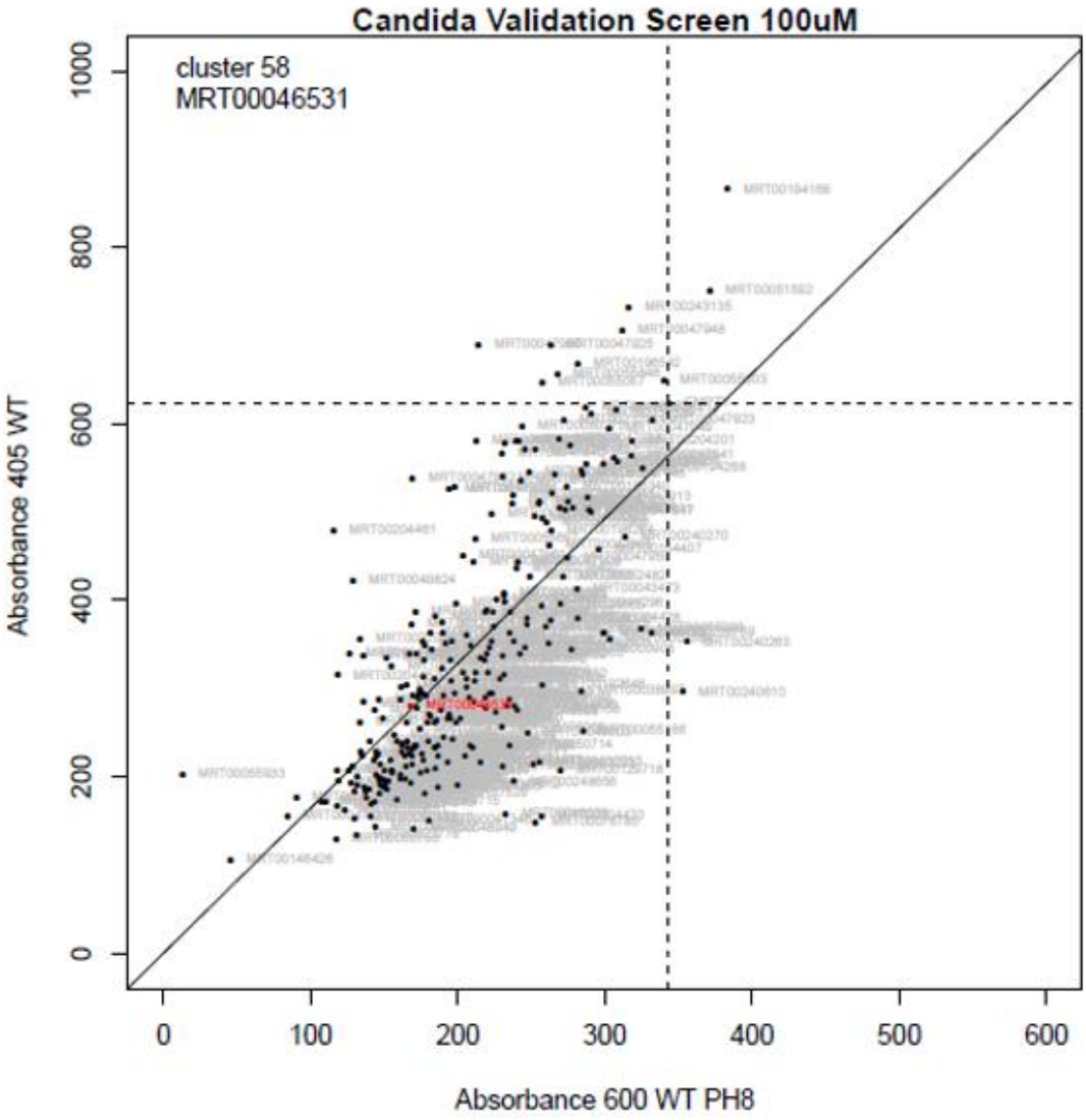

Cluster 58: 100 µM Secondary Screen: pH8 as a readout for PHO Pathway activity.
Plot of OD_{600} *wt* cells grown in pH 8 vs. OD_{405} of *wt* cells. Cells were grown to log phase in YPD before being washed 3 times in pH8 media and diluted back to OD_{600} = 0.05 then seeded into 384 well plates containing 100 µM of compound. Absorbance of 600 nm is used for growth at pH and 405 for secreted acid phosphatase activity. Red hits represent those from cluster 58.

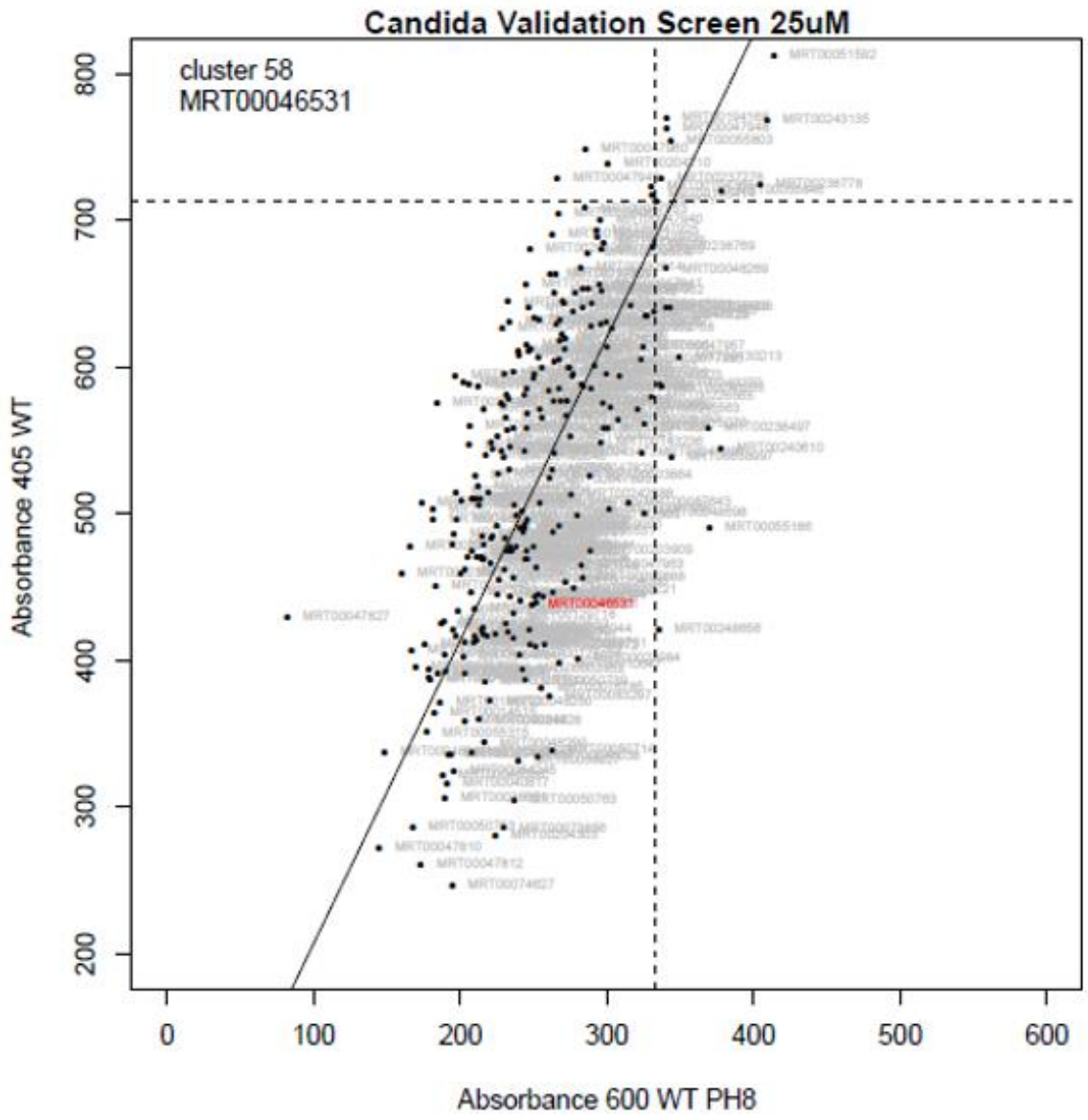

Cluster 58: 25 µM Secondary Screen: pH8 as a readout for PHO Pathway activity.
Plot of OD_{600} *wt* cells grown in pH 8 vs. OD_{405} of *wt* cells. Cells were grown to log phase in YPD before being washed 3 times in pH8 media and diluted back to OD_{600} = 0.05 then seeded into 384 well plates containing 25 µM of compound. Absorbance of 600 nm is used for growth at pH and 405 for secreted acid phosphatase activity. Red hits represent those from cluster 58.

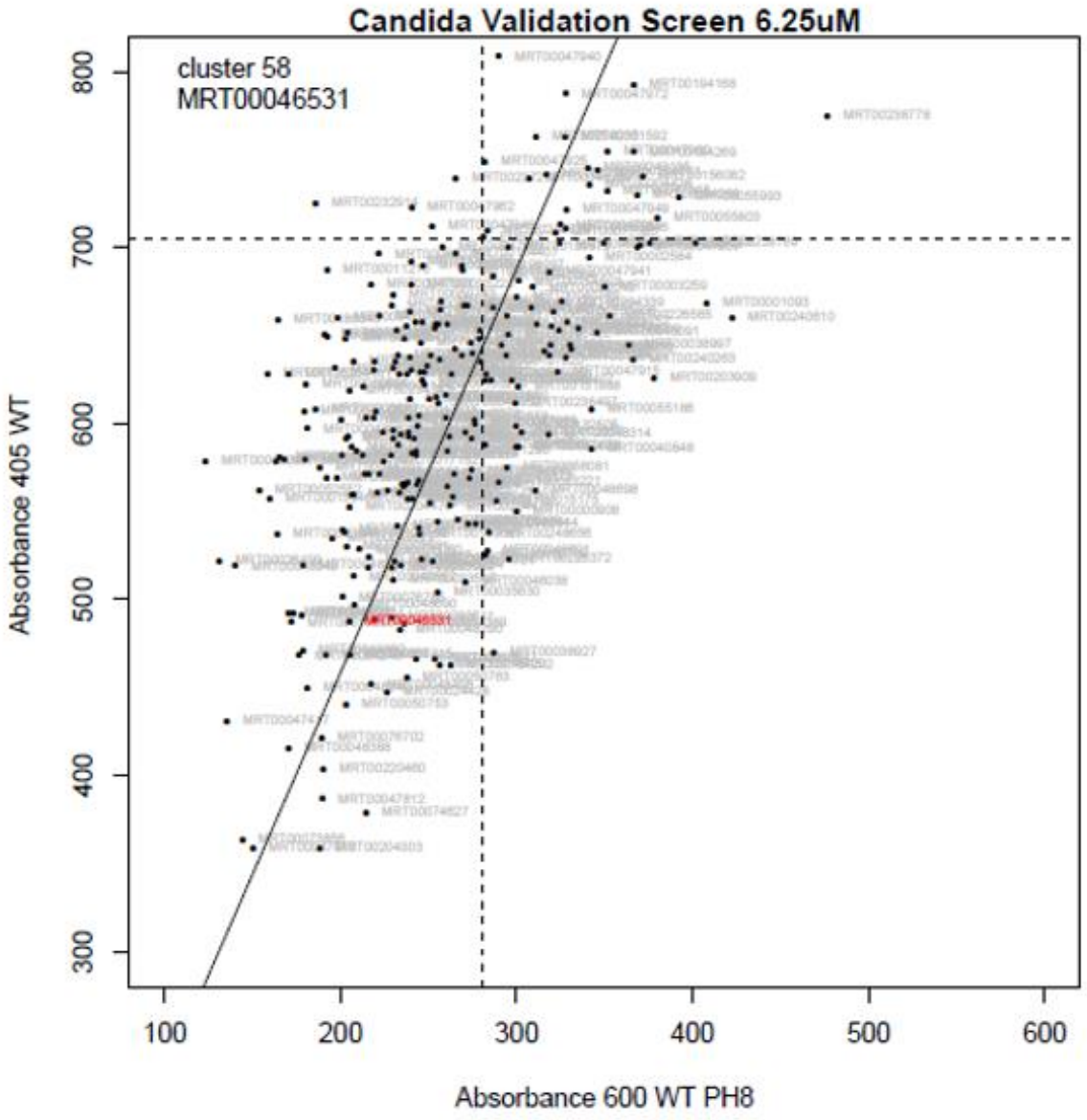

Cluster 58: 6.25 µM Secondary Screen: pH8 as a readout for PHO Pathway activity.
Plot of OD_{600} *wt* cells grown in pH 8 vs. OD_{405} of *wt* cells. Cells were grown to log phase in YPD before being washed 3 times in pH8 media and diluted back to OD_{600} = 0.05 then seeded into 384 well plates containing 6.25 µM of compound. Absorbance of 600 nm is used for growth at pH and 405 for secreted acid phosphatase activity. Red hits represent those from cluster 58.

Cluster 81

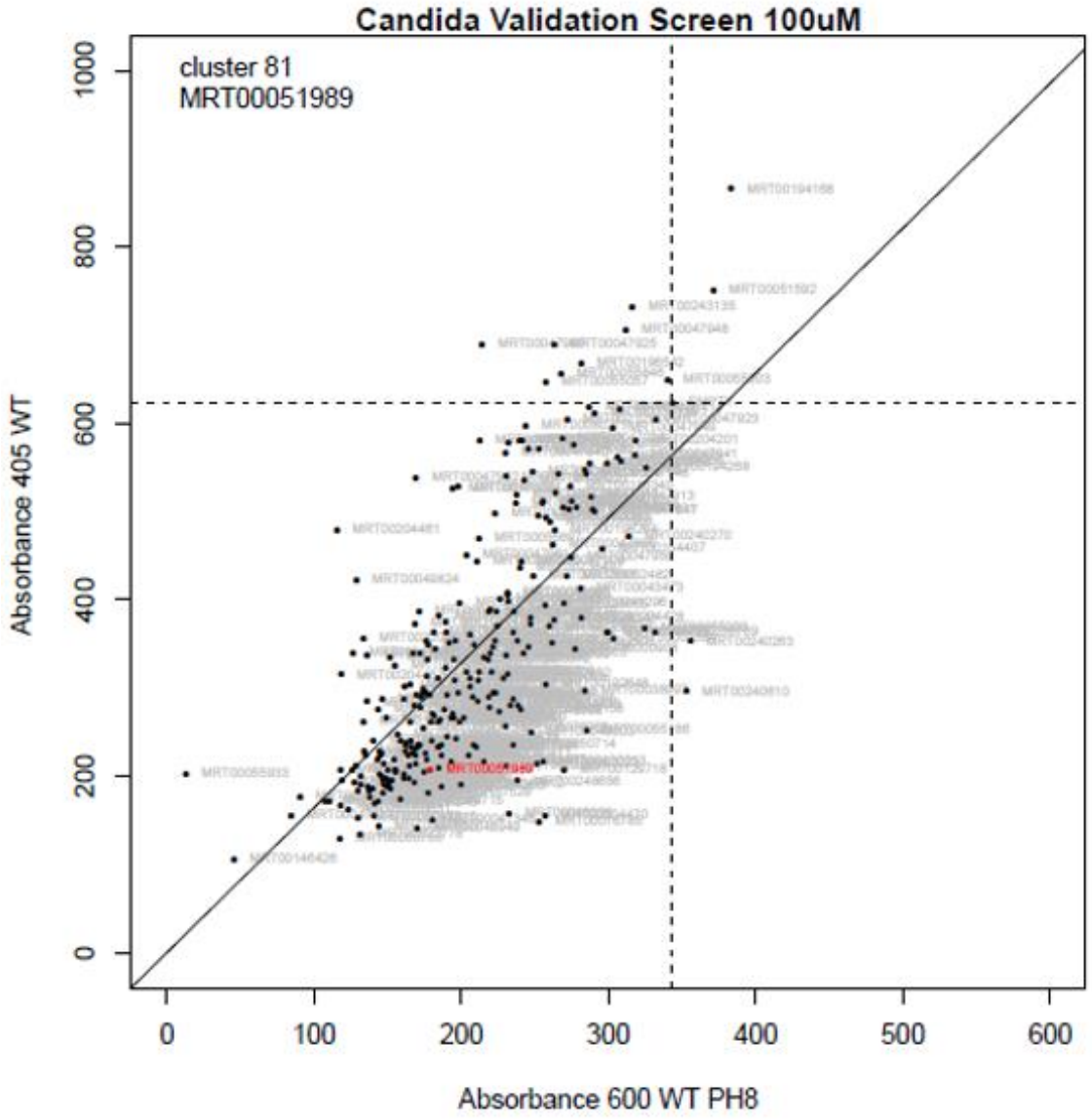

Cluster 81: 100 µM Secondary Screen: pH8 as a readout for PHO Pathway activity.
Plot of OD_{600} *wt* cells grown in pH 8 vs. OD_{405} of *wt* cells. Cells were grown to log phase in YPD before being washed 3 times in pH8 media and diluted back to OD_{600} = 0.05 then seeded into 384 well plates containing 100 µM of compound. Absorbance of 600 nm is used for growth at pH and 405 for secreted acid phosphatase activity. Red hits represent those from cluster 81.

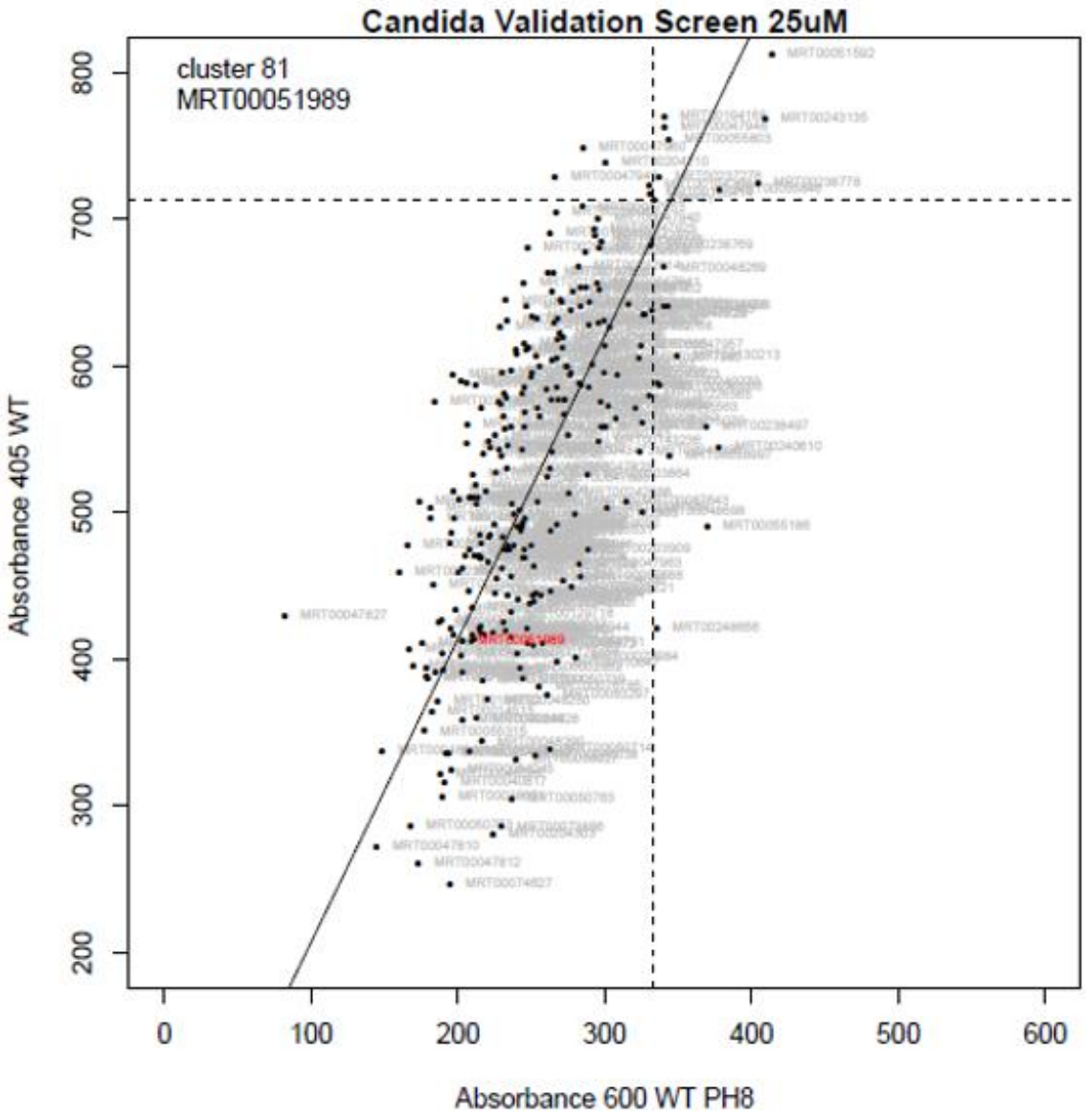

Cluster 81: 25 µM Secondary Screen: pH8 as a readout for PHO Pathway activity.
Plot of OD_{600} *wt* cells grown in pH 8 vs. OD_{405} of *wt* cells. Cells were grown to log phase in YPD before being washed 3 times in pH8 media and diluted back to OD_{600} = 0.05 then seeded into 384 well plates containing 25 µM of compound. Absorbance of 600 nm is used for growth at pH and 405 for secreted acid phosphatase activity. Red hits represent those from cluster 81.

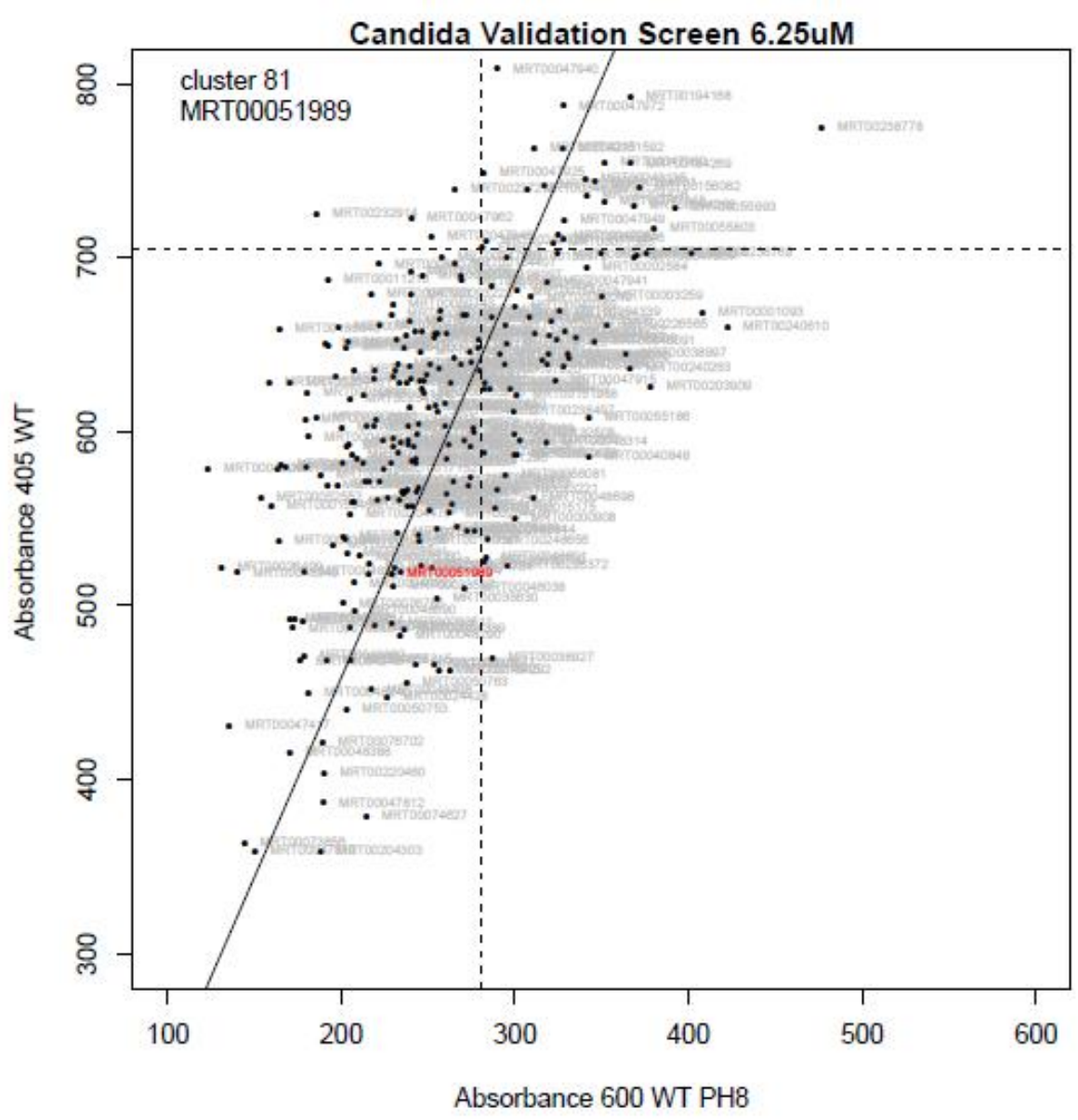

Cluster 81: 6.25 µM Secondary Screen: pH8 as a readout for PHO Pathway activity.
Plot of OD_{600} *wt* cells grown in pH 8 vs. OD_{405} of *wt* cells. Cells were grown to log phase in YPD before being washed 3 times in pH8 media and diluted back to OD_{600} = 0.05 then seeded into 384 well plates containing 6.25 µM of compound. Absorbance of 600 nm is used for growth at pH and 405 for secreted acid phosphatase activity. Red hits represent those from cluster 81.

Cluster 82

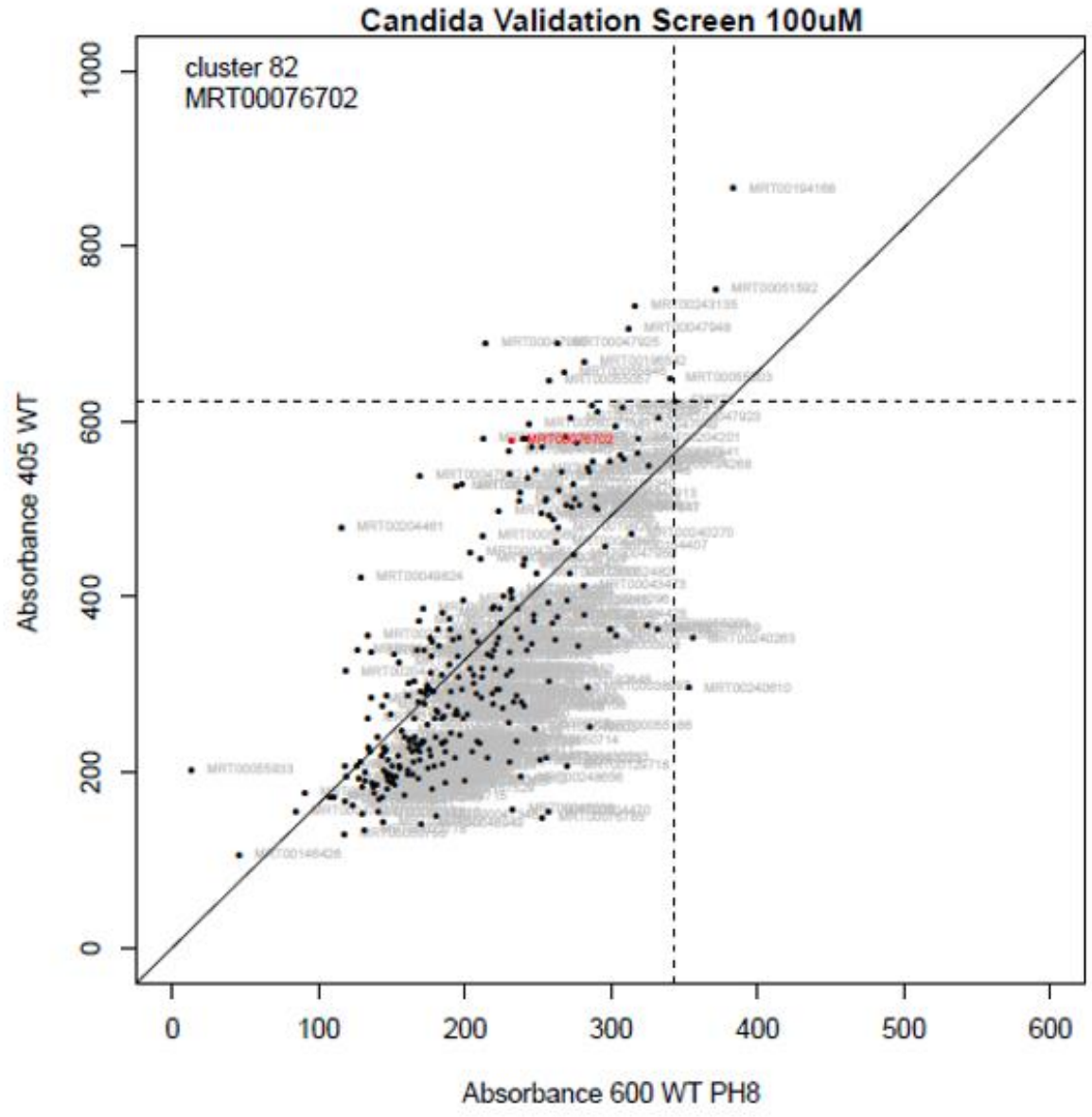

Cluster 82: 100 µM Secondary Screen: pH8 as a readout for PHO Pathway activity.
Plot of OD_{600} *wt* cells grown in pH 8 vs. OD_{405} of *wt* cells. Cells were grown to log phase in YPD before being washed 3 times in pH8 media and diluted back to OD_{600} = 0.05 then seeded into 384 well plates containing 100 µM of compound. Absorbance of 600 nm is used for growth at pH and 405 for secreted acid phosphatase activity. Red hits represent those from cluster 82.

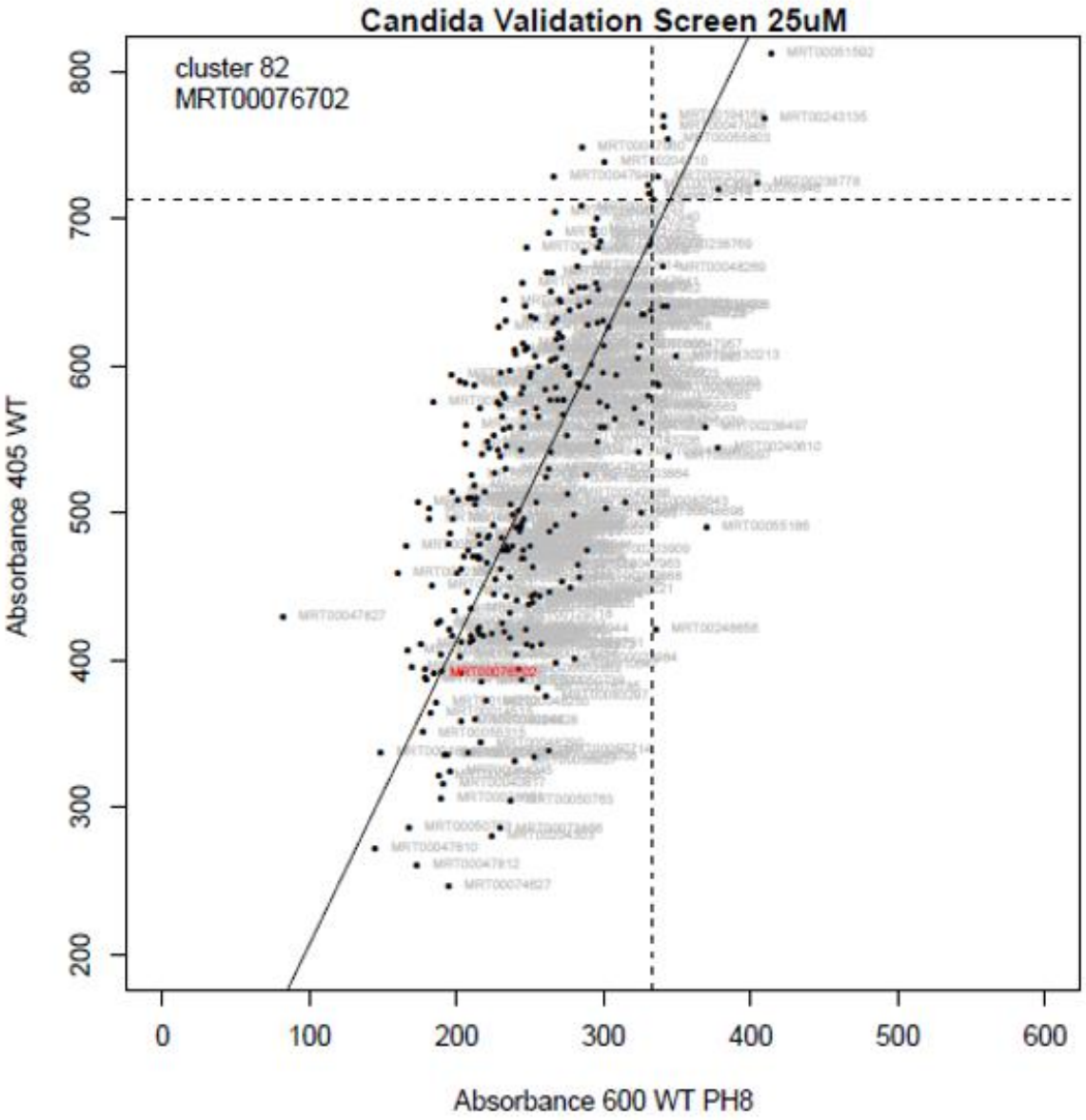

Cluster 82: 25 µM Secondary Screen: pH8 as a readout for PHO Pathway activity.
Plot of OD_{600} *wt* cells grown in pH 8 vs. OD_{405} of *wt* cells. Cells were grown to log phase in YPD before being washed 3 times in pH8 media and diluted back to OD_{600} = 0.05 then seeded into 384 well plates containing 25 µM of compound. Absorbance of 600 nm is used for growth at pH and 405 for secreted acid phosphatase activity. Red hits represent those from cluster 82.

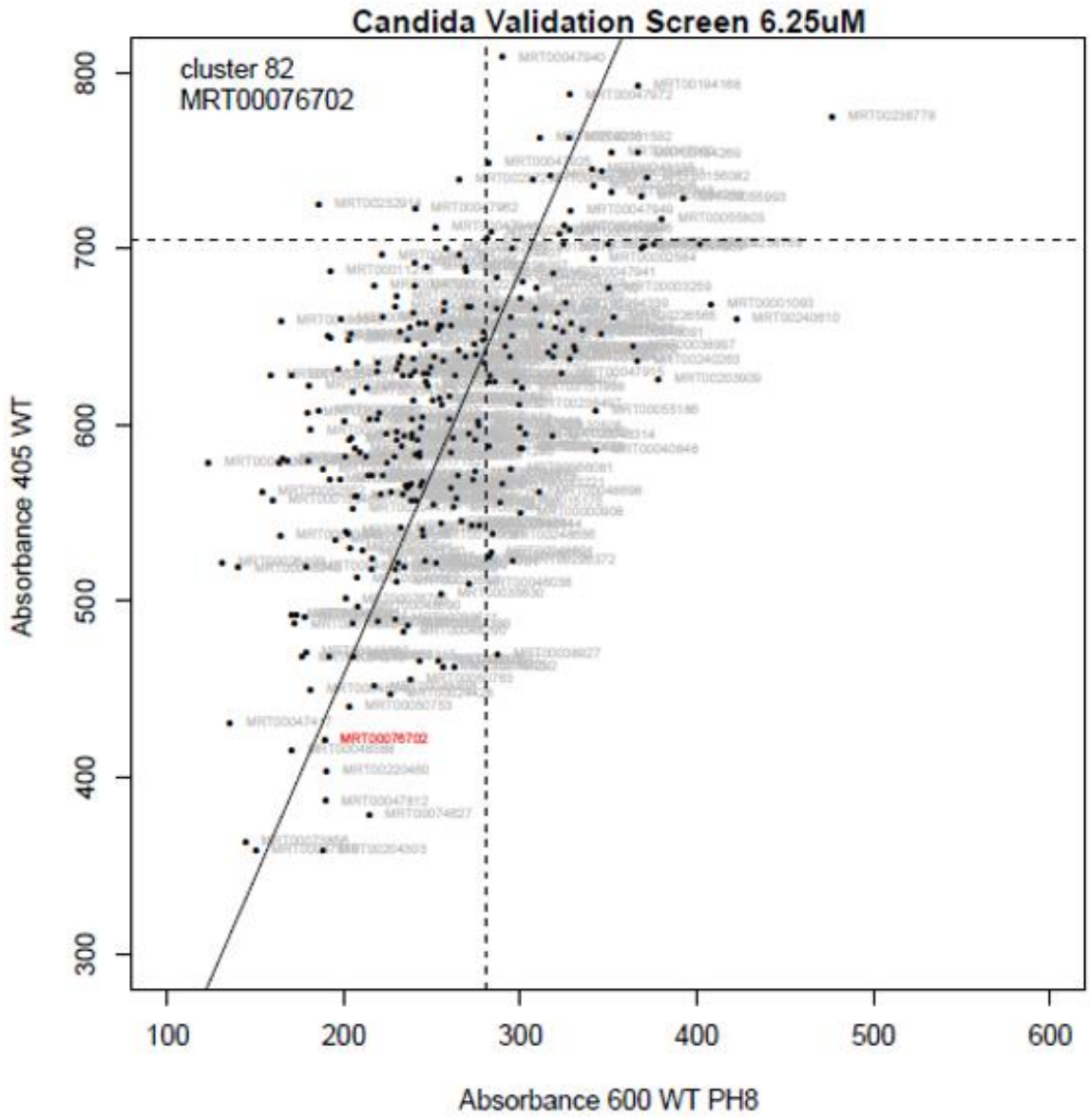

Cluster 82: 6.25 µM Secondary Screen: pH8 as a readout for PHO Pathway activity.
Plot of OD_{600} *wt* cells grown in pH 8 vs. OD_{405} of *wt* cells. Cells were grown to log phase in YPD before being washed 3 times in pH8 media and diluted back to OD_{600} = 0.05 then seeded into 384 well plates containing 6.25 µM of compound. Absorbance of 600 nm is used for growth at pH and 405 for secreted acid phosphatase activity. Red hits represent those from cluster 82.

Cluster 92

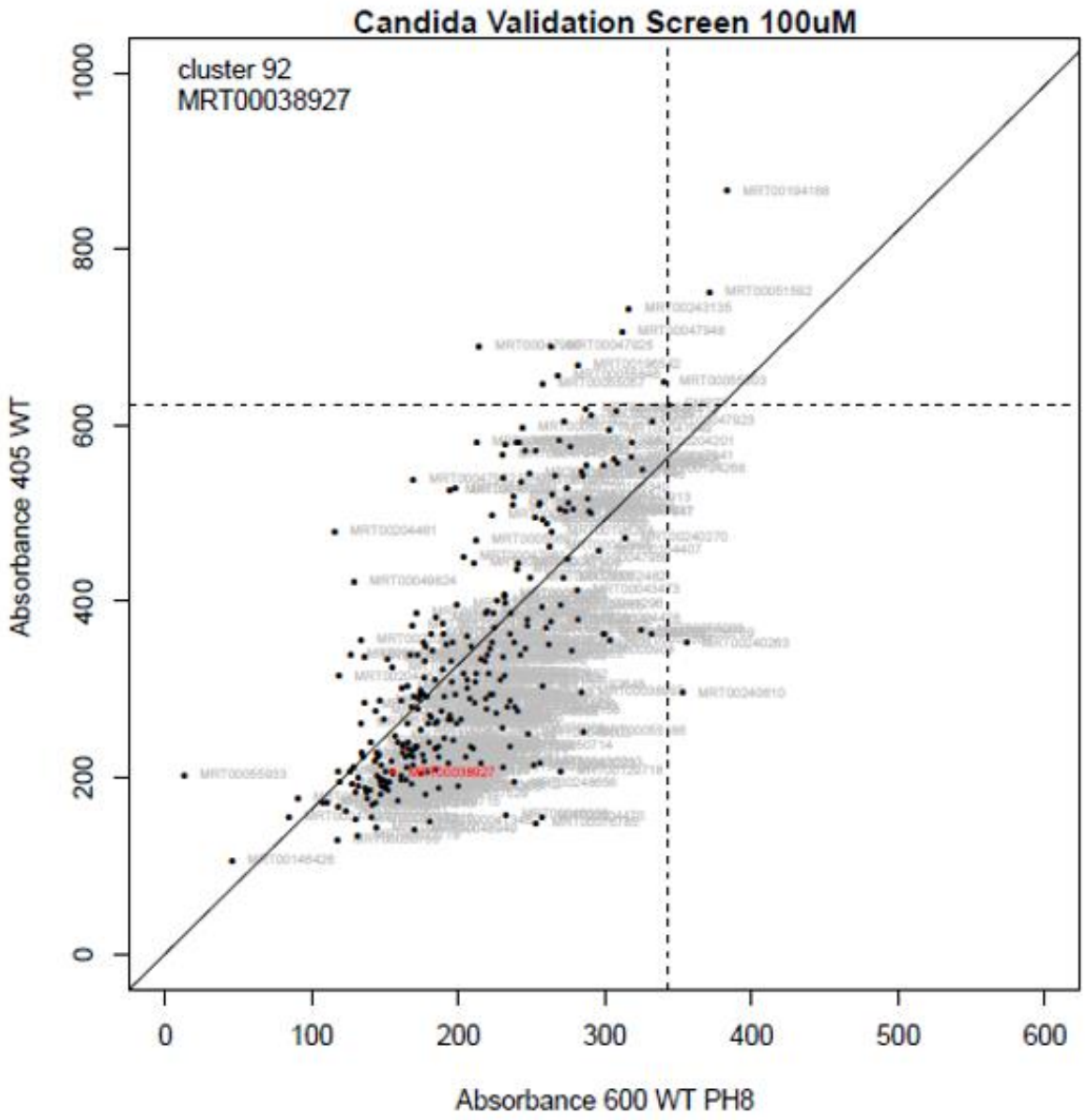

Cluster 92: 100 µM Secondary Screen: pH8 as a readout for PHO Pathway activity.
Plot of OD_{600} *wt* cells grown in pH 8 vs. OD_{405} of *wt* cells. Cells were grown to log phase in YPD before being washed 3 times in pH8 media and diluted back to OD_{600} = 0.05 then seeded into 384 well plates containing 100 µM of compound. Absorbance of 600 nm is used for growth at pH and 405 for secreted acid phosphatase activity. Red hits represent those from cluster 92.

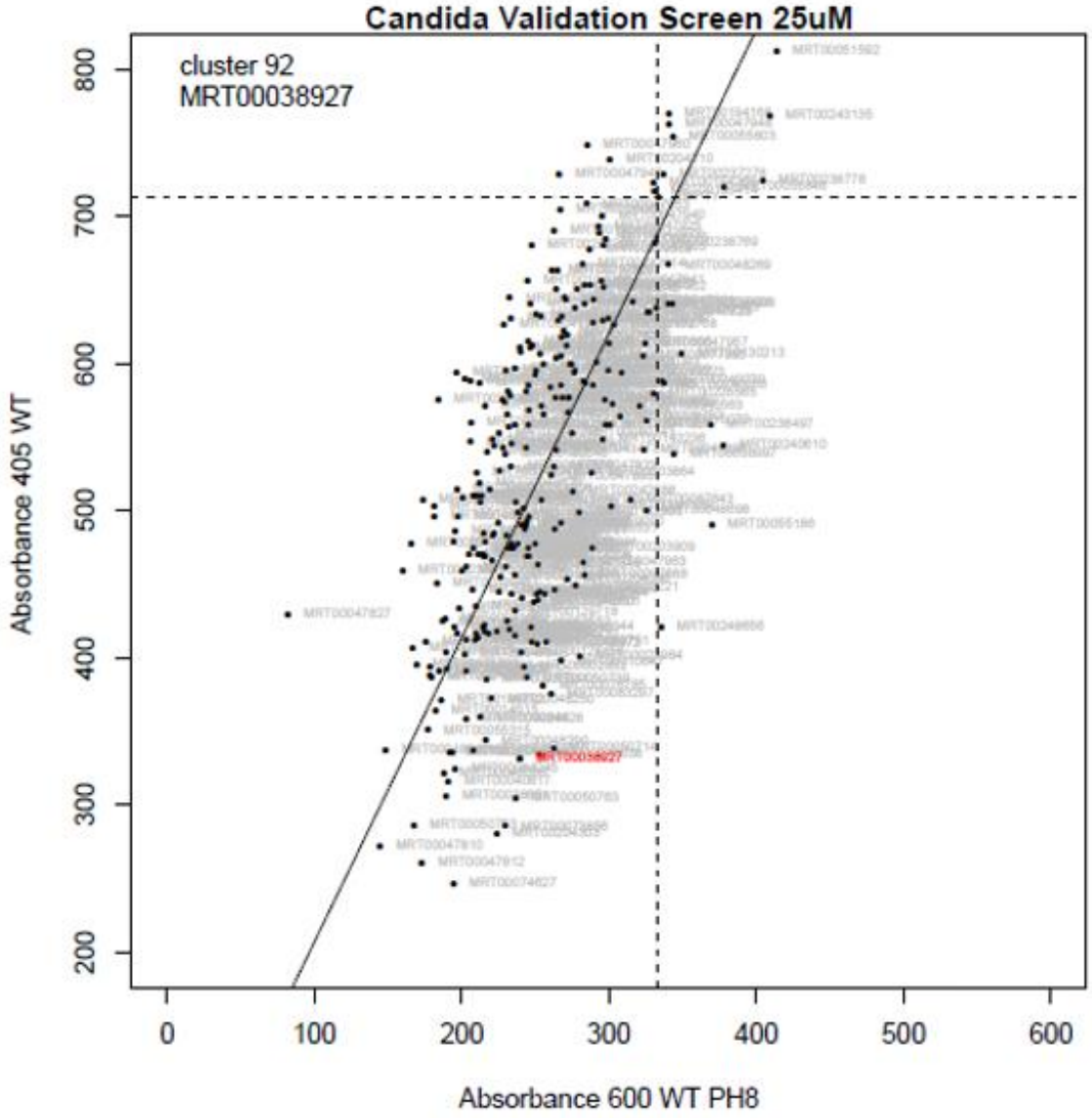

Cluster 92: 25 µM Secondary Screen: pH8 as a readout for PHO Pathway activity.
Plot of OD_{600} *wt* cells grown in pH 8 vs. OD_{405} of *wt* cells. Cells were grown to log phase in YPD before being washed 3 times in pH8 media and diluted back to OD_{600} = 0.05 then seeded into 384 well plates containing 25 µM of compound. Absorbance of 600 nm is used for growth at pH and 405 for secreted acid phosphatase activity. Red hits represent those from cluster 92.

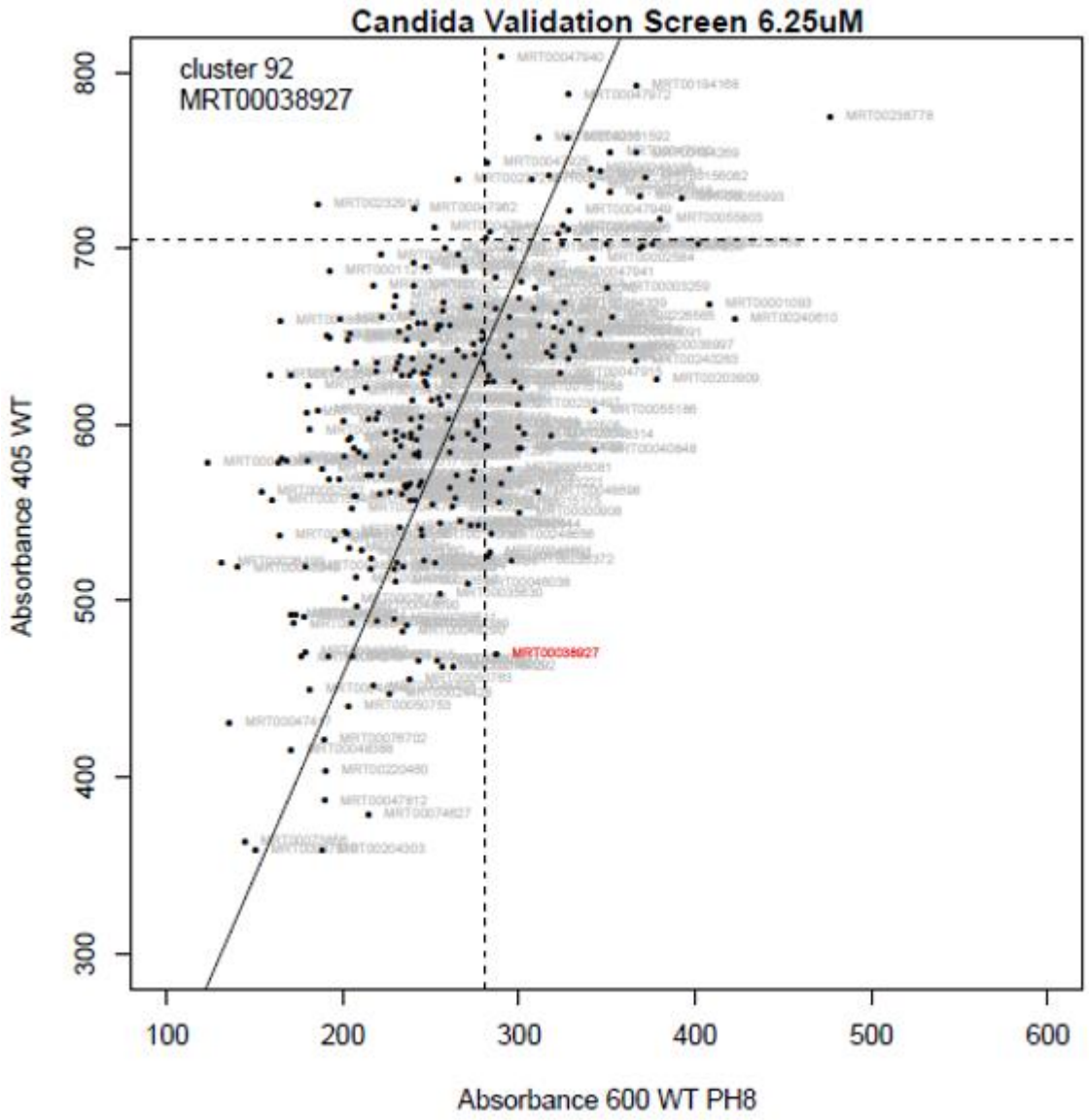

Cluster 92: 6.25 µM Secondary Screen: pH8 as a readout for PHO Pathway activity.
Plot of OD_{600} *wt* cells grown in pH 8 vs. OD_{405} of *wt* cells. Cells were grown to log phase in YPD before being washed 3 times in pH8 media and diluted back to OD_{600} = 0.05 then seeded into 384 well plates containing 6.25 µM of compound. Absorbance of 600 nm is used for growth at pH and 405 for secreted acid phosphatase activity. Red hits represent those from cluster 92.

Cluster 96

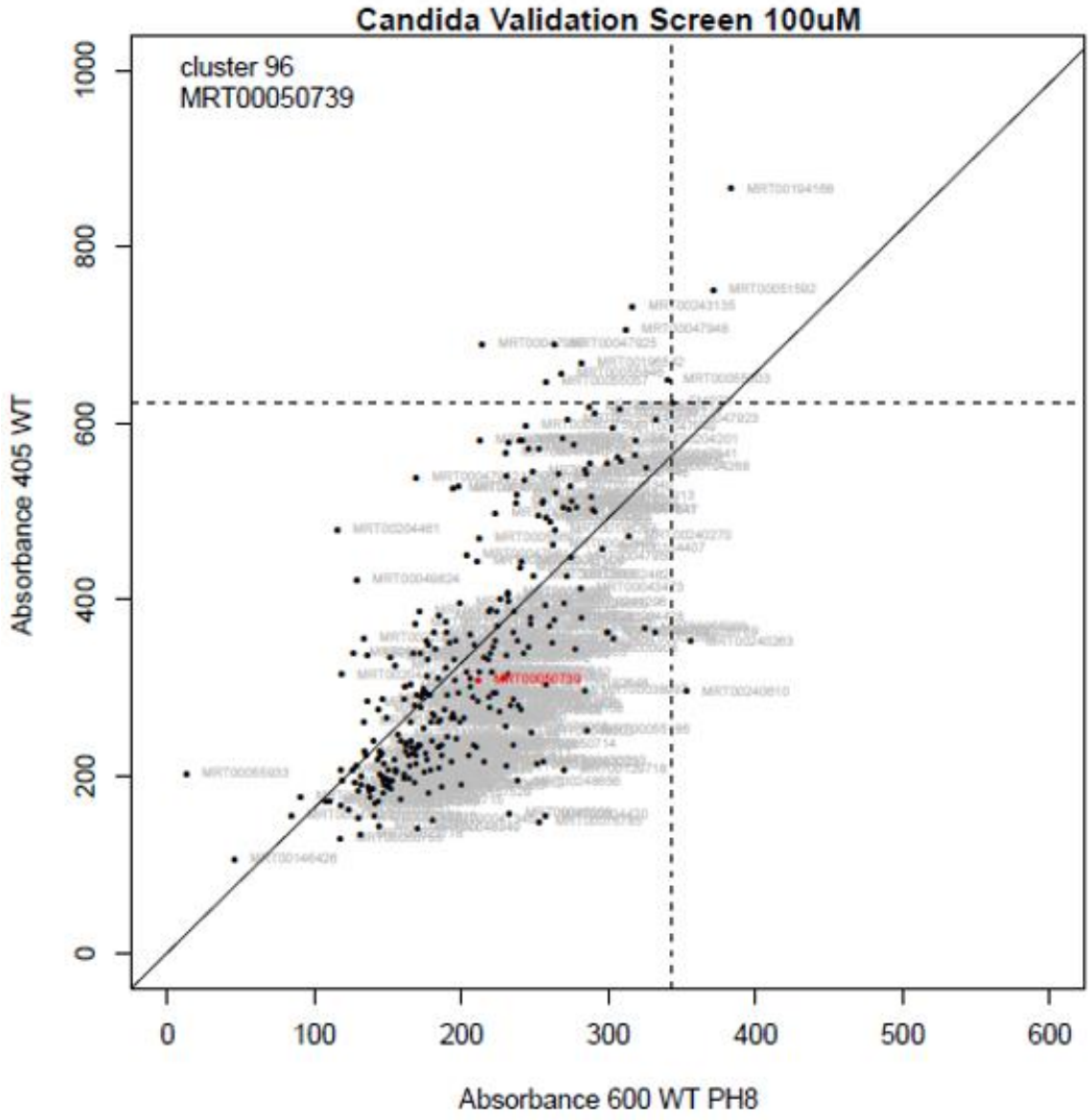

Cluster 96: 100 µM Secondary Screen: pH8 as a readout for PHO Pathway activity.
Plot of OD_{600} *wt* cells grown in pH 8 vs. OD_{405} of *wt* cells. Cells were grown to log phase in YPD before being washed 3 times in pH8 media and diluted back to OD_{600} = 0.05 then seeded into 384 well plates containing 100 µM of compound. Absorbance of 600 nm is used for growth at pH and 405 for secreted acid phosphatase activity. Red hits represent those from cluster 96.

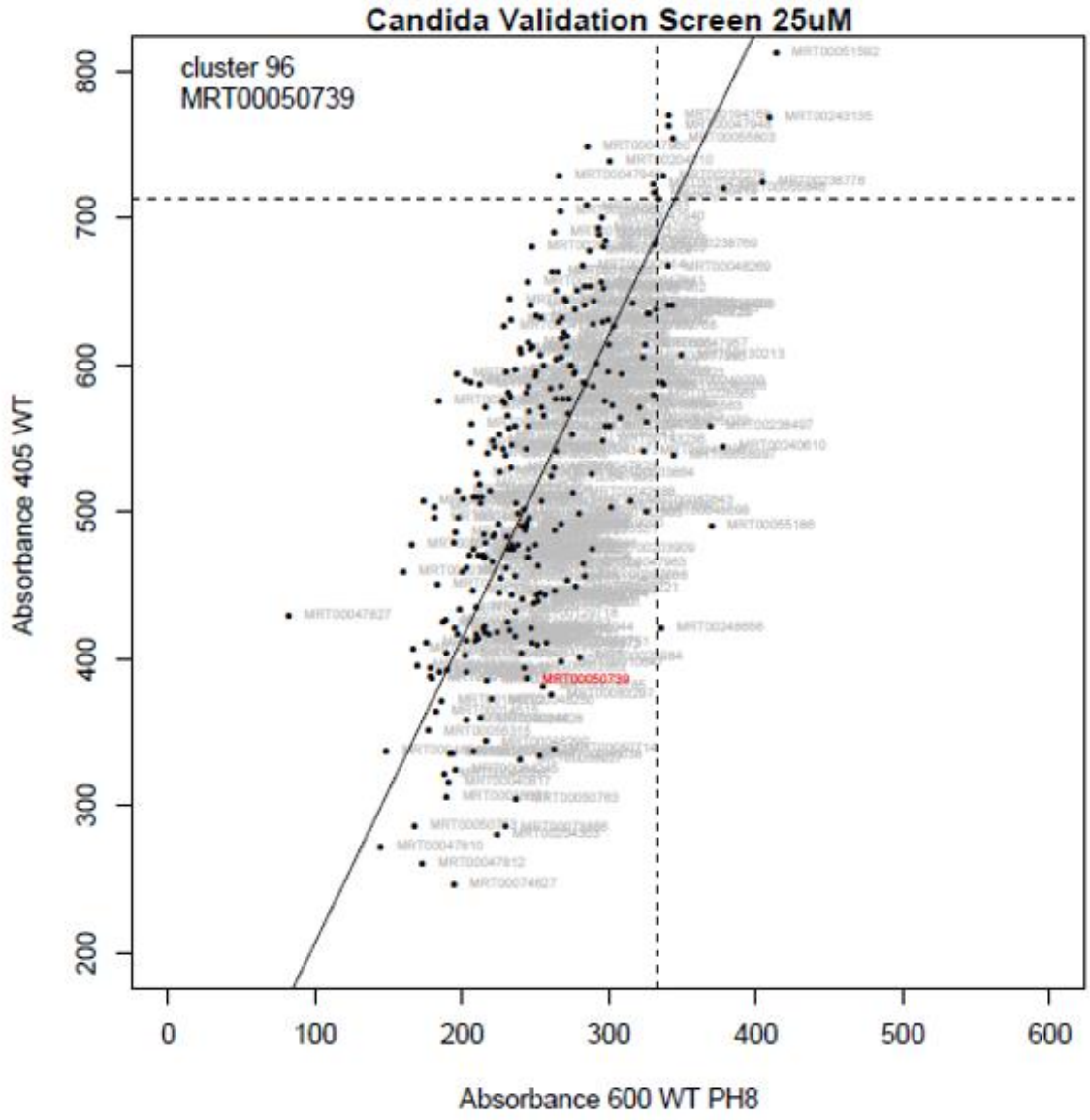

Cluster 96: 25 µM Secondary Screen: pH8 as a readout for PHO Pathway activity.
Plot of OD_{600} *wt* cells grown in pH 8 vs. OD_{405} of *wt* cells. Cells were grown to log phase in YPD before being washed 3 times in pH8 media and diluted back to OD_{600} = 0.05 then seeded into 384 well plates containing 25 µM of compound. Absorbance of 600 nm is used for growth at pH and 405 for secreted acid phosphatase activity. Red hits represent those from cluster 96.

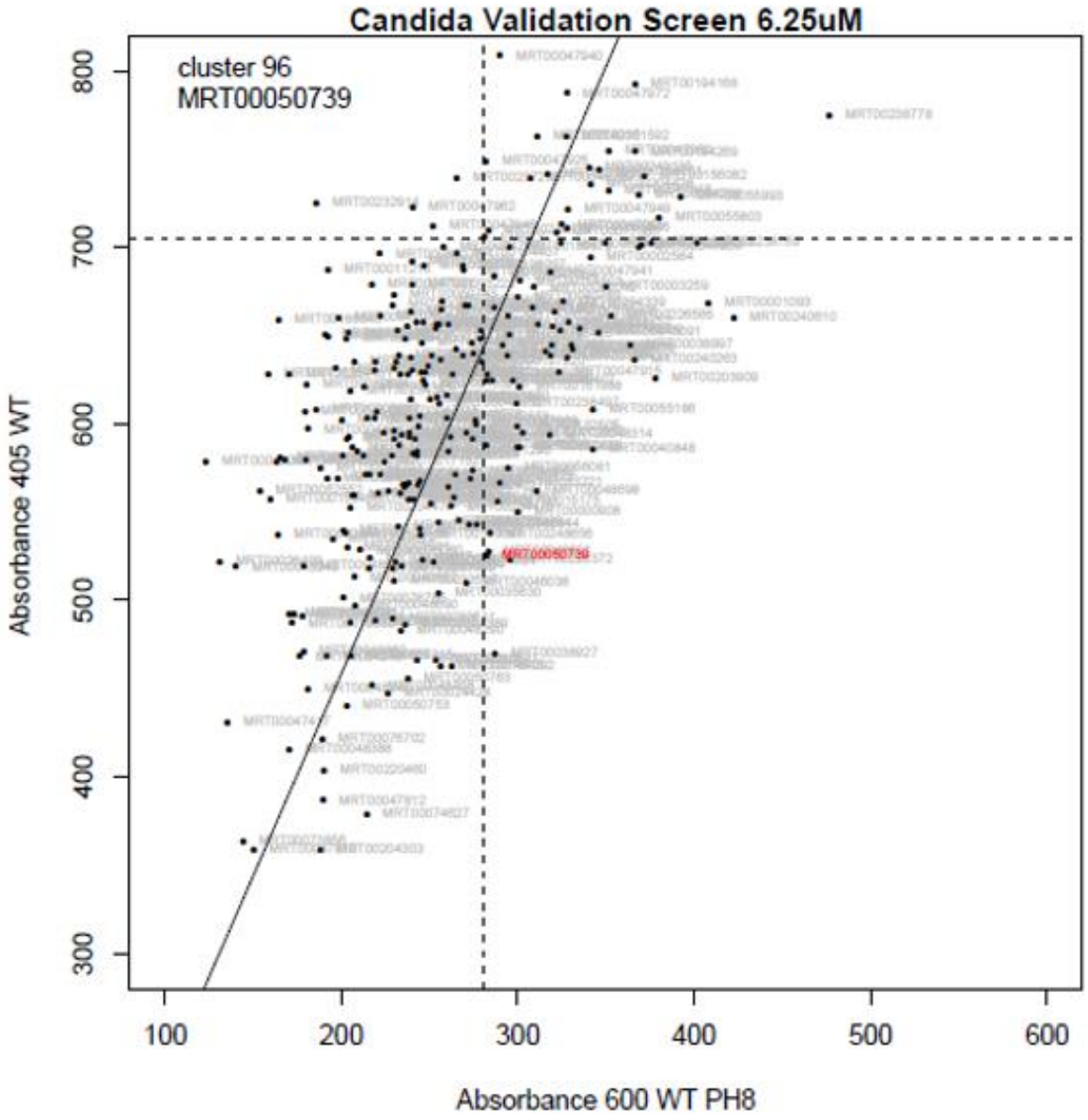

Cluster 96: 6.25 µM Secondary Screen: pH8 as a readout for PHO Pathway activity.
Plot of OD_{600} *wt* cells grown in pH 8 vs. OD_{405} of *wt* cells. Cells were grown to log phase in YPD before being washed 3 times in pH8 media and diluted back to OD_{600} = 0.05 then seeded into 384 well plates containing 6.25 µM of compound. Absorbance of 600 nm is used for growth at pH and 405 for secreted acid phosphatase activity. Red hits represent those from cluster 96.

Cluster 104

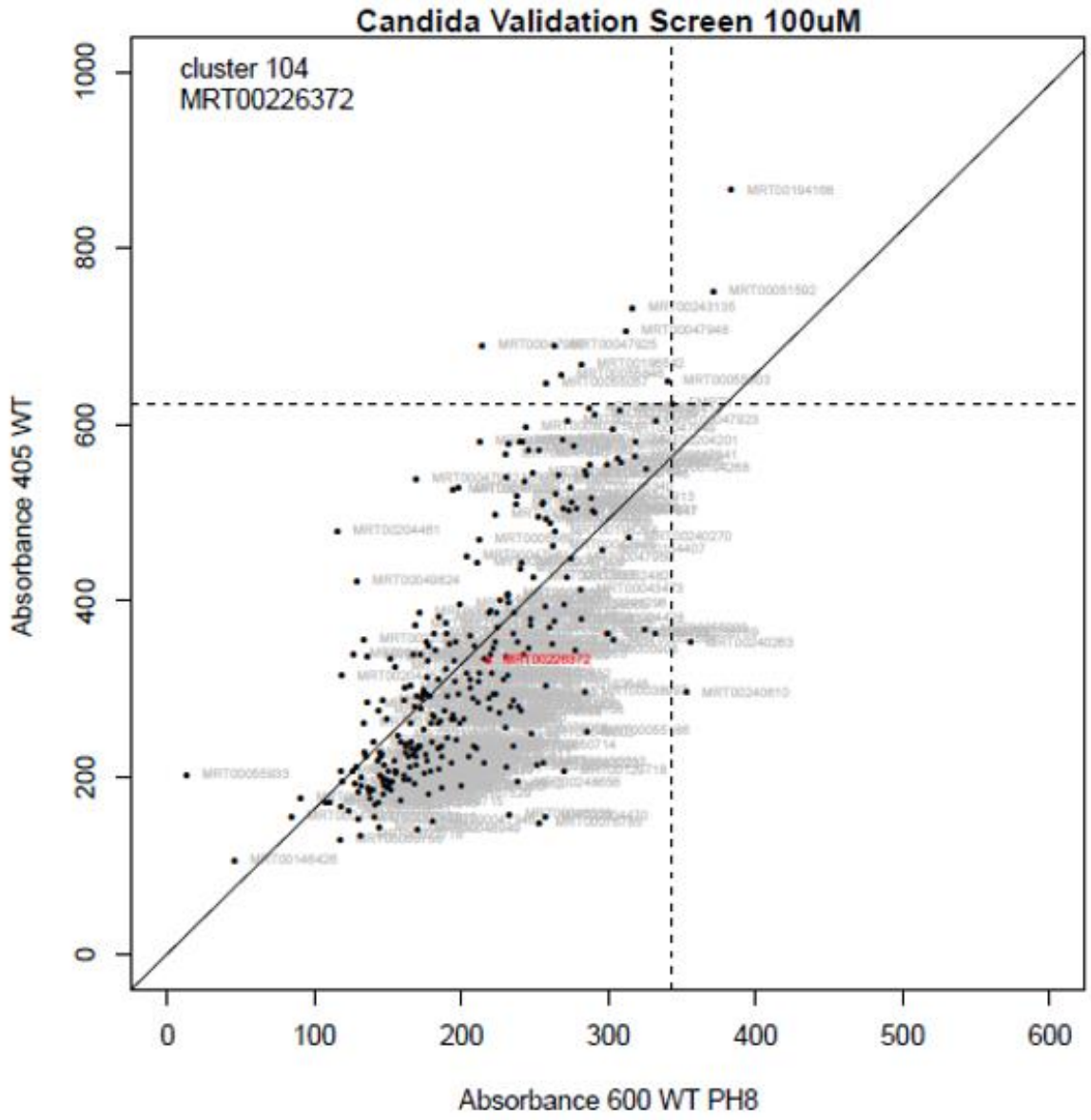

Cluster 104: 100 µM Secondary Screen: pH8 as a readout for PHO Pathway activity.
Plot of OD_{600} *wt* cells grown in pH 8 vs. OD_{405} of *wt* cells. Cells were grown to log phase in YPD before being washed 3 times in pH8 media and diluted back to OD_{600} = 0.05 then seeded into 384 well plates containing 100 µM of compound. Absorbance of 600 nm is used for growth at pH and 405 for secreted acid phosphatase activity. Red hits represent those from cluster 104.

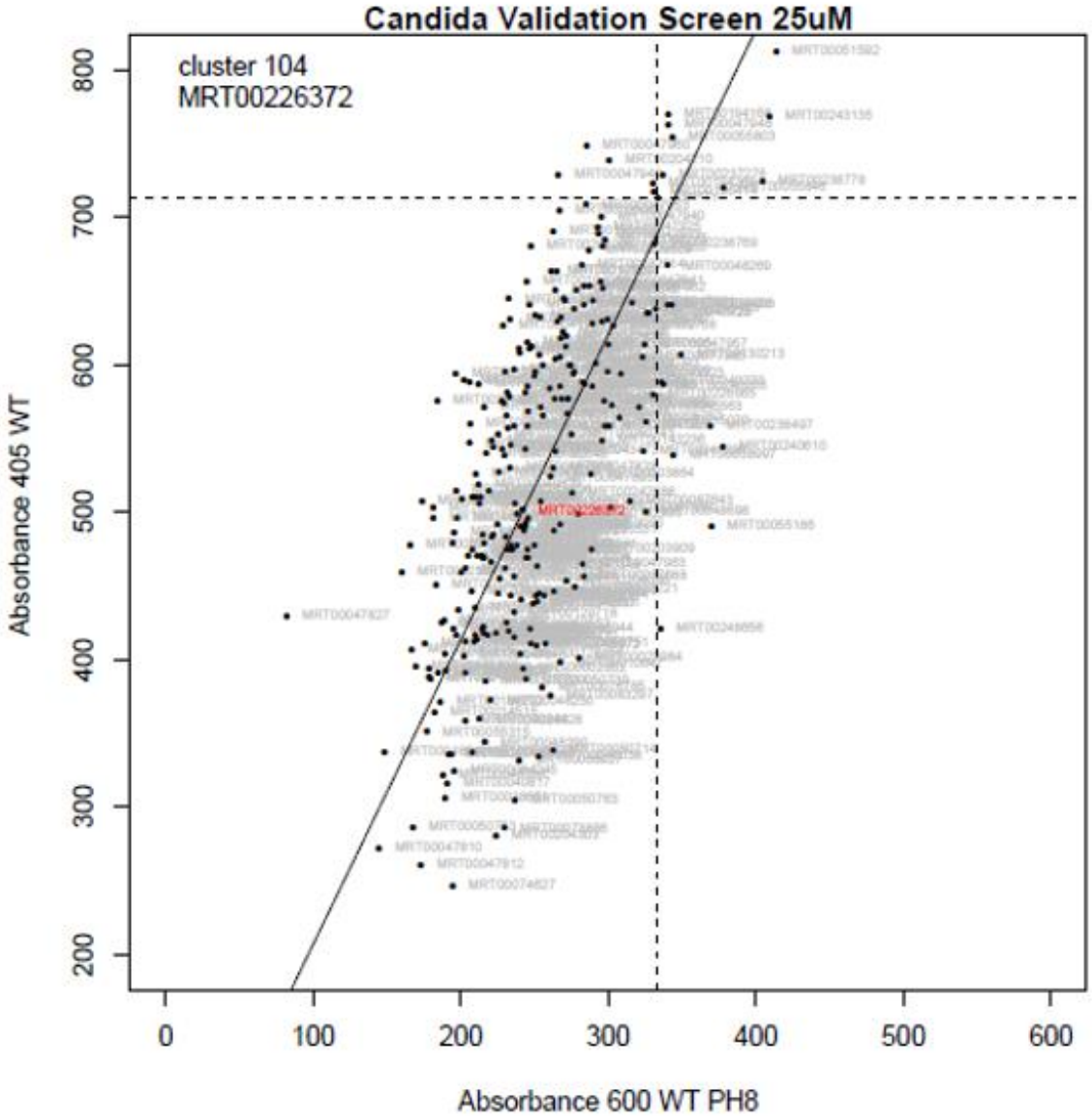

Cluster 104: 25 µM Secondary Screen: pH8 as a readout for PHO Pathway activity.
Plot of OD_{600} *wt* cells grown in pH 8 vs. OD_{405} of *wt* cells. Cells were grown to log phase in YPD before being washed 3 times in pH8 media and diluted back to OD_{600} = 0.05 then seeded into 384 well plates containing 25 µM of compound. Absorbance of 600 nm is used for growth at pH and 405 for secreted acid phosphatase activity. Red hits represent those from cluster 104.

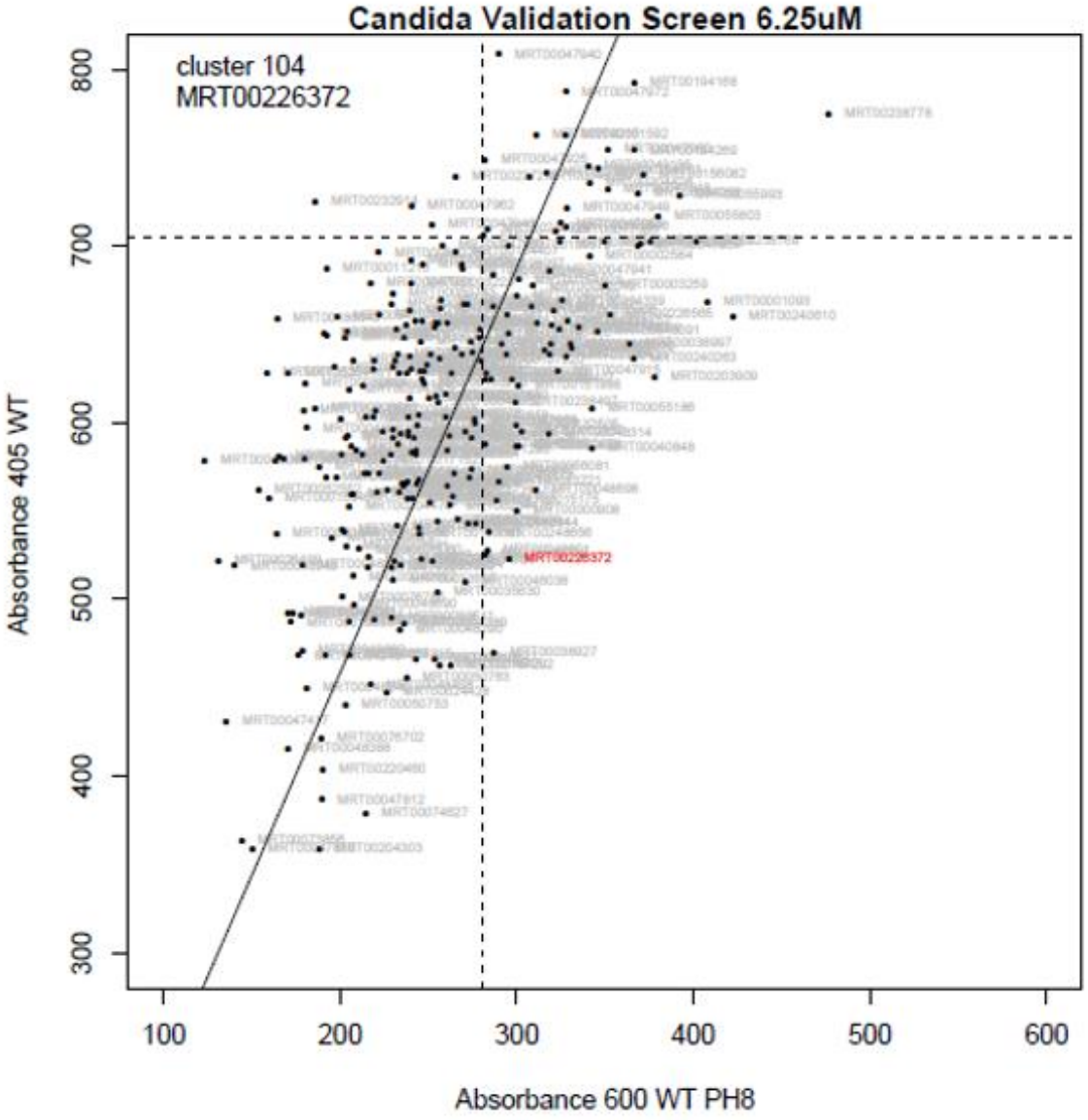

Cluster 104: 6.25 µM Secondary Screen: pH8 as a readout for PHO Pathway activity.
Plot of OD_{600} *wt* cells grown in pH 8 vs. OD_{405} of *wt* cells. Cells were grown to log phase in YPD before being washed 3 times in pH8 media and diluted back to OD_{600} = 0.05 then seeded into 384 well plates containing 6.25 µM of compound. Absorbance of 600 nm is used for growth at pH and 405 for secreted acid phosphatase activity. Red hits represent those from cluster 104.

Cluster 109

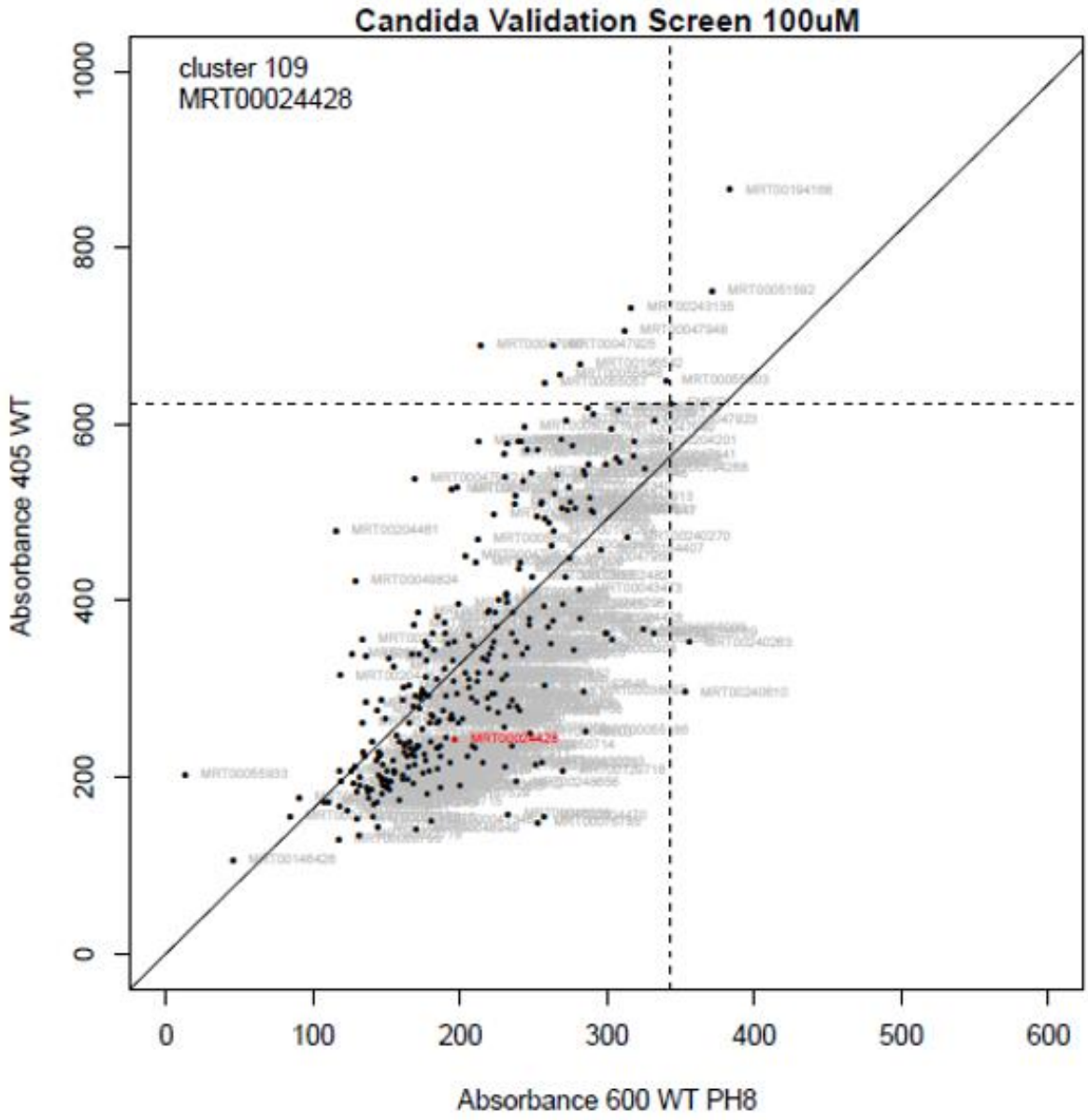

Cluster 109: 100 µM Secondary Screen: pH8 as a readout for PHO Pathway activity.
Plot of OD_{600} *wt* cells grown in pH 8 vs. OD_{405} of *wt* cells. Cells were grown to log phase in YPD before being washed 3 times in pH8 media and diluted back to OD_{600} = 0.05 then seeded into 384 well plates containing 100 µM of compound. Absorbance of 600 nm is used for growth at pH and 405 for secreted acid phosphatase activity. Red hits represent those from cluster 109.

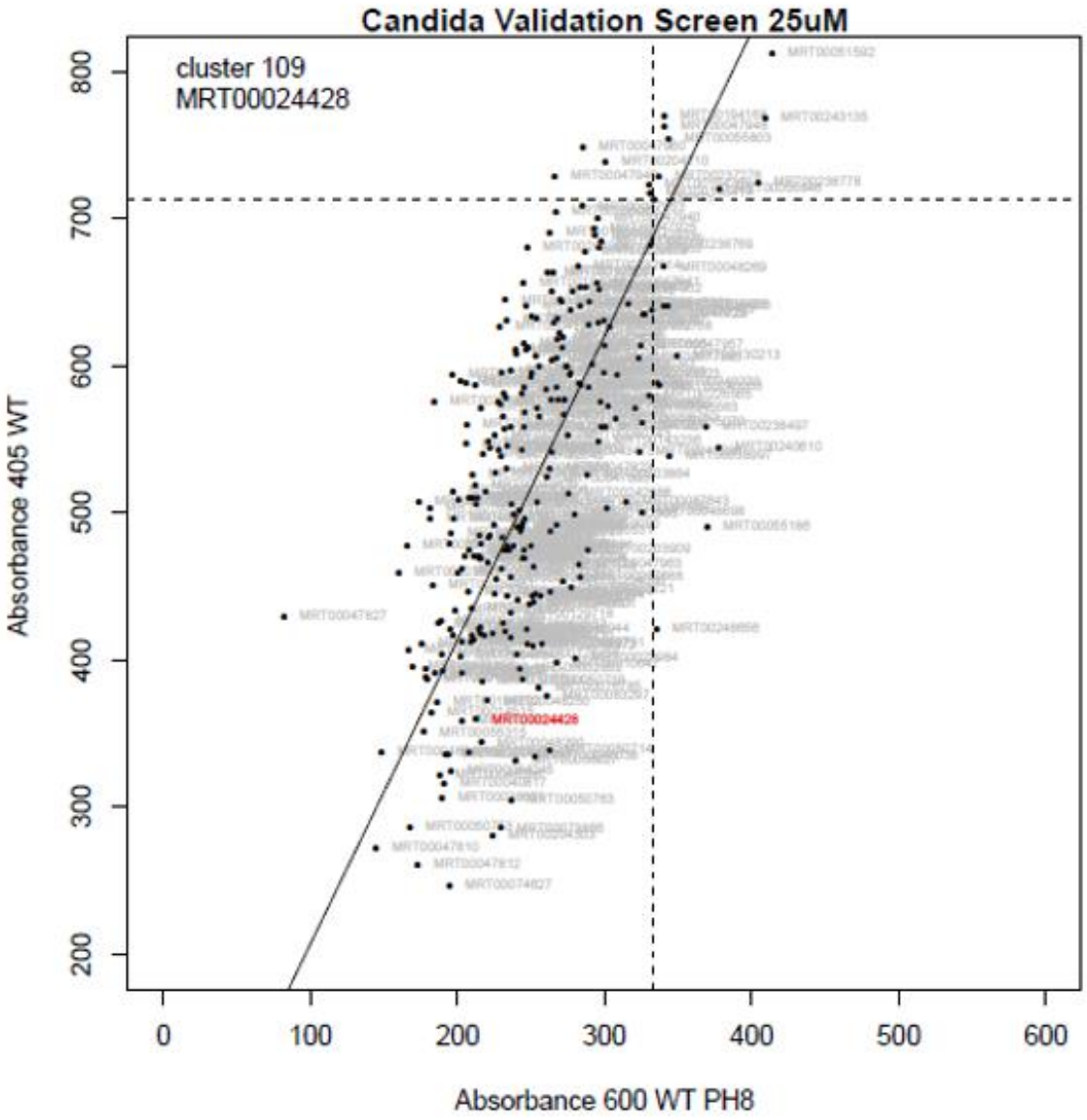

Cluster 109: 25 µM Secondary Screen: pH8 as a readout for PHO Pathway activity.
Plot of OD_{600} *wt* cells grown in pH 8 vs. OD_{405} of *wt* cells. Cells were grown to log phase in YPD before being washed 3 times in pH8 media and diluted back to OD_{600} = 0.05 then seeded into 384 well plates containing 25 µM of compound. Absorbance of 600 nm is used for growth at pH and 405 for secreted acid phosphatase activity. Red hits represent those from cluster 109.

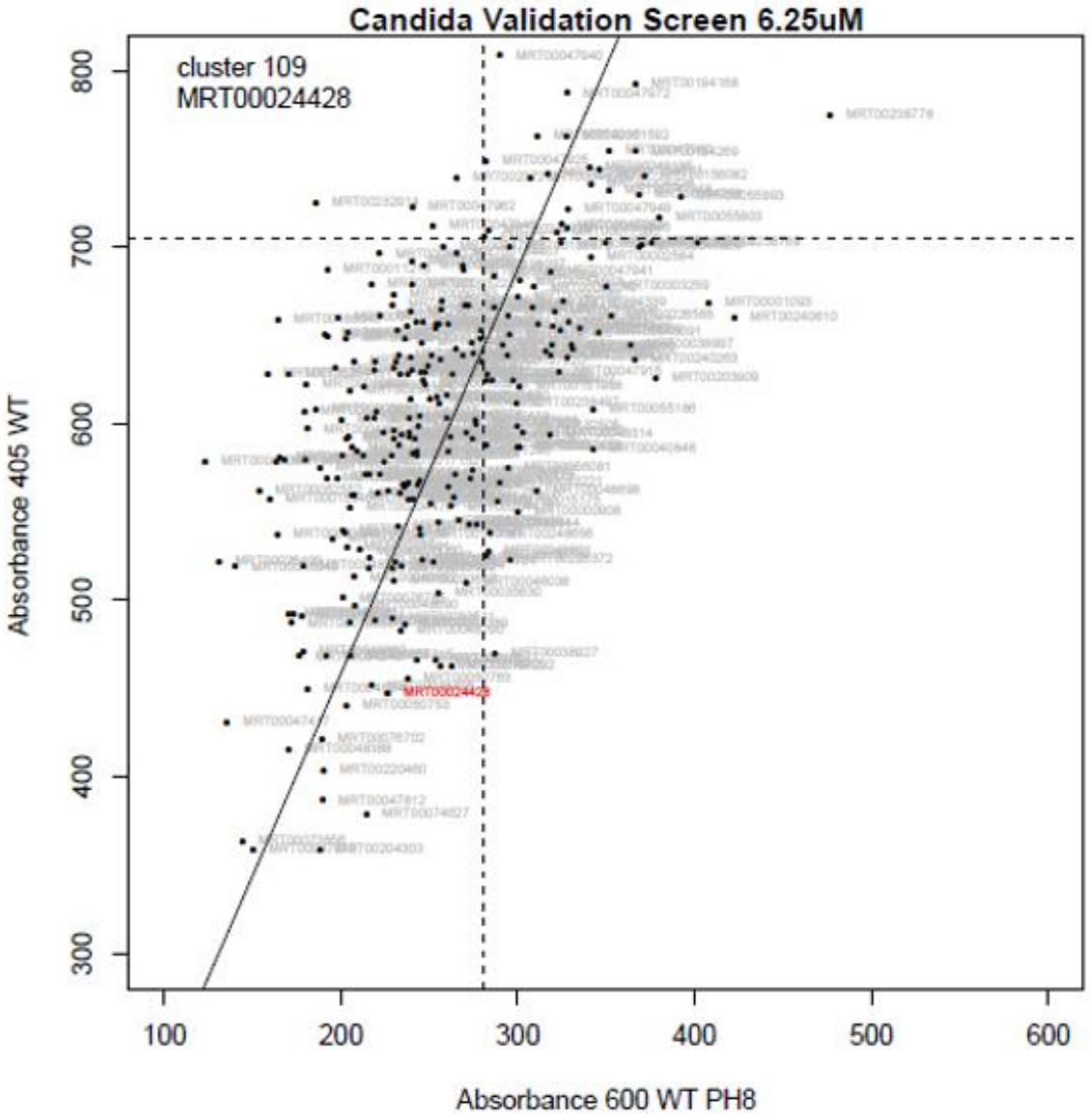

Cluster 109: 6.25 µM Secondary Screen: pH8 as a readout for PHO Pathway activity.
Plot of OD_{600} *wt* cells grown in pH 8 vs. OD_{405} of *wt* cells. Cells were grown to log phase in YPD before being washed 3 times in pH8 media and diluted back to OD_{600} = 0.05 then seeded into 384 well plates containing 6.25 µM of compound. Absorbance of 600 nm is used for growth at pH and 405 for secreted acid phosphatase activity. Red hits represent those from cluster 109.

Cluster 114

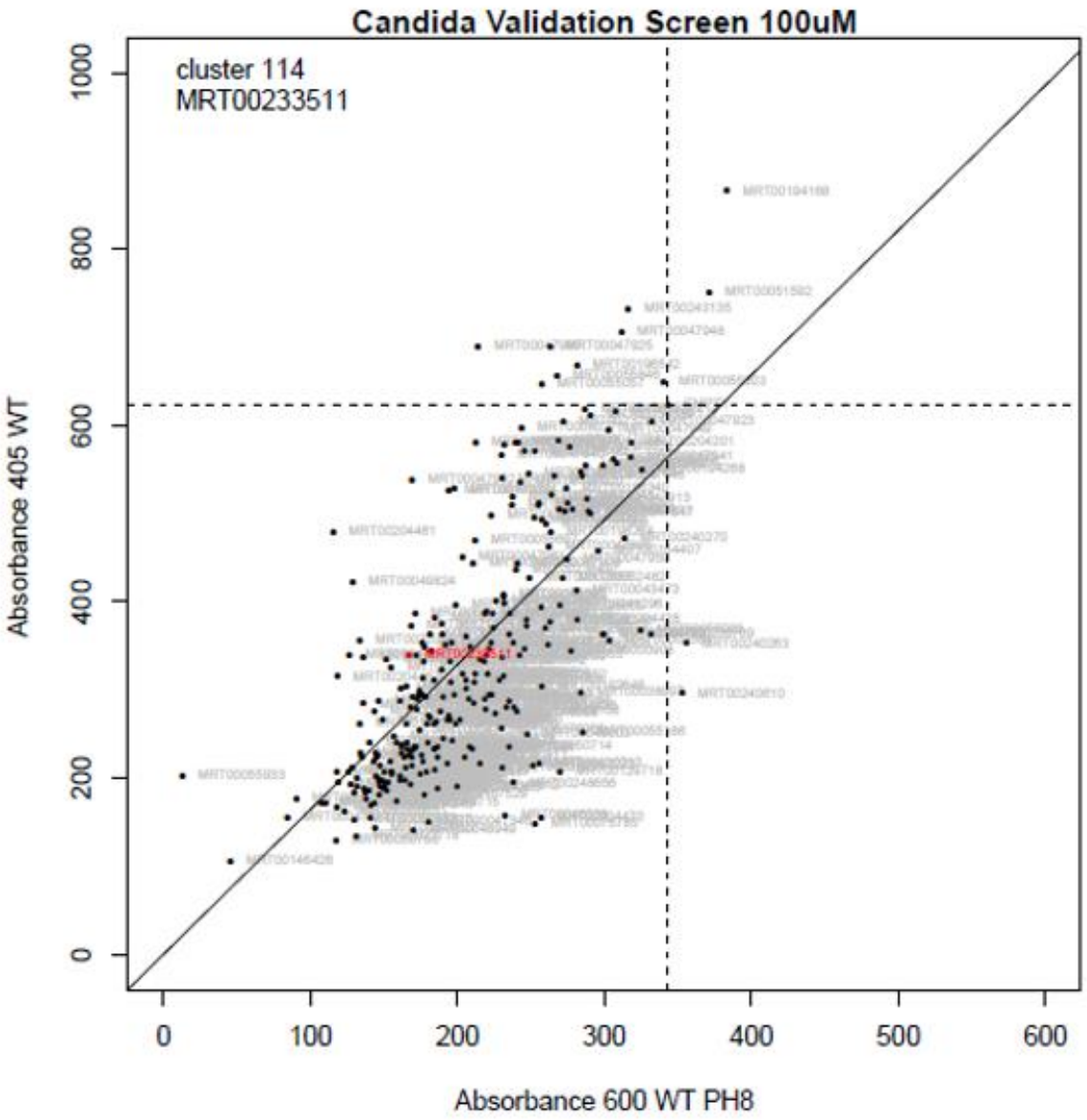

Cluster 114: 100 µM Secondary Screen: pH8 as a readout for PHO Pathway activity.
Plot of OD_{600} *wt* cells grown in pH 8 vs. OD_{405} of *wt* cells. Cells were grown to log phase in YPD before being washed 3 times in pH8 media and diluted back to OD_{600} = 0.05 then seeded into 384 well plates containing 100 µM of compound. Absorbance of 600 nm is used for growth at pH and 405 for secreted acid phosphatase activity. Red hits represent those from cluster 114.

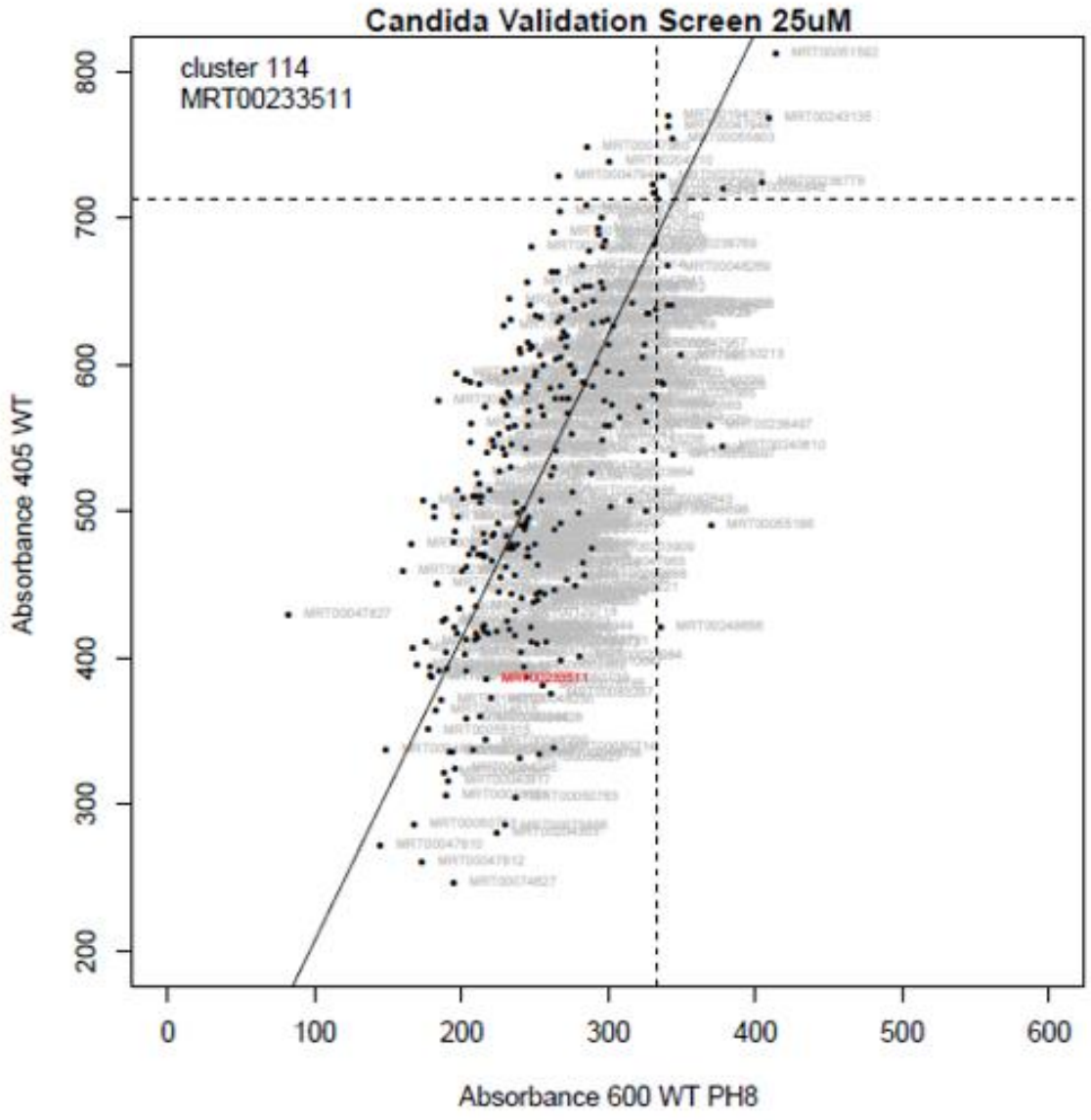

Cluster 114: 25 µM Secondary Screen: pH8 as a readout for PHO Pathway activity.
Plot of OD_{600} *wt* cells grown in pH 8 vs. OD_{405} of *wt* cells. Cells were grown to log phase in YPD before being washed 3 times in pH8 media and diluted back to OD_{600} = 0.05 then seeded into 384 well plates containing 25 µM of compound. Absorbance of 600 nm is used for growth at pH and 405 for secreted acid phosphatase activity. Red hits represent those from cluster 114.

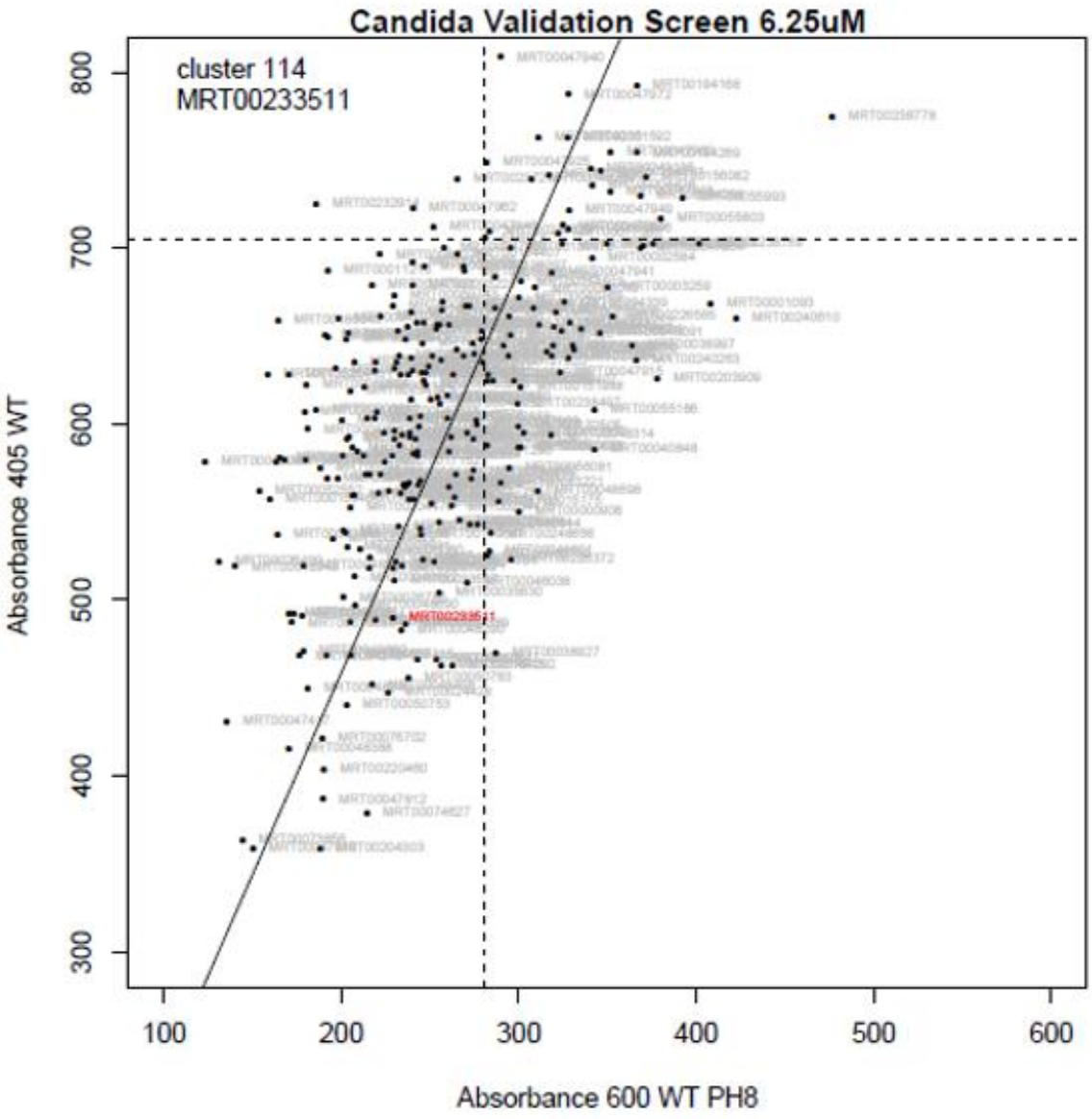

Cluster 114: 6.25 µM Secondary Screen: pH8 as a readout for PHO Pathway activity.
Plot of OD_{600} *wt* cells grown in pH 8 vs. OD_{405} of *wt* cells. Cells were grown to log phase in YPD before being washed 3 times in pH8 media and diluted back to OD_{600} = 0.05 then seeded into 384 well plates containing 6.25 µM of compound. Absorbance of 600 nm is used for growth at pH and 405 for secreted acid phosphatase activity. Red hits represent those from cluster 114.

Cluster 123

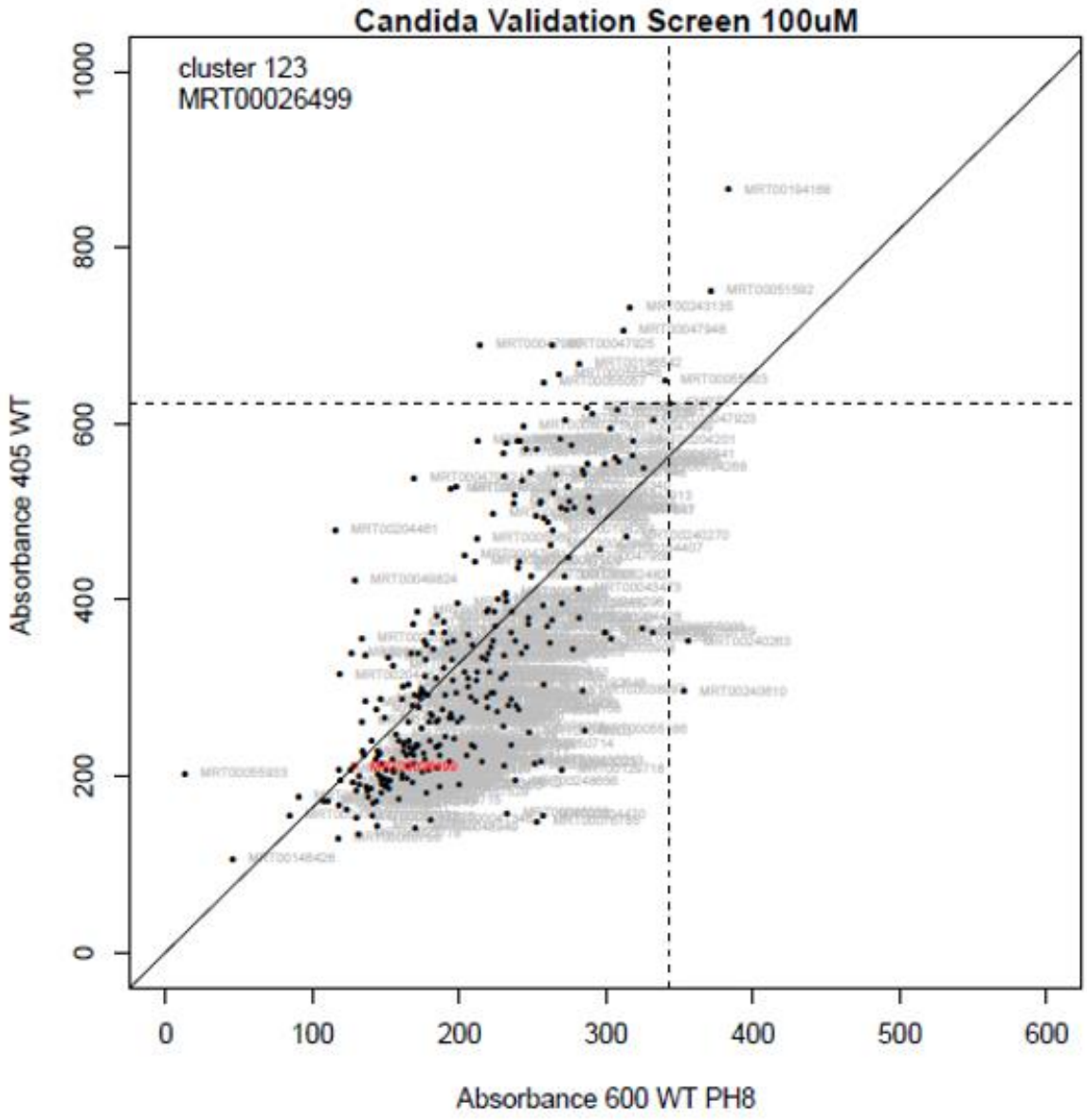

Cluster 123: 100 µM Secondary Screen: pH8 as a readout for PHO Pathway activity.
Plot of OD_{600} *wt* cells grown in pH 8 vs. OD_{405} of *wt* cells. Cells were grown to log phase in YPD before being washed 3 times in pH8 media and diluted back to OD_{600} = 0.05 then seeded into 384 well plates containing 100 µM of compound. Absorbance of 600 nm is used for growth at pH and 405 for secreted acid phosphatase activity. Red hits represent those from cluster 123.

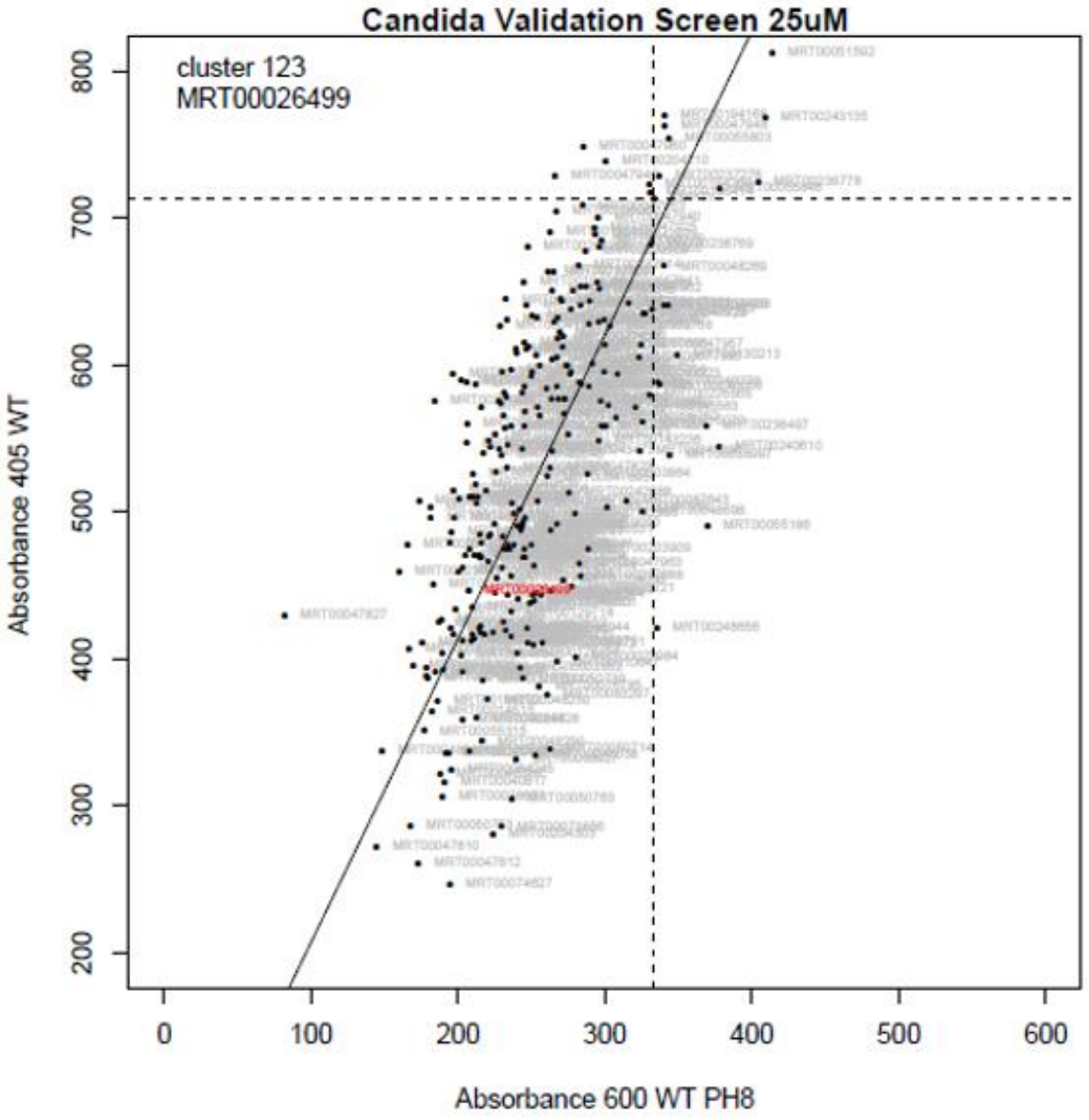

Cluster 123: 25 µM Secondary Screen: pH8 as a readout for PHO Pathway activity.
Plot of OD_{600} *wt* cells grown in pH 8 vs. OD_{405} of *wt* cells. Cells were grown to log phase in YPD before being washed 3 times in pH8 media and diluted back to OD_{600} = 0.05 then seeded into 384 well plates containing 25 µM of compound. Absorbance of 600 nm is used for growth at pH and 405 for secreted acid phosphatase activity. Red hits represent those from cluster 123.

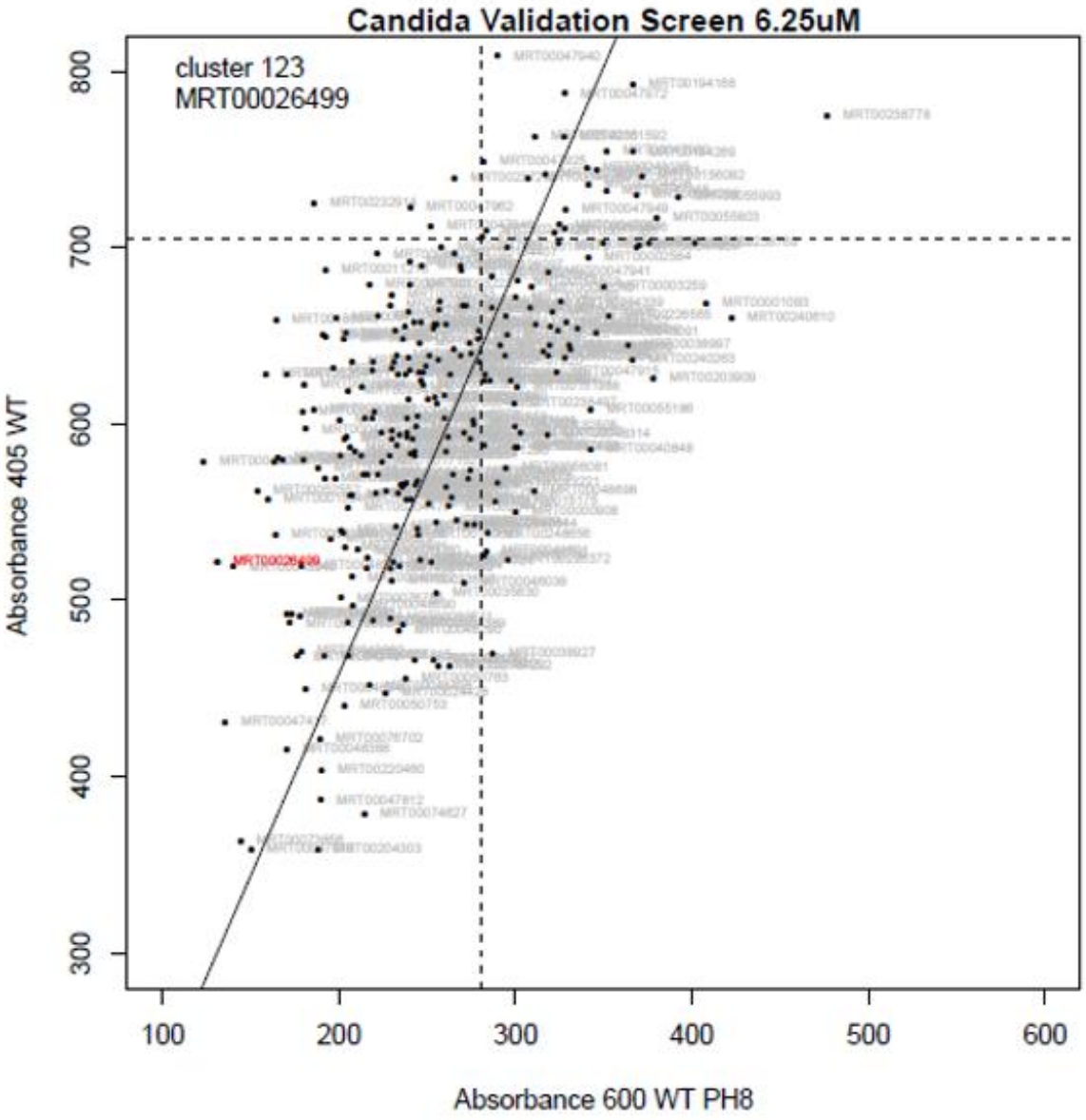

Cluster 123: 6.25 µM Secondary Screen: pH8 as a readout for PHO Pathway activity.
Plot of OD_{600} *wt* cells grown in pH 8 vs. OD_{405} of *wt* cells. Cells were grown to log phase in YPD before being washed 3 times in pH8 media and diluted back to OD_{600} = 0.05 then seeded into 384 well plates containing 6.25 µM of compound. Absorbance of 600 nm is used for growth at pH and 405 for secreted acid phosphatase activity. Red hits represent those from cluster 123.

Cluster 124

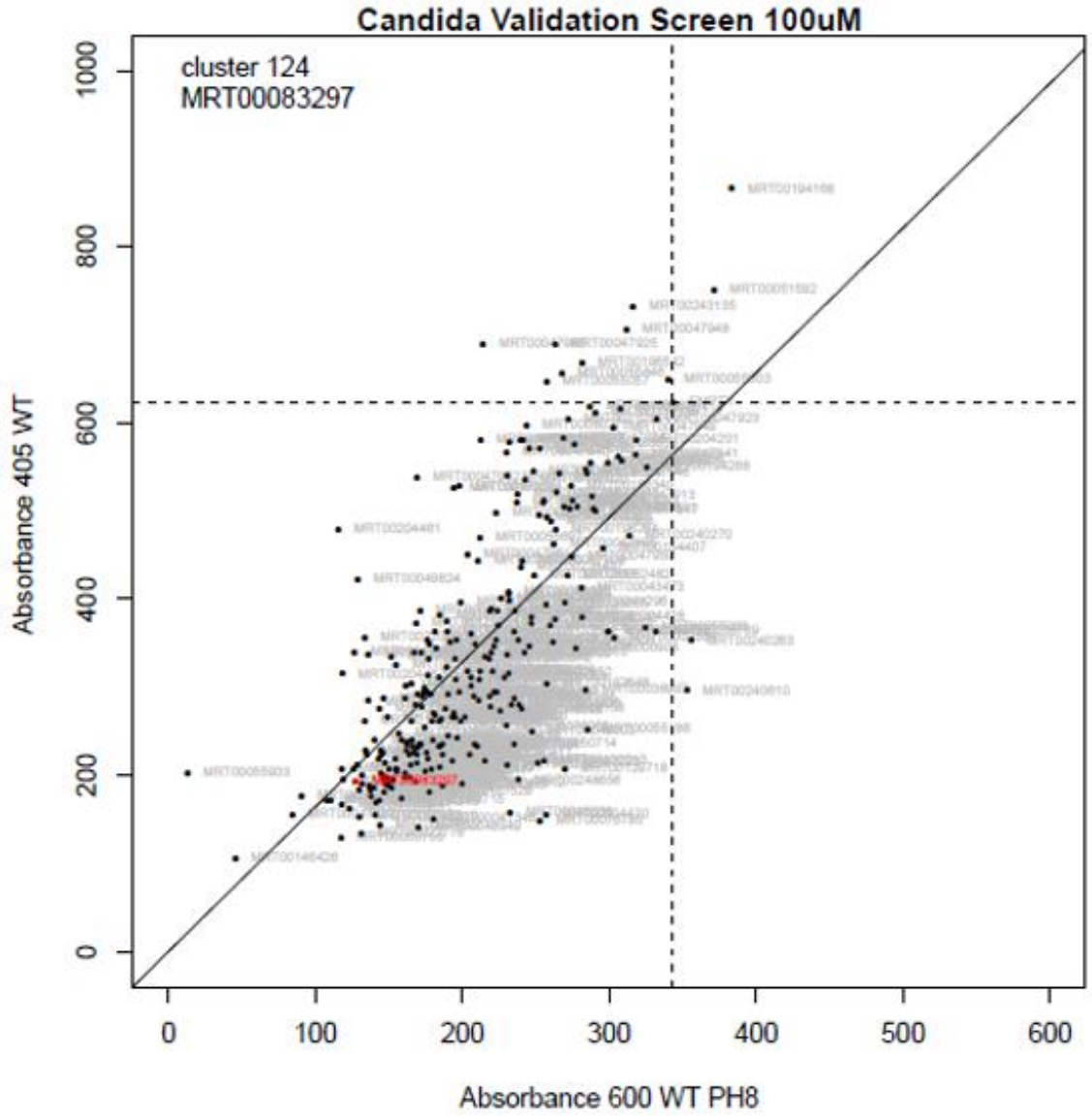

Cluster 124: 100 µM Secondary Screen: pH8 as a readout for PHO Pathway activity.
Plot of OD_{600} *wt* cells grown in pH 8 vs. OD_{405} of *wt* cells. Cells were grown to log phase in YPD before being washed 3 times in pH8 media and diluted back to OD_{600} = 0.05 then seeded into 384 well plates containing 100 µM of compound. Absorbance of 600 nm is used for growth at pH and 405 for secreted acid phosphatase activity. Red hits represent those from cluster 124.

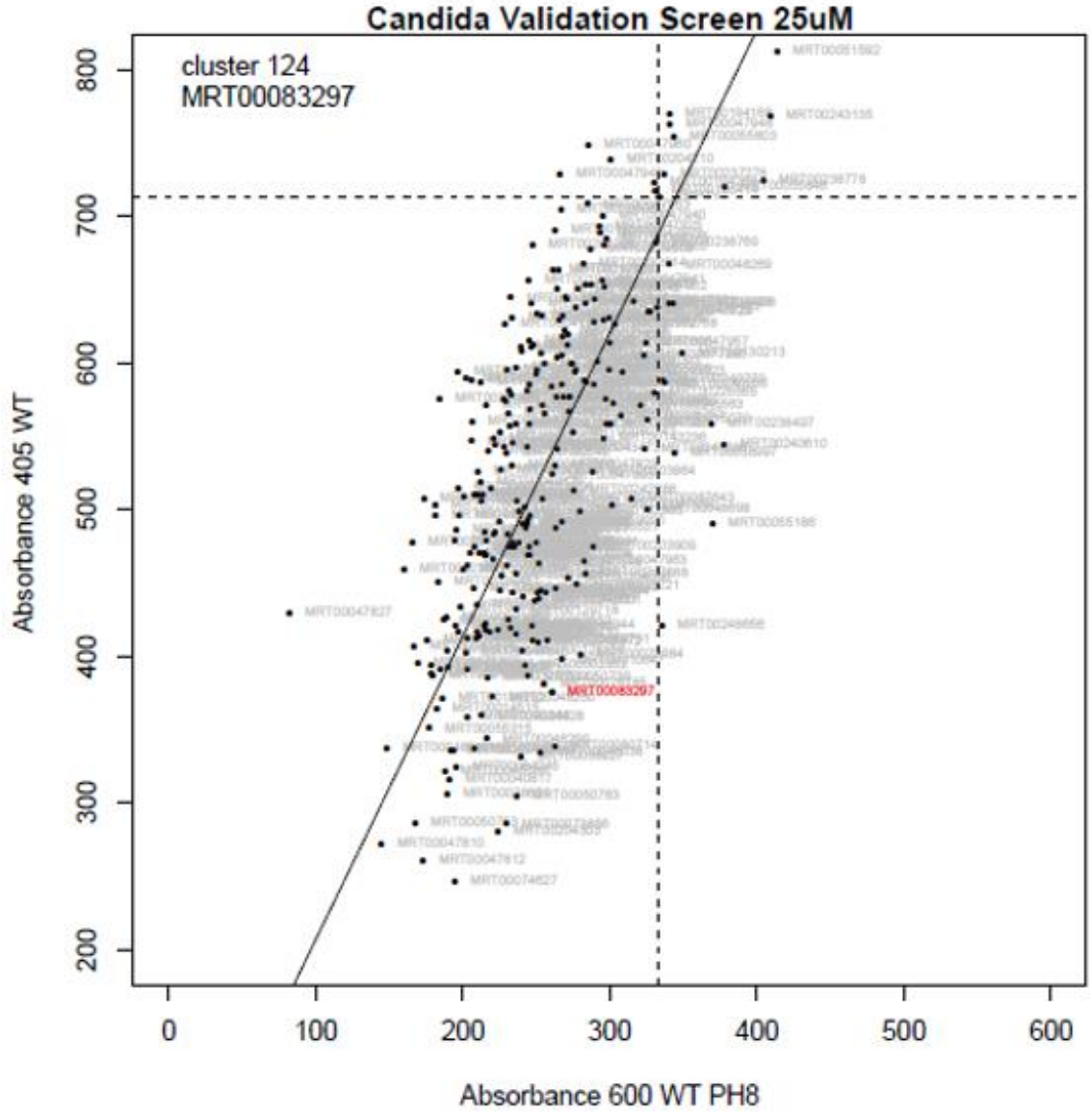

Cluster 124: 25 µM Secondary Screen: pH8 as a readout for PHO Pathway activity.
Plot of OD_{600} *wt* cells grown in pH 8 vs. OD_{405} of *wt* cells. Cells were grown to log phase in YPD before being washed 3 times in pH8 media and diluted back to OD_{600} = 0.05 then seeded into 384 well plates containing 25 µM of compound. Absorbance of 600 nm is used for growth at pH and 405 for secreted acid phosphatase activity. Red hits represent those from cluster 124.

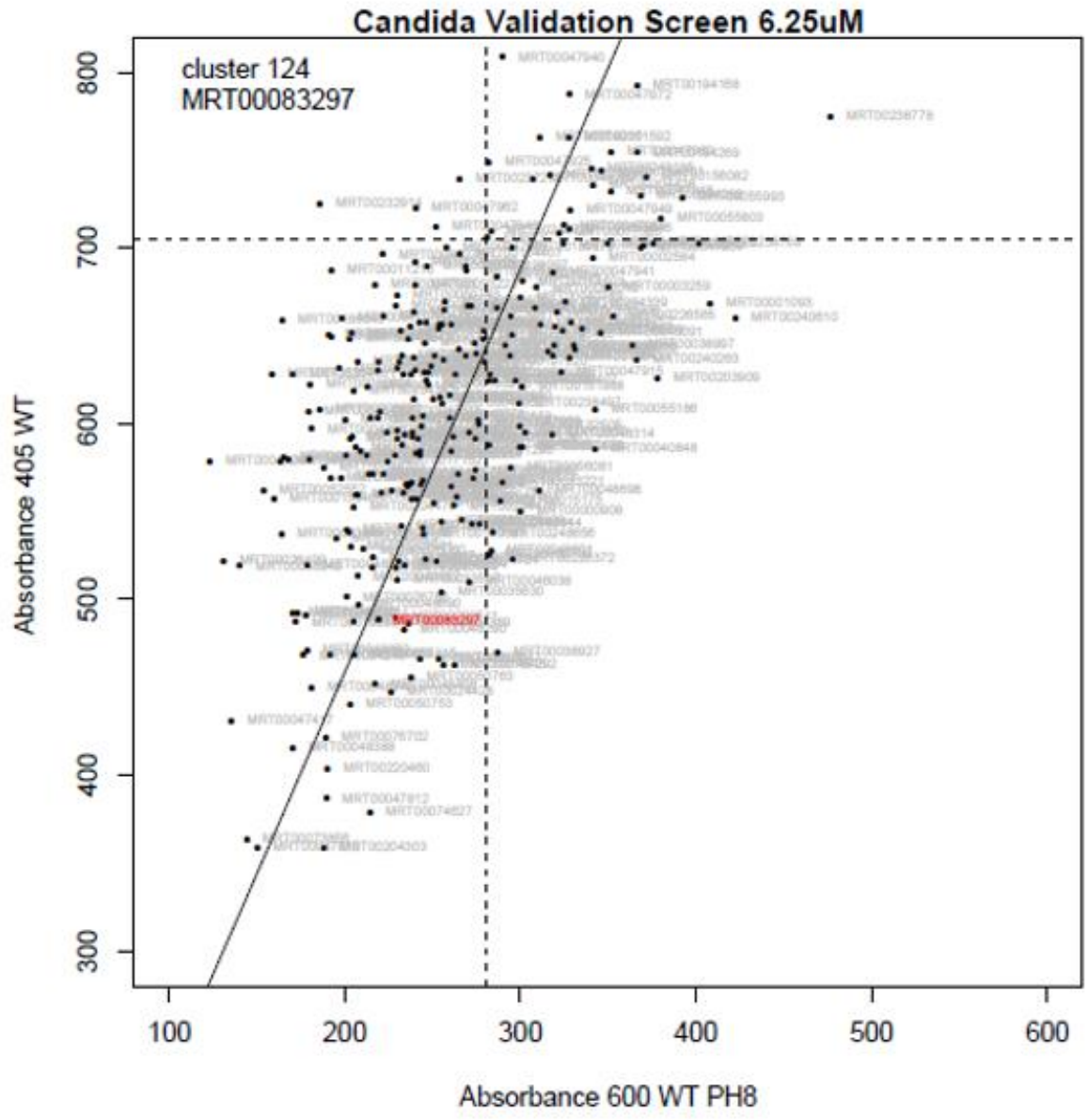

Cluster 123: 6.25 µM Secondary Screen: pH8 as a readout for PHO Pathway activity.
Plot of OD_{600} *wt* cells grown in pH 8 vs. OD_{405} of *wt* cells. Cells were grown to log phase in YPD before being washed 3 times in pH8 media and diluted back to OD_{600} = 0.05 then seeded into 384 well plates containing 6.25 µM of compound. Absorbance of 600 nm is used for growth at pH and 405 for secreted acid phosphatase activity. Red hits represent those from cluster 123.

Cluster 144

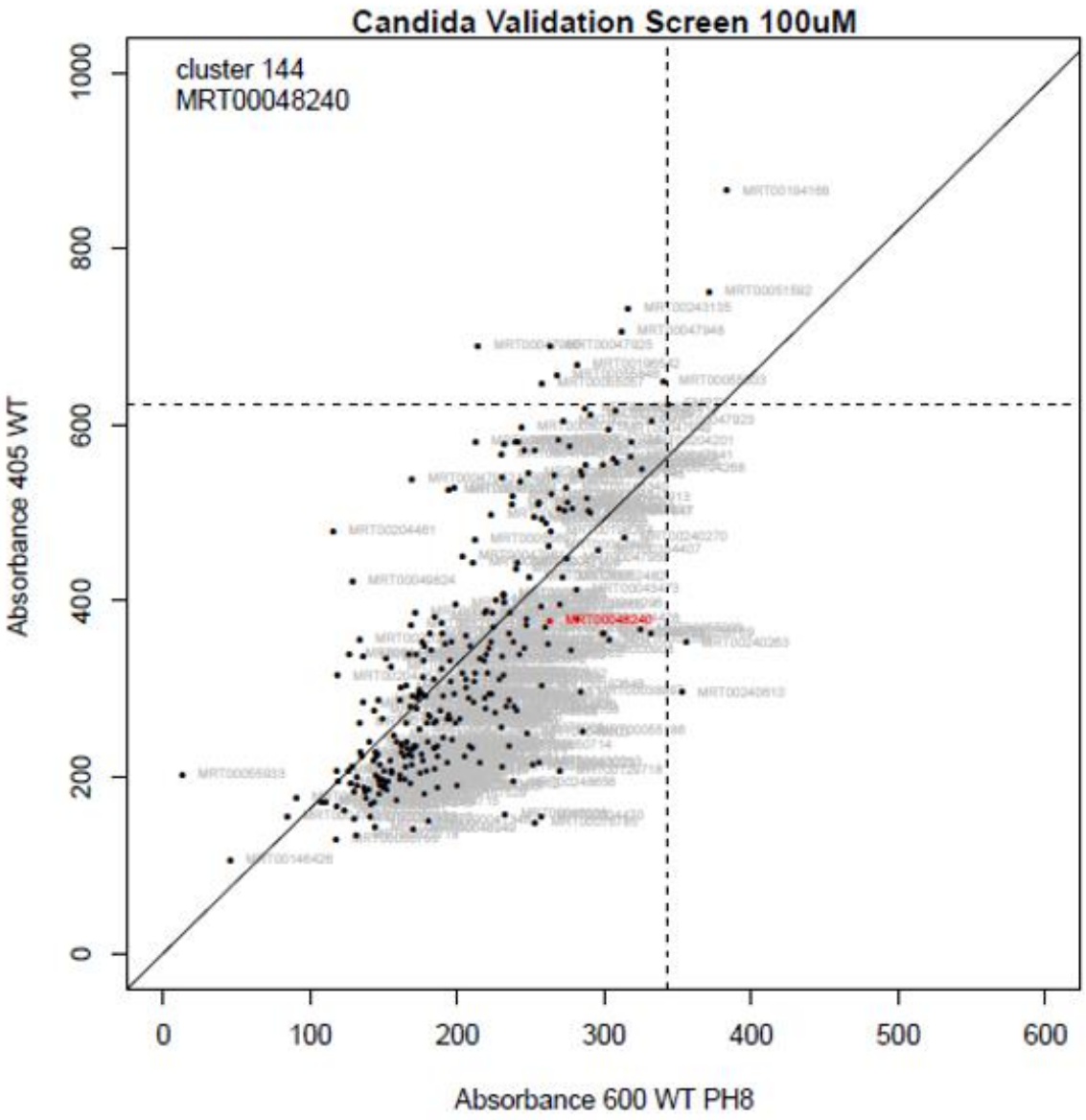

Cluster 144: 100 µM Secondary Screen: pH8 as a readout for PHO Pathway activity.
Plot of OD_{600} *wt* cells grown in pH 8 vs. OD_{405} of *wt* cells. Cells were grown to log phase in YPD before being washed 3 times in pH8 media and diluted back to OD_{600} = 0.05 then seeded into 384 well plates containing 100 µM of compound. Absorbance of 600 nm is used for growth at pH and 405 for secreted acid phosphatase activity. Red hits represent those from cluster 144.

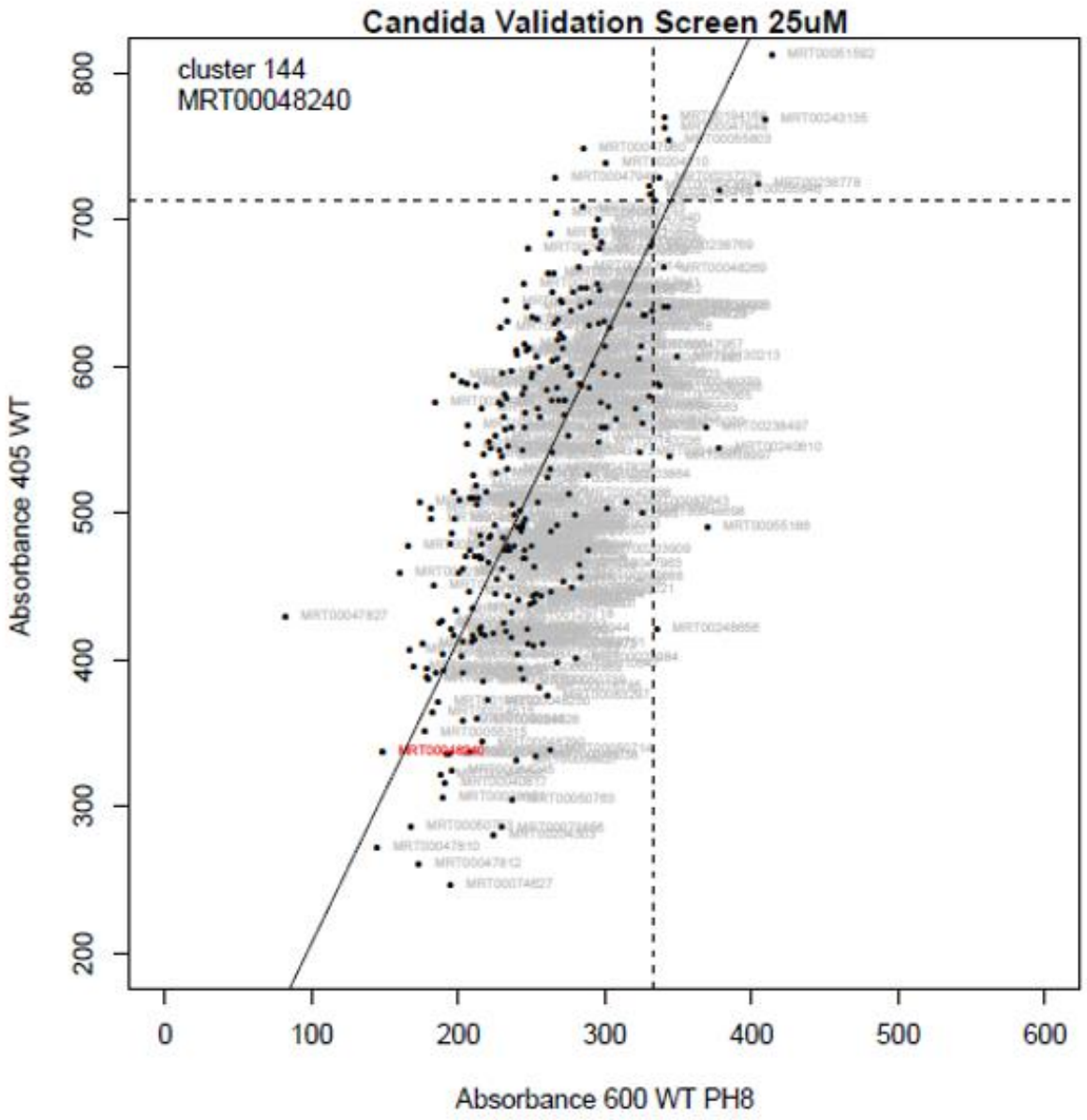

Cluster 144: 25 µM Secondary Screen: pH8 as a readout for PHO Pathway activity.
Plot of OD_{600} *wt* cells grown in pH 8 vs. OD_{405} of *wt* cells. Cells were grown to log phase in YPD before being washed 3 times in pH8 media and diluted back to OD_{600} = 0.05 then seeded into 384 well plates containing 25 µM of compound. Absorbance of 600 nm is used for growth at pH and 405 for secreted acid phosphatase activity. Red hits represent those from cluster 144.

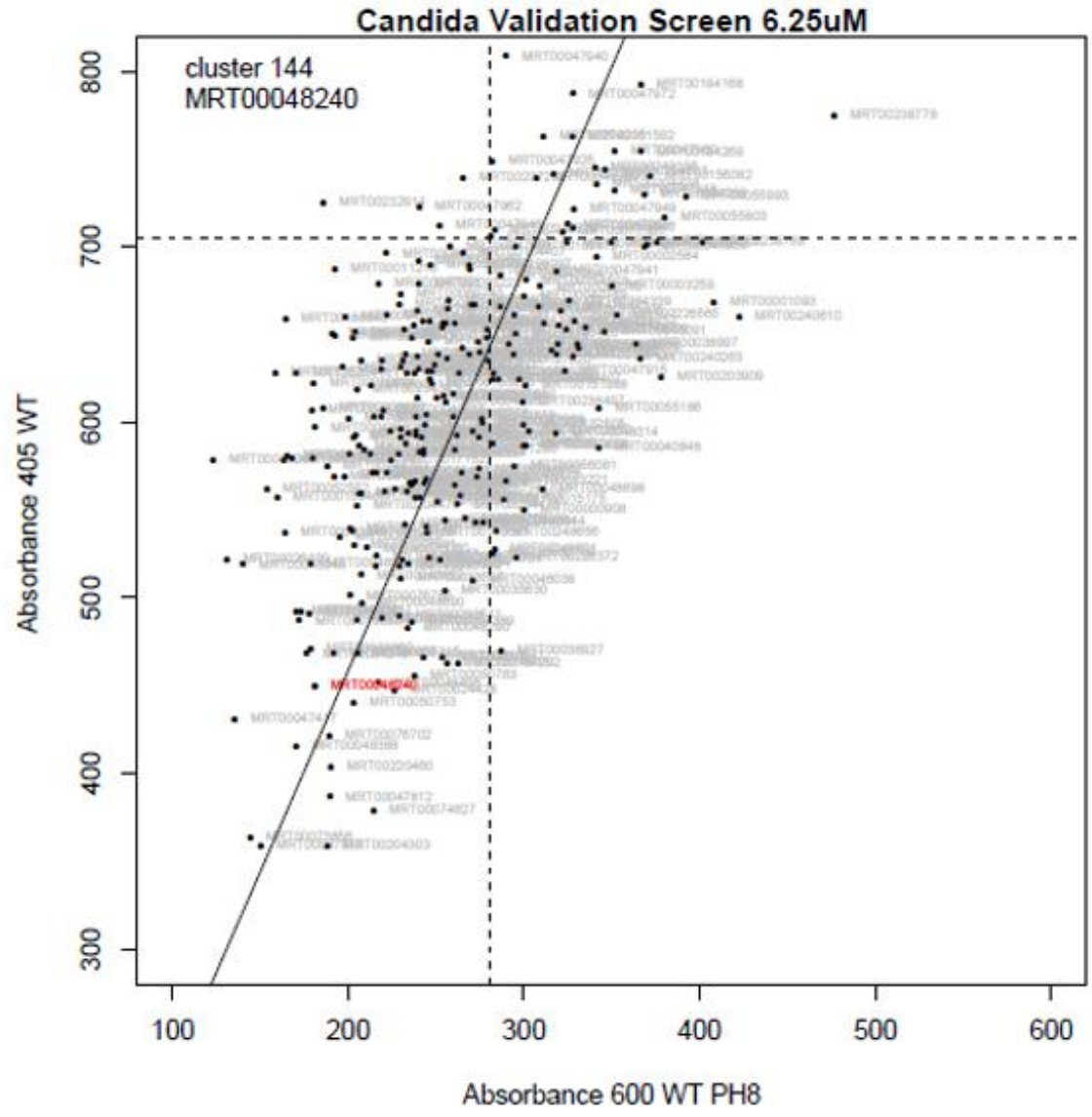

Cluster 144: 6.25 µM Secondary Screen: pH8 as a readout for PHO Pathway activity.
Plot of OD_{600} *wt* cells grown in pH 8 vs. OD_{405} of *wt* cells. Cells were grown to log phase in YPD before being washed 3 times in pH8 media and diluted back to OD_{600} = 0.05 then seeded into 384 well plates containing 6.25 µM of compound. Absorbance of 600 nm is used for growth at pH and 405 for secreted acid phosphatase activity. Red hits represent those from cluster 144.

Cluster 159

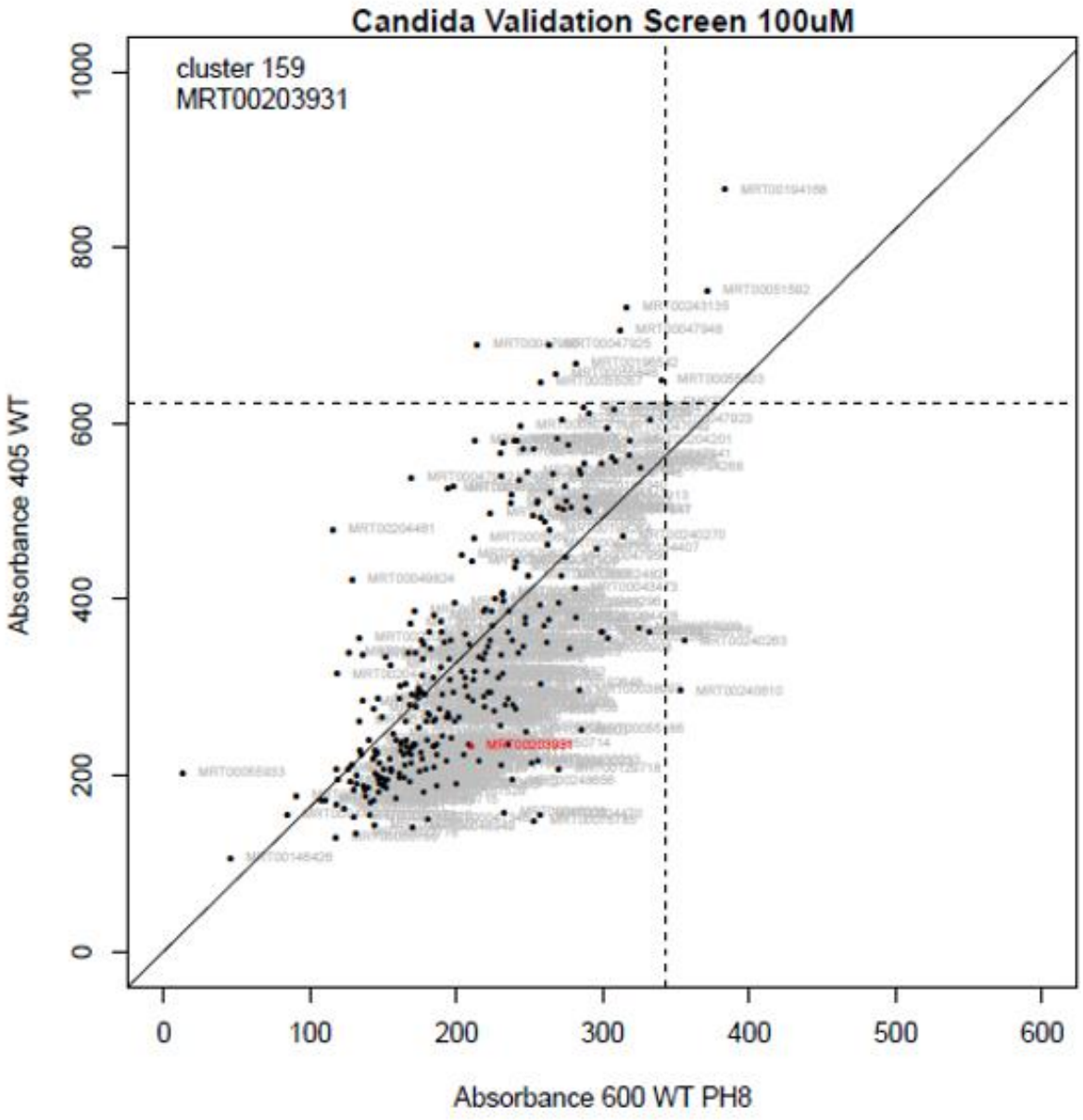

Cluster 159: 100 µM Secondary Screen: pH8 as a readout for PHO Pathway activity.
Plot of OD_{600} *wt* cells grown in pH 8 vs. OD_{405} of *wt* cells. Cells were grown to log phase in YPD before being washed 3 times in pH8 media and diluted back to OD_{600} = 0.05 then seeded into 384 well plates containing 100 µM of compound. Absorbance of 600 nm is used for growth at pH and 405 for secreted acid phosphatase activity. Red hits represent those from cluster 159.

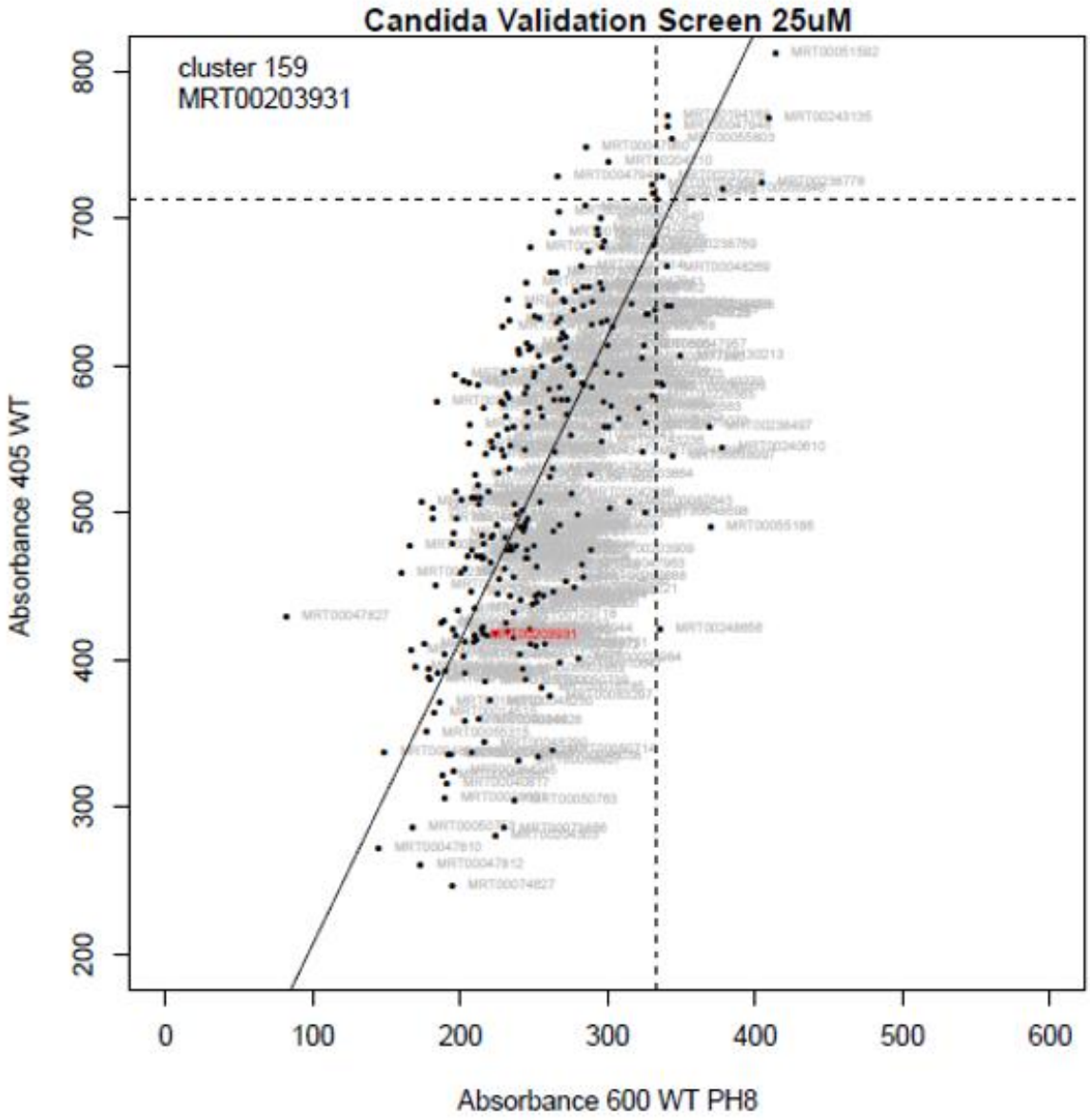

Cluster 159: 25 µM Secondary Screen: pH8 as a readout for PHO Pathway activity.
Plot of OD_{600} *wt* cells grown in pH 8 vs. OD_{405} of *wt* cells. Cells were grown to log phase in YPD before being washed 3 times in pH8 media and diluted back to OD_{600} = 0.05 then seeded into 384 well plates containing 25 µM of compound. Absorbance of 600 nm is used for growth at pH and 405 for secreted acid phosphatase activity. Red hits represent those from cluster 159.

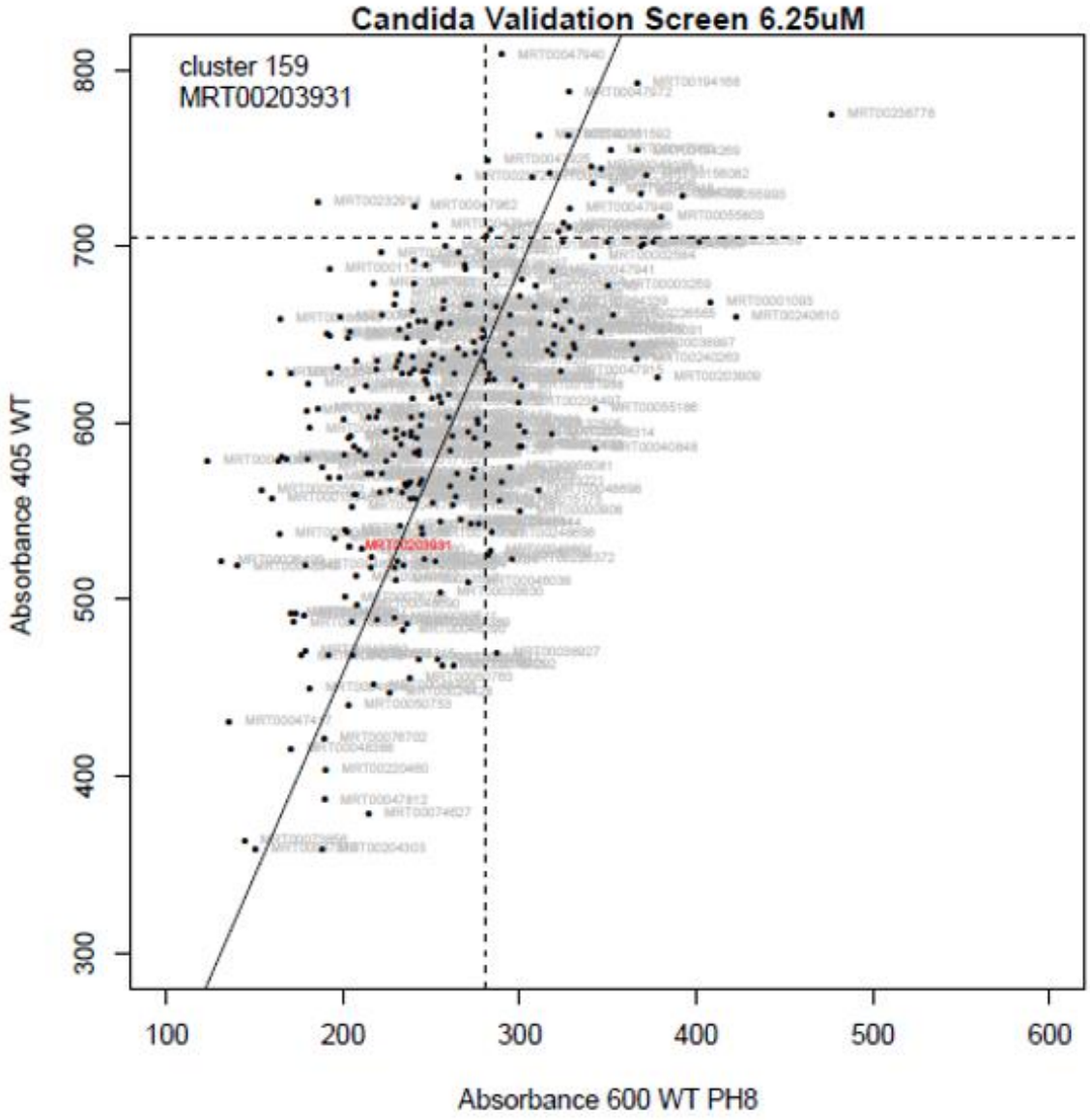

Cluster 159: 6.25 µM Secondary Screen: pH8 as a readout for PHO Pathway activity.
Plot of OD_{600} *wt* cells grown in pH 8 vs. OD_{405} of *wt* cells. Cells were grown to log phase in YPD before being washed 3 times in pH8 media and diluted back to OD_{600} = 0.05 then seeded into 384 well plates containing 6.25 µM of compound. Absorbance of 600 nm is used for growth at pH and 405 for secreted acid phosphatase activity. Red hits represent those from cluster 159.

Cluster 161

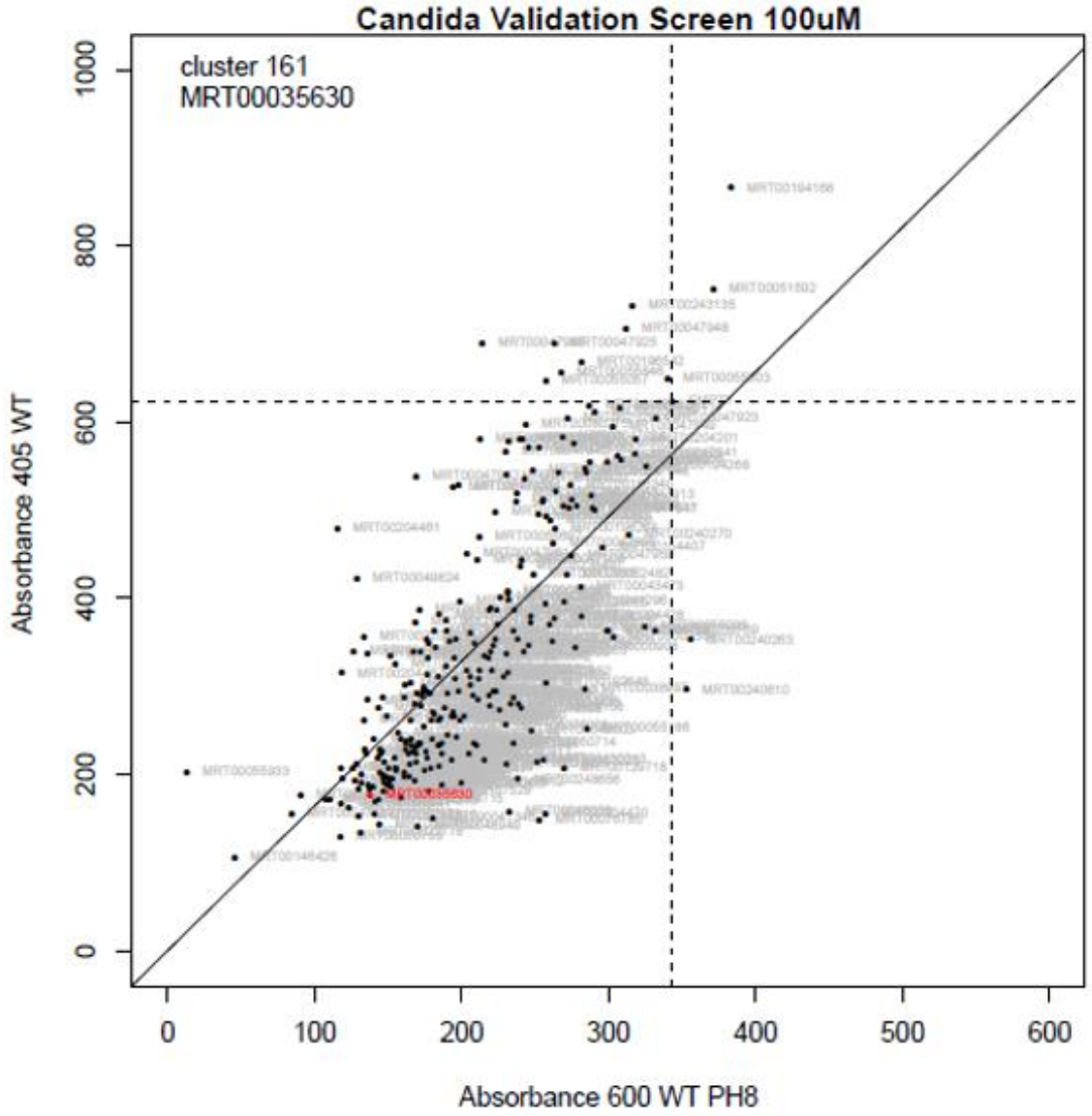

Cluster 161: 100 µM Secondary Screen: pH8 as a readout for PHO Pathway activity.
Plot of OD_{600} *wt* cells grown in pH 8 vs. OD_{405} of *wt* cells. Cells were grown to log phase in YPD before being washed 3 times in pH8 media and diluted back to OD_{600} = 0.05 then seeded into 384 well plates containing 100 µM of compound. Absorbance of 600 nm is used for growth at pH and 405 for secreted acid phosphatase activity. Red hits represent those from cluster 161.

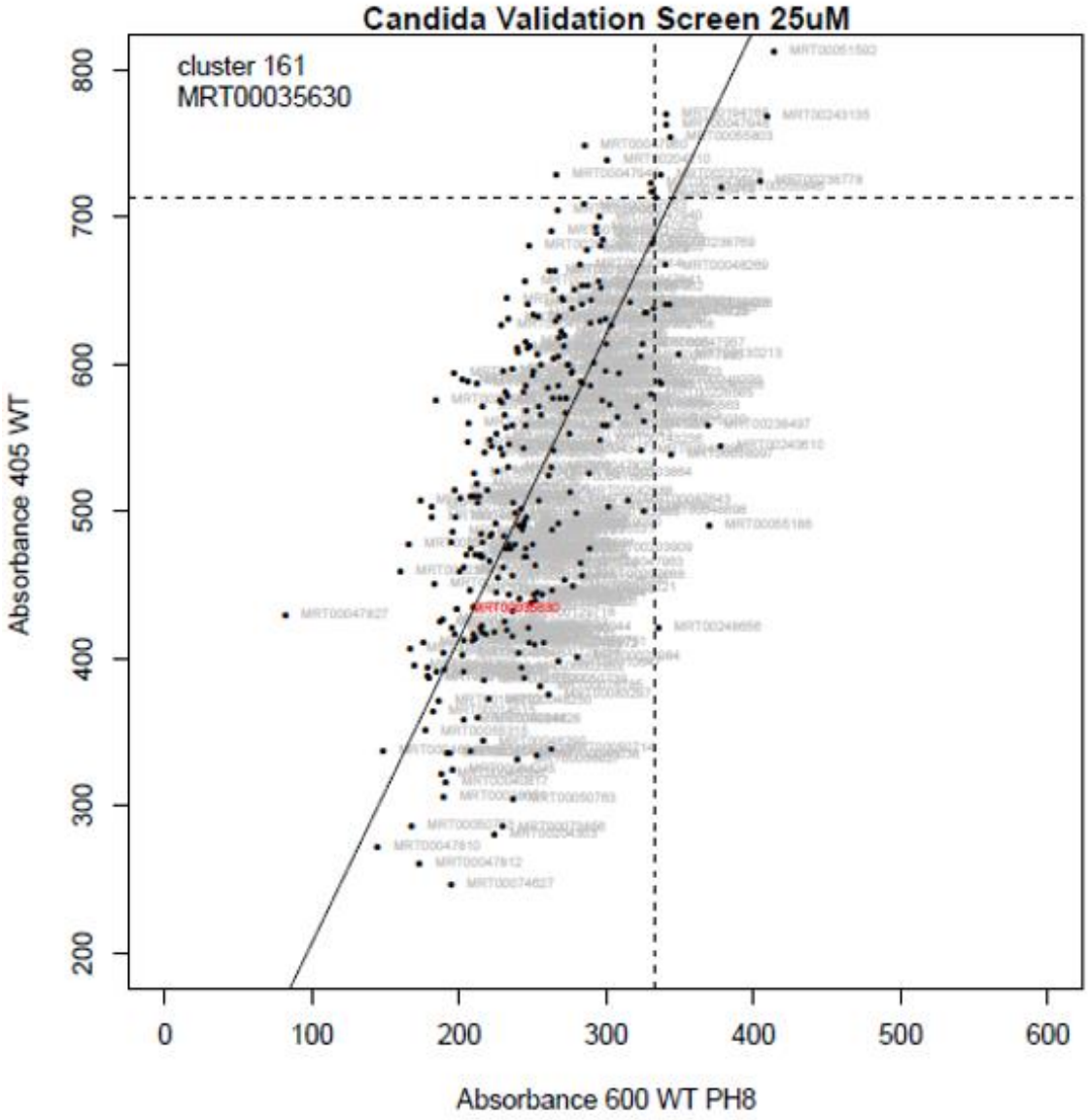

Cluster 161: 25 µM Secondary Screen: pH8 as a readout for PHO Pathway activity.
Plot of OD_{600} *wt* cells grown in pH 8 vs. OD_{405} of *wt* cells. Cells were grown to log phase in YPD before being washed 3 times in pH8 media and diluted back to OD_{600} = 0.05 then seeded into 384 well plates containing 25 µM of compound. Absorbance of 600 nm is used for growth at pH and 405 for secreted acid phosphatase activity. Red hits represent those from cluster 161.

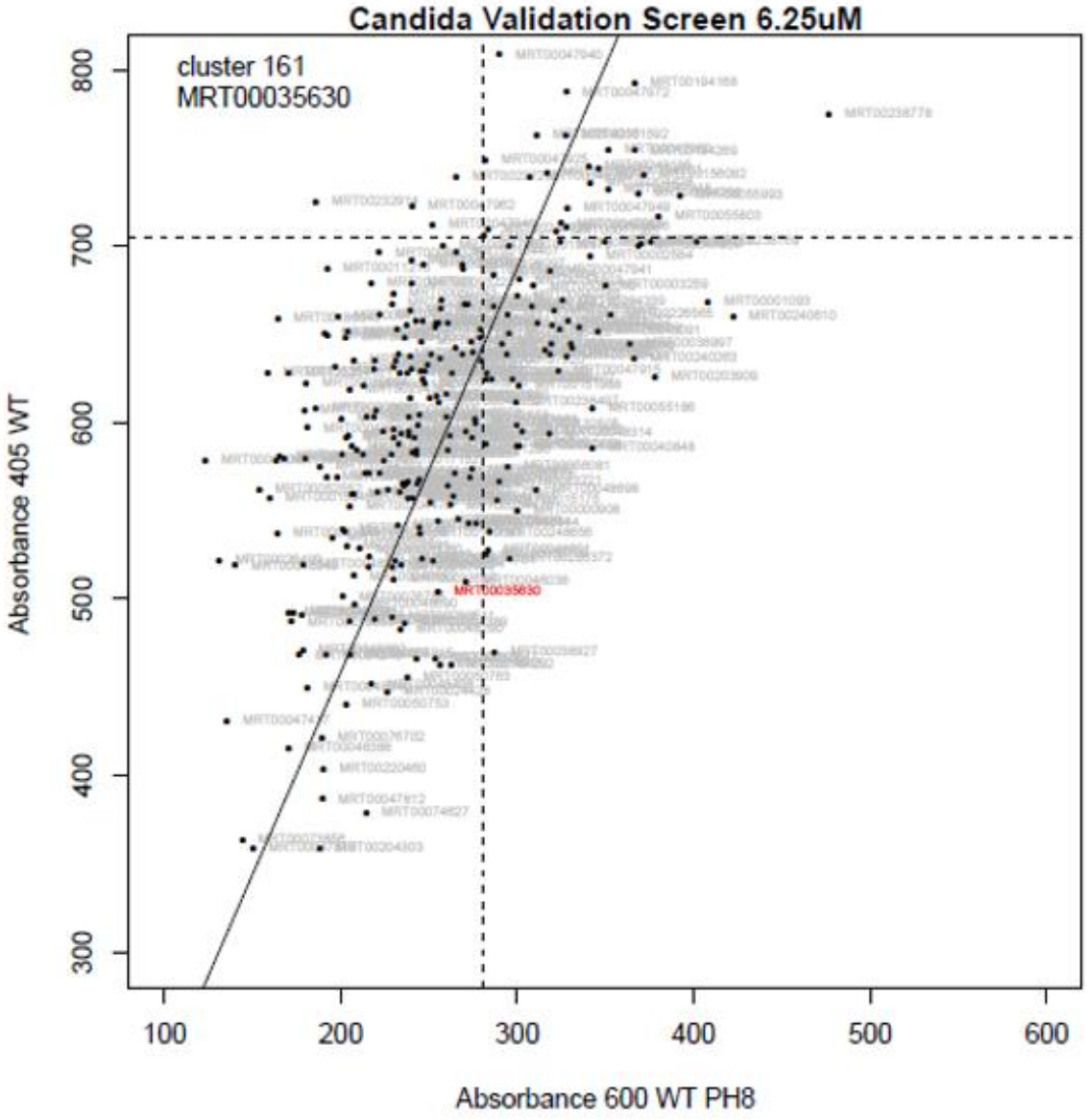

Cluster 161: 100 µM Secondary Screen: pH8 as a readout for PHO Pathway activity.
Plot of OD_{600} *wt* cells grown in pH 8 vs. OD_{405} of *wt* cells. Cells were grown to log phase in YPD before being washed 3 times in pH8 media and diluted back to OD_{600} = 0.05 then seeded into 384 well plates containing 6.25 µM of compound. Absorbance of 600 nm is used for growth at pH and 405 for secreted acid phosphatase activity. Red hits represent those from cluster 161.

Cluster 170

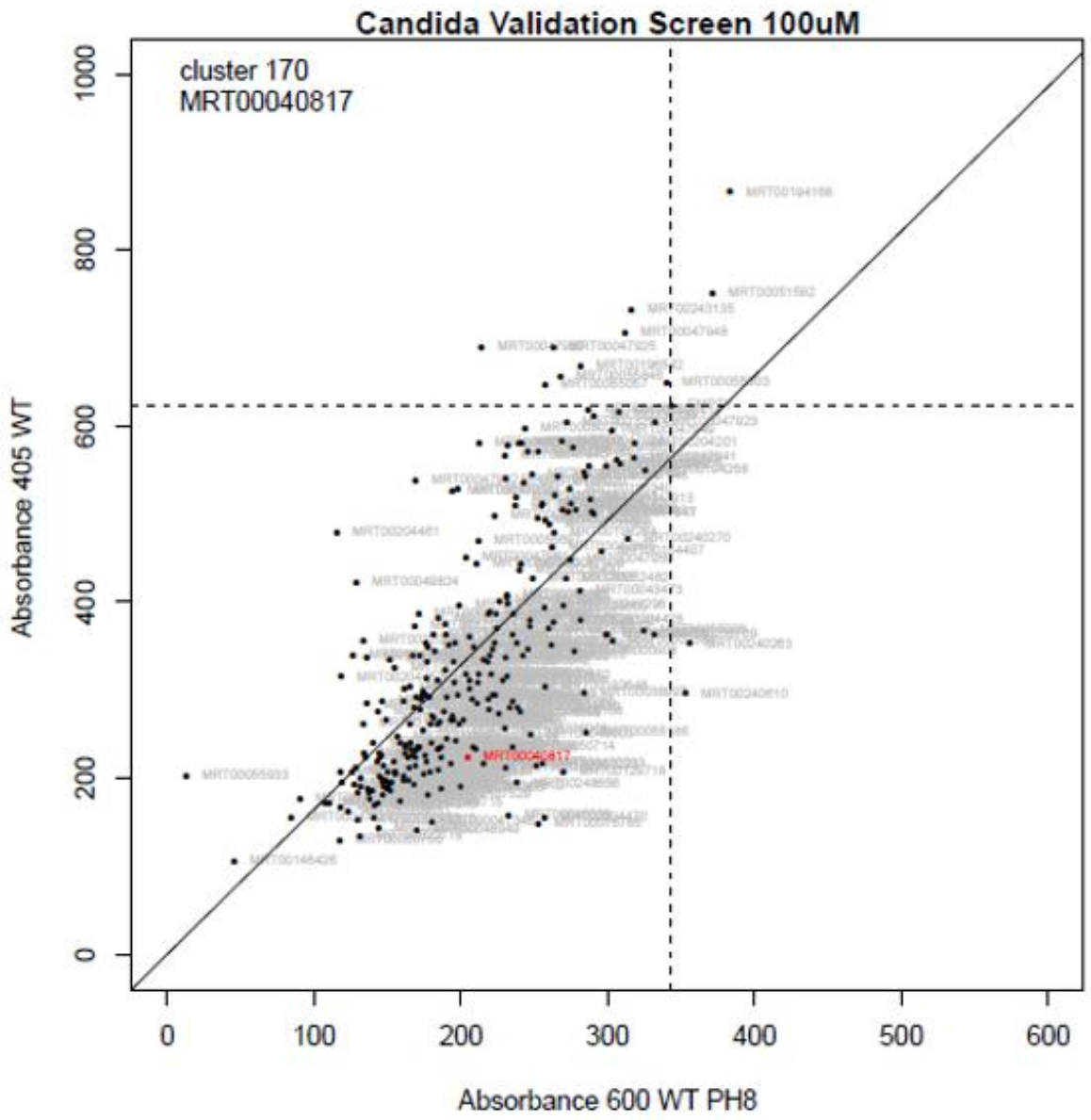

Cluster 170: 100 µM Secondary Screen: pH8 as a readout for PHO Pathway activity.
Plot of OD_{600} *wt* cells grown in pH 8 vs. OD_{405} of *wt* cells. Cells were grown to log phase in YPD before being washed 3 times in pH8 media and diluted back to OD_{600} = 0.05 then seeded into 384 well plates containing 100 µM of compound. Absorbance of 600 nm is used for growth at pH and 405 for secreted acid phosphatase activity. Red hits represent those from cluster 170.

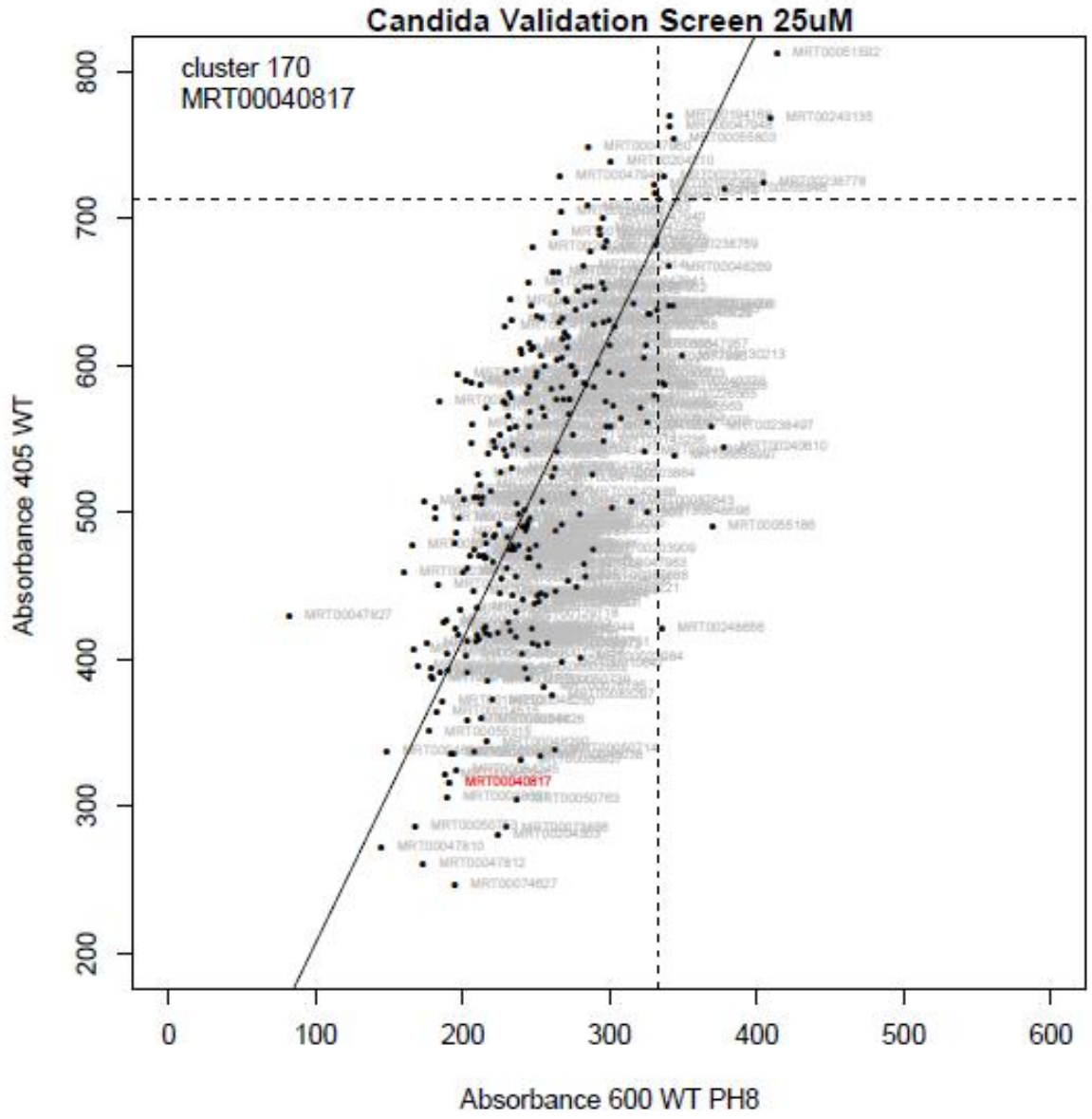

Cluster 170: 25 µM Secondary Screen: pH8 as a readout for PHO Pathway activity.
Plot of OD_{600} *wt* cells grown in pH 8 vs. OD_{405} of *wt* cells. Cells were grown to log phase in YPD before being washed 3 times in pH8 media and diluted back to OD_{600} = 0.05 then seeded into 384 well plates containing 25 µM of compound. Absorbance of 600 nm is used for growth at pH and 405 for secreted acid phosphatase activity. Red hits represent those from cluster 170.

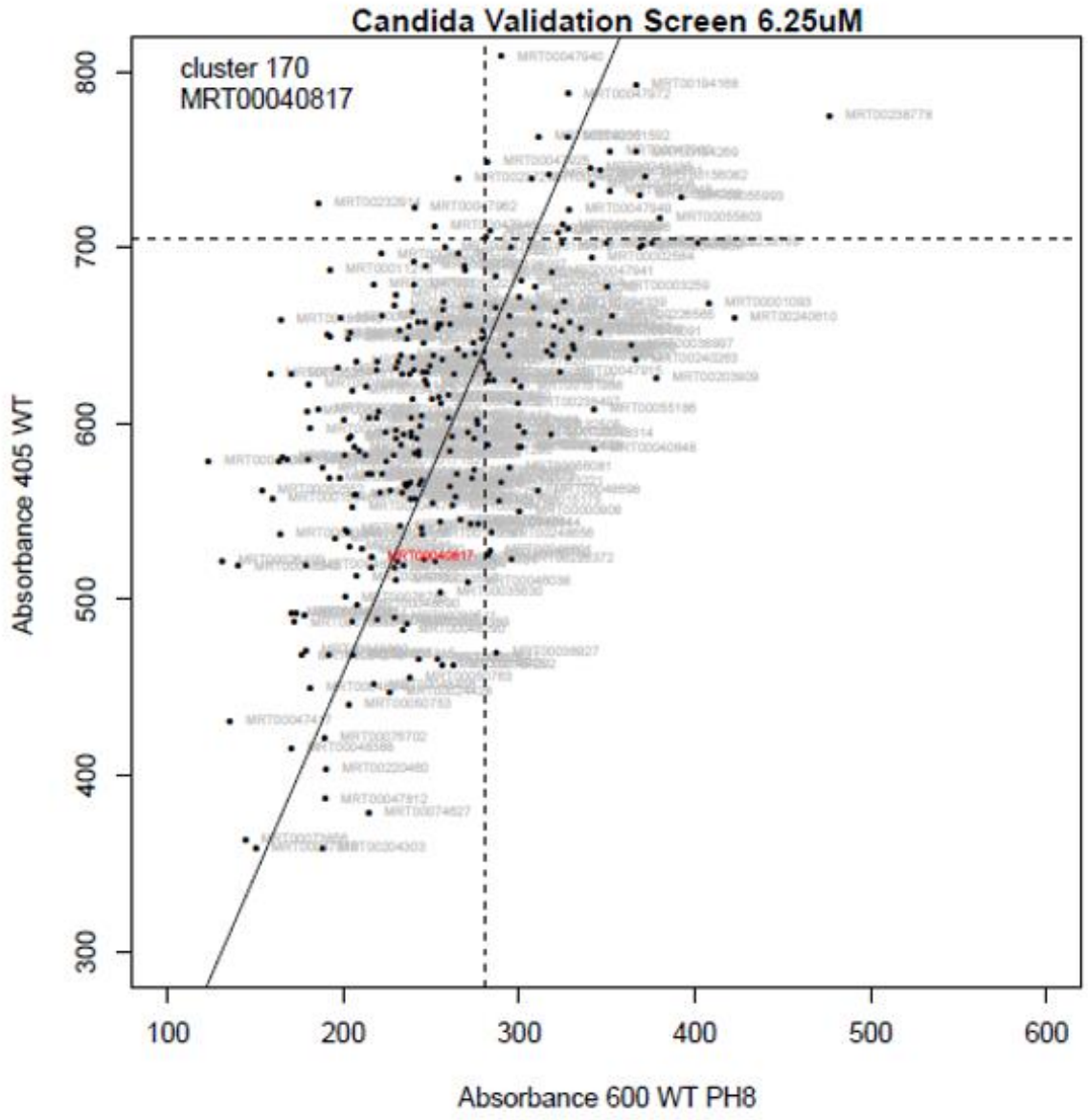

Cluster 170: 6.25 µM Secondary Screen: pH8 as a readout for PHO Pathway activity.
Plot of OD_{600} *wt* cells grown in pH 8 vs. OD_{405} of *wt* cells. Cells were grown to log phase in YPD before being washed 3 times in pH8 media and diluted back to OD_{600} = 0.05 then seeded into 384 well plates containing 6.25 µM of compound. Absorbance of 600 nm is used for growth at pH and 405 for secreted acid phosphatase activity. Red hits represent those from cluster 170.